Molecular mechanisms of the transcriptional regulation by PGC-1α/β in skeletal muscle

Inauguraldissertation

zur

Erlangung der Würde eines Doktors der Philosophie

vorgelegt der

Philosophisch-Naturwissenschaftlichen Fakultät

der Universität Basel

von

Barbara Heim-Kupr

aus Birsfelden (BL), Schweiz

Basel, 2018

Genehmigt von der Philosophisch-Naturwissenschaftlichen Fakultät

auf Antrag von

Prof. Dr. Christoph Handschin und Prof. Dr. Markus Rüegg

Basel, den 26.06.2018

Prof. Dr. Martin Spiess, Dekan

Table of contents

Abstract

Skeletal muscle (SKM) is an energetic organ with a high degree of plasticity. Different environmental stimuli as exercise or cold, but also physical inactivity, lead to complex molecular regulations that result in metabolic adaptations of the SKM and the whole body. Key factors in SKM plasticity and whole body energy homeostasis are the peroxisome proliferator-activated receptor (PPAR) γ coactivator-1 (PGC-1) family including three members, PGC-1α, PGC-1β and PGC-related coactivator (PRC). The PGC-1s are coactivators and hence use transcription factor binding partners (TFBP) in order to regulate their target genes. The complexity of transcriptional control might even be increased by epigenetic alterations, mainly DNA methylation.

The aim of my thesis was to study the regulation of global molecular mechanisms by SKM PGC-1α and PGC-1β leading to muscle plasticity in various environmental contexts. We combined diverse experimental, computational and multi-omics approaches such as chromatin immunoprecipitation sequencing (ChIPseq), RNA sequencing (RNAseq), reduced representation bisulfite sequencing (RRBS) and CRISPR (clustered regularly interspaced short palindromic repeats)/Cas (CRISPR-associated proteins) genome editing technology in skeletal muscle systems *in vitro* and *in vivo* and investigated the effect of external stimuli as cold or exercise in different PGC-1α/β genotypes.

Our data show that various interventions like acute and chronic exercise have different methylation profiles or combined with cold-induced muscle shivering, individual transcript profiles in wild type (WT) mice. A time-dependent correlation of DNA methylation with gene expression was observed, however dissimilar in acute and chronic exercise. Furthermore, we dissected potential memory marks on the DNA by methylation following chronic training in mice. In addition, we could show for the first time a role of PGC-1α, not only in exercise performance but as well in altered transcriptome and methylome profiles subsequent to exercise and changed transcription profile to cold stimulation, by using muscle-specific PGC-1α knockout (MKO) mice. Thus, PGC-1α is a major contributor in global metabolic control by the regulation of a transcriptional network through multiple TF interactions and its involvement in epigenetic alterations.

To further investigate the PGC-1α network, the Ppargc1a locus multiplex epitope tag knock-in mouse, which we generated by the CRISPR/Cas technology, will serve as a platform for future studies. This genetic mouse model allows now detailed evaluation of PGC-1α isoforms as well as the identification of new TFBPs under diverse contexts and in different tissues, due to non-tissue-specific epitope tags at the proximal PGC-1α promoter. However, in C2C12 myotubes we could show that PGC-1α regulates its target genes either by direct TF binding or indirectly. Even more, the genomic context of guanine-cytosine (GC) and cytosine-phosphate-guanine (CpG) amount affects PGC-1α recruitment and allows the estrogen-related receptor α (ERRα), a known TFBP of PGC-1α in the regulation of mitochondrial biogenesis, to regulate PGC-

1α target genes without coactivation by PGC-1α but by interaction with the TF specificity protein 1 (SP1). Contrarily, we observed that PGC-1β acts mostly indirect on its target genes and only to a very small extent direct on the DNA by TF binding.

Taken together, our data provide new knowledge of the functional role of PGC-1α and PGC-1β in SKM metabolism. The involvement of transcriptional regulation and epigenetic control under basal, acute and chronic exercise conditions as well as in cold-induced muscle shivering, adds a next piece of puzzle to the complex network regulated by these coactivators. Our findings help to understand the mechanism of SKM plasticity and open new signaling pathways and targets, which will, complemented with further studies, support the development of novel therapeutic strategies to cure myopathies and fight against metabolic disorders and other pathophysiological conditions.

Abbreviations

5hmC	5-hydroxymethylcytosine
5mC	5-methylcytosine
aa	Amino acid
AD	Activation domain
AMP	Adenosine monophosphate
AMPK	AMP-activated protein kinase
ARC	activator-recruited co-factor
ATP	Adenosine triphosphate
β2-AR	β2-adrenergic receptor
BAF60a	BRG1-assocated factor 60a
BAT	Brown adipose tissue
bp	Base pair
cAMP	cyclic adenosine monophosphate
CaMKIV	Calcium/calmodulin-dependent protein kinase IV
Cas	CRISPR-associated protein
CBP	CREB binding protein
CE	Cold exposure
CH_3	methyl group
ChIPseq	Chromatin immunoprecipitation sequencing
crRNA	CRISPR RNA
Crunch	Completely Automated Analysis of ChIP-seq Data
CnA	Calcineurin A
CpG	cytosine-phosphate-guanine
CREB	cAMP-response element-binding protein
CRISPR	clustered regularly interspaced short palindromic repeats
DE	differentially expressed
Dio2	Deiodinase 2
DM	differentiation medium
DMR	differentially methylated region
DNMT	DNA methyltransferases
DSB	double strand break

ES cells	Embryonic stem cells
ERα	Estrogen receptor α
ERRα	Estrogen-related receptor α
FC	fold change
FDR	false discovery rate
FOXO3	Fork-head transcription factor O3
GABP	GA-binding protein
GC	guanine-cytosine
GCN	Gastrocnemius muscle
GCN5	General control of amino acid synthesis 5
gDNA	genomic DNA
gRNA	guide RNA
GM	growth medium
GO	gene ontology
GSK3β	Glycogen synthase kinase 3β
HAT	Histone acetyltransferase
HCF	Host cell factor
HDAC	Histone deacetylase
HDR	homology directed repair
HS	horse serum
HSP	heat shock protein
i.p.	intraperitoneal
ISMARA	integrated motif activity response analysis
IU	International unit
kb	kilo base
KI	Knock-in
LB	lysogeny broth
LXRα	liver X receptor α
MAFbx	Muscle atrophy F-box
MEF2C/D	Myocyte enhancer factor 2C/D
MKO	skeletal muscle-specific PGC-1α knockout mouse
mTORC1	mammalian target of rapamycin complex 1

MuRF1	Muscle RING-finger protein-1
MyHC	Myosin heavy chain
MyoD	Myogenic Factor 3
NAD+ / NADH	Nicotinamide adenine dinucleotide
NFκB	Nuclear factor-kappaB
NHEJ	nonhomologues end joining
NLS	Nuclear localization signal
NMJ	Neuromuscular junction
NR	Nuclear receptor
NRF	nuclear respiratory factor
NT-PGC-1α	N-Terminal truncated PGC-1α
p38 MAPK	p38 mitogen-activated protein kinase
p160 MBP	p160 myb binding protein
PAM	protospacer adjacent motif
PCA	principal component analysis
PDK4	pyruvate dehydrogenase kinase 4
PGC-1	PPARγ coactivator-1
PPAR	Peroxisome proliferator-activated receptor
PRC	PGC-related coactivator
PRMT1	protein arginine methyltransferase 1
PTM	Posttranslational modification
RE	Restriction enzyme
redox	reduction–oxidation reaction
RIP140	receptor interaction protein 140
RNAseq	RNA sequencing
RRBS	reduced representation bisulfite sequencing
RRM	RNA recognition motif
RS	Arginine/Serine-rich domain
RT	room temperature
Quad	Quadriceps muscle
qRT-PCR	quantitative real-time polymerase chain reaction
S6K	S6 kinase

SAM	S-adenosyl methionine
SCF cdc4	Skp1/Cullin/F-box
SEM	standard errors of the means
SIRT1	Sirtuin 1
SKM	Skeletal muscle
SRC-1	steroid receptor coactivator-1
T2D	Type 2 diabetes
TET	Ten-Eleven-Translocation oxygenases
TF	Transcription factor
TFAM	Mitochondrial transcription factor A
TFBP	Transcription factor binding partner
TFBS	Transcription factor binding site
Tg	skeletal muscle-specific PGC-1α overexpressing mice
TRAP/DRIP	Thyroid hormone receptor-associated protein/ vitamin D receptor interacting protein
trcrRNA	trans-activating crRNA
TSS	Transcription start site
UCP	Uncoupling protein
VEGF	Vascular endothelial growth factor
WT	Wild type mice

1. Introduction

1.1 Skeletal muscle and body metabolism

Skeletal muscle (SKM), approximately 40% of the body mass, is the largest and most abundant organ in the corpus with a central function in the modulation of whole body homeostasis and thus, health status. During maximal physical activity SKM can account up to 90% of whole body energy expenditure, while at sedentary state, only 20-30% of the resting energy expenditure are used (Egan and Zierath, 2013; Summermatter and Handschin, 2012; Zurlo et al., 1990). SKM is the main place of energy expenditure, glycogen storage and insulin-stimulated glucose uptake and has thus, a significant impact on whole body metabolism and displays a high degree of plasticity in response to stimuli (Egan and Zierath, 2013). Hence, physical inactivity has been linked to metabolic disorders like type 2 diabetes (T2D), obesity, cardiovascular diseases, cancer and others, which could be prevented by physical activity (Booth et al., 2012; Colberg et al., 2010b; Egan and Zierath, 2013; Haskell et al., 2007).

1.1.1 Skeletal muscle plasticity

SKM is composed of a heterogeneous myofiber population with different metabolic and functional properties, slow-oxidative (type 1) and fast-glycolytic (type 2) fibers, with type 2 subdivided into 2A, 2B and 2X fibers. Type 1 oxidative fibers appear red in color due to a high myoglobin content, have a high mitochondrial portion and oxidative capacity, are characterized by slow-twitch properties, dominantly express myosin heavy chain 1 (MyHC-1) and are resistant to fatigue (Schiaffino and Reggiani, 2011). On the other hand, type 2 glycolytic fibers, mainly 2B and 2X, exhibit glycolytic metabolism, have low mitochondrial content, fast-twitch properties and are low fatigue resistant. 2A fibers have intermediate characteristics between type 1 and type 2B/2X. Rodent type 2 fibers are expressing MyHC-2A, MyHC-2B or MyHC-2X, respectively, while human SKM do not have type 2B myofibers (Schiaffino and Reggiani, 2011). This heterogeneity in muscle fibers allows the muscle to be plastic in a high degree and ensures tight regulation dependent on a variety of activities, from supporting the skeleton for upright standing to explosive movements during a sprint. Hence, this plasticity can be influenced by external stimuli such as specific exercise training or nutrients.

Endurance or aerobic exercise is defined as performing exercise for a long period against low load. There, fatty acids coming from intramuscular and adipose tissue triglyceride stores and carbohydrates in form of glucose, emerging from the circulation and intramuscular glycogen supply, provide energy demand. Repeated bouts of endurance exercise induces a wide range of beneficial metabolic adaptations such as increased maximal oxygen consumption, improved body composition, neovascularization, higher insulin

sensitivity and cardiovascular functions leading collectively to enhanced endurance performance and improved metabolic health (Egan and Zierath, 2013; Haskell et al., 2007). Endurance exercise causes a shift in SKM physiology towards more oxidative, slow-type phenotype, which is tightly regulated by a very wide and complex range of molecules and pathways converging in gene transcription as main player (Coffey and Hawley, 2007; Egan et al., 2016; Egan and Zierath, 2013; Gundersen, 2011). It was demonstrated that endurance athletes show an endurance finger print gene profile with main functions in mitochondrial and oxidative metabolism (Stepto et al., 2009). All these changes on a single bout of exercise can collectively over time induce a transient change on mRNA level of metabolic genes leading to a long-term increase in protein content and enzyme activity, finally resulting in improved exercise performance and whole body metabolism (Coffey and Hawley, 2007; Egan et al., 2016; Egan and Zierath, 2013; Perry et al., 2010).

Resistance exercise is a high load training for a short period of time leading to increased muscle mass, called hypertrophy, enhanced strength and power (Egan and Zierath, 2013). Resistance training is thus thought to be an effective treatment against muscle wasting-associated diseases (Egan and Zierath, 2013; Glass and Roubenoff, 2010). As already mentioned for endurance exercise, adaptations after resistance training are mainly settled by transcriptional changes, seen in increased genes responsible for protein synthesis and decreased genes for protein degradation (Stepto et al., 2009).

Both exercise types play a key role in SKM remodeling and promote health benefits. A mutual combination of training types would probably be the most effective treatment against metabolic disorders (Iepsen et al., 2015; Jorge et al., 2011; Skrypnik et al., 2015).

1.2 Transcriptional coregulators and their role in skeletal muscle plasticity

A highly regulated and coordinated interaction between TFs and coregulators is needed for gene transcription. TFs are proteins that bind DNA on specific sites called transcription factor binding site (TFBS) or response elements that can be at the promoter or at enhancer sites. This binding close to the transcription start site (TSS) of the gene helps to form the transcription initiation complex leading to gene activation, in contrast to silencer, which inhibit complex formation and hence, lead to decreased gene expression (Adcock and Caramori, 2009; Maston et al., 2006). However, transcriptional coregulators are not able to bind DNA directly, they form multiprotein complexes that interact with TFs. Dependent on the coregulator, coactivator or corepressor, the interaction with the same TF can lead to different outputs regarding gene transcription. Hence, there is a variety of mechanisms by which coregulators function. Coactivators can interact with histone acetyltransferases (HATs), which cooperate with multiple TFs and other proteins to facilitate chromatin opening and thus, accessibility of proteins to DNA. Opposite, corepressors interact with histone deacetylases (HDACs) to make the chromatin structure inaccessible for

TF binding (Hermanson et al., 2002; Spiegelman and Heinrich, 2004). Some coactivators are part of the thyroid hormone receptor-associated protein/ vitamin D receptor interacting protein (TRAP/DRIP), also called mediator complex, and the activator-recruited co-factor (ARC) complex, together TRAP/DRIP/Mediator/ARC complex, which contain proteins that bind TFs, recruit RNA polymerase II and initiate transcription. Additionally, the SWitch/Sucrose Non-Fermentable (SWI/SNF) chromatin remodeling complex induces accessibility of proteins to DNA in an adenosine triphosphate (ATP)-dependent manner and thus, increase transcription (Spiegelman and Heinrich, 2004). Coregulators serve as a central platform to bring TFs and chromatin modifying-enzymes together and accordingly regulate the transcriptional outcome (Figure 1). Interestingly, some TFs as for example the nuclear receptors (NRs) are upon ligand binding able to release the bound corepressor and recruit instead a coactivator, hence, changing transcription of targets (Glass and Rosenfeld, 2000; Spiegelman and Heinrich, 2004).

The PGC-1 family of coregulators are interacting with most NRs amongst other TFs and were shown to play an essential role in the regulation of energy metabolism and SKM plasticity (Knutti and Kralli, 2001; Kupr and Handschin, 2015; Kupr et al., 2017; Puigserver and Spiegelman, 2003). The next sections will focus on the PGC-1 family of coregulators and their role in SKM.

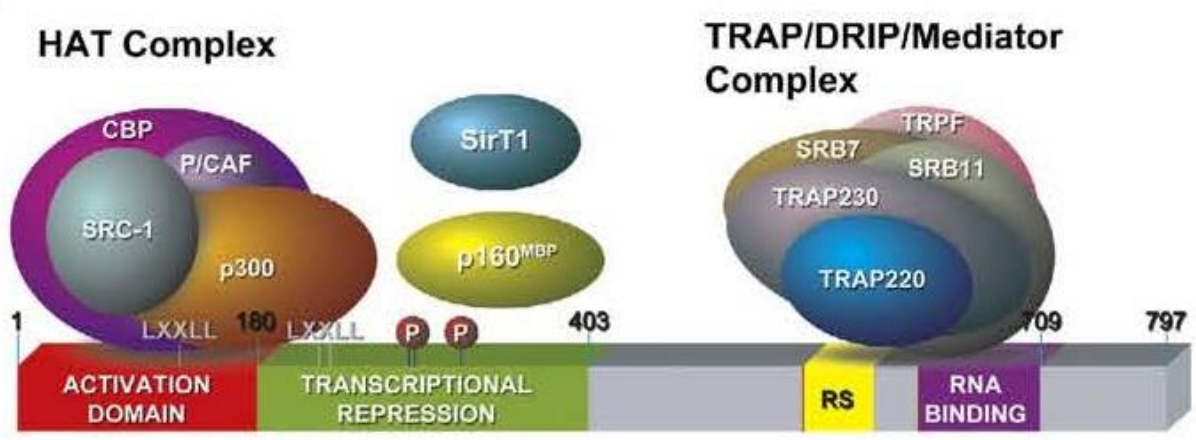

Figure 1

Main components of the multi-protein complex associated with PGC-1α. PGC-1α binds to the HAT and TRAP/DRIP/Mediator complex at the N- and C-Terminus, respectively. The conserved domains including the activation domain (AD), Arginine/Serine-rich domain (RS) and RNA binding/RNA-recognition motif are indicated (RRM). Nuclear receptor binding sites are indicated by LXXLL motifs (Lin et al., 2005).

1.2.1 The PGC-1 family of transcriptional coregulators

The PGC-1 family consists of three members: PGC-1α, PGC-1β and PRC (Figure 2). PGC-1α was first discovered and initially described as a coactivator of PPARγ, inducing uncoupling protein 1 (UCP1) in brown adipose tissue (BAT) to regulate adaptive thermogenesis (Puigserver et al., 1998). PGC-1β (Kressler et al., 2002b; Lin et al., 2002a) and PRC (Andersson and Scarpulla, 2001) were identified later and not much is known about those coactivators yet.

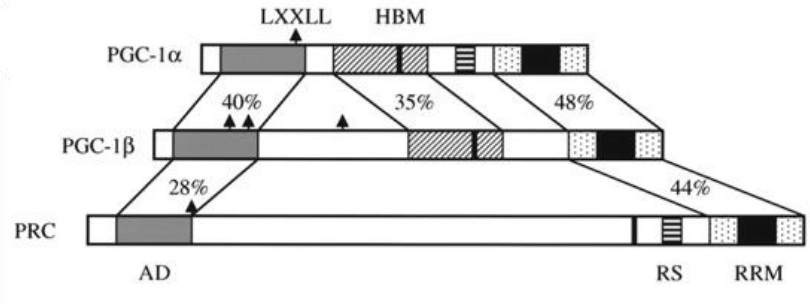

Figure 2

Sequence identity of the three PGC-1 family members PGC-1α, PGC-1β and PRC. Conserved domains/motifs are indicated including the AD, LXXLL motifs, host cell factor (HCF)-binding motif (HBM), Arginine/Serine-rich domain (RS) and RRM (Lin et al., 2002a).

1.2.2 PGC-1α coactivator, a regulatory nexus

PGC-1α is expressed at high levels in energy demanding organs like SKM, BAT, brain, heart and kidney (Lin et al., 2005; Puigserver et al., 1998). Notably, PGC-1α can be induced by several different external stimuli such as cold exposure in BAT and SKM (Puigserver et al., 1998), fasting in liver (Handschin et al., 2005; Yoon et al., 2001) and exercise in SKM (Baar et al., 2002; Pilegaard et al., 2003; Ruas et al., 2012; Terada and Tabata, 2004). Consequently, PGC-1α serves as a sensor for external stimuli converting them in to organ-specific gene programs, mainly mitochondrial functions and oxidative metabolism, leading to PGC-1α being a master regulator of energy homeostasis.

The Ppargc1a gene is located on chromosome 5 in the mouse genome and encodes 797 amino acids (aa) resulting in PGC-1α protein. PGC-1α interacts with several TFs, including most members of NRs (Kupr et al., 2017; Puigserver and Spiegelman, 2003; Puigserver et al., 1998). The interaction takes place via the LXXLL motif of which three are located in the activation domain (AD) at the N-Terminus of PGC-1α (Figure 1 + 2) (Knutti et al., 2000; Kupr and Handschin, 2015; Lin et al., 2005; Puigserver et al., 1998). The AD interacts with cyclic adenosine monophosphate (cAMP)-response element-binding protein (CREB) binding protein (CBP), p300 and the steroid receptor coactivator-1 (SRC-1), thereby enhancing the effect on gene

transcription (Puigserver et al., 1999; Wallberg et al., 2003b). PGC-1α is not able to acetylate histones itself but it interacts with HATs, thus modifying histones to make the chromatin more accessible for the TFs and the transcriptional machinery. The C-Terminus of PGC-1α binds to the TRAP/DRIP/Mediator complex, interacting with the RNA polymerase II and the transcription initiation complex (Figure 1) (Wallberg et al., 2003b). An additional coactivation boost of PGC-1α is given via the interplay of the SWI/SNF chromatin remodeling complex, which binds via BRG1-assocated factor 60a (BAF60a) to PGC-1α (Li et al., 2008). Moreover, the C-Terminus is composed of Arginine/Serine-rich domain (RS) and a RNA recognition motif (RRM), linking PGC-1α to mRNA processing (Figure 1 + 2) (Monsalve et al., 2000).

PGC-1α is a docking platform for a multi-protein complex regulating gene transcription. PGC-1α binds to TFs and brings them together with HATs, the mediator chromatin remodeling complex and proteins for mRNA processing forming a large network of transcriptional regulation.

1.2.3 PGC-1α isoforms and splice variants

PGC-1α transcription can be initiated by three TSSs on two alternative promoters. There is a proximal and a distal promoter, later one being around 13.8 kilo base (kb) upstream (Figure 3). Additionally, RNA processing further increases the quantity of PGC-1α transcripts and thus, protein variants (Martinez-Redondo et al., 2015; Miura et al., 2008; Ruas et al., 2012). Whether the alternative promoter usage is directly linked to the transcription of the PGC-1α isoforms as well as the functional consequences is not known yet. The proximal (classical) promoter seems to transcribe the basal and robust PGC-1α1 isoform whereas the distal (alternative) promoter appears to have a higher dynamic range in regard to PGC-1α gene expression (Figure 3) (Martinez-Redondo et al., 2015). In the first description from Miura et al., 2008, the full length PGC-1α isoform transcribed from the proximal promoter was termed as PGC-1α-a (named PGC-1α1 in Ruas et al., 2012), the isoforms from the distal promoter, which vary only in their N-Terminus, as PGC-1α-b and PGC-1α-c (Figure 3) (Miura et al., 2008). Those three variants differ in their response to stimuli and tissue expression levels. All three versions are induced by exercise but PGC-1α-a seems to be the major form in SKM (Miura et al., 2008; Tadaishi et al., 2011). The distal promoter additionally transcribes a N-Terminal truncated PGC-1α (NT-PGC-1α) variant (Figure 3) (Zhang et al., 2009). NT-PGC-1α is only 270 aa long and is produced by alternative 3’ splicing. The C-Terminal motifs for nuclear localization signal (NLS), the nuclear receptor binding domain as well as the RS and the RRM domains are all lacking in the NT-PGC-1α variant. Consequently, the protein-protein interactions as well the recruitment to target promoters and the subcellular localization, mostly cytoplasmic, are unique (Zhang et al., 2009).

As already mentioned, the distal alternative promoter has higher range of PGC-1α variants (Martinez-Redondo et al., 2015). Next to the PGC-1a-b/c isoforms described by Miura et al., 2008, Ruas et al., 2012,

discovered a new truncated isoform called PGC-1α4, transcribed from the distal promoter and including the same 3' splicing as the NT-PGC-1α version (Figure 3). Opposite to so far all other discussed isoforms, PGC-1α1 (from proximal promoter) and PGC-1α2, PGC-1α3 and NT-PGC-1α (all from distal promoter), PGC-1α4 plays a role in exercise adaptation to resistance training resulting in fiber hypertrophy (Ruas et al., 2012). PGC-1α4 does not regulate genes in mitochondrial and metabolic processes like the full length PGC-1α1 and the NT-PGC-1α isoforms do. So far, not much is known about the two other discovered transcripts by Ruas et al., 2012, PGC-1α2 and PGC-1α3. They contain a novel exon 1 transcript (exon 1b and exon 1c) and can follow two different splicing options leading to 12 aa (for PGC-1α2) and 3 aa (for PGC-1α3) long exon 1, respectively, shorter than exon 1a (16 aa) from the proximal promoter (Figure 3) (Chinsomboon et al., 2009; Martinez-Redondo et al., 2015; Ruas et al., 2012).

In any case, the high flexibility in gene structure and transcript processing of PGC-1α generates an additional layer of functional and regulatory specificity (Handschin and Spiegelman, 2006; Kupr and Handschin, 2015).

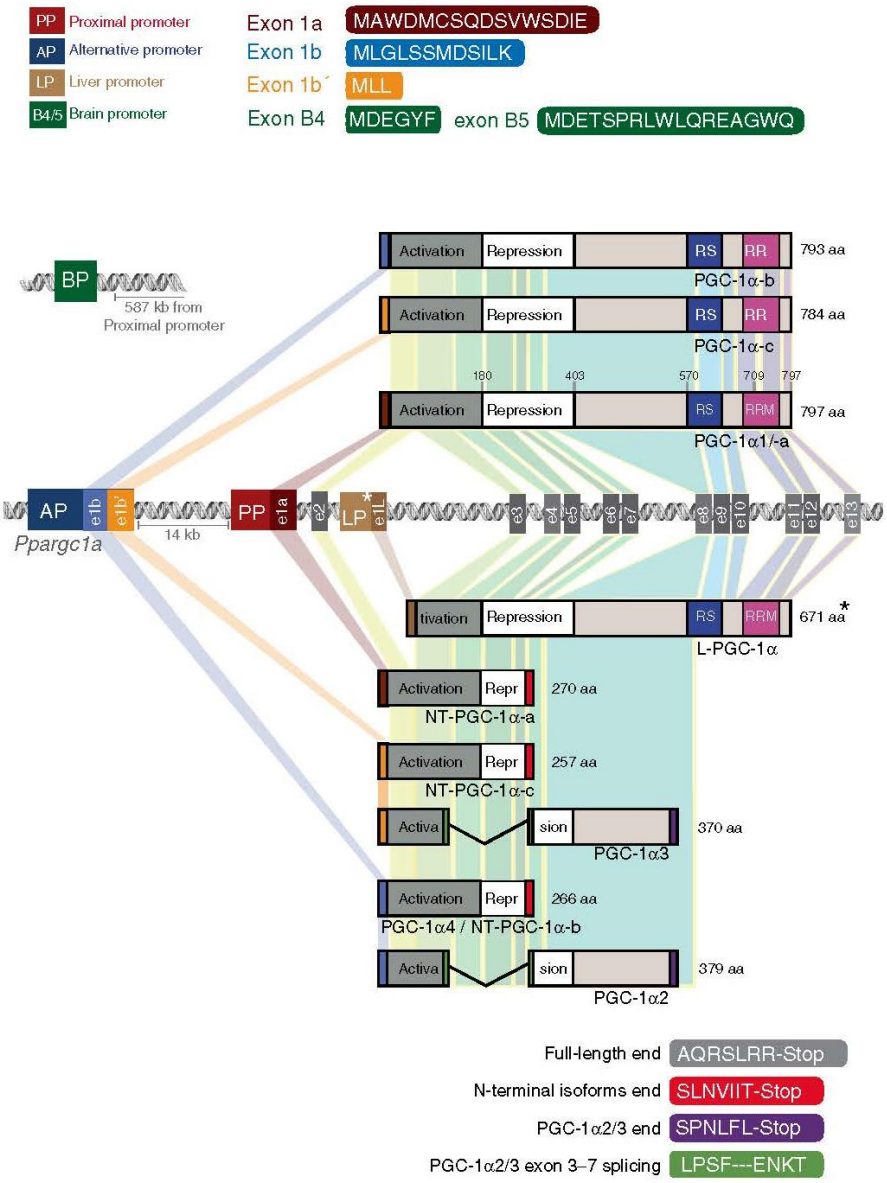

Figure 3

PGC-1α isoform structure and promoter location. The upstream alternative promoter (AP) (in this thesis called distal promoter) of the Ppargc1a gene results in new exon 1b or exon 1b' (in this thesis called exon 1b and exon 1c), which encodes distinct N-Termini. The proximal promoter (PP) encodes the canonical exon 1a. In addition, a human liver-specific promoter (LP) located in intron 2 encoding for the exon 1L (e1L) and a brain-specific promoter (BP) exists. (Martinez-Redondo et al., 2015).

1.2.4 Regulation of PGC-1α expression, activity and stability

Several upstream signaling pathways tightly regulate PGC-1α transcription, activity and stability. PGC-1α senses the environmental energetic changes following different stress situations like fasting in liver (Yoon et al., 2001), cold in BAT or exercise in SKM (Baar et al., 2002; Puigserver et al., 1998), and is itself induced by those stimuli and drives the main regulations for a proper energy metabolism.

Upon muscle contraction, mechanical stress, tissue physoxia, the endocrine milieu and the metabolic demands are changed and affect several signaling pathways all converging on PGC-1α, promoting its transcriptional induction or posttranslational modification (PTM) of the protein (Figure 4). PTMs can be phosphorylation by various kinases on different phosphorylation sites, acetylation, methylation, sumoylation, ubiquitination, and acetylglucosamination (Fernandez-Marcos and Auwerx, 2011; Kupr and Handschin, 2015). Some of the PTMs alter the stability of the PGC-1α protein, while others modulate the interaction with TFs or other coregulators. The adenosine monophosphate (AMP)-activated protein kinase (AMPK) is an intracellular energy sensor sensitive for the AMP/ATP ratio and is activated after ATP need e.g. energy deficit following exercise. Activated AMPK phosphorylates PGC-1α, thereby increases its activity and positively leads to the transcriptional induction of mitochondrial genes in SKM (Jager et al., 2007). Next to energy demand and exercise, the reduction-oxidation (redox) status, namely reduced and oxidized nicotinamide adenine dinucleotide (NAD+ / NADH) levels activate sirtuin 1 (SIRT1). SIRT1 is a NAD+ sensitive deacetylase, which is induced by exercise and able to deacetylate PGC-1α, hence increasing its activity (Cantó and Auwerx, 2009). Contrary, acetylation of PGC-1α by histone general control of amino acid synthesis 5 (GCN5) decreases PGC-1α expression by increasing the association of PGC-1α with inactive transcriptional domains in the nucleus (Lerin et al., 2006). AMPK was shown to increase intracellular NAD+ levels and thus, increasing deacetylation activity of SIRT1 on PGC-1α. In addition, the direct phosphorylation of PGC-1α by AMPK has two important outcomes, direct gene expression regulation of PGC-1α and necessity for stimulated deacetylation by SIRT1 (Cantó and Auwerx, 2009; Canto et al., 2009). Supplemental, phosphorylation of PGC-1α by p38 mitogen-activated protein kinase (p38 MAPK) increases stability of the protein by preventing ubiquitination and thus, prolong the very short half-life of PGC-1α of around 2.5h (Olson et al., 2008; Puigserver et al., 2001). Even more, the phosphorylation by p38 MAPK protects the coactivator from interaction with the repressor p160 myb binding protein (p160 MBP) and consequently, increases its transcriptional activity (Fan et al., 2004). PTMs change not only the stability and activity of PGC-α but as well the ability to interact with TFs or other coactivators (Handschin and Spiegelman, 2006). The interaction of PGC-1α with nuclear respiratory factor 2 (NRF2) (also known as GA-binding protein: GABP) is boosted by neuregulin, coming from neuromuscular junctions (NMJs), inducing NMJ gene transcripts (Handschin et al., 2007b). PGC-1α can as well be sumoylated, which happens at the

same residue as the acetylation by GCN5 and leads to the repression of its activity by promoting the interaction with the repressor receptor interaction protein 140 (RIP140) (Rytinki and Palvimo, 2009). Also methylation of PGC-1α on all three arginine residues by protein arginine methyltransferase 1 (PRMT1) was shown to promote the coactivator activity (Teyssier et al., 2005). Additionally, PGC-1α promoter, it still has to be clarified whether both promoters are affected or not, is hypomethylated by acute exercise in human SKM leading to changes in its own and target gene transcription (Barres et al., 2009; Barres et al., 2012; Lochmann et al., 2015b). Further, ubiquitination targets PGC-1α for its degradation. This can be performed by the E3 ligases Skp1/Cullin/F-box (SCF cdc4) complex and is supported by the phosphorylation of PGC-1α by p38 MAPK and glycogen synthase kinase 3β (GSK3β), which was shown to target PGC-1α for proteasomal degradation (Anderson et al., 2008; Olson et al., 2008). Next to PTMs, different signaling pathways that are stimulated following muscle contraction converge on PGC-1α by regulating its expression. As already mentioned, PGC-1α transcript is induced subsequent to exercise and reduced during physical inactivity (Egan et al., 2016; Egan and Zierath, 2013). Calcium/calmodulin-dependent protein kinase IV (CaMKIV) and calcineurin A (CnA) manage the increased calcium levels during exercise and supplementary increase PGC-1α expression. They act upstream of the coactivator and involve cAMP, which stimulates CREB on the PGC-1α promoter (Handschin et al., 2003; Olson and Williams, 2000). In addition, the gene expression of PGC-1α can be controlled by tissue-specific TF interactions, as it is e.g. myocyte enhancer factor 2C/D (MEF2C/D) in muscle cells. Interestingly, there is an autoregulatory loop of coactivation on the MEF2 promoter by PGC-1α, which further controls the appropriate transcription of PGC-1α (Handschin et al., 2003; Pérez-Schindler, 2013). Finally, in SKM the β2-adrenergic receptor (β2-AR) together with cAMP induces PGC-1α expression (Miura et al., 2007).

This enormous variety of regulations on different layers makes the PGC-1α coactivator a tightly regulated sensor for environmental changes that are converted into transcriptional regulations of many different target genes. The possibilities to change activity, stability and expression of PGC-1α indicate the importance of this factor and the significance to be not only turned on or off, but also to collect inputs from a multiplicity of signaling pathways and initiate cellular changes dependent on the metabolic needs in a fine-tuned manner.

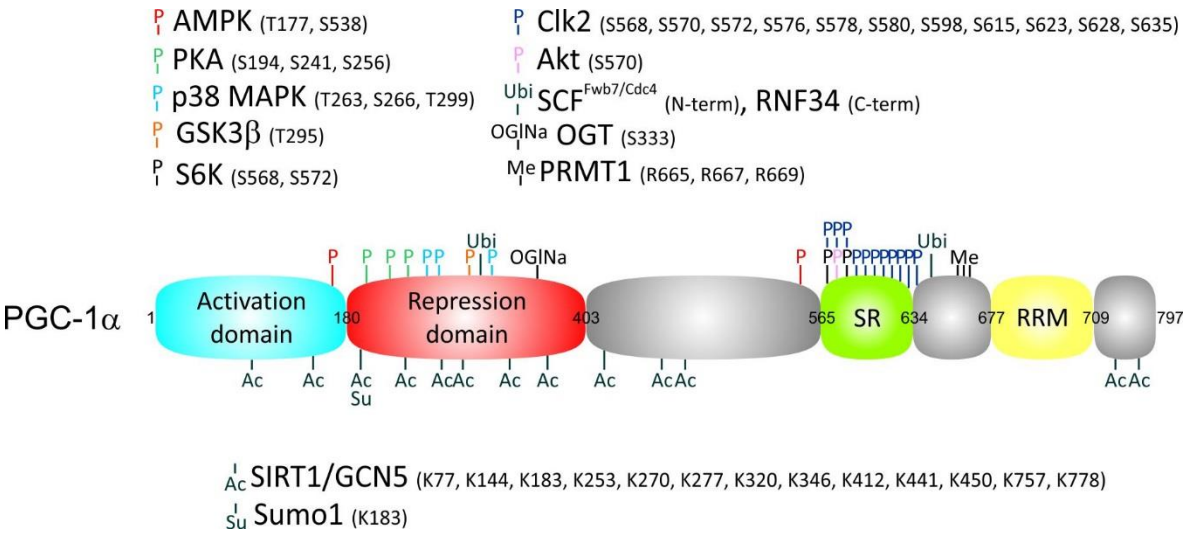

Figure 4

Posttranslational modification (PTM) of the PGC-1α protein. Ac, acetylation; Akt, protein kinase B; AMPK, AMP-activated protein kinase; Clk2, Cdc2-like kinase 2; Gsk3β, glycogen synthase kinase 3 beta; OGlNa, O-linked β-N-acetylglucosamination; OGT, O-linked β-N-acetylglucosamine transferase; p38 MAPK, p38 mitogen-activated protein kinase; PKA, protein kinase A; P, phosphorylation; PRMT1, protein arginine methyltransferase 1; RNF34, ring finger protein 34; S6K, S6-kinase; $SCF^{Fwb7/Cdc4}$, SCF ubiquitin ligase complex subunit Fwb7/Cdc4; SIRT1, sirtuin-1; Su, sumoylation; Sumo1, small ubiquitin related modifier 1; Ubi, ubiquitination (Kupr and Handschin, 2015).

1.2.5 Transcriptional network regulated by PGC-1α in skeletal muscle

As described above, external stimuli and metabolic changes activate numerous signaling pathways that converge on PGC-1α. Those events result in induced expression or protein modification of PGC-1α, which lead to activation or degradation of the coactivator. When PGC-1α is active, it binds to its transcriptional partners, hence regulate tissue-specific gene programs.

In SKM, PGC-1α is known to be the master regulator of mitochondrial biogenesis. A very important transcriptional partner of PGC-1α is ERRα. PGC-1α together with ERRα and NRF2 was shown to regulate nearly the whole mitochondrial and oxidative phosphorylation gene program (Huss et al., 2002; Mootha et al., 2004; Schreiber et al., 2004). In addition, the interaction of PGC-1α and ERRα regulates angiogenesis in SMK by inducing vascular endothelial growth factor (VEGF) (Arany et al., 2008). Further, by coactivating NRF1 and NRF2, mitochondrial transcription factor A (TFAM), a main regulator of mitochondrial DNA transcription and replication, is induced and thus, mitochondrial genes regulated not directly but indirectly by PGC-1α (Lin et al., 2005; Wu et al., 1999). Besides, PGC-1α is able to increase in a mammalian target of

rapamycin complex 1 (mTORC1)-dependent manner the transcription of Yin Yang 1 and consequently, boost SKM oxidative metabolism (Blattler et al., 2012; Cunningham et al., 2007). Also, lipid storage in SKM can be regulated by PGC-1α via interaction with the liver X receptor α (LXRα) (Summermatter et al., 2010). Next to the activation of gene programs, PGC-1α is able to play a repressing role as well. PGC-1α decreases the expression of fork-head transcription factor O3 (FOXO3) and nuclear factor-kappaB (NFκB), which prevent SKM atrophy (Brault et al., 2010; Sandri et al., 2006). FOXO3 is important for the induction of the E3 ubiquitin ligases muscle RING-finger protein-1 (MuRF1, also known as Trim63) and muscle atrophy F-box (MAFbx, also known as atrogene 1 or Fbx32), which are atrogenes and main regulators involved in muscle atrophy (Bodine et al., 2001; Sandri et al., 2006). Recently, the PGC-1α4 transcript was shown to be involved in SKM hypertrophy (Ruas et al., 2012). Thus, PGC-1α seems to have a very versatile function in many different biological functions, acting as coactivator or corepressor at the same time in numerous ways, dependent on the metabolic situation. So far, no “PTM code” has been found for most of the modifications on PGC-1α protein leading to the combinatorial complexity that determines transcriptional interaction specificity (Handschin and Spiegelman, 2006; Lonard and O'Malley, 2007). A prototypical example of this diversity is the interaction of PGC-1α with S6 kinase (S6K) in the liver. S6K phosphorylates PGC-1α after feeding and selectively maintains the ability of PGC-1α to enhance fatty acid oxidation and mitochondrial functions while reducing its effect on hepatic gluconeogenesis (Lustig et al., 2011).
The coactivator PGC-1α is a very tight and complex regulatory nexus converging a multitude of signaling pathways and transforming them in a variety of specific biological functions dependent on the metabolic changes stimulating PGC-1α.

1.2.6 PGC-1β and PRC coactivators

As already mentioned, next to PGC-1α there are two other PGC-1 family members of coactivators (Figure 2). Ppargc1b is located on chromosome 18 in the mouse genome and is 1014 aa long leading to the protein called PGC-1β. PGC-1β shares general sequence similarities with PGC-1α, the N-Terminal AD, LXXLL motif and the C-Terminal RRM, but it lacks the RS domain and its role in regulating metabolism is less understood and studied so far (Brault et al., 2010; Kressler et al., 2002b; Lin et al., 2002a; Scarpulla, 2008). PGC-1β was first discovered as an interaction partner of PPARα, estrogen receptor α (ERα) and host cell factor (HCF) involved in the regulation of hepatic fasting, viral infection and proliferation (Kressler et al., 2002b; Lin et al., 2002a). Same as for PGC-1α, PGC-1β is involved in mitochondrial biogenesis, energy homeostasis and cellular respiration and hence, found in high energy demanding organs (Lin et al., 2002a; Scarpulla, 2008; St-Pierre et al., 2003). Via interaction of PGC-1β with some TFs like NRF1, MEF2, ERRα, and PPARα specific gene programs are induced leading to increased oxidative capacity and other adaptations to

environmental changes (Arany et al., 2007). As already observed for PGC-1α, PGC-1β is as well reduced by disused SKM in old individuals (Suetta et al., 2012). Interestingly and contrarily to PGC-1α, mitochondrial biogenesis and high PGC-1β levels are associated with the induction of type 2X oxidative muscle fibers (Arany et al., 2007). Also opposing, PGC-1β is not induced subsequent to exercise or cold exposure in SKM (Mortensen et al., 2007; Sonoda et al., 2007) but upon fasting and short-term high fat diet in the liver (Koves et al., 2005; Lin et al., 2002a; Lin et al., 2003).

Nearly nothing is known about the third member of the PGC-1 family, PRC. PRC is ubiquitously expressed and responds to several metabolic stresses by regulating genes involved in mitochondrial biogenesis, inflammation, proliferation and metabolic reprogramming (Andersson and Scarpulla, 2001; Philp et al., 2011; Vercauteren et al., 2009; Vercauteren et al., 2006). Like PGC-1α, PRC is induced after endurance exercise in human SKM (Russell et al., 2005).

Further studies are necessary to elucidate the role of PGC-1β and PRC in energy metabolism and SKM plasticity.

1.2.7 The role of PGC-1α and PGC-1β in skeletal muscle plasticity

The coactivators PGC-1α and PGC-1β are associated with SKM oxidative metabolism and adaptions to external stimuli mainly due to the induction of the TFs NRF1, NRF2 and ERRα (Arany et al., 2007; Miura et al., 2008; Scarpulla, 2008; St-Pierre et al., 2003). SKM-specific overexpression of PGC-1α promotes the formation of slow-fiber type MyHC-1 and MyHC-2A (Lin et al., 2002b), whereas PGC-1β induces MyHC-2X fibers that are oxidative but have fast-twitch properties (Arany et al., 2007). Furthermore, overexpression of either of the PGC-1s leads to improved exercise performance due to improved oxidative capacity (Arany et al., 2007; Lee et al., 2017; Lin et al., 2002b) and induced angiogenesis by VEGF (Arany et al., 2008; Chinsomboon et al., 2009; Rowe et al., 2011). A role in protecting SKM from atrophy by PGC-1α or PGC-1β via reducing the transcript levels of FOXO3 and NFκB and thus, decreasing proteolysis, was found as well (Brault et al., 2010; Sandri et al., 2006). Opposite, SKM-specific knockout of either coactivator results in a shift towards fast-glycolytic fibers (Gali Ramamoorthy et al., 2015; Handschin et al., 2007a; Rowe et al., 2013). Additionally, single or double SKM knockout of the PGC-1s conduct in a drastic reduced mitochondrial respiration with severe effect on exercise capacity (Gali Ramamoorthy et al., 2015; Handschin et al., 2007a; Rowe et al., 2013; Zechner et al., 2010a). Double knockout of PGC-1α/β in SKM revealed blunted oxidative capacity and hence, reduced exercise performance but normal mitochondrial density, fiber type distribution and basal muscle function (Lai et al., 2008; Lin et al., 2004a; Rowe et al., 2013). Interestingly, global PGC-1α knockout animals are viable and hyperactive and remarkably, show no deficit in mitochondrial biogenesis but reduced respiratory capacity, which points towards that PGC-1α is

important but not required and compensatory mechanisms as e.g. by PGC-1β, exist (Arany et al., 2005; Leone et al., 2005). Global PGC-1β knockout animals are viable and do not have significant changes in energy homeostasis and overall substrate usage but they have an increased overall metabolic rate and reduced mitochondrial number and gene expression resulting in a leaner phenotype (Lelliott et al., 2006). As already seen for the PGC-1α global knockout animals, there are compensatory pathways reducing the dramatic effect on mitochondrial metabolism in both global knockout models. Contrary to individual whole-body knockout, global deletion of both coactivators leads to prenatal death due to heart failure (Lai et al., 2008).

It seems that the PGC-1 family are important regulators for energy homeostasis but as well that they are dispensable for basal energy metabolism but serve as a boosting platform in stress situations as exercise.

1.3 Epigenetic control by DNA methylation

Epigenetics are heritable modifications in gene function that do not involve changes in the DNA sequence, namely DNA methylation, histone modification, microRNA etc. (Howlett and McGee, 2016; Xu et al., 2016b). In the last years, it was shown that epigenetic changes play an important role in transducing external stimuli into a transcriptional response and are essential for proper maintenance of cellular metabolism (Howlett and McGee, 2016). On the other hand, epigenetics can be influenced itself by external stimuli (Xu et al., 2016b). DNA methylation is an epigenetic mechanism involving the transfer of a methyl group (CH_3) onto the C5 position of the cytosine on the genomic DNA leading to the generation of 5-methylcytosine (5mC). These DNA methylation changes have an important biological role and are essential for mammalian development and the adaptation to environmental signals (Moore et al., 2013; Smith and Meissner, 2013). Abnormal DNA methylation leads to increased risk of cancer and neurological disorders since DNA methylation is often associated with regulation of gene expression by blocking the binding of TFs or affecting the chromatin structure (Jones and Takai, 2001; Robertson, 2005; Schubeler, 2015; Siegfried and Simon, 2010). Importantly, DNA methylation is a heritable and reversible epigenetic mark on the genomic DNA without changing its genetic information (Schubeler, 2015; Stadler et al., 2011). As already mentioned, eukaryotic DNA methylation occurs mainly on cytosine residues that precedes a guanine nucleotide, called GC site, or a cytosine-phosphate-guanine (CpG) site, although recent findings showed that methylation can occur as well on adenine, like already known from prokaryotes (Iyer et al., 2016; Luo et al., 2015). DNA methylation varies across organisms from very high methylation levels as in the mammalian genome to very low ones like in invertebrates such as Drosophila (Lyko et al., 2000). The mammalian genome contains around 28 million CpGs of which 60-80% are methylated. The CpGs are not found at GC-rich regions on the genome, only around 10% are at GC-dense sites and are called CpG islands

(Smith and Meissner, 2013). The CpG islands are located at TSSs and are mainly protected from DNA methylation, thus hypomethylated (Smith and Meissner, 2013; Yong et al., 2016). Overall, there is only around 1% of 5mC in the mammalian genome due to high mutagenic potential of 5mC, which can deaminate to thymine, consequently leading to an underrepresentation of CpG dinucleotides in the genome (Moore et al., 2013).

1.3.1 DNA methyltransferases (DNMTs) and demethyltransferases (TETs)

In mammals, DNA methylation is regulated by a conserved family of DNA methyltransferases (DNMTs) that transfer a CH_3 group from a S-adenosyl methionine (SAM) to the fifth carbon of a cytosine residue to form 5mC (Figure 5). The mammalian DNMT family consists of three members: DNMT1, DNMT3a and DNMT3b. DNMT1 was first reported in 1975 as an important enzyme during development and the dominant methyltransferase preferable acting on hemimethylated DNA (Holliday and Pugh, 1975; Riggs, 1975). It is a maintenance methyltransferase ensuring proper copy of the DNA methylation pattern from the parental DNA strand to the newly synthesized daughter strand during cell division, where DNA replication occurs. In addition to maintain DNA methylation and contrary to DNMT1, DNMT3a and DNMT3b establish new methylation patterns on nonmethylated or hemimethylated DNA and are thus called *de novo* DNMTs. All three DNMTs are involved in embryonic development and in mice the deletion of these enzymes results in embryonic lethality for DNMT1 and DNMT3b, or postnatal death for DNMT3a (Jin et al., 2011; Li et al., 1993; Li et al., 1992; Okano et al., 1999). The levels of the methyltransferases decrease after differentiation, except in the brain (Feng et al., 2005), an indication of stable methylation patterns after development (Moore et al., 2013). Opposite to the DNMTs are the Ten-Eleven-Translocation (TET) oxygenases, which convert 5mCs into 5-hydroxymethylcytosine (5hmC), the first step towards demethylation, hence also called demethyltransferases (Figure 5) (Dahl et al., 2011; Moore et al., 2013). It was shown that the level of 5hmC is tissue-specific and tend to be more associated with transcriptional activation than the 5mC, although this theory is controversial (Moore et al., 2013; Munzel et al., 2011). The family of TETs consists of three members, TET1, TET2 and TET3 (Tahiliani et al., 2009). TET1 acts on fully- and hemimethylated DNA and deletion of TET1 in embryonic stem (ES) cells results in the lack of self-renewal capacity (Dahl et al., 2011). Contrary, TET2 and TET3 deletion in ES cells had no effect, fitting the observation that the TETs are expressed differentially in diverse mouse tissues, however TET2 is the most abundant one (Dahl et al., 2011; Ito et al., 2010; Langemeijer et al., 2009).

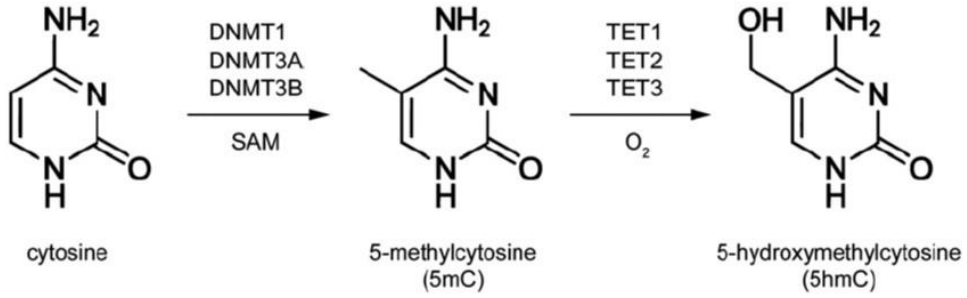

Figure 5

Cytosine methylation and demethylation in mammalian DNA. 5-methylcytosine (5mC) is formed by addition of a methyl group (CH_3) to cytosine through the action of DNA methyltransferases (DNMT) via S-adenosyl methionine (SAM) as methyl donor. 5-hydroxymethylcytosine (5hmC) is formed through the action of Ten-Eleven-Translocation (TET) oxygenase proteins with oxygen (O_2) to transfer a hydroxyl (OH) group to 5mC (Dahl et al., 2011).

1.3.2 DNA methylation and its role in skeletal muscle

Several studies implicated methylation profiles in myogenic differentiation and found a demethylation pattern occurring during development from myoblasts to myotubes with high methylation changes going on early and only few in the later stage. Thus, DNA methylation is important for lineage- and tissue-specific finding and differentiation (Carrió and Suelves, 2015; Hupkes et al., 2011) as e.g. Myogenic Factor 3 (MyoD) promoter demethylation was shown to be key for myogenic lineage decision (Brunk et al., 1996; Taylor and Jones, 1979). In addition, myogenin, an important gene during myogenesis, becomes demethylated at the onset of myoblast differentiation (Lucarelli et al., 2001). Next to myogenesis and self-renewal capacity in SKM, DNA methylation was also brought in contact with fiber-type specificity, exercise adaptations and SKM plasticity (Barres et al., 2012; Begue et al., 2017; Nitert et al., 2012). SKM-specific epigenetic modifications, here DNA methylation, was shown to play an important role in gene profile changes leading not only to SKM but as well to whole body adaptations (Cedar and Bergman, 2009; Nitert et al., 2012).

1.3.3 PGC-1α coactivator and DNA methylation following exercise

A limited number of studies discussed the role of DNA methylation changes upon environmental stimuli e.g. exercise in SKM (McGee and Walder, 2017). Since PGC-1α is a key regulator in the adaptive response to exercise in SKM, the question rises whether the complex transcriptional network regulated by PGC-1α

might be further fine-tuned by DNA methylation on several key factors involved in SKM plasticity and of PGC-1α itself (Bajpeyi et al., 2017; Barres et al., 2009; Barres et al., 2012; Lochmann et al., 2015b). The proximal promoter of PGC-1α has a methylation site -260nt upstream of the TSS (Bajpeyi et al., 2017; Barres et al., 2009). It was shown that the -260nt site is required for the action of DNMT3b on the PGC-1α promoter (Barres et al., 2009). The epigenetic regulation at the -260nt site might occur through alteration in the nucleosome (N) positioning within the PGC-1α promoter region, with -1N position over the regulatory -260nt methylation site leading to hypermethylation in association with decreased PGC-1α transcript level. When -1N is repositioned away from the -260nt site, PGC-1α is hypomethylated and its gene expression induced (Bajpeyi et al., 2017; Barres et al., 2009; Henagan et al., 2014). An acute bout of exercise shifts the -1N position farther from the TSS and away from the regulatory methylation -260nt site leading to promoter hypomethylation and increased PGC-1α mRNA levels (Bajpeyi et al., 2017; Barres et al., 2009; Barres et al., 2012). Going in line, Barres et al., 2012, showed a global DNA methylation decrease upon an acute bout of high intensity exercise but not after low intensity exercise in humans SKM (Barres et al., 2012). Striking, important metabolic gene promoters as PGC-1α were hypomethylated, inversely correlated with increased mRNA levels of the gene itself (Barres et al., 2012). Contrary, Lochmann et al., 2015, concluded in their mouse study that PGC-1α promoter methylation status remains unchanged after acute exercise (Lochmann et al., 2015b). Although both studies performed acute exercise, one study was in humans and the other one in mice, which could explain the discrepancies. Lochmann et al., 2015, discussed the effect of DNA methylation as a long-term adaptation process with consequent changes on gene transcription, therefore they do not see DNA methylation changes after only one acute exercise test (Lochmann et al., 2015b). Contradictory, Barres et al., 2012, discuss the genomic adaptation by DNA methylation also after acute environmental stimuli. In addition, the Barres et al. checked methylation status immediately or 3h after exercise, while Lochmann et al. 1h post exercise (Barres et al., 2012; Lochmann et al., 2015b). Furthermore, there might be differences in regard to the two promoters, proximal and distal, existing for PGC-1α, since the DNA methylation level varies across the promoters (Lochmann et al., 2015b). Low DNA methylation at the distal promoter leads to high basal PGC-1α1 mRNA levels and high DNA methylation at the proximal promoter goes in line with low PGC-1α2/3 transcripts (Lochmann et al., 2015b). Under exercise condition, the different isoforms are differentially induced, mainly transcript PGC-1α2 and PGC-1α3 and only mildly PGC-1α1 (Barres et al., 2012; Lochmann et al., 2015b). Opposite to exercise, increased PGC-1α promoter methylation is observed subsequent to forced bed rest, which goes in line with decreased transcripts involved in mitochondrial functions. This hypermethylation could be reversed by 4-week exercise training, leading to reduced PGC-1α promoter methylations and increased transcript levels (Alibegovic et al., 2010). Studies with long-term endurance

exercise revealed as well changes on DNA methylation into both directions, hyper- and hypomethylation to similar extent (Kanzleiter et al., 2015; Lindholm et al., 2014). In T2D patients, hypermethylated PGC-1α promoter and a negative correlation with PGC-1α mRNA levels were found (Barres et al., 2009; Egan and Zierath, 2013; Nitert et al., 2012). Exercise changed the gene expression profile and DNA methylation in SKM of T2D patients and sedentary healthy individuals towards reduced DNA methylation and increased gene expression in many pathways associated with metabolic diseases (Nitert et al., 2012).

Different studies revealed conflicting changes in the DNA methylation pattern after exercise. There is controversy about muscle type, acute versus chronic exercise as well as about hyper- or hypomethylation leading to gene up- or downregulation after exercise. Taken together, physical exercise modify DNA methylation and transcript levels and thus, regulate SKM plasticity and whole body adaptations. Further studies need to be done to elucidate the role of DNA methylation in SKM, analyzing acute versus chronic exercise and key regulators of SKM plasticity and energy metabolism as PGC-1α.

2. Aims of the thesis

Transcriptional coregulators are important metabolic sensors and effectors in the control of gene transcription and thus, skeletal muscle plasticity in the context of physical activity and inactivity as well as metabolic diseases. Different signaling events in skeletal muscle converge on the PGC-1 family of transcriptional coactivators, mainly PGC-1α, affecting their expression or activity and stability by PTMs. The combination of these different events on the coactivator itself together with the epigenetic manipulation of DNA and the use of diverse TFs allows to regulate an enormous complexity of gene programs. Therefore, the aim of this work is to understand the fine-tuned complex regulatory network of PGC-1α and PGC-1β in skeletal muscle cells. The thesis is dissected into following aims:

1. **Characterize the PGC-1α - transcription factor binding partner (TFBP) interaction and define the transcriptional control on PGC-1α target genes in skeletal muscle cells (chapter 3).**
   Coactivator - transcription factor (TF) interaction increases the diversity of transcriptional control. In a previous study from our group (Baresic et al., 2014), we observed that PGC-1α regulates many target genes by collaboration with the estrogen-related receptor α (ERRα) but interestingly that ERRα might regulate PGC-1α target genes as well without PGC-1α. Thus, we performed a follow-up study by a combined ChIPseq approach of PGC-1α and ERRα in context of PGC-1α target genes to elucidate further the interaction of PGC-1α and ERRα.
2. **Describe the transcriptional network regulated by PGC-1β and identify TFBPs involved in the regulation of PGC-1β target genes in skeletal muscle cells (chapter 4).**
   Nearly nothing is known about the transcriptional network of PGC-1β, its TFBP usage as well as the functional relevance. Even more, similar or distinct role between PGC-1α and PGC-1β was not well studied yet. Therefore, we performed ChIPseq and RNAseq analysis of PGC-1β in skeletal muscle cells to define the regulatory network, identify new binding partners and clarify its role compared to PGC-1α.
3. **Define the impact of acute and chronic exercise on the transcriptome and the methylome in diverse PGC-1α *in vivo* and *in vitro* model systems in skeletal muscle (chapter 5.1).**
   Exercise induces many metabolic changes and adaptations, which are acute and local but might involve as well long-term memory alterations. Accordingly, the interaction of epigenetic modifications and transcriptional changes such as the underlying mechanism is not clear yet. Therefore, we analyzed the transcription and methylation response subsequent to an acute exercise time course and a chronic training combined with various PGC-1α models in skeletal muscle.

4. **Determine the role of PGC-1α and PGC-1β on the transcriptome and the methylome in skeletal muscle cells (chapter 5.2).**

   The PGC-1 family of coactivators are important regulators in whole body energy homeostasis. So far, the role of the coactivators was mainly studied on the transcriptional level by diverse TF interactions, which explain the complexity of the network. However, the large transcriptional network has to be tightly controlled in a fine-tuned manner. Thus, we hypothesize a possible epigenetic control by the PGC-1 family, which could serves as an additional layer of control. Hence, we used RRBS together with RNAseq data in PGC-1α/β overexpressing muscle cells to define the role of the coactivators on the methylome and the transcriptome.

5. **Describe the skeletal muscle transcriptional profile and contractile response following an acute exercise time course or cold-induced muscle shivering in various PGC-1α genotypes (chapter 6).** Skeletal muscle contraction can be induced by several external stimuli. Nevertheless, muscle contraction following exercise has a different output then muscle contraction by cold-induced shivering. Thus, we used RNAseq to understand the molecular mechanism of skeletal muscle contraction under acute exercise and acute cold exposure combined with the role of PGC-1α in skeletal muscle.

6. **Generate a multiplex epitope tag knock-in mouse at the proximal and distal PGC-1α promoter by the CRISPR/Cas genome editing technology (chapter 7).**

   PGC-1α as a coactivator interacts with numerous TFs that allows to regulate a complex network. In addition, PGC-1α contains multiple isoforms, which are transcribed from a proximal and a distal promoter, dependent on the stimulus. Due to technical difficulties, a global and detailed isoform and promoter usage analysis was not done so far. However, it is of interest to dissect the various isoforms and their biological function since PGC-1α plays an important metabolic regulatory role and might be a therapeutic candidate. For this reason, we aimed to designed an epitope tag knock-in mouse with individual tags for each promoter region at the PGC-1α locus by the non-tissue-specific CRISPR/Cas genome editing technology.

3. The Genomic Context and Corecruitment of SP1 Affect ERRα Coactivation by PGC-1α in Muscle Cells

ORIGINAL RESEARCH

The Genomic Context and Corecruitment of SP1 Affect ERRα Coactivation by PGC-1α in Muscle Cells

Silvia Salatino,* Barbara Kupr,* Mario Baresic, Erik van Nimwegen, and Christoph Handschin

Focal Area Growth and Development (S.S., B.K., M.B., C.H.) and Focal Area Computational and Systems Biology (S.S., E.N.), Biozentrum, University of Basel, and Swiss Institute of Bioinformatics (S.S., E.N.), CH-4056 Basel, Switzerland

The peroxisome proliferator-activated receptor-γ coactivator 1α (PGC-1α) coordinates the transcriptional network response to promote an improved endurance capacity in skeletal muscle, eg, by coactivating the estrogen-related receptor-α (ERRα) in the regulation of oxidative substrate metabolism. Despite a close functional relationship, the interaction between these 2 proteins has not been studied on a genomic level. We now mapped the genome-wide binding of ERRα to DNA in a skeletal muscle cell line with elevated PGC-1α and linked the DNA recruitment to global PGC-1α target gene regulation. We found that, surprisingly, ERRα coactivation by PGC-1α is only observed in the minority of all PGC-1α recruitment sites. Nevertheless, a majority of PGC-1α target gene expression is dependent on ERRα. Intriguingly, the interaction between these 2 proteins is controlled by the genomic context of response elements, in particular the relative GC and CpG content, monomeric and dimeric repeat-binding site configuration for ERRα, and adjacent recruitment of the transcription factor specificity protein 1. These findings thus not only reveal a novel insight into the regulatory network underlying muscle cell plasticity but also strongly link the genomic context of DNA-response elements to control transcription factor-coregulator interactions. (***Molecular Endocrinology*** **30: 809–825, 2016)**

Skeletal muscle cells have an enormous capacity to respond to external stimuli, eg, altered levels of physical activity, temperature, oxygen, nutrient composition, and supply, by modulating metabolic and contractile properties (1, 2). Accordingly, skeletal muscle cell plasticity entails a biological program with an enormous complexity. Thus, not surprisingly, the molecular mechanisms that control this program are still largely elusive. In recent years, however, the peroxisome proliferator-activated receptor-γ coactivator 1α (PGC-1α) has emerged as a regulatory nexus in the phenotypic adaptation of skeletal muscle to endurance training (3). The expression of individual or groups of target genes is positively or negatively affected by specific interactions of PGC-1α with a substantial repertoire of different transcription factors (TFs) (4). The dynamism and flexibility of a coactivator-controlled transcriptional network could therefore provide an explanation regarding how PGC-1α expression in muscle is not only sufficient to induce a high endurance phenotype in this tissue (5, 6) but also to control related processes such as angiogenesis (7) or post- and presynaptic neuromuscular junction plasticity (8).

The estrogen-related receptor-α (ERRα) (nuclear receptor 3B1) plays a prominent role in regulating cellular metabolism that is highly reminiscent of the function of PGC-1α to boost mitochondrial biogenesis and oxidative substrate utilization (9). Indeed, a close relationship between ERRα and PGC-1α in the regulation of the expression of metabolic and other genes has been described in muscle and other tissues (10, 11). Unbiased motif prediction in promoters of genes that exhibit PGC-1α-depen-

ISSN Print 0888-8809 ISSN Online 1944-9917
Printed in USA.

Received March 15, 2016. Accepted May 5, 2016.
First Published Online May 16, 2016

* S.S. and B.K. authors contributed equally to this work.

Abbreviations: AP-1, activator protein 1; ChIP-Seq, chromatin immunoprecipitation followed by deep sequencing; DMSO, dimethyl sulfoxide; ERRα, estrogen-related receptor-α; ERRE, ERR-response element; GFP, green fluorescent protein; ISMARA, Integrated Motif Activity Response Analysis; log2FC, log2 fold change; MitA, mithramycin A; MKO, muscle-specific PGC-1α knockout; mTg, PGC-1α muscle-specific transgenic; PCA, principal component analysis; PGC-1α, peroxisome proliferator-activated receptor-γ coactivator 1α; qPCR, semiquantitative real-time PCR; shRNA, small hairpin RNA; SP1, specificity protein 1; SRC, steroid receptor coactivator; TA, tibialis anterior; TF, transcription factor; TFBS, TF-binding site; TSS, transcription start site.

dent changes in expression furthermore implied coactivation of ERRα by PGC-1α as a central regulatory paradigm in the control of mitochondrial oxidative phosphorylation gene expression (12). Intriguingly, at least in some crystal structures, the ligand-binding pocket of ERRα is almost completely occupied by bulk amino acid side chains, and thereby, binding of putative endogenous ligands in the ligand binding pocket might be almost impossible (13). Instead, fluorescence polarization-based binding assay of the ERRα ligand-binding domain together with a coactivator peptide from PGC-1α revealed that these 2 partners exhibit a particularly high interaction affinity, as well as a change of the ERRα ligand-binding domain into a transcriptionally active conformation in a ligand-independent manner (13). These data imply a "special relationship" between ERRα and PGC-1α to constitute the mechanistic core of PGC-1α- and ERRα-controlled gene expression whereby PGC-1α could act as the effective "ligand" of ERRα (14).

Recently, we have investigated the global DNA recruitment pattern of PGC-1α to the mouse genome in muscle cells related to PGC-1α-controlled gene transcription (4). To our surprise, a computational analysis of regulatory sites in positively regulated PGC-1α target genes not only suggested ERRα as an important TF in the regulation of direct but also to be involved in the induction of indirect PGC-1α target genes, implying a role for ERRα in the absence of coactivation (4). To rule out the possibility of false positive computational prediction or spurious assignment of different nuclear receptor-binding sites as ERRα-response elements, we now studied genome-wide binding of endogenous ERRα to the mouse genome in muscle cells upon activation of PGC-1α. As in our previous study, cultured muscle cells were chosen based on their low expression of endogenous PGC-1α and hence a high signal to noise ratio upon adenoviral overexpression of this coactivator. Furthermore, exogenous expression of PGC-1α allowed the introduction of an epitope tag, which not only further enhances the selectivity of the immunoprecipitation, but also circumvents the problem of the currently existing low affinity antibodies that hamper an analysis of endogenous, untagged PGC-1α in cells or muscle tissue in vivo. Thus, by comparing genomic loci bound by endogenous ERRα in muscle cells that overexpress PGC-1α with those occupied by PGC-1α using chromatin immunoprecipitation followed by deep sequencing (ChIP-Seq), we aimed at identifying shared and individual recruitment sites for these 2 proteins in the context of PGC-1α-controlled muscle gene expression in the same cellular context. We now experimentally confirmed a role for ERRα in the regulation of PGC-1α-mediated transcription, thus after overexpression of PGC-1α, in the absence of PGC-1α corecruitment. Importantly, we identified several parameters describing the genomic context of DNA-response elements that differentiate between ERRα/PGC-1α coactivation and exclusive ERRα DNA binding. In particular, monomeric/dimeric DNA-binding site configuration for ERRα, GC and CpG content of the binding region, and corecruitment of the specificity protein 1 (SP1) predict the interaction between PGC-1α and ERRα. Collectively, these findings not only significantly expand our insights into the regulation of the PGC-1α-controlled transcriptional network involved in muscle cell plasticity but, at the same time, provide distinctive molecular links between genomic elements and TF-coregulator interactions.

Materials and Methods

Cell culture, small hairpin RNA (shRNA) knockdown of ERRα, and RNA isolation

C2C12 cell culture, shRNA-mediated knockdown and RNA isolation were performed as described (4). The adenoviral vectors for the modulation of ERRα were a generous gift from Professor A. Kralli from the Scripps Research Institute in La Jolla, CA. For the ERRα knockdown gene expression arrays, the RNAs from the following 3 conditions were used: AV-sh-green fluorescent protein (GFP) + AV-GFP + vehicle (0.02% dimethyl sulfoxide, DMSO); AV-shGFP + AV-flag-PGC-1α + vehicle (0.02% DMSO); and AV-shERRα + AV-flag-PGC-1α + 2μM XCT-790. Briefly, myoblasts were differentiated into myotubes for 4 days, infected with adenoviral constructs and treated with XCT-790 for 2 additional days with daily medium change before harvesting. XCT-790 was used in the experiment to inhibit residual ERRα activity, because the AV-shERRα knockdown alone was incomplete (at ~20% control levels) (data not shown). Because modulation of PGC-1α and ERRα could potentially affect the myogenic program, the degree of differentiation of the cells was visually assessed before each experiment. Affymetrix Mouse Genome 430 2.0 arrays were used for the gene expression analysis.

ChIP and ChIP-Seq

The ERRα ChIP-Seq was done in cells overexpressing PGC-1α using the exact same conditions and methodology as described for the PGC-1α ChIP-Seq experiments (4), and the ChIP-Seq data for PGC-1α were used from previous work (4) to assess DNA binding of ERRα in the context of PGC-1α-regulated gene expression. For the immunoprecipitation of ERRα, magnetic beads (Dynabeads Protein G; Invitrogen) were coated with the monoclonal anti-ERRα antibody (ERRα rabbit monoclonal antibody, clone ID: EPR46Y; Epitomics). For the ChIP of SP1, the magnetic beads were coated with the polyclonal anti-SP1 antibody (ChIPAb+ Sp1 rabbit polyclonal antibody, 17–601; Millipore).

doi: 10.1210/me.2016-1036

High-throughput sequencing, read mapping, and peak calling

The ERRα ChIP-Seq experiment in C2C12 cells undergoing PGC-1α overexpression was performed at the joint Quantitative Genomics core facility of the University of Basel and the Department of Biosystems Science and Engineering of the Eidgenössische Technische Hochschule Zurich in Basel on a Illumina HiSeq2000 sequencer as described (4).

The sequenced reads underwent a quality filter which retained all reads having Phred score of more than or equal to 20, read length of more than or equal to 25 bp, and ambiguous nucleotides per read of less than or equal to 2. The reads that passed the filter were used as input for Bowtie version 0.12.7 (15) and aligned to the University of California Santa Cruz mm9 mouse genome assembly. Moreover, to avoid PCR amplification errors, which might have arisen during sample preparation, we removed redundant reads mapping to the same location with the same orientation, and we kept at most one read per position. Consequently, we obtained 2 155 507 covered positions for the IP and 84 175 472 covered positions for the whole-cell extract. Peak calling was performed as described using sliding windows (4). For the ERRα ChIP-Seq experiment, all consecutive windows having a Z-score greater than 3.5 were merged and the top scoring one from each window cluster was considered as the peak summit and used for further analyses.

TF-binding site (TFBS) overrepresentation and principal component analysis (PCA)

Analysis of TFBS overrepresentation and PCA was done as described (4). Briefly, TFBS occurrence was compared with a randomized background set of regions and overrepresentations of TFBSs calculated based on occurrence in peaks vs that in the shuffled, randomized background. The PCA was based on an input matrix N containing the total number of predicted TFBSs in each of the peaks for the 190 mammalian regulatory motifs that were defined.

Gene expression array analysis and gene ontology

Microarray probes were associated to a comprehensive collection of mouse promoters that was downloaded from the SwissRegulon database (16) as described (4). For each promoter, the log2 fold change (log2FC) was compared between the following conditions: overexpressed PGC-1α (treatment) and GFP (control); ERRα knockdown with the addition of XCT-790 (treatment) and overexpressed PGC-1α (control). The significance of the expression change was assessed by a Z-score, which was computed as:

$$Z = \frac{\bar{E}_{treatment} - \bar{E}_{control}}{\sqrt{\frac{\sigma^2_{treatment}}{n} + \frac{\sigma^2_{control}}{n}}}$$

where n = 3 was the number of replicate samples, $\bar{E}_{treatment}$ is the mean log2 expression across the treatment samples, $\bar{E}_{control}$ is the mean log2 expression across the control samples, and $\sigma^2_{treatment}$ and $\sigma^2_{control}$ are the variances of log2 expression levels across the replicates for the treatment and control samples, respectively. A log2FC threshold of ±0.585 (corresponding, in a more commonly used notation, to 1.5-fold change) and a Z-score cutoff of ±3 were used to identify significantly up-/down-regulated promoters. The criterion used to associate peaks and genes was proximity. For each gene with 1 or more differentially regulated promoters, we checked whether there was a peak located within 10 kb from any of the gene's associated promoters. Gene ontology analysis was performed as described using a false discovery rate-adjusted $P \leq .05$ for enrichment.

Motif activity-response analysis

An extended version of Integrated Motif Activity Response Analysis (ISMARA) (17) to separately model the direct and indirect regulatory effects that ERRα and PGC-1α was performed as described (4) using the following linear model with e_{ps} denoting the log-expression of promoter p, ie, the total log-expression of transcripts expressed from that promoter, and N_{pm} denoting the total number of predicted TFBSs for regulatory motif m in the proximal promoter p (running from −500 to +500 relative to the transcription start site [TSS]):

$$e_{ps} = c_p + c_s + \sum_m N_{pm} A_{ms}$$

In this model, c_p describes the basal expression of promoter p, c_s a sample-dependent normalization constant, and A_{ms} is the regulatory activity of motif m in sample s, which is inferred by the model. To extend this model to now incorporate PGC-1α and ERRα-binding data, we recognized that the motif activities A_{ms} of a given regulatory motif m may be modulated by the nearby binding of PGC-1α and/or ERRα. We thus distinguished the effect A_{ms} of a regulatory site for motif m that occurs outside of the binding of PGC-1α/ERRα from the effect A^*_{ms} of the motif when it occurs within a binding peak of either PGC-1α or ERRα. To model our gene expression data, we applied the standard MARA model above to promoters that lacked an associated PGC-1α-binding peak. The gene expression changes observed at these promoters upon knockdown of ERRα and/or overexpression of PGC-1α indicate indirect regulatory effects of ERRα, PGC-1α, or both of them on the activities A_{ms}. In contrast, for each "direct target" promoter p that has an associated binding peak (which could be an ERRα, a PGC-1α or an overlapping ERRα/PGC-1α peak) within 10 kb, we modeled its expression in terms of the predicted TFBSs in the binding peak, ie,

$$e_{ps} = c_p + c_s + \sum_m N^*_{pm} A^*_{ms}$$

where N^*_{pm} is the number of predicted TFBSs for motif m in the peak associated with promoter p, and A_{ms} is the motif activity of regulator m in sample s when this motif occurs in the context of either ERRα binding, PGC-1α recruitment, or both. Besides motif activities, ISMARA also calculates error bars δ_{ms} for each motif m in each sample s. Using these, ISMARA calculates, for each motif m, an overall significance measure for the variation in motif activities across the samples analogous to a z-statistic:

$$Z_m = \sqrt{\frac{1}{S}\sum_{S=1}^{S}\left(\frac{A_{ms}}{\delta_{ms}}\right)^2}$$

For each motif, we calculate a z-score Z_m associated with its indirect activity changes, a z-score $Z^*_{m,ERR\alpha}$ associated with its direct activity changes in the context of ERRα binding, a z-score $Z^*_{m,PGC1\alpha}$ associated with its direct activity changes in the context of PGC-1α recruitment, and a z-score $Z^*_{m,BOTH}$ associated

with its direct activity changes in the context of both ERRα binding and PGC-1α recruitment.

Quantitative real-time PCR and statistical analysis

Semiquantitative real-time PCR (qPCR) was used to validate the efficiency of the ERRα knockdown in regard to gene expression and to verify that the ChIP of ERRα and the ChIP of SP1 were successful. The sequences of all primers used for qPCR are listed in Supplemental Table 1. Previously described ERRα-response elements in PGC-1α target gene promoters and known ERRα/PGC-1α target genes were used as positive controls for the validation of the ChIP and gene expression, respectively. Regarding the statistical analysis of qPCR datasets, the values are presented as the mean ± SEM. Student's *t* tests were performed, and $P < .05$ was considered as significant; *, $P < .05$; **, $P < .01$; ***, $P < .001$.

Animal experiments

Mice were housed in a conventional facility with a 12-hour light, 12-hour dark cycle with free access to chow diet pellet and water. For the experiments, male, 10- to 13-week-old skeletal muscle-specific PGC-1α knockout (MKO) mice (18) and PGC-1α muscle-specific transgenic (mTg) animals (5) were used. All experiments were performed according to the criteria outlined for the care and use of laboratory animals and with approval of the veterinary office of the Basel canton and the Swiss authorities. Injections were performed under sevoflurane (QN01AB08; Provet) anesthesia. Mice were injected i.m. with either PBS + DMSO vehicle (30 μL/TA (tibialis anterior)) or mithramycin A (MitA) (1 μg/TA, 11434; Cayman Chemical) dissolved in DMSO in both TA muscles. Mice were sacrificed 6 hours after injection and the TAs isolated for further analysis. As for data access, the Gene Expression Omnibus SuperSeries accession number for the ChIP-Seq and gene expression array data reported in this article is GSE80522.

Results

ERRα is recruited to DNA together with and independently of PGC-1α

Following up on several previous publications that implied a strong, direct codependence of ERRα and PGC-1α in the control of PGC-1α-regulated metabolic gene expression (10, 12), we previously performed an unbiased, genome-wide analysis of PGC-1α recruitment to the mouse genome (4). The results of this study suggested a role for ERRα in controlling PGC-1α target gene expression in the absence of coactivation by PGC-1α (4). To verify these predictions and to identify all regions that are bound by this TF genome wide in skeletal muscle cells after overexpression of PGC-1α, we performed a ChIP-Seq of endogenous ERRα in differentiated C2C12 murine myotubes that overexpressed epitope-tagged PGC-1α. Thus, importantly, our experiments were not designed to map ERRα recruitment per se, but specifically the involvement of ERRα in the regulation of PGC-1α muscle target genes in the exact same cellular context as the previous mapping of PGC-1α recruitment (4). We then compared the identified ERRα-binding sites with this set of PGC-1α recruitment regions that we identified previously (4). In order to identify all genomic locations significantly enriched in ERRα binding, we passed a sliding window along the genome and compared the local IP read density with the background read density from whole-cell extract for each consecutive window and quantified the significance of the enrichment by Z-score. All regions with a Z-score bigger than 3.5 were merged into a final total of 3225 peaks, which included binding regions near known ERRα target genes (Supplemental Figure 1A), like the *isocitrate dehydrogenase 3 [nicotinamide adenine dinucleotide+]-α* and the *pyruvate dehydrogenase lipoamide kinase isozyme 4* (19). The enrichment of IP fragments from the ChIP-Seq experiment was validated for some of these ERRα target genes by quantitative real-time PCR (Supplemental Figure 1B).

When we compared the genome-wide ERRα binding and PGC-1α DNA recruitment (Figure 1A), we noticed that most ERRα peaks (~60%) are not overlapping a PGC-1α peak, suggesting that the so-far believed concept of symbiotic cooperation between these 2 proteins is in fact restricted to only a subset of their identified targets (~40% for ERRα and ~18% for PGC-1α), at least at the specific time point of analysis chosen in our experiments. It obviously is possible that the overlap between the 2 sets of peaks differs in a temporal manner. Moreover, the number of the PGC-1α peaks that overlap ERRα-binding sites (~18%) could in part be due to the high overexpression of PGC-1α. Finally, the 2 ChIP-Seq experiments most likely differ in terms of specificity and efficacy of the antibody-antigen interaction, and thus, interpretation of negative data could be hampered in the analysis. Nevertheless, the small overlap between the ERRα and PGC-1α peaks was not necessarily expected based on the literature. Some examples of the differential regulation are depicted in Figure 1B. Of the 1321 ERRα peaks overlapping a PGC-1α site (that is, sharing at least one base pair), the vast majority of them is well centered on the closest PGC-1α peak at a distance of a couple of dozen base pairs (Figure 1C), which could be interpreted as direct coactivation of ERRα by PGC-1α in most cases of ERRα/PGC-1α peak overlap. Notably, a larger fraction of ERRα peaks (~12%) resides within 100 bp from a mouse promoter region (Figure 1D), compared with the PGC-1α peaks (~2%), which we previously found to be more distally located (4).

doi: 10.1210/me.2016-1036

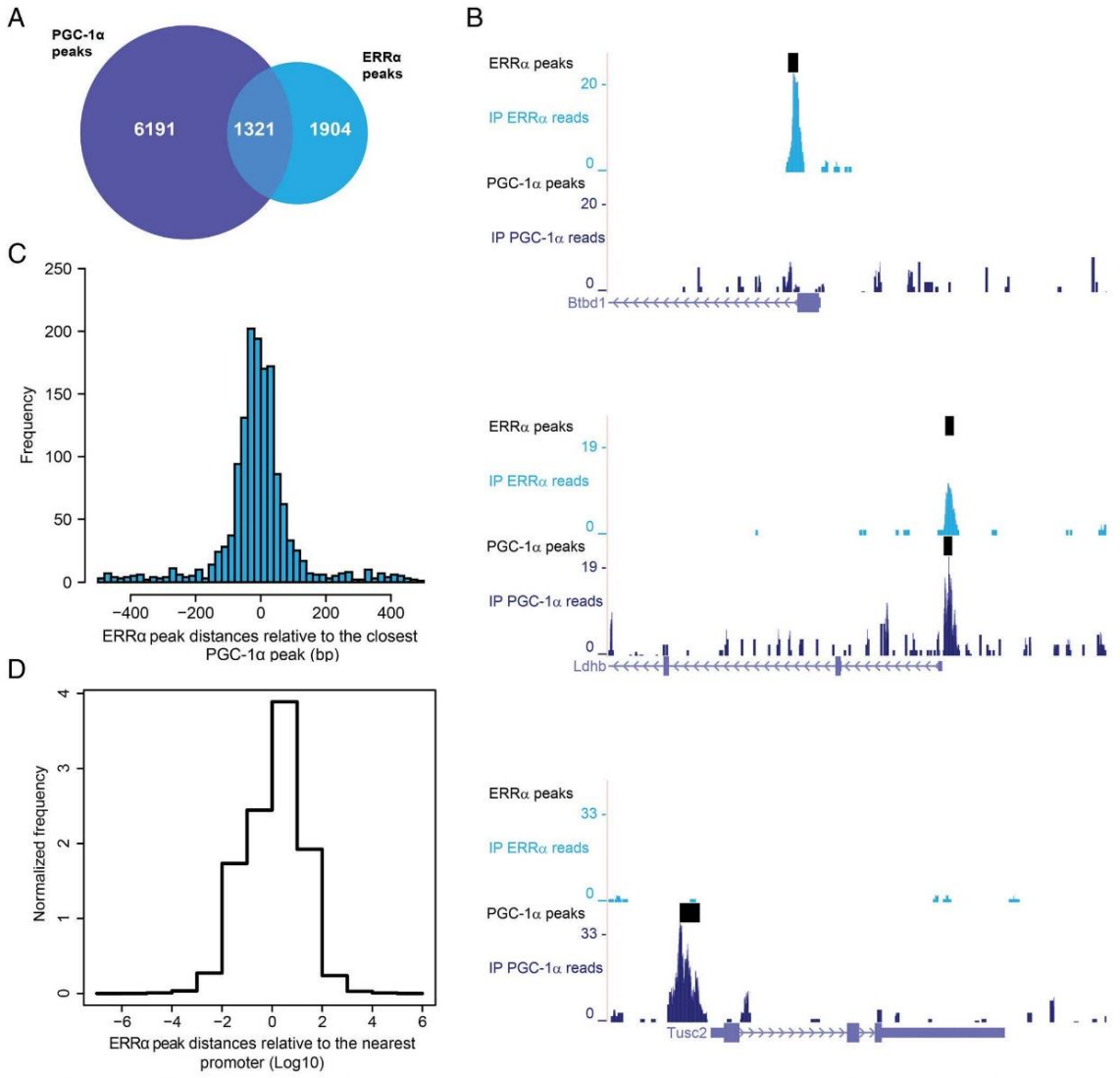

Figure 1. ERRα and PGC-1α are recruited to both shared and distinct sets of DNA elements and target genes. A, Venn diagram depicting the number of ChIP-Seq-binding peaks for PGC-1α (blue) and for ERRα (cyan). B, PGC-1α and ERRα read densities around the TSS of the genes Btbd1 (only ERRα peak), Ldhb (overlapping ERRα/PGC-1α peaks), and Tusc2 (only PGC-1α peak) obtained from the University of California Santa Cruz Genome Browser. C, Distribution of ERRα peaks relative to their closest PGC-1α peaks. D, Distribution of all ERRα peaks from the nearest mouse promoter region.

ERRα function is required for the regulation of many PGC-1α target genes

Based on DNA-binding data alone, we cannot estimate how many of the non-PGC-1α overlapping ERRα peaks are nonfunctional. Therefore, to integrate the results obtained from the ChIP-Seq experiment with functional data in terms of PGC-1α-dependent gene expression, we further analyzed the impact of ERRα on gene expression changes downstream of PGC-1α in differentiated muscle cells using the following conditions: 1) shGFP-transfected control cells expressing shRNA targeted at GFP; 2) shGFP-transfected cells expressing PGC-1α; and 3) shERRα-transfected cells expressing PGC-1α in addition to shRNA against ERRα combined with the ERRα inverse agonist XCT-790 (12) to completely abolish ERRα activity. By comparing conditions 1) and 2), we are able to identify gene expression changes downstream of PGC-1α induction, whereas comparing conditions 2)

with 3) allows us to quantify the impact of ERRα on PGC-1α-mediated gene expression: for example, we observed a strong reduction of PGC-1α-controlled induction of *Acadm*, a known ERRα/PGC-1α target gene, in cells with abolished ERRα activity (Figure 2A). After mapping the microarray probes to known transcripts and, through these, to a reference set of mouse promoters (16), we noticed that more promoters were significantly up-regulated (1863, corresponding to 1164 genes) than down-regulated (658, corresponding to 468 genes) after PGC-1α overexpression; in contrast, we observed the opposite effect in the ERRα knockdown cells: 910 promoters (corresponding to 597 genes) were significantly induced, whereas 1952 promoters (corresponding to 1203 genes) were repressed, demonstrating a strong role for ERRα in PGC-1α-mediated up-regulation of gene expression (Figure 2B). Then, a region of ±10-kb distance from each promoter was chosen to assign peaks to promoters and hence divide target genes into direct (harboring at least on peak within this region) vs indirect (without a peak within this region) genes, which obviously underestimates more long-range regulatory interactions. This stratification of the positively regulated PGC-1α target genes in terms of presence and absence of PGC-1α and ERRα peaks revealed several interesting findings: first, of the up-regulated PGC-1α target genes with a PGC-1α peak within 10 kb from any of their associated promoters, which constitute roughly 40% of all up-regulated PGC-1α targets, the number of genes with an overlap of ERRα and PGC-1α peaks (179 peaks, 15.4% of all up-regulated target genes) is lower than that of genes with only a PGC-1α peak (198 genes with only a PGC-1α peak and 57 genes that harbor distinct ERRα and PGC-1α peaks, thus combined representing 255 or 22% of all up-regulated genes) (Figure 2C). Importantly, ERRα recruitment is observed in a significant number of indirectly up-regulated PGC-1α target genes (166 genes, corresponding to 22.7% of all indirect PGC-1α targets). These data suggest that, based on DNA binding, ERRα indeed plays a substantial role in PGC-1α target gene regulation, both when coactivated by PGC-1α, but equally significant when binding in the absence of this coactivator. Notably, the PGC-1α-mediated down-regulation of gene expression is almost exclusively indirect (439 out of 468 down-regulated PGC-1α target genes, corresponding to 93.8%), and the DNA binding of ERRα seems to likewise play a minor role in this process with ERRα peaks occurring in only 17 of down-regulated genes (3.6%) (Supplemental Figure 2A). Of note, 62% of the 1321 overlapping PGC-1α/ERRα peaks (Figure 1A) where not associated to any gene within a distance of ±10 kb of the TSS, whereas 25% of these peaks were linked to nonchanging genes.

DNA recruitment of TFs or coregulators typically only partially correlates with transcriptional changes, eg, as indicated by a large number of PGC-1α peaks that were not assigned to regulated genes (4). Inversely, gene regulation can be brought about in an indirect manner and, therefore, might not require a peak adjacent to the gene promoter region, as seen for 48.5% of up-regulated PGC-1α target genes without a PGC-1α or ERRα peak, respectively (Figure 2C). We classified genes that exhibit up-regulation in response to PGC-1α induction into 4 categories based on whether they were associated with a PGC-1α-binding peak, ie, direct vs indirect PGC-1α targets, and whether the up-regulation was dependent on ERRα. According to this classification, approximately two thirds of the up-regulated PGC-1α-controlled genes were dependent on the presence of functional ERRα protein, irrespective of whether they were direct or indirect targets of PGC-1α (Figure 2, D and E).

We next investigated whether the different classes of PGC-1α targets were overrepresented for genes from different functional categories. As expected, most of the enriched categories for ERRα-dependent up-regulated target genes were related to mitochondria and oxidative energy metabolism (Figure 2, F and G). Notably, as we observed previously (4), the same functional categories show enrichment regardless of direct or indirect PGC-1α involvement. Moreover, similar gene ontology terms were found when using the ERRα-independent PGC-1α targets as input for FatiGO (Figure 2, F and G). The different categories of PGC-1α target genes were confirmed by qPCR showing 2 ERRα-dependent (*Aim1l* and *Twf2*) and 2 ERRα-independent (*Atg9b* and *Ifrd1*) PGC-1α target genes (Figure 2, H and I, respectively).

Finally, we also checked dependency of transcriptional regulation on functional ERRα for PGC-1α down-regulated targets. Peak-gene association clearly indicates that most genes whose transcription is repressed by PGC-1α lack peaks for either PGC-1α or ERRα within 10 kb of the gene promoters (~94% of all down-regulated PGC-1α target genes) (Supplemental Figure 2A). Out of these 439 indirectly down-regulated genes, about 23% (101 down-regulated, indirect PGC-1α targets) were dependent on ERRα meaning that PGC-1α-mediated repression was significantly alleviated by ERRα knockdown (Supplemental Figure 2B). Thus, ERRα markedly contributes to boost an indirect inhibitory mechanism that is involved in PGC-1α-controlled transcriptional repression. Nevertheless, most PGC-1α-mediated inhibition of gene expression is ERRα-independent and thus using alternative mediators, such as, for example, the indirect inhibition of the nuclear factor κB (20).

doi: 10.1210/me.2016-1036 press.endocrine.org/journal/mend 815

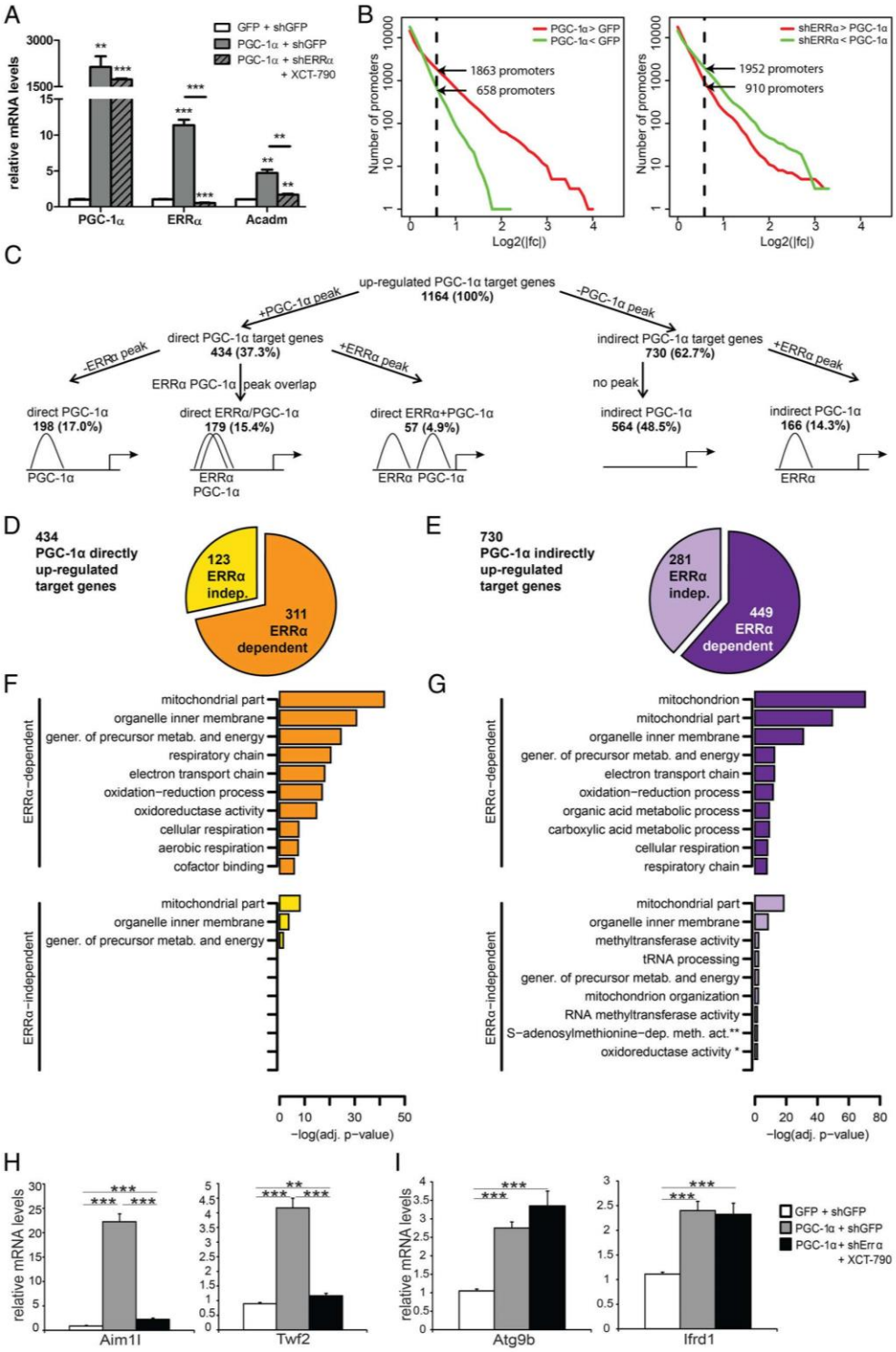

Figure 2. PGC-1α directly up-regulates both in an ERRα-dependent and -independent manner. A, qPCR analysis of PGC-1α, ERRα, and Acadm mRNA levels in response to PGC-1α overexpression (OV) and shERRα knockdown (KD) + XCT-790. Data are normalized to mRNA levels in GFP-

Coactivation specificity of monomeric vs dimeric ERRα-binding elements

In light of the postulated intimate relationship between ERRα and PGC-1α, our data depicting a high degree of independence of these 2 proteins in the regulation of PGC-1α target genes in muscle cells are quite surprising. In particular, it is unclear by what molecular mechanisms PGC-1α is recruited to ERRα-binding sites at some genomic loci, but not to others. ERRα can bind to a 9 nucleotide-long element with the consensus sequence TNAAGGTCA called an ERR-response element (ERRE) (21). In addition, binding of ERRα to repeats of ERREs and potentially other response elements has also been proposed (22). In both cases, ERRα has been proposed to bind as homo- or heterodimer, even to single ERREs (23). Importantly, data based on in vitro experiments implied that the base at the N position of the ERRE controls coactivation by PGC-1α with a preference for PGC-1α to interact with ERRα on ERREs with a T at the N position (TTAAGGTCA), whereas a C (TCAAGGTCA) favors reduced coactivation by PGC-1α (22). Because these in vitro studies were severely limited in terms of scope, we now investigated whether similar sequence variations can be detected in a genome-wide analysis of ERRα DNA-binding elements identified by ChIP-Seq. We therefore split the ERRα and PGC-1α peaks into 3 distinct groups: "only ERRα," "overlapping ERRα/PGC-1α," and "only PGC-1α" peak regions and computationally derived separate binding motifs for each set of regions. Instead of inferring standard position-specific weight matrix motifs, we employed a novel approach, recently developed in our group (S. Omidi and E. van Nimwegen, personal communication), which extends position-specific weight matrix models to so-called dinucleotide weight tensors, which allow arbitrary dependencies between the positions within the binding sites.

First, both the only ERRα and the overlapping ERRα/PGC-1α peak-associated motifs exhibited a more determined 5′ extension of the hexamer half-site as expected for an ERRE compared with the only PGC-1α peak regions (Figure 3, A–C). Intriguingly, the only ERRα motif harbors a stronger preference for C at position 5 when compared with the overlapping ERRα/PGC-1α peaks, even though the preference for this nucleotide is relatively small. However, even more strikingly, we noticed that although there are internal dependencies between the nucleotides at positions 4–6 in every peak group, the dependencies between the initial and final positions (1–2 and 13–14) of the motif are only observed for overlapping ERRα/PGC-1α and only PGC-1α peaks but not for only ERRα peaks (Figure 3, A–C).

Dependencies at the ends of the motif could imply that the TF is more often binding DNA as a dimer at these sites, suggesting that ERRα-binding site repeats may be more likely to recruit coactivation by PGC-1α than monomeric, extended half-sites. To test whether these motifs indeed differ in terms of hexamer repeat configuration, we next used the core recognition motif "AGGTCA" of the ESRRA weight matrix to identify nuclear receptor dimers in direct, everted or inverted configurations with a variable spacing between half-sites that ranged from 1 to 10 nucleotides around the core motif in the different peak groups. Remarkably, we found a striking difference in the relative occurrence of monomers and dimers of nuclear receptor hexamer half-sites between the only ERRα and the overlapping ERRα/PGC-1α peak sets (Figure 3D). In the first group, the ratio of monomers to dimers was markedly higher compared with the overlapping ERRα/PGC-1α peaks (0.63 vs 0.32), further supporting that dimeric ERRα-binding sites are more likely to enable coactivation by PGC-1α. Furthermore, even when the number of monomers is normalized to the sum of monomers and dimers in each peak set, the only ERRα peaks showed the highest fraction of nuclear receptor monomers (39%) of the 3 groups (Figure 3D). It should be noted, however, that despite these differences, the presence of a monomeric half-site in a ERRα peak is only a weak predictor of PGC-1α corecruitment, as in both groups only a marginally higher proportion of only ERRα peaks contain a monomer compared with overlapping ERRα/PGC-1α (only ERRα, 440 out of 1904 peaks corresponding to 23.1%; overlapping ERRα/PGC-1α, 266 out of 1321 peaks in total corresponding to 20.1%). It is therefore

Figure 2 (Continued). infected cells. Error bars represent ±SEM; *, $P < .05$; **, $P < .01$; ***, $P < .001$. B, Reverse cumulative distribution of log2FCs for all mouse promoters in the PGC-1α OV condition vs GFP control (left panel) and in the PGC-1α OV + shERRα KD + XCT-790 vs PGC-1α OV (right panel). Promoters are colored in red (up-regulation) when their fold change is bigger than 1.5 and in green (down-regulation) when their fold change is smaller than −1.5 (obtained by taking the inverse of the linear binding ratio). C, Tree diagram of all PGC-1α up-regulated target genes, distinguished in different subgroups according to peak presence/absence. D, Pie-chart representing the classification of directly up-regulated PGC-1α target genes in ERRα-dependent (orange) and ERRα-independent (yellow) targets. E, Pie-chart representing the classification of indirectly up-regulated PGC-1α target genes in ERRα-dependent (violet) and ERRα-independent (lilac) targets. F and G, Subset of the top significantly enriched Gene Ontology terms identified for ERRα-dependent and ERRα-independent PGC-1α directly (F) or indirectly (G) induced target genes. gener., generation; metab., metabolites; *, oxidoreductase activity, acting on a sulfur group, disulfide as acceptor; **, S-adenosylmethionine-dependent methyltransferase activity. H and I, qPCR analysis of 2 ERRα-dependent (H) or ERRα-independent (I) PGC-1α target genes, in response to PGC-1α OV and shERRα KD + XCT-790. Data are normalized to mRNA levels in GFP-infected cells. Error bars represent ±SEM; *, $P < .05$; **, $P < .01$; ***, $P < .001$.

doi: 10.1210/me.2016-1036

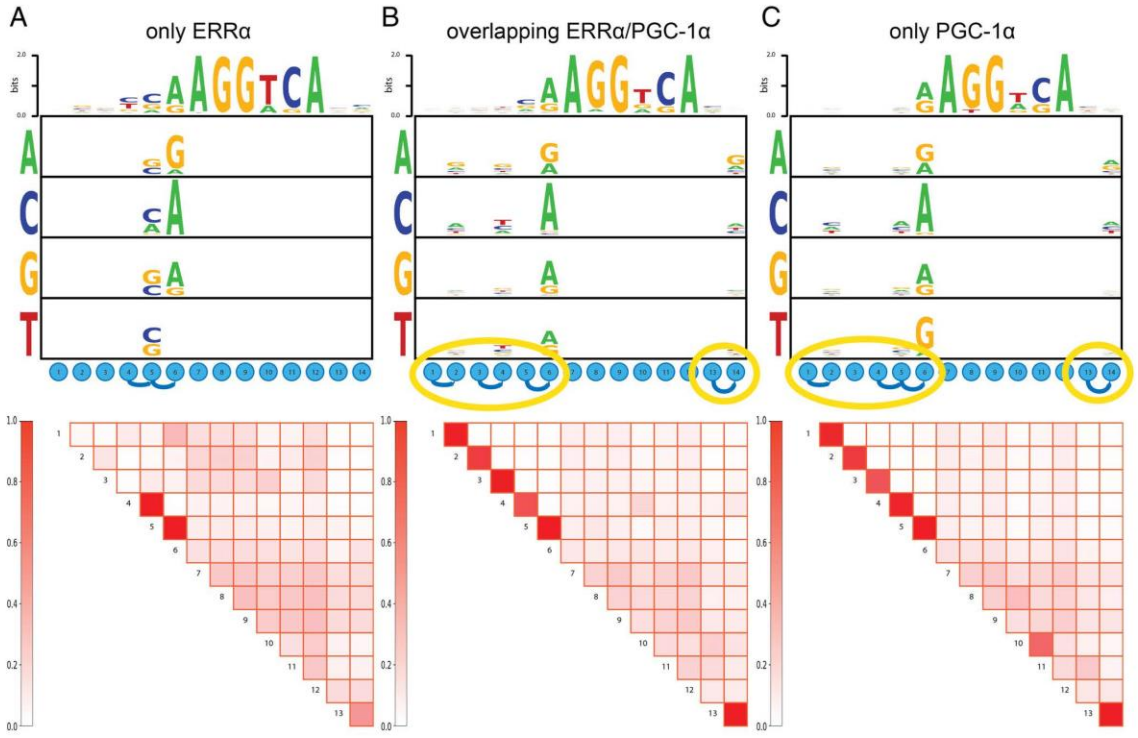

D

	only ERRα peaks	ovl. ERRα/PGC-1α peaks	only PGC-1α peaks
posterior sum dimers	599.15	1354.69	3475.18
posterior sum monomers	378.88	432.60	1456.84
ratio monomers/dimers	0.63	0.32	0.42
ratio monomers/(monomers+dimers)	0.39	0.24	0.30

Figure 3. In the absence of a direct coactivation by PGC-1α, ERRα prefers to bind to monomeric DNA elements. A–C, Motif logo showing the interdependencies between the different positions of the ESRRA weight matrix identified in only ERRα, overlapping ERRα/PGC-1α, and only PGC-1α. Dependencies between positions are indicated by a blue curved line, whereas yellow ellipses highlight the dependencies which are in overlapping ERRα/PGC-1α and only PGC-1α peaks but not in only ERRα peaks. D, Table showing the posterior sum and the fraction of nuclear receptor hexamer half-site monomers and dimers across our 3 peak sets.

very likely that the sequence specificity and the monomeric/dimeric configuration favor, but by themselves are not sufficient to entirely control coactivation of ERRα by PGC-1α.

ERRα-binding regions without PGC-1α recruitment are enriched for SP1 binding

To identify additional predictors of the ERRα/PGC-1α interaction, we next analyzed the occurrence of TF DNA-binding motifs within all of the ERRα peaks. We used the software MotEvo to predict TFBSs for a set of 190 known mammalian regulatory motifs (24). In order to explain most of the binding site variation observed across the ERRα peaks, we then applied PCA to a site-count matrix N, whose elements N_{pm} represent the number of predicted TFBSs for each motif m in each ERRα peak region p. Out of a total of 190, the first component was accounting for approximately 10% of the total variation in the dataset (Figure 4A). The distribution of motif projections on the first 2 principal components clearly indicates 2 distinct clusters of motifs that are associated with variation along the first and second principal components (Figure 4B). The first group includes ESRRA and other nuclear receptors which have binding motifs that are very similar to that of the ERRα motif. This cluster reflects the most abundant sites which can be found within the ERRα-binding regions. Interestingly, besides these expected nuclear receptor motifs, the second group of motifs consists of GC-rich motifs which often are found in

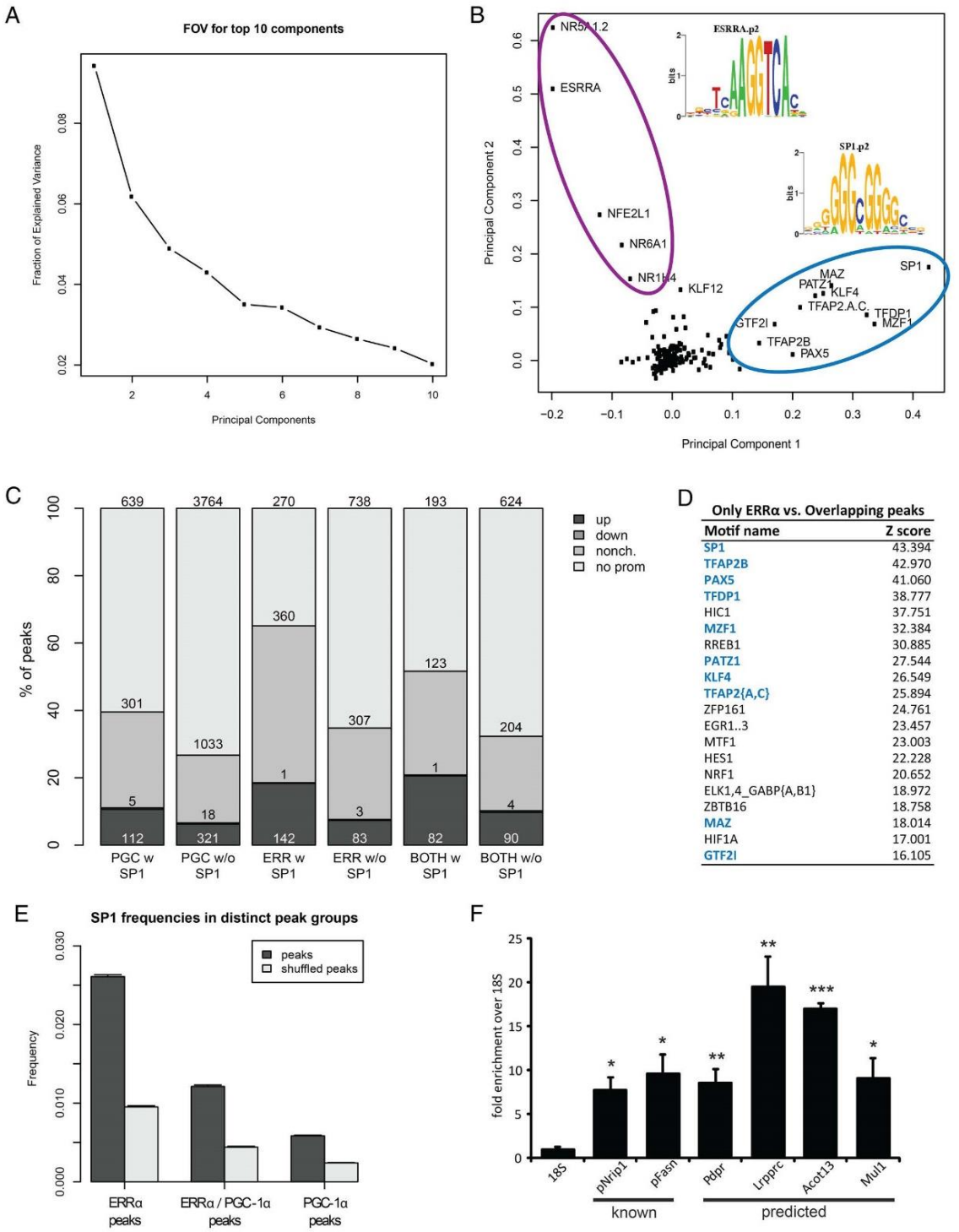

Figure 4. SP1 is the top TF partner for ERRα in skeletal muscle. A, Fraction of explained variance of the top 10 PCA components. B, PCA analysis of the 3225 ERRα peaks. The names of the motifs with the largest projections on the first 2 principal components are indicated. Purple and light blue ellipses highlight motif clusters, as identified by principal component 1, of nuclear hormone receptor-like motifs and SP1-like motifs,

doi: 10.1210/me.2016-1036

the proximity of transcriptional start sites. The motif with the highest score along the first principal component describes binding elements of SP1. The activity of this protein can be significantly affected by posttranslational modifications, resulting in SP1 to either act as an activator or as a repressor (25). Moreover, a functional link between the occurrence of SP1-binding sites and ERRα activity, albeit without consideration of coactivation by PGC-1α, has been proposed previously (26). We thus subsequently investigated the activity of SP1 in the context of PGC-1α target gene regulation. The different classes of peaks (only ERRα, only PGC-1α, overlapping ERRα/PGC-1α) were therefore combined with the regulation of their assigned promoters ("up," "down," "nonchanging," and "no promoter assigned") as shown in Figure 4C. Strikingly, whenever a site for SP1 is present within a peak, it is more likely for the assigned promoter to be up-regulated, strongly suggesting that in the context of PGC-1α overexpression, SP1 plays a role as an activator. This effect is particularly enhanced when SP1 is found in an ERRα peak compared with the PGC-1α peaks. Similarly, when analyzing TFBS predictions that differ between the only ERRα and the overlapping ERRα/PGC-1α groups, SP1 emerges as the top-scoring motif and thus strongly associates with only ERRα peaks (Figure 4D). The specific enrichment of SP1 motifs in the only ERRα group was also confirmed by comparing the enrichment of predicted SP1-binding sites, relative to its occurrence in a set of randomized peak sequences, in only ERRα peaks with the enrichment in overlapping ERRα/PGC-1α and only PGC-1α peaks. Although SP1 sites are more frequent in all peak sets relative to randomized regions, the enrichment is by far strongest in only ERRα peaks (Figure 4E). Next, we experimentally validated the presence of SP1 both at the promoters of the known target genes *RIP140/Nrip1* and *Fasn* (27, 28) and in ERRα peaks with an adjacent predicted SP1-binding site in the proximity of 4 distinct genes by ChIP (Figure 4F). Finally, we studied the functional consequence of SP1 on muscle target gene expression of endogenous and overexpressed PGC-1α in gain- and loss-of-function animal models in vivo (Supplemental Figure 3). First, we validated a set of target genes belonging to all 4 binding categories (genes with only ERRα recruitment with SP1 motifs, only ERRα recruitment without SP1-binding sites, PGC-1α/ERRα overlapping peaks with SP1 motifs and PGC-1α/ERRα overlapping peaks without SP1-binding sites). As shown in Figure 5, the expression of genes from all 4 categories was reduced in skeletal MKO animals and elevated in skeletal mTg mice. Thus, at least these genes are not only regulated by overexpressed PGC-1α in cultured muscle cells, but also by endogenous and overexpressed PGC-1α in mouse muscle in vivo. Subsequently, we aimed at testing the functional involvement of SP1 in the predicted subcategories of PGC-1α target genes using the specific pharmacological SP1 inhibitor MitA (29). First, efficacy of SP1 inhibition was demonstrated by the reduction of the known SP1 target genes *Sp1* and *Vegfa* (Supplemental Figure 4). Surprisingly, however, MitA not only reduced the ability of PGC-1α to induce target genes that harbor an SP1 motif but also those without a predicted SP1-binding site (Supplemental Figure 4). Most likely, the expected selectivity of the functional involvement of SP1 is lost due to an inhibition of endogenous and transgenic PGC-1α expression by MitA (Supplemental Figure 4). Similarly, small interfering RNA-mediated knockdown of SP1 in cultured muscle cells likewise reduced the expression of PGC-1α (data not shown). Indeed, putative SP1-binding sites were found both in the proximal as well as in the distal/alternative promoter regions of PGC-1α (Supplemental Figure 4). Thus, even though we found a significant functional involvement of SP1 in the regulation of PGC-1α target gene expression in mouse muscle in vivo, we were unable to validate our prediction based on the presence of SP1 motifs in a subset of these genes, most likely due to the observation of PGC-1α itself being an SP1 target.

Figure 4 (Continued). respectively. C, Bar chart representing the different classes of peaks (only ERRα, only PGC-1α, "overlapping ERRα/PGC-1α) together with the regulation of their associated promoters (up, down, nonchanging, and no promoter assigned). Numbers shown on top of each box represent the absolute peak counts. D, Top scoring results of motif search obtained by comparing the TFBSs predictions within the only ERRα peaks with those in the overlapping ERRα/PGC-1α. The motifs corresponding to the SP1 group in the PCA are colored in blue. E, TFBSs posterior sum for SP1 in only ERRα, overlapping ERRα/PGC-1α and only PGC-1α peaks. For each dataset, TFBS occurrences were compared against binding site predictions performed on the corresponding background set of shuffled peaks. F, qPCR validation of the ChIP enrichment measured at the promoter of a set of SP1 known target genes and around the predicted SP1 site within the ERRα peaks associated to the genes Pdpr, Lrpprc, Acot13, and Mul1. Bars represent fold enrichment over that of the 18S rRNA gene, error bars represent SEM; *, $P < .05$; **, $P < .01$; ***, $P < .001$.

ERRα peaks without PGC-1α corecruitment exhibit higher GC and CpG content

Intriguingly, the amount of predicted SP1 TFBSs (in terms of posterior sum) was much lower in PGC-1α randomized (shuffled) peaks compared with the ERRα shuffled peak dataset (Figure 4E). Because SP1 is known to bind GC-rich regions, these results might reflect a different nucleotide composition between the peak sets. Accordingly, we analyzed the GC and CpG content of all ERRα and PGC-1α peaks. Interestingly, in contrast to the

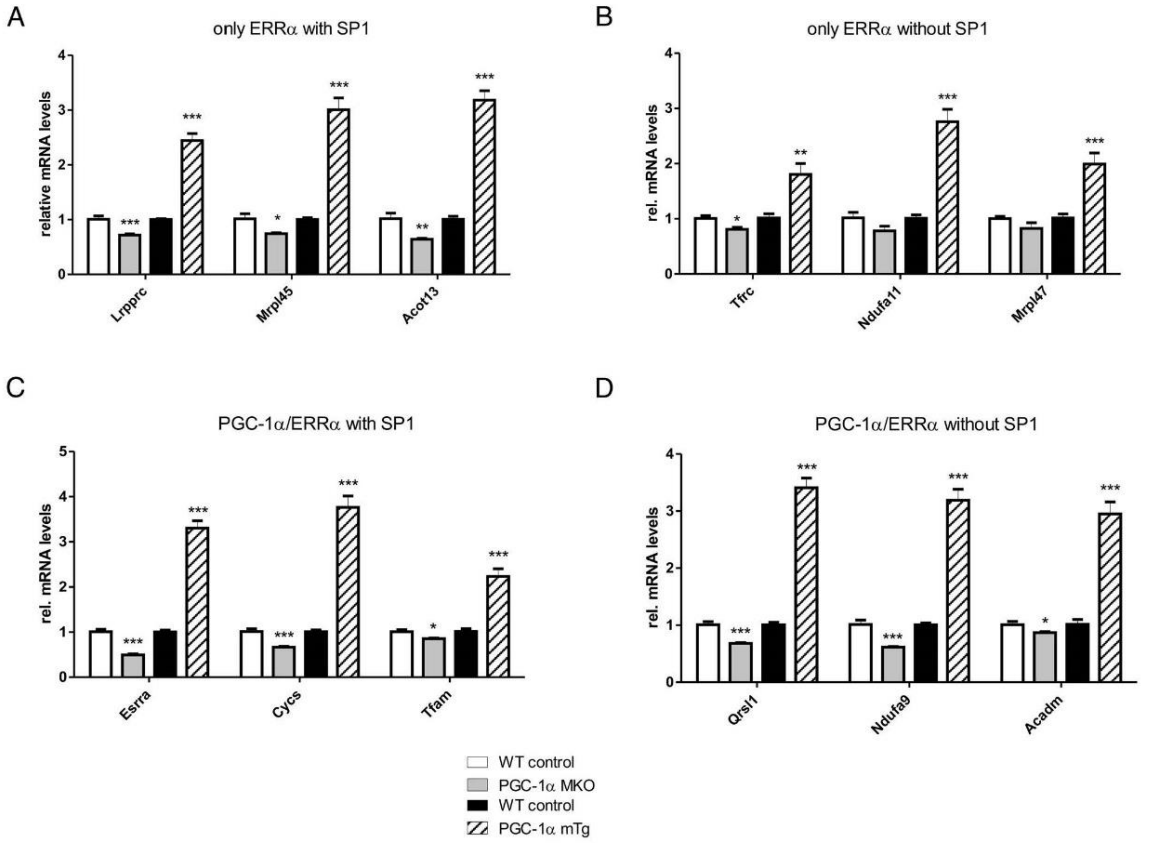

Figure 5. Target genes of all 4 binding categories are regulated by endogenous and overexpressed PGC-1α in mouse muscle in vivo. A–D, The expression of PGC-1α target genes with only ERRα DNA binding with (A) and without (B) adjacent SP1 motifs as well as of PGC-1α target genes with overlapping PGC-1α and ERRα peaks with (C) and without (D) SP1-binding sites was validated in skeletal MKO and mTg mice compared with the respective wild-type littermate controls.

overlapping ERRα/PGC-1α peaks, and even more to the only PGC-1α peaks, the only ERRα peaks separated into 2 distinct populations, one with high and the second with lower GC content (Figure 6, A–C). Even more strikingly, these 2 populations in the only ERRα peak group also differed in the CpG content and therefore potential CpG islands. Subsequently, each peak set was further subdivided into proximal and distal-binding regions, where proximal referred to peaks within 1 kb from their associated gene promoter and "distal" to peaks located farther away. As clearly shown in Figure 6, D–F, the only ERRα peaks host more CpG dinucleotides with respect to only PGC-1α peaks; moreover, the fraction of only ERRα proximal peaks is much higher (~1/3) than the corresponding fraction of only PGC-1α peaks (~1/10). Importantly, although most of this difference stems from the CpG content in proximal peaks, even the more distal ERRα peak distribution curve exhibits shoulders towards higher CpG content that are completely missing in the PGC-1α peaks. These results suggest a preference for high GC and CpG content in ERRα DNA recruitment sites, whereas PGC-1α in the absence of ERRα is bound to response elements with a relatively lower GC and CpG content. Importantly, the overlapping ERRα/PGC-1α peaks behave in an intermediary manner (Figure 6E).

Strikingly, the combination of all 3 parameters, monomeric binding, high CpG content and presence of an SP1-binding site, synergize in discriminating between only ERRα and overlapping ERRα/PGC-1α peaks. For example, as depicted in Figure 6, G and H, the percentage of peaks harboring at least 2 features are 2-fold more frequent in the only ERRα compared with the overlapping ERRα/PGC-1α group, whereas those with all 3 features are even 5 times more frequent. Notably, SP1 cooccurrence with high CpG content is particularly enriched in the only ERRα group with 15.7% of peaks, as opposed to only 4.5% in the overlapping ERRα/PGC-1α peak group. Similarly, the combination of all the 3 criteria accounts

doi: 10.1210/me.2016-1036 press.endocrine.org/journal/mend 821

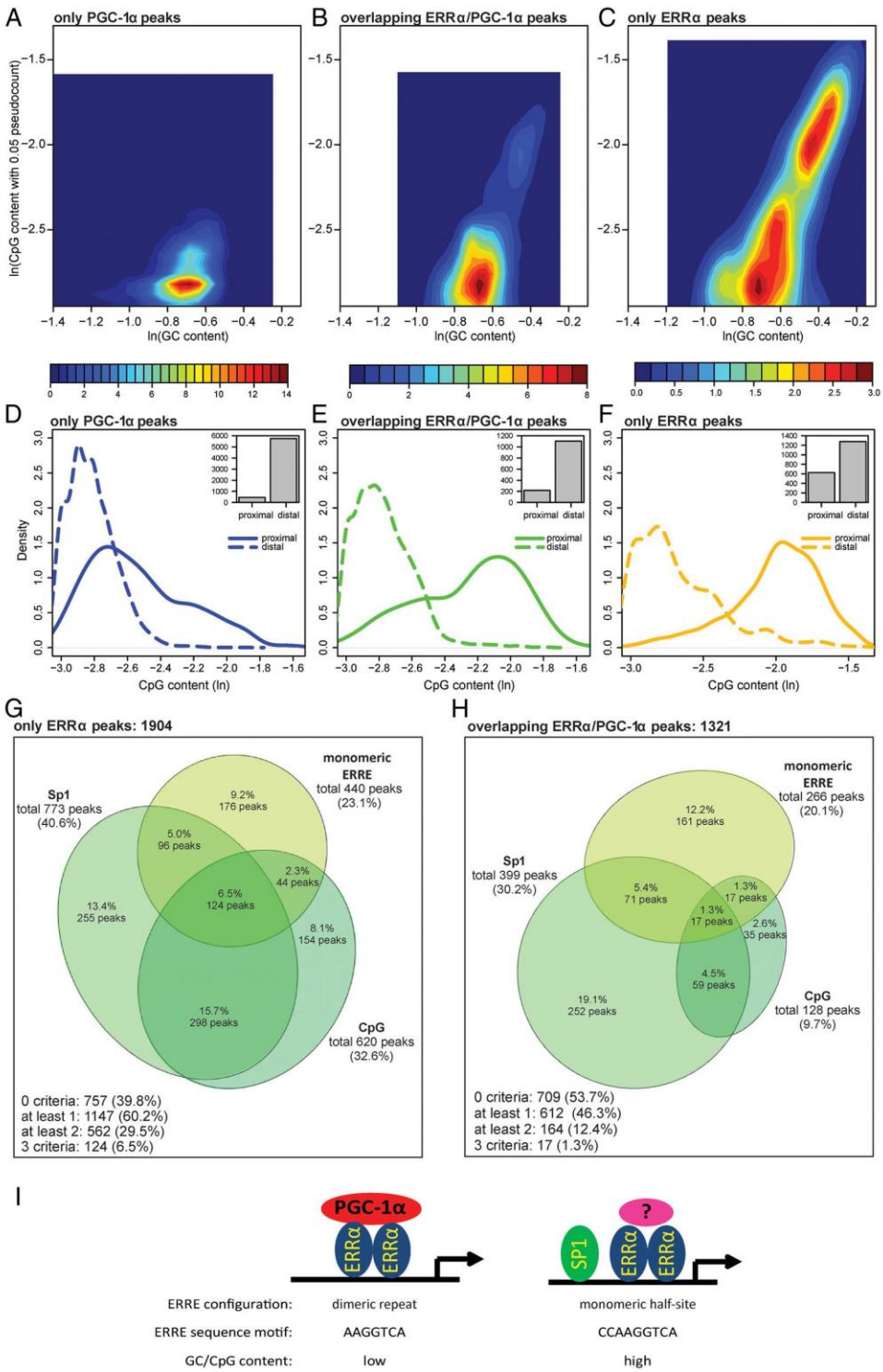

Figure 6. Only ERRα peaks prefer to occur as ERRE monomers and to bind high CpG content regions A–C, Two-dimensional histogram (shown as a heat map) of the GC base content (horizontal axis) and CpG dinucleotide content (vertical axis) of only PGC-1α (A), overlapping ERRα/PGC-1α

for 6.5% of only ERRα peaks, whereas they are found in only 1.3% of overlapping ERRα/PGC-1α peaks. Indeed, the CpG content, which is present in 32.6% of the only ERRα peaks (ie, 3-fold higher than in the other dataset), is the feature which determines the biggest fraction of overlap among the 3 criteria that we focused on.

Discussion

Control of complex biological programs by coregulator proteins has emerged as a regulatory paradigm in higher organisms in recent years. For example, the 3 members of the steroid receptor coactivator (SRC) family SRC-1, SRC-2, and SRC-3 play a major role in modulating systems metabolism (30). Coregulator control of biological programs exhibits several advantages over individual TFs (31, 32): by binding to and modulating the activity of several different TFs, coregulators usually have a broader repertoire in target gene transcriptional regulation (33). Second, the possibility of coordinating the regulation of genes within a specific transcriptional program provides kinetic advantages to accelerate the output of specific pathways beyond the possibilities of individual gene regulation (34). Furthermore, transcriptional regulation, transcript variants and a myriad of posttranslational modifications allow a combinatorial control of coregulator stability and specificity and thereby enable dynamic control of complex cellular plasticity in a highly context-dependent manner (35). Many of these mechanistic principles are illustrated by the regulation and function of PGC-1α in the control of cellular energy homeostasis. However, mechanistic insights into the dynamic TF-coregulator interactions remain rudimentary. Following our previous report predicting ERRα activity both in the presence and absence of direct PGC-1α coactivation based on motif representation (4), we now provide experimental and computational evidence for a contribution of the genomic context of DNA-response elements to control the corecruitment of PGC-1α and ERRα in the context of PGC-1α-controlled muscle gene expression. Our findings are particularly surprising, because historically, ERRα has been thought to strongly rely on PGC-1α coactivation to regulate PGC-1α target gene expression (10, 12). Interestingly, the DNA binding of PGC-1α and ERRα have been analyzed in a previous study by Charos et al (36). Notably, several important differences compared with our experimental system exist: for example, Charos et al (36) analyzed human proteins in the human hepatoma cell line HepG2 and studied ERRα DNA binding in the absence of activated/elevated PGC-1α. Nevertheless, in both studies, a similar number of ERRα peaks were found (3786 by Charos et al compared with 3225 reported here), and even more importantly, the overlap between PGC-1α and ERRα peaks was likewise small: of the 3193 and 1741 multiple regulatory factor-binding regions of ERRα and PGC-1α, respectively, only 535 were shared between these 2 factors (36).

Intriguingly, the decision between ERRα coactivation by PGC-1α and distinct DNA binding is to a certain extent determined by several aspects of the DNA composition of the enhancer and promoter regions (Figure 6I). In particular, the ERRα-binding element configuration as a monomeric half-site, adjacent recruitment of SP1 and a high CpG content appear to discourage corecruitment of PGC-1α. Assuming that ERRα activity seems largely determined by coactivator action due to the small ligand-binding pocket observed in some crystallographic studies (13), the context of PGC-1α-regulated gene expression implies that separate ERRα DNA binding not only precludes association of PGC-1α, but instead favors coactivation by other coregulators. Indeed, the transcriptional activity of human ERR1, the human ortholog of the murine ERRα, is enhanced in a ligand-independent manner by the activator of thyroid and retinoic acid receptors, the glucocorticoid receptor-interacting protein 1, and SRC-1 (37). Whether any of these coactivators are involved in ERRα-dependent muscle gene regulation by PGC-1α remains to be investigated. Intriguingly, such a shift in coactivator preference from PGC-1α towards binding of glucocorticoid receptor-interacting protein 1 to the glucocorticoid receptor could be achieved by using pharmacological means (38). Furthermore, an inverse agonist was discovered to specifically reduce the interaction between PGC-1α and ERRα but not other TF binding partners (12, 39). However, future studies will have to aim at determining how the genomic context translates into conformational changes in a TF that then affects interaction with distinct coregulators. Importantly, at least part of this genomic context might be amenable to dynamic regulation, for example, by the overall availability or post-

Figure 6 (Continued). (B), and only ERRα peaks (C). The values shown on both axes are expressed as logarithms. D–F, Density plots of the CpG content of only ERRα (D), overlapping ERRα/PGC-1α (E), and only PGC-1α (F) peaks, located either proximally (≤1 kb) or distally (>1 kb) from the closest promoter. Each inset shows the bar plot of the number of proximal and distal peaks. G and H, Euler diagram of only ERRα peaks (G) and of overlapping ERRα/PGC-1α peaks (H). Peaks were subdivided according to 3 different criteria: presence of SP1-binding sites, presence of monomers and high CpG content (defined as GC content ≥ 50% and CpG content ≥ 65%). I, Model of ERRα regulation of PGC-1α target genes in muscle cells. A combination of SP1 corecruitment, monomeric vs dimeric ERRα-binding site configuration, nucleotide preference of the ERRE, and GC/CpG content affect coactivation of ERRα by PGC-1α in the regulation of PGC-1α target genes in muscle cells.

doi: 10.1210/me.2016-1036

translational control of the activity of SP1. Unfortunately, due to the potent effect of SP1 on PGC-1α transcription, we were unable to validate our predictions of increased presence of SP1-binding sites in ERRα only regulated PGC-1α target genes. Second, the cytosines in CpG sites are potential targets for DNA methylation and thereby mediate epigenetic regulation of gene expression (40). Even though our conclusions rely to a large extent on computational prediction and therefore, future experiments will have to further validate and expand these findings, it is intriguing to speculate that DNA methylation may not only generally repress transcription by limiting TF binding, but maybe in a more fine-tuned manner also modulate TF-coregulator interactions. Moreover, based on the reports of epigenetic modifications in exercise, including DNA hypomethylation of the PGC-1α promoter itself (41), it thus will be interesting to study how exercise-induced epigenetic changes affect not only the expression, but also the DNA recruitment and TF coactivation pattern of this key regulator of endurance exercise adaptation in muscle.

Besides the more general implication of our results on the mechanistic aspects of genomic context, TF binding and coregulator recruitment, a second highly surprising finding emerged from the data related to the function of ERRα and PGC-1α in muscle cells. Specifically, ERRα was described as the central partner for PGC-1α in the regulation of mitochondrial oxidative phosphorylation gene expression (10, 12). Our results, however, now reveal a much more diverse manner by which PGC-1α regulates the expression of these and other, related metabolic pathways. Ontological analysis of the PGC-1α target genes devoid of an ERRα and PGC-1α peak demonstrate that other TFs also significantly contribute to the regulation of genes encoding enzymes in the same metabolic pathways. Importantly, in light of the close similarity of DNA-binding elements and target gene activation, it is possible that some of the predicted ERREs could also be activated by ERRγ. Moreover, as implied by the prediction of TF-binding motifs to be associated with PGC-1α-dependent transcriptional regulation, there might be a number of additional TFs that work with PGC-1α in controlling muscle cell plasticity, many of which have not been studied in the context of PGC-1α-mediated transcriptional control so far. Intriguingly, a certain degree of functional redundancy seems to exist: for example, inhibition of ERRα reduces the PGC-1α-induced expression of *Vegfa* (7). Likewise, however, small interfering RNA-mediated knockdown of components of the activator protein 1 (AP-1) TF complex or of SP1 also decreases the ability of PGC-1α to increase vascular endothelial growth factor gene expression (4). Thus, PGC-1α-controlled muscle cell plasticity might combine 2 mechanistic principles: on the one hand, a "regulon" to tightly coordinate the concurrent expression of genes that belong to a specific transcriptional program while, on the other hand, providing a more distributed transcriptional network using a variety of different TFs, both directly as well as indirectly, to add regulatory robustness as well as flexibility to control the expression of these genes in different cellular contexts. ERRα most likely is the central factor for PGC-1α to control a bioenergetic regulon using several modulators including SP1 and potentially others such as prospero homeobox 1 (42) to affect ERRα-PGC-1α interactions. Inversely, AP-1 and other TFs could complement the action of ERRα, for example, by triggering muscle vascularization in different contexts such as local tissue hypoxia for AP-1 as opposed to altered metabolic demand for ERRα (4).

In conclusion, we elucidated to what extent the nuclear receptor ERRα contributes to PGC-1α target gene expression in a muscle cell line. Even though our experiments were restricted to the analysis of endogenous ERRα in the context of overexpressed PGC-1α in cultured muscle cells, several interesting mechanistic findings emerged. Intriguingly, despite a relatively low overlap in DNA binding, ERRα is crucial for the regulation of a majority of PGC-1α target genes in a muscle cell line. Moreover, the genome-wide DNA-binding patterns of ERRα and PGC-1α demonstrated that coactivation of this TF by PGC-1α depends on different aspects of the genomic context of the DNA-response element. Importantly, however, the postulated criteria do not provide a binary distinction between coactivation and noncoactivation. Parameters with a higher predictive power might be identified in a temporal analysis of PGC-1α and ERRα DNA recruitment to PGC-1α target genes in muscle cells. Nevertheless, these findings not only provide important mechanistic insights into the regulation of complex biological programs by coregulator proteins but could also help to specifically modulate such networks in order to selectively address dysregulation of genes in pathological settings. In the future, studies on endogenous proteins in murine and human contexts in vivo will help to further unravel the complex mechanisms of coactivator-controlled transcriptional networks.

Acknowledgments

We thank Dr A. Kralli for the generous gift of control and shERRα adenoviral vectors.

Address all correspondence and requests for reprints to: Christoph Handschin, Biozentrum, University of Basel, Klingelbergstrasse 50/70, CH-4056 Basel, Switzerland. E-mail: christoph.handschin@unibas.ch; or Erik van Nimwegen, Biozentrum, University of Basel, Klingelbergstrasse 50/70, CH-4056 Basel, Switzerland. E-mail: erik.vannimwegen@unibas.ch.

Present address for S.S.: Wellcome Trust Centre for Human Genetics, Roosvelt Drive, Oxford OX3 7BN, United Kingdom.

Present address for M.B.: Schweizerische Arbeitsgemeinschaft für Klinische Krebsforschung, CH-3008 Bern, Switzerland.

This work was supported by the European Research Council Consolidator Grant 616830-MUSCLE_NET, the Swiss National Science Foundation, SystemsX.ch, the Swiss Society for Research on Muscle Diseases, the Neuromuscular Research Association Basel, the Gebert-Rüf Foundation Rare Diseases Program, the Novartis Stiftung für medizinisch-biologische Forschung, the Biozentrum Basel International PhD Program "Fellowships for Excellence," the University of Basel, and the Biozentrum.

Disclosure Summary: The authors have nothing to disclose.

References

1. Hoppeler H, Baum O, Lurman G, Mueller M. Molecular mechanisms of muscle plasticity with exercise. *Compr Physiol*. 2011;1(3):1383–1412.
2. Blaauw B, Schiaffino S, Reggiani C. Mechanisms modulating skeletal muscle phenotype. *Compr Physiol*. 2013;3(4):1645–1687.
3. Pérez-Schindler J, Handschin C. New insights in the regulation of skeletal muscle PGC-1α by exercise and metabolic diseases. *Drug Discov Today Dis Models*. 2013;10(2):e79–e85.
4. Baresic M, Salatino S, Kupr B, van Nimwegen E, Handschin C. Transcriptional network analysis in muscle reveals AP-1 as a partner of PGC-1α in the regulation of the hypoxic gene program. *Mol Cell Biol*. 2014;34(16):2996–3012.
5. Lin J, Wu H, Tarr PT, et al. Transcriptional co-activator PGC-1 α drives the formation of slow-twitch muscle fibres. *Nature*. 2002;418(6899):797–801.
6. Handschin C, Chin S, Li P, et al. Skeletal muscle fiber-type switching, exercise intolerance, and myopathy in PGC-1α muscle-specific knock-out animals. *J Biol Chem*. 2007;282(41):30014–30021.
7. Arany Z, Foo SY, Ma Y, et al. HIF-independent regulation of VEGF and angiogenesis by the transcriptional coactivator PGC-1α. *Nature*. 2008;451(7181):1008–1012.
8. Arnold AS, Gill J, Christe M, et al. Morphological and functional remodelling of the neuromuscular junction by skeletal muscle PGC-1α. *Nat Commun*. 2014;5:3569.
9. Eichner LJ, Giguère V. Estrogen related receptors (ERRs): a new dawn in transcriptional control of mitochondrial gene networks. *Mitochondrion*. 2011;11(4):544–552.
10. Schreiber SN, Emter R, Hock MB, et al. The estrogen-related receptor α (ERRα) functions in PPARγ coactivator 1α (PGC-1α)-induced mitochondrial biogenesis. *Proc Natl Acad Sci USA*. 2004;101(17):6472–6477.
11. Huss JM, Kopp RP, Kelly DP. Peroxisome proliferator-activated receptor coactivator-1α (PGC-1α) coactivates the cardiac-enriched nuclear receptors estrogen-related receptor-α and -γ. Identification of novel leucine-rich interaction motif within PGC-1α. *J Biol Chem*. 2002;277(43):40265–40274.
12. Mootha VK, Handschin C, Arlow D, et al. Errα and Gabpa/b specify PGC-1α-dependent oxidative phosphorylation gene expression that is altered in diabetic muscle. *Proc Natl Acad Sci USA*. 2004;101(17):6570–6575.
13. Kallen J, Schlaeppi JM, Bitsch F, et al. Evidence for ligand-independent transcriptional activation of the human estrogen-related receptor α (ERRα): crystal structure of ERRα ligand binding domain in complex with peroxisome proliferator-activated receptor coactivator-1α. *J Biol Chem*. 2004;279(47):49330–49337.
14. Handschin C, Mootha VK. Estrogen-related receptor α (ERRα): a novel target in type 2 diabetes. *Drug Discov Today Ther Strateg*. 2005;2(2):151–156.
15. Langmead B, Trapnell C, Pop M, Salzberg SL. Ultrafast and memory-efficient alignment of short DNA sequences to the human genome. *Genome Biol*. 2009;10(3):R25.
16. Pachkov M, Balwierz PJ, Arnold P, Ozonov E, van Nimwegen E. SwissRegulon, a database of genome-wide annotations of regulatory sites: recent updates. *Nucleic Acids Res*. 2013;41(Database issue):D214–D220.
17. Balwierz PJ, Pachkov M, Arnold P, Gruber AJ, Zavolan M, van Nimwegen E. ISMARA: automated modeling of genomic signals as a democracy of regulatory motifs. *Genome Res*. 2014;24(5):869–884.
18. Pérez-Schindler J, Summermatter S, Santos G, Zorzato F, Handschin C. The transcriptional coactivator PGC-1α is dispensable for chronic overload-induced skeletal muscle hypertrophy and metabolic remodeling. *Proc Natl Acad Sci USA*. 2013;110(50):20314–20319.
19. Zhang Y, Ma K, Sadana P, et al. Estrogen-related receptors stimulate pyruvate dehydrogenase kinase isoform 4 gene expression. *J Biol Chem*. 2006;281(52):39897–39906.
20. Eisele PS, Salatino S, Sobek J, Hottiger MO, Handschin C. The peroxisome proliferator-activated receptor γ coactivator 1α/β (PGC-1) coactivators repress the transcriptional activity of NF-κB in skeletal muscle cells. *J Biol Chem*. 2013;288(4):2246–2260.
21. Sladek R, Bader JA, Giguère V. The orphan nuclear receptor estrogen-related receptor α is a transcriptional regulator of the human medium-chain acyl coenzyme A dehydrogenase gene. *Mol Cell Biol*. 1997;17(9):5400–5409.
22. Barry JB, Laganière J, Giguère V. A single nucleotide in an estrogen-related receptor α site can dictate mode of binding and peroxisome proliferator-activated receptor γ coactivator 1α activation of target promoters. *Mol Endocrinol*. 2006;20(2):302–310.
23. Horard B, Vanacker JM. Estrogen receptor-related receptors: orphan receptors desperately seeking a ligand. *J Mol Endocrinol*. 2003;31(3):349–357.
24. Arnold P, Erb I, Pachkov M, Molina N, van Nimwegen E. MotEvo: integrated Bayesian probabilistic methods for inferring regulatory sites and motifs on multiple alignments of DNA sequences. *Bioinformatics*. 2012;28(4):487–494.
25. Chu S. Transcriptional regulation by post-transcriptional modification–role of phosphorylation in Sp1 transcriptional activity. *Gene*. 2012;508(1):1–8.
26. Castet A, Herledan A, Bonnet S, Jalaguier S, Vanacker JM, Cavaillès V. Receptor-interacting protein 140 differentially regulates estrogen receptor-related receptor transactivation depending on target genes. *Mol Endocrinol*. 2006;20(5):1035–1047.
27. Nichol D, Christian M, Steel JH, White R, Parker MG. RIP140 expression is stimulated by estrogen-related receptor α during adipogenesis. *J Biol Chem*. 2006;281(43):32140–32147.
28. Samson SL, Wong NC. Role of Sp1 in insulin regulation of gene expression. *J Mol Endocrinol*. 2002;29(3):265–279.
29. Malek A, Nunez LE, Magistri M, et al. Modulation of the activity of Sp transcription factors by mithramycin analogues as a new strategy for treatment of metastatic prostate cancer. *PLoS One*. 2012;7(4):e35130.
30. Stashi E, York B, O'Malley BW. Steroid receptor coactivators: servants and masters for control of systems metabolism. *Trends Endocrinol Metab*. 2014;25(7):337–347.

31. Mouchiroud L, Eichner LJ, Shaw RJ, Auwerx J. Transcriptional coregulators: fine-tuning metabolism. *Cell Metab*. 2014;20(1):26–40.
32. Dasgupta S, Lonard DM, O'Malley BW. Nuclear receptor coactivators: master regulators of human health and disease. *Annu Rev Med*. 2014;65:279–292.
33. Handschin C, Spiegelman BM. Peroxisome proliferator-activated receptor γ coactivator 1 coactivators, energy homeostasis, and metabolism. *Endocr Rev*. 2006;27(7):728–735.
34. Spiegelman BM, Heinrich R. Biological control through regulated transcriptional coactivators. *Cell*. 2004;119(2):157–167.
35. Lonard DM, O'malley BW. Nuclear receptor coregulators: judges, juries, and executioners of cellular regulation. *Mol Cell*. 2007; 27(5):691–700.
36. Charos AE, Reed BD, Raha D, Szekely AM, Weissman SM, Snyder M. A highly integrated and complex PPARGC1A transcription factor binding network in HepG2 cells. *Genome Res*. 2012;22(9): 1668–1679.
37. Xie W, Hong H, Yang NN, et al. Constitutive activation of transcription and binding of coactivator by estrogen-related receptors 1 and 2. *Mol Endocrinol*. 1999;13(12):2151–2162.
38. Coghlan MJ, Jacobson PB, Lane B, et al. A novel antiinflammatory maintains glucocorticoid efficacy with reduced side effects. *Mol Endocrinol*. 2003;17(5):860–869.
39. Willy PJ, Murray IR, Qian J, et al. Regulation of PPARγ coactivator 1α (PGC-1α) signaling by an estrogen-related receptor α (ERRα) ligand. *Proc Natl Acad Sci USA*. 2004;101(24):8912–8917.
40. Blattler A, Farnham PJ. Cross-talk between site-specific transcription factors and DNA methylation states. *J Biol Chem*. 2013; 288(48):34287–34294.
41. Barrès R, Yan J, Egan B, et al. Acute exercise remodels promoter methylation in human skeletal muscle. *Cell Metab*. 2012;15(3): 405–411.
42. Charest-Marcotte A, Dufour CR, Wilson BJ, et al. The homeobox protein Prox1 is a negative modulator of ERRα/PGC-1α bioenergetic functions. *Genes Dev*. 2010;24(6):537–542.

Supplemental figures and tables

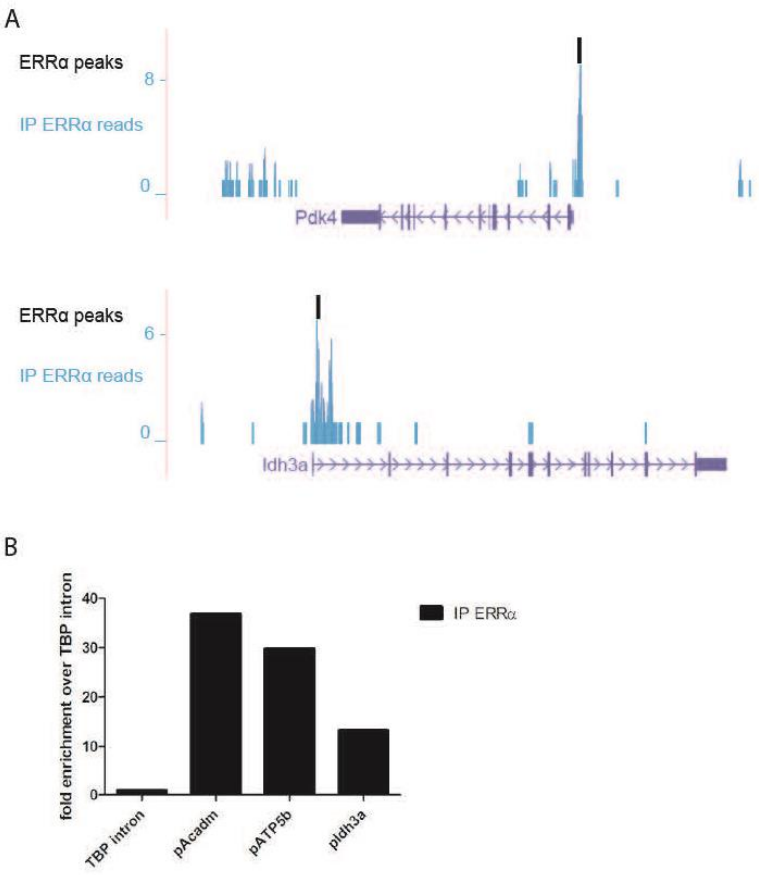

Suppl. Figure S1. (**A**) ERRα read densities around the TSS of the known target genes Pdk4 and Idh3a, as displayed by the UCSC Genome Browser. (**B**) Real-time semiquantiative PCR validation of the ChIP enrichment measured at the promoter of a set of ERRα target genes. Bars represent fold enrichment over that of the TBP intron.

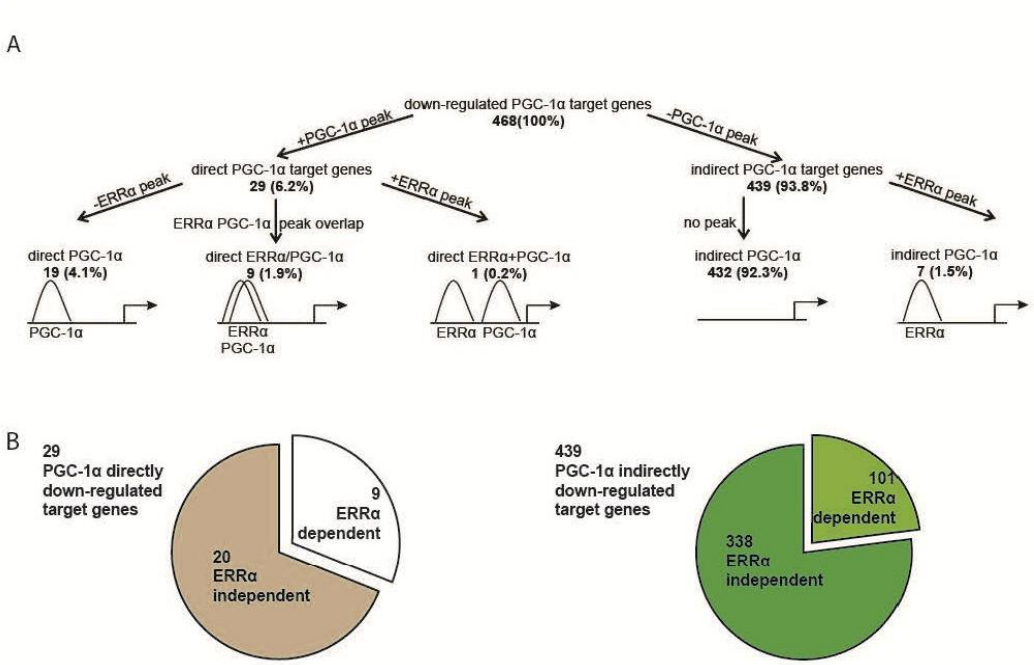

Suppl. Figure S2. (**A**) Tree diagram of all PGC-1α down-regulated target genes, distinguished in different subgroups according to peak presence/absence. (**B**) Piechart representing the classification of directly (grey/white) and indirectly (dark green/light green) down-regulated PGC-1α target genes, either ERRα-dependent or ERRα-independent targets.

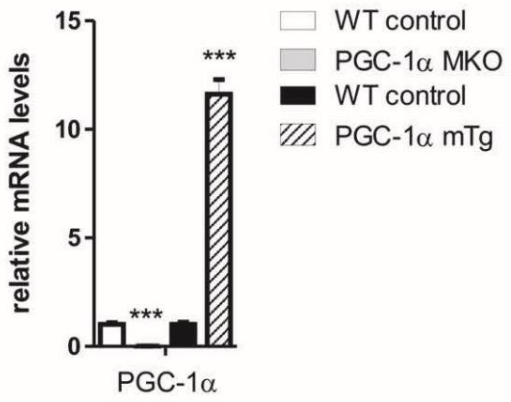

Suppl. Figure S3. Gene expression of PGC-1α in muscle-specific knockout mice (MKO), muscle-specific transgenic animals (mTg) and their respective wildtype control littermates.

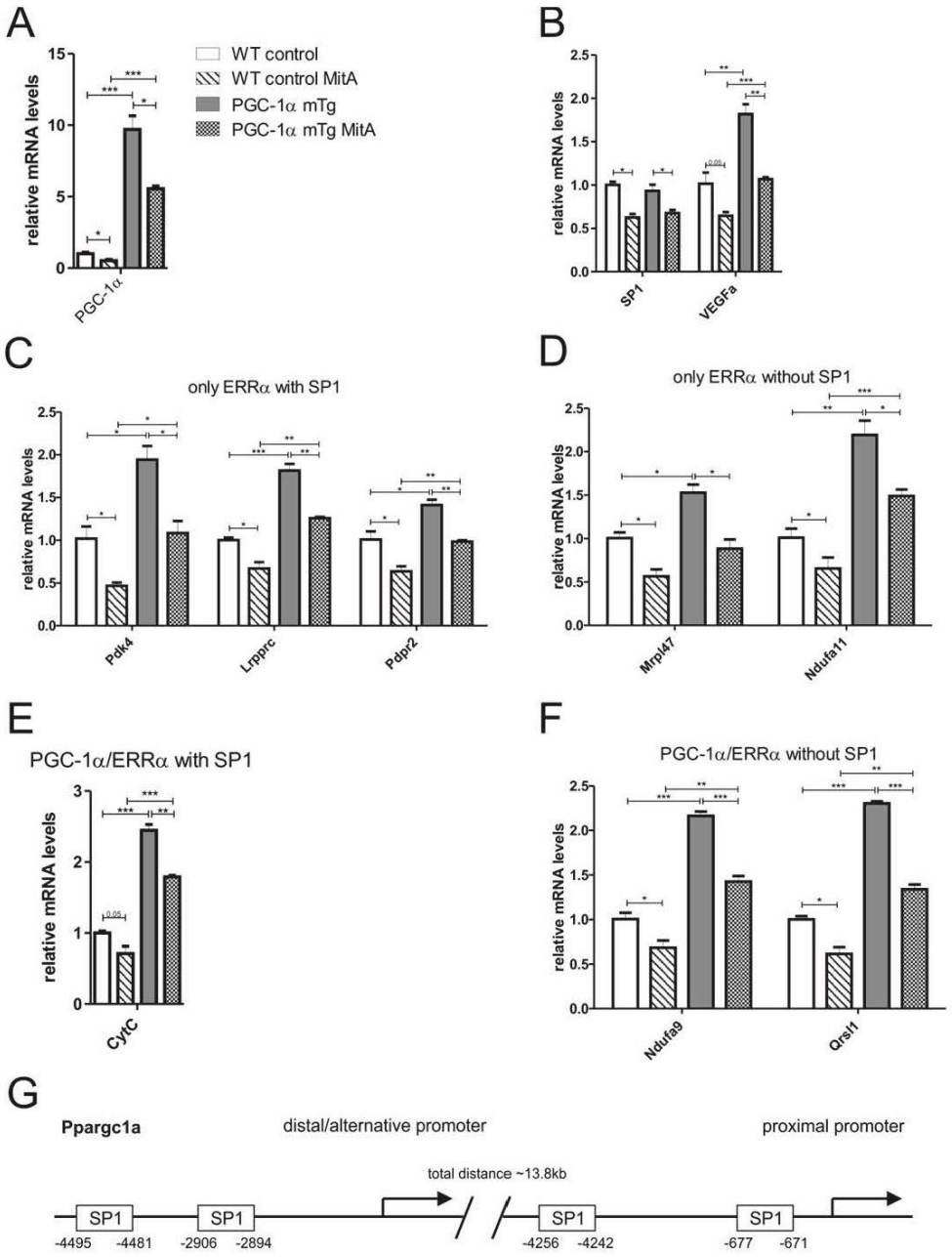

Suppl. Figure S4. Gene expression changes upon pharmacological inhibition of SP1 with Mithramycin A (MitA) in mouse muscles *in vivo*. **(A)** Expression of endogenous and transgenic PGC-1α in muscle-specific transgenic mice (mTg) and wildtype littermate controls with and without MitA, respectively. **(B)** Inhibition of known SP1 target genes by MitA (see Suppl. Refs. (1-3). **(C-F)** Regulation of PGC-1α-controlled gene expression by inhibition of SP1 with only ERRα peaks and SP1 binding sites **(C)**, only ERRα peaks without SP1 binding sites **(D)**, overlapping PGC-1α/ERRα peaks with SP1 binding sites **(E)** and overlapping PGC-1α/ERRα peaks without SP1 binding sites **(F)**, respectively. **(G)** Representation of predicted SP1 binding sites in the proximal and distal PGC-1α promoter regions. Predictions were made with MatInspector and PROMO (see Suppl. Refs. 4,5).

Suppl. Table 1. Real-time qPCR primer sequences

Real-time qPCR primers for ChIP validation		
Gene promoter or intron	*Forward primer*	*Reverse primer*
TBP intron	TGTGAGCTCCTTGGCTTTTT	ATAGTTGCCCAGCAATCAGG
promoter of Acadm	CCTTGCCCGAGCCTAAAC	GTCTGGCTGCGCCCTCT
promoter of ATP5b	CTGGAAACTTCCACCCTCACTA	GAGAGGTTTTTGGCGGAACTA
promoter of Idh3a	GGACGGCGTCAAGGTCAAG	GCCTAGGTGGCCTGTCTGTG
pNrip1	CACGCCATTCAGCTCTTCAG	GTGACAATGGGAGGGAGGG
pFasn	CTGGAGCACAAGGAACGC	GGACAGAGATGAGGGCGTC
Pdpr	CACACTCGTCGTCAACCAG	GTGCGCTTGTTTGGGTCTC
Lrpprc	ACAACACCCCTCCACTTTGA	CGGTGTCGCTCCTAGTTG
Acot13	TCACTCTTTAGCGCCCCAG	AAGACCGCCCTCTCTGGT
Mul1	ACTCCATATACCGGCAGAAGG	GAGCTGCCAGTGAGACCG
Real-time qPCR primers for testing the knockdown of ERRα		
Gene	*Forward primer*	*Reverse primer*
18S	AGTCCCTGCCCTTTGTACACA	CGATCCGAGGGCCTCACTA
PGC-1α	TGATGTGAATGACTTGGATACAGACA	GCTCATTGTTGTACTGGTTGGATATG
ERRα	ACTGCAGAGTGTGTGGATGG	GCCCCCTCTTCATCTAGGAC
Acadm	AACACTTACTATGCCTCGATTGCA	CCATAGCCTCCGAAAATCTGAA
Aim1l	CCTGTTGCGTCCATAAGGGT	GCTCTGAGTTCCACATCCCC
Twf2	TGCTACCTCCTCTTCCGACT	ATAGCATCTTCAGCCGCACC
Atg9b	TGGCATCACATCCAGAACCT	CATTGTAATCCACGCAGCGA
Ifrd1	GACAAGAGAAAGCAGCGGTC	GGTACTGCATCCCTGATCCA
Real-time qPCR primers used to analyze gene expression in mouse muscle *in vivo*		
Gene	*Forward primer*	*Reverse primer*
Acadm	AACACTTACTATGCCTCGATTGCA	CCATAGCCTCCGAAAATCTGAA
Acot13	TCACTCTTTAGCGCCCCAG	AAGACCGCCCTCTCTGGT
Cycs	GCAAGCATAAGACTGGACCAAA	TTGTTGGCATCTGTGTAAGAGAATC
CytC	TGCCCAGTGCCACACTGT	CTGTCTTCCGCCCGAACA
Esrra	ACTGCAGAGTGTGTGGATGG	GCCCCCTCTTCATCTAGGAC
Lrpprc	ACAACACCCCTCCACTTTGA	CGGTGTCGCTCCTAGTTG
Mrpl45	CCAGAGGGTGATGCTCGAAT	TTCGGATTGCCAGCTGTGAT
Mrpl47	CTCGGGGTAAGTGGTGAGAG	CTCAGGACTCCTCGGAAACC
Ndufa9	TTCTGTGGCTCATCCCATCG	TGTAGCCCCAAACACAGTGG
Ndufa11	TGGTGATGTAGGTCTTGCGA	GCGTCCAAGGCGTTCAATAA
Pdk4	AAAATTTCCAGGCCAACCAA	CGAAGAGCATGTGGTGAAGGT
Pdpr2	ATGAACTCTGCTGGCCTGTC	AAGCGCTGCAAATCCAACTC
PGC-1α ex2	TGATGTGAATGACTTGGATACAGACA	GCTCATTGTTGTACTGGTTGGATATG
PGC-1 ex3-5	AGCCGTGACCACTGACAACGAG	GCTGCATGGTTCTGAGTGCTAAG
PolR2a	AATCCG CATCATGAACAGTG	CAGCATGTTGGACTCAATGC
Qrsl1	GTTGGATCAGGGTGCCCTAC	GGGGTTTCTAACTGGCCCAA
SP1	GACCTCATCTCCGAGCAC	GAAGCTCGTCCGAACGTGTA
Tfam	GAGCGTGCTAAAAGCACTGG	GCTACCCATGCTGGAAAAACA
Tfrc	AGCTTTGTCCTTTTCAGCTGT	TGTGGGGAGCCGCTGTAC
VEGFα	CACGACAGAAGGAGAGCAGA	GGGCTTCATCGTTACAGCAG

Supplemental references

1. Xie L, Collins JF. Transcription factors Sp1 and Hif2alpha mediate induction of the copper-transporting ATPase (Atp7a) gene in intestinal epithelial cells during hypoxia. *J Biol Chem*. 2013;288(33):23943-23952.
2. Malek A, Nunez LE, Magistri M, Brambilla L, Jovic S, Carbone GM, Moris F, Catapano CV. Modulation of the activity of Sp transcription factors by mithramycin analogues as a new strategy for treatment of metastatic prostate cancer. *PLoS One*. 2012;7(4):e35130.
3. Rosol TJ, Capen CC. The effect of low calcium diet, mithramycin, and dichlorodimethylene bisphosphonate on humoral hypercalcemia of malignancy in nude mice transplanted with the canine adenocarcinoma tumor line (CAC-8). *J Bone Miner Res*. 1987;2(5):395-405.
4. Quandt K, Frech K, Karas H, Wingender E, Werner T. MatInd and MatInspector: new fast and versatile tools for detection of consensus matches in nucleotide sequence data. *Nucleic Acids Res*. 1995;23(23):4878-4884.
5. Messeguer X, Escudero R, Farre D, Nunez O, Martinez J, Alba MM. PROMO: detection of known transcription regulatory elements using species-tailored searches. *Bioinformatics*. 2002;18(2):333-334.

4. Skeletal muscle-specific transcriptional network analysis revealed PGC-1β as important indirect regulator of the metabolic gene program

Barbara Heim[1], Anne Krämer[1, 2], Erik van Nimwegen[1, 2] and Christoph Handschin[1*]

[1]Biozentrum, [2]Computational and Systems Biology, University of Basel, Klingelbergstrasse 50/70, 4056 Basel, Switzerland

[*]Corresponding author: christoph.handschin@unibas.ch / Biozentrum, University of Basel, Klingelbergstrasse 50/70, CH-4056 Basel / Phone: +41 61 207 23 78

Abstract

Skeletal muscle is a large and energy demanding organ with enormous plasticity dependent on stimuli. The underlying mechanism of this extraordinary cellular plasticity is still poorly understood. A regulatory nexus of many metabolic adaptions is the peroxisome proliferator-activated receptor γ coactivator-1 (PGC-1) family. In this study, we elucidated the regulatory role of PGC-1β in skeletal muscle cells overexpressing PGC-1β. Chromatin immunoprecipitation (ChIP) followed by sequencing (ChIPseq) combined with computational approaches was used to understand the transcriptional network regulated by PGC-1β in skeletal muscle cells. We found a small fraction of transcription factor binding sites (TFBS) directly occupied by PGC-1β, whereas the largest fraction of PGC-1β target genes seemed to be indirectly controlled by PGC-1β. The directly controlled PGC-1β target genes were regulated by a complex including nuclear receptors (NR) with Estrogen related receptor α (ERRα) as top partner managing mitochondrial biogenesis. Also Ets-like transcription factors (TFs) involved in developmental and cell homeostasis pathways as well as Hox-like TFs that played a role in biosynthetic processes and endocytosis. Our findings revealed skeletal muscle PGC-1β as an important metabolic regulator but contrary to PGC-1α, most of the actions were done indirectly.

Abbreviations

AMPK, AMP-dependent protein kinase; ARC, activator-recruited co-factor ; Crunch, Completely Automated Analysis of ChIP-seq Data; DE, differentially expressed; DM, differentiation medium; ERRα, estrogen-related receptor α; FC, fold change; FDR, false discovery rate; GM, growth medium; GO, gene ontology; HS, horse serum; ISMARA, integrated motif activity response analysis; MAPK, mitogen-activated protein kinase; MyHC, myosin heavy chain; NFκB , nuclear factor kappa B; NR, nuclear receptor; PCA, principal component analysis; PGC-1, peroxisome proliferator-activated receptor γ coactivator-1; PTM, posttranslational modification; qRT-PCR, quantitative real-time polymerase chain reaction; SEM, standard errors of the means, Sirt1, sirtuin 1; TRAP, thyroid hormone receptor-associated protein

Introduction

The balance between energy intake and energy expenditure needs to be tightly regulated. Skeletal muscle has one of the highest rates of energy expenditure amongst tissues, as well as insulin-stimulated glucose uptake and glycogen storage. Thus, skeletal muscle has a significant impact on whole body metabolism and displays a high degree of plasticity in response to stimuli as e.g. exercise (Egan and Zierath, 2013). Hence, physical inactivity has been linked to metabolic disorders like type 2 diabetes, obesity, cardiovascular diseases, cancer and others which could be prevented by physical activity (Booth et al., 2012; Colberg et al., 2010b; Egan and Zierath, 2013; Haskell et al., 2007). The beneficial effect of exercise is due to enormous adaptation capability of the muscle tissue. Since muscle is a heterogeneous organ composed of different muscle fiber types, type 1 slow-twitch oxidative and type 2 fast-twitch glycolytic fibers, the organ is very plastic and able to adapt to many different conditions (Schiaffino and Reggiani, 2011). Endurance exercise is known to improve mitochondrial capacity, insulin sensitivity and cardiovascular functions leading to improved endurance performance and metabolic health (Egan and Zierath, 2013; Haskell et al., 2007). Many different signaling pathways are involved in the very complex regulation of skeletal muscle plasticity. Exercise leads to the activation of energy sensors in the cell, such as the AMP-dependent protein kinase (AMPK) and sirtuin 1 (Sirt1) (Canto and Auwerx, 2009; Canto et al., 2009; Jager et al., 2007). Following exercise, intracellular calcium and hence p38 mitogen-activated kinase (p38 MAPK) increases, which leads to phosphorylation of its target (Puigserver et al., 2001). All these exercise-mediated signaling pathways converge on the peroxisome proliferator-activated receptor γ coactivator-1 (PGC-1) family, which induces its gene expression, modify the posttranslational modifications (PTMs) and hence, change the activity or repression function, or the stability of the protein (Canto and Auwerx, 2009; Canto et al., 2009; Handschin, 2010; Jager et al., 2007; Olson et al., 2008; Puigserver et al., 2001). Most of those controlling actions in skeletal muscle are described for PGC-1α, less is known about PGC-1β and its regulatory role in skeletal muscle plasticity (Kressler et al., 2002a; Lin et al., 2002a). PGC-1β has been implicated to play a role in skeletal muscle mitochondrial homeostasis, angiogenesis and fiber type determination (Arany et al., 2007; Gali Ramamoorthy et al., 2015; Rowe et al., 2011; Zechner et al., 2010b). Opposite to PGC-1α, PGC-1β is not induced after exercise but contributes to skeletal muscle as well as whole body adaptations subsequent to metabolic stress. Skeletal muscle-specific overexpression of PGC-1β lead to increased myosin heavy chain (MyHC) type 2X fibers and improved exercise performance due to improved oxidative capacity and angiogenesis (Arany, 2008; Arany et al., 2008; Arany et al., 2007; Lee et al., 2017; Lin et al., 2002a). In addition, PGC-1β is able to protect skeletal muscle from atrophy by reducing the transcript levels of nuclear factor kappa B (NFκB) and forkhead box O (FOXO) 3 and hence, reducing proteolysis (Brault et al., 2010; Sandri et al., 2006; Sandri et al., 2004).

Contrarily, muscle-specific knockout of PGC-1β results in a fiber type shift towards glycolytic fibers and reduced oxygen capacity affecting exercise performance (Gali Ramamoorthy et al., 2015; Rowe et al., 2011; Zechner et al., 2010b). Given the fact that PGC-1β is an important regulator of skeletal muscle and whole body metabolism, we aimed to elucidate how the transcriptional network of PGC-1β is regulated and which TFs are used in skeletal muscle. Same as PGC-1α, PGC-1β is part of a multiprotein complex needed to translate the external stimuli into promoter and enhancer activities by modulating histones and the chromatin structure with the thyroid hormone receptor-associated protein (TRAP), part of the mediator complex, contain proteins that bind TFs, recruit RNA polymerase II and initiate transcription (Lin et al., 2005; Liu and Lin, 2011; Wallberg et al., 2003a). Which other factors are involved to recruit PGC-1β has not been studied yet. The dynamic assembly as well as the multiplicity of coregulators and TFs used, results in an enormous variety and complexity of different outputs (Spiegelman and Heinrich, 2004). Thus, the very complex but tightly and specific control by the PGC-1 family of coactivators might explain the plastic character of skeletal muscle upon exercise. As PGC-1α, PGC-1β might not only play a role in skeletal muscle adaptations following exercise because it is not induced but in whole body metabolism (Egan and Zierath, 2013; Gali Ramamoorthy et al., 2015; Lee et al., 2017; Lin et al., 2005). Therefore, it would be of great interest to understand the molecular mechanism involved and possibly identify new therapeutic targets in this pathway.

This study aimed to reveal a global picture of the transcriptional network regulated by the coactivator PGC-1β in skeletal muscle cells. We combined genome-wide binding data from ChIPseq experiments with computational predictions of TFBSs and RNAseq gene expression profiles in response to PGC-1β overexpression in muscle cells to uncover the TFBPs needed to regulate a specific biological function. Our results show that PGC-1β is an important metabolic regulator but that most of its target genes are regulated in an indirect manner. To directly regulate PGC-1β target genes, nuclear receptors, mainly ERRα regulating mitochondrial biogenesis, as well as Ets-like and Hox-like TFs are used to regulate in addition genes involved in development, biosynthetic processes and endocytosis.

Results

Genome-wide PGC-1β recruitment to the mouse genome in skeletal muscle cells

Not much is known about PGC-1β dependent gene transcription. We performed chromatin immunoprecipitation followed by deep sequencing (ChIPseq) of C2C12 myotubes infected with adenoviral GFP control or flag tagged PGC-1β. ChIPseq allows to identify genomic regions were PGC-1β is recruited to coactivate TFs, which directly bind to DNA. The genomic sites where PGC-1β is binding to were identified by the Crunch software (Berger et al., 2016). Brief, the read density of the ChIP was compared across the

genome by a 500bp sliding window for the immunoprecipitation (IP) compared to a 2000bp sliding window for the background, whole cell extract. Only regions with a z-score higher than 4.15 and a false discovery rate (FDR) of 0.1 were considered as significant. Each condition was performed and analyzed in triplicates. By this cutoff we identified 673 peaks. Using the IGV genome browser we included top peak regions (Figure 1A) as well as binding regions within the promoter of known PGC-1 target genes such as Aco2 and Idh3a regulating energy metabolism (Suppl. Figure 1A) (Baresic et al., 2014; Huss et al., 2004; Tiraby et al., 2011). The enrichment of the IP fractions was validated by qRT-PCR in the PGC-1β compared to GFP infected myotubes. The enrichment of known target genes was only observed in the PGC-1β ChIP and not in the GFP control data (Figure 1B). Even more, the top peak regions found in the ChIPseq analysis could be validated by qRT-PCR as enriched fraction in the PGC-1β but not the GFP ChIP (Figure 1C).

Analyzing the distribution of peaks from the closest promoter, we found 62% of all peaks within a region of 50kb from the promoter site (Figure 1D). Next, we associated 225 genes to the 673 peak, taking the shortest distance of peak to promoter into account (Figure 1E).

Taken together, this data show a genome-wide recruitment of PGC-1β in skeletal muscle cells, sharing same regions with PGC-1α.

Small but strong overlap of ChIPseq and RNAseq showing specific functionality in PGC-1β stimulated muscle cells

Additionally to the ChIPseq, we performed RNAseq from the same experimental setup using C2C12 myotubes infected either with adenoviral GFP control or with PGC-1β to characterize further the functionality of the identified ChIPseq peaks. As already described, we found 225 genes being associated with the 673 peaks (Figure 1E). Differential expression (DE) was set by a cutoff of log2 fold change (FC) </> 0.6 and a FDR < 0.01 for the RNAseq. This cutoff narrowed the number to 70 significantly and directly regulated target genes by PGC-1β (Figure 1E). Those 70 genes were subdivided into 54 upregulated and 16 downregulated targets (Figure 1F). The RNAseq analysis revealed a total of 5729 DE genes, 3265 up- and 2464 downregulated (Figure 1G). Considering this number, it seemed that PGC-1β acts mostly indirect on its target regulation, indicated by only 70 genes with a binding site for PGC-1β in contrast to 5659 indirectly regulated ones. Generally and as already shown for PGC-1α, also PGC-1β acts more as a coactivator than a corepressor, since most genes are upregulated (Figure 1F + G). This observation goes in hand with previous reports and work from our group regarding the PGC-1α genome-wide recruitment in C2C12 myotubes, where higher number of PGC-1α target genes were indirectly regulated and most of the direct regulated targets were upregulated (Baresic et al., 2014).

Taken together, this data indicate that PGC-1β mainly upregulates its target genes and this in an indirect way. Due to our cutoffs for the ChIPseq and the RNAseq data, a large fraction of target genes was associated to peaks, around 69%, but not set as significant. This large number of targets might come due to our cutoffs, wrongly assigned peaks or no functionality of those genes in our cell culture system at the moment of the experiment.

Directly regulated PGC-1β targets are important for energy metabolism

We assessed the biological functions of the 70 direct PGC-1β targets (Figure 2F). Gene ontology (GO) and Kegg pathway analysis revealed strong association with the energy metabolism as well with cytoskeletal organization for PGC-1β target genes (Figure 2A). The majority of GO terms associated with energy homeostasis were supported by the Kegg analysis, where diseases associated with a proper mitochondrial homeostasis appeared (Figure 2B). The GO and Kegg terms dealing with energy homeostasis were mainly regulated by upregulated PGC-1β target genes whereas the 16 downregulated ones were widely distributed and no Kegg terms could be identified (Figure 2E).

In summary, these results indicate that only a small fraction of PGC-1β target genes are regulated directly but those ones are very tightly and strongly regulated by PGC-1β and its TFs to precisely play a role in energy metabolism.

TFBS and their activity in PGC-1β muscle cells

We wanted to clarify, which TFs are used by PGC-1β to bind DNA and regulate its target genes. We used ISMARA (Balwierz et al., 2014) to identify TFBS occurrence under the PGC-1β peaks and predict the activity of a specific TFBS according to its occupancy in the IP compared to the background. We got a list of 568 TFBS motifs for the PGC-1β ChIP, 40% (235 motifs) had a predicted active function (Figure 3A). Only 5%, which were 27 motifs, had a z-score > 2 and were set as significant (Figure 3B). As we could already observe in our previous work for PGC-1α in muscle cells and as it is highly reported in other studies, the most famous PGC-1 partner is ERRα. The top motif we found for PGC-1β was “Esrra_Esrrb” with a z-score of 7.5 (Figure 3B). In agreement to its well-studied family member PGC-1α, the most motifs associated with PGC-1β were nuclear receptors, here 8 motifs out of the top 27 (Figure 3B, blue). Having a closer look on the motifs, 60% were positively regulated motifs and only 1/3 was repressed comparing PGC-1β to GFP ChIP (Figure 3C-E). This data indicate that PGC-1β plays a role as coactivator and corepressor but the strongest interaction partners like the ERRs are more involved in coactivation than corepression.

To further characterize the TFs interacting with PGC-1β, we compared the predicted target genes from each motif with the genes directly coactivated by PGC-1β. “Maz_Mta3” motif contained most of the direct

PGC-1β targets (Figure 4A). Maz TF is a high G-containing motif (Figure 4B) and was shown to play an important role in skeletal muscle gene transcription and is itself increased in transcription and DNA-binding activity during skeletal myocyte differentiation (Himeda et al., 2008). Interestingly, the first half of the top motifs, the majority of them were nuclear receptors (Figure 3B), accumulated most of the directly regulated PGC-1β targets, indicating the strength of those motifs in the interaction with PGC-1β to regulate directly the targets (Figure 4A).

Taken together, the ChIPseq analysis of PGC-1β in skeletal muscle cells supports the assumption that the PGC family of coregulators are strongly involved in the regulation of cell energy homeostasis.

The Nuclear receptors and "Ets-like" TFs are the main partners of PGC-1β in skeletal muscle cells

We used principal component analysis (PCA) to further describe our motif findings in the PGC-1β ChIP. The fraction of variance in the principal components showed the first two components with the highest variance in our data set with 15.5% for PC1 and 13.2% for PC2, respectively (Figure 5A). Comparing PC1 and PC2 we got three sets of motifs (Figure 5B). The most striking one, having positive projections on PC1 and on PC2, and a very good control for the experiment were the "Esrr-like motifs" containing nuclear receptors, which were also found to be top in the ISMARA analysis and were mostly associated with energy homeostasis GO terms (Figure 5B, blue). Furthermore, it is known from previous PGC-1α studies that ERRα as well as other nuclear receptors are known binding partners (Baresic et al., 2014; Huss et al., 2004; Salatino et al., 2016b; Schreiber et al., 2004). The second interesting set of motifs with positive PC1 but negative PC2 projections were the "Hox-like motifs" (Figure 5B, green). The third motif cluster we found in the PCA with negative projections for both components were the "Ets-like motifs" (Figure 5B, red). Remarkably, Ems (also known as Etv5), was shown to be involved in the subsynaptic gene expression at the neuromuscular junction (NMJ) (Hippenmeyer et al., 2007) and was one of the factors in our PCA "Ets-like-motifs" cluster.

Surrounding the "Hox-like motifs" were the motifs for "Maf" and "Rest", which had a complete different weight matrix than the Hox-TFs (Figure 5C-E), therefore we did not add them into the "Hox-like motif" cluster. Additionally, we put the PC3 with a variance of 9.9% into account. Comparing PC1 and PC3 (Figure 5F) as well as PC2 with PC3 (Figure 5G). we observed now a clear separation of the "Maf" and "Rest" motif (Figure 5F + G, orange) from the "Hox-like-motifs" (Figure 5F + G, green), going in line with the different motif logos they have (Figure 5C-E). It seemed that PC3 focused on those two motifs, Maf and Rest, which have the sequence "TGCTGA" in common (Figure 5D + E).

To characterize further those TF binding partners of PGC-1β in skeletal muscle cells we assigned the TF identified by ISMARA to the peaks and the nearest TF motif as well to the associated genes. We found that

PGC-1β coactivates mostly the nuclear receptors or the “Ets-like” TFs to regulated its target genes (Figure 5H). Performing GO and Kegg analysis with the TFs associated genes we further strengthen the relationship of the PGC-1 coactivators with the nuclear receptors in the regulation of energy metabolism (Suppl. Figure 5A–G).

This data indicate that next to the known nuclear receptors with the ERRs also the Ets TFs are functional partners of PGC-1β in skeletal muscle cells.

Figure 1

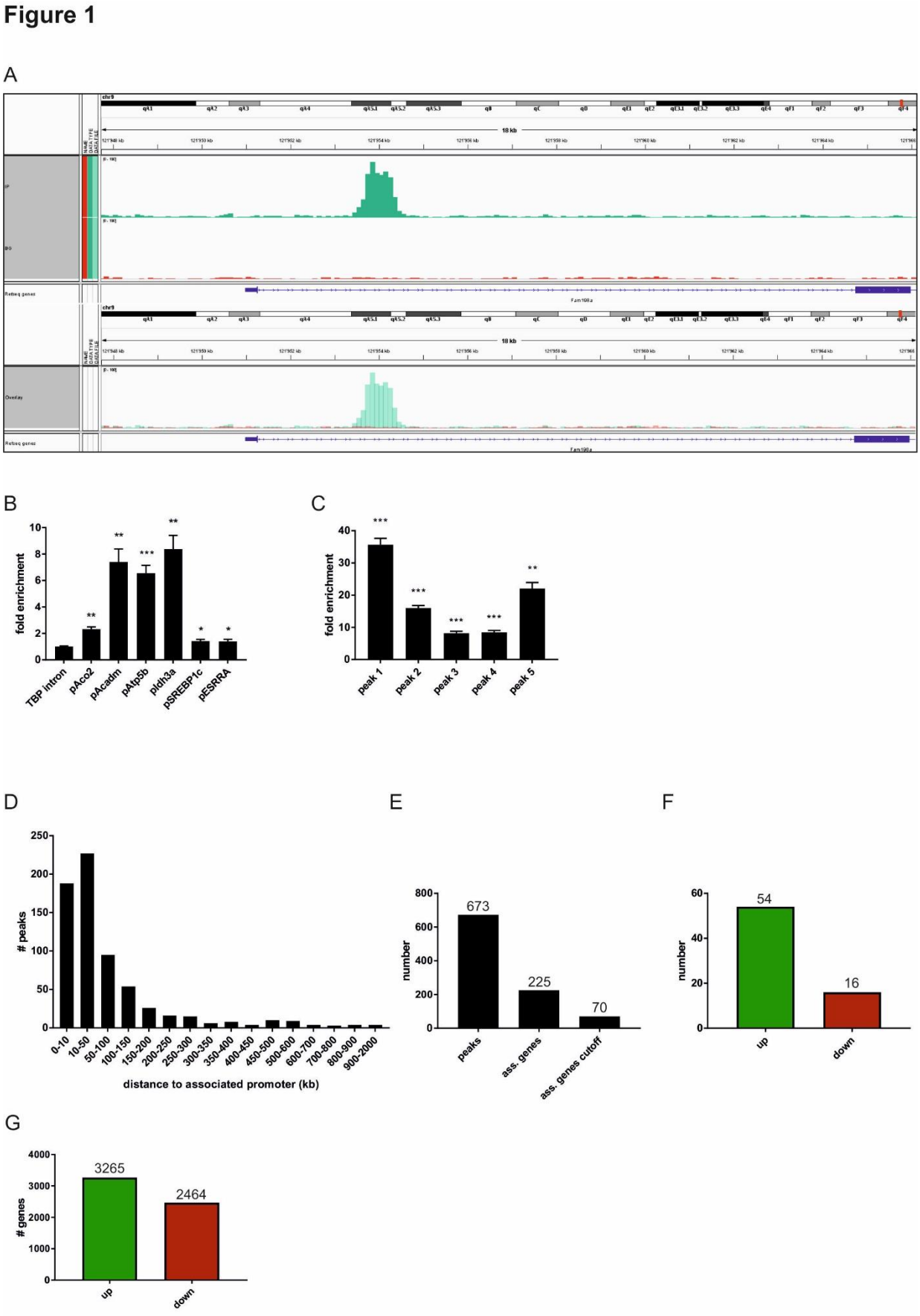
A
chr9
18 kb
Refseq genes
Fam198a
Overlay
B
fold enrichment
TBP intron
pAco2
pAcadm
pAtp5b
pIdh3a
pSREBP1c
pESRRA
C
fold enrichment
peak 1
peak 2
peak 3
peak 4
peak 5
D
peaks
distance to associated promoter (kb)
0-10
10-50
50-100
100-150
150-200
200-250
250-300
300-350
350-400
400-450
450-500
500-600
600-700
700-800
800-900
900-2000
E
number
673
225
70
peaks
ass. genes
ass. genes cutoff
F
number
54
16
up
down
G
genes
3265
2464
up
down

Figure 1. Genome-wide PGC-1β recruitment with small peak fraction but strong transcript impact

A) Top PGC-1β ChIPseq binding peaks obtained from the IGV Genome Browser.

B) ChIP enrichment validation measured by qRT-PCR at the promoter of a set of PGC-1β target genes. Bars represent mean fold enrichment of PGC-1β compared to GFP ChIPs, both performed in triplicates, and normalized to TBP intron. Error bars represent SEM: *p < 0.05; ** p < 0.01; *** p < 0.001.

C) Chip peak validation by qRT-PCR. Bars represent mean fold enrichment of PGC-1β compared to GFP ChIPs, both performed in triplicates. Error bars represent SEM: *p < 0.05; ** p < 0.01; *** p < 0.001.

D) Bar graph representing the total peak number in the PGC-1β ChIP with a z-score > 4.15 and a FDR of 0.1 and the distance to the associated promoter in kilo base pairs (kb).

E) Bar graph shown the identified number of peaks, nearest associated genes (ass. genes) and the number of genes with a cutoff of FDR < 0.01, log2 FC 0.6 in the RNAseq (ass. genes cutoff).

F) Bar graph of the significant associated genes subdivided in up- and downregulated according to RNAseq.

G) Bar graph of the differentially expressed (DE) genes in the RNAseq data.

Figure 2

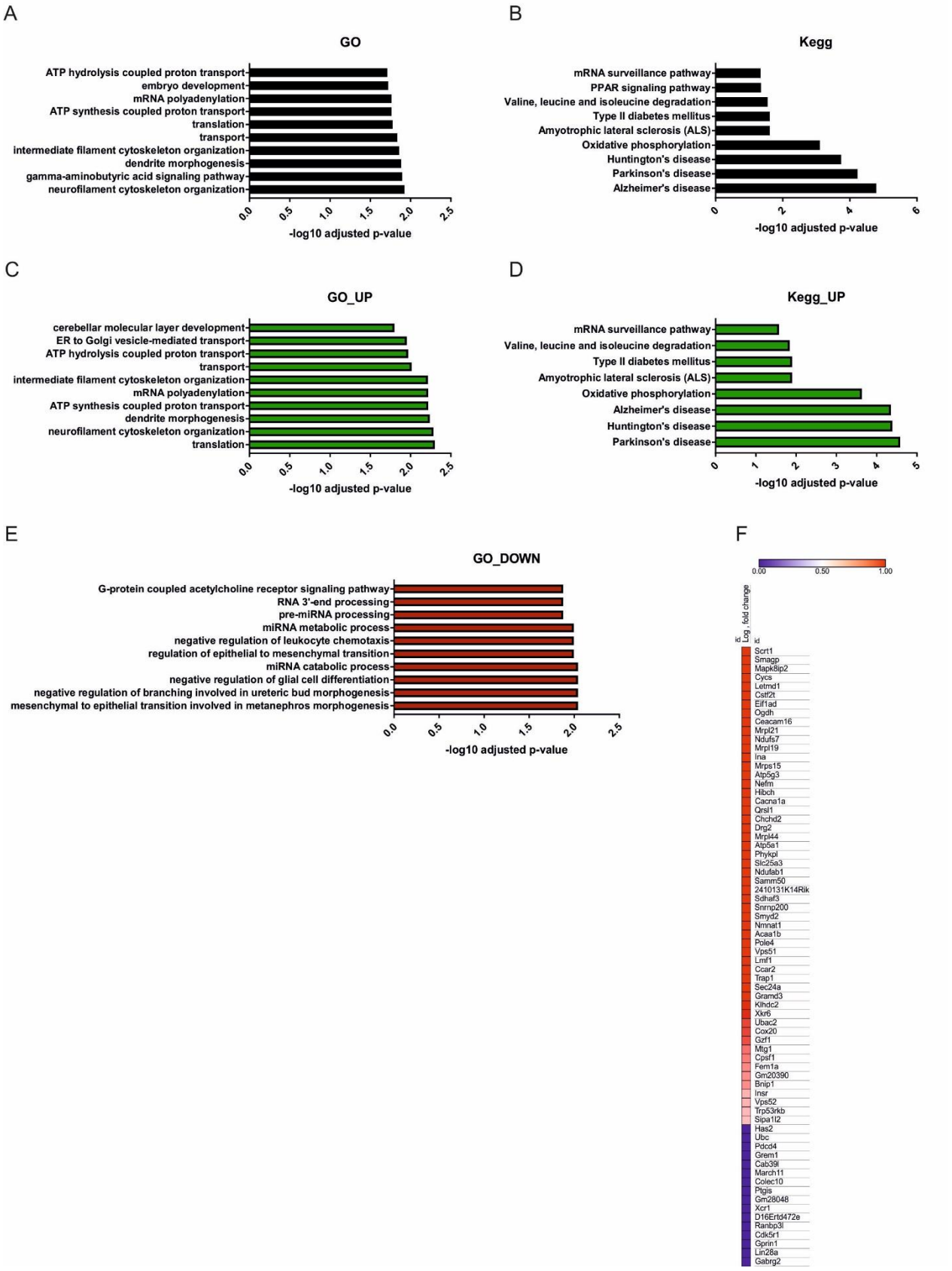
A
GO
ATP hydrolysis coupled proton transport
embryo development
mRNA polyadenylation
ATP synthesis coupled proton transport
translation
transport
intermediate filament cytoskeleton organization
dendrite morphogenesis
gamma-aminobutyric acid signaling pathway
neurofilament cytoskeleton organization
0.0 0.5 1.0 1.5 2.0 2.5
-log10 adjusted p-value
B
Kegg
mRNA surveillance pathway
PPAR signaling pathway
Valine, leucine and isoleucine degradation
Type II diabetes mellitus
Amyotrophic lateral sclerosis (ALS)
Oxidative phosphorylation
Huntington's disease
Parkinson's disease
Alzheimer's disease
0 2 4 6
-log10 adjusted p-value
C
GO_UP
cerebellar molecular layer development
ER to Golgi vesicle-mediated transport
ATP hydrolysis coupled proton transport
transport
intermediate filament cytoskeleton organization
mRNA polyadenylation
ATP synthesis coupled proton transport
dendrite morphogenesis
neurofilament cytoskeleton organization
translation
0.0 0.5 1.0 1.5 2.0 2.5
-log10 adjusted p-value
D
Kegg_UP
mRNA surveillance pathway
Valine, leucine and isoleucine degradation
Type II diabetes mellitus
Amyotrophic lateral sclerosis (ALS)
Oxidative phosphorylation
Alzheimer's disease
Huntington's disease
Parkinson's disease
0 1 2 3 4 5
-log10 adjusted p-value
E
GO_DOWN
G-protein coupled acetylcholine receptor signaling pathway
RNA 3'-end processing
pre-miRNA processing
miRNA metabolic process
negative regulation of leukocyte chemotaxis
regulation of epithelial to mesenchymal transition
miRNA catabolic process
negative regulation of glial cell differentiation
negative regulation of branching involved in ureteric bud morphogenesis
mesenchymal to epithelial transition involved in metanephros morphogenesis
0.0 0.5 1.0 1.5 2.0 2.5
-log10 adjusted p-value
F
0.00 0.50 1.00
Log2 fold change
Id
Scrt1
Smagp
Mapk8ip2
Cycs
Letmd1
Cstf2t
Eif1ad
Ogdh
Ceacam16
Mrpl21
Ndufs7
Mrpl19
Ina
Mrps15
Atp5g3
Nefm
Hibch
Cacna1a
Qrsl1
Chchd2
Drg2
Mrpl44
Atp5a1
Phykpl
Slc25a3
Ndufab1
Samm50
2410131K14Rik
Sdhaf3
Snrnp200
Smyd2
Nmnat1
Acaa1b
Pole4
Vps51
Lmf1
Ccar2
Trap1
Sec24a
Gramd3
Klhdc2
Xkr6
Ubac2
Cox20
Gzf1
Mtg1
Cpsf1
Fem1a
Gm20390
Bnip1
Insr
Vps52
Trp53rkb
Sipa1l2
Has2
Ubc
Pdcd4
Grem1
Cab39l
March11
Colec10
Ptgis
Gm28048
Xcr1
D16Ertd472e
Ranbp3l
Cdk5r1
Gprin1
Lin28a
Gabrg2

Figure 2. PGC-1β directly regulate energy metabolism

A) Top 10 Geneonthology (GO) terms of all directly regulated genes. X-axis represents -log10 of the adjusted p-value.

B) All Kegg pathway terms of all directly regulated genes. X-axis represents -log10 of the adjusted p-value.

C) Top 10 GO terms of the directly upregulated genes. X-axis represents -log10 of the adjusted p-value.

D) All Kegg pathway terms of the directly upregulated genes. X-axis represents -log10 of the adjusted p-value.

E) Top 10 GO terms of the directly downregulated genes. X-axis represents -log10 of the adjusted p-value.

F) Heatmap of the directly regulated PGC-1β genes with their log2 FC. Scale goes from downregulated (blue) to upregulated (red).

Figure 3

A

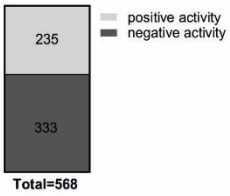

B

motif	z value
Esrrb_Esrra	7.586935
Esr2	6.577819
Snai1_Zeb1_Snai2	6.203734
Taf1	5.010193
Hoxb7	4.846334
Ybx1_Nfya_Nfyb_Nfyc_Cebpz	4.315675
Nr5a2	4.07482
Esr1	3.575141
Rarg	3.497699
Nr2f1_Nr4a1	3.447743
Tfdp1_Wt1_Egr2_Chd1_Pml	3.412146
Ebf1	3.408837
Tead3_Tead4	3.33354
Sox2	3.292406
Mef2d_Mef2a	3.265399
Irf2_Irf1_Irf8_Irf9_Irf7	2.94288
Mef2c	2.902636
Pparg_Rxrg	2.851445
AAGGCAC	2.64915
Hic2	2.552869
Maf_Nrl	2.486112
Nr1i2	2.445262
Hcfc1_Six5	2.345203
Maz_Mta3	2.322096
Hoxa6	2.283378
Rad21_Smc3	2.26283
Yy1	2.179365

C

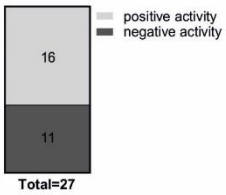

D

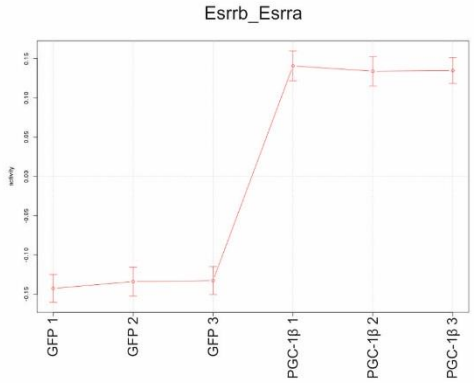

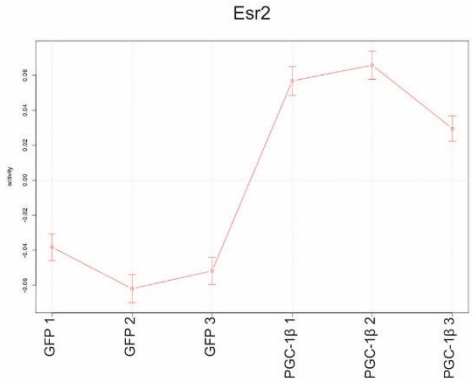

E

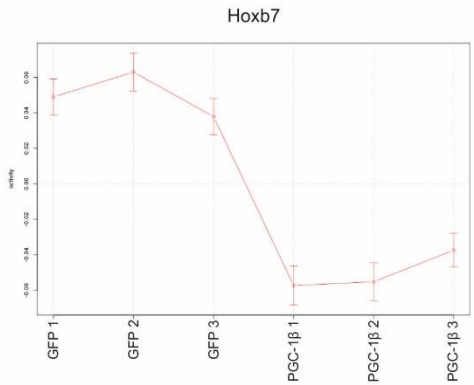

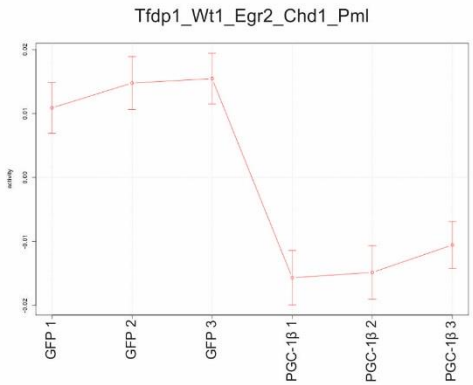

Figure 3. Transcription factor binding site activity in muscle cells

A) Total number of motifs received from ISMARA analysis classified into positive and negative activity profile.

B) Table with predicted 27 motifs having a z-score > 2. Blue: nuclear receptors motifs, green “Hox-like” motifs.

C) Histogram of the top 27 motifs split into positive and negative activity profiles.

D) Positive activity plot of the motifs Esrrb_Esrra (left) and Esr2 (right) as predicted by ISMARA comparing GFP to PGC-1β ChIP.

E) Negative activity plot of the motifs Hoxb7 (left) and Tfdp1_Wt1_Egr2_Chd1_Pml (right) as predicted by ISMARA comparing GFP to PGC-1β ChIP.

Figure 4

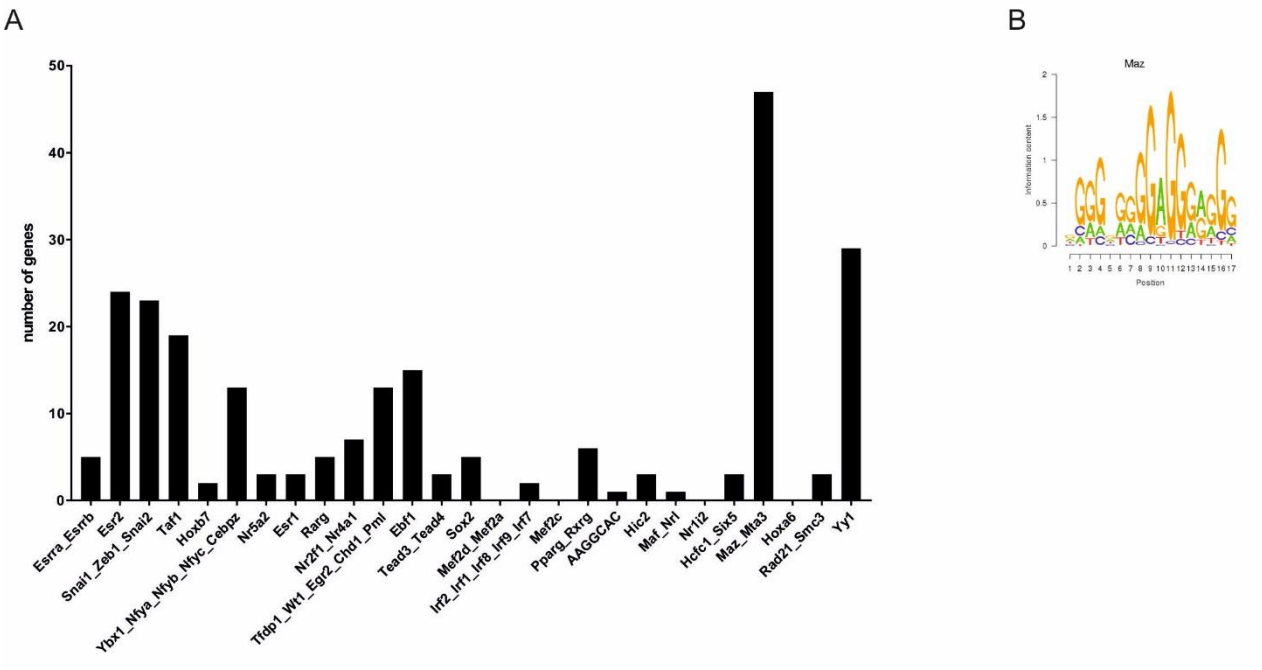

Figure 4. Motif and gene expression comparison regulated by PGC-1β

A) Bar graph showing the predicted target genes from each motif identified by ISMARA and associated with the direct genes identified in the ChIPseq.

B) Sequence logo of Maz motif.

Figure 5

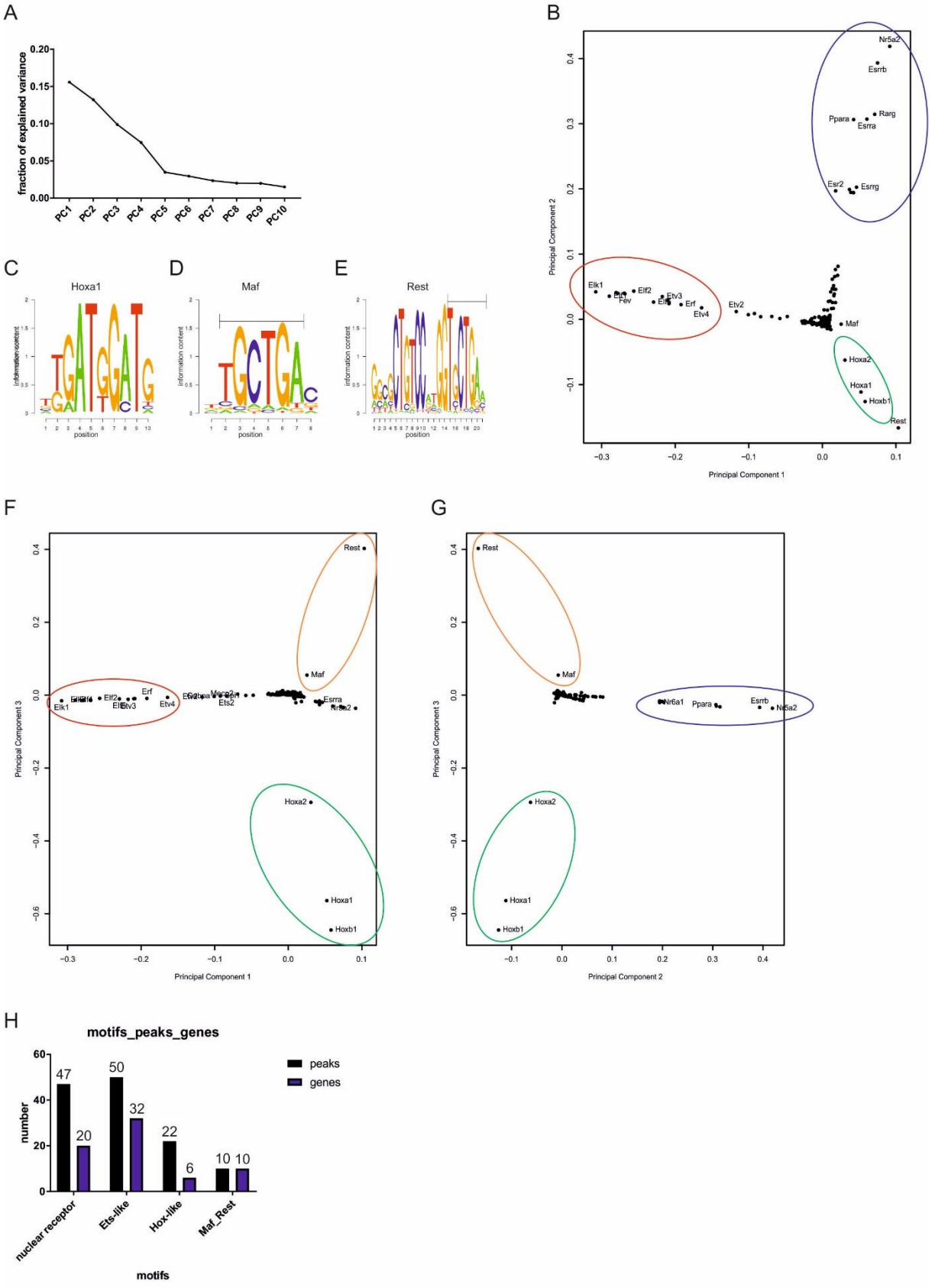
A
fraction of explained variance
PC1
PC2
PC3
PC4
PC5
PC6
PC7
PC8
PC9
PC10
B
Principal Component 1
Principal Component 2
Nr5a2
Esrrb
Ppara
Rarg
Esrra
Esr2
Esrrg
Elk1
Fev
Elf2
Etv3
Erf
Etv4
Etv2
Maf
Hoxa2
Hoxa1
Hoxb1
Rest
C
Hoxa1
D
Maf
E
Rest
information content
position
F
Principal Component 1
Principal Component 3
G
Principal Component 2
Principal Component 3
H
motifs_peaks_genes
peaks
genes
number
47
20
50
32
22
6
10
10
nuclear receptor
Ets-like
Hox-like
Maf_Rest
motifs

Figure 5. Transcription factor binding partner of PGC-1 b in muscle cells

A) Fraction of explained variance of the top 10 principal component analysis (PCA) components.

B) PCA of the 673 PGC-1β peaks. Motif scores across principal component (PC) 1 and PC2 are shown. Circles point the motif clusters identified. Blue: nuclear receptors, red: “Ets-like” motifs, green: “Hox-like” motifs.

C) Sequence logo of Hoxa1 motif.

D) Sequence logo of Maf motif.

E) Sequence logo of Rest motif.

F) PCA of the 673 PGC-1β peaks. Motif scores across PC1 and PC3 are shown. Circles point the motif clusters identified. Red: “Ets-like” motifs, green: “Hox-like” motifs, orange: Maf and Rest motifs.

G) PCA of the 673 PGC-1β peaks. Motif scores across PC2 and PC3 are shown. Circles point the motif clusters identified. Blue: nuclear receptors, green: “Hox-like” motifs, orange: Maf and Rest motifs.

H) Bar graph of the number of peaks and genes associated with the TF motifs identified by PCA.

Suppl. Figure 1

A

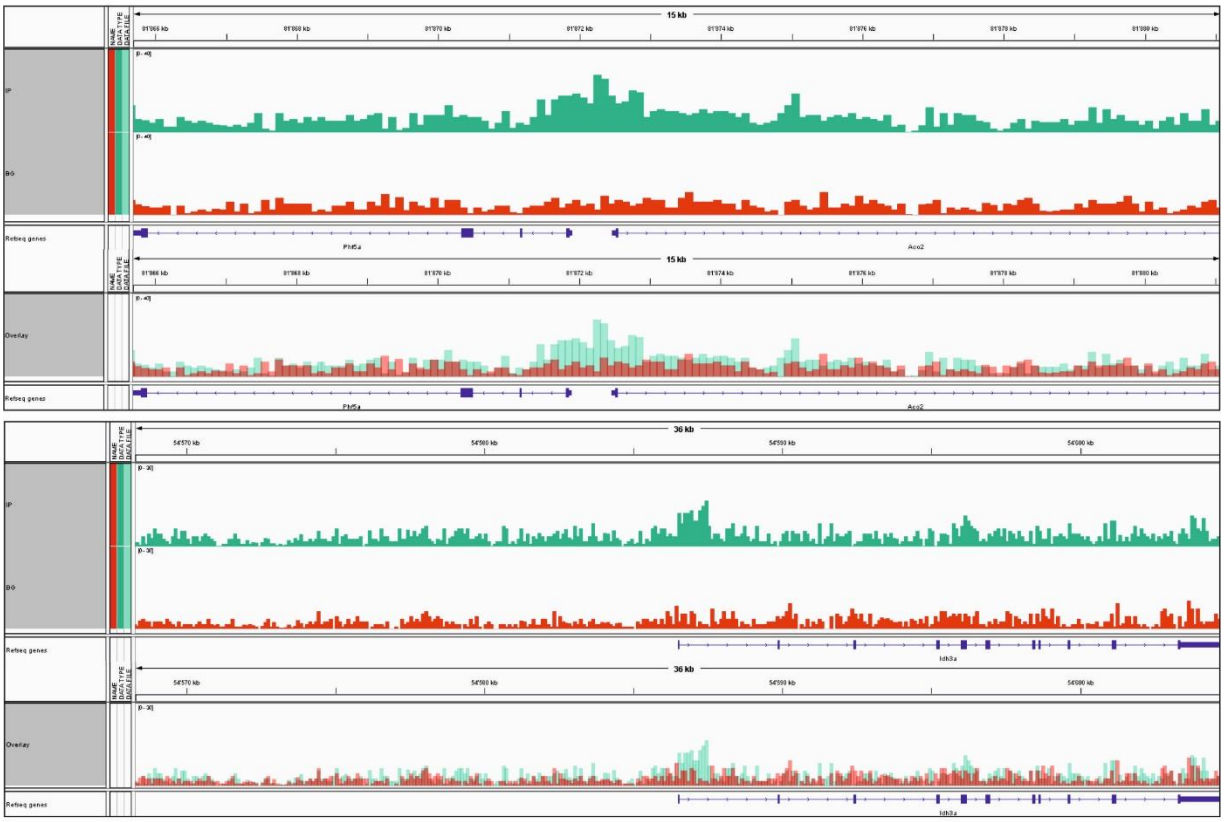

B

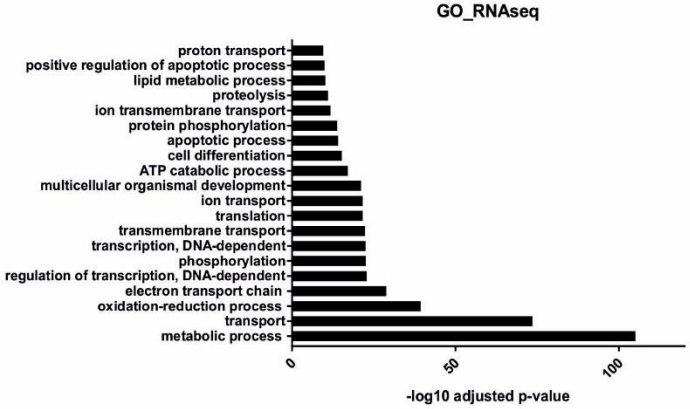

C

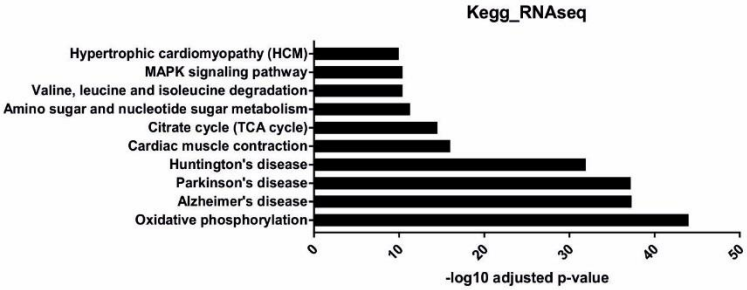

Supplemental Figure 1. PGC-1β binding regions and biological functions in muscle cells

A) PGC-1β ChIPseq binding peaks around the TSSs of the genes Aco2 and Idh3a obtained from the IGV Genome Browser.

B) GO terms of DE genes of PGC-1β overexpression in C2C12 myotubes. X-axis represents -log10 of the adjusted p-value.

C) Kegg pathway terms of DE genes of PGC-1β overexpression in C2C12 myotubes. X-axis represents -log10 of the adjusted p-value.

Suppl. Figure 5

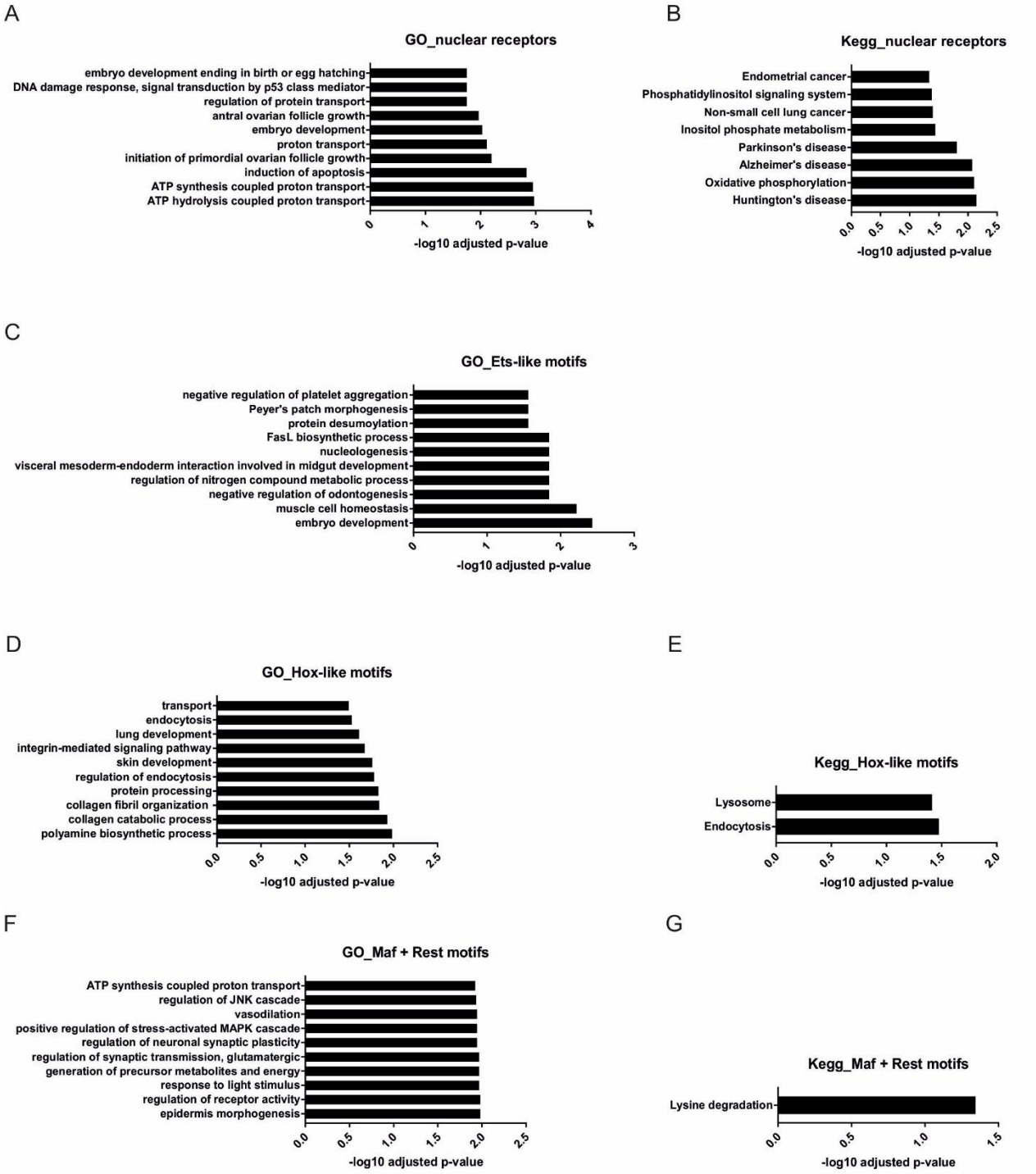

Supplemental Figure 5. Nuclear receptors and Ets-like transcription factors are functional binding partners of PGC-1β

A) Top 10 GO terms of genes associated with the nuclear receptor motifs. X-axis represents -log10 of the adjusted p-value.

B) All Kegg pathway terms of genes associated with the nuclear receptor motifs. X-axis represents -log10 of the adjusted p-value.

C) Top 10 GO terms of genes associated with the Ets-like motifs. X-axis represents -log10 of the adjusted p-value. D: All Kegg pathway terms of genes associated with the Ets-like motifs. X-axis represents -log10 of the adjusted p-value.

E) Top 10 GO terms of genes associated with the Hox-like motifs. X-axis represents -log10 of the adjusted p-value.

F) All Kegg pathway terms of genes associated with the Hox-like motifs. X-axis represents -log10 of the adjusted p-value.

G) Top 10 GO terms of genes associated with the Maf and Rest motifs. X-axis represents -log10 of the adjusted p-value.

H) All Kegg pathway terms of genes associated with the Maf and Rest motifs. X-axis represents -log10 of the adjusted p-value.

Discussion

Skeletal muscle is an organ with high plasticity, especially after physical activity. This adaptations and modifications are very complex biological programs that involves many factors and numerous cellular changes. Since the PGC-1 family of coactivators have a strong link to many skeletal muscle changes but as well whole body adaptions, we dissected the role of the so far not well-studied PGC-1β coactivator-controlled transcriptional network in skeletal muscle cells.

Our study revealed a genome-wide recruitment of PGC-1β to the mouse genome (673 peaks), although to our surprise to a lesser extent then we observed in our previous study performed for PGC-1α in skeletal muscle cells (Baresic et al., 2014). Since the ChIP experiment showed only a snapshot of recruitment, it might be that the moment of cell harvesting lead to the smaller recruitment of PGC-1β to the DNA than expected. It was obvious from our gene expression profile that PGC-1β played an important metabolic role since we observed 5729 differentially expressed genes under PGC-1β overexpression in muscle cells. In addition, it might be that some PGC-1β targets were transcriptionally silent due to additional binding factors needed for activation but those were not present at the moment of harvest. Setting our cutoffs for the ChIPseq data in combination with the RNAseq data left only few genes. Those direct PGC-1β genes were mostly upregulated and involved in the regulation of the energy metabolism, confirming literature (Gali Ramamoorthy et al., 2015; Scarpulla, 2011; Shao et al., 2010). Using ISMARA to predict TFBSs occupancy, we identified the nuclear receptors with ERRα as main motif in out PGC-1β setup, similar as already observed for PGC-1α (Baresic et al., 2014). Most of the TFBSs identified by ISMARA were positively regulated by PGC-1β, indicating once again, PGC-1β to be more a coactivator than e corepressor. Combining the ISMARA results with PCA analysis revealed a clear pattern of preferred TF partners of PGC-1β in muscle cells. We confirmed the nuclear receptors, which were the main cluster of factors in the PC1, regulating the pathways of energy metabolism. Interestingly, PC2 showed a new, so far unexplored branch of TFs in combination with the PGC-1s, which were the Ets-like TFs. Several studies implicated the involvement of the Ets-TFs in the NMJ regulation and formation (Hippenmeyer et al., 2007; Sapru, 2001) and we found the PGC-1β-Ets TF-axis played a role in skeletal muscle development and cell homeostasis. PC3 revealed Hox-like TFs as possible binding partners of PGC-1β in muscle cells and thus, regulation of biosynthetic processes and endocytosis. From literature it is known that Hox TFs are important for skeletal muscle differentiation and DNA methylation (Tsumagari et al., 2013a) and that Hox TFs increase their binding affinity when associated with a cofactor, which could be PGC-1β in skeletal muscle (Svingen and Tonissen, 2006).

One of the main functions of PGC-1β is to boost mitochondrial biogenesis, which we could confirm in our findings. Interestingly, although mitochondrial homeostasis seemed to be one of the key regulatory

functions of PGC-1β, we found most of the genes involved in mitochondrial gene regulation indirectly controlled by PGC-1β. This was already obserbed in our previous study about PGC-1α in skeletal muscle cells (Baresic et al., 2014) and could again reflect the moment of experiment, which was chosen leading to the observed result.

Taken together, it is of great importance to dissect in a clean and unbiased manner the very complex regulatory transcriptional network of PGC-1α and PGC-1β in skeletal muscle cells. The molecular mechanism controlling and influencing not only skeletal muscle plasticity but as well whole bod homeostasis could help to find new therapeutic targets for metabolic diseases.

Materials and Methods

Cell culture

C2C12 myoblasts were grown in proliferation medium (GM) (DMEM, 10% FetalClone Serum [FCS, SH30066.03, GE Healthcare Life Sciences], 1% Penicillin/Streptomycin [15140122, Thermo Scientific]) until confluency and then medium was switched to differentiation medium (DM) (DMEM, 2% horse serum [HS, 16050122, Thermo Scientific]) for 4 days. Myotubes were infected with adenoviral (AD) GFP control and PGC-1β-Flag for 24h, and then the infection medium was changed to differentiation medium for 24h before cells were collected according to the experiment that was performed.

ChIPseq data analysis

The genomic sites where PGC-1β is binding to via a TF were identified by the Crunch software (Berger et al., 2016). Brief, the read density of the ChIP was compared across the genome by a 500bp sliding window for the immunoprecipitation (IP) compared to a 2000bp sliding window for the background (input). Only regions with a z-score higher than 4.15 and a FDR of 0.1 were considered as significant. Each condition was performed and analyzed in triplicates.

ISMARA was used to predict enriched TFBS (Balwierz et al., 2014). Motifs with a z-score > 2 were considered as significant.

Gene ontology analysis

Gene ontology (GO) analysis was executed by the use of GeneCodis (Carmona-Saez et al., 2007; Nogales-Cadenas et al., 2009; Tabas-Madrid et al., 2012). Enriched GO terms were furthermore sorted by (-log10) adjusted p-value.

qRT-PCR validation of ChIP enrichment and peak validation

Assumed target genes of PGC-1β as well as top peaks found in the PGC-1β ChIP were chosen for ChIP enrichment and peak validation, respectively. Primer sequences used are depicted in table 1. Relative mRNA levels were measured by quantitative real-time PCR (qRT-PCR) on a StepOnePlus system (Applied Biosystems) using Power SYBR green PCR master mix (4367659, Thermo Scintific).

RNA isolation and real-time qPCR

Total RNA was isolated from C2C12 myotubes with 1 mL TRI reagent (T9424, Sigma) according to the manufacturer's instructions. RNA concentration was measured with a NanoDrop OneC spectrophotometer (Thermo Scientific), treated with DNase I (18068015, Thermo Scientific) and then reverse transcribed using hexanucleotide mix (11277081001, Sigma) and SuperScript II reverse transcriptase (18064022, Thermo Scientific).

The level of relative mRNA was quantified by qRT-PCR on a Light Cycler 480 II system (Roche) using Fast Start Essential DNA Green Master mix (06924204001, Roche).

mRNA sequencing and analysis

Total RNA was isolated from C2C12 myotubes with TRI reagent (T9424, Sigma) according to the manufacturer's instructions. RNA concentration was measured with a NanoDrop OneC spectrophotometer (Thermo Scientific). RNA was further purified with the direct-zol RNA MiniPrep Kit (R2050, Zymo Research) according to the manufacturer's instructions. For RNAseq library preparation 1 µg of purified RNA was used and libraries prepared with the TruSeq RNA library Prep Kit (Illumina) according to the manufacturer's instructions. Single read sequencing was performed with a HighSeq 2500 machine (50 cycles, Illumina). Fastq files were mapped to the mouse genome (mm10) and statistical analysis performed with the CLC Genomics Workbench Software (Qiagen).

References

Arany, Z. (2008). PGC-1 coactivators and skeletal muscle adaptations in health and disease. Current opinion in genetics & development *18*, 426-434.

Arany, Z., Foo, S.Y., Ma, Y., Ruas, J.L., Bommi-Reddy, A., Girnun, G., Cooper, M., Laznik, D., Chinsomboon, J., Rangwala, S.M., et al. (2008). HIF-independent regulation of VEGF and angiogenesis by the transcriptional coactivator PGC-1alpha. Nature *451*, 1008-1012.

Arany, Z., Lebrasseur, N., Morris, C., Smith, E., Yang, W., Ma, Y., Chin, S., and Spiegelman, B.M. (2007). The transcriptional coactivator PGC-1beta drives the formation of oxidative type IIX fibers in skeletal muscle. Cell metabolism *5*, 35-46.

Balwierz, P.J., Pachkov, M., Arnold, P., Gruber, A.J., Zavolan, M., and van Nimwegen, E. (2014). ISMARA: automated modeling of genomic signals as a democracy of regulatory motifs. Genome research *24*, 869-884.

Baresic, M., Salatino, S., Kupr, B., van Nimwegen, E., and Handschin, C. (2014). Transcriptional network analysis in muscle reveals AP-1 as a partner of PGC-1alpha in the regulation of the hypoxic gene program. Molecular and cellular biology *34*, 2996-3012.

Berger, S., Omidi, S., Pachkov, M., Arnold, P., Kelley, N., Salatino, S., and van Nimwegen, E. (2016). Crunch: Completely Automated Analysis of ChIP-seq Data. In bioRvix.

Booth, F.W., Roberts, C.K., and Laye, M.J. (2012). Lack of exercise is a major cause of chronic diseases. Comprehensive Physiology *2*, 1143-1211.

Brault, J.J., Jespersen, J.G., and Goldberg, A.L. (2010). Peroxisome proliferator-activated receptor gamma coactivator 1alpha or 1beta overexpression inhibits muscle protein degradation, induction of ubiquitin ligases, and disuse atrophy. The Journal of biological chemistry *285*, 19460-19471.

Canto, C., and Auwerx, J. (2009). PGC-1alpha, SIRT1 and AMPK, an energy sensing network that controls energy expenditure. Current opinion in lipidology *20*, 98-105.

Canto, C., Gerhart-Hines, Z., Feige, J.N., Lagouge, M., Noriega, L., Milne, J.C., Elliott, P.J., Puigserver, P., and Auwerx, J. (2009). AMPK regulates energy expenditure by modulating NAD+ metabolism and SIRT1 activity. Nature *458*, 1056-1060.

Carmona-Saez, P., Chagoyen, M., Tirado, F., Carazo, J.M., and Pascual-Montano, A. (2007). GENECODIS: a web-based tool for finding significant concurrent annotations in gene lists. Genome biology *8*, R3.

Colberg, S.R., Sigal, R.J., Fernhall, B., Regensteiner, J.G., Blissmer, B.J., Rubin, R.R., Chasan-Taber, L., Albright, A.L., Braun, B., American College of Sports, M., et al. (2010). Exercise and type 2 diabetes: the American College of Sports Medicine and the American Diabetes Association: joint position statement executive summary. Diabetes care *33*, 2692-2696.

Egan, B., and Zierath, J.R. (2013). Exercise metabolism and the molecular regulation of skeletal muscle adaptation. Cell metabolism *17*, 162-184.

Gali Ramamoorthy, T., Laverny, G., Schlagowski, A.I., Zoll, J., Messaddeq, N., Bornert, J.M., Panza, S., Ferry, A., Geny, B., and Metzger, D. (2015). The transcriptional coregulator PGC-1beta controls mitochondrial function and anti-oxidant defence in skeletal muscles. Nature communications *6*, 10210.

Handschin, C. (2010). Regulation of skeletal muscle cell plasticity by the peroxisome proliferator-activated receptor gamma coactivator 1alpha. Journal of receptor and signal transduction research *30*, 376-384.

Haskell, W.L., Lee, I.M., Pate, R.R., Powell, K.E., Blair, S.N., Franklin, B.A., Macera, C.A., Heath, G.W., Thompson, P.D., Bauman, A., et al. (2007). Physical activity and public health: updated recommendation for adults from the American College of Sports Medicine and the American Heart Association. Circulation *116*, 1081-1093.

Himeda, C.L., Ranish, J.A., and Hauschka, S.D. (2008). Quantitative proteomic identification of MAZ as a transcriptional regulator of muscle-specific genes in skeletal and cardiac myocytes. Molecular and cellular biology *28*, 6521-6535.

Hippenmeyer, S., Huber, R.M., Ladle, D.R., Murphy, K., and Arber, S. (2007). ETS transcription factor Erm controls subsynaptic gene expression in skeletal muscles. Neuron *55*, 726-740.

Huss, J.M., Torra, I.P., Staels, B., Giguere, V., and Kelly, D.P. (2004). Estrogen-related receptor alpha directs peroxisome proliferator-activated receptor alpha signaling in the transcriptional control of energy metabolism in cardiac and skeletal muscle. Molecular and cellular biology *24*, 9079-9091.

Jager, S., Handschin, C., St-Pierre, J., and Spiegelman, B.M. (2007). AMP-activated protein kinase (AMPK) action in skeletal muscle via direct phosphorylation of PGC-1alpha. Proceedings of the National Academy of Sciences of the United States of America *104*, 12017-12022.

Kressler, D., Schreiber, S.N., Knutti, D., and Kralli, A. (2002). The PGC-1-related protein PERC is a selective coactivator of estrogen receptor alpha. The Journal of biological chemistry *277*, 13918-13925.

Lee, S., Leone, T.C., Rogosa, L., Rumsey, J., Ayala, J., Coen, P.M., Fitts, R.H., Vega, R.B., and Kelly, D.P. (2017). Skeletal muscle PGC-1beta signaling is sufficient to drive an endurance exercise phenotype and to counteract components of detraining in mice. American journal of physiology. Endocrinology and metabolism *312*, E394-E406.

Lin, J., Handschin, C., and Spiegelman, B.M. (2005). Metabolic control through the PGC-1 family of transcription coactivators. Cell metabolism *1*, 361-370.

Lin, J., Puigserver, P., Donovan, J., Tarr, P., and Spiegelman, B.M. (2002). Peroxisome proliferator-activated receptor gamma coactivator 1beta (PGC-1beta), a novel PGC-1-related transcription coactivator associated with host cell factor. The Journal of biological chemistry *277*, 1645-1648.

Liu, C., and Lin, J.D. (2011). PGC-1 coactivators in the control of energy metabolism. Acta biochimica et biophysica Sinica *43*, 248-257.

Nogales-Cadenas, R., Carmona-Saez, P., Vazquez, M., Vicente, C., Yang, X., Tirado, F., Carazo, J.M., and Pascual-Montano, A. (2009). GeneCodis: interpreting gene lists through enrichment analysis and integration of diverse biological information. Nucleic acids research *37*, W317-322.

Olson, B.L., Hock, M.B., Ekholm-Reed, S., Wohlschlegel, J.A., Dev, K.K., Kralli, A., and Reed, S.I. (2008). SCFCdc4 acts antagonistically to the PGC-1alpha transcriptional coactivator by targeting it for ubiquitin-mediated proteolysis. Genes & development *22*, 252-264.

Puigserver, P., Rhee, J., Lin, J., Wu, Z., Yoon, J.C., Zhang, C.Y., Krauss, S., Mootha, V.K., Lowell, B.B., and Spiegelman, B.M. (2001). Cytokine stimulation of energy expenditure through p38 MAP kinase activation of PPARgamma coactivator-1. Molecular cell *8*, 971-982.

Rowe, G.C., Jang, C., Patten, I.S., and Arany, Z. (2011). PGC-1beta regulates angiogenesis in skeletal muscle. American journal of physiology. Endocrinology and metabolism *301*, E155-163.

Salatino, S., Kupr, B., Baresic, M., van Nimwegen, E., and Handschin, C. (2016). The Genomic Context and Corecruitment of SP1 Affect ERRα Coactivation by PGC-1α in Muscle Cells. Molecular Endocrinology *30*, 809-825.

Sandri, M., Lin, J., Handschin, C., Yang, W., Arany, Z.P., Lecker, S.H., Goldberg, A.L., and Spiegelman, B.M. (2006). PGC-1alpha protects skeletal muscle from atrophy by suppressing FoxO3 action and atrophy-specific gene transcription. Proceedings of the National Academy of Sciences of the United States of America *103*, 16260-16265.

Sandri, M., Sandri, C., Gilbert, A., Skurk, C., Calabria, E., Picard, A., Walsh, K., Schiaffino, S., Lecker, S.H., and Goldberg, A.L. (2004). Foxo transcription factors induce the atrophy-related ubiquitin ligase atrogin-1 and cause skeletal muscle atrophy. Cell *117*, 399-412.

Sapru, M.K. (2001). Neuregulin-1 regulates expression of the Ets-2 transcription factor. Life sciences *69*, 2663-2674.

Scarpulla, R.C. (2011). Metabolic control of mitochondrial biogenesis through the PGC-1 family regulatory network. Biochimica et biophysica acta *1813*, 1269-1278.

Schiaffino, S., and Reggiani, C. (2011). Fiber types in mammalian skeletal muscles. Physiological reviews *91*, 1447-1531.

Schreiber, S.N., Emter, R., Hock, M.B., Knutti, D., Cardenas, J., Podvinec, M., Oakeley, E.J., and Kralli, A. (2004). The estrogen-related receptor alpha (ERRalpha) functions in PPARgamma coactivator 1alpha (PGC-1alpha)-induced mitochondrial biogenesis. Proceedings of the National Academy of Sciences of the United States of America *101*, 6472-6477.

Shao, D., Liu, Y., Liu, X., Zhu, L., Cui, Y., Cui, A., Qiao, A., Kong, X., Liu, Y., Chen, Q., et al. (2010). PGC-1 beta-regulated mitochondrial biogenesis and function in myotubes is mediated by NRF-1 and ERR alpha. Mitochondrion *10*, 516-527.

Spiegelman, B.M., and Heinrich, R. (2004). Biological control through regulated transcriptional coactivators. Cell *119*, 157-167.

Svingen, T., and Tonissen, K.F. (2006). Hox transcription factors and their elusive mammalian gene targets. Heredity *97*, 88-96.

Tabas-Madrid, D., Nogales-Cadenas, R., and Pascual-Montano, A. (2012). GeneCodis3: a non-redundant and modular enrichment analysis tool for functional genomics. Nucleic acids research *40*, W478-483.

Tiraby, C., Hazen, B.C., Gantner, M.L., and Kralli, A. (2011). Estrogen-related receptor gamma promotes mesenchymal-to-epithelial transition and suppresses breast tumor growth. Cancer research *71*, 2518-2528.

Tsumagari, K., Baribault, C., Terragni, J., Chandra, S., Renshaw, C., Sun, Z., Song, L., Crawford, G.E., Pradhan, S., Lacey, M., et al. (2013). DNA methylation and differentiation: HOX genes in muscle cells. Epigenetics & chromatin *6*, 25.

Wallberg, A.E., Yamamura, S., Malik, S., Spiegelman, B.M., and Roeder, R.G. (2003). Coordination of p300-mediated chromatin remodeling and TRAP/mediator function through coactivator PGC-1alpha. Molecular cell *12*, 1137-1149.

Zechner, C., Lai, L., Zechner, J.F., Geng, T., Yan, Z., Rumsey, J.W., Collia, D., Chen, Z., Wozniak, D.F., Leone, T.C., et al. (2010). Total skeletal muscle PGC-1 deficiency uncouples mitochondrial derangements from fiber type determination and insulin sensitivity. Cell metabolism *12*, 633-642.

5.1 Acute and chronic exercise regulate skeletal muscle DNA methylation and transcription in a time- and PGC-1α-dependent manner

Barbara Heim-Kupr[1], Karl Nordström[2], Svenia Schnyder[1], Regula Furrer[1], Stefan Steurer[1], Jörn Walter[2] and Christoph Handschin[1*]

[1]Biozentrum, University of Basel, Klingelbergstrasse 50/70, CH-4056 Basel, Switzerland

[2]Department of Biological Sciences, Genetics/Epigenetics, Saarland University, Saarbrücken, Saarland, Germany

[*]Corresponding author: christoph.handschin@unibas.ch / Biozentrum, University of Basel, Klingelbergstrasse 50/70, CH-4056 Basel / Phone: +41 61 207 23 78

Abstract

Skeletal muscle (SKM) contraction is a tightly controlled molecular mechanism important to adapt to increased energy expenditure, which involves changes in SKM and whole body metabolism. Exercise lead to plastic adaptations in SKM and is a well-established treatment against many metabolic diseases and myopathies. The peroxisome proliferator-activated receptor γ coactivator-1α (PGC-1α) is a main driver of energy homeostasis and SKM plasticity. Nevertheless, the molecular mechanism underlying SKM plasticity is not fully understood yet. We used a combined approach of RNAseq and reduced representation bisulfite sequencing (RRBS) in acute and chronic exercised mice together with various PGC-1α genotypes. Our data show that acute and chronic exercise regulate distinct transcriptome and methylome profiles. Even more, PGC-1α is involved in the exercise-induced response on methylation and transcription level, which is diminished in skeletal muscle-specific PGC-1α knockout animals. Our findings reveal novel insides in the control of SKM metabolism and open new doors for therapeutic strategies to cure myopathies and fight against pathophysiological conditions.

Abbreviations

5hmC, 5-hydroxymethylcytosine; 5mC, 5-methylcytosine; BAT, brown adipose tissue; CH_3, methyl group; CpG, cytosine-phosphate-guanine; DE, differentially expressed; DM, differentiation medium; DMR, differentially methylated region; DNMT, DNA methyltransferase; ES, embryonic stem cells; FC, fold change; FDR, false discovery rate; GC, guanine-cytosine; gDNA, genomic DNA; GM, growth medium; GO, gene ontology; HS, horse serum; MKO, skeletal muscle-specific PGC-1α knockout mice; PGC-1, peroxisome proliferator-activated receptor γ coactivator-1; Quad, Quadriceps muscle; qRT-PCR, quantitative real-time polymerase chain reaction; RNAseq, RNA sequencing; RRBS, reduced representation bisulfite sequencing; SEM, standard errors of the means; SKM, skeletal muscle; Tg, skeletal muscle-specific PGC-1α overexpressing mice; TET, Ten-Eleven-Translocation oxygenases; TF, transcription factor; TSS, transcription start sites; WT, wild type mice

Introduction

Exercise induces muscle contractions, which include many tightly controlled molecular mechanisms that are needed to adapt to increased energy expenditure and involve changes in SKM and whole body metabolism (Egan and Zierath, 2013). Improved cardio vascular functions and antagonize type 2 diabetes or obesity by physical activity is an accepted therapeutic strategy (Colberg et al., 2010a; Haskell et al., 2007). Even more, exercise was reviewed to have beneficial effects and improve quality of life in myopathies as well as in sarcopenia (Egan and Zierath, 2013; Gill et al., 2018; Law et al., 2016b; Phillips and Mastaglia, 2000). Therefore, it is of importance to understand the molecular mechanism underlying not only SKM plasticity but as well whole body adaptations. Especially, the observation of faster response of retraining subsequent to disuse due to injury or off-season in sport opened the discussion of possible memory effect in trained SKM (Bruusgaard et al., 2010; Gundersen, 2016; Lindholm et al., 2016; Mutin-Carnino et al., 2014; Seaborne et al., 2018; Sharples et al., 2016). The term of muscle memory is defined as that the SKM is able to respond more favorably to stimuli that have already been faced in the past. Previous studies showed morphological and functional different response of SKM detraining and retraining in untrained versus trained muscle (Sharples et al., 2016; Taaffe et al., 2009). The morphological changes could be associated with retained myonuclei after regular exercise, mainly upon resistance exercise (Bruusgaard et al., 2010; Gundersen, 2016). Additionally, the SKM reaction could as well be related to epigenetic adaptations following acute and chronic endurance as well as resistance exercise, specifically DNA methylation (Barres et al., 2012; Ntanasis-Stathopoulos et al., 2013; Seaborne et al., 2018; Sharples et al., 2016; Voisin et al., 2015). However, the connection of DNA methylation, transcriptional changes and muscle memory could not be defined yet. Since exercise is used as treatment strategy, it is of interest to understand the mechanism of SKM plasticity and the role of muscle memory to improve and personalize physical activity as treatment strategy for various patients with diverse severities of diseases and thus, use the discovered pathways also for patients which are not anymore able to perform exercise. A key player in the control of muscle plasticity and whole body adaptations following physical activity is the peroxisome proliferator-activated receptor γ coactivator-1α (PGC-1α) (Akimoto et al., 2005; Handschin et al., 2007a; Jager et al., 2007; Wu et al., 2002). PGC-1α is a master regulator of mitochondrial biogenesis and induced upon physical activity, additionally its target genes (Lin et al., 2005), the protein stability (Canto et al., 2009; Jager et al., 2007; Puigserver et al., 2001) and the methylation status of its promoter is modified (Barres et al., 2012). As PGC-1α is a coactivator, it interacts with many different transcription factors (TFs) to regulate a complex transcriptional network. Nevertheless, a global picture of regulatory power by PGC-1α following exercise stimuli was mostly done on transcriptional level and less on epigenetic site, which might be involved in acute (Barres et al., 2012; Lochmann et al., 2015a; Nitert et al., 2012) and long-term

adaptations, namely muscle memory (Seaborne et al., 2018; Sharples et al., 2016). Several studies implicated that DNA methylation is able to manipulate PGC-1α levels and consequently its target genes (Bajpeyi et al., 2017; Barres et al., 2009; Lochmann et al., 2015b; Salatino et al., 2016a). The methyl group (CH_3) that is added on the cytosine of the DNA can block the binding of TFs or change the chromatin structure and subsequently change gene expression (Jones and Takai, 2001; Schubeler, 2015; Siegfried and Simon, 2010). However, the link of methylation adaptations and transcriptional changes following various exercise stimuli and the consequences on SKM and the body metabolism are not analyzed yet. In addition, the role of PGC-1α on the methylome after exercise is unknown. Therefore, we performed a combined analysis of RNA sequencing (RNAseq) and reduced representation bisulfite sequencing (RRBS) data subsequent to an acute exercise time course and chronic exercise in wild type (WT) and skeletal muscle-specific PGC-1α knockout (MKO) mice. In addition, we used *in vivo* and *in vitro* gain-of-function models to investigate further the role of PGC-1α on DNA methylation. Our findings show that acute and chronic exercise have distinct transcriptome and methylome profiles. We discovered large methylation adaptions but mild transcription alterations by chronic exercise, indicating potential memory effect after chronic training. Even more, we observed that MKO mice have a blunted transcription and methylation exercise response. Finally, our findings show changed transcriptome and methylome in PGC-1α gain-of-function models *in vivo* and *in vitro*, strengthen the role of PGC-1α in epigenetic manipulations.

Our data help to understand the acute and chronic exercise-induced SKM adaptation and display the role of PGC-1α in the regulation of SKM metabolism. The new knowledge will help to optimize the use of physical activity as a therapeutic treatment not only against metabolic diseases but as well to help patients with myopathies or sarcopenia.

Results

Acute exercise modulates DNA methylation and transcription in skeletal muscle

Exercise is involved in many adaptations not only in SKM but also in whole body homeostasis. This complex molecular mechanism might involve a combined regulation by DNA methylation and gene transcription (Barres et al., 2012; Lochmann et al., 2015a; Nitert et al., 2012). To elucidate the role of exercise on DNA methylation and the effect of methylation changes on transcript profile, we performed a time course of acute exercise until exhaustion and killed the WT mice immediately, 0h, or 4h, 6h and 8h after the exhaustion test (Suppl. Figure 1A-C). Quadriceps (Quad) muscle was taken and RNAseq analysis of the whole acute exercise time course preformed. Additionally, we implemented RRBS of the 0h and 4h time points of the exercise time course to measure the acutely induced DNA methylation alterations and their effect on gene expression over a time course. For RNAseq a cutoff of false discovery rate (FDR) < 0.05 was

used and revealed large portion of differentially expressed (DE) genes after acute exercise in all time points in WT animals, mainly upregulated ones (Figure 1A). The highest fraction of DE genes was observed 6h post exercise (Figure 1A), which we do not know the reason for but goes in line with better performance in those mice (data not shown). Next, RRBS was analyzed in the acute exercise WT 0h and WT 4h cohort with a cutoff of q-value < 0.01 and differentially methylated region (DMR) of ± 10%. Interestingly, most of the DMRs were hypomethylated upon acute exercise (Figure 1B), comparable to previous studies analyzing DNA methylation status after acute exercise (Barres et al., 2012; Kanzleiter et al., 2015). This data already suggested that exercise induces not only transcriptional changes but as well DNA methylation adaptations. Therefore, we combined the RRBS with the RNAseq data for all time points to analyze further the functional output of DNA methylation on mRNA level. The DMRs were associated to the closest gene allowing gene comparison of the data sets. Venn diagram of WT animals with DMRs at 0h and DE genes to any time point (101 genes) or DMRs at 4h and DE genes at any time point (130 genes) revealed around 1/3 overlap between the genes significantly changed in DNA methylation and transcript level (Figure 1C). Interestingly, the overlap was dissected in 16 hypermethylated genes at 0h, whereas at 4h three of them were hypomethylated, and 22 hypomethylated genes at 0h, while six were hypermethylated at 4h. However, gene expression direction was not affected. Gene ontology (GO) analysis of each individual fraction of the Venn diagram exposed very mild GO terms for the WT 0h only group with the term for transcriptional regulation marginal significant (Figure 1D). Remarkably, the GO analysis of the overlap (Figure 1E) and of the WT 4h only (Figure 1F) group showed transcriptional regulation as top terms. However, the same GO terms contained different genes, many of them TFs (Figure 1G), which were identified by the Animal TFDB2.0 software (Zhang et al., 2012; Zhang et al., 2015). To catch a global overview of DNA methylation and gene transcription we combined the DMRs of the WT 0h with the WT 4h and all DE genes to all time points and analyzed for transcriptional and methylation changes in a time course dependent manner, represented in a heatmap (Figure 2A). The largest pattern in the heatmap belonged to hypomethylation at 0h and 4h, which correlated with gene induction. Even more, some genes were only changed in methylation at 0h and not at 4h but the gene expression was changed either at a specific or at any time point. Similar was observed for the 4h time point. Finally, a small fraction of regions was found to be affected at both methylation stages after exercise but the pattern of DNA methylation could be different resulting in a very mild FC of those genes compared to the genes, which had methylation changes into the same direction at any time point (Figure 1G). The correlation of hypomethylation at a specific time point with gene induction could be validated by Pearson correlation with good correlation coefficients for WT 0h (R = -0.6317) and WT 4h (R = -0.7252) (Figure 2B + C). Furthermore, the heatmap was dissected into different parts of up- and downregulated genes and GO analysis conducted. Most of

the upregulated genes, which were mainly hypomethylated at the WT 0h time point, were highly significant and involved in the transcriptional regulation (Suppl. Figure 2A). Contrarily, the downregulated genes, mostly hypermethylated, do not contain a significant GO Term (Suppl. Figure 2B). Similar was observed for WT 4h GO analysis (Suppl. Figure 2C + D). This data show that the combination of DNA methylation and transcript changes upon acute exercise in SKM come along with each other in a time-dependent manner.

PGC-1α controls DNA methylation and transcription following acute exercise

To characterize further the molecular mechanism of exercise on transcript and epigenetic level, we brought the master regulator of mitochondrial biogenesis and important player in SKM plasticity into the game, namely PGC-1α (Akimoto et al., 2005; Barres et al., 2012; Handschin et al., 2007a; Lin et al., 2005; Lin et al., 2002b; Puigserver et al., 1998). PGC-1α is a major contributor to SKM plasticity and controls a very complex transcriptional network (Kupr and Handschin, 2015). It was shown that PGC-1α interacts with different TFs and regulate its target genes dependent on the genomic GC content (Salatino et al., 2016a), hence DNA methylation might be an additional level of control. Therefore, we used WT control as well as MKO mice and performed RNAseq (Figure 3A) and RRBS (Figure 3B) from acute exercised time course Quad muscle as already described before. Interestingly, both analysis in the MKO mice showed lower number of DE genes and DMRs, respectively, when compared to the WT animals (Figure 1A + B, Figure 3A + B). Even more striking and contrarily to the WT animals, the MKO mice displayed DMRs towards hypermethylation upon acute exercise (Figure 3B). We combined WT acute exercise data found to be significant to any RRBS and RNAseq time point (193 genes) with the similar approach used in the MKO mice (77 genes) (Figure 3C). There was only very little overlap of 25 genes (Figure 3C), clearly depicted in the heatmap over all acute exercise measurements and genotypes (Figure 3D). GO analysis of each fraction from the Venn diagram in Figure 3C depicted deficits in transcriptional regulation in the MKO mice compared to the WT mice (Suppl. Figure 3A-C). Although the overlap (core) contained the GO terms for transcriptional regulation, however additional genes found only in the WT group were missing in the MKO cohort (Suppl. Figure 3D-F). Even more, the overlap revealed that most of the methylation adaptations in the MKO mice were done at the 0h time point, which was not observed in the WT animals (Suppl. Figure 3F). However, gene expression direction was not affected, only the FC was diminished in the MKO animals (Suppl. Figure 3F).

Distinct DNA methylation patterns subsequent to acute and chronic exercise

DNA methylation is often thought to be a stable and long-range adaptation. Therefore, we assessed a one month chronically trained group of WT animals (Suppl. Figure 4A + B) and performed RNAseq (Figure 4A) and RRBS (Figure 4B) from Quad muscle, using the same cutoffs as for the acute exercise group. Contrarily to the methylome, the effect on transcription by chronic exercise was low, especially when we combined the two approaches to measure the functional relevance, which resulted in 19 genes (Figure 4C + Suppl. Figure 4C). Opposed to the acute exercise procedure, no involvement in transcriptional regulation could be found from GO evaluation (Suppl. Figure 4D), matching the low number of DE genes found (Figure 4A). Upon chronic exercise, muscle memory could play an important role due to long-term epigenetic alterations (Seaborne et al., 2018; Sharples et al., 2016). Thus in a next step, we combined the RRBS data from the chronic exercise group with the RNAseq data of the acute exercise cohort to all time points (Figure 4D). We found good overlap of chronic DMRs and acute DE genes, namely 142 genes, indicating potential memory effect in the chronic trained unit. Opposite to the above-mentioned GO analysis of chronic exercise data only, GO evaluation of the overlap revealed a large involvement of transcriptional regulation (Figure 4E). We further dissected and compared the genes found in the GO terms associated with transcription to the genes detected in the GO notions transcriptional regulation in the acute exercise RRBS and RNAseq analysis, which resulted in three groups of transcriptional associated genes (Suppl. Figure 4E + F). A heatmap with all acute and chronic DMRs as well as the DE genes showed distinct methylation patterns in acute and chronic exercised mice and the very low transcriptional response following chronic exercise (Figure 4F). Interestingly, the pattern of hypomethylation leading mostly to gene induction and vice versa could be, as already observed during acute exercise, also discovered in the chronic exercise DMRs compared to acute exercise RNAseq data, nicely depicted by Pearson correlation (Figure 4G). Furthermore, the overlap of chronic exercise DMRs with acute exercise RNAseq data was split into up and down regulated genes, correlating mostly with hypo- and hypermethylation, respectively. GO analysis of those groups revealed evidently the transcriptional regulation as main term in the upregulated, hence hypomethylated genes (Suppl. Figure 4G + H), which was in strong contrast to the analysis of the complete chronic exercise data set (Suppl. Figure 4D). The downregulated genes could not be associated with significant GO terms (Suppl. Figure 4H).

PGC-1α controls the distinct DNA methylation pattern after acute and chronic exercise

As PGC-1α plays a critical role in the methylome and transcriptome control subsequent to acute exercise, we further elucidated its impact in chronic exercised animals. We used MKO mice, which were trained one month on running wheels (Suppl. Figure 4A + B). RNAseq (Suppl. Figure 5A) and RRBS (Suppl. Figure 5B)

from Quad muscle was performed and the same cutoffs used as for the WT animals. As already observed in the WT mice (Figure 4A), very mild transcriptional changes could be observed upon chronic training in the MKO animals (Suppl. Figure 5A). Contrarily, strong methylation changes were detected (Suppl. Figure 5B). The combination of RRBS and RNAseq resulted in only one hypermethylated and three hypomethylated genes (Suppl. Figure 5C). Therefore, the chronic DMRs were compared to the acute DE genes in the MKO animals, as it was already done in the WT animals. Interestingly, also the MKO mice showed good overlap of 110 genes (Suppl. Figure 5D), playing mainly a role in transcriptional regulation (Suppl. Figure 5E). Heatmap was performed with all DMRs and DE genes from the acute time course and the chronic exercise training that revealed distinct methylation patterns in acute versus chronic exercise MKO mice (Suppl. Figure 5F). However, Pearson correlation of chronic DMRs and acute RNAseq information showed again nice correlation of hypomethylation leading to gene induction and vice versa (Suppl. Figure 5G). We further evaluated the role of PGC-1α in chronic exercise and potential in muscle memory by the comparison of all genes found in the overlap of chronic DMRs with acute RNAseq in WT (142 genes, Figure 4D) to MKO (110 genes, Suppl. Figure 5D) mice. A small overlap of 22 genes, which were independent of PGC-1α, was discovered (Figure 5A). Importantly, the distribution of hyper- and hypomethylation in the overlap between the genotypes could be altered (Figure 5B), however not affecting gene expression direction (Figure 5A).

Skeletal muscle methylome and transcriptome is also regulated by PGC-1α in gain-of-function models

Our data showed that PGC-1α plays a major role in the control of DNA methylation and the linked gene expression adaptations upon exercise. To find a potential mechanism, we used gain-of-function models *in vivo* and *in vitro*. RNAseq and RRBS from the Quad muscles of skeletal muscle-specific PGC-1α overexpressing mice (Tg) and their corresponding littermate WT controls was performed. Using the same limits as for the previous analysis, we observed massive DE genes (Figure 6A) and a large impact on the DNA methylation status in those mice, with higher proportion of hypomethylation (Figure 6B). The combination of DMRs with DE genes revealed still a bigger proportion of hypomethylated genes tending towards mRNA upregulation (Figure 6C). The opposite was observed for genes, which were hypermethylated (Figure 6C). GO analysis discovered strong impact in transcriptional regulation (Figure 6D + E) together with cell differentiation and interestingly, Wnt signaling pathway including the GO term of catenin import into nucleus (Figure 6D). A link between PGC-1α and the Wnt signaling pathway was found in osteoblasts and brown adipose tissue (BAT), where PGC-1α is regulated by the Wnt pathway but has in addition, a positive feedback loop to regulate catenin, a main player in the Wnt signaling pathway (Canto et al., 2010; Kang et al., 2005). To dissect further the role of PGC-1α in SKM DNA methylation a

second gain-of-function model, C2C12 myotubes where adenoviral PGC-1α and GFP control was applied, was used. RNAseq (Figure 6F) and RRBS (Figure 6G) was performed and the data analyzed with the same thresholds as used for the *in vivo* analysis. The transcriptional investigation of DE genes resulted in massive mRNA changes upon PGC-1α overexpression in myotubes, mostly upregulation (Figure 6F). Contrary to the *in vivo* gain-of-function model, not much DMRs could be detected in the *in vitro* system and the distribution of hyper- to hypomethylation was roughly equal (Figure 6G). The functional output by combining RNAseq with RRBS data reduced the number of significant genes even more, with higher fraction of hypermethylation but equal gene expression direction (Figure 6H). GO analysis of all combined genes tended towards neuronal regulation and low p-values (Figure 6I).

Figure 1

A

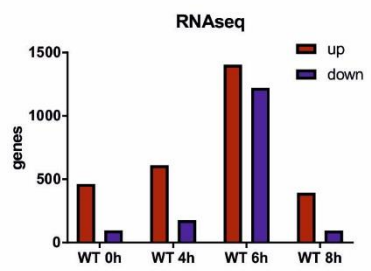

B

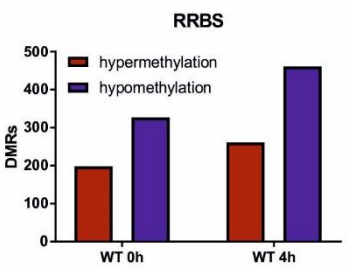

C

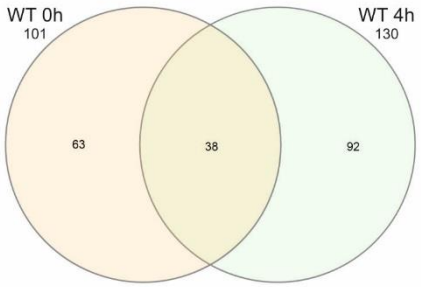

D

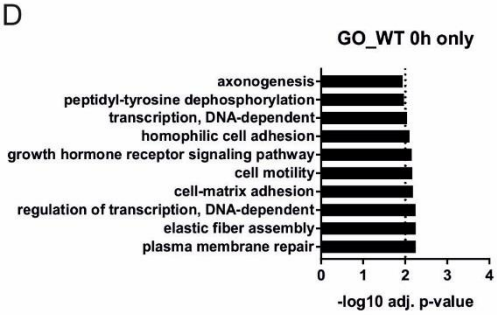

E

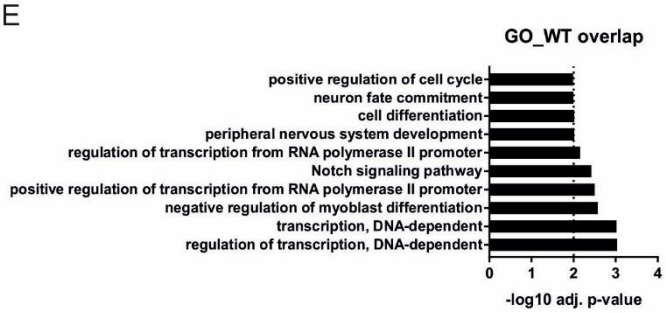

F

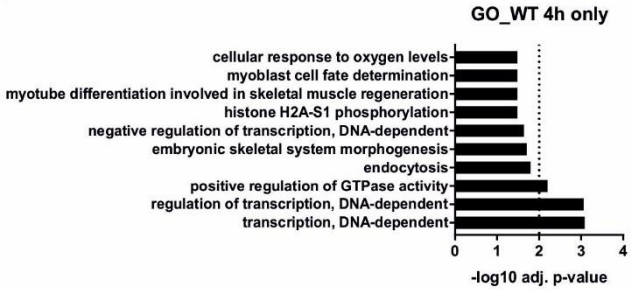

G

WT 0h only	DMR WT 0h	DMR WT 4h	0h Log2 FC	4h Log2 FC	6h Log2 FC	8h Log2 FC	TF
Zfp219	12.05				0.4		TF
Kctd1	25.88				1.5		
Hira	10.36				-0.45		
Dedd2	10.17		0.94	0.7	0.41		
Cebpg	-12.76				0.43		TF
Foxo6	-21.09				-0.59	-0.83	TF
Esrrb	-19.92				1.15		TF
Vgll2	-12.50			0.62	0.44		
Esrrg	-11.38				0.7		TF
Eng	-14.76			0.7	0.7		
Dnmt3a	-11.72			-0.44	-0.36		

overlap	DMR WT 0h	DMR WT 4h	0h Log2 FC	4h Log2 FC	6h Log2 FC	8h Log2 FC	TF
Gata2	12.43	12.19	0.58		0.53		TF
Tbx2	21.00	12.04			0.93		TF
Nfatc4	13.80	14.81			1.1		TF
Tcf3	23.92	11.29			0.37		TF
Tgfb1	14.20	15.10			0.82		
Rai1	11.55	10.12			0.77		
Nr4a3	-11.47	-15.61	2.94	4.38	2.73	2.31	TF
Notch3	-10.30	-19.34			0.97		
Zfp503	-21.55	-10.61			1.28	0.76	
Casz1	-11.56	-24.18			0.43		
Egr3	-21.76	-22.32	4.21	3.5	3.82		TF
Heyl	-20.79	-30.86			0.95		TF

WT 4h only	DMR WT 0h	DMR WT 4h	0h Log2 FC	4h Log2 FC	6h Log2 FC	8h Log2 FC	TF
Gli1		15.37			1.66		TF
Sox13		23.34			0.36		TF
Hdac7		18.49		0.61	0.76		
Zfp329		10.27			-0.48		TF
Phf21a		31.55			-0.39		
Rps6ka5		18.08		-0.72	-1.15	-1.9	
Rreb1		-19.70		-0.59	-0.72	-0.83	TF
Tbx15		-11.82			-0.48		TF
Zzz3		-15.34			-0.43		TF
Pcgf2		-48.23			0.79		
Myod1		-13.68		1.85	1.37	1.61	TF
Baz1a		-34.18	0.85				
Hspa8		-12.29		0.75	0.5		
Sox10		-15.01			1.38		TF
Med26		-26.44	0.79				
Cbx4		-12.98			0.97		
Cdk5r1		-19.38		2.87	1.74	2.71	

Figure 1: Acute exercise changes DNA methylation and transcript levels in skeletal muscle

A): Bar graph of DE genes in WT mice upon acute exercise time course measured 0h, 4h, 6h or 8h post exercise. DE genes are subdivided into up- (red) and downregulated (blue). DE genes: FDR < 0.05.

B): Bar graph of DMRs in WT mice upon acute exercise time course measured 0h or 4h post exercise. DMRs genes are subdivided into hyper- (red) and hypomethylated (blue). DMR: q-value < 0.01, ±10 methylation change.

C): Venn diagram of combined DE genes from total time course and DMRs in WT mice 0h post acute exercise (orange) or 4h post acute exercised (green).

D-F): Gene ontology (GO) of all genes from the Venn diagram fractions for WT 0h only (D), overlap (E) and WT 4h only (F). Top 10 GO terms are shown. X-axis: (-)log10 adjusted p-value. Dotted line represents significance: (-)log10 adjusted p-value > 2.

G): Table of genes found in the GO terms associated with transcriptional regulation for WT 0h only, overlap and WT 4h only. DMR of each time point as well gene expression in log2 FC is indicated at each acute exercise time point, 0h, 4h, 6h and 8h. Last column shows if the genes are transcription factors (TF), identified by Animal TFDB2.0 software (Zhang et al., 2012; Zhang et al., 2015).

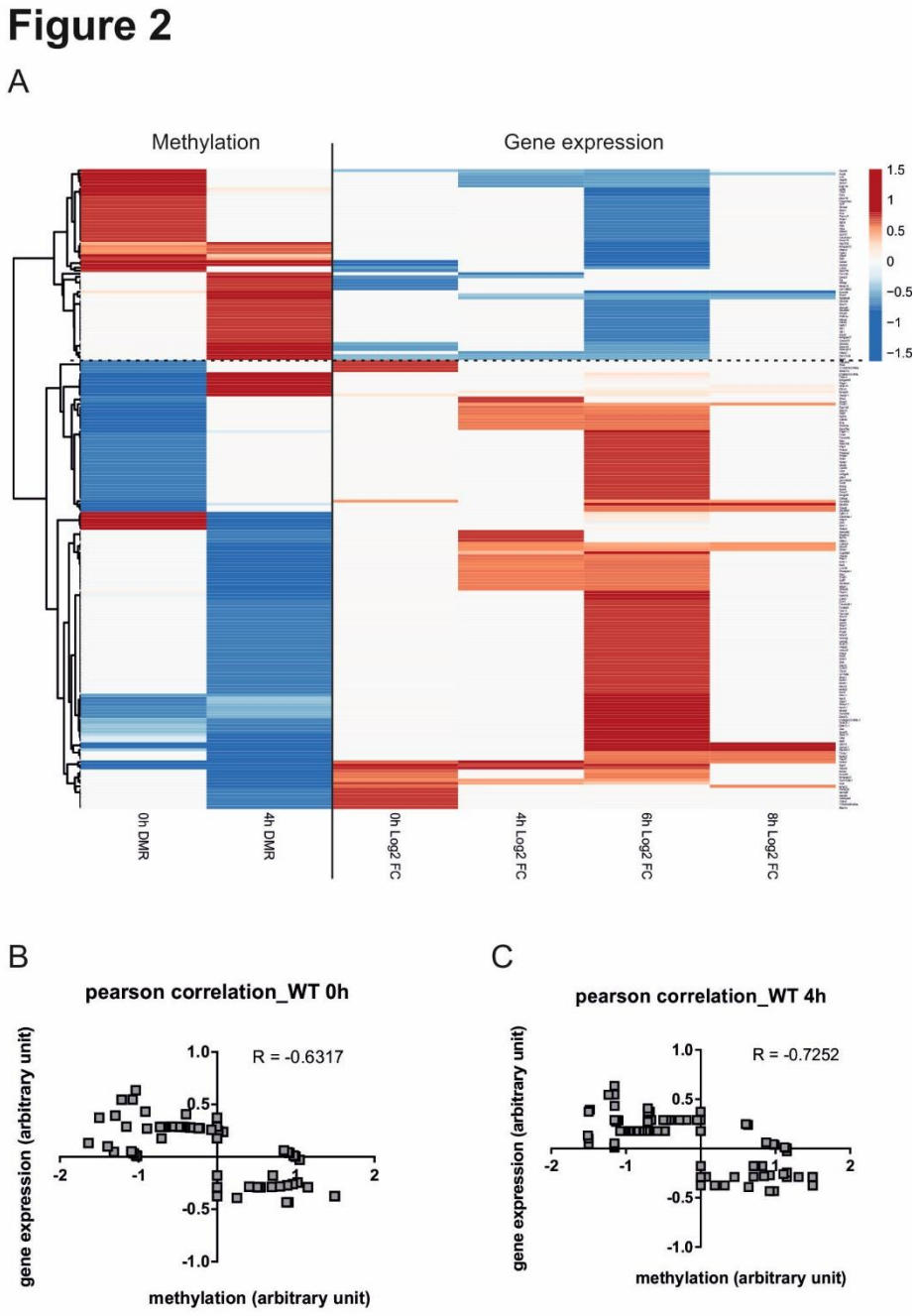

Figure 2: Acute exercise lead mostly to hypomethylation and gene induction

A): Heatmap of all genes in acute exercised WT animals found to be significant at either 0h or 4h post exercise at methylation level or at any time point in the RNAseq data, 0h, 4h, 6h and 8h. Straight line separates methylation from gene expression. Dotted line indicates clusters. Scale is according to processed values by the ClustVis software (Metsalu and Vilo, 2015), hypermethylation and gene upregulation are red, hypomethylation and gene downregulation blue, white corresponds to no data.

B-C): Pearson correlation calculated by processed values from the heatmap for WT 0h (B) DMRs with RNAseq 6h time point and WT 4h (C) respectively.

Figure 3

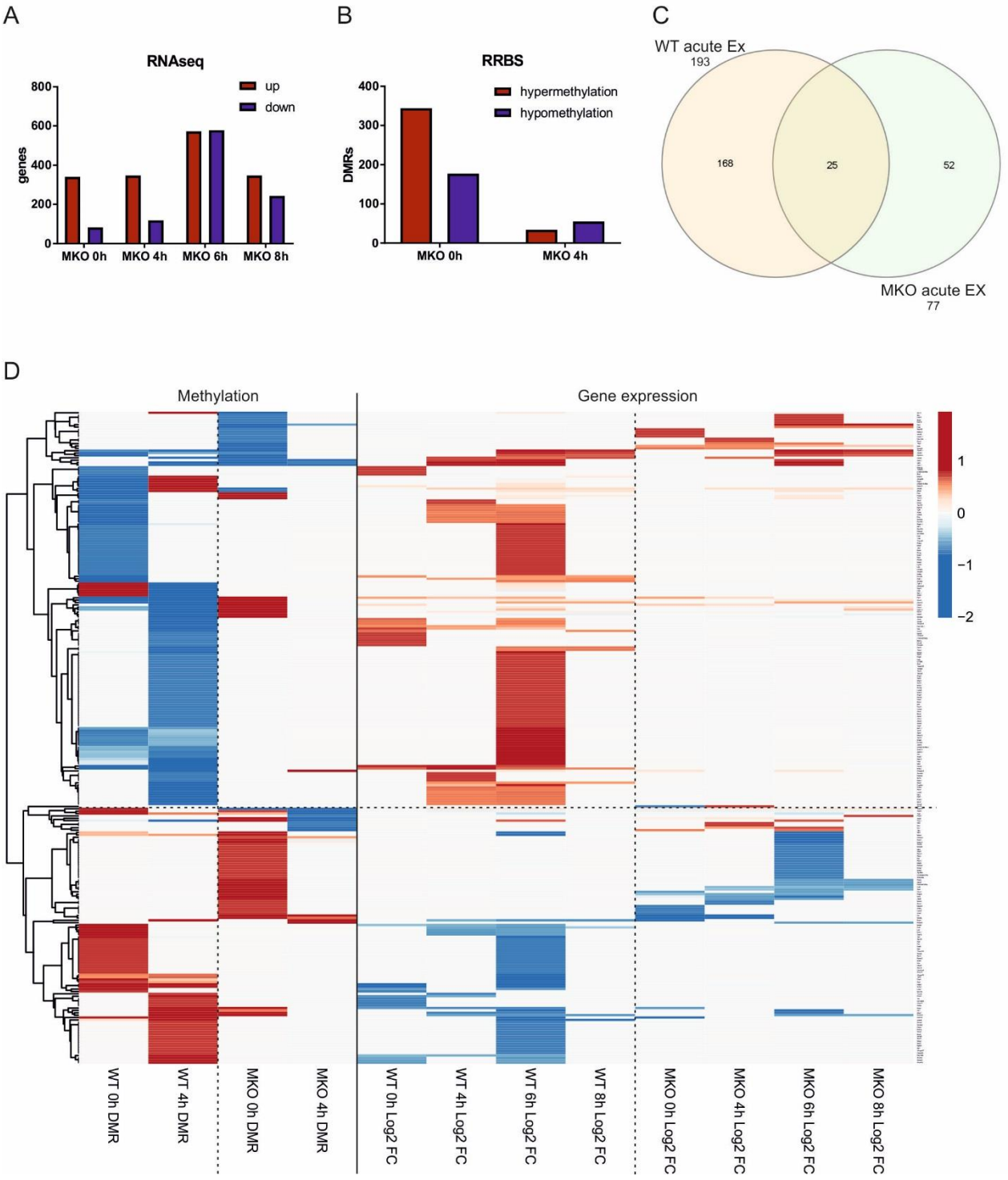
A
RNAseq
up
down
genes
800
600
400
200
0
MKO 0h
MKO 4h
MKO 6h
MKO 8h
B
RRBS
hypermethylation
hypomethylation
DMRs
400
300
200
100
0
MKO 0h
MKO 4h
C
WT acute Ex
193
168
25
52
MKO acute EX
77
D
Methylation
Gene expression
1
0
−1
−2
WT 0h DMR
WT 4h DMR
MKO 0h DMR
MKO 4h DMR
WT 0h Log2 FC
WT 4h Log2 FC
WT 6h Log2 FC
WT 8h Log2 FC
MKO 0h Log2 FC
MKO 4h Log2 FC
MKO 6h Log2 FC
MKO 8h Log2 FC

Figure 3: PGC-1α plays a major role in DNA methylation and transcriptional control upon acute exercise

A): Bar graph of DE genes in muscle-specific PGC-1α knockout (MKO) mice upon acute exercise time course measured 0h, 4h, 6h or 8h post exercise. DE genes are subdivided into up- (red) and downregulated (blue). DE genes: FDR < 0.05.

B): Bar graph of DMRs in MKO mice upon acute exercise time course measured 0h or 4h post exercise. DMRs genes are subdivided into hyper- (red) and hypomethylated (blue). DMR: q-value < 0.01, ±10 methylation change.

C): Venn diagram of combined DE genes and DMRs in all acute WT animals to any time point (orange) and all acute MKO animals to any time point (green).

D): Heatmap of all genes in acute exercised WT and MKO animals to all time points. Straight line separates methylation from gene expression. Dotted line vertical separates WT and MKO mice, dotted line horizontal indicates clusters. Scale is according to processed values by the ClustVis software (Metsalu and Vilo, 2015), hypermethylation and gene upregulation are red, hypomethylation and gene downregulation blue, white corresponds to no data.

Figure 4

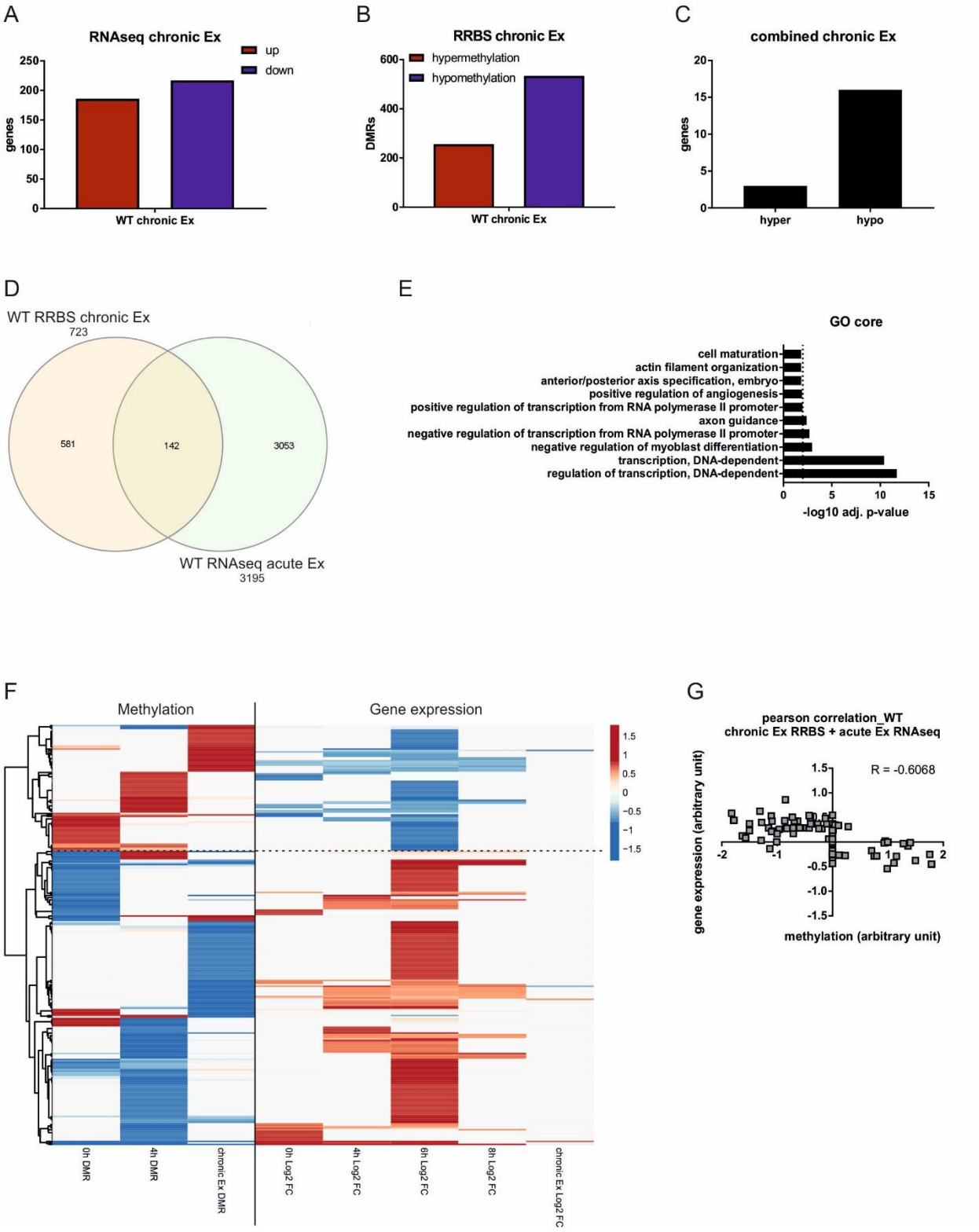
A
RNAseq chronic Ex
up
down
genes
WT chronic Ex
B
RRBS chronic Ex
hypermethylation
hypomethylation
DMRs
WT chronic Ex
C
combined chronic Ex
genes
hyper
hypo
D
WT RRBS chronic Ex
723
581
142
3053
WT RNAseq acute Ex
3195
E
GO core
cell maturation
actin filament organization
anterior/posterior axis specification, embryo
positive regulation of angiogenesis
positive regulation of transcription from RNA polymerase II promoter
axon guidance
negative regulation of transcription from RNA polymerase II promoter
negative regulation of myoblast differentiation
transcription, DNA-dependent
regulation of transcription, DNA-dependent
-log10 adj. p-value
F
Methylation
Gene expression
0h DMR
4h DMR
chronic Ex DMR
0h Log2 FC
4h Log2 FC
6h Log2 FC
8h Log2 FC
chronic Ex Log2 FC
G
pearson correlation_WT
chronic Ex RRBS + acute Ex RNAseq
R = -0.6068
gene expression (arbitrary unit)
methylation (arbitrary unit)

Figure 4: Different DNA methylation patterns upon acute and chronic exercise

A): Bar graph of DE genes in WT mice upon chronic exercise. DE genes are subdivided into up- (red) and downregulated (blue). DE genes: FDR < 0.05.

B): Bar graph of DMRs in WT mice upon chronic exercise. DMRs genes are subdivided into hyper- (red) and hypomethylated (blue). DMR: q-value < 0.01, ±10 methylation change.

C): Bar graph of combined DMRs and DE genes from chronic exercised WT mice, subdivided into hyper- and hypomethylated genes.

D): Venn diagram of combined DMRs from the chronic exercised WT group (orange) with the DE genes from the acute exercise time course (green) WT mice.

E): GO analysis of the core overlap of DMRs from the chronically trained WT mice and the acutely trained DE genes in WT mice. Top 10 GO terms are shown. X-axis: (-)log10 adjusted p-value. Dotted line represents significance: (-)log10 adjusted p-value > 2.

F): Heatmap of all genes from the acute and chronic exercised WT animals RRBS and RNAseq data. Straight line separates methylation from gene expression. Dotted line indicates clusters. Scale is according to processed values by the ClustVis software (Metsalu and Vilo, 2015), hypermethylation and gene upregulation are red, hypomethylation and gene downregulation blue, white corresponds to no data.

G): Pearson correlation calculated by processed values from the heatmap for WT chronic exercised DMRs and WT acute exercised DE genes 6h time point.

Figure 5

A

overlap	WT chronic Ex DMR	MKO chronic Ex DMR	WT 0h Log2 FC	WT 4h Log2 FC	WT 6h Log2 FC	WT 8h Log2 FC	WT chronic Ex Log2 FC	MKO 0h Log2 FC	MKO 4h Log2 FC	MKO 6h Log2 FC	MKO 8h Log2 FC	MKO chronic Ex Log2 FC
F3	-10.24	-11.94			0.78					0.73		
Oprd1	-10.40	-12.24	4.11	5.37	3.84	4.7	-2.35			1.99		
Dusp4	-11.03	-11.05		0.83	0.67					0.69		
Tmem88	-14.37	-15.04			0.73					0.52		
Eng	-14.67	-11.50		0.7	0.7						-0.34	
Ssx2ip	-17.95	-22.67			-0.51					-0.41		
Zfhx3	-19.96	-10.06			-0.59	-0.56				-0.59		
Aatk	-27.13	-12.33		0.67	1.1					0.52		
Grb10	-28.59	-31.76			-0.51	-0.6				-0.46	-0.43	
Hlx	-11.35	10.02			0.64				0.65			
Mmp11	-11.61	20.05			1.01				0.85	0.98		
Fzd5	-11.65	22.00		1.59	1.35	2.16			1.33	1.21	1.51	
Irx3	-13.74	34.31		0.95	0.62	0.87			0.94	0.8	0.91	
Lzts2	-15.19	20.96	0.48		0.43			0.49				
Zfp503	-16.81	26.56			1.28	0.76				1.16	0.75	
Klhl30	-19.64	24.17		1.16	0.9	0.74			0.88	0.57	0.48	
Fam110a	-20.95	10.87			0.88					0.62		
Zzz3	-21.02	20.70			-0.43					-0.31		
Pear1	11.78	16.63		0.63	0.93				0.53	0.7		
Casz1	42.17	-13.02			0.43						0.36	
Runx1	17.12	-10.32		1.64	0.9	1.86	-1.7		1.33			
Gltscr1	16.34	-10.79			0.44						0.48	

B

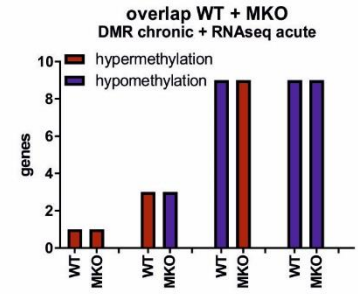

Figure 5: PGC-1α controls the distinct DNA methylation pattern upon acute and chronic exercise

A): Table of genes from the overlap of WT and MKO animals of combined chronic RRBS and acute RNAseq data. DMR (red: hypermethylation, blue: hypomethylation) and gene expression in log2 FC (red: upregulation, blue: downregulation) is indicated.

B): Bar graph of the methylation pattern detected in the overlap of WT and MKO animals of combined chronic RRBS and acute RNAseq data. red: hypermethylation, blue: hypomethylation.

Figure 6

A

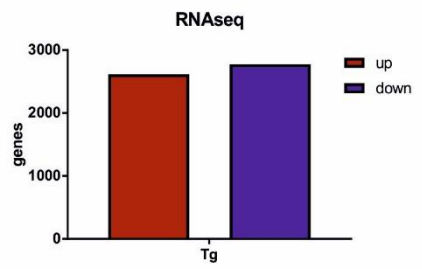

B

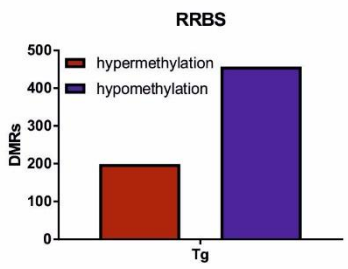

C

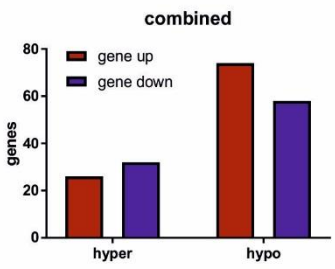

D

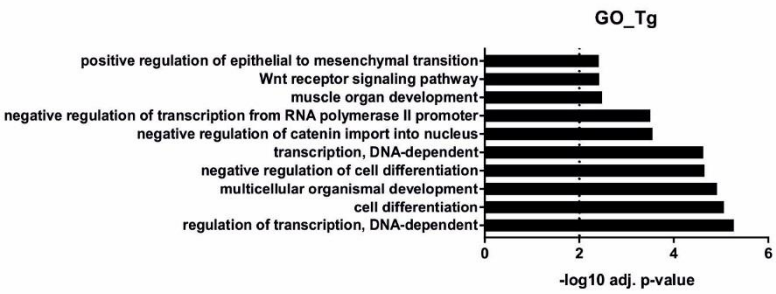

E

Tg	DMR	Log2 FC	TF
Mafa	33.17	-0.54	TF
Sik1	22.12	-0.84	
Mnt	18.67	-0.41	TF
Patz1	16.60	-0.54	TF
Zfp521	16.08	-0.51	TF
Atf4	14.57	-0.31	TF
Dab2ip	13.86	-0.43	
Tbx2	12.94	0.8	TF
Twist1	12.48	-1.24	TF
Foxp4	12.21	-0.64	TF
Zfp503	10.45	-0.69	
Scx	10.42	-1.8	TF
Satb1	-10.08	-0.96	TF
Lrpprc	-10.97	0.82	
Tbx1	-12.67	-0.58	TF
Abcg1	-12.81	0.84	
Notch3	-12.86	0.27	
Sim2	-12.98	-0.57	
Phf2	-13.56	-0.55	
Hoxc4	-14.04	-0.52	TF
Hmg20b	-15.02	1.05	TF
Srebf1	-18.31	-1.85	TF
Rara	-18.84	0.48	TF
Bmi1	-19.63	-0.47	
Axin2	-20.51	-0.42	
Lbx1	-23.87	-0.35	TF
Cbx7	-28.45	-0.33	

F

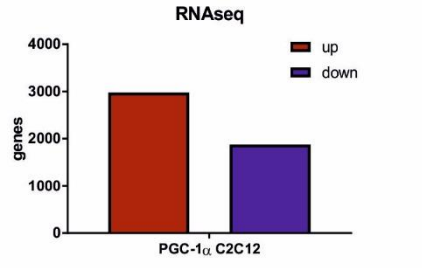

G

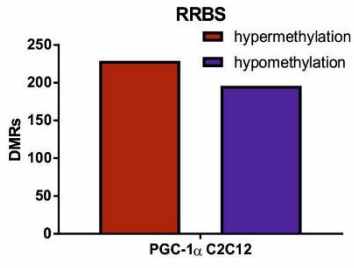

H

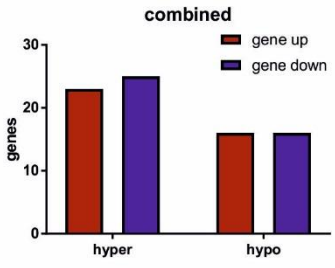

I

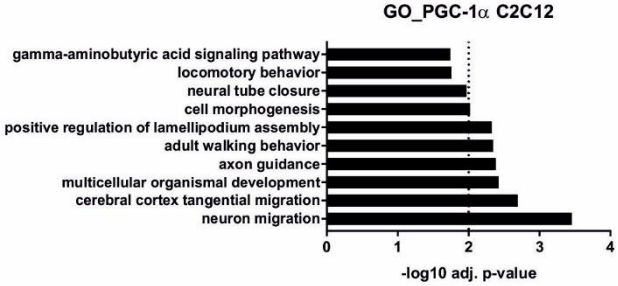

Figure 6: Skeletal muscle methylome and transcriptome is regulated by PGC-1α in vivo and in vitro

A): Bar graph of DE genes in muscle-specific PGC-1α overexpressing (Tg) mice. DE genes are subdivided into up- (red) and downregulated (blue). DE genes: FDR < 0.05.

B): Bar graph of DMRs in Tg. DMRs genes are subdivided into hyper-(red) and hypomethylated (blue). DMR: q-value < 0.01, ±10 methylation change.

C): Bar graph of combined DMRs and DE genes in Tg animals divided into hyper- and hypomethylation as well as up- (red) and downregulated (blue).

D): GO analysis of DMRs and DE genes combined in Tg animals. Top 10 GO terms are shown.

X-axis: (-)log10 adjusted p-value. Dotted line represents significance: (-)log10 adjusted p-value > 2.

D): Table of genes associated with the GO term transcriptional regulation in the Tg animals. DMR as well gene expression in log2 FC is indicated. Last column shows if the genes are transcription factors (TF), identified by Animal TFDB2.0 software (Zhang et al., 2012; Zhang et al., 2015).

F): Bar graph of DE genes C2C12 myotubes overexpressing PGC-1α. DE genes are subdivided into up- (red) and downregulated (blue). DE genes: FDR < 0.01, log2 FC </> 0.6.

G): Bar graph of DMRs in C2C12 myotubes overexpressing PGC-1α. DMRs genes are subdivided into hyper-(red) and hypomethylated (blue). DMR: q-value < 0.01, ±10 methylation change.

H): Bar graph of combined DMRs and DE genes in C2C12 myotubes overexpressing PGC-1α divided into hyper- and hypomethylation as well as up- (red) and downregulated (blue).

I): GO analysis of DMRs and DE genes combined in C2C12 myotubes overexpressing PGC-1α. Top 10 GO terms are shown. X-axis: (-)log10 adjusted p-value. Dotted line represents significance: (-)log10 adjusted p-value > 2.

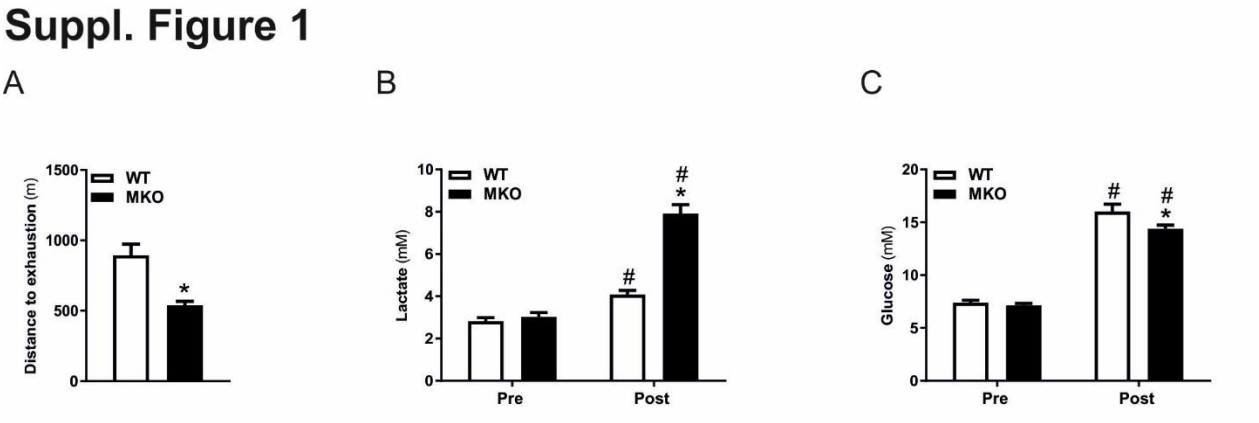

Supplemental Figure 1

A): Distance until exhaustion of acutely treadmill run WT and MKO mice.

B-C): Pre- and post-lactate (B) and –glucose (C) plasma values of acutely treadmill run WT and MKO mice.

Suppl. Figure 2

A

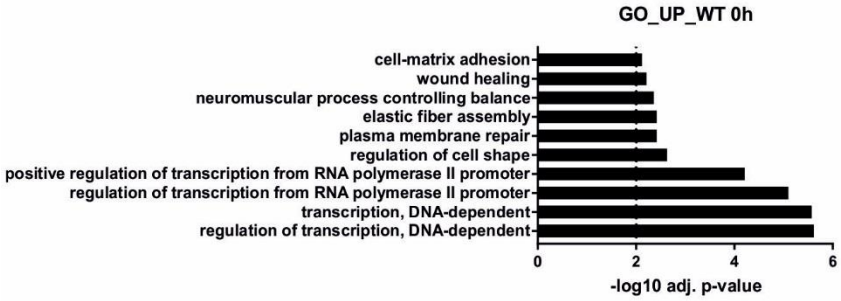

B

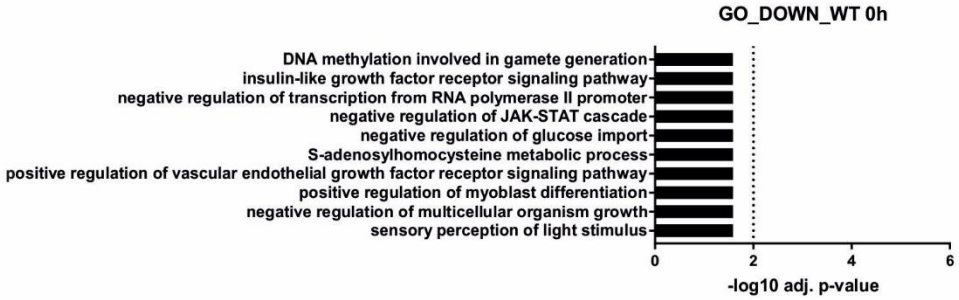

C

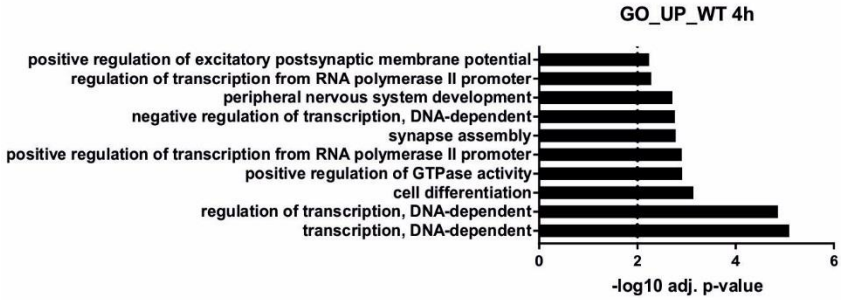

D

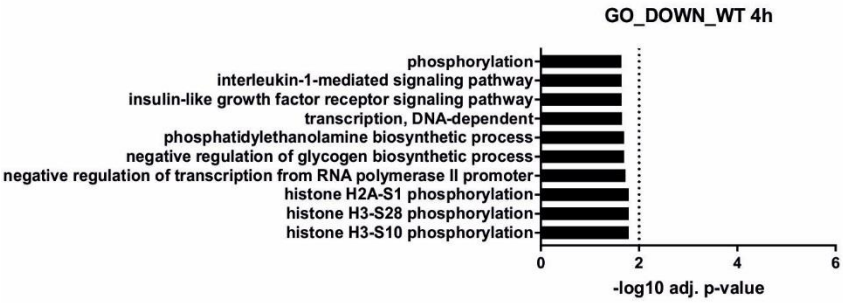

Supplemental Figure 2

A-D): GO analysis of genes from the acute exercised WT animals found in the heatmap Figure 2A. GO analysis is divided into WT 0h DMR and upregulated genes (A), WT 0h DMR and downregulated genes (B), WT 4h DMR upregulated genes (C) and WT 4h DMR downregulated genes (D). Top 10 GO terms are shown. X-axis: (-)log10 adjusted p-value. Dotted line represents significance: (-)log10 adjusted p-value > 2.

Suppl. Figure 3

A

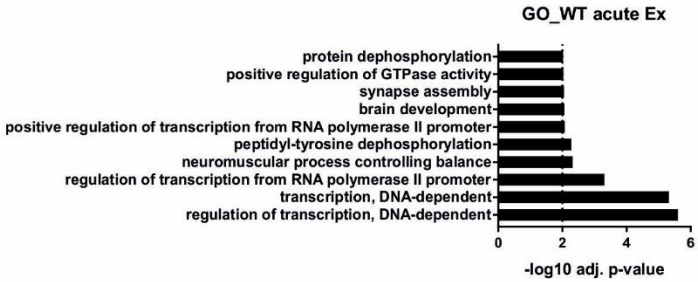

D

WT acute Ex	0h DMR	4h DMR	0h Log2 FC	4h Log2 FC	6h Log2 FC	8h Log2 FC	TF
Kctd1	25.88				1.05		
Tcf3	23.92	11.29			0.37		TF
Tgfb1	14.20	15.19			0.82		
Gata2	12.43	12.19	0.59		0.53		TF
Zfp219	12.05				0.4		TF
Rai1	11.55	10.12			0.77		
Fzd5	10.49			1.59	1.35	2.16	
Hira	10.36				-0.45		
Dedd2	10.17		0.94	0.7	0.41		
Jak3	-10.06				0.54		
Notch3	-10.30	-19.34			0.97		
Esrrg	-11.39				0.7		TF
Nr4a3	-11.47	-15.61	2.94	4.38	2.73	2.31	TF
Dnmt3a	-11.72			-0.44	-0.36		
Vgll2	-12.50			0.62	0.44		
Cebpg	-12.76				0.43		TF
Eng	-14.76			0.7	0.7		
Esrrb	-19.92				1.15		TF
Heyl	-20.79	-30.86			0.95		TF
Fzd2	-30.22				1.06		
Zzz3		-15.34			-0.43		TF
Zfp329		10.21			-0.48		TF
Tbx15		-11.82			-0.48		TF
Sox13		23.34			0.38		TF
Sox10		-15.01			1.38		TF
Rreb1		-19.70		-0.59	-0.72	-0.83	TF
Phf21a		31.55			-0.39		
Pcgf2		-48.23			0.79		
Nfatc1		-14.70		0.54			TF
Med26		-26.44	0.73				
Hspa8		-12.29		0.75	0.5		
Cbx4		-12.96			0.97		
Baz1a		-34.18	0.85				

B

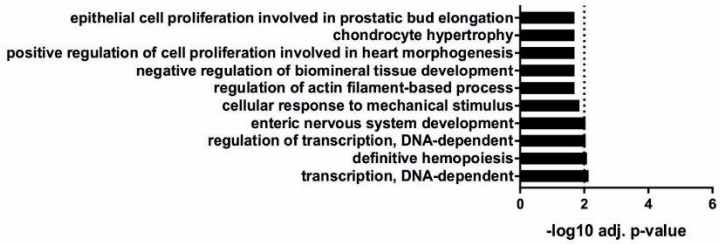

E

MKO acute Ex	0h DMR	4h DMR	0h Log2 FC	4h Log2 FC	6h Log2 FC	8h Log2 FC	TF
Hoxb3	24.63	10.77			0.98		TF
Runx1	21.86			1.33			TF
Zfp46	18.25			-0.84	-0.74		TF
Sox9	15.13	-18.49	1.24	2.59	1.04		TF
Hlx	13.31	13.89	0.65	0.65			TF
Ncor2	10.37			0.51			TF
Maff	10.15		3.54	1.57	0.72		TF
Esr1	-18.76	-13.72			-0.65	-0.61	TF
Hic1		-10.87		-0.89	0.56		TF
Mnt		-38.28		0.96			TF

C

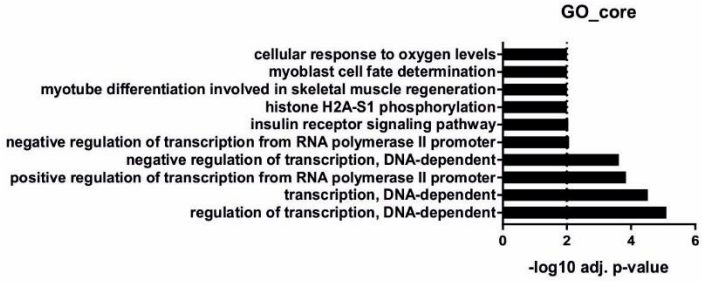

F

	WT						MKO						
overlap	0h DMR	4h DMR	0h Log2 FC	4h Log2 FC	6h Log2 FC	8h Log2 FC	0h DMR	4h DMR	0h Log2 FC	4h Log2 FC	6h Log2 FC	8h Log2 FC	TF
Tbx2	21.00	12.09			0.93		10.07	-16.52			1.15		TF
Nfatc4	13.80	14.81			1.01		21.04				0.72		TF
Casz1	-11.56	-24.18			0.43		20.65					0.36	
Zfhx3	-20.05	13.69			-0.59	-0.56	-11.87				-0.59		TF
Foxo6	-21.09				-0.59	-0.83	12.12				-0.68		TF
Zfp503	-21.55	-10.61			1.28	0.76	-11.70				1.16	0.75	
Egr3	-21.76	-22.32	4.21	3.05	3.82		13.67		4.22	1.72			TF
Gli1		15.37			1.66		11.45				1		TF
Myod1		-13.68		1.85	1.37	1.61	12.64			1.12	0.66		TF
Hdac7		18.46		0.61	0.76		13.34				0.38		
Rps6ka5		18.08		-0.72	-1.15	-1.09	12.33				-0.88	-0.63	
Agap2		-16.25			1.05	1.06	27.36					0.87	
Cdk5r1		-19.36		2.87	1.74	2.71	-21.32			1.91			

Supplemental Figure 3

A-C): GO analysis of combined data of DMRs and DE genes from acute exercised WT (A), MKO (B) and the overlap (C) identified in the Venn diagram Figure 4C. Top 10 GO terms are shown. X-axis: (-)log10 adjusted p-value. Dotted line represents significance: (-)log10 adjusted p-value > 2.

D-F): Table of genes of combined data of DMRs and DE genes from acute exercised WT (D), MKO (E) and the overlap (F) identified in the Venn diagram Figure 4C. DMR (red: hypermethylation, blue: hypomethylation) and gene expression in log2 FC (red: upregulation, blue: downregulation) is indicated. Last column shows if the genes are transcription factors (TF), identified by Animal TFDB2.0 software (Zhang et al., 2012; Zhang et al., 2015).

Suppl. Figure 4

A

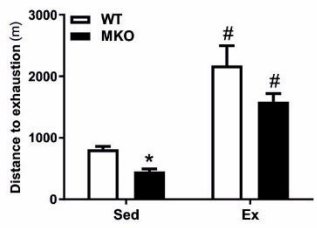

B

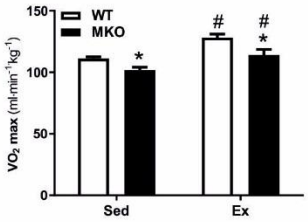

C

Genes	DMR	Log2 FC
Col6a2	17.12	-1.45
Runx1	17.12	-1.70
Slc26a10	10.03	1.84
Bcl9l	-10.04	1.30
Srebf1	-10.16	1.35
Otud1	-10.40	-2.35
Nr4a3	-10.41	-4.52
Adamtsl5	-11.12	1.48
Fndc3a	-11.72	-1.27
Ccbl2	-12.83	1.37
Vegfb	-13.08	1.27
Cdh22	-13.46	2.89
Mn1	-13.63	1.36
Glrx5	-15.75	1.27
Atp2a2	-16.14	1.46
Mn1	-17.65	1.36
Fndc3a	-21.30	-1.27
Chad	-26.37	-2.39
Impact	-27.91	-1.43

D

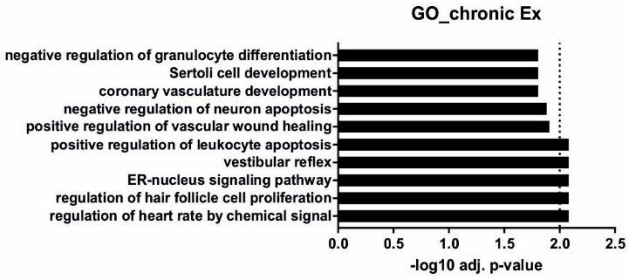

E

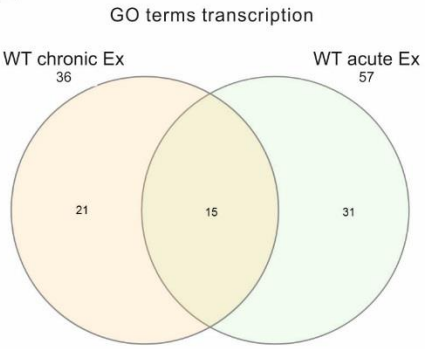

F

Genes WT chronic Ex	Genes overlap	Genes WT acute Ex
Ppp1r13l	Zfhx3	Cebpg
Hic1	Nr4a3	Tgfb1
Prrxl1	Tbx15	Notch3
Runx1	Zzz3	Vgll2
Cic	Foxo6	Zfp219
Tbx3	Esrrb	Kctd1
Hlx	Zfp503	Tbx2
Lhx6	Casz1	Esrrg
Jund	Gata2	Egr3
Ets2	Zfp329	Nfatc4
Hmg20b	Eng	Heyl
Sox9	Hira	Tcf3
Maml1	Cbx4	Dnmt3a
Zfp513	Dedd2	Rai1
Nsd1	Fzd5	Fzd2
Pkn1		Jak3
Spen		Rreb1
Zfp574		Gli1
Nfil3		Sox13
Irx3		Pcgf2
Fgfr3		Myod1
		Hdac7
		Baz1a
		Hspa8
		Sox10
		Phf21a
		Med26
		Rps6ka5
		Agap2
		Nfatc1
		Cdk5r1

G

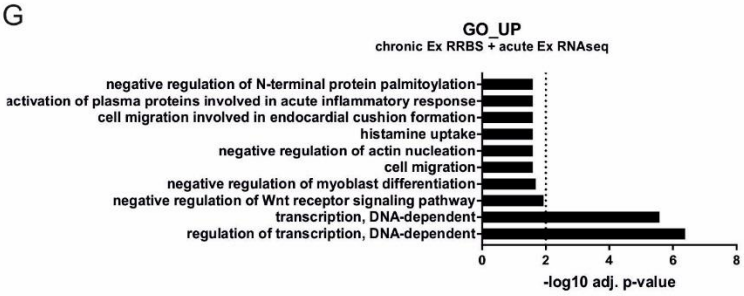

H

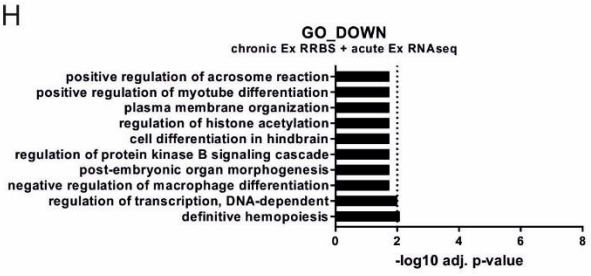

Supplemental Figure 4

A): Distance until exhaustion of sedentary (sed) and chronically trained (Ex) WT and MKO mice.

B): Maximal oxygen consumption (VO_{2max}) of sed and chronically trained (Ex) WT and MKO mice.

C): Table of genes of combined RRBS and RNAseq of the chronic excised WT animals. DMR (red: hypermethylation, blue: hypomethylation) and gene expression in log2 FC (red: upregulation, blue: downregulation) is indicated.

D): GO analysis of combined data, RRBS and RNAseq, in the chronic exercised WT mice. Top 10 GO terms are shown. X-axis: (-)log10 adjusted p-value. Dotted line represents significance: (-)log10 adjusted p-value > 2.

E): Venn diagram of all genes found in the top 10 GO terms associated with transcriptional regulation in the combined data of DMRs from WT chronic trained mice(orange) with the RNAseq from the acute exercise time course (green).

F): Table of genes associated with the GO term transcription identified in the Venn diagram from Suppl. Figure 3E.

G-H): GO analysis of combined data of DMRs from WT chronic trained mice with the RNAseq from the acute exercise time course divided into up- (G) and downregulated (H) genes identified in the heatmap Figure 3F. Top 10 GO terms are shown. X-axis: (-)log10 adjusted p-value. Dotted line represents significance: (-)log10 adjusted p-value > 2.

Suppl. Figure 5

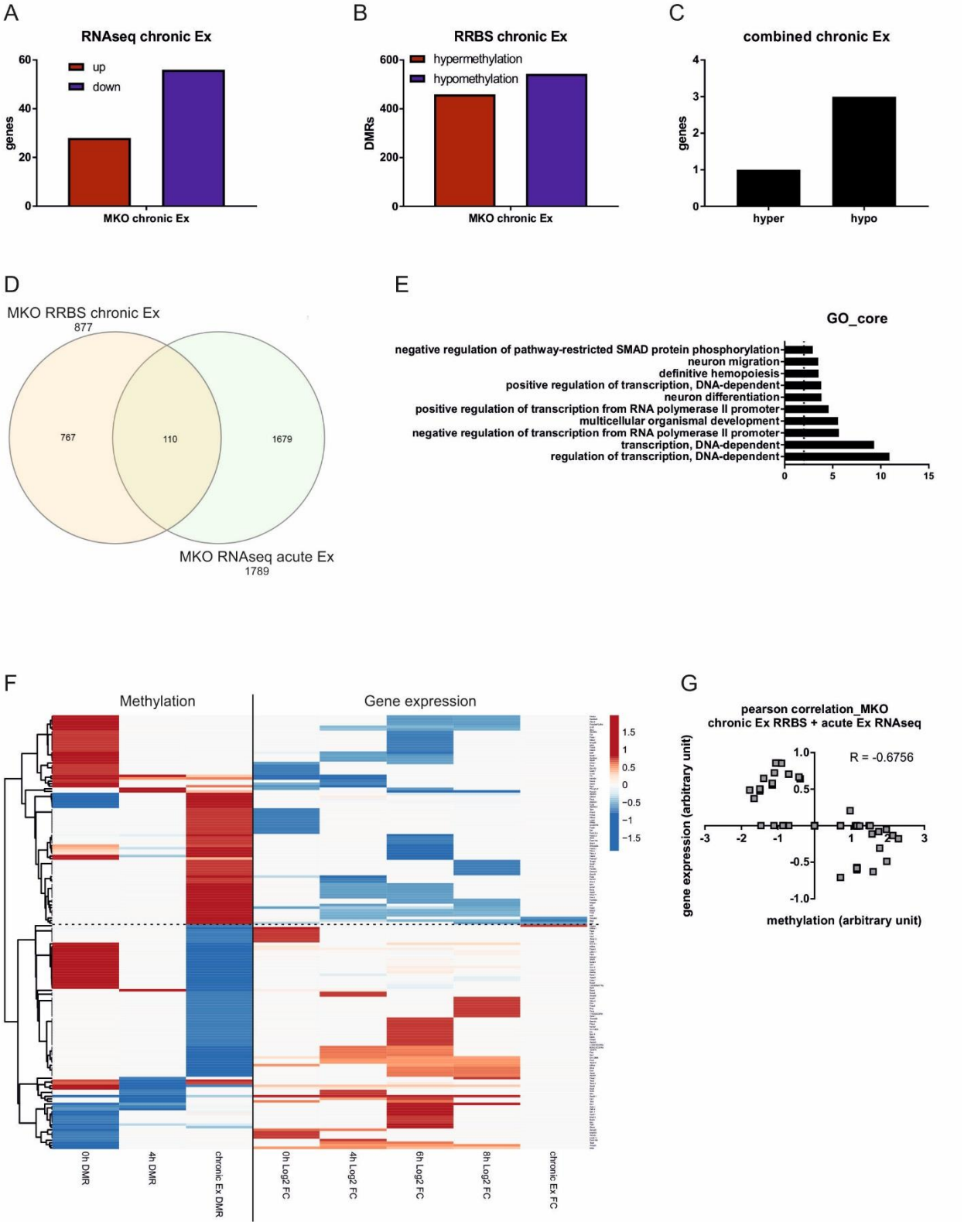

Supplemental Figure 5

A): Bar graph of DE genes in MKO mice upon chronic exercise. DE genes are subdivided into up- (red) and downregulated (blue). DE genes: FDR < 0.05.

B): Bar graph of DMRs in MKO mice upon chronic exercise. DMRs genes are subdivided into hyper- (red) and hypomethylated (blue). DMR: q-value < 0.01, ±10 methylation change.

C): Bar graph of combined DMRs and DE genes from chronic exercised MKO mice, subdivided into hyper- and hypomethylated genes.

D): Venn diagram of combined DMRs from the chronic exercised MKO group (orange) with the DE genes from the acute exercise time course (green) MKO mice.

E): GO analysis of the core overlap of DMRs from the chronically trained MKO mice and the acutely trained DE genes in MKO mice. Top 10 GO terms are shown. X-axis: (-)log10 adjusted p-value. Dotted line represents significance: (-)log10 adjusted p-value > 2.

F): Heatmap of all genes from the acute and chronic exercised MKO animals RRBS and RNAseq data. Straight line separates methylation from gene expression. Dotted line indicates clusters. Scale is according to processed values by the ClustVis software (Metsalu and Vilo, 2015), hypermethylation and gene upregulation are red, hypomethylation and gene downregulation blue, white corresponds to no data.

G): Pearson correlation calculated by processed values from the heatmap for MKO chronic exercised DMRs and MKO acute exercised DE genes 6h time point.

Discussion

Several studies reported a link of transcriptional adaptations to environmental stimuli with epigenetic changes as DNA methylation (Barres et al., 2012; Kanzleiter et al., 2015; Lochmann et al., 2015a; Nitert et al., 2012). Especially exercise seems to have not only a large impact on the transcriptome but also on the methylome following acute and chronic endurance as well as resistance exercise (Barres et al., 2012; Kanzleiter et al., 2015; Ntanasis-Stathopoulos et al., 2013; Seaborne et al., 2018; Sharples et al., 2016; Voisin et al., 2015). However, the connection of DNA methylation, transcriptional changes, potential muscle memory and a key mediator of all those alterations could not be defined yet.

Our data show the first time distinct transcriptome and methylome profiles in acute and chronic exercise. We observed strong DNA methylation alteration after chronic exercise but only mild gene expression changes. However, the overlap with the acutely measured transcriptome was large. Thus, we hypothesize that chronic exercise might induce muscle memory marks on the DNA, hence allowing a quicker exercise-induced transcriptional response. Nevertheless, further studies need to be done to prove the concept of muscle memory subsequent to chronic training either by training-detraining-retraining studies or by a final time course exhaustion test after the chronic exercise period to evaluate the transcriptional profile of acute exercise-induced genes to chronically induced genomic alterations. Furthermore, our results show strong involvement of PGC-1α on the transcriptome and the methylome by altered transcriptional response in the MKO mice after exercise. So far, most studies elucidated the impact of DNA methylation on PGC-1α and its target genes and whether the effects can be altered by exercise stimulus (Barres et al., 2012; Lochmann et al., 2015a). We could now discover that PGC-1α not only regulate transcription by multiple TF usage (Handschin and Spiegelman, 2006; Kupr and Handschin, 2015) but in addition, is able to manipulate DNA methylation of its target genes. This new knowledge helps to dissect further the complex network controlled by PGC-1α and to identify pathways regulated by this coactivator under different contexts, which can be used specifically for therapeutic treatments. In a next step, the role of PGC-1α on the regulation of the methylation enzymes, the DNA methyltransferases (DNMTs) and the Ten-Eleven-Translocation oxygenases (TETs) should be evaluated. Combined approaches of exercise studies with altered DNMT or TET activities by pharmacological treatment or plasmid electroporation in different PGC-1α background mice would reveal the influence of PGC-1α on the enzymes and the impact on the methylome and the transcriptome under stimulated conditions. Even more, we observed acute and chronic exercise-induced hyper- and hypomethylation, which was correlated with gene repression and gene induction, respectively. In majority, we detected hypomethylation and gene activation after exercise, going in line with current literature (Barres et al., 2012; Kanzleiter et al., 2015). Remarkably, this effect was shifted towards hypermethylation and gene repression in the MKO mice following acute or chronic

exercise, showing once more the importance of PGC-1α in a normal exercise response. To further point the significance of PGC-1α in the regulation of the methylome and the transcriptome, a muscle memory setup should be performed with the MKO mice to elucidate, whether they are able to generate muscle memory to the same extend as WT animals. Thus, chronic training followed by detraining and retraining should be performed and the transcriptome analyzed in WT and MKO mice combined with morphological and functional readouts. Finally, we could demonstrate in gain-of-function models of PGC-1α *in vivo* and *in vitro* significantly altered DNA methylation and gene expression, implicating the regulatory role of PGC-1α on those mechanisms in skeletal muscle.

Our data provide new insides into the close correlation of exercise, transcription and epigenetics. The importance of the exercise intervention, acute versus chronic, as well as the time dependency of DNA methylation and transcriptional output is an important feature, which has to be considered also in future studies. Even more, we could show that chronic endurance exercise might lead to muscle memory by foot printing the genome by methylation. Finally, we discovered PGC-1α as a major player in the controlled and regulated muscle adaptation leading to SKM plasticity by transcription and methylation manipulation following acute and chronic exercise. These new aspects in the control of molecular mechanisms in SKM by diverse exercise conditions and PGC-1α will help to adjust interventions and treatments used against metabolic disease or to cure patients with myopathies and sarcopenia.

Materials and Methods

Animals

Experiments were performed with the approval of the Swiss authorities on adult male mice (15-20 weeks old) for all the experiment and n = 5-6 per condition. Mice had free access to food and water and were housed in a conventional facility with a 12 h light/12 h dark cycle. The PGC-1α muscle-specific knockout (MKO) mice used in this study were generated as described in (Handschin et al., 2007a) and floxed littermates were used as controls (WT). Additionally, the PGC-1α muscle-specific overexpression (Tg) mice, generated and described in (Lin et al., 2002b) and their littermates as WT controls were used.

Exercise training protocols

For the acute exercise time course study, mice were acclimatized to treadmill running (Columbus Instruments) as described in Table 1 of the Supplemental Material. Two days after acclimatization, the test started at 0 m/min for 5 min, 5 m/min for 5 min and 8 m/min for 5 min with a 5° incline and the speed was increased 2 m/min every 15 min until 26 m/min and exhaustion. Blood lactate and glucose were measured from tail blood with a lactate plus meter (Nova Biomedical, Labor-Systeme Flükiger AG) or glucose meter

(Accu-Chek, Roche), respectively, before and after the treadmill test. Immediately (0h), 4h, 6h and 8h after the test mice were killed by CO_2 and tissues collected. Sedentary mice were not exposed to any treadmill running.

For chronic training, mice were acclimatized to treadmill running and treadmill training was carried out 5 times a week for four weeks as described in Table 2A and B of the Supplemental Material. Endurance capacity of the mice was determined on an open treadmill as described above. VO_2max was measured in a closed treadmill (Columbus Instruments) and the test started at 0 m/min for 5 min and 10 m/min for 3 min with a 15° incline and the speed was increased 2 m/min every 3 min until exhaustion. Chronically trained mice were killed by CO_2 18h after the last training session and organs were removed.

Cell culture

C2C12 myoblasts were grown in proliferation medium (GM) (DMEM, 10% FetalClone Serum [FCS, SH30066.03, GE Healthcare Life Sciences], 1% Penicillin/Streptomycin [15140122, Thermo Scientific]) until confluency and then medium was switched to differentiation medium (DM) (DMEM, 2% horse serum [HS, 16050122, Thermo Scientific]) for 4 days. Myotubes were infected with adenoviral (AD) GFP control or PGC-1α-Flag for 24h, and then the infection medium was changed to differentiation medium for 24h before cells were collected according to the experiment, which will be performed.

Genomic DNA isolation

Around 15mg of powdered Quadriceps (Quad) muscle was used for genomic DNA (gDNA) isolation. Tissue was digested overnight in proteinase K (20mg/ml) (V302, Promega) and DNA lysis buffer (50mM Tris-HCl pH-8.0, 100mM NaCl, 10mM EDTA, 0.5% Nonidet P-40) at 55°C on a shaker. Next day proteinase K was inactivated at 95°C for 10min. Phenol-chloroform-isoamyl alcohol (PCI) (P3803, Sigma-Aldrich) was added in a 1:1 ratio. Sample was vortexed and centrifuged at room temperature (RT), 13000rpm, 4min. Upper phase was collected and same amount of PCI as in the first step added, vortexed and centrifuged as described above. Upper phase was collected. 1/10 volume 3M Na-Acetate pH 5.0 and 6/10 volume Isopropanol was added. Vortex and let sit at RT for 5min. Centrifuge at RT, 15min and maximum speed (20000rpm). Keep pellet and wash with 70% ethanol and centrifuge again at RT, 5min, maximum speed. Pellet was dried for 10min at RT and then resuspended nuclease free H2O. DNA quality and concentration was measured with a NanoDrop OneC spectrophotometer (Thermo Scientific). The isolated gDNA was further purified according to manufacturer's protocol (DNeasy Blood & Tissue Kit, 69504, Qiagen). gDNA quality and concentration was measured by NanoDrop OneC spectrophotometer (Thermo Scientific).

C2C12 myotubes were collected by trypsin and centrifugation to collect cell pellet. gDNA was isolated by the QIAamp DNA Mini Kit (#51304, Qiagen) according to the manufacturers protocol. The level and quality of isolated gDNA was measured with a NanoDrop OneC spectrophotometer (Thermo Scientific).

Reduced Representation Bisulfite Sequencing (RRBS) library and sequencing

RRBS library was performed with the Premium Reduced Representation Bisulfite Sequencing Kit (C02030032, Diagenode) according to the manufacturer's instructions. 100ng of gDNA was used as starting material. Quality and fragment size was checked by Bioanalyzer (Agilent) measurements. Single read sequencing was performed with a HiSeq2500 machine (51 cycles, Illumina).

RRBS analysis

The reads were quality- and adapter trimmed with the Trim Galore! wrapper of cutadapt (Martin, 2011). The trimmed reads were controlled with FastQC (http://www.bioinformatics.bbsrc.ac.uk/projects/fastqc/). Conversion rates were calculated with custom scripts, counting the amount of G's and C's in non-GC context resulting in values above 99% for all libraries. The reads were mapped to the mm10 version of the mouse genome with BWA (Li and Durbin, 2009) and methylCtools (Hovestadt et al., 2014) after why a slightly extended Bis-SNP pipeline (Liu et al., 2012). The reads were locally realigned and the quality values were recalibrated before calling the methylation levels. The mm10 SNPs and InDels from dbSNP v138 (Smigielski et al., 2000) was used in this process. An initial quality control and exploratory analysis was done with R package RnBeads (Assenov et al., 2014). Differential loci was detected with MethylKit (Akalin et al., 2012) testing in 500bp sliding windows with at least 3 CpGs, only including those with a coverage of at least 10x. Differentially methylated regions (DMR) were defined as +/- 10% with a q-value > 0.01.

mRNA sequencing and analysis

Total RNA was isolated from Quadriceps muscle with TRI reagent (T9424, Sigma) according to the manufacturer's instructions. RNA concentration was measured with a NanoDrop OneC spectrophotometer (Thermo Scientific). 7500 ng RNA was further purified with the Direct-zol RNA MiniPrep Kit (R2050, Zymo Research) according to the manufacturer's instructions. For RNAseq library preparation, 1 µg of purified RNA was used and libraries prepared with the TruSeq RNA library Prep Kit (Illumina) according to the manufacturer's instructions. Single read sequencing was performed with a HighSeq 2500 machine (50 cycles, Illumina). Fastq files were mapped to the mouse genome (mm10) and RNAseq and statistical analysis performed with the CLC Genomics Workbench Software (Qiagen).

Venn diagram, gene ontology, heatmap analysis, Pearson correlation

Differentially expressed (DE) genes, DMRs or the combination of both analysis were pictured in a Venn diagram with the use of the interactiVenn web-based tool (Heberle et al., 2015). Gene ontology (GO) analysis was executed by the usage of GeneCodis (Carmona-Saez et al., 2007; Nogales-Cadenas et al., 2009; Tabas-Madrid et al., 2012). Enriched GO terms were furthermore sorted by (-)log10 adjusted p-value. Dotted line represents significance, (-)log10 adjusted p-value > 2. Heatmap was conducted by ClustVis (Metsalu and Vilo, 2015) using standard parameters and average Pearson correlation for data clustering. Processed values from the heatmap software were used to evaluate Pearson correlation by GraphPad Prism 7. For RNAseq data from acute exercise time course the 6h time point was chosen due to highest level of DE genes.

Statistical analysis

Values are expressed as means ± standard errors of the means (SEM) and statistical significance was determined with unpaired two tailed t-tests using Excel software. An asterisk (*) indicates significant differences between genotypes or the conditions.

Supplemental Material

Table 1. Acclimatization protocol for treadmill running of acute time course study at 5° inclination.

Day 1	5 min 0 m/min	5 min 5 m/min	5 min 8 m/min	10 min 10 m/min		
Day 2	5 min 0 m/min	5 min 5 m/min	5 min 8 m/min	15 min 10 m/min	5 min 12 m/min	
Day 3	5 min 0 m/min	5 min 5 m/min	5 min 8 m/min	15 min 10 m/min	5 min 12 m/min	2 min 14 m/min
Day 4	5 min 0 m/min	5 min 5 m/min	5 min 8 m/min	15 min 10 m/min	10 min 12 m/min	2 min 14 m/min
Day 5	5 min 0 m/min	5 min 5 m/min	5 min 8 m/min	15 min 10 m/min	10 min 12 m/min	5 min 14 m/min

Table 2A. Acclimatization protocol for treadmill running of chronically trained mice.

Day 1	0° inclination	5 min 0 m/min	5 min 5 m/min	5 min 8 m/min	5 min 10 m/min
Day 2	5° inclination	5 min 0 m/min	5 min 5 m/min	5 min 8 m/min	5 min 10 m/min

Table 2B. Training protocol for chronic treadmill exercise.

	Day 1	**Day 2**	**Day 3**	**Day 4**	**Day 5**
Week 1	10 m/min	10.5 m/min	11 m/min	11.5 m/min	12 m/min
Week 2	12.5 m/min	13 m/min	13.5 m/min	14 m/min	14.5 m/min
Week 3	15 m/min	15.5 m/min	16 m/min	16.5 m/min	17 m/min
Week 4	17.5 m/min	18 m/min	18.5 m/min	Rest	Exercise test
Week 5	Exercise test	18.5 m/min	18.5 m/min	Sacrifice	

References

Akalin, A., Kormaksson, M., Li, S., Garrett-Bakelman, F.E., Figueroa, M.E., Melnick, A., and Mason, C.E. (2012). methylKit: a comprehensive R package for the analysis of genome-wide DNA methylation profiles. Genome biology *13*, R87.

Akimoto, T., Pohnert, S.C., Li, P., Zhang, M., Gumbs, C., Rosenberg, P.B., Williams, R.S., and Yan, Z. (2005). Exercise stimulates Pgc-1alpha transcription in skeletal muscle through activation of the p38 MAPK pathway. The Journal of biological chemistry *280*, 19587-19593.

Assenov, Y., Muller, F., Lutsik, P., Walter, J., Lengauer, T., and Bock, C. (2014). Comprehensive analysis of DNA methylation data with RnBeads. Nature methods *11*, 1138-1140.

Bajpeyi, S., Covington, J.D., Taylor, E.M., Stewart, L.K., Galgani, J.E., and Henagan, T.M. (2017). Skeletal Muscle PGC1α −1 Nucleosome Position and −260 nt DNA Methylation Determine Exercise Response and Prevent Ectopic Lipid Accumulation in Men. Endocrinology *158*, 2190-2199.

Barres, R., Osler, M.E., Yan, J., Rune, A., Fritz, T., Caidahl, K., Krook, A., and Zierath, J.R. (2009). Non-CpG methylation of the PGC-1alpha promoter through DNMT3B controls mitochondrial density. Cell metabolism *10*, 189-198.

Barres, R., Yan, J., Egan, B., Treebak, J.T., Rasmussen, M., Fritz, T., Caidahl, K., Krook, A., O'Gorman, D.J., and Zierath, J.R. (2012). Acute exercise remodels promoter methylation in human skeletal muscle. Cell metabolism *15*, 405-411.

Bruusgaard, J.C., Johansen, I.B., Egner, I.M., Rana, Z.A., and Gundersen, K. (2010). Myonuclei acquired by overload exercise precede hypertrophy and are not lost on detraining. Proceedings of the National Academy of Sciences of the United States of America *107*, 15111-15116.

Canto, C., Gerhart-Hines, Z., Feige, J.N., Lagouge, M., Noriega, L., Milne, J.C., Elliott, P.J., Puigserver, P., and Auwerx, J. (2009). AMPK regulates energy expenditure by modulating NAD+ metabolism and SIRT1 activity. Nature *458*, 1056-1060.

Canto, C., Jiang, L.Q., Deshmukh, A.S., Mataki, C., Coste, A., Lagouge, M., Zierath, J.R., and Auwerx, J. (2010). Interdependence of AMPK and SIRT1 for metabolic adaptation to fasting and exercise in skeletal muscle. Cell metabolism *11*, 213-219.

Carmona-Saez, P., Chagoyen, M., Tirado, F., Carazo, J.M., and Pascual-Montano, A. (2007). GENECODIS: a web-based tool for finding significant concurrent annotations in gene lists. Genome biology *8*, R3.

Colberg, S.R., Sigal, R.J., Fernhall, B., Regensteiner, J.G., Blissmer, B.J., Rubin, R.R., Chasan-Taber, L., Albright, A.L., Braun, B., American College of Sports, M., et al. (2010). Exercise and type 2 diabetes: the American College of Sports Medicine and the American Diabetes Association: joint position statement. Diabetes Care *33*, e147-167.

Egan, B., and Zierath, J.R. (2013). Exercise metabolism and the molecular regulation of skeletal muscle adaptation. Cell metabolism *17*, 162-184.

Gill, J.F., Santos, G., Schnyder, S., and Handschin, C. (2018). PGC-1alpha affects aging-related changes in muscle and motor function by modulating specific exercise-mediated changes in old mice. Aging cell *17*.

Gundersen, K. (2016). Muscle memory and a new cellular model for muscle atrophy and hypertrophy. The Journal of experimental biology *219*, 235-242.

Handschin, C., Chin, S., Li, P., Liu, F., Maratos-Flier, E., Lebrasseur, N.K., Yan, Z., and Spiegelman, B.M. (2007). Skeletal muscle fiber-type switching, exercise intolerance, and myopathy in PGC-1alpha muscle-specific knock-out animals. The Journal of biological chemistry *282*, 30014-30021.

Handschin, C., and Spiegelman, B.M. (2006). Peroxisome proliferator-activated receptor gamma coactivator 1 coactivators, energy homeostasis, and metabolism. Endocrine reviews *27*, 728-735.

Haskell, W.L., Lee, I.M., Pate, R.R., Powell, K.E., Blair, S.N., Franklin, B.A., Macera, C.A., Heath, G.W., Thompson, P.D., Bauman, A., et al. (2007). Physical activity and public health: updated recommendation for adults from the American College of Sports Medicine and the American Heart Association. Circulation *116*, 1081-1093.

Heberle, H., Meirelles, G.V., da Silva, F.R., Telles, G.P., and Minghim, R. (2015). InteractiVenn: a web-based tool for the analysis of sets through Venn diagrams. BMC bioinformatics *16*, 169.

Hovestadt, V., Jones, D.T., Picelli, S., Wang, W., Kool, M., Northcott, P.A., Sultan, M., Stachurski, K., Ryzhova, M., Warnatz, H.J., et al. (2014). Decoding the regulatory landscape of medulloblastoma using DNA methylation sequencing. Nature *510*, 537-541.

Jager, S., Handschin, C., St-Pierre, J., and Spiegelman, B.M. (2007). AMP-activated protein kinase (AMPK) action in skeletal muscle via direct phosphorylation of PGC-1alpha. Proceedings of the National Academy of Sciences of the United States of America *104*, 12017-12022.

Jones, P.A., and Takai, D. (2001). The role of DNA methylation in mammalian epigenetics. Science *293*, 1068-1070.

Kang, S., Bajnok, L., Longo, K.A., Petersen, R.K., Hansen, J.B., Kristiansen, K., and MacDougald, O.A. (2005). Effects of Wnt signaling on brown adipocyte differentiation and metabolism mediated by PGC-1alpha. Molecular and cellular biology *25*, 1272-1282.

Kanzleiter, T., Jahnert, M., Schulze, G., Selbig, J., Hallahan, N., Schwenk, R.W., and Schurmann, A. (2015). Exercise training alters DNA methylation patterns in genes related to muscle growth and differentiation in mice. Am J Physiol Endocrinol Metab *308*, E912-920.

Kupr, B., and Handschin, C. (2015). Complex Coordination of Cell Plasticity by a PGC-1alpha-controlled Transcriptional Network in Skeletal Muscle. Frontiers in physiology *6*, 325.

Law, T.D., Clark, L.A., and Clark, B.C. (2016). Resistance Exercise to Prevent and Manage Sarcopenia and Dynapenia. Annu Rev Gerontol Geriatr *36*, 205-228.

Li, H., and Durbin, R. (2009). Fast and accurate short read alignment with Burrows-Wheeler transform. Bioinformatics (Oxford, England) *25*, 1754-1760.

Lin, J., Handschin, C., and Spiegelman, B.M. (2005). Metabolic control through the PGC-1 family of transcription coactivators. Cell metabolism *1*, 361-370.

Lin, J., Wu, H., Tarr, P.T., Zhang, C.Y., Wu, Z., Boss, O., Michael, L.F., Puigserver, P., Isotani, E., Olson, E.N., et al. (2002). Transcriptional co-activator PGC-1 alpha drives the formation of slow-twitch muscle fibres. Nature *418*, 797-801.

Lindholm, M.E., Giacomello, S., Werne Solnestam, B., Fischer, H., Huss, M., Kjellqvist, S., and Sundberg, C.J. (2016). The Impact of Endurance Training on Human Skeletal Muscle Memory, Global Isoform Expression and Novel Transcripts. PLoS genetics *12*, e1006294.

Liu, Y., Siegmund, K.D., Laird, P.W., and Berman, B.P. (2012). Bis-SNP: combined DNA methylation and SNP calling for Bisulfite-seq data. Genome biology *13*, R61.

Lochmann, T.L., Thomas, R.R., Bennett, J.P., Jr., and Taylor, S.M. (2015a). Epigenetic Modifications of the PGC-1alpha Promoter during Exercise Induced Expression in Mice. PLoS One *10*, e0129647.

Lochmann, T.L., Thomas, R.R., Bennett, J.P., and Taylor, S.M. (2015b). Epigenetic Modifications of the PGC-1α Promoter during Exercise Induced Expression in Mice. PLoS ONE *10*, e0129647.

Martin, M. (2011). Cutadapt removes adapter sequences from high-throughput sequencing reads. EMBnet.journal *17*.

Metsalu, T., and Vilo, J. (2015). ClustVis: a web tool for visualizing clustering of multivariate data using Principal Component Analysis and heatmap. Nucleic acids research *43*, W566-570.

Mutin-Carnino, M., Carnino, A., Roffino, S., and Chopard, A. (2014). Effect of muscle unloading, reloading and exercise on inflammation during a head-down bed rest. International journal of sports medicine *35*, 28-34.

Nitert, M.D., Dayeh, T., Volkov, P., Elgzyri, T., Hall, E., Nilsson, E., Yang, B.T., Lang, S., Parikh, H., Wessman, Y., et al. (2012). Impact of an exercise intervention on DNA methylation in skeletal muscle from first-degree relatives of patients with type 2 diabetes. Diabetes *61*, 3322-3332.

Nogales-Cadenas, R., Carmona-Saez, P., Vazquez, M., Vicente, C., Yang, X., Tirado, F., Carazo, J.M., and Pascual-Montano, A. (2009). GeneCodis: interpreting gene lists through enrichment analysis and integration of diverse biological information. Nucleic acids research *37*, W317-322.

Ntanasis-Stathopoulos, J., Tzanninis, J.G., Philippou, A., and Koutsilieris, M. (2013). Epigenetic regulation on gene expression induced by physical exercise. Journal of musculoskeletal & neuronal interactions *13*, 133-146.

Phillips, B.A., and Mastaglia, F.L. (2000). Exercise therapy in patients with myopathy. Current opinion in neurology *13*, 547-552.

Puigserver, P., Rhee, J., Lin, J., Wu, Z., Yoon, J.C., Zhang, C.Y., Krauss, S., Mootha, V.K., Lowell, B.B., and Spiegelman, B.M. (2001). Cytokine stimulation of energy expenditure through p38 MAP kinase activation of PPARgamma coactivator-1. Molecular cell *8*, 971-982.

Puigserver, P., Wu, Z., Park, C.W., Graves, R., Wright, M., and Spiegelman, B.M. (1998). A cold-inducible coactivator of nuclear receptors linked to adaptive thermogenesis. Cell *92*, 829-839.

Salatino, S., Kupr, B., Baresic, M., van Nimwegen, E., and Handschin, C. (2016). The Genomic Context and Corecruitment of SP1 Affect ERRalpha Coactivation by PGC-1alpha in Muscle Cells. Molecular endocrinology *30*, 809-825.

Schubeler, D. (2015). Function and information content of DNA methylation. Nature *517*, 321-326.

Seaborne, R.A., Strauss, J., Cocks, M., Shepherd, S., O'Brien, T.D., van Someren, K.A., Bell, P.G., Murgatroyd, C., Morton, J.P., Stewart, C.E., et al. (2018). Human Skeletal Muscle Possesses an Epigenetic Memory of Hypertrophy. Scientific reports *8*, 1898.

Sharples, A.P., Stewart, C.E., and Seaborne, R.A. (2016). Does skeletal muscle have an 'epi'-memory? The role of epigenetics in nutritional programming, metabolic disease, aging and exercise. Aging cell *15*, 603-616.

Siegfried, Z., and Simon, I. (2010). DNA methylation and gene expression. Wiley interdisciplinary reviews. Systems biology and medicine *2*, 362-371.

Smigielski, E.M., Sirotkin, K., Ward, M., and Sherry, S.T. (2000). dbSNP: a database of single nucleotide polymorphisms. Nucleic acids research *28*, 352-355.

Taaffe, D.R., Henwood, T.R., Nalls, M.A., Walker, D.G., Lang, T.F., and Harris, T.B. (2009). Alterations in muscle attenuation following detraining and retraining in resistance-trained older adults. Gerontology *55*, 217-223.

Tabas-Madrid, D., Nogales-Cadenas, R., and Pascual-Montano, A. (2012). GeneCodis3: a non-redundant and modular enrichment analysis tool for functional genomics. Nucleic acids research *40*, W478-483.

Voisin, S., Eynon, N., Yan, X., and Bishop, D.J. (2015). Exercise training and DNA methylation in humans. Acta physiologica (Oxford, England) *213*, 39-59.

Wu, H., Kanatous, S.B., Thurmond, F.A., Gallardo, T., Isotani, E., Bassel-Duby, R., and Williams, R.S. (2002). Regulation of mitochondrial biogenesis in skeletal muscle by CaMK. Science *296*, 349-352.

Zhang, H.M., Chen, H., Liu, W., Liu, H., Gong, J., Wang, H., and Guo, A.Y. (2012). AnimalTFDB: a comprehensive animal transcription factor database. Nucleic acids research *40*, D144-149.

Zhang, H.M., Liu, T., Liu, C.J., Song, S., Zhang, X., Liu, W., Jia, H., Xue, Y., and Guo, A.Y. (2015). AnimalTFDB 2.0: a resource for expression, prediction and functional study of animal transcription factors. Nucleic acids research *43*, D76-81.

5.2 Supplemental Project: PGC-1α/β control the transcriptome and methylome in differentiated myotubes

Barbara Heim-Kupr[1], Karl Nordström[2], Jörn Walter[2] and Christoph Handschin[1*]

[1]Biozentrum, University of Basel, Klingelbergstrasse 50/70, CH-4056 Basel, Switzerland

[2]Department of Biological Sciences, Genetics/Epigenetics, Saarland University, Saarbrücken, Saarland, Germany

[*]Corresponding author: christoph.handschin@unibas.ch / Biozentrum, University of Basel, Klingelbergstrasse 50/70, CH-4056 Basel / Phone: +41 61 207 23 78

Abstract

Skeletal muscle (SKM) is a very plastic organ able to adapt to multiple stimuli affecting whole body homeostasis. The peroxisome proliferator-activated receptor γ coactivator-1 (PGC-1) family of coactivators are involved in the regulation of a large and complex transcriptional network allowing the SKM to adapt functionally and morphologically. We could show the first time that PGC-1α and PGC-1β play an important role not only in the control and regulation of SKM transcriptional profile but as well in the DNA methylation alterations. Even more, we could demonstrate that both coactivators regulate some methyl- and demethyltransferases and hence, allow DNA methylation control by PGC-1 α/β. Our data provide further insides in the molecular mechanism of PGC-1α and PGC-1β controlled SKM plasticity and connects the transcriptome with the methylome in SKM cells.

Abbreviations

5mC, 5-methylcytosine; CH_3, methyl group; CpG, cytosine-phosphate-guanine; DE, differentially expressed; DM, differentiation medium; DMR, differentially methylated region; DNMT, DNA methyltransferase; FC, fold change; FDR, false discovery rate; GC, guanine-cytosine; gDNA, genomic DNA; GM, growth medium; GO, gene ontology; PGC-1, peroxisome proliferator-activated receptor γ coactivator-1; Quad, qRT-PCR, quantitative real-time polymerase chain reaction; RNAseq, RNA sequencing; RRBS, reduced representation bisulfite sequencing; SEM, standard errors of the means; SKM, skeletal muscle; TET, Ten-Eleven-Transloction oxygenases; TF, transcription factor

Introduction

In the mammalian genome, DNA methylation is a heritable and reversible enzyme-mediated epigenetic mechanism involving the transfer of a methyl group (CH_3) onto the C5 position of the cytosine leading to the generation of 5-methylcytosine (5mC) (Schubeler, 2015; Stadler et al., 2011). This methylation changes are essential for mammalian development and the adaptation to environmental signals (Moore et al., 2013; Smith and Meissner, 2013). Additionally, it was shown that abnormal DNA methylation leads to increase risk of cancer and neurological disorders (Robertson, 2005) because DNA methylation is often associated with regulation of gene expression by blocking the binding of transcription factors (TF) or impacting the chromatin structure (Jones and Takai, 2001; Schubeler, 2015; Siegfried and Simon, 2010). In mammals, DNA methylation is delivered to the DNA by a conserved family of DNA methyltransferases (DNMTs), which consists of three members: DNMT1, DNMT3a and DNMT3b. DNMT1 is a maintenance methyltransferase and was the first reported DNMT, important during development (Holliday and Pugh, 1975; Riggs, 1975), which acts mainly on hemimethylated DNA. In contrast, DNMT3a and DNMT3b assemble new methylation pattern on nonmethylated or hemimethylated DNA and are therefore called *de novo* DNMTs. All three DNMTs are involved in embryonic development and their level decrease after differentiation, indication stable methylation models after development. The Ten-Eleven-Translocation (TET) oxygenases are involved in the DNA demethylation (Dahl et al., 2011; Moore et al., 2013), leading to hypomethylated DNA, which is often associated with gene activation (Moore et al., 2013; Munzel et al., 2011). The family of TETs consists of three members, TET1, TET2 and TET3 (Tahiliani et al., 2009), most of them perform during development (Dahl et al., 2011; Ito et al., 2010; Langemeijer et al., 2009). In SKM, the most studies discuss the role of DNA methylation in the differentiation of myoblasts into myotubes. It was shown that DNA methylation plays an important role in the satellite cells during myogenesis, as it was already reported for general cell differentiation (Carrio and Suelves, 2015; Okano et al., 1999). Interestingly, several investigations observed different methylation pattern in SKM compared to other tissues but the exact role of DNA methylation in differentiated SKM cells is still unclear (Carrio and Suelves, 2015). Next to myogenesis and self-renewal capacity in SKM, DNA methylation was brought in contact with fiber-type specificity, exercise adaptations and SKM plasticity (Barres et al., 2012; Begue et al., 2017; Heim-Kupr et al., 2018 (not published yet); Nitert et al., 2012). Different studies revealed changes in DNA methylation design after exercise, although there is controversy about muscle type, acute versus chronic exercise as well about hyper- or hypomethylation after exercise. A previous study from our group in C2C12 myotubes, which overexpressed PGC-1α, indicated a potential interaction of the PGC-1 coactivators with DNA methylation (Salatino et al., 2016a). It is known that there is an interplay between site-specific TFs and gene regulation (Blattler and Farnham, 2013) and our results indicated different recruitment of PGC-

1α dependent on the genomic guanine-cytosine (GC) and cytosine-phosphate-guanine (CpG) content and thus, specific target gene regulation. Since PGC-1α is a key regulator in mitochondrial biogenesis and SKM plasticity and main regulator of a very complex transcriptional network, DNA methylation might be an additional layer of control. So far, not much is known about the role of PGC-1β in SKM plasticity as well about its transcriptional network and the epigenetic manipulation (Arany et al., 2007; Brault et al., 2010; Gali Ramamoorthy et al., 2015; Lee et al., 2017; Lin et al., 2002a; Rowe et al., 2011; St-Pierre et al., 2003). The conclusions from our previous study by Salatino et al. was mainly based on computational predictions. Therefore, the aim of the current study was to elucidate the role of DNA methylation in differentiated C2C12 SKM cells and to further characterize and validate the previous findings, to be able to conclude about the role of PGC-1α and PGC-1β on DNA methylation, consequences in TF-coregulator interaction and gene regulation in SKM cells. The role of PGC-1α in DNA methylation and transcriptional regulation in SKM *in vivo* and *in vitro* is discussed in detail in the main chapter 5.1. In this supplemental chapter, we focus on the role of PGC-1α and mainly PGC-1β in DNA methylation and gene expression in SKM cells *in vitro* and their interplay with the methyl- and demethyltransferases by RNA sequencing (RNAseq) and reduced representation bisulfite sequencing (RRBS) data analysis.

Results

PGC-1α/β regulate mitochondrial biogenesis and oxidative phosphorylation in skeletal muscle cells

We investigated the role of SKM PGC-1α and PGC-1β on DNA methylation and transcription in an *in vitro* model using C2C12 myotubes. PGC-1α or PGC-1β was overexpressed by adenovirus and GFP was used as control in differentiated myotubes. RNAseq was performed to analyze the transcriptional profile of myotubes overexpressing PGC-1α/β. Differentially expressed (DE) genes were defined by a false discovery rate (FDR) < 0.01 and a log2 fold change (FC) </> 0.6, which revealed large amount of DE genes for both coactivators. PGC-1α lead to 2978 up- and 1876 downregulated genes (data shown in main chapter 5.1, Figure 5F). Gene ontology (GO) analysis of all PGC-1α DE genes exposed main involvement in general “metabolic process”, “oxidation-reduction process” and “electron transport chain” (Suppl. Figure 1A). The GO investigation was supported by Kegg analysis, where “oxidative phosphorylation” was followed by “Parkinson’s, Alzheimer’s and Huntington’s diseases” (Suppl. Figure 1B), all diseases associated with mitochondrial dysfunction (Lin and Beal, 2006). PGC-1β showed 3265 upregulated and 2464 downregulated DE genes (Figure 1A). GO analysis discovered the same terms as observed for PGC-1α, namely “metabolic process”, “oxidation-reduction process”, “electron transport chain” and transcriptional regulation (Figure 1B). The Kegg pathway analysis discovered “oxidative phosphorylation” as top term,

followed by terms associated with mitochondrial dysfunction as “Alzheimer’s, Parkinson’s and Huntington’s disease”, which supports the GO analysis (Figure 1C) (Lin and Beal, 2006).

PGC-1β regulates DNA methylation in skeletal muscle cells

To identify DNA methylation in our model system, RRBS was chosen as a random approach for large-scale high-resolution DNA methylation analysis, which selects for CpG-rich regions and thus captures the majority of the CpG islands and promoters (Meissner et al., 2005). A cutoff of q-value < 0.01 and differentially methylated region (DMR) of ± 10% was set. RRBS from PGC-1α overexpressed myotubes as well as the follow-up combined with RNAseq was discussed in the main chapter 5.1, Figure 5G + H. RRBS from PGC-1β infected myotubes revealed 380 hypermethylated and 219 hypomethylated regions (Figure 1D).

Mild association of the methylome and transcriptome in differentiated myotubes overexpressing PGC-1β

To validate the functionality and consequences of DNA methylation on transcript level, RRBS and RNAseq data were combined. The DMRs were associated to their closest genes and those once compared with the DE genes identified in the RNAseq data. The number of genes dropped massively by the combined approach, resulting in 92 hypermethylated and 49 hypomethylated genes with significant gene expression changes (Figure 1E). GO analysis was conducted and resulted in weak and general terms involved in development, differentiation and immune response (Figure 1F).

PGC-1α and PGC-1β regulate some methyl- and demethyltransferases in myotubes

Finally, the regulators of DNA methylation, the DNMTs and TETs were measured by qRT-PCR in differentiated myotubes overexpressing either PGC-1α (Figure 2A) or PGC-1β (Figure 2B). Interestingly, PGC-1α induced DNMT1 and DNMT3a whereas PGC-1β only upregulated DNMT3a but repressed DNMT3b (Figure 2A + B). Remarkably, all three TET members were decreased on transcript level by PGC-1β (Figure 2B) while PGC-1α repressed TET2 and TET3 (Figure 2A).

Small effect on differentially expressed gene number by siRNA-based knockdown of DNMTs and TETs under PGC-1α/β overexpression in myotubes

Further mechanistic analysis was executed by using siRNA against all DNMTs and TETs in myotubes either overexpressing PGC-1α or PGC-1β and GFP as control. Due to their regulation by PGC-1α and PGC-1β in myotubes at baseline (Figure 2A + B), DNMT1, DNMT3a, which were induced, and TET1, chosen as contrary control, were selected for knockdown and advance comprehensive analysis by RNAseq and qRT-PCR

validation (Figure 3A-D, Figure 4A-D). Importantly, the level of PGC-1α or PGC-1β mRNA was not affected by the performed knockdown (Figure 3A + 4A). DE genes were analyzed with a cutoff of FDR < 0.01 and a log2 FC of </> 0.6. Comparison of PGC-1α or PGC-1β to GFP under control condition (sictrl) revealed 4886 DE genes for PGC-1α and 5422 DE genes for PGC-1β (Figure 3E + 4E). Next, we focused on the identified PGC-1α- or PGC-1β-dependent genes and compared to the siRNA-based knockdown DE genes under PGC-1α or PGC-1β overexpression conditions. Interestingly, the knockdown of DNMT1, DNMT3a or TET1 in each condition affected the number of PGC-1α- or PGC-1β-dependent DE genes only mild (Figure 3E + 4E).

Figure 1

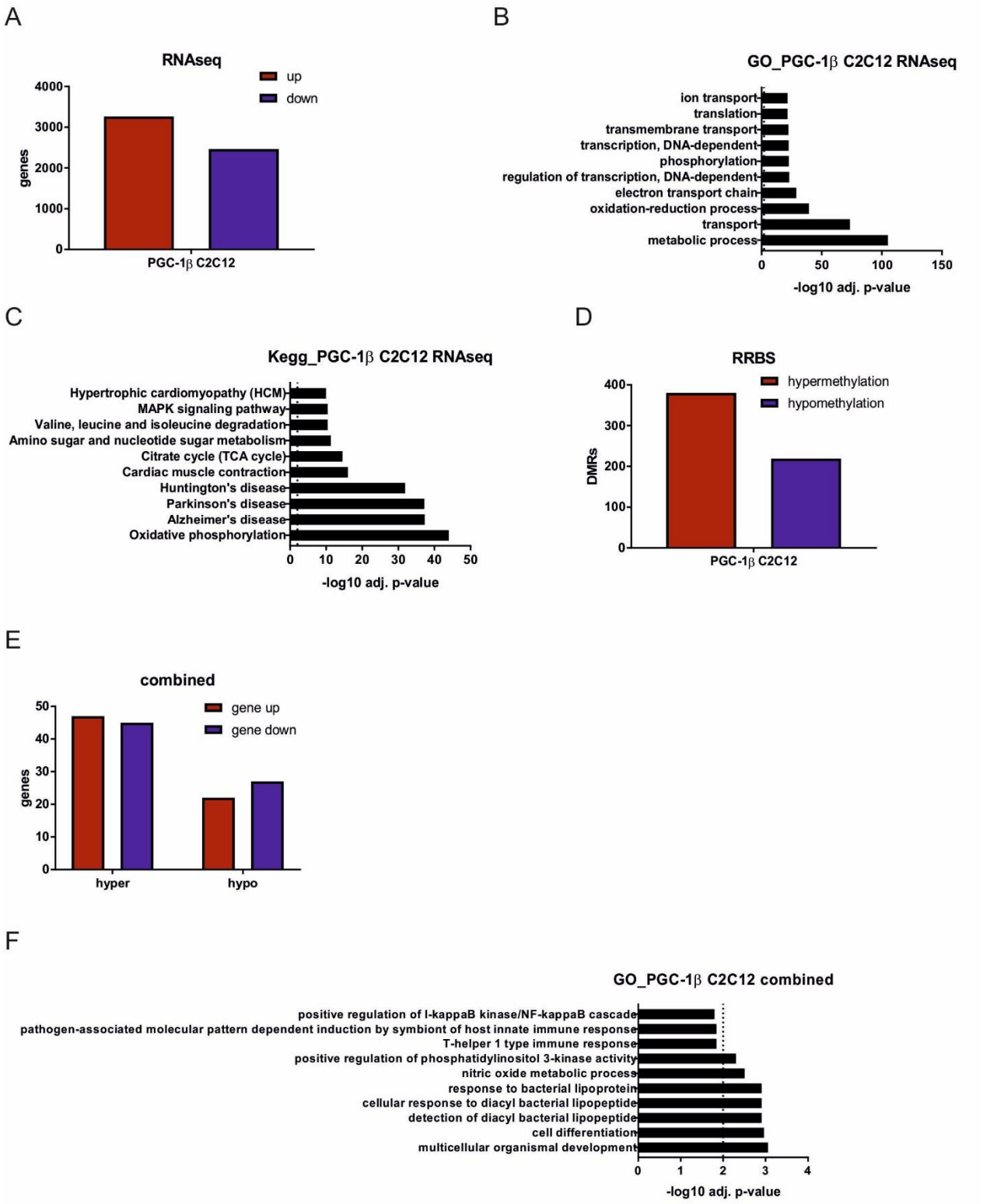
A
RNAseq
up
down
genes
4000
3000
2000
1000
0
PGC-1β C2C12
B
GO_PGC-1β C2C12 RNAseq
ion transport
translation
transmembrane transport
transcription, DNA-dependent
phosphorylation
regulation of transcription, DNA-dependent
electron transport chain
oxidation-reduction process
transport
metabolic process
0
50
100
150
-log10 adj. p-value
C
Kegg_PGC-1β C2C12 RNAseq
Hypertrophic cardiomyopathy (HCM)
MAPK signaling pathway
Valine, leucine and isoleucine degradation
Amino sugar and nucleotide sugar metabolism
Citrate cycle (TCA cycle)
Cardiac muscle contraction
Huntington's disease
Parkinson's disease
Alzheimer's disease
Oxidative phosphorylation
0
10
20
30
40
50
-log10 adj. p-value
D
RRBS
hypermethylation
hypomethylation
DMRs
400
300
200
100
0
PGC-1β C2C12
E
combined
gene up
gene down
genes
50
40
30
20
10
0
hyper
hypo
F
GO_PGC-1β C2C12 combined
positive regulation of I-kappaB kinase/NF-kappaB cascade
pathogen-associated molecular pattern dependent induction by symbiont of host innate immune response
T-helper 1 type immune response
positive regulation of phosphatidylinositol 3-kinase activity
nitric oxide metabolic process
response to bacterial lipoprotein
cellular response to diacyl bacterial lipopeptide
detection of diacyl bacterial lipopeptide
cell differentiation
multicellular organismal development
0
1
2
3
4
-log10 adj. p-value

Figure 1: PGC-1α/β regulate mitochondrial biogenesis and oxidative phosphorylation in skeletal muscle cells

A): Bar graph of DE genes C2C12 myotubes overexpressing PGC-1β. DE genes are subdivided into up- (red) and downregulated (blue). DE genes: FDR < 0.01, log2 FC </> 0.6.

B): GO analysis of DE genes in C2C12 myotubes overexpressing PGC-1β. Top 10 GO terms are shown. X-axis: (-)log10 adjusted p-value. Dotted line represents significance: (-)log10 adjusted p-value > 2.

C): Kegg analysis of D DE genes combined in C2C12 myotubes overexpressing PGC-1β. Top 10 Kegg terms are shown. X-axis: (-)log10 adjusted p-value. Dotted line represents significance: (-)log10 adjusted p-value > 2.

D): Bar graph of DMRs in C2C12 myotubes overexpressing PGC-1β. DMRs genes are subdivided into hyper- (red) and hypomethylated (blue). DMR: q-value < 0.01, ±10 methylation change.

E): Bar graph of combined DMRs and DE genes in C2C12 myotubes overexpressing PGC-1β divided into hyper- and hypomethylation as well as up- (red) and downregulated (blue) genes.

F): GO analysis of combined DMRs and DE genes in C2C12 myotubes overexpressing PGC-1β. Top 10 GO terms are shown. X-axis: (-)log10 adjusted p-value. Dotted line represents significance: (-)log10 adjusted p-value > 2.

Figure 2

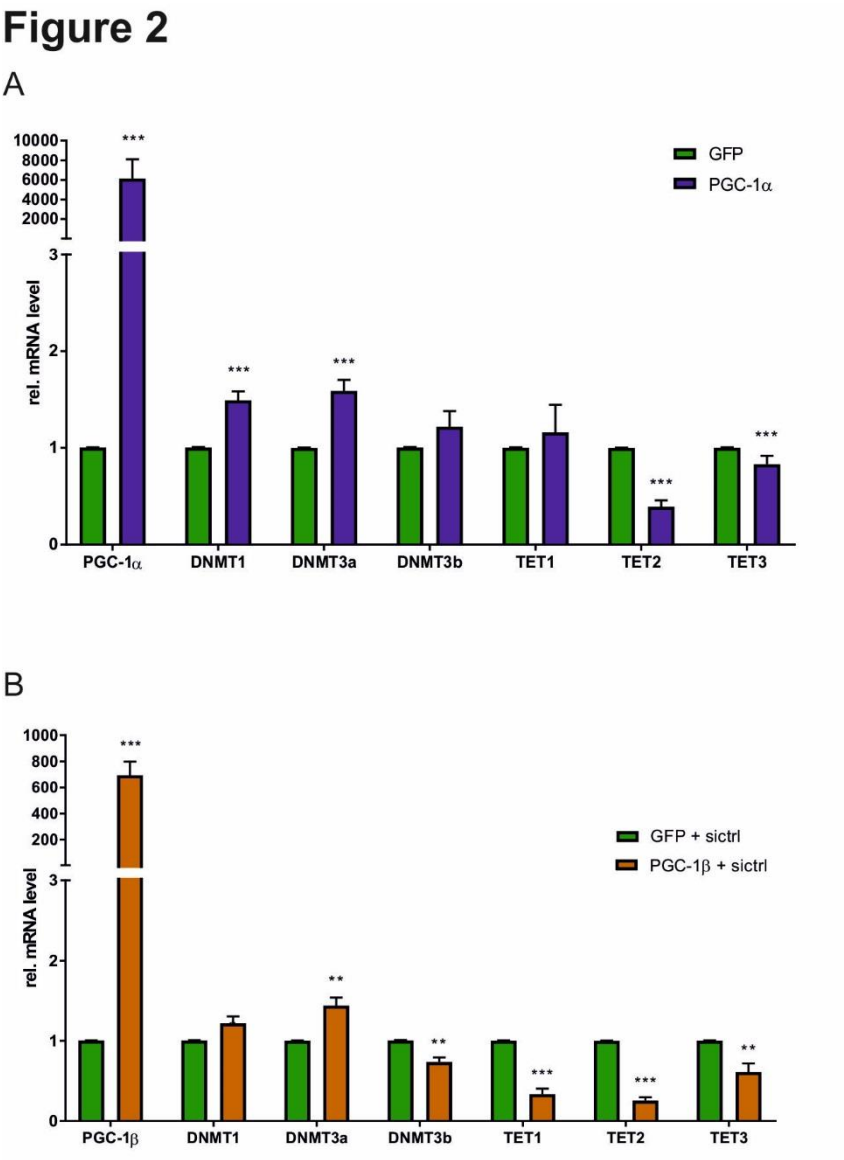

Figure 2: PGC-1α/β regulate some methyl- and demethyltransferases in myotubes

A-B): qRT-PCR in C2C12 myotubes overexpressing PGC-1α or GFP control (A) or PGC-1β and GFP control (B) was measured for the indicated genes. The analysis of the mRNA was performed by the comparative CT method using TATA binding protein (TBP) as endogenous control. Data was normalized to the condition of GFP of each gene. Bar graphs represent relative mean mRNA level, error bars represent SEM p* < 0.05, p* < 0.01, p*** < 0.001.

Figure 3

A

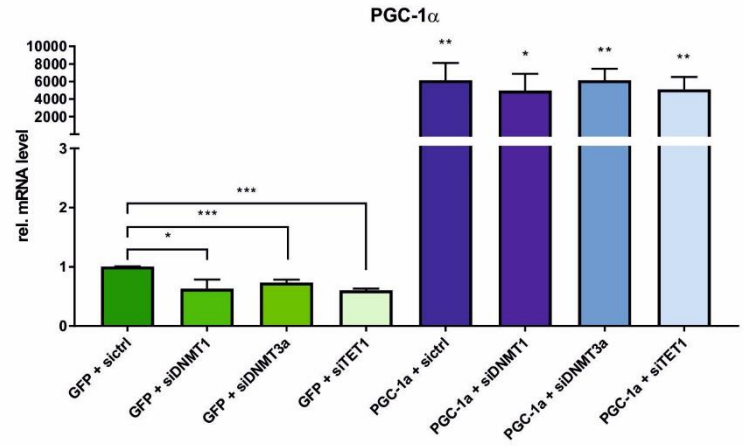

B

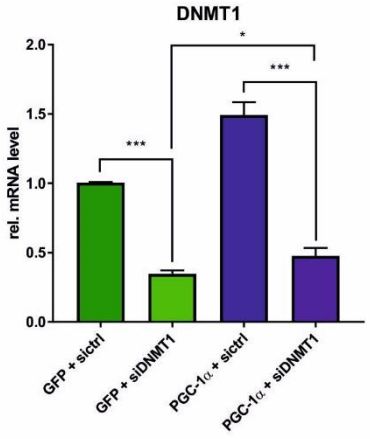

C

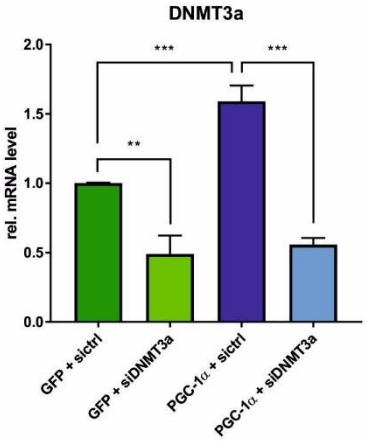

D

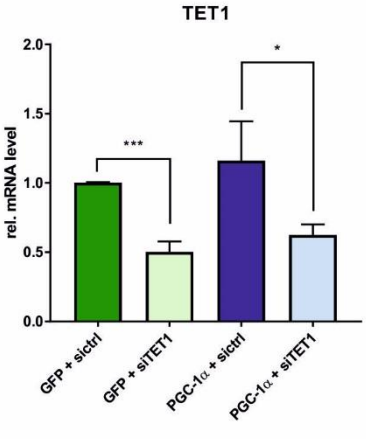

E

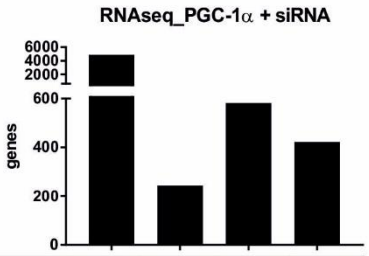

PGC-1α	+	+	+	+
sictrl	+	+	+	+
siDNMT1		+		
siDNMT3a			+	
siTET1				+

Figure 3: siRNA-based knockdown of DNMTs and TETs in myotubes overexpressing PGC-1α

A-D): qRT-PCR in C2C12 myotubes overexpressing PGC-1α or GFP control as well as combined with siRNA against non-targeted control (sictrl), DNMT1, DNMT3a and TET1 was measured for PGC-1α (A), DNMT1 (B), DNMT3a (C) and TET1 (D). The analysis of the mRNA was performed by the comparative CT method using TATA binding protein (TBP) as endogenous control. Data was normalized to the condition of GFP + sictrl. Bar graphs represent relative mean mRNA level, error bars represent SEM p* < 0.05, p* < 0.01, p*** < 0.001.

E): Number of DE genes in different conditions. From left to right: C2C12 myotubes overexpressing (OE) PGC-1α + sictrl against GFP + sictrl, PGC-1α OE + siDNMT1 against PGC-1α OE + sictrl, PGC-1α OE + siDNMT3a against PGC-1α OE + sictrl, PGC-1α OE + siTET1 against PGC-1α OE + sictrl. DE genes: FDR < 0.01, log2 FC </> 0.6.

Figure 4

A

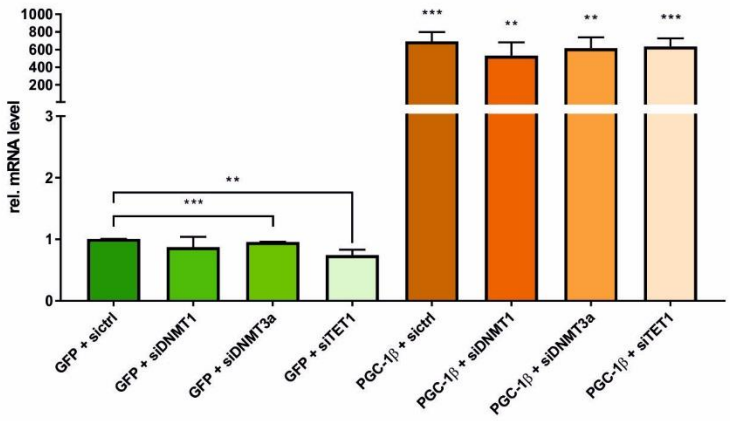

B

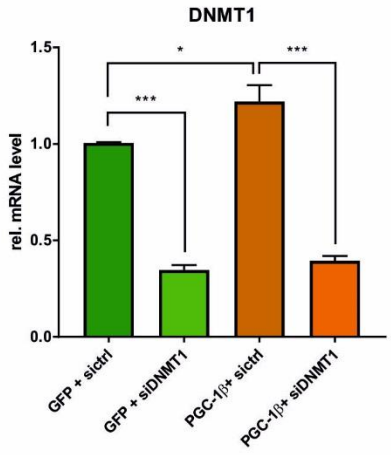

C

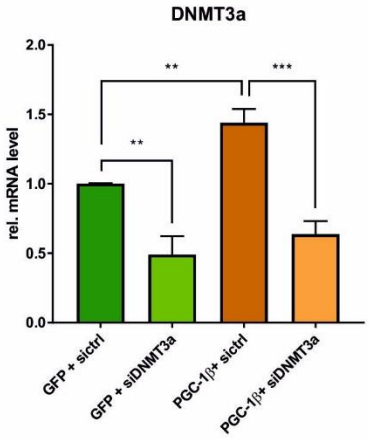

D

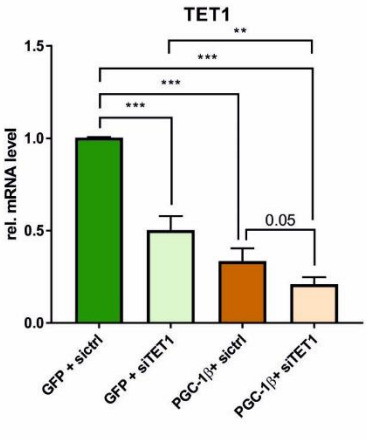

E

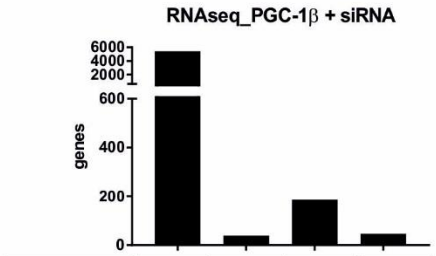

PGC-1β	+	+	+	+
sictrl	+	+	+	+
siDNMT1		+		
siDNMT3a			+	
siTET1				+

Figure 4: siRNA-based knockdown of DNMTs and TETs in myotubes overexpressing PGC-1β

A-D): qRT-PCR in C2C12 myotubes overexpressing PGC-1β or GFP control as well as combined with siRNA against non-targeted control (sictrl), DNMT1, DNMT3a and TET1 was measured for PGC-1β (A), DNMT1 (B), DNMT3a (C) and TET1 (D). The analysis of the mRNA was performed by the comparative CT method using TATA binding protein (TBP) as endogenous control. Data was normalized to the condition of GFP + sictrl. Bar graphs represent relative mean mRNA level, error bars represent SEM p* < 0.05, p* < 0.01, p*** < 0.001.

E): Number of DE genes in different conditions. From left to right: C2C12 myotubes overexpressing (OE) PGC-1β + sictrl against GFP + sictrl, PGC-1β OE + siDNMT1 against PGC-1β OE + sictrl, PGC-1β OE + siDNMT3a against PGC-1β OE + sictrl, PGC-1β OE + siTET1 against PGC-1β OE + sictrl. DE genes: FDR < 0.01, log2 FC </> 0.6.

F): Bar graph indicating the gene number difference in the indicated conditions of PGC-1β OE combined with siRNA to the control condition of PGC-1β OE + sictrl against GFP + sictrl.

Suppl. Figure 1

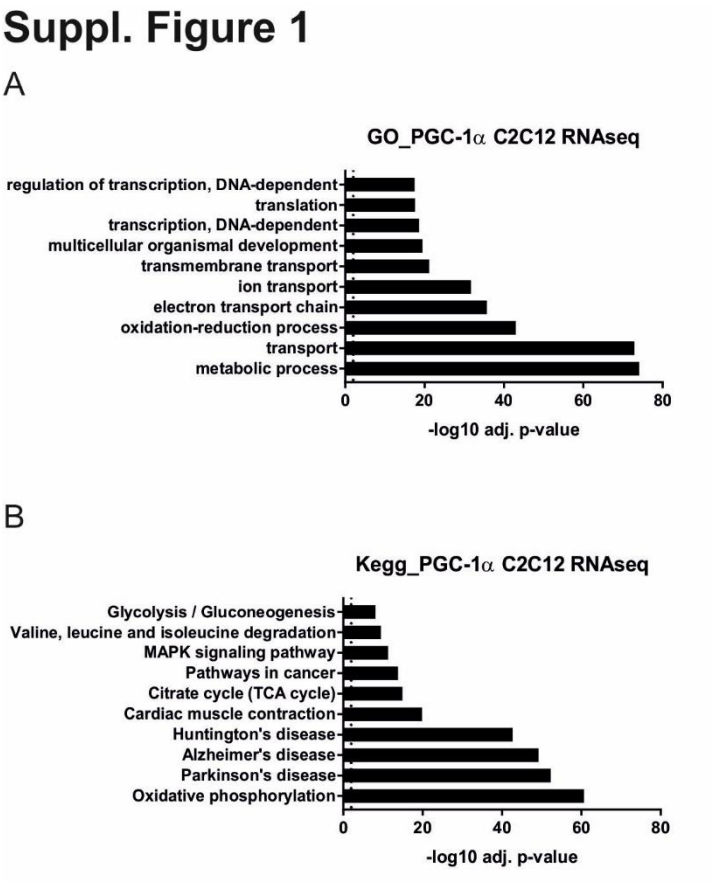

Supplemental Figure 1

A): GO analysis of DE genes in C2C12 myotubes overexpressing PGC-1α. Top 10 GO terms are shown. X-axis: (-)log10 adjusted p-value. Dotted line represents significance: (-)log10 adjusted p-value > 2.

B): Kegg analysis of D DE genes combined in C2C12 myotubes overexpressing PGC-1α. Top 10 Kegg terms are shown. X-axis: (-)log10 adjusted p-value. Dotted line represents significance: (-)log10 adjusted p-value > 2.

Discussion

Several studies reported a relationship of DNA methylation and transcriptional regulation (Blattler and Farnham, 2013; Deaton and Bird, 2011; Herman and Baylin, 2003; Holliday and Pugh, 1975; Moore et al., 2013; Ntanasis-Stathopoulos et al., 2013; Siegfried and Simon, 2010; Song et al., 2005). Most of the literature focused on epigenetic adaptations during development (Feng et al., 2005; Holliday and Pugh, 1975; Li et al., 1993; Li et al., 1992; Okano et al., 1999; Reik et al., 2001; Smith and Meissner, 2013). In SKM, only few studies discussed about the role of DNA methylation in differentiated muscle cells (Barres et al., 2009; Barres et al., 2012; Kanzleiter et al., 2015; Lochmann et al., 2015a), mostly, the myogenic process was investigated (Brunk et al., 1996; Carrio and Suelves, 2015; Hupkes et al., 2011; Tsumagari et al., 2013b). Especially environmental stimuli as e.g. exercise or nutrients are associated with epigenetic and transcriptional adaptations (Barres et al., 2012; Kanzleiter et al., 2015; Lochmann et al., 2015a; Moore et al., 2013). The PGC-1 family of coactivators are key players in the metabolic control of the whole body as well as tissue-specific adaptations, as e.g. SKM plasticity (Kupr and Handschin, 2015; Lin et al., 2005; Lin et al., 2002a; Puigserver et al., 1998; Schnyder and Handschin, 2015; Schnyder et al., 2017a). We elucidated the methylome and transcriptome of PGC-1α and PGC-1β in SKM by a combined approach of RNAseq and RRBS. The detailed *in vivo* and *in vitro* analysis of PGC-1α in SKM combined with exercise stimuli was discussed in chapter 5.1. In our study here, we elucidated the transcriptional and the DNA methylation profile in an *in vitro* system using C2C12 myotubes overexpressing PGC-1α or PGC-1β combined with siRNA-based knockdown for DNMTs and TETs. Our data showed regulation of the DNMTs and TETs by both PGC-1 coactivators in SKM cells and thus, supports the idea of an additional control layer by DNA methylation in the complex transcriptional network regulated by the PGC-1 family of coactivators. A comparison of PGC-1α and PGC-1β regulated target genes and DMRs would help to observe the overlapping as well as the distinct control and hence, help to define the function of each PGC-1 member in more detail. Furthermore, knockdown of one coactivator would indicate, whether there is compensatory mechanism by the other family member in regard of DNA methylation and the corresponding gene regulation. Nevertheless, PGC-1β alone regulated large amount of transcripts in SKM, which was already known for PGC-1α (Baresic et al., 2014; Kupr and Handschin, 2015; Lin et al., 2005; Salatino et al., 2016a). Even more, both members controlled DNA methylation, although not to such a large extend as the transcriptome. This might be due the reduced methylation activity after development (Moore et al., 2013; Okano et al., 1999; Reik et al., 2001; Smith and Meissner, 2013). Especially in the myogenic lineage, demethylation was shown to play a critical role to define muscle tissue and induce differentiation (Brunk et al., 1996; Hupkes et al., 2011; Lucarelli et al., 2001; Montesano et al., 2013; Tsumagari et al., 2013b). However, this was in contrast to the large number of DMRs observed *in vivo* and

discussed in chapter 5.1. In addition to the study mentioned before, it would be interesting to analyze the role of muscle PGC-1β in an *in vivo* system combined with external stimuli as e.g. fasting, which was shown to be an important stimulus in regard of the control of PGC-1β target genes involved in muscle atrophy (Schnyder et al., 2018 (not published yet)). Although we observed regulation of DNMTs and TETs by PGC-1α/β *in vitro*, siRNA-based knockdown of the enzymes had only mild effect on the PGC-1α- and PGC-1β-dependent DE genes, respectively. Nevertheless, the impact of the PGC-1s on the DNMTs and TETs *in vivo* would give the final global overview of this network.

Our data help to increase the knowledge in the field of combined control of transcription and DNA methylation, which allows a fine-tuned regulation of a large and complex transcriptional network in SKM cells by PGC-1α/β.

Materials and Methods

Cell culture and siRNA DNMT and TET

C2C12 myoblasts were grown in proliferation medium (GM) (DMEM, 10% FetalClone Serum [FCS, SH30066.03, GE Healthcare Life Sciences], 1% Penicillin/Streptomycin [15140122, Thermo Scientific]) until confluency and then medium was switched to differentiation medium (DM) (DMEM, 2% horse serum [HS, 16050122, Thermo Scientific]) for 4 days. Myotubes were infected with adenoviral (AD) GFP control or PGC-1α-Flag or PGC-1β-Flag for 24h, and then the infection medium was changed to differentiation medium for 24h before cells were collected according to the experiment, which will be performed.

For siRNA, C2C12 myotubes were differentiated for 3 days in DM and then treated for 24hours with 25nM siRNA for DNMT1 (M-056796-01-0005, Dharmacon), DNMT3a (M-065433-01-0005, Dharmacon), TET1 (M-062861-01-0005, Dharmacon) and non-targeted control (D-001206-13-05, Dharmacon) according to manufacturer's instructions. After 24h siRNA treatment, media was changed to infection media containing AD GFP or PGC-1α-Flag or PGC-1β-Flag for 24h that was then changed for another 24h into DM. siRNA experiments were performed in technical and biological triplicates.

Genomic DNA isolation

C2C12 myotubes were collected by trypsin and centrifugation to collect cell pellet. Genomic DNA (gDNA) was isolated by the QIAamp DNA Mini Kit (#51304, Qiagen) according to the manufacturers protocol. The level and quality of isolated gDNA was measured with a NanoDrop OneC spectrophotometer (Thermo Scientific).

Reduced Representation Bisulfite Sequencing (RRBS) library and sequencing

RRBS library was performed with the Premium Reduced Representation Bisulfite Sequencing Kit (C02030032, Diagenode) according to the manufacturer's instructions. 100ng of gDNA was used as starting material. Quality and fragment size was checked by Bioanalyzer (Agilent) measurements. Single read sequencing was performed with a HiSeq2500 machine (51 cycles, Illumina).

RRBS analysis

The reads were quality- and adapter trimmed with the Trim Galore! wrapper of cutadapt (Martin, 2011). The trimmed reads were controlled with FastQC (http://www.bioinformatics.bbsrc.ac.uk/projects/fastqc/). Conversion rates were calculated with custom scripts, counting the amount of G's and C's in non-GC context resulting in values above 99% for all libraries. The reads were mapped to the mm10 version of the mouse genome with BWA (Li and Durbin, 2009) and methylCtools (Hovestadt et al., 2014) after why a slightly extended Bis-SNP pipeline (Liu et al., 2012). The reads were locally realigned and the quality values were recalibrated before calling the methylation levels. The mm10 SNPs and InDels from dbSNP v138 (Smigielski et al., 2000) was used in this process. An initial quality control and exploratory analysis was done with R package RnBeads (Assenov et al., 2014). Differential loci was detected with MethylKit (Akalin et al., 2012) testing in 500bp sliding windows with at least 3 CpGs, only including those with a coverage of at least 10x. Differentially methylated regions (DMR) were defined as +/- 10% with a q-value > 0.01.

mRNA sequencing and analysis

Total RNA was isolated from C2C12 myotubes TRI reagent (T9424, Sigma) according to the manufacturer's instructions. RNA concentration was measured with a NanoDrop OneC spectrophotometer (Thermo Scientific). 7500 ng RNA was further purified with the Direct-zol RNA MiniPrep Kit (R2050, Zymo Research) according to the manufacturer's instructions. For RNAseq library preparation, 1 µg of purified RNA was used and libraries prepared with the TruSeq RNA library Prep Kit (Illumina) according to the manufacturer's instructions. Single read sequencing was performed with a HighSeq 2500 machine (50 cycles, Illumina). Fastq files were mapped to the mouse genome (mm10) and RNAseq and statistical analysis performed with the CLC Genomics Workbench Software (Qiagen).

Gene ontology

Gene ontology (GO) analysis was executed by the usage of GeneCodis (Carmona-Saez et al., 2007; Nogales-Cadenas et al., 2009; Tabas-Madrid et al., 2012). Enriched GO terms were furthermore sorted by (-)log10 adjusted p-value. Dotted line represents significance: (-)log10 adjusted p-value > 2.

Quantitative real-time PCR (qRT-PCR)

Total RNA was isolated from C2C12 cells as described above. The RNA was treated with DNase I (18068015, Thermo Scientific) and then reverse transcribed using hexanucleotide mix (11277081001, Sigma) and SuperScript II reverse transcriptase (18064022, Thermo Scientific). The level of relative mRNA was quantified by the Light Cycler 480 II system (Roche) using Fast Start Essential DNA Green Master mix (06924204001, Roche). The analysis of the mRNA was performed by the comparative CT method using TATA binding protein (TBP) as endogenous control. Primer sequences are listed in Table 1 of the Supplemental Material.

Statistical analysis

Values are expressed as means ± standard errors of the means (SEM) and statistical significance was determined with unpaired two tailed t-tests using Excel software. An asterisk (*) indicates significant differences between the conditions.

Supplemental Material

Table 1. qPCR primer sequences.

Gene Name	Forward primer	Reverse primer
DNMT1	CTCTTGCCCTGTGTGGTACA	GCAGGTTGCAGACGACAGAA
DNMT3a	GCCGAATTGTGTCTTGGTGGATGACA	CCTGGTGGAATGCACTGCAGAAGGA
DNMT3b	GAACATGCGCCTGCAAGA	GCACAGACTTCGGAGGCAAT
PGC-1α	TGATGTGAATGACTTGGATACAGACA	GCTCATTGTTGTACTGGTTGGATATG
PGC-1β	ATGCTTCCCTCACACCTCAG	GCTTTTGCCTTGTAGGCTTG
TBP	TGCTGTTGGTGATTGTTGGT	CTGGCTTGTGTGGGAAAGAT
TET1	TCATTCCAGACCGCAAGACC	TGACACCAGAGAAAGGACGC
TET2	ATATTGATGCGGAGGCGAGG	CAAATCCTACAGGGCAGCCA
TET3	GGGCAGGCAGCGTAGC	ATGAGGTGAGCCAATGGGTG

References

Akalin, A., Kormaksson, M., Li, S., Garrett-Bakelman, F.E., Figueroa, M.E., Melnick, A., and Mason, C.E. (2012). methylKit: a comprehensive R package for the analysis of genome-wide DNA methylation profiles. Genome biology *13*, R87.

Arany, Z., Lebrasseur, N., Morris, C., Smith, E., Yang, W., Ma, Y., Chin, S., and Spiegelman, B.M. (2007). The transcriptional coactivator PGC-1beta drives the formation of oxidative type IIX fibers in skeletal muscle. Cell metabolism *5*, 35-46.

Assenov, Y., Muller, F., Lutsik, P., Walter, J., Lengauer, T., and Bock, C. (2014). Comprehensive analysis of DNA methylation data with RnBeads. Nature methods *11*, 1138-1140.

Baresic, M., Salatino, S., Kupr, B., van Nimwegen, E., and Handschin, C. (2014). Transcriptional network analysis in muscle reveals AP-1 as a partner of PGC-1alpha in the regulation of the hypoxic gene program. Molecular and cellular biology *34*, 2996-3012.

Barres, R., Osler, M.E., Yan, J., Rune, A., Fritz, T., Caidahl, K., Krook, A., and Zierath, J.R. (2009). Non-CpG methylation of the PGC-1alpha promoter through DNMT3B controls mitochondrial density. Cell metabolism *10*, 189-198.

Barres, R., Yan, J., Egan, B., Treebak, J.T., Rasmussen, M., Fritz, T., Caidahl, K., Krook, A., O'Gorman, D.J., and Zierath, J.R. (2012). Acute exercise remodels promoter methylation in human skeletal muscle. Cell metabolism *15*, 405-411.

Begue, G., Raue, U., Jemiolo, B., and Trappe, S. (2017). DNA methylation assessment from human slow- and fast-twitch skeletal muscle fibers. Journal of applied physiology *122*, 952-967.

Blattler, A., and Farnham, P.J. (2013). Cross-talk between site-specific transcription factors and DNA methylation states. The Journal of biological chemistry *288*, 34287-34294.

Brault, J.J., Jespersen, J.G., and Goldberg, A.L. (2010). Peroxisome proliferator-activated receptor gamma coactivator 1alpha or 1beta overexpression inhibits muscle protein degradation, induction of ubiquitin ligases, and disuse atrophy. The Journal of biological chemistry *285*, 19460-19471.

Brunk, B.P., Goldhamer, D.J., and Emerson, C.P., Jr. (1996). Regulated demethylation of the myoD distal enhancer during skeletal myogenesis. Developmental biology *177*, 490-503.

Carmona-Saez, P., Chagoyen, M., Tirado, F., Carazo, J.M., and Pascual-Montano, A. (2007). GENECODIS: a web-based tool for finding significant concurrent annotations in gene lists. Genome biology *8*, R3.

Carrio, E., and Suelves, M. (2015). DNA methylation dynamics in muscle development and disease. Frontiers in aging neuroscience *7*, 19.

Dahl, C., Gronbaek, K., and Guldberg, P. (2011). Advances in DNA methylation: 5-hydroxymethylcytosine revisited. Clinica chimica acta; international journal of clinical chemistry *412*, 831-836.

Deaton, A.M., and Bird, A. (2011). CpG islands and the regulation of transcription. Genes & development *25*, 1010-1022.

Feng, J., Chang, H., Li, E., and Fan, G. (2005). Dynamic expression of de novo DNA methyltransferases Dnmt3a and Dnmt3b in the central nervous system. Journal of neuroscience research *79*, 734-746.

Gali Ramamoorthy, T., Laverny, G., Schlagowski, A.I., Zoll, J., Messaddeq, N., Bornert, J.M., Panza, S., Ferry, A., Geny, B., and Metzger, D. (2015). The transcriptional coregulator PGC-1beta controls mitochondrial function and anti-oxidant defence in skeletal muscles. Nature communications *6*, 10210.

Heim-Kupr, B., Nordström, K., Schnyder, S., Furrer, R., Steurer, S., Walter, J., and Handschin, C. (2018 (not published yet)). Acute and chronic exercise regulate skeletal muscle DNA methylation and transcription in a time and PGC-1α dependent manner. not published yet.

Herman, J.G., and Baylin, S.B. (2003). Gene silencing in cancer in association with promoter hypermethylation. The New England journal of medicine *349*, 2042-2054.

Holliday, R., and Pugh, J.E. (1975). DNA modification mechanisms and gene activity during development. Science *187*, 226-232.

Hovestadt, V., Jones, D.T., Picelli, S., Wang, W., Kool, M., Northcott, P.A., Sultan, M., Stachurski, K., Ryzhova, M., Warnatz, H.J., et al. (2014). Decoding the regulatory landscape of medulloblastoma using DNA methylation sequencing. Nature *510*, 537-541.

Hupkes, M., Jonsson, M.K., Scheenen, W.J., van Rotterdam, W., Sotoca, A.M., van Someren, E.P., van der Heyden, M.A., van Veen, T.A., van Ravestein-van Os, R.I., Bauerschmidt, S., et al. (2011). Epigenetics: DNA demethylation promotes skeletal myotube maturation. FASEB journal : official publication of the Federation of American Societies for Experimental Biology *25*, 3861-3872.

Ito, S., D'Alessio, A.C., Taranova, O.V., Hong, K., Sowers, L.C., and Zhang, Y. (2010). Role of Tet proteins in 5mC to 5hmC conversion, ES-cell self-renewal and inner cell mass specification. Nature *466*, 1129-1133.

Jones, P.A., and Takai, D. (2001). The role of DNA methylation in mammalian epigenetics. Science *293*, 1068-1070.

Kanzleiter, T., Jahnert, M., Schulze, G., Selbig, J., Hallahan, N., Schwenk, R.W., and Schurmann, A. (2015). Exercise training alters DNA methylation patterns in genes related to muscle growth and differentiation in mice. American journal of physiology. Endocrinology and metabolism *308*, E912-920.

Kupr, B., and Handschin, C. (2015). Complex Coordination of Cell Plasticity by a PGC-1alpha-controlled Transcriptional Network in Skeletal Muscle. Frontiers in physiology *6*, 325.

Langemeijer, S.M., Aslanyan, M.G., and Jansen, J.H. (2009). TET proteins in malignant hematopoiesis. Cell cycle *8*, 4044-4048.

Lee, S., Leone, T.C., Rogosa, L., Rumsey, J., Ayala, J., Coen, P.M., Fitts, R.H., Vega, R.B., and Kelly, D.P. (2017). Skeletal muscle PGC-1beta signaling is sufficient to drive an endurance exercise phenotype and to counteract components of detraining in mice. American journal of physiology. Endocrinology and metabolism *312*, E394-e406.

Li, E., Beard, C., Forster, A.C., Bestor, T.H., and Jaenisch, R. (1993). DNA methylation, genomic imprinting, and mammalian development. Cold Spring Harbor symposia on quantitative biology *58*, 297-305.

Li, E., Bestor, T.H., and Jaenisch, R. (1992). Targeted mutation of the DNA methyltransferase gene results in embryonic lethality. Cell *69*, 915-926.

Li, H., and Durbin, R. (2009). Fast and accurate short read alignment with Burrows-Wheeler transform. Bioinformatics (Oxford, England) *25*, 1754-1760.

Lin, J., Handschin, C., and Spiegelman, B.M. (2005). Metabolic control through the PGC-1 family of transcription coactivators. Cell metabolism *1*, 361-370.

Lin, J., Puigserver, P., Donovan, J., Tarr, P., and Spiegelman, B.M. (2002). Peroxisome proliferator-activated receptor gamma coactivator 1beta (PGC-1beta), a novel PGC-1-related transcription coactivator associated with host cell factor. The Journal of biological chemistry *277*, 1645-1648.

Lin, M.T., and Beal, M.F. (2006). Mitochondrial dysfunction and oxidative stress in neurodegenerative diseases. Nature *443*, 787-795.

Liu, Y., Siegmund, K.D., Laird, P.W., and Berman, B.P. (2012). Bis-SNP: combined DNA methylation and SNP calling for Bisulfite-seq data. Genome biology *13*, R61.

Lochmann, T.L., Thomas, R.R., Bennett, J.P., Jr., and Taylor, S.M. (2015). Epigenetic Modifications of the PGC-1alpha Promoter during Exercise Induced Expression in Mice. PLoS One *10*, e0129647.

Lucarelli, M., Fuso, A., Strom, R., and Scarpa, S. (2001). The dynamics of myogenin site-specific demethylation is strongly correlated with its expression and with muscle differentiation. The Journal of biological chemistry *276*, 7500-7506.

Martin, M. (2011). Cutadapt removes adapter sequences from high-throughput sequencing reads. EMBnet.journal *17*.

Meissner, A., Gnirke, A., Bell, G.W., Ramsahoye, B., Lander, E.S., and Jaenisch, R. (2005). Reduced representation bisulfite sequencing for comparative high-resolution DNA methylation analysis. Nucleic acids research *33*, 5868-5877.

Montesano, A., Luzi, L., Senesi, P., and Terruzzi, I. (2013). Modulation of cell cycle progression by 5-azacytidine is associated with early myogenesis induction in murine myoblasts. International journal of biological sciences *9*, 391-402.

Moore, L.D., Le, T., and Fan, G. (2013). DNA methylation and its basic function. Neuropsychopharmacology : official publication of the American College of Neuropsychopharmacology *38*, 23-38.

Munzel, M., Lischke, U., Stathis, D., Pfaffeneder, T., Gnerlich, F.A., Deiml, C.A., Koch, S.C., Karaghiosoff, K., and Carell, T. (2011). Improved synthesis and mutagenicity of oligonucleotides containing 5-hydroxymethylcytosine, 5-formylcytosine and 5-carboxylcytosine. Chemistry *17*, 13782-13788.

Nitert, M.D., Dayeh, T., Volkov, P., Elgzyri, T., Hall, E., Nilsson, E., Yang, B.T., Lang, S., Parikh, H., Wessman, Y., et al. (2012). Impact of an exercise intervention on DNA methylation in skeletal muscle from first-degree relatives of patients with type 2 diabetes. Diabetes *61*, 3322-3332.

Nogales-Cadenas, R., Carmona-Saez, P., Vazquez, M., Vicente, C., Yang, X., Tirado, F., Carazo, J.M., and Pascual-Montano, A. (2009). GeneCodis: interpreting gene lists through enrichment analysis and integration of diverse biological information. Nucleic acids research *37*, W317-322.

Ntanasis-Stathopoulos, J., Tzanninis, J.G., Philippou, A., and Koutsilieris, M. (2013). Epigenetic regulation on gene expression induced by physical exercise. Journal of musculoskeletal & neuronal interactions *13*, 133-146.

Okano, M., Bell, D.W., Haber, D.A., and Li, E. (1999). DNA methyltransferases Dnmt3a and Dnmt3b are essential for de novo methylation and mammalian development. Cell *99*, 247-257.

Puigserver, P., Wu, Z., Park, C.W., Graves, R., Wright, M., and Spiegelman, B.M. (1998). A cold-inducible coactivator of nuclear receptors linked to adaptive thermogenesis. Cell *92*, 829-839.

Reik, W., Dean, W., and Walter, J. (2001). Epigenetic reprogramming in mammalian development. Science *293*, 1089-1093.

Riggs, A.D. (1975). X inactivation, differentiation, and DNA methylation. Cytogenetics and cell genetics *14*, 9-25.

Robertson, K.D. (2005). DNA methylation and human disease. Nature reviews. Genetics *6*, 597-610.

Rowe, G.C., Jang, C., Patten, I.S., and Arany, Z. (2011). PGC-1beta regulates angiogenesis in skeletal muscle. American journal of physiology. Endocrinology and metabolism *301*, E155-163.

Salatino, S., Kupr, B., Baresic, M., van Nimwegen, E., and Handschin, C. (2016). The Genomic Context and Corecruitment of SP1 Affect ERRalpha Coactivation by PGC-1alpha in Muscle Cells. Molecular endocrinology *30*, 809-825.

Schnyder, S., and Handschin, C. (2015). Skeletal muscle as an endocrine organ: PGC-1alpha, myokines and exercise. Bone *80*, 115-125.

Schnyder, S., Heim-Kupr, B., Beer, M., Mittal, N., Ehrenfeuchter, N., and Handschin, C. (2018 (not published yet)). PGC-1β is involved in the response to fasting-induced skeletal muscle atrophy by inhibiting Nfatc1 activity. not published yet.

Schnyder, S., Kupr, B., and Handschin, C. (2017). Coregulator-mediated control of skeletal muscle plasticity - A mini-review. Biochimie *136*, 49-54.

Schubeler, D. (2015). Function and information content of DNA methylation. Nature *517*, 321-326.

Siegfried, Z., and Simon, I. (2010). DNA methylation and gene expression. Wiley interdisciplinary reviews. Systems biology and medicine *2*, 362-371.

Smigielski, E.M., Sirotkin, K., Ward, M., and Sherry, S.T. (2000). dbSNP: a database of single nucleotide polymorphisms. Nucleic acids research *28*, 352-355.

Smith, Z.D., and Meissner, A. (2013). DNA methylation: roles in mammalian development. Nature reviews. Genetics *14*, 204-220.

Song, F., Smith, J.F., Kimura, M.T., Morrow, A.D., Matsuyama, T., Nagase, H., and Held, W.A. (2005). Association of tissue-specific differentially methylated regions (TDMs) with differential gene expression. Proceedings of the National Academy of Sciences of the United States of America *102*, 3336-3341.

St-Pierre, J., Lin, J., Krauss, S., Tarr, P.T., Yang, R., Newgard, C.B., and Spiegelman, B.M. (2003). Bioenergetic analysis of peroxisome proliferator-activated receptor gamma coactivators 1alpha and 1beta (PGC-1alpha and PGC-1beta) in muscle cells. The Journal of biological chemistry *278*, 26597-26603.

Stadler, M.B., Murr, R., Burger, L., Ivanek, R., Lienert, F., Scholer, A., van Nimwegen, E., Wirbelauer, C., Oakeley, E.J., Gaidatzis, D., et al. (2011). DNA-binding factors shape the mouse methylome at distal regulatory regions. Nature *480*, 490-495.

Tabas-Madrid, D., Nogales-Cadenas, R., and Pascual-Montano, A. (2012). GeneCodis3: a non-redundant and modular enrichment analysis tool for functional genomics. Nucleic acids research *40*, W478-483.

Tahiliani, M., Koh, K.P., Shen, Y., Pastor, W.A., Bandukwala, H., Brudno, Y., Agarwal, S., Iyer, L.M., Liu, D.R., Aravind, L., et al. (2009). Conversion of 5-methylcytosine to 5-hydroxymethylcytosine in mammalian DNA by MLL partner TET1. Science *324*, 930-935.

Tsumagari, K., Baribault, C., Terragni, J., Varley, K.E., Gertz, J., Pradhan, S., Badoo, M., Crain, C.M., Song, L., Crawford, G.E., et al. (2013). Early de novo DNA methylation and prolonged demethylation in the muscle lineage. Epigenetics *8*, 317-332.

6. PGC-1α dependent and distinct skeletal muscle adaptations in acute exercise and shivering thermogenesis

Barbara Heim-Kupr[1], Svenia Schnyder[1], Regula Furrer[1], Stefan Steurer[1] and Christoph Handschin[1*]

[1]Biozentrum, University of Basel, Klingelbergstrasse 50/70, CH-4056 Basel, Switzerland

[*]Corresponding author: christoph.handschin@unibas.ch / Biozentrum, University of Basel, Klingelbergstrasse 50/70, CH-4056 Basel / Phone: +41 61 207 23 78

Abstract

Skeletal muscle (SKM) contraction is a tightly controlled molecular mechanism important to adapt to increased energy expenditure, which involves changes in SKM and whole body metabolism. Exercise leads to massive plastic adaptations in SKM and is a well-established treatment against many metabolic diseases and myopathies but cannot be executed by all patients due to their health condition. Thus, it is of great importance to elucidate the mechanism and transcriptional profile of SKM contraction subsequent to different physiological stimuli such as exercise and cold exposure, leading to shivering, hence, to have alternative treatments. We could show by RNA sequencing (RNAseq) that the transcriptional profile of acute exercise-induced muscle contraction is distinct to the shivering muscle contraction induced following acute cold exposure. Even more, our data demonstrate the importance of the master regulator peroxisome proliferator-activated receptor γ coactivator-1α (PGC-1α) in the regulation of a proper and healthy acute muscle contraction response. Our data increase the knowledge in the field of SKM contraction following external stimuli and helps to identify new pathways for the development of novel treatments for patients with metabolic diseases or myopathies.

Abbreviations

BAT, brown adipose tissue; CE, cold exposure; DE, differentially expressed; Dio2, Deiodinase 2; DM, differentiation medium; ERRα, estrogen-related receptor α; FC, fold change; FDR, false discovery rate; GCN, Gastrocnemius muscle; GM, growth medium; GO, gene ontology; HS, horse serum; HSP, heat shock protein; MKO, skeletal muscle-specific PGC-1α knockout mice; PCA, principal component analysis; PDK4, pyruvate dehydrogenase kinase 4; PGC-1, peroxisome proliferator-activated receptor γ coactivator-1; PPARα, peroxisome proliferator-activated receptor α; Quad, Quadriceps muscle; qRT-PCR, quantitative real-time polymerase chain reaction; RT, room temperature; SEM, standard errors of the means; SKM, skeletal muscle; TF, transcription factor; UCP, uncoupling protein; WT, wild type control mice

Introduction

SKM is a very plastic organ and a major contributor to whole body energy metabolism, in particular through strenuous physical activity. During muscle contractions, many tightly controlled molecular mechanisms are regulated to adapt to increased energy expenditure, which involves changes in SKM and whole body metabolism (Egan and Zierath, 2013). These adaptations subsequent to repeated bouts of exercise have been shown to counteract metabolic diseases such as obesity or type 2 diabetes and improve cardio vascular functions but also advance quality of life in myopathies or sarcopenia (Egan and Zierath, 2013; Gill et al., 2018; Law et al., 2016a; Phillips and Mastaglia, 2000). Hence, regular physical activity is widely accepted as therapeutic strategy (Colberg et al., 2010a; Haskell et al., 2007). Interestingly, repeated muscle contractions are not only triggered by exercise but also during cold-induced SKM shivering. Thermogenesis is an important evolutionary conserved regulatory mechanism including organs like brown adipose tissue (BAT) and SKM. To withstand prolonged cold exposure and maintain body temperature, heat is produced by non-shivering thermogenesis in BAT via mitochondrial uncoupling and by shivering in SKM. Surprisingly, SKM shivering and its underlying mechanisms is still largely unexplored. In addition, it is unknown if the SKM adaptations during cold exposure are similar to the exercise-induced plasticity and molecular changes in muscle metabolism. Interestingly, the transcriptional coactivator peroxisome proliferator-activated receptor γ coactivator-1α (PGC-1α) is involved in muscle adaptations upon exercise as well as shivering (Lin et al., 2004b; Puigserver et al., 1998). PGC-1α was found to regulate uncoupling protein 1 (UCP1) and hence, thermogenesis in BAT, which makes up around 60% of the heat generated by non-shivering, adaptive thermogenesis. PGC-1α deficient mice are not able to keep their body temperature after 6h of cold exposure, showing the important role of this master regulator of mitochondrial biogenesis and energy homeostasis (Lin et al., 2004b). In SKM, PGC-1α can be induced by cold and exercise and is a central regulator of oxidative metabolism and therefore, main driver of SKM adaptations following exercise (Akimoto et al., 2005; Handschin et al., 2007a; Jager et al., 2007; Oliveira et al., 2004; Puigserver et al., 1998). Even more, its methylation status (Barres et al., 2012), protein stability (Canto et al., 2009; Jager et al., 2007; Puigserver et al., 2001) and its target genes (Lin et al., 2005) are modified after exercise. Since PGC-1α is a coactivator, it interacts with many different transcription factors (TFs) to regulate the stimuli-induced adaptations as angiogenesis (Arany et al., 2008), fiber type switch (Handschin et al., 2007a; Lin et al., 2002b) and as already mentioned, mitochondrial biogenesis and oxidative metabolism (Egan and Zierath, 2013; Lin et al., 2005). Many studies have explored the context of SKM exercise metabolism and the role of PGC-1α but so far no complete picture of the molecular mechanisms underlying all these modifications and adaptations has been elucidated. Even less is known about SKM shivering and the adaptive thermogenesis and hence, the molecular pathways regulated in this

context. It is established that each bout of muscle contraction during exercise alters the transcript levels, which over time accumulates in increased protein abundance, leading to improved exercise performance and SKM functions (Egan and Zierath, 2013; Gabriel and Zierath, 2017; Robinson et al., 2017; Yang et al., 2005). However, the time course of transcriptional changes as well as the chronically trained-induced adaptions in SKM are not analyzed yet. In addition, it is not clear if muscle contraction has a general transcript profile, independent of the triggering stimuli as acute cold or acute exercise.

Thus, the aim of our study was to understand the general transcript profile of SKM as well as the PGC-1α-dependency of 6h acute cold exposure and its effect on SKM shivering. Additionally, we aimed to elucidate if the contractions during muscle shivering are comparable with exercise-induced muscle contraction. Therefore, the cold exposed animals were compared with exercised animals, in an acute exercise time course. For each study, wild type control (WT) as well as skeletal muscle-specific PGC-1α knockout (MKO) animals were used and RNAseq from the Quadriceps (Quad) muscle performed to compare the transcript profile of each condition and genotype. Our data demonstrate that muscle shivering is distinct from acute exercise-induced muscle contraction. Even more, we could show that PGC-1α is not essential to cope with cold or exercise but it is of crucial importance to keep a proper and healthy response during SKM contraction.

Results

Acute cold exposure induces stress in PGC-1α muscle-specific knockout animals

To elucidate the role of SKM shivering thermogenesis, animals were exposed to cold at 4 degrees. A time course of cold exposure, 1h, 3h, 6h, and 12h compared to room temperature (RT), was performed and body temperature, body weight and gene expression levels of known cold-induced target genes in Gastrocnemius (GCN) muscle measured to validate the optimal length for an acute cold exposure experiment (Suppl. Figure 1A-C). After 6h of cold exposure, the highest level of PGC-1α, peroxisome proliferator-activated receptor α (PPARα) as well as of UCP2 and UCP3 could be measured while body temperature was unchanged compared to RT exposed mice (Suppl. Fig. 1A + C). Since we were interested in SKM shivering and PGC-1α is an important and well-studied regulator of muscle plasticity, we used WT as well as MKO animals and exposed them to RT or 6h of cold (CE). Both genotypes could keep the body temperature at normal level (Suppl. Figure 1D), as it was already known from our time course experiment for WT animals (Suppl. Figure 1A). BAT was used as control tissue to measure the thermogenic response in the WT and MKO animals. PGC-1α, UCP1 and Deiodinase2 (Dio2) mRNA levels were induced after 6h CE (Figure 1A). Quad muscle was used from the same WT and MKO mice to analyze the cold response in SKM tissue. We confirmed our time course experiment by qRT-PCR as well as literature (Puigserver et al., 1998)

and observed induction of PGC-1α, UCP2, UCP3, PPARα and pyruvate dehydrogenase kinase 4 (PDK4) following 6h CE, although there was no genotype effect (Figure 1B). To get a global overview of the transcriptional profile in SKM upon CE in WT and MKOs, we performed RNAseq analysis from the Quad muscle. Principal component analysis (PCA) showed a clear distinct pattern in regard of the genotype and the conditions (Figure 1C). PC2 displayed the genotype effect, whereas PC1 the difference between RT and CE (Figure 1C). Further analysis was done to get the differentially expressed (DE) genes between the genotypes and conditions. We used a cutoff of false discovery rate (FDR) > 0.01 and a log2 fold change (FC) of < -0.6 and > 0.6. Interestingly, there was around the same number of DE genes comparing WT to MKO mice at RT (403 DE genes) to the group at CE (405 DE genes) (Figure 1D). Twice as much genes were differentially expressed comparing the conditions within the same genotype, making up 907 DE genes in WT animals and 851 DE genes in MKOs (Figure 1D). Additionally, we observed that more genes were induced than repressed by CE in WT and MKO animals (Figure 1D). We elucidated, whether the transcriptional cold response in the MKO animals was the same as in the WT mice. Around 2/3 (588) of the MKO DE genes following CE were overlapping with the WT cold response (Figure 2A). Those overlapping 588 genes represented the “core” cold response, including the induction of PGC-1α as well as the uncoupling proteins UCP1, 2, and 3 (Figure 2B). Interestingly, PGC-1β expression level showed a mild reduction in WT and MKO mice, probably as compensation for the PGC-1α induction (Figure 2B). In addition we dissected the regions from the Venn diagram into a cold “core” response (588 DE genes), independent of PGC-1α, and into “WT only” (319 DE genes) as well as “MKO only” (263 DE genes) genes, which were all regulated upon acute cold exposure (Figure 2A). Gene ontology (GO) was performed to further characterize the cold “core” as well as the distinct “WT only” and “MKO only” cold responses, respectively. The “core” cold response was mostly responsible for the regulation of general transcription, phosphorylation and apoptotic processes (Figure 2C). The “WT only” cold response was concerning the GO terms like the “core” cold response (Suppl. Figure 2A). The top GO terms in the “MKO only” cold response was again transcriptional regulation but additionally, the term “apoptotic process” was one of the top candidates and thus, more important than in the other groups (Suppl. Figure 2B). Apoptotic process appeared as well in the “core” and “WT only” cold response but not within the top three (Figure 2C + Suppl. Figure 2A). To dissect the PGC-1α-dependent differences in regard of the acute cold response, we further analyzed the genes from the GO terms in the “WT only” and “MKO only”. Recent studies implicated muscle-derived cytokines, called myokines, following exercise (Bostrom et al., 2012; Rao et al., 2014), hence we analyzed for signal peptides by the PrediSI software (Hiller et al., 2004). Signal peptides have a short peptide marker at the N-Terminus and are mostly proteins fated towards signaling pathways. Interestingly, we found that a large fraction, around 90% of all GO associated genes, belonged to signal

peptides. Within the “WT only” associated GO terms a total of 129 signal peptides were found, 52 being induced and 77 being repressed during acute cold (Figure 2D). The top up- or downregulated signal peptide genes in WT animals were involved in the GO terms “transcription”, “signal transduction” and “transport” (Figure 2E). In MKO animals, we found 75 of the total GO associated genes to be signal peptides. These could be dissected into 45 up- and 30 downregulated genes in our RNAseq data (Figure 2D). The top regulated signal peptide genes in MKO mice were involved in “transport”, “apoptotic process” and “response to stress” GO terms (Figure 2F). The MKO mice had more problems to deal with the acute CE by inducing apoptotic processes and responses to stress. To strengthen further this observation, we compared the genotype effect within the different conditions. At RT, 403 genes were differentially regulated between MKO and WT animals, acute cold lead to 405 DE genes between the genotypes (Figure 1D). A Venn diagram showed the overlap of 249 genes, which were independent of temperature but dependent on PGC-1α (Suppl. Figure 2C). GO analysis of this overlap presented general terms as “metabolic process”, “transport” and “apoptotic process”, although with low p-values (Suppl. Figure 2D). No significant GO terms were found for the 156 DE between MKO and WT animals during cold (“CE only”). This data indicate clearly that the WT and MKO mice have not only different genes recruited after acute cold exposure but also that different biological processes are regulated, reflected by the distinct GO terms in the “WT only” and “MKO only” categories.

Acute exercise time course in WT and MKO animals

In a next step, we elucidated whether the muscle contraction induced by cold exposure or acute exercise underlies the same transcriptional regulation and thus, the same molecular mechanism. Therefore, we analyzed transcriptional changes after an acute bout of exercise in a time course experiment. For this purpose, WT and MKO mice were run on an open treadmill until exhaustion and then killed 0h, 4h, 6h or 8h after the exercise test. MKO mice run significantly less and lactate as well as glucose levels were increased in WT and MKO animals after the exhaustion test but not to the same extend, which confirmed the current literature (Figure 3A-C) (Handschin et al., 2007a; Summermatter et al., 2013). To be able to compare the different muscle responses upon contraction, Quad muscle was used for RNAseq analysis of all acute exercise time points in WT and MKO animals as it was done in the CE experiment. PCA examination of the acute exercise time course revealed a clear separation between genotypes but not such a strong discrimination between the different time points (Figure 3D). Interestingly, and contrary to the CE DE genes, the MKO mice showed less DE genes than the WT animals over all time points (854 versus 1339), proposing that PGC-1α contributed to many transcript changes induced after acute exercise (Figure 3E + F). Venn diagram analysis of all time points showed an overlap of 56 DE genes in the WT animals

(Figure 3E) and of 25 DE genes in the MKO mice (Figure 3F). We defined the overlapping DE genes as “acute core exercise response”. Next, the question rose, whether PGC-1α is needed for the “acute core exercise response”.

PGC-1α is involved in the acute core exercise response in skeletal muscle

To characterize the “acute core exercise response” and check for its PGC-1α dependency, we executed Venn diagram analysis of the “acute core exercise response” DE genes found in WT and MKO animals (Figure 4A). There was an overlap of 14 genes, which were similar between the genotypes and thus, represented the PGC-1α independent “acute core exercise response”. GO analysis of the overlap revealed ion and zinc homeostasis as top terms, followed by nitric oxide signaling and interestingly, “response to stress” and “response to heat” containing the heat shock proteins (HSP) Hspa1a, Hspa1b and Dnajb1 (also known as Hsp40) (Figure 4B). However, the “acute core exercise response” only found in WT animals belonged to the biological processes of calcium handling, transcription and surprisingly, “response to stress” including other HSPs than found in the overlap “acute core exercise response”, namely Hsp90aa1 and Hspb1 (Figure 4C). In contrast, the MKO “acute core exercise response” contained only very few genes, consequently, these ones were only loosely associated to GO terms (Figure 4D). Importantly, we could not find any HSPs in the GO term associated list in the MKO animals. Even more, the HSPs found in the overlap were blunted in the MKO animals compared to the WT mice (Figure 4E-G). This suggests an incomplete acute exercise response in the PGC-1α muscle-specific knockout animals and supports the PGC-1α importance.

Distinct skeletal muscle transcriptional profiles after acute cold exposure and acute exercise

Our results from the acute cold and acute exercise experiments suggested PGC-1α dependent responses in the Quad muscle under each condition. The aim of this study was to elucidate the transcriptional profile upon muscle contraction in acute cold and acute exercise to get an answer whether the mechanisms are comparable to each other. Therefore, we compared now the RNAseq data from the acute CE experiment with the data from the acute exercise time course. In a first step, we associated DE genes from WT animals CE versus RT to all individual acute exercise time points (Suppl. Figure 5A). There was a small core group of 31 genes (“core 31”), which were overlapping between CE and all time points during acute exercise. GO analysis pointed towards genes involved in “apoptotic processes” and transcriptional regulation (Suppl. Figure 5B). Interestingly, we did not observe any specific acute exercise time point where we had a dominant overlap with the acute cold DE genes (Suppl. Figure 5C-F). Since we were interested in the general overlap of muscle contraction between acute cold-induced shivering and exercise-induced muscle

contraction, we combined all DE genes that were overlapping to any acute exercised time point with the CE DE genes in the WT animals (Figure 5A). Around 1/3 (305) of the CE DE genes (907) were overlapping with the acute exercise DE genes (1339). We termed the genes being DE in acute cold and acute exercise as “core SKM contractile component”. GO analysis revealed the “core SKM contractile component” mainly involved in the biological processes of transcriptional regulation (Figure 5B). The individual CE response consisted of 602 DE genes (“CE only”), which had their main functions in transcriptional regulation as well as apoptosis and cell death (Figure 5C). Contrary, the 1034 transcripts found only in the acute exercise group (“EX only”) belonged again to the GO terms transcription, but importantly, also to angiogenesis and cell differentiation (Figure 5D). It is known from literature that exercise improves angiogenesis (Arany et al., 2008; Hoier et al., 2012; Rowe et al., 2011) and moreover, angiogenesis in SKM seems to be dependent on both coactivators PGC-1α and PGC-1β (Arany et al., 2008; Rowe et al., 2011). The “EX only” group showed a variety of transcription categories as the top GO terms, however, composed of different genes, not overlapping in the Venn diagram (Figure 5A and D). Importantly, as we found the GO term “response to stress” as a significant factor in the “acute core exercise response”, specifically in the acute exercise time course, we checked the term in the acute cold versus acute exercise response. Remarkably, the GO term “response to stress” was only found in the “EX only” group at the 11th GO term position but still highly significant. As already observed in the acute time course, the GO term mainly contained HSPs (Figure 5E). Taken together, this data indicate that muscle contraction upon acute cold exposure is clearly distinct from the response after acute exercise and that the response to heat including HSPs is exclusively needed under acute exercise-induced muscle contraction.

Distinct transcription factor response in acute cold and acute exercised skeletal muscle

The main regulatory functions subsequent to acute muscle contraction, by either cold or exercise, lead to transcriptional changes and regulations. Thus, we had a closer look on the individual DE genes and found 10% of the “CE only”, 14% of the “core SKM contractile component” and 11% of the “EX only” DE genes were TFs (Figure 6A), identified by the AnimalTFDB 2.0 software (Zhang et al., 2012; Zhang et al., 2015). Importantly, the “EX only” group contained the nuclear receptor TFs Esr1, Esrrb, Esrrg, Nr3c2, which are known to be important players in the proper control of mitochondrial biogenesis and hence, energy homeostasis, mainly together with the PGC-1 family of transcriptional coactivators (Scarpulla, 2011; Scarpulla et al., 2012; Schreiber et al., 2004). Interestingly, the overlapping “core SKM contractile response” contained the TFs of the nuclear receptor subfamily 4 with Nr4a1 (Nur77), Nr4a2 (Nurr1), and Nr4a3 (Nor1), which are known to play a role in exercise SKM metabolism (Chao et al., 2012; Kupr et al., 2017; Mahoney et al., 2005; Pearen et al., 2008; Tontonoz et al., 2015). This indicated that an important

function upon acute muscle contraction is the maintenance of energy balance in the muscle and the whole body. Remarkably, Kegg pathway analysis from the TFs revealed strong impact in circadian rhythm in the "CE only" TFs (Figure 6B) and osteoclast differentiation in the "core SKM contractile component" (Figure 6C). No significant pathways were found in the "EX only" group. Previous studies already linked circadian rhythm with thermogenic adaptations in muscle and other tissues (Chappuis et al., 2013; Gerhart-Hines et al., 2013; Lee et al., 2013). Here in our study, the regulation of circadian genes seemed to be acute cold specific. The common function of osteoclast differentiation regulated by TFs and myokines, respectively, in acute cold and exercise was mentioned in literature, although not much is known about that (Deng et al., 2015; Hamrick et al., 2010). Further studies need to be done to understand the role of circadian rhythm in cold as well as the general interaction of muscle and bone following contraction.

Skeletal muscle contraction is distinct in acute cold exposure and acute exercise in PGC-1α muscle-specific knockout mice

Since PGC-1α was shown to play a key role in the regulation of exercise-induced transcriptional regulation as well as in thermogenesis and whole body energy homeostasis (Bostrom et al., 2012; Liang and Ward, 2006; Oliveira et al., 2004), we compared RNAseq data in the PGC-1α muscle-specific KO animals from cold exposed against acute exercised mice. Same as for the WT mice, we first analyzed CE DE genes against all DE genes in the individual acute exercise time points (not shown). As already observed in the WT animals, also in the MKO mice, no significant time point stood out and in addition, there was only a very small group of 14 genes, which symbolize the core response in cold and all acute exercise time points (not shown). Thus, to get an overview of the general transcriptional regulation during cold and in acute exercise in the MKO mice, we took all genes, which overlapped to any time point with the cold response and compared those ones (Figure 7A). We found a total of 851 CE DE genes and 854 DE genes in the acute exercise response in the MKO animals (Figure 7A). The high number of DE genes in both conditions indicated a clear response to acute muscle contraction stimuli in the muscle-specific PGC-1α knockout animals. The "core SKM contractile component" of 228 genes belonged to the GO terms transcriptional regulation (Figure 7B). The independent 623 CE genes ("CE only") played a major role in the apoptotic and inflammatory response (Figure 7C), clearly indicating that the MKO animals had much more problems to overcome a healthy response to the contraction induced stress by cold. Contrary, the 626 genes, which were only present during acute exercise ("EX only"), were, as it was already observed in the WT animals, involved in the transcriptional regulation and angiogenesis but as well in apoptosis (Figure 7D).

This data show that MKO animals can deal with acute cold and exercise responses but they are more severely affected by different stress pathways as apoptosis and inflammation, mainly upon cold exposure.

Figure 1

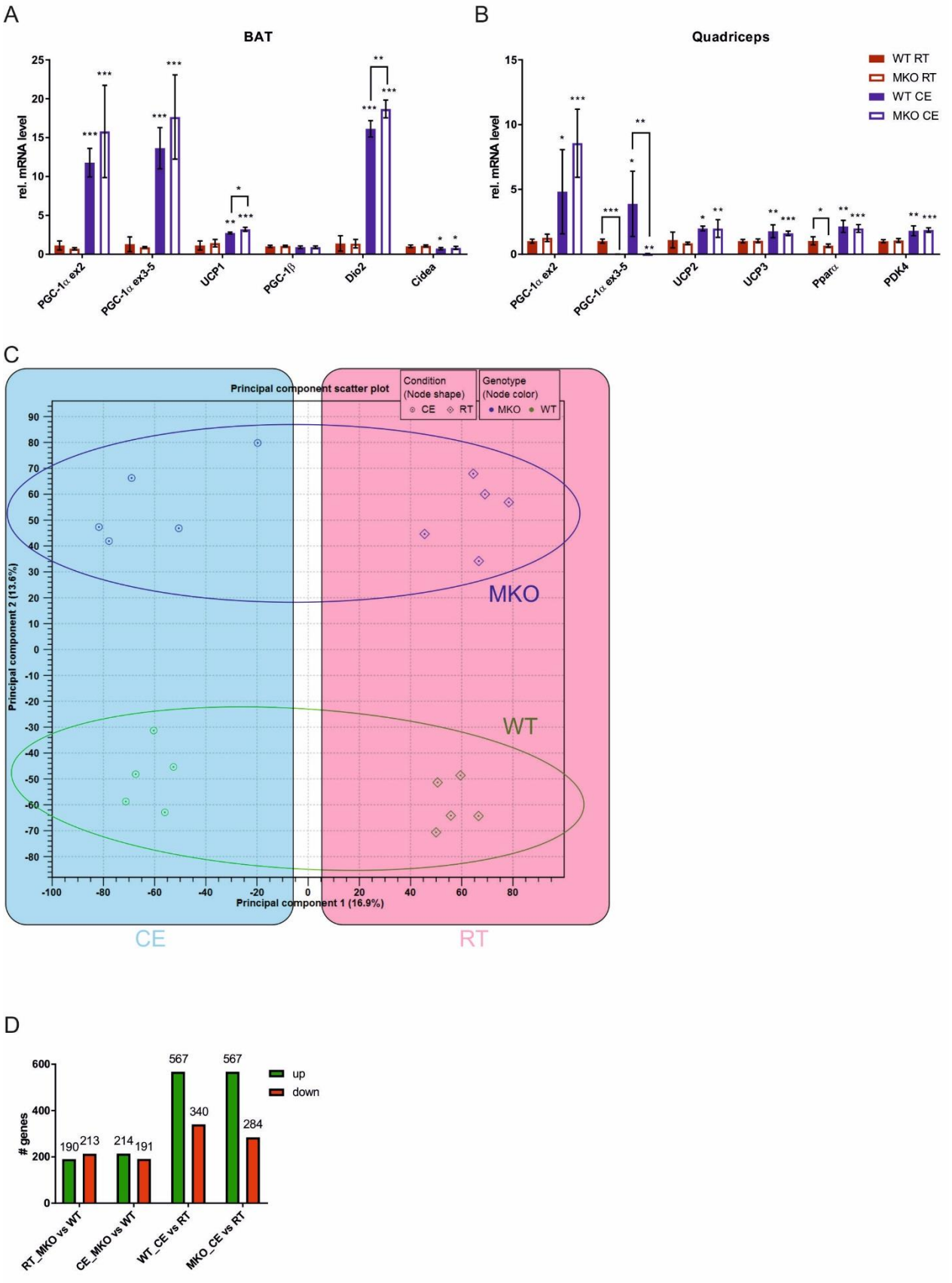
A
BAT
rel. mRNA level
PGC-1α ex2
PGC-1α ex3-5
UCP1
PGC-1β
Dio2
Cidea
B
Quadriceps
WT RT
MKO RT
WT CE
MKO CE
PGC-1α ex2
PGC-1α ex3-5
UCP2
UCP3
Pparα
PDK4
C
Principal component scatter plot
Condition (Node shape)
CE
RT
Genotype (Node color)
MKO
WT
Principal component 2 (13.6%)
Principal component 1 (16.9%)
MKO
WT
CE
RT
D
genes
up
down
190
213
214
191
567
340
567
284
RT_MKO vs WT
CE_MKO vs WT
WT_CE vs RT
MKO_CE vs RT

Figure 1. Acute 6h cold exposure induces cold-specific genes in WT and MKO animals

A) Gene expression of peroxisome proliferator-activated receptor γ coactivator-1α (PGC-1α) exon 2 and exon 3-5, uncoupling protein (UCP) 1, PGC-1β, Deiodinase 2 (Dio2) and Cidea relative to TATA binding protein (TBP) and normalized to WT RT measured by qRT-PCR in brown adipose tissue (BAT) of 6h acute cold exposed (CE) or room temperature (RT) kept WT and MKO mice (n=5). Bar graphs represent relative mean mRNA level, error bars represent SEM p* < 0.05, p* < 0.01, p*** < 0.001.

B) Gene expression of PGC-1α exon 2 and exon 3-5, UCP2, UCP3, peroxisome proliferator-activated receptor α (PPARα) and pyruvate dehydrogenase kinase 4 (PDK4) relative to TBP and normalized to WT RT measured by qRT-PCR in Quadriceps muscle (Quad) of CE or RT kept WT and MKO mice (n=5). Bar graphs represent relative mean mRNA level, error bars represent SEM p* < 0.05, p* < 0.01, p*** < 0.001.

C) Principal component analysis (PCA) in Quad of CE or RT kept WT and MKO mice (n=5).

D) Total differentially expressed (DE) genes divided into up- or downregulated in Quad of WT and MKO CE or kept at RT (n=5). Different conditions and genotypes were compared. From left: MKO against WT at RT, MKO against WT at cold, in WT mice cold against RT, in MKO animals cold against RT. A False discovery rate (FDR) < 0.01 and a log2 fold change (FC) < -0.6 and > 0.6 was used.

Figure 2

A

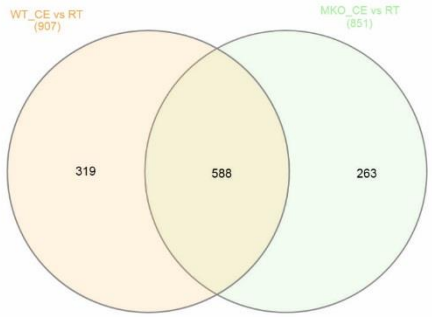

B

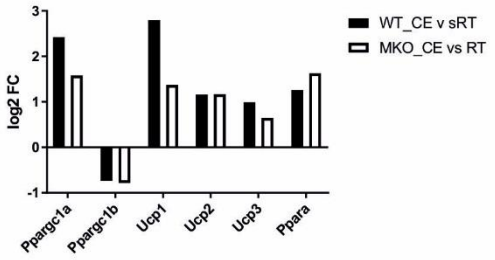

C

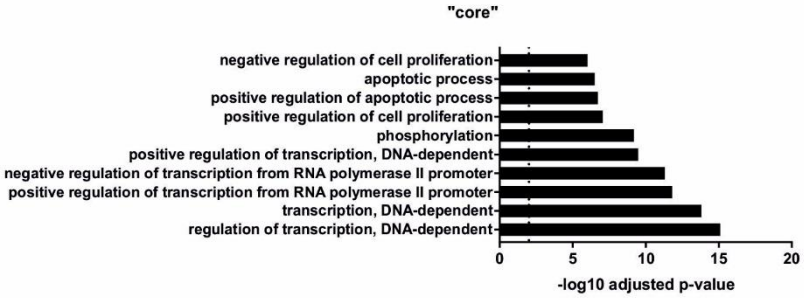

D

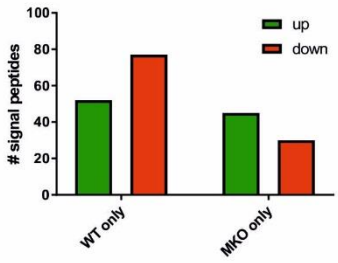

E

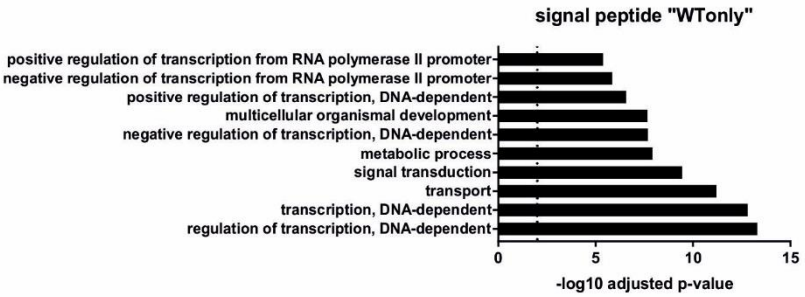

F

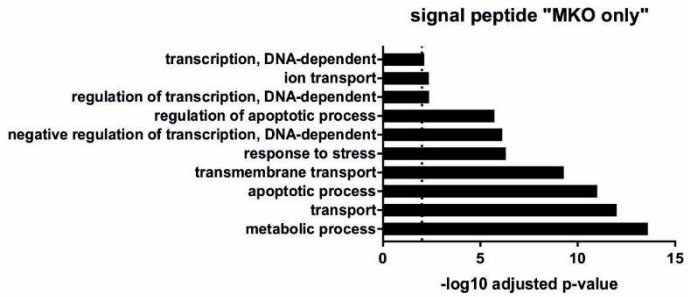

Figure 2. Distinct gene profile during acute cold exposure compared to room temperature

A) Venn diagram of DE genes in Quad of WT mice compared CE to RT and MKO mice compared CE to RT (n=5). FDR < 0.01 and log2 FC < -0.6 and > 0.6.

B) RNAseq log 2 FC of cold-specific genes PGC-1α (Ppargc1a), PGC-1β (Pargc1b), UCP1, UCP2, UCP3 and PPARα in WT mice compared CE to RT and MKO mice compared CE to RT (n=5).

C) Gene ontology (GO) analysis of DE genes in Quad of the overlap of WT and MKO animals compared CE to RT called “core” (n=5). X-axis: (-)log10 adjusted p-value. Dotted line represents significance: (-)log10 adjusted p-value > 2.

D) Bar graph representing number of signal peptides found in the GO term associated genes of the comparison between CE and RT in WT and MKO animals (n=5). Signal peptides only found in WT (WT only) or only found in MKO (MKO only) are shown.

E-F) GO analysis of the signal peptides in Quad found in the WT only (E) or the MKO (F) only group after comparing CE to RT (n=5). X-axis: (-)log10 adjusted p-value. Dotted line represents significance: (-)log10 adjusted p-value > 2.

Figure 3

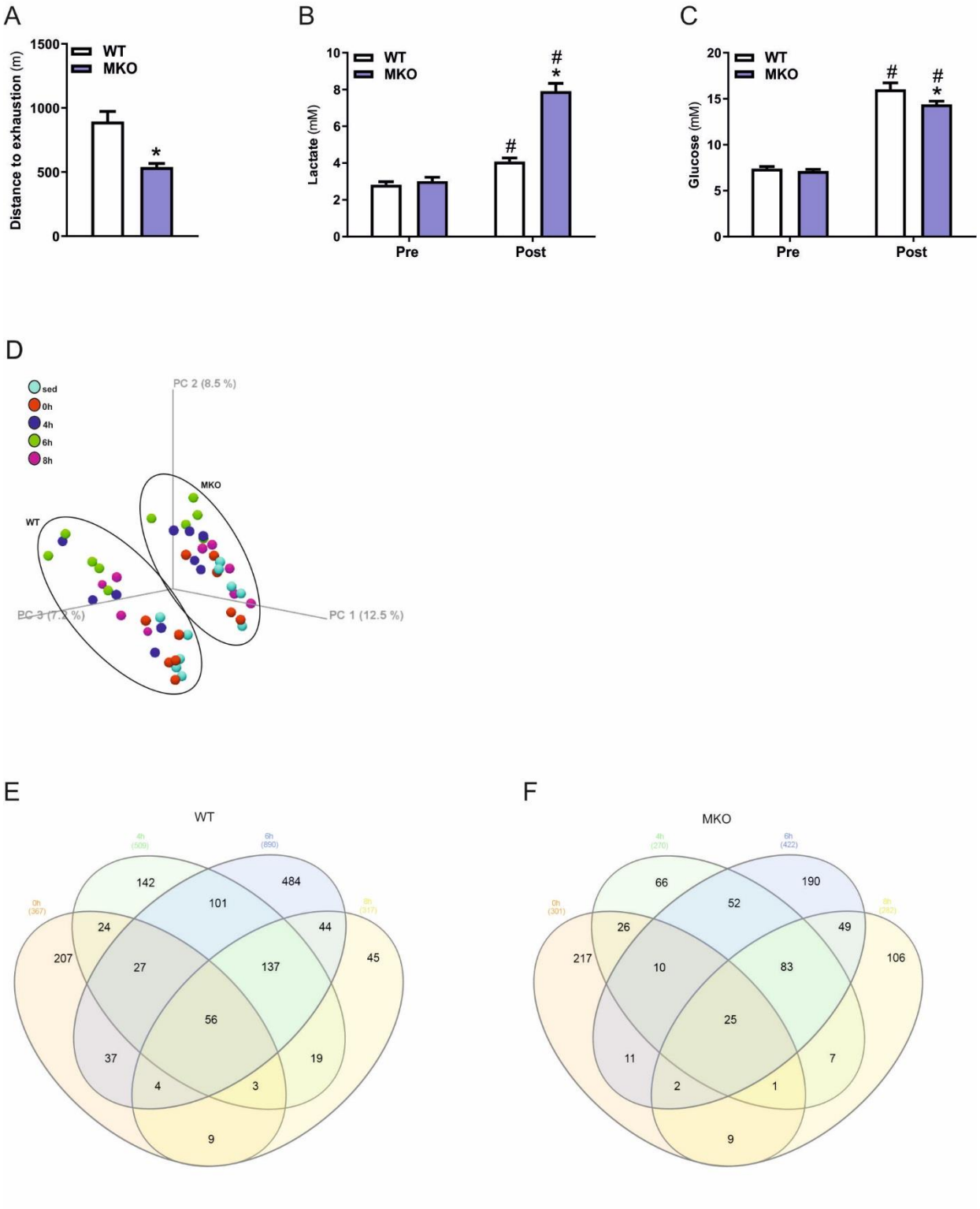
A
Distance to exhaustion (m)
1500
1000
500
0
WT
MKO
*
B
Lactate (mM)
10
8
6
4
2
0
WT
MKO
#
*
Pre
Post
C
Glucose (mM)
20
15
10
5
0
WT
MKO
#
*
Pre
Post
D
sed
0h
4h
6h
8h
PC 2 (8.5 %)
MKO
WT
PC 3 (7.2 %)
PC 1 (12.5 %)
E
WT
4h (509)
6h (890)
0h (367)
8h (917)
142
484
101
24
44
207
27
137
45
56
37
19
4
3
9
F
MKO
4h (270)
6h (422)
0h (301)
8h (282)
66
190
52
26
49
217
10
83
106
25
11
7
2
1
9

Figure 3. PGC-1α substantially contributes to gene expression changes after acute treadmill running

A) Distance until exhaustion of acutely treadmill run WT and MKO mice (n=24).

B-C) Pre- and post-lactate (B) and –glucose (C) plasma values of acutely treadmill run WT and MKO mice (n=24).

D) PCA in Quadriceps muscle of WT and MKO mice killed 0h, 4h, 6h, or 8h after acute treadmill test (n=5).

E-F) Venn diagram of DE genes in Quad of WT (E) and MKO (F) mice killed 0h, 4h, 6h, or 8h after acute treadmill test compared to sedentary mice. FDR < 0.01 and log2 FC < -0.6 and > 0.6 (n=5).

Figure 4

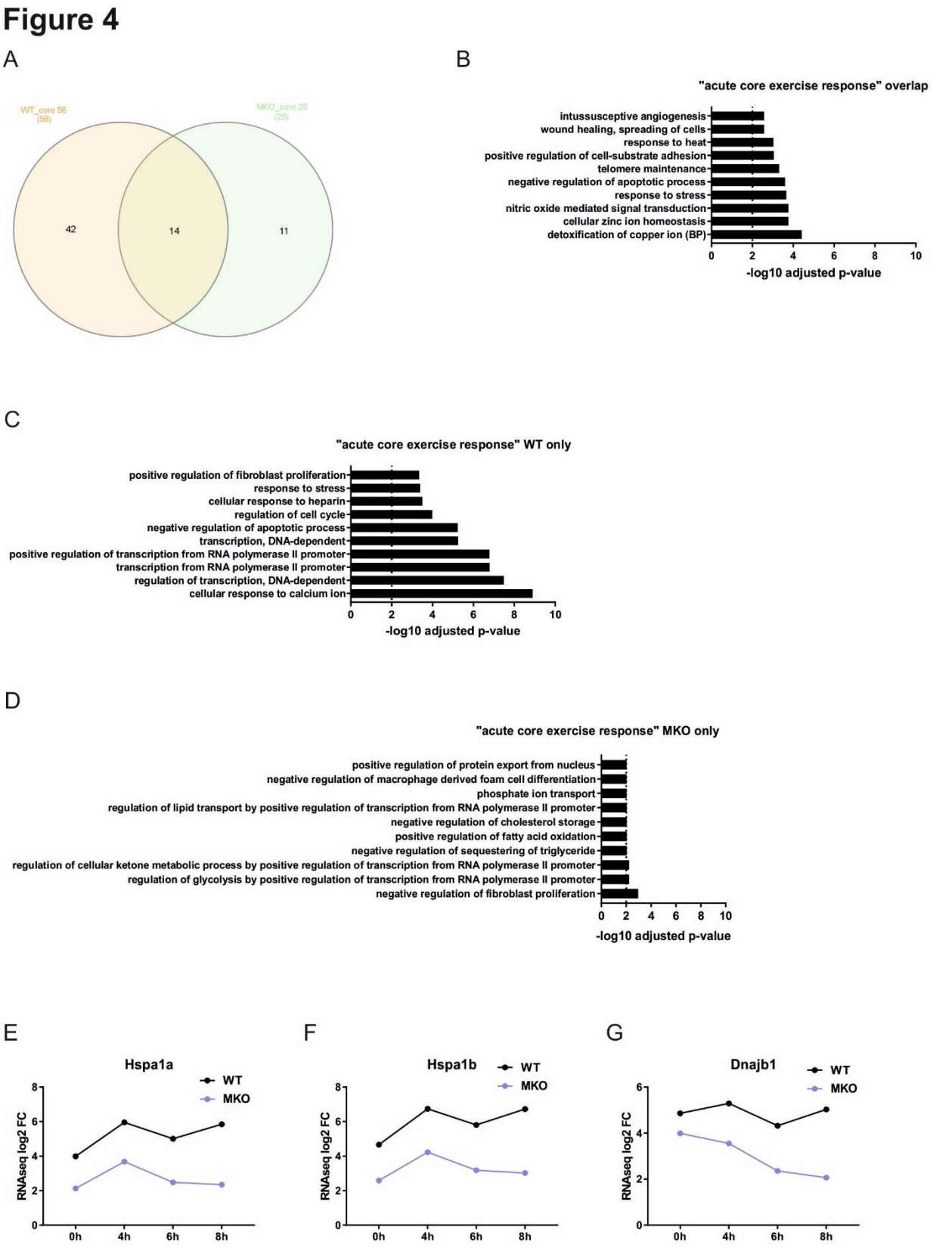
A
WT_core 56
(56)
MKO_core 25
(25)
42
14
11
B
"acute core exercise response" overlap
intussusceptive angiogenesis
wound healing, spreading of cells
response to heat
positive regulation of cell-substrate adhesion
telomere maintenance
negative regulation of apoptotic process
response to stress
nitric oxide mediated signal transduction
cellular zinc ion homeostasis
detoxification of copper ion (BP)
0 2 4 6 8 10
-log10 adjusted p-value
C
"acute core exercise response" WT only
positive regulation of fibroblast proliferation
response to stress
cellular response to heparin
regulation of cell cycle
negative regulation of apoptotic process
transcription, DNA-dependent
positive regulation of transcription from RNA polymerase II promoter
transcription from RNA polymerase II promoter
regulation of transcription, DNA-dependent
cellular response to calcium ion
0 2 4 6 8 10
-log10 adjusted p-value
D
"acute core exercise response" MKO only
positive regulation of protein export from nucleus
negative regulation of macrophage derived foam cell differentiation
phosphate ion transport
regulation of lipid transport by positive regulation of transcription from RNA polymerase II promoter
negative regulation of cholesterol storage
positive regulation of fatty acid oxidation
negative regulation of sequestering of triglyceride
regulation of cellular ketone metabolic process by positive regulation of transcription from RNA polymerase II promoter
regulation of glycolysis by positive regulation of transcription from RNA polymerase II promoter
negative regulation of fibroblast proliferation
0 2 4 6 8 10
-log10 adjusted p-value
E
Hspa1a
WT
MKO
RNAseq log2 FC
0 2 4 6 8
0h 4h 6h 8h
F
Hspa1b
WT
MKO
RNAseq log2 FC
0 2 4 6 8
0h 4h 6h 8h
G
Dnajb1
WT
MKO
RNAseq log2 FC
0 2 4 6
0h 4h 6h 8h

Figure 4. PGC-1α dependent acute exercise response in skeletal muscle

A) Venn diagram of the overlap of DE genes in Quad of WT (core 56) and MKO (core 25) mice killed 0h, 4h, 6h, or 8h after the acute treadmill test compared to sedentary mice (n=5).FDR < 0.01 and a log2 FC < -0.6 and > 0.6.

B-D) GO analysis of each individual DE fraction found in the Venn diagram and called “acute core exercise response” in the overlap (B), only found the WT animals (C) and only found in the MKO mice (D) (n=5). X-axis: (-)log10 adjusted p-value. Dotted line represents significance: (-)log10 adjusted p-value > 2.

E-G) RNAseq log 2 FC of heat shock protein (HSP) Hspa1a (E), Hspa1b (F) and Dnajb1 (G) in Quad of WT and MKO mice killed 0h, 4h, 6h, or 8h after the acute treadmill test compared to sedentary mice (n=5).

Figure 5

A

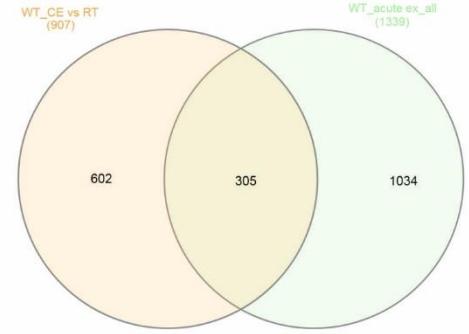

B

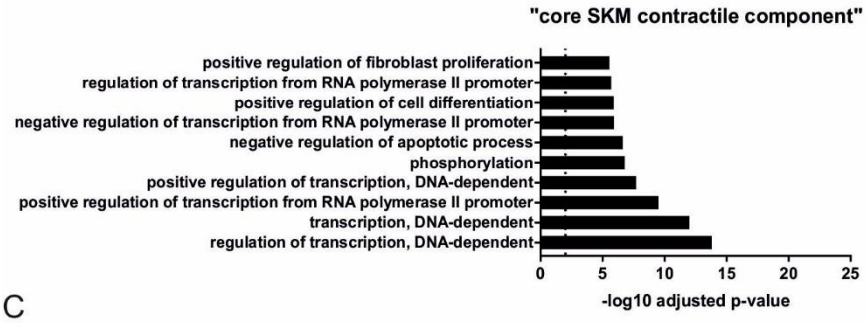

C

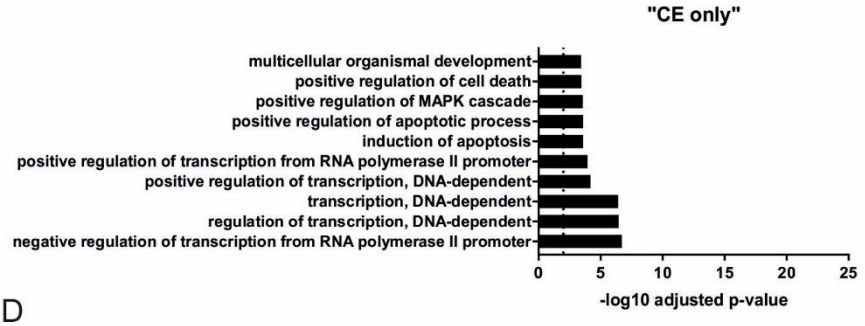

D

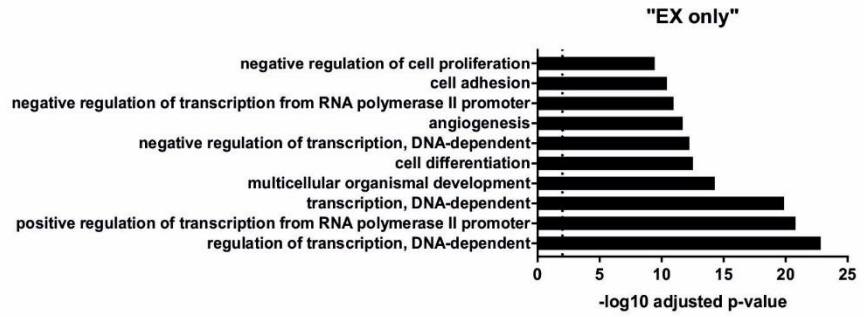

E

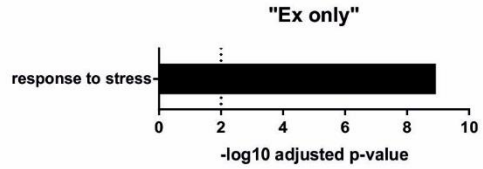

Hsf2bp,Sult1a1,Hsp90aa1,Hspb7,Hspa1l,Serpinh1,Hspe1,Hspb8,Hspa8,Hspa1a, Adra1a, Hspb1,Rps6ka5,Hspb2,Avil,Hspb3,Sod3,Dnajb1,Hsf2,Ahr,Hspa1b

Figure 5. Distinct skeletal muscle transcript profile following acute exercise and acute cold

A) Venn diagram of all DE genes overlapping to any time point in Quad of WT mice killed 0h, 4h, 6h, or 8h after the acute treadmill test compared to sedentary mice with the CE WT mice (n=5). FDR < 0.01 and a log2 FC < -0.6 and > 0.6.

B-D) GO analysis of each individual DE fraction found in the Venn diagram called “core SKM contractile component” for the overlap (B), only found in the CE WT animals (C), only found in the acute exercised WT mice (D) (n=5). X-axis: (-)log10 adjusted p-value. Dotted line represents significance: (-)log10 adjusted p-value > 2.

E) GO term found only in the acute exercised WT fraction at the 11th position with the corresponding genes. X-axis: (-)log10 adjusted p-value. Dotted line represents significance: (-)log10 adjusted p-value > 2.

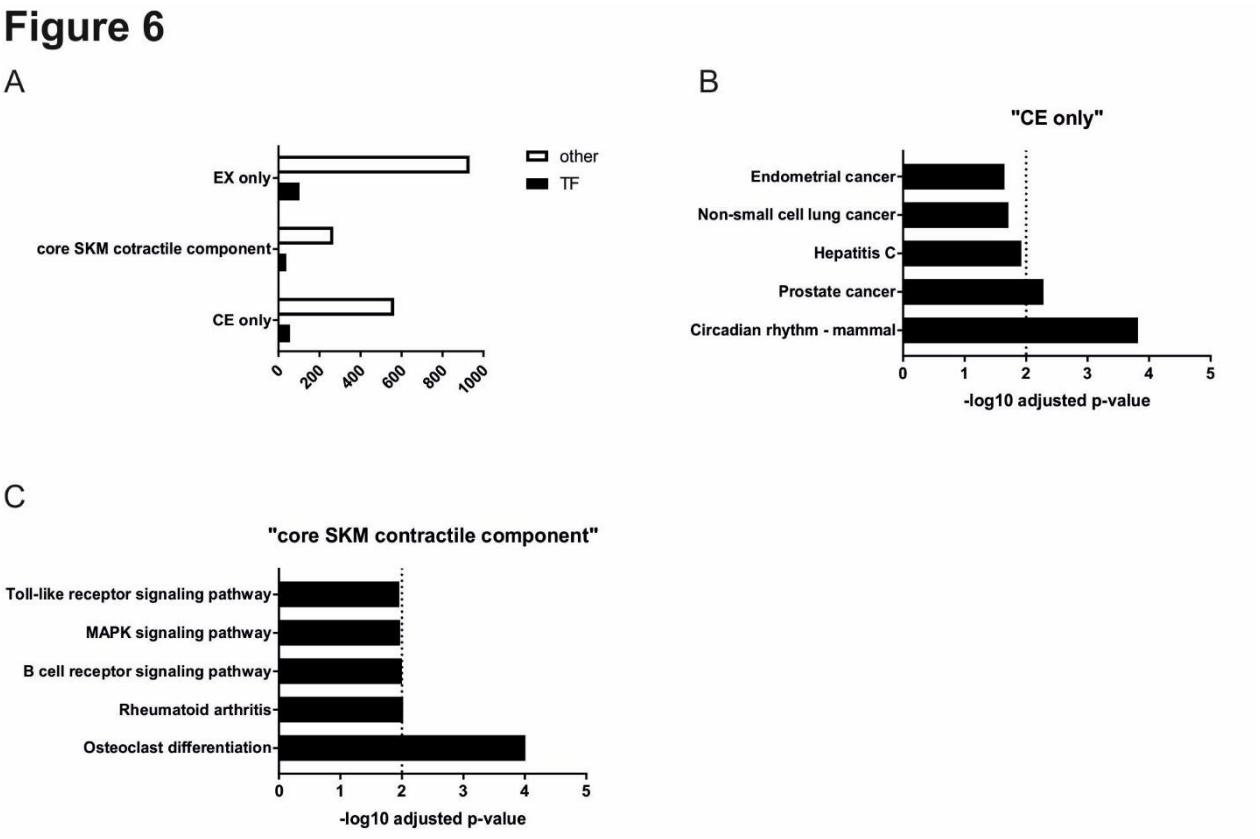

Figure 6. Acute cold and acute exercise induce a different transcription factor response

A) Bar graph represents number of DE genes divided in transcription factors (TF) and all other genes (other) found in the comparison between all DE genes overlapping to any time point in Quad of WT mice killed 0h, 4h, 6h, or 8h after the acute treadmill test compared to sedentary mice with the CE WT mice compared to RT (n=5). Fractions of genes found only in the acute exercised (EX only), in the overlap of acute exercise and CE (core SKM contractile component) or only found in the cold expose WT animals (CE only). FDR < 0.01 and a log2 FC < -0.6 and > 0.6.

B-C) Kegg pathway analysis of the TFs found in the comparison between all DE genes overlapping to any time point in Quad of WT mice killed 0h, 4h, 6h, or 8h after the acute treadmill test compared to sedentary mice with the CE WT mice compared to RT (n=5). TFs only present in the CE fraction (B) and TF found in the overlap of acute exercise and CE WT animals (C). X-axis: (-)log10 adjusted p-value. Dotted line represents significance: (-)log10 adjusted p-value > 2.

Figure 7

A

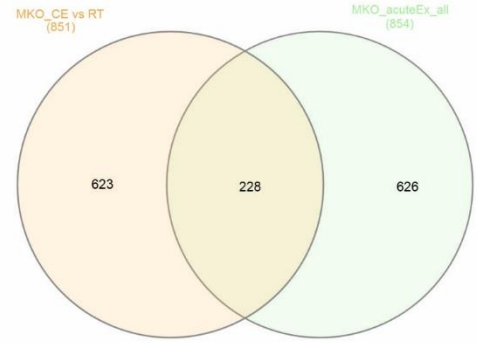

B

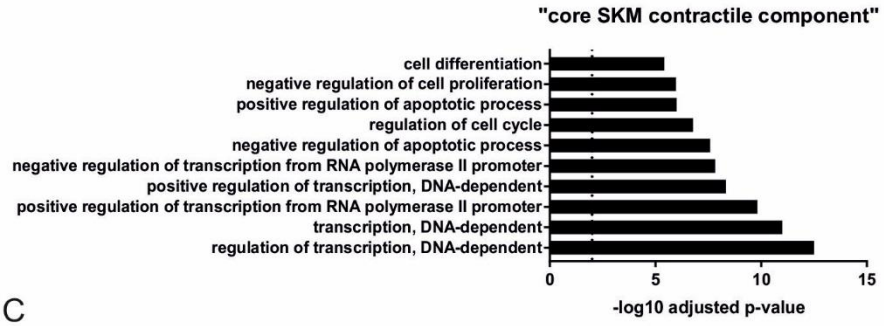

C

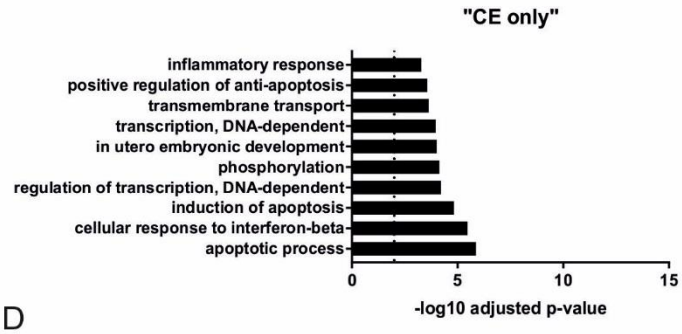

D

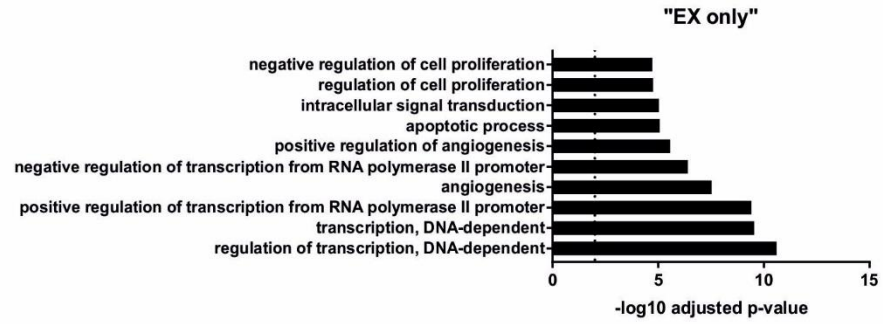

Figure 7. PGC-1α muscle specific knockout animals react differently during acute cold and acute exercise muscle contraction

A) Venn diagram of all DE genes overlapping to any time point in Quad of MKO mice killed 0h, 4h, 6h, or 8h after the acute treadmill test compared to sedentary mice with the CE MKO mice (n=5). FDR < 0.01 and a log2 FC < -0.6 and > 0.6.

B-D) GO analysis of each individual DE fraction found in the Venn diagram called “core SKM contractile component” for the overlap (B), only found in the CE MKO animals (C), only found in the acute exercised MKO mice (D) (n=5). X-axis: (-)log10 adjusted p-value. Dotted line represents significance: (-)log10 adjusted p-value > 2.

Suppl. Figure 1

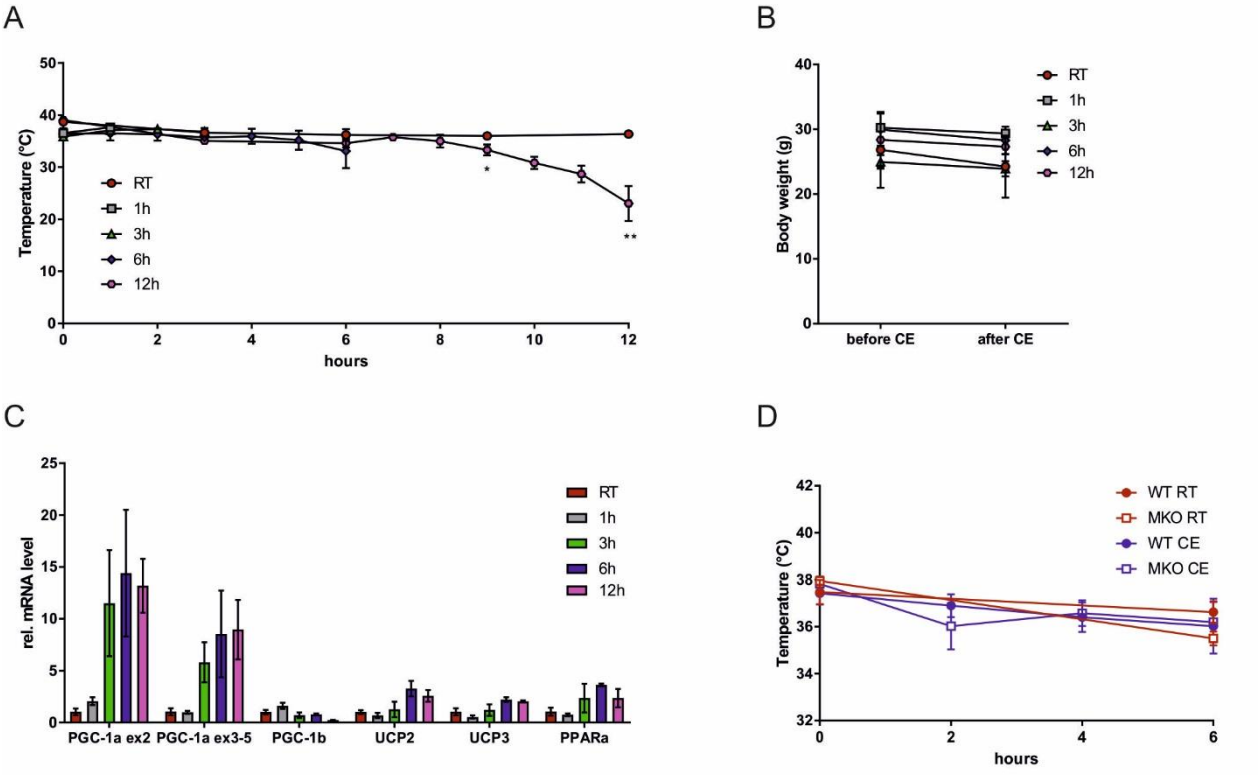

Supplemental Figure 1. Stable body temperature and cold-specific gene induction after 6h cold exposure

A) Body temperature (°C) of WT mice at RT or kept 1h, 3h, 6h or 12h at cold (n=3). Graphs represent relative mean, error bars represent SEM p* < 0.05, p* < 0.01, p*** < 0.001.

B) Body weight (g) of WT mice at RT or kept 1h, 3h, 6h or 12h at cold (n=3). Graphs represent relative mean, error bars represent SEM p* < 0.05, p* < 0.01, p*** < 0.001.

C) Gene expression of PGC-1α exon 2 and exon 3-5, PGC-1β, UCP2, UCP3 and PPARα relative TBP and normalized to RT measured by qRT-PCR in Gastrocnemius muscle (GCN) of WT mice at RT or kept 1h, 3h, 6h or 12h at cold (n=5). Bar graphs represent relative mean mRNA level, error bars represent SEM p* < 0.05, p* < 0.01, p*** < 0.001.

D) Body temperature (°C) of WT and MKO mice CE for 6h or kept at RT (n=5) Graphs represent relative mean, error bars represent SEM p* < 0.05, p* < 0.01, p*** < 0.001.

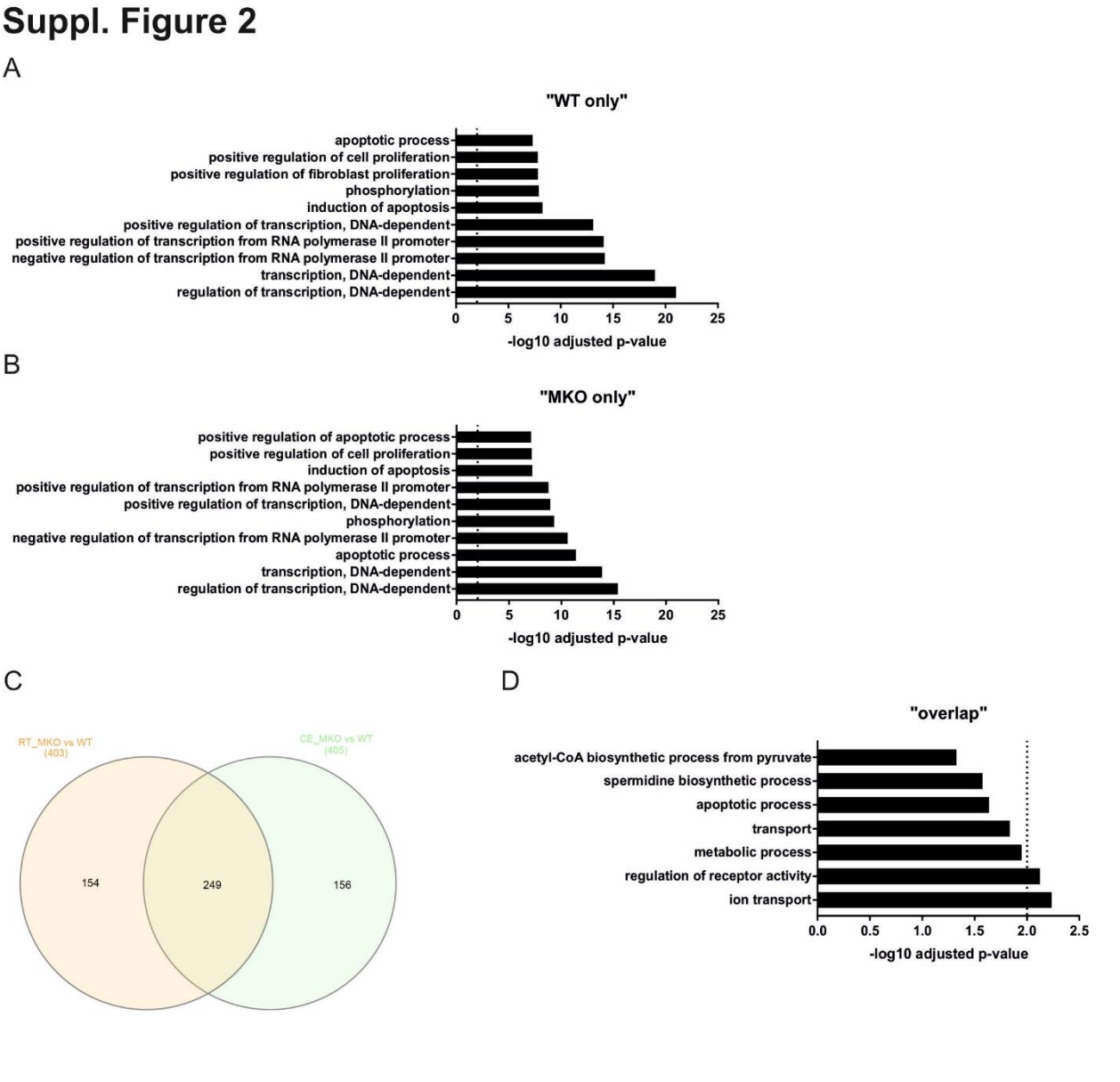

Supplemental Figure 2. Cold exposure dominantly induce transcriptional changes in WT and MKO mice

A-B) GO analysis of DE genes in Quad of the WT only (A) and MKO only (B) animals compared CE to RT (n=5). X-axis: (-)log10 adjusted p-value. Dotted line represents significance: (-)log10 adjusted p-value > 2.

C) Venn diagram of DE genes in Quad of RT mice compared MKO to WT and of CE mice MKO to WT (n=5). FDR < 0.01 and log2 FC < -0.6 and > 0.6.

D) GO analysis of DE genes in Quad of the overlap of RT mice compared MKO to WT and of CE mice MKO to WT (n=5). X-axis: (-)log10 adjusted p-value. Dotted line represents significance: (-)log10 adjusted p-value > 2.

Suppl. Figure 5

A

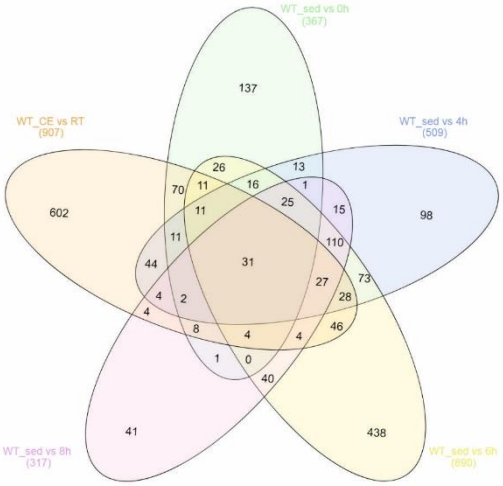

B

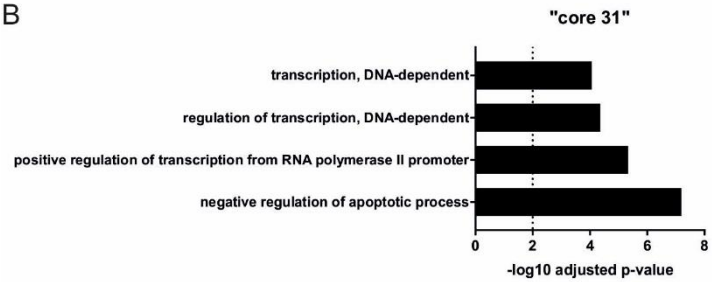

C

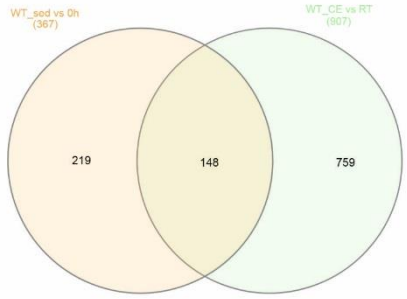

D

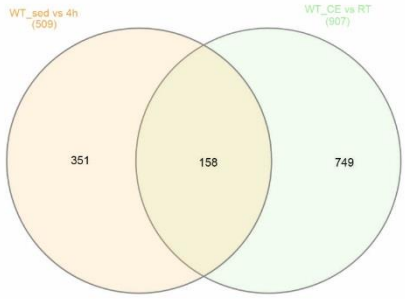

E

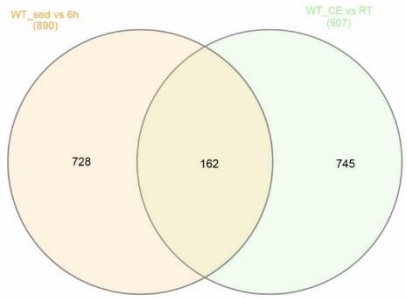

F

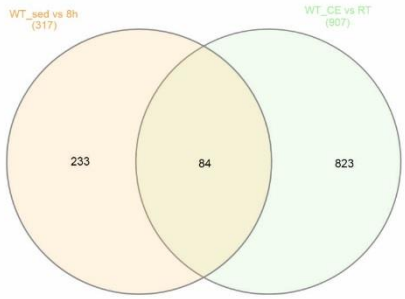

Supplemental Figure 5. No specific acute exercise time point overlap with cold exposure

A) Venn diagram of the DE genes in Quad of WT mice killed 0h, 4h, 6h, or 8h after the acute treadmill test compared to sedentary mice and of CE WT mice (n=5). FDR < 0.01 and a log2 FC < -0.6 and > 0.6.

B) GO analysis of the overlap (core 31) of the DE genes in Quad of WT mice killed 0h, 4h, 6h, or 8h after the acute treadmill test compared to sedentary mice and to CE WT mice compared to RT (n=5).

X-axis: (-)log10 adjusted p-value. Dotted line represents significance: (-)log10 adjusted p-value > 2.

C-F) Venn diagram of DE genes in Quad of acute exercise and CE WT mice killed 0h (C), 4h (D), 6h (E), or 8h (F) after the acute treadmill test compared to sedentary mice with the CE WT mice (n=5). FDR < 0.01 and a log2 FC < -0.6 and > 0.6.

Discussion

Exercise is an accepted and widely used treatment to positively affect metabolic diseases (Colberg et al., 2010a; Haskell et al., 2007) but also to have beneficial effects and improve life performance in myopathies as well as in sarcopenia (Egan and Zierath, 2013; Gill et al., 2018; Law et al., 2016a; Phillips and Mastaglia, 2000). Many of the exercise-induced effects on whole body metabolism are mediated by SKM metabolic and molecular changes (Egan and Zierath, 2013). These adaptations include alterations in mitochondrial and metabolic functions (Green et al., 1992; Spina et al., 1996), in the contractile apparatus (Adams et al., 1993; Widrick et al., 2002), signaling cascades (Benziane et al., 2008) and transcriptional responses (Pilegaard et al., 2003). Importantly, repeated muscle contractions are not only triggered following exercise but also by cold-induced SKM shivering. One of the most important mediators of the transcriptional adaptations to exercise and cold is PGC-1α (Catoire et al., 2012; Egan and Zierath, 2013; Puigserver et al., 1998). However, the underlying mechanism of SKM contraction subsequent to exercise or cold is still largely unexplored and hence, it is not clear whether the same mechanisms and pathways are involved. In addition, it is not known whether there are different functional outputs as force or heat generation following diverse muscle contractions. We now defined for the first time the transcriptional profile of SKM during acute exercise in a time course dependent manner together with the acute cold transcriptional response. Furthermore, the acute exercise and the acute cold response in SKM are clearly distinct from each other, showing that muscle contraction uses different molecular mechanisms dependent on the stimuli and biological output needed. Finally, we found PGC-1α as a key player in both responses to guarantee a healthy and proper contractile answer during acute exercise and acute cold exposure. It is well known that PGC-1α is involved in muscle adaptations upon exercise as well as cold-induced shivering (Lin et al., 2004b; Puigserver et al., 1998). Thus, it is not surprising that PGC-1α was increased by acute cold in BAT and Quad as well as in Quad after acute exercise. Previous studies showed that PGC-1α-Null mice survive not more than 6h when they were cold exposed (Lin et al., 2004b), which fits with our performed time course, where PGC-1α mRNA levels peaked after 6h of cold exposure. Furthermore, PGC-1α was important for a healthy response to acute cold exposure, as observed in a distinct PCA and GO pattern between the genotypes upon cold. Contrary to the PGC-1α-Null mice, the MKO animals were able to induce the mitochondrial uncoupling response in BAT and Quad, hence, they were capable to survive an acute cold exposure of 6h without losing normal body temperature. The transcriptional program, which was regulated during cold, was 2/3 similar to the control animals. However, compared to the WT animals, which regulated on first hand their transcription to cope with the stress induced by cold, the MKO mice seemed to have more problems to handle the cold, depicted by the GO terms “apoptotic process” and “response to stress”. Some studies already linked the lack of PGC-1α to

increased inflammation and apoptotic susceptibility (Adhihetty et al., 2009; Chen et al., 2011; Eisele et al., 2015; Handschin and Spiegelman, 2008). Thus, PGC-1α was important to deal with the switch from RT to cold in a normal, healthy manner, as it is known and important regarding the evolutionary significance of adaptive thermogenesis (Rowland et al., 2015). Since we could not observe any deficits as decreased body temperature after acute cold exposure, it would be interesting to characterize whether the increased stress and apoptotic levels in the MKO animals would have detrimental effects subsequent to either chronic cold exposure or following repetitive acute cold exposure bouts.

As already mentioned, exercise and the induction of PGC-1α are going hand in hand (Lin et al., 2004b; Puigserver et al., 1998). MKO animals were not able to run as long as WT animals and they had massive lactate induction upon acute exercise (Handschin et al., 2007a; Summermatter et al., 2013). Importantly, both genotypes showed enormous transcript changes in a time course dependent manner after acute exercise until exhaustion. This result clearly depicted the importance to take the temporal aspect of gene transcription into account when performing exercise studies. So far, most investigations decided for one specific time point and performed the molecular analysis based on this single snapshot (Egan and Zierath, 2013; Gabriel and Zierath, 2017). In disregard of the time point, the core exercise response in WT animals was “cellular response to calcium ion”. This is not astonishing since it is known that neuronal stimulation increases cytoplasmic calcium levels and hence, activates different cascades such as Ca^{2+}/calmodulin-dependent protein kinases (Gehlert et al., 2015). Furthermore, the GO term “response to stress” including some HSPs was also strongly enriched in the WT core response. Moreover, the overlap in the exercise core responses between WT and MKO animals was likewise highly associated with the term “response to stress”, however, involving different HSPs than in the WT core exercise response. HSPs are chaperons that help to correctly fold newly synthesized proteins or to prevent protein aggregation and they have been shown to be upregulated by an acute bout of exercise in different tissues, including SKM (Henstridge et al., 2016; Lancaster et al., 2004; Noble and Shen, 2012; Tsuzuki et al., 2017). Next to heat-stress, physiological stressors induced by exercise such as hypoxia, energy depletion, calcium level changes or ischemia regulate HSPs as well (Henstridge et al., 2016; Kregel, 2002). So whether the core exercise response of HSP induction found in our exercise model was only due to mechanical heat-stress or a mix of the mentioned stressors above is not clear yet and would need to be further analyzed. Therefore, an exercise experiment in a temperature-controlled environment should be performed to monitor and prevent overheating of SKM by mechanical contraction and hence, elucidate the role of the HSPs. Our data showed clearly a functional important role of PGC-1α in the regulation of the HSPs upon exercise due to blunted induction of Hspa1a, Hspa1b and Dnajb1 and the absent gene induction of the HSPs Hsp90aa1 and Hspb1 in the MKO animals. A recent study linked PGC-1α with the TF heat shock factor 1 (HSF1) and

showed their involvement in the induction of the HSPs, which might explain the reduced response in the MKO animals (Xu et al., 2016a).

Our study aimed to dissect the mechanism of SKM contraction following acute cold and acute exercise. The comparison of the transcriptional profile to the mentioned physiological stimuli revealed a distinct transcriptional pattern. The discovered "core SKM contractile component" response in WT animals overlapped 1/3 between the cold-regulated genes and all acute exercise transcripts. This core response was mainly involved in transcriptional regulation and "apoptotic process". Contrary, the main functions during cold exposure was mostly associated, next to transcriptional regulation, with apoptotic processes and cell death whereas the exercise response exhibited the key functions in transcriptional control, angiogenesis and cell differentiation. Earlier studies already connected exercise to improved angiogenesis, even more, the effect seems to be PGC-1 dependent (Arany et al., 2008; Hoier et al., 2012; Rowe et al., 2011). Interestingly, our data demonstrated the "response to stress" including HSPs as a specific exercise feature, which could not be found in the acute cold response. A common attribute of general muscle contraction was the term of transcription, which was depicted by a fraction of TFs that were either specific for exercise or cold or involved in the general "core SKM contractile component". Exercise and the involvement of TFs, mostly nuclear receptors, have been associated previously, mainly in combination with the PGC-1 family (Scarpulla, 2011; Scarpulla et al., 2012; Schreiber et al., 2004). Interestingly, the "core SKM contractile response" important during cold and exercise, contained the TFs Nr4a1 (Nur77), Nr4a2 (Nurr1), and Nr4a3 (Nor1), which are known to play a role in SKM metabolism and so far, have only been related to exercise-induced muscle contraction but not to shivering thermogenesis (Chao et al., 2012; Kupr et al., 2017; Mahoney et al., 2005; Pearen et al., 2008; Tontonoz et al., 2015). This indicated that an important function upon acute muscle contraction was the maintenance of energy balance in the muscle and the whole body. Remarkably and contrary to the acute exercise specific response of HSPs, the specific cold response revealed an involvement in the regulation of circadian rhythm. Previous studies linked circadian rhythm with thermogenic adaptations in SKM and other tissues but not much is known about this relationship (Chappuis et al., 2013; Gerhart-Hines et al., 2013; Lee et al., 2013). Finally, we showed the importance of PGC-1α in the normal and healthy response to acute muscle contraction as induced by cold or exercise. Muscle-specific PGC-1α knockout animals could fight against acute cold and acute exercise but they were more affected by different stress pathways as apoptosis, mostly upon cold exposure.

Altogether, this data show that muscle contraction subsequent to different stimuli is distinct from each other. A variety of molecular pathways is involved in the regulation of muscle shivering after acute cold exposure compared to the muscle contraction induced during acute exercise. Even more, the role of the master coregulator PGC-1α in the proper and healthy regulation of both stimuli, acute cold- and acute

exercise-induced muscle contraction, is important and needed for a balanced metabolism and a normal output as exercise performance and cold protection over time. Since physical activity is already a well-established treatment against metabolic diseases, our results could help to improve and adapt treatments containing muscle contraction, such as exercise and cold, to improve further patients' quality of life.

Materials and Methods

Animals

Experiments were performed with the approval of the Swiss authorities on adult male mice (15-20 weeks old) for all the experiment and n = 5-6 per condition. Mice had free access to food and water and were housed in a conventional facility with a 12 h light/12 h dark cycle. The PGC-1α muscle-specific knockout (MKO) mice used in this study were generated as described in (Handschin et al., 2007a) and floxed littermates were used as controls (WT).

Exercise training protocols

For the acute exercise time course study mice were acclimatized to treadmill running (Columbus Instruments) as described in Table 1 of the Supplemental Material. Two days after acclimatization, the test started at 0 m/min for 5 min, 5 m/min for 5 min and 8 m/min for 5 min with a 5° incline and the speed was increased 2 m/min every 15 min until 26 m/min and exhaustion. Blood lactate and glucose were measured from tail blood with a lactate plus meter (Nova Biomedical, Labor-Systeme Flükiger AG) or glucose meter (Accu-Chek, Roche), respectively, before and after the treadmill test. Immediately (0h), 4h, 6h and 8h after the test mice were killed by CO_2 and tissues collected. Sedentary mice were not exposed to any treadmill running.

For chronic training mice were acclimatized to treadmill running and treadmill training was carried out 5 times a week for four weeks as described in Table 2A and B of the Supplemental Material. Endurance capacity of the mice was determined on an open treadmill as described above. VO_2max was measured in a closed treadmill (Columbus Instruments) and the test started at 0 m/min for 5 min and 10 m/min for 3 min with a 15° incline and the speed was increased 2 m/min every 3 min until exhaustion. Chronically trained mice were killed by CO_2 18h after the last training session and organs were removed.

Cold exposure

WT and MKO animals were kept at room temperature or at 4 degree 1h, 3h, 6h or 12h for the pilot experiment. Main experiment was performed with 6h cold exposure. Animals were in single cages with

bedding and water but no food during experiment. Mice were killed by CO_2 immediately after 6h cold at 4 degrees and organs were removed.

mRNA sequencing and analysis

Total RNA was isolated from Quadriceps muscle with TRI reagent (T9424, Sigma) according to the manufacturer's instructions. RNA concentration was measured with a NanoDrop OneC spectrophotometer (Thermo Scientific). 7500 ng RNA was further purified with the Direct-zol RNA MiniPrep Kit (R2050, Zymo Research) according to the manufacturer's instructions. For RNAseq library preparation, 1 µg of purified RNA was used and libraries prepared with the TruSeq RNA library Prep Kit (Illumina) according to the manufacturer's instructions. Single read sequencing was performed with a HighSeq 2500 machine (50 cycles, Illumina). Fastq files were mapped to the mouse genome (mm10) and RNAseq and statistical analysis performed with the CLC Genomics Workbench Software (Qiagen).

Venn diagram, gene ontology, principal component analysis, signal peptides

Differentially expressed (DE) genes were pictured in a Venn diagram with the use of the interactiVenn web-based tool (Heberle et al., 2015). Gene ontology (GO) analysis of biological processes was executed by the usage of GeneCodis (Carmona-Saez et al., 2007; Nogales-Cadenas et al., 2009; Tabas-Madrid et al., 2012). Enriched GO terms were furthermore sorted by (-)log10 adjusted p-value. Dotted line represents significance, (-)log10 adjusted p-value > 2. Principal component analysis (PCA) was performed by the CLC Genomic Workbench Software (Qiagen). Signal peptides were analyzed by the PrediSI software (Hiller et al., 2004).

Quantitative real-time PCR (qRT-PCR)

Total RNA was isolated from tissue as described above. The RNA was treated with DNase I (18068015, Thermo Scientific) and then reverse transcribed using hexanucleotide mix (11277081001, Sigma) and SuperScript II reverse transcriptase (18064022, Thermo Scientific). The level of relative mRNA was quantified by real-time PCR on a StepOnePlus system (Applied Biosystems) using Power SYBR green PCR master mix (4367659, Thermo Scientific) or by a Light Cycler 480 II system (Roche) using Fast Start Essential DNA Green Master mix (06924204001, Roche). The analysis of the mRNA was performed by the comparative CT method using TATA binding protein (TBP) as endogenous control. Primer sequences are listed in Table 3 of the Supplemental Material.

Statistical analysis

Values are expressed as means ± standard errors of the means (SEM) and statistical significance was determined with unpaired two tailed t-tests using Excel software. An asterisk (*) indicates significant differences between genotypes or the conditions.

Supplemental Material

Table 1. Acclimatization protocol for treadmill running of acute time course study at 5° inclination.

Day 1	5 min 0 m/min	5 min 5 m/min	5 min 8 m/min	10 min 10 m/min		
Day 2	5 min 0 m/min	5 min 5 m/min	5 min 8 m/min	15 min 10 m/min	5 min 12 m/min	
Day 3	5 min 0 m/min	5 min 5 m/min	5 min 8 m/min	15 min 10 m/min	5 min 12 m/min	2 min 14 m/min
Day 4	5 min 0 m/min	5 min 5 m/min	5 min 8 m/min	15 min 10 m/min	10 min 12 m/min	2 min 14 m/min
Day 5	5 min 0 m/min	5 min 5 m/min	5 min 8 m/min	15 min 10 m/min	10 min 12 m/min	5 min 14 m/min

Table 2A. Acclimatization protocol for treadmill running of chronically trained mice.

Day 1	0° inclination	5 min 0 m/min	5 min 5 m/min	5 min 8 m/min	5 min 10 m/min
Day 2	5° inclination	5 min 0 m/min	5 min 5 m/min	5 min 8 m/min	5 min 10 m/min

Table 2B. Training protocol for chronic treadmill exercise.

	Day 1	**Day 2**	**Day 3**	**Day 4**	**Day 5**
Week 1	10 m/min	10.5 m/min	11 m/min	11.5 m/min	12 m/min
Week 2	12.5 m/min	13 m/min	13.5 m/min	14 m/min	14.5 m/min
Week 3	15 m/min	15.5 m/min	16 m/min	16.5 m/min	17 m/min
Week 4	17.5 m/min	18 m/min	18.5 m/min	Rest	Exercise test
Week 5	Exercise test	18.5 m/min	18.5 m/min	Sacrifice	

Table 3. qPCR primer sequences.

Gene Name	Forward primer	Reverse primer
Cidea	TGGGATTGCAGACTAAGAAGGTC	CGGTCATGGTTTGAAACTCGAAA
Dio2	GAGGAAGGAAGAAGAGGAAGCAA	TTCTTCCAGTGTTTTGGACATGC
PDK4	AAAATTTCCAGGCCAACCAA	CGAAGAGCATGTGGTGAAGGT
PGC-1α exon2	TGATGTGAATGACTTGGATACAGACA	GCTCATTGTTGTACTGGTTGGATATG
PGC-1α exon3-5	AGCCGTGACCACTGACAACGAG	GCTGCATGGTTCTGAGTGCTAAG
PGC-1β	ATGCTTCCCTCACACCTCAG	GCTTTTGCCTTGTAGGCTTG
PPARα	GCGTACGGCAATGGCTTTAT	ACAGAACGGCTTCCTCAGGTT
TBP	TGCTGTTGGTGATTGTTGGT	CTGGCTTGTGTGGGAAAGAT
UCP1	GTCCCCTGCCATTTACTGTCA	TTGGATACTGTCCTGGCAGAGA
UCP2	TGCCCGTAATGCCATTGTC	AGTGGCAAGGGAGGTCATCT
UCP3	TTTTGCGGACCTCCTCACTT	TGGATCTGCAGACGGACCTT

References

Adams, G.R., Hather, B.M., Baldwin, K.M., and Dudley, G.A. (1993). Skeletal muscle myosin heavy chain composition and resistance training. Journal of applied physiology *74*, 911-915.

Adhihetty, P.J., Uguccioni, G., Leick, L., Hidalgo, J., Pilegaard, H., and Hood, D.A. (2009). The role of PGC-1alpha on mitochondrial function and apoptotic susceptibility in muscle. American journal of physiology. Cell physiology *297*, C217-225.

Akimoto, T., Pohnert, S.C., Li, P., Zhang, M., Gumbs, C., Rosenberg, P.B., Williams, R.S., and Yan, Z. (2005). Exercise stimulates Pgc-1alpha transcription in skeletal muscle through activation of the p38 MAPK pathway. The Journal of biological chemistry *280*, 19587-19593.

Arany, Z., Foo, S.Y., Ma, Y., Ruas, J.L., Bommi-Reddy, A., Girnun, G., Cooper, M., Laznik, D., Chinsomboon, J., Rangwala, S.M., et al. (2008). HIF-independent regulation of VEGF and angiogenesis by the transcriptional coactivator PGC-1alpha. Nature *451*, 1008-1012.

Barres, R., Yan, J., Egan, B., Treebak, J.T., Rasmussen, M., Fritz, T., Caidahl, K., Krook, A., O'Gorman, D.J., and Zierath, J.R. (2012). Acute exercise remodels promoter methylation in human skeletal muscle. Cell metabolism *15*, 405-411.

Benziane, B., Burton, T.J., Scanlan, B., Galuska, D., Canny, B.J., Chibalin, A.V., Zierath, J.R., and Stepto, N.K. (2008). Divergent cell signaling after short-term intensified endurance training in human skeletal muscle. American journal of physiology. Endocrinology and metabolism *295*, E1427-1438.

Bostrom, P., Wu, J., Jedrychowski, M.P., Korde, A., Ye, L., Lo, J.C., Rasbach, K.A., Bostrom, E.A., Choi, J.H., Long, J.Z., et al. (2012). A PGC1-alpha-dependent myokine that drives brown-fat-like development of white fat and thermogenesis. Nature *481*, 463-468.

Canto, C., Gerhart-Hines, Z., Feige, J.N., Lagouge, M., Noriega, L., Milne, J.C., Elliott, P.J., Puigserver, P., and Auwerx, J. (2009). AMPK regulates energy expenditure by modulating NAD+ metabolism and SIRT1 activity. Nature *458*, 1056-1060.

Carmona-Saez, P., Chagoyen, M., Tirado, F., Carazo, J.M., and Pascual-Montano, A. (2007). GENECODIS: a web-based tool for finding significant concurrent annotations in gene lists. Genome Biol *8*, R3.

Catoire, M., Mensink, M., Boekschoten, M.V., Hangelbroek, R., Muller, M., Schrauwen, P., and Kersten, S. (2012). Pronounced effects of acute endurance exercise on gene expression in resting and exercising human skeletal muscle. PLoS One *7*, e51066.

Chao, L.C., Wroblewski, K., Ilkayeva, O.R., Stevens, R.D., Bain, J., Meyer, G.A., Schenk, S., Martinez, L., Vergnes, L., Narkar, V.A., et al. (2012). Skeletal muscle Nur77 expression enhances oxidative metabolism and substrate utilization. Journal of lipid research *53*, 2610-2619.

Chappuis, S., Ripperger, J.A., Schnell, A., Rando, G., Jud, C., Wahli, W., and Albrecht, U. (2013). Role of the circadian clock gene Per2 in adaptation to cold temperature. Molecular Metabolism *2*, 184-193.

Chen, S.-D., Yang, D.-I., Lin, T.-K., Shaw, F.-Z., Liou, C.-W., and Chuang, Y.-C. (2011). Roles of Oxidative Stress, Apoptosis, PGC-1α and Mitochondrial Biogenesis in Cerebral Ischemia. International Journal of Molecular Sciences *12*, 7199-7215.

Colberg, S.R., Sigal, R.J., Fernhall, B., Regensteiner, J.G., Blissmer, B.J., Rubin, R.R., Chasan-Taber, L., Albright, A.L., Braun, B., American College of Sports, M., et al. (2010). Exercise and type 2 diabetes: the American College of Sports Medicine and the American Diabetes Association: joint position statement. Diabetes Care *33*, e147-167.

Deng, C., Wang, P., Zhang, X., and Wang, Y. (2015). Short-term, daily exposure to cold temperature may be an efficient way to prevent muscle atrophy and bone loss in a microgravity environment. Life sciences in space research *5*, 1-5.

Egan, B., and Zierath, J.R. (2013). Exercise metabolism and the molecular regulation of skeletal muscle adaptation. Cell metabolism *17*, 162-184.

Eisele, P.S., Furrer, R., Beer, M., and Handschin, C. (2015). The PGC-1 coactivators promote an anti-inflammatory environment in skeletal muscle in vivo. Biochemical and biophysical research communications *464*, 692-697.

Fernandez-Marcos, P.J., and Auwerx, J. (2011). Regulation of PGC-1α, a nodal regulator of mitochondrial biogenesis. The American Journal of Clinical Nutrition *93*, 884S-890S.

Gabriel, B.M., and Zierath, J.R. (2017). The Limits of Exercise Physiology: From Performance to Health. Cell metabolism *25*, 1000-1011.

Gehlert, S., Bloch, W., and Suhr, F. (2015). Ca2+-dependent regulations and signaling in skeletal muscle: from electro-mechanical coupling to adaptation. Int J Mol Sci *16*, 1066-1095.

Gerhart-Hines, Z., Feng, D., Emmett, M.J., Everett, L.J., Loro, E., Briggs, E.R., Bugge, A., Hou, C., Ferrara, C., Seale, P., et al. (2013). The nuclear receptor Rev-erbalpha controls circadian thermogenic plasticity. Nature *503*, 410-413.

Gill, J.F., Santos, G., Schnyder, S., and Handschin, C. (2018). PGC-1alpha affects aging-related changes in muscle and motor function by modulating specific exercise-mediated changes in old mice. Aging cell *17*.

Green, H.J., Helyar, R., Ball-Burnett, M., Kowalchuk, N., Symon, S., and Farrance, B. (1992). Metabolic adaptations to training precede changes in muscle mitochondrial capacity. Journal of applied physiology *72*, 484-491.

Hamrick, M.W., McNeil, P.L., and Patterson, S.L. (2010). Role of muscle-derived growth factors in bone formation. Journal of musculoskeletal & neuronal interactions *10*, 64-70.

Handschin, C., Chin, S., Li, P., Liu, F., Maratos-Flier, E., Lebrasseur, N.K., Yan, Z., and Spiegelman, B.M. (2007). Skeletal muscle fiber-type switching, exercise intolerance, and myopathy in PGC-1alpha muscle-specific knock-out animals. The Journal of biological chemistry *282*, 30014-30021.

Handschin, C., and Spiegelman, B.M. (2008). The role of exercise and PGC1alpha in inflammation and chronic disease. Nature *454*, 463-469.

Haskell, W.L., Lee, I.M., Pate, R.R., Powell, K.E., Blair, S.N., Franklin, B.A., Macera, C.A., Heath, G.W., Thompson, P.D., Bauman, A., et al. (2007). Physical activity and public health: updated recommendation for adults from the American College of Sports Medicine and the American Heart Association. Circulation *116*, 1081-1093.

Heberle, H., Meirelles, G.V., da Silva, F.R., Telles, G.P., and Minghim, R. (2015). InteractiVenn: a web-based tool for the analysis of sets through Venn diagrams. BMC Bioinformatics *16*, 169.

Henstridge, D.C., Febbraio, M.A., and Hargreaves, M. (2016). Heat shock proteins and exercise adaptations. Our knowledge thus far and the road still ahead. Journal of applied physiology *120*, 683-691.

Hiller, K., Grote, A., Scheer, M., Munch, R., and Jahn, D. (2004). PrediSi: prediction of signal peptides and their cleavage positions. Nucleic acids research *32*, W375-379.

Hoier, B., Nordsborg, N., Andersen, S., Jensen, L., Nybo, L., Bangsbo, J., and Hellsten, Y. (2012). Pro- and anti-angiogenic factors in human skeletal muscle in response to acute exercise and training. The Journal of Physiology *590*, 595-606.

Jager, S., Handschin, C., St-Pierre, J., and Spiegelman, B.M. (2007). AMP-activated protein kinase (AMPK) action in skeletal muscle via direct phosphorylation of PGC-1alpha. Proceedings of the National Academy of Sciences of the United States of America *104*, 12017-12022.

Kregel, K.C. (2002). Heat shock proteins: modifying factors in physiological stress responses and acquired thermotolerance. Journal of applied physiology *92*, 2177-2186.

Kupr, B., Schnyder, S., and Handschin, C. (2017). Role of Nuclear Receptors in Exercise-Induced Muscle Adaptations. Cold Spring Harbor perspectives in medicine *7*.

Lancaster, G.I., Møller, K., Nielsen, B., Secher, N.H., Febbraio, M.A., and Nybo, L. (2004). Exercise induces the release of heat shock protein 72 from the human brain in vivo. Cell Stress & Chaperones *9*, 276-280.

Law, T.D., Clark, L.A., and Clark, B.C. (2016). Resistance Exercise to Prevent and Manage Sarcopenia and Dynapenia. Annual review of gerontology & geriatrics *36*, 205-228.

Lee, P., Brychta, R.J., Linderman, J., Smith, S., Chen, K.Y., and Celi, F.S. (2013). Mild Cold Exposure Modulates Fibroblast Growth Factor 21 (FGF21) Diurnal Rhythm in Humans: Relationship between FGF21 Levels, Lipolysis, and Cold-Induced Thermogenesis. The Journal of Clinical Endocrinology & Metabolism *98*, E98-E102.

Liang, H., and Ward, W.F. (2006). PGC-1alpha: a key regulator of energy metabolism. Advances in physiology education *30*, 145-151.

Lin, J., Handschin, C., and Spiegelman, B.M. (2005). Metabolic control through the PGC-1 family of transcription coactivators. Cell metabolism *1*, 361-370.

Lin, J., Wu, H., Tarr, P.T., Zhang, C.Y., Wu, Z., Boss, O., Michael, L.F., Puigserver, P., Isotani, E., Olson, E.N., et al. (2002). Transcriptional co-activator PGC-1 alpha drives the formation of slow-twitch muscle fibres. Nature *418*, 797-801.

Lin, J., Wu, P.H., Tarr, P.T., Lindenberg, K.S., St-Pierre, J., Zhang, C.Y., Mootha, V.K., Jager, S., Vianna, C.R., Reznick, R.M., et al. (2004). Defects in adaptive energy metabolism with CNS-linked hyperactivity in PGC-1alpha null mice. Cell *119*, 121-135.

Mahoney, D.J., Parise, G., Melov, S., Safdar, A., and Tarnopolsky, M.A. (2005). Analysis of global mRNA expression in human skeletal muscle during recovery from endurance exercise. FASEB journal : official publication of the Federation of American Societies for Experimental Biology *19*, 1498-1500.

Noble, E.G., and Shen, G.X. (2012). Impact of Exercise and Metabolic Disorders on Heat Shock Proteins and Vascular Inflammation. Autoimmune Diseases *2012*, 836519.

Nogales-Cadenas, R., Carmona-Saez, P., Vazquez, M., Vicente, C., Yang, X., Tirado, F., Carazo, J.M., and Pascual-Montano, A. (2009). GeneCodis: interpreting gene lists through enrichment analysis and integration of diverse biological information. Nucleic acids research *37*, W317-322.

Oliveira, R.L., Ueno, M., de Souza, C.T., Pereira-da-Silva, M., Gasparetti, A.L., Bezzera, R.M., Alberici, L.C., Vercesi, A.E., Saad, M.J., and Velloso, L.A. (2004). Cold-induced PGC-1alpha expression modulates muscle glucose uptake through an insulin receptor/Akt-independent, AMPK-dependent pathway. American journal of physiology. Endocrinology and metabolism *287*, E686-695.

Pearen, M.A., Myers, S.A., Raichur, S., Ryall, J.G., Lynch, G.S., and Muscat, G.E.O. (2008). The Orphan Nuclear Receptor, NOR-1, a Target of β-Adrenergic Signaling, Regulates Gene Expression that Controls Oxidative Metabolism in Skeletal Muscle. Endocrinology *149*, 2853-2865.

Phillips, B.A., and Mastaglia, F.L. (2000). Exercise therapy in patients with myopathy. Current opinion in neurology *13*, 547-552.

Pilegaard, H., Saltin, B., and Neufer, P.D. (2003). Exercise induces transient transcriptional activation of the PGC-1alpha gene in human skeletal muscle. J Physiol *546*, 851-858.

Puigserver, P., Rhee, J., Lin, J., Wu, Z., Yoon, J.C., Zhang, C.Y., Krauss, S., Mootha, V.K., Lowell, B.B., and Spiegelman, B.M. (2001). Cytokine stimulation of energy expenditure through p38 MAP kinase activation of PPARgamma coactivator-1. Mol Cell *8*, 971-982.

Puigserver, P., Wu, Z., Park, C.W., Graves, R., Wright, M., and Spiegelman, B.M. (1998). A cold-inducible coactivator of nuclear receptors linked to adaptive thermogenesis. Cell *92*, 829-839.

Robinson, M.M., Dasari, S., Konopka, A.R., Johnson, M.L., Manjunatha, S., Esponda, R.R., Carter, R.E., Lanza, I.R., and Nair, K.S. (2017). Enhanced Protein Translation Underlies Improved Metabolic and Physical Adaptations to Different Exercise Training Modes in Young and Old Humans. Cell metabolism *25*, 581-592.

Rowe, G.C., Jang, C., Patten, I.S., and Arany, Z. (2011). PGC-1beta regulates angiogenesis in skeletal muscle. American journal of physiology. Endocrinology and metabolism *301*, E155-163.

Rowland, L.A., Bal, N.C., and Periasamy, M. (2015). The role of skeletal-muscle-based thermogenic mechanisms in vertebrate endothermy. Biological reviews of the Cambridge Philosophical Society *90*, 1279-1297.

Scarpulla, R.C. (2011). Metabolic control of mitochondrial biogenesis through the PGC-1 family regulatory network. Biochimica et biophysica acta *1813*, 1269-1278.

Scarpulla, R.C., Vega, R.B., and Kelly, D.P. (2012). Transcriptional integration of mitochondrial biogenesis. Trends in endocrinology and metabolism: TEM *23*, 459-466.

Schreiber, S.N., Emter, R., Hock, M.B., Knutti, D., Cardenas, J., Podvinec, M., Oakeley, E.J., and Kralli, A. (2004). The estrogen-related receptor alpha (ERRalpha) functions in PPARgamma coactivator 1alpha (PGC-1alpha)-induced mitochondrial biogenesis. Proceedings of the National Academy of Sciences of the United States of America *101*, 6472-6477.

Spina, R.J., Chi, M.M., Hopkins, M.G., Nemeth, P.M., Lowry, O.H., and Holloszy, J.O. (1996). Mitochondrial enzymes increase in muscle in response to 7-10 days of cycle exercise. Journal of applied physiology *80*, 2250-2254.

Summermatter, S., Santos, G., Perez-Schindler, J., and Handschin, C. (2013). Skeletal muscle PGC-1alpha controls whole-body lactate homeostasis through estrogen-related receptor alpha-dependent activation of LDH B and repression of LDH A. Proceedings of the National Academy of Sciences of the United States of America *110*, 8738-8743.

Tabas-Madrid, D., Nogales-Cadenas, R., and Pascual-Montano, A. (2012). GeneCodis3: a non-redundant and modular enrichment analysis tool for functional genomics. Nucleic acids research *40*, W478-483.

Tontonoz, P., Cortez-Toledo, O., Wroblewski, K., Hong, C., Lim, L., Carranza, R., Conneely, O., Metzger, D., and Chao, L.C. (2015). The orphan nuclear receptor Nur77 is a determinant of myofiber size and muscle mass in mice. *35*, 1125-1138.

Tsuzuki, T., Kobayashi, H., Yoshihara, T., Kakigi, R., Ichinoseki-Sekine, N., and Naito, H. (2017). Attenuation of exercise-induced heat shock protein 72 expression blunts improvements in whole-body insulin resistance in rats with type 2 diabetes. Cell Stress Chaperones *22*, 263-269.

Widrick, J.J., Stelzer, J.E., Shoepe, T.C., and Garner, D.P. (2002). Functional properties of human muscle fibers after short-term resistance exercise training. Am J Physiol Regul Integr Comp Physiol *283*, R408-416.

Wu, H., Kanatous, S.B., Thurmond, F.A., Gallardo, T., Isotani, E., Bassel-Duby, R., and Williams, R.S. (2002). Regulation of mitochondrial biogenesis in skeletal muscle by CaMK. Science *296*, 349-352.

Xu, L., Ma, X., Bagattin, A., and Mueller, E. (2016). The transcriptional coactivator PGC1alpha protects against hyperthermic stress via cooperation with the heat shock factor HSF1. Cell Death Dis *7*, e2102.

Yang, Y., Creer, A., Jemiolo, B., and Trappe, S. (2005). Time course of myogenic and metabolic gene expression in response to acute exercise in human skeletal muscle. Journal of applied physiology *98*, 1745-1752.

Zhang, H.M., Chen, H., Liu, W., Liu, H., Gong, J., Wang, H., and Guo, A.Y. (2012). AnimalTFDB: a comprehensive animal transcription factor database. Nucleic acids research *40*, D144-149.

Zhang, H.M., Liu, T., Liu, C.J., Song, S., Zhang, X., Liu, W., Jia, H., Xue, Y., and Guo, A.Y. (2015). AnimalTFDB 2.0: a resource for expression, prediction and functional study of animal transcription factors. Nucleic acids research *43*, D76-81.

7. Generation of a multiplex epitope tag knock-in mouse at the Ppargc1a locus by CRISPR/Cas genome editing technology

Barbara Heim-Kupr[1], Pawel Pelczar[2] and Christoph Handschin[1*]

[1]Biozentrum, University of Basel, Klingelbergstrasse 50/70, CH-4056 Basel, Switzerland

[2]Center for Transgenic Models (CTM) Basel, Mattenstrasse 22, CH-4002 Basel, Switzerland

[*]Corresponding author: christoph.handschin@unibas.ch / Biozentrum, University of Basel, Klingelbergstrasse 50/70, CH-4056 Basel / Phone: +41 61 207 23 78

Abstract

The CRISPR/Cas genome engineering technology is a new developing method allowing precise and fast manipulation of the genome in a multiple fashion. We created two multiplex epitope tagged constructs to generate epitope tagged knock-in mice at the proximal and distal peroxisome proliferator-activated receptor γ coactivator 1α (PGC-1α) promoter transcriptional start site (TSS). Each single stranded DNA construct was injected individually with the corresponding gRNA and Cas9 into male pronuclei of fertilized mouse oocytes. Surviving embryos were transferred into pseudopregnant females, breeding the genetically modified mice. Finally, the born mice were analyzed for correct knock-in by genotyping and sequencing. The applied method allowed the generation of knock-in mice harboring multiple epitope tags at once. Here, we successfully generated a mouse harboring multiplex epitopes at the proximal TSS at the exon 1a of PGC-1α. This new model allows for the first time a detailed analysis of PGC-1α promoter usage, isoform generation and protein level detection in every single cell of the body.

Abbreviations

bp	Base pair
Cas	CRISPR-associated
CRISPR	clustered regularly interspaced short palindromic repeats
crRNA	CRISPR RNA
DSB	double strand break
ES	embryonic stem cells
gRNA	guide RNA
HDR	homology directed repair
i.p.	intraperitoneal
IU	International unit
kb	kilo base
KI	Knock-in
LB	lysogeny broth
NHEJ	nonhomologues end joining
PAM	protospacer adjacent motif
PGC-1α	peroxisome proliferator-activated receptor γ coactivator 1α
RE	Restriction enzyme
trcrRNA	trans-activating crRNA
TSS	transcription start site
WT	Wild type

Introduction

Precise and effective gene editing tools are important to drive today's research in the biology field further. The new clustered regularly interspaced short palindromic repeats (CRISPR) and CRISPR-associated (Cas) proteins technology, which rises from the prokaryote type II CRISPR/Cas system providing bacteria with an adaptive immunity to viruses and plasmids, gives the basis for state of the art genome editing (Hille et al., 2018; Horvath and Barrangou, 2010; Wiedenheft et al., 2012). The endonuclease Cas9 originating from Streptococcus pyogenes type II CRISPR/Cas system is one of the most used enzymes for precise sequence-specific DNA double strand breaks (DSB) (Jinek et al., 2012). A 20 nucleotide single guide RNA (gRNA) sequence within an RNA duplex consisting of the trans-activating crRNA (trcrRNA) and CRISPR RNA (crRNA), trcrRNA:crRNA, form a ribonucleocomplex and base pairs with the DNA target sequence (Gasiunas et al., 2012; Jinek et al., 2012). In addition, the gRNA needs to contain a protospacer adjacent motif (PAM), which is a NGG for Cas9 from Streptococcus pyogenes. Thus, Cas9 is able to introduce a site-specific DSB in the DNA at a precise position, within the target DNA and around 3-4 nucleotides upstream of the PAM sequence (Doudna and Charpentier, 2014; Hille et al., 2018). The CRISPR/Cas technology allows by changes in the sequence of the gRNA to direct the Cas9 and thus, to target any DNA sequence of interest, hence a huge capacity of genome editing is possible. The DSB on the DNA is by nature repaired either by nonhomologues end joining (NHEJ) or by homology directed repair (HDR). NHEJ is the most frequent repair mechanism, which can be used for deletions or insertions but is less precise and often occurs with imprecise DSB repair missing or adding 1-3 nucleotides (Su et al., 2016; Wang et al., 2013; Yang et al., 2013). HDR on the other hand, is a rare event but allows a very precise insertion at the cut site by supplementing the CRISPR/Cas system with a donor sequence containing homology arms to the end flanking regions of the DSB (Cong et al., 2013; Wang et al., 2013; Yang et al., 2013). Several studies implicated the CRISPR/Cas system as very efficient and easy to us for gene deletion as well for reporter gene insertions, not only in simpler organism but as well in rodents (Sternberg and Doudna, 2015; Yang et al., 2014; Yang et al., 2013). This is in contrast to the classical and time-consuming approach of electroporation of a target construct into embryonic stem (ES) cells and targeted homologues recombination, which first generates e chimeric and not clean mouse. According to literature, the usage of the CRISPR/Cas system is very quick and clean, the reagents needed can be directly injected into fertilized mouse eggs and the first CRISPR-based founder mouse is ready after around 3 months (Wang et al., 2013; Yang et al., 2014; Yang et al., 2013).

The goal of this study was to generate an epitope tag knock-in (KI) mouse by using the CRISPR/Cas genome editing technology. We aimed to insert a multiplex epitope tag at the promoter site of the Ppargc1a gene located on chromosome 5 in the mouse genome. Ppargc1a leads to the generation of the peroxisome

proliferator-activated receptor γ coactivator 1α (PGC-1α) protein. Importantly, PGC-1α can be transcribed from two promoters, a proximal and a distal promoter, later one located 13.8 kilo base (kb) upstream (Martinez-Redondo et al., 2015; Miura et al., 2007; Ruas et al., 2012). Dependent on the promoter usage, different isoforms are generated, leading to diverse biological outputs. To date, it is not proven what isoform is generated by which promoter under changing conditions (Martinez-Redondo et al., 2016; Martinez-Redondo et al., 2015; Miura et al., 2007; Popov et al., 2015; Ruas et al., 2012; Ydfors et al., 2013b). Because of the distance of 13.8kb between the promoters, we designed two constructs for each promoter site, which had to be inserted separately into animals. Once a construct is successfully integrated, this mouse can be used for insertion of the second construct. The two constructs designed, contained each a common epitope tag for every transcribed exon 1 from each promoter as well as individual epitope tags for all exon 1s. The different exon 1s are called exon 1a coming from the proximal promoter and exon 1b and exon 1c from the distal promoter. Dependent on which promoter is used, different exon 1s can be transcribed leading to different isoforms (Martinez-Redondo et al., 2015; Miura et al., 2007). By introducing epitope tags at the N-Terminus, next to the TSS of the Ppargc1a promoters, we will be able to define the role of the different promoters as well as the corresponding isoforms. Furthermore, we will be capable to look at protein levels, which was not possible so far due to bad antibodies. Finally, the CRISPR/Cas based knock-in is not cell type specific, allowing a whole body investigation of the individual PGC-1α isoforms and biological functions.

Methods and Results

Knock-in epitope construct strategy

To be able to detect the individual isoforms developing from the two distinct promoters of Ppargc1a, two epitope containing constructs were designed, which we aimed to integrate into the mouse genome at the N-Terminus of the Ppargc1a gene. Each construct contained a common epitope tag for any transcribed exon 1 from any promoter as well as individual epitope tags for each individual exon 1 (Figure 1 + Table 1). This construct allows to study all PGC-1α forms together, total PGC-1α, as well as to distinguish between the promoters and the corresponding isoforms. To enhance the epitopes strength, each epitope was introduced twice with individual sequences resulting in one epitope protein sequence. Especially, each HA epitope, which is the common tag for all translated exon 1s and is present twice at each exon 1 N-Terminus site, is specific as well, finalizing in six individual HA sequences (Table 1). This individuality diminished the risk of miss matches due to similar sequences. Those six specific HA sequences were adapted by changing the Wobble nucleotide leading to unchanged amino acid translation (Crick, 1966) (Table 1). Furthermore, the HA tags were separated by an artificial methionine (ATG) sequence, guaranteeing the correct

transcription of the Ppargc1a gene in case of mismatching at the original TSS in front of the first HA tag (Figure 1).

Proximal promoter epitope construct - exon 1a

An Ultramer DNA oligo (Integrated DNA Technology) of 200 base pairs (bp) was designed for the proximal promoter exon 1a epitope tag (Figure 1). 48bp of the upstream genomic DNA was used as homology arm to allow homologues recombination at the Ppargc1a position of interest. Next, the original TSS (ATG) was followed by the first 27bp HA tag sequence (exon 1a HA Nr.1). Then an artificial methionine (ATG) was placed continued by the second HA tag (exon 1a HA Nr.2). Afterwards, two specific Flag tag sequences each of 24bp (exon 1a Flag Nr1. + Nr.2) were following by 44bp of the genomic DNA containing the exon 1a as homology arm. Finally, the Kozak sequence in front of the original ATG was changed from GG nucleotides to CC due to the risk of miss cutting by the Cas enzyme, which uses an NGG as PAM recognition site.

gRNA for the proximal promoter exon 1a construct

We used the Cas9 enzyme for DSB in our CRISPR/Cas system. Cas needs next to a gRNA to be guided to the place of interest in the genome, a NGG as PAM recognition site. We used the CRISPOR gRNA design tool to generate our gRNA needed (http://crispor.tefor.net/). The best guide was chosen according to the programs calculated score and the cutting site. The selected guide contained a GGG as PAM and cut the DNA after the TSS of the exon 1a (Table 2).

Distal promoter epitope construct - exon 1b and exon 1c

A Megamer DNA oligo (Integrated DNA Technology) of 1100bp was designed for the distal promoter exon 1b and exon 1c epitope tags (Figure 1). The Megamer started with 590bp of the genomic DNA, which was used as homology arm. Then, the original TSS (ATG) was followed by the first HA tag sequence (exon 1b HA Nr.1). Next, a fake methionine (ATG) was placed neighboring by the second HA tag (exon 1b HA Nr.2). Subsequently, two specific V5 tag sequences each of 42bp (exon 1b V5 Nr1. + Nr.2) were followed by 33bp sequence of the exon 1b. Then, a 41bp intron sequence was adjacent to the TSS (ATG) of the exon 1c. Next, two specific HA tags (exon 1c HA Nr.1 + Nr.2) were followed by two distinct Myc tags (exon 1c Myc Nr.1 + Nr.2), each 30bp in length. Finally, the exon 1c sequence of only six nucleotides was used and 171bp of the genomic DNA as homology arm.

gRNA for the distal promoter exon 1b and exon 1c construct

As already used for the proximal promoter construct, Cas protein was used in the CRISPR system. Hence, a gRNA containing NGG as PAM was designed with the CRISPOR gRNA design tool (http://crispor.tefor.net/) according to the score and the site of DSB. The gRNA for the exon 1b and exon 1c construct was a reverse complement sequence, containing a TGG as PAM and cut around 2-3 nucleotides before the TSS of the exon 1c (Table 2).

Genotyping strategy

A precise genotyping strategy had to be used to elucidate the success of the knock-in by CRISPR/Cas into the mouse genome. Offspring toe biopsies were digested in proteinase K (20mg/ml) (V302, Promega) and DNA lysis buffer (50mM Tris-HCl pH-8.0, 100mM NaCl, 10mM EDTA, 0.5% Nonidet P-40) and genotyping was performed (TaKaRa Ex Taq Mg^{2+} free Buffer, RR01AM, Takara Clontech) (Table 3 + 4). Different primer combinations were used to elucidate the correct KI of the epitope sequences and additionally to reveal the genomic location, to check whether the KI took place at the right chromosome or if there were off-targets (Table 5 + 6). In addition, as positive controls a plasmid with the insert and wild type (WT) biopsies were used. Furthermore, genotyping revealing both products, WT and KI bands, as well as genotyping giving only a product in case of KI were considered. An additional critical point was the fact of heterogeneity within a mouse. Thus, the genotyping of a successful KI can reveal a WT and KI band. Even more difficult, we might have the KI on only one allele instead of both alleles. Hence, the genotyping products of interest had to be sequenced to proof the correct nucleotide insertion but still not guarantee the KI on both alleles. Since there was the possibility of heterogeneous samples, the PCR product had to be cleaned by TA cloning (NEB PCR Cloning Kit, E1202). Brief, a PCR product was cloned into a plasmid vector containing ampicillin resistant cassette and hence, allowing selection of cloned products. The cloning product was transformed into competent E.coli bacteria (SURE 2 Supercompetent Cells, 200152, Agilent Techonolgies). Bacteria were plated overnight on lysogeny broth (LB) Agar (BD Difco LB Agar, 244520, Miller) containing ampicillin (A9518, Sigma). Next day, positive colonies were selected and PCR screened for the correct PCR product insertion into the plasmid vector on one hand and replicated in LB medium (NZY Broth, BP2465-500, Fisher Scientific) containing ampicillin overnight on the other hand. PCR screening allowed further selection of possible positive clones used for sequencing. Next, the probes identified as potentially positive for a correct KI by right PCR size detection of the PCR screen were purified for their plasmid and sent for sequencing by using the classical T7 and SP6 primers.

Genotyping for the proximal promoter exon 1a construct

Successful KI of the exon 1a construct was checked by a combination of primers (Figure 2A + Table 6). The primer pair $P1_{ex1a}$ and $P2_{ex1a}$ revealed a band for WT and KI animals. Thus, a control for successful PCR was additionally included. Even more, this primer combination allowed the effective recognition of the integration at the correct position in the genome, due to the fact that the primers were located outside the homology arms of the Ultramer DNA oligo. As positive controls, WT samples from other animals as well as plasmid samples containing the KI sequence were used individually or in a mixed sample to mimic heterogeneity (Figure 3A). The Plasmid was generated by the Bluescript vector (pBS) and Gibson Assembly (Barnes, 1994; Gibson et al., 2010; Gibson et al., 2009). In addition, the genotyping could already give an idea about the gRNA activity due to smeared bands at WT level (Figure 3A, sample 4). Supplementary, a primer combination of $P1_{ex1a}$ with $P4_{ex1a}$ and $P3_{ex1a}$ with $P2_{ex1a}$ was used revealing a band at requested level if a KI happened or no band for WT animals (Figure 3B + Table 6). Thus, the amount of biopsies to further test downstream by TA cloning could already be diminished massively.

Genotyping for the distal promoter exon 1b and exon 1c construct

The same genotyping strategy can be applied for the construct of exon 1b and exon 1c, although there, the PCR products are much larger compared to the exon 1a KI construct (Table 6). So far, the focus was on the generation of the KI at the proximal promoter. The first CRISPR/Cas tests for the KI at the distal promoter were with other previously designed constructs and not successful. The new, here explained construct, was not used so far and thus, the $P3_{ex1bc}$ and $P4_{ex1bc}$ primers still have to be designed and tested accordingly. Therefore, no results are available yet.

gRNA activity detection

It is of huge importance to elucidate the quality of the gRNA as well as the cutting efficiency of the Cas enzyme. Hence, one of the genotyping products was used to check for gRNA activity. Therefore, a PCR product was chosen, which contained the total KI construct including the site of DSB. The sequence of interest was analyzed for restriction sites at the position of DSB induced by Cas. By the use of restriction enzymes (RE), the cutting efficiency could be screened. In case of successful DSB, the restriction recognition site is lost. If the gRNA was inactive, the PCR product can be digested by the RE and the original PCR product is gone.

gRNA activity for the proximal promoter exon 1a construct

FokI, which has GGATG as restriction site, was identified as perfect RE to detect the activity of the gRNA for exon 1a construct. The genotyping product generated with the primer pair $P1_{ex1a}$ and $P2_{ex1a}$ was used for RE digest (Figure 3A + Table 6 + 7). Before digest, the product had to be PCR purified (Qiagen MiniElute PCR purification Kit Cat No./ID:28004). If the gRNA was not active, then the PCR product will be digested into two pieces of 106bp and 93bp, respectively. If there was cutting by Cas and hence the gRNA active, the original PCR product size remains.

gRNA activity for the distal promoter exon 1b and exon 1c construct

XcmI, having CCANNNNNNNNNTGG as restriction site, was found to be ideal for the activity measurement of the gRNA for exon 1b and exon 1c. The purified genotyping product generated with the primer pair $P1_{ex1bc}$ and $P2_{ex1bc}$ was used for RE digest (Table 6 + 7). The digested PCR pieces are 110bp and 76bp in size, respectively.

Pronuclear microinjection of the knock-in sequence and Cas9/CRISP into fertilized mouse oocytes

The desired modification of the exon1a sequence at the Ppargc1a locus was carried out using Cas9/CRISP directly in fertilised mouse oocytes. C57BL/6J female mice underwent ovulation induction by intraperitoneal (i.p.) injection of 5 interantional unit (IU) equine chorionic gonadotrophin (PMSG; Folligon–InterVet), followed by i.p. injection of 5 IU human chorionic gonadotropin (Pregnyl–Essex Chemie) 48h later. For the recovery of zygotes, C57BL/6J females were mated with males of the same strain immediately after the administration of human chorionic gonadotropin. All zygotes were collected from oviducts 24h after the human chorionic gonadotropin injection, and were then freed from any remaining cumulus cells by a 1–2min treatment of 0.1% hyaluronidase (Sigma-Aldrich) dissolved in M2 medium (Sigma-Aldrich). Mouse embryos were cultured in M16 medium (Sigma-Aldrich) at 37°C and 5% CO_2. For micromanipulation, embryos were transferred into M2 medium. All microinjections were performed using a microinjection system comprised of an inverted microscope equipped with Nomarski optics (Nikon), a set of micromanipulators (Narashige), and a FemtoJet microinjection unit (Eppendorf). Injection solution containing trcrRNA annealed to the crRNA targeting the sequence attcgggagctggatggctt (Table 2, gRNA exon 1a) (20ng/ul), Cas9 protein (20ng/µl) and ssDNA homologous recombination template (Ultramer DNA oligo with epitope construct exon 1a) (10ng/ul) (all reagents obtained from IDT) was microinjected into the male pronuclei of fertilized mouse oocytes until 20-30% distension of the organelle was observed. Embryos that survived the microinjection were transferred on the same day into the oviducts of 8–16-wk-old pseudopregnant Crl:CD1(ICR) females (0.5d used after coitus) that had been mated with sterile

genetically vasectomized males the day before embryo transfer (Haueter et al., 2010). Pregnant females were allowed to deliver and raise their pups until weaning age. Offspring toe biopsies were taken around one week after birth.

Cassy, a multiplex PGC-1α exon 1a epitope tag knock-in mouse

Cassy was born on 27th December 2017 in the CTM Basel (Figure 4). She is a healthy female mouse containing all epitope tags and the artificial ATG at the correct genomic locus of the Ppargc1a proximal promoter. She developed in the injection series 13 performed with the designed sense construct for exon 1a described above.

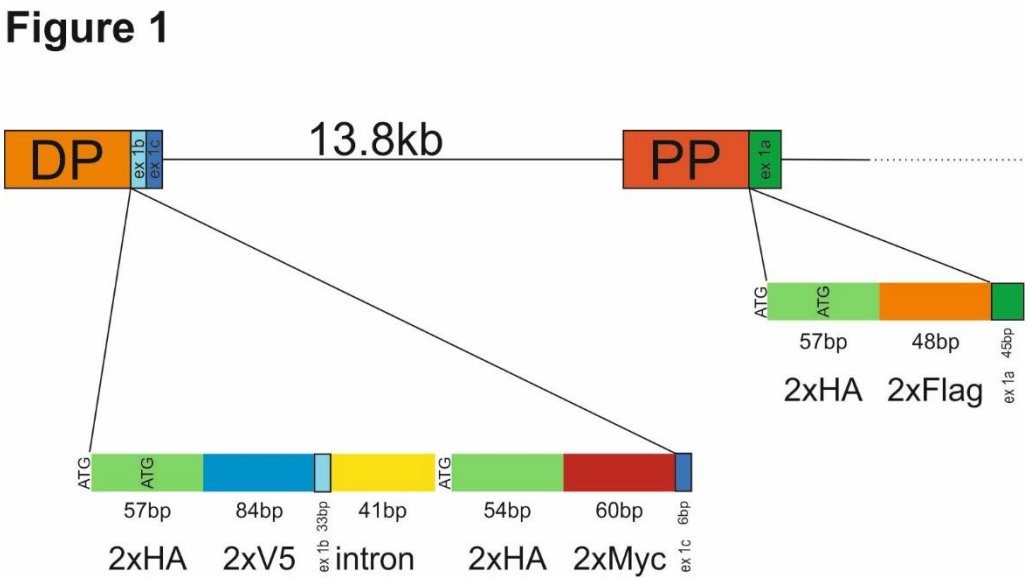

Figure 1

Schematic representation of the proximal (PP) and distal (DP) promoter of PGC-1α and the multiplex epitope constructs for exon1a as well as exon 1b and exon 1c, which will be inserted by CRISPR/Cas technology at the transcription start sites. The two promoters are separated by 13.8kb.

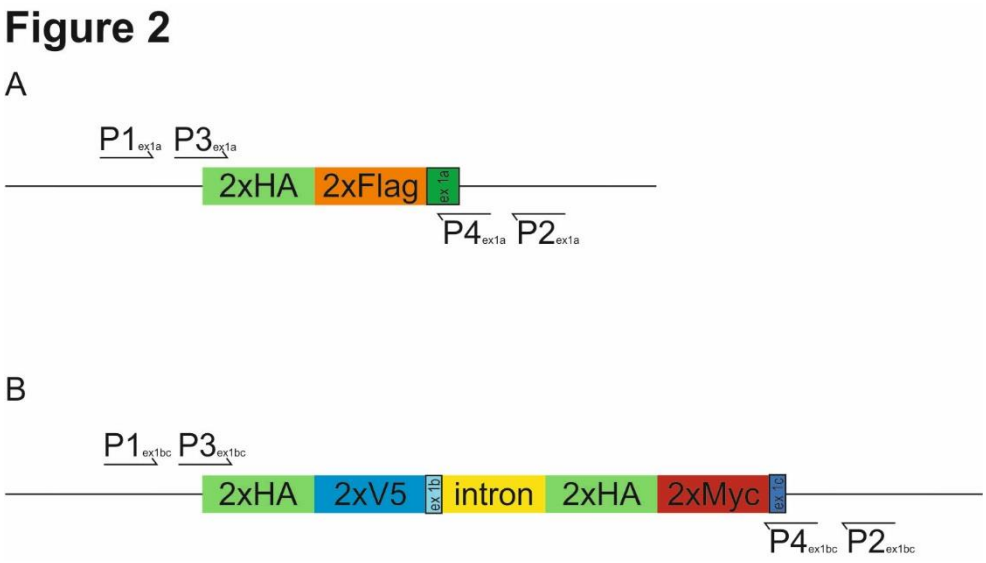

Figure 2

Overview of primer location used for genotyping of exon 1a construct (A) and exon 1b and exon 1c construct (B).

Figure 3

A

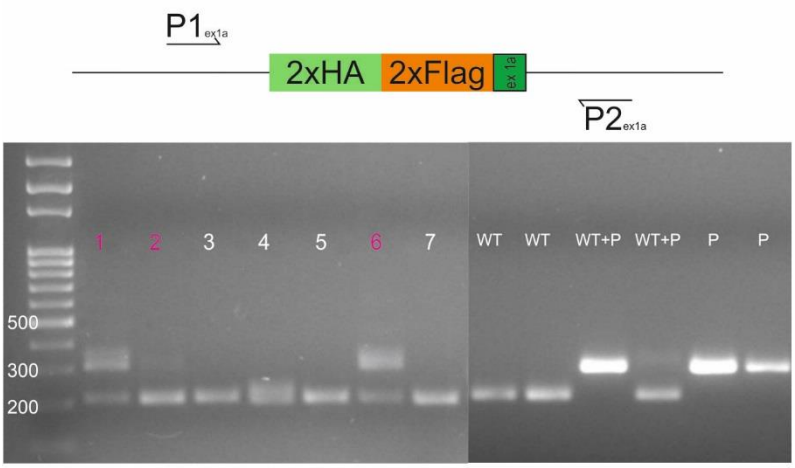

B

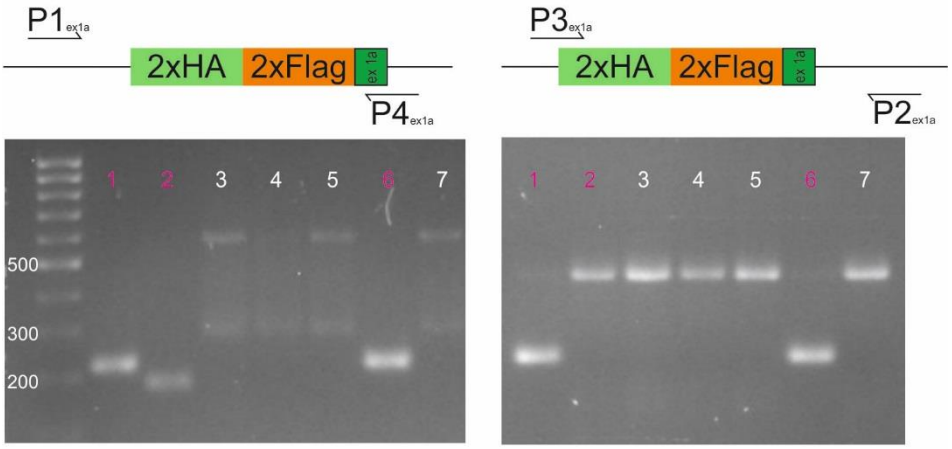

C

Primer combination	PCR product WT	PCR product KI
P1ex1a - P2ex1a	199bp	304bp
P1ex1a - P4ex1a	No band	215bp
P3ex1a - P2ex1a	No band	221bp

Figure 3

Agarose gel picture of exon 1a genotyping performed with primer $P1_{ex1a}$ and $P2_{ex1a}$ (A) and with primer $P1_{ex1a}$ and $P4_{ex1a}$ (B: left) and $P3_{ex1a}$ and $P2_{ex1a}$ (B: right). Seven samples (1-7) as well as wild type (WT), mixture of WT and plasmid (P) and P alone are shown. Pink color indicates possible samples containing the knock-in. C: Table of primer combinations and resulting PCR product.

Figure 4

Three pictures of the first multiplex epitope tagged PGC-1α proximal promoter mouse called Cassy.

Discussion

CRISPR/Cas technology is a new rising tool for genome editing. It allows precise and fast manipulation of the genome leading to deletions or insertions at specific locations of interest. The quick and direct delivery allows fast generation of new animal models (Sternberg and Doudna, 2015; Wang et al., 2013; Yang et al., 2014; Yang et al., 2013). The aim of this study was to generate a KI mouse model containing multiplex epitope tags at the Ppargc1a proximal and distal promoter. Thus, the promoter usage and the transcribed isoforms of PGC-1α can be studied in detail subsequent to different stimuli and in different tissues. So far, the CRISPR/Cas technology was mostly used in simpler organism as Drosophila or Zebrafish or for knockout in mouse models. Only few studies report successful KI at the mouse genome (Singh et al., 2015; Wang et al., 2013; Yang et al., 2014). For the first time a multiplex epitope tag KI mouse at the proximal PGC-1α promoter was generated. Excitingly, the epitope tags at the TSS of the proximal PGC-1α promoter are non-tissue-specific. This allows to study the role of PGC-1α isoforms from the proximal promoter in each cell of the body under diverse stimuli. However, in a first step, the generated mouse has to be bred with WT animals to further transfer the KI to the next generation. Once the PGC-1α exon 1a tag construct is stable integrated in a clean homozygous mouse line, first experiments and characterizations of the animal can be performed. It has to be proven that the mouse is still behaving as a WT animal and is not disordered by the genomic manipulation performed. In addition, this mouse line can be later used to insert the epitope tag KI construct for the exon 1b and exon 1c by the CRISPR/Cas technology. The final goal of this whole project would be a mouse containing both epitope constructs for both promoters at once, to have the full power of promoter and isoform dissection of the PGC-1α protein. By the meanwhile, a successful KI of the exon 1b and exon 1c construct will be continued independently, in an individual mouse line. The generation of the PGC-1α epitope tag KI mouse opens novel study opportunities in regard of the understanding of PGC-1α regulation and functional output. For the first time, isoform specific protein levels can be evaluated under basal and stimulated conditions in different tissues. Detailed promoter usage and isoform generation can be achieved and analysed by diverse approaches such as ChIPseq, IP and Western blot. Finally, the CRISPR generated PGC-1α epitope tag KI mouse will further help to understand the regulatory role of PGC-1α in body metabolism.

Tables

Table 1: Epitope tag sequences used for construct exon 1a and exon 1b + exon 1c

epitope	sequence
exon 1a HA Nr.1	TACCCCTATGACGTTCCCGATTACGCC
exon 1a HA Nr.2	TACCCATACGATGTTCCAGATTACGCT
exon 1a Flag Nr.1	GATTATAAGGACGATGATGACAAA
exon 1a Flag Nr.2	GACTACAAAGACGATGACGACAAG
exon 1b HA Nr.1	TATCCATACGACGTCCCTGACTACGCA
exon 1b HA Nr.2	TACCCTTACGATGTACCCGATTATGCT
exon 1b V5 Nr.1	GGCAAGCCCATCCCCAACCCCCTGCTGGGCCTGGACAGCACC
exon 1b V5 Nr.2	GGTAAACCTATCCCTAACCCCCTTCTCGGTCTGGACAGTACT
exon 1c HA Nr.1	TACCCGTATGATGTGCCGGACTATGCT
exon 1c HA Nr.2	TATCCATATGACGTCCCAGATTATGCC
exon 1c Myc Nr.1	GAACAAAAACTCATCTCAGAAGAGGATCTG
exon 1c Myc Nr.2	AGCAAAAGCTTATTTCAGAAGAAGATCTC

Table 2: gRNA sequence including PAM

gRNA + PAM	sequence
gRNA exon 1a	ATTCGGGAGCTGG**ATG**GCTT GGG
gRNA exon 1b + exon 1c	CCTACATACCAGCAG**CAT**AG TGG

*gRNA exon 1b + exon 1c is reverse complement

**bolt: ATG (CAT is reverse complement) of the exon 1

Table 3: Genotyping PCR mix (final volume 25ul)

Reagents	Volume (µl)
Tag Buffer Mg^{2+} free	2.5
$MgCl_2$	2
dNTP	2
Primer (each)	0.1
Ex tag polymerase	0.125
H2O	17.275
DNA	1

Table 4: Genotyping Program

Temperature	Time
95°C	2min
95°C	30s
58°C	30s
72°C	1min (go to step 2, 34x)
72°C	5min

Table 5: Primer sequences used for genotyping

Primer	Sequence
$P1_{ex1a}$	TCTCAGTAAGGGGCTGGTTG
$P2_{ex1a}$	CAGGAATCATTGCATCTGAG
$P3_{ex1a}$	ACATGTCCCAAGCCTTGTCG
$P4_{ex1a}$	TCGGGAGCTCCATGTACCCC
$P1_{ex1bc}$	ATCTGCACTCCAGCAGAATG
$P2_{ex1bc}$	CAGTCTCCTGATCTTATGTC

Table 6: Primer combinations used for genotyping

Primer combination	PCR product WT	PCR product KI
$P1_{ex1a}$ – $P2_{ex1a}$	199bp	304bp
$P1_{ex1a}$ – $P4_{ex1a}$	No band	215bp
$P3_{ex1a}$ – $P2_{ex1a}$	No band	221bp
$P1_{ex1bc}$ – $P2_{ex1bc}$	186bp	441bp
$P1_{ex1bc}$ – $P4_{ex1bc}$	Not done yet	Not done yet
$P3_{ex1bc}$ – $P2_{ex1bc}$	Not done yet	Not done yet

Table 7: Restriction enzyme (RE) digest

Master Mix	Volume (µl)
H2O	7
RE Buffer	2
RE	1
DNA	10

*digestion was performed 1h at 37°C.

Reference

Barnes, W.M. (1994). PCR amplification of up to 35-kb DNA with high fidelity and high yield from lambda bacteriophage templates. Proceedings of the National Academy of Sciences *91*, 2216-2220.

Cong, L., Ran, F.A., Cox, D., Lin, S.L., Barretto, R., Habib, N., Hsu, P.D., Wu, X.B., Jiang, W.Y., Marraffini, L.A., et al. (2013). Multiplex Genome Engineering Using CRISPR/Cas Systems. Science *339*, 819-823.

Crick, F.H. (1966). Codon--anticodon pairing: the wobble hypothesis. Journal of molecular biology *19*, 548-555.

Doudna, J.A., and Charpentier, E. (2014). The new frontier of genome engineering with CRISPR-Cas9. Science *346*.

Gasiunas, G., Barrangou, R., Horvath, P., and Siksnys, V. (2012). Cas9–crRNA ribonucleoprotein complex mediates specific DNA cleavage for adaptive immunity in bacteria. Proceedings of the National Academy of Sciences *109*, E2579-E2586.

Gibson, D.G., Smith, H.O., Hutchison, C.A., 3rd, Venter, J.C., and Merryman, C. (2010). Chemical synthesis of the mouse mitochondrial genome. Nature methods *7*, 901-903.

Gibson, D.G., Young, L., Chuang, R.Y., Venter, J.C., Hutchison, C.A., 3rd, and Smith, H.O. (2009). Enzymatic assembly of DNA molecules up to several hundred kilobases. Nature methods *6*, 343-345.

Haueter, S., Kawasumi, M., Asner, I., Brykczynska, U., Cinelli, P., Moisyadi, S., Burki, K., Peters, A.H., and Pelczar, P. (2010). Genetic vasectomy-overexpression of Prm1-EGFP fusion protein in elongating spermatids causes dominant male sterility in mice. Genesis (New York, N.Y. : 2000) *48*, 151-160.

Hille, F., Richter, H., Wong, S.P., Bratovic, M., Ressel, S., and Charpentier, E. (2018). The Biology of CRISPR-Cas: Backward and Forward. Cell *172*, 1239-1259.

Horvath, P., and Barrangou, R. (2010). CRISPR/Cas, the Immune System of Bacteria and Archaea. Science *327*, 167-170.

Jinek, M., Chylinski, K., Fonfara, I., Hauer, M., Doudna, J.A., and Charpentier, E. (2012). A Programmable Dual-RNA–Guided DNA Endonuclease in Adaptive Bacterial Immunity. Science *337*, 816-821.

Martinez-Redondo, V., Jannig, P.R., Correia, J.C., Ferreira, D.M., Cervenka, I., Lindvall, J.M., Sinha, I., Izadi, M., Pettersson-Klein, A.T., Agudelo, L.Z., et al. (2016). Peroxisome Proliferator-activated Receptor gamma Coactivator-1 alpha Isoforms Selectively Regulate Multiple Splicing Events on Target Genes. The Journal of biological chemistry *291*, 15169-15184.

Martinez-Redondo, V., Pettersson, A.T., and Ruas, J.L. (2015). The hitchhiker's guide to PGC-1alpha isoform structure and biological functions. Diabetologia *58*, 1969-1977.

Miura, S., Kawanaka, K., Kai, Y., Tamura, M., Goto, M., Shiuchi, T., Minokoshi, Y., and Ezaki, O. (2007). An increase in murine skeletal muscle peroxisome proliferator-activated receptor-gamma coactivator-1alpha (PGC-1alpha) mRNA in response to exercise is mediated by beta-adrenergic receptor activation. Endocrinology *148*, 3441-3448.

Popov, D.V., Lysenko, E.A., Kuzmin, I.V., Vinogradova, V., and Grigoriev, A.I. (2015). Regulation of PGC-1α Isoform Expression in Skeletal Muscles. Acta Naturae *7*, 48-59.

Ruas, J.L., White, J.P., Rao, R.R., Kleiner, S., Brannan, K.T., Harrison, B.C., Greene, N.P., Wu, J., Estall, J.L., Irving, B.A., et al. (2012). A PGC-1alpha isoform induced by resistance training regulates skeletal muscle hypertrophy. Cell *151*, 1319-1331.

Singh, P., Schimenti, J.C., and Bolcun-Filas, E. (2015). A Mouse Geneticist's Practical Guide to CRISPR Applications. Genetics *199*, 1-U402.

Sternberg, S.H., and Doudna, J.A. (2015). Expanding the Biologist's Toolkit with CRISPR-Cas9. Mol Cell *58*, 568-574.

Su, T., Liu, F., Gu, P., Jin, H., Chang, Y., Wang, Q., Liang, Q., and Qi, Q. (2016). A CRISPR-Cas9 Assisted Non-Homologous End-Joining Strategy for One-step Engineering of Bacterial Genome. Scientific reports *6*, 37895.

Wang, H.Y., Yang, H., Shivalila, C.S., Dawlaty, M.M., Cheng, A.W., Zhang, F., and Jaenisch, R. (2013). One-Step Generation of Mice Carrying Mutations in Multiple Genes by CRISPR/Cas-Mediated Genome Engineering. Cell *153*, 910-918.

Wiedenheft, B., Sternberg, S.H., and Doudna, J.A. (2012). RNA-guided genetic silencing systems in bacteria and archaea. Nature *482*, 331-338.

Yang, H., Wang, H.Y., and Jaenisch, R. (2014). Generating genetically modified mice using CRISPR/Cas-mediated genome engineering. Nat Protoc *9*, 1956-1968.

Yang, H., Wang, H.Y., Shivalila, C.S., Cheng, A.W., Shi, L.Y., and Jaenisch, R. (2013). One-Step Generation of Mice Carrying Reporter and Conditional Alleles by CRISPR/Cas-Mediated Genome Engineering. Cell *154*, 1370-1379.

Ydfors, M., Fischer, H., Mascher, H., Blomstrand, E., Norrbom, J., and Gustafsson, T. (2013). The truncated splice variants, NT-PGC-1α and PGC-1α4, increase with both endurance and resistance exercise in human skeletal muscle. Physiological Reports *1*, e00140.

8. Discussion

Skeletal muscle (SKM) has enormous capacity to adapt to diverse external stimuli and disease associated changes, leading to SKM plasticity and whole body adaptations (Egan and Zierath, 2013). Hence, physical inactivity has been linked to metabolic disorders like T2D, obesity, cardiovascular diseases, cancer and others, which could be prevented by physical activity (Booth et al., 2012; Colberg et al., 2010b; Egan and Zierath, 2013; Haskell et al., 2007). The molecular mechanism how SKM is able to regulate the transcriptional as well as the morphological and functional adaptations are not fully understood yet (Egan and Zierath, 2013; Schiaffino and Reggiani, 2011). Key regulators in energy homeostasis, SKM plasticity and whole body metabolism are the PGC-1 coactivators (Arany et al., 2007; Baresic et al., 2014; Cantó and Auwerx, 2009; Chinsomboon et al., 2009; Fernandez-Marcos and Auwerx, 2011; Gali Ramamoorthy et al., 2015; Handschin et al., 2007a; Handschin et al., 2007b; Handschin and Spiegelman, 2006; Knutti and Kralli, 2001; Kressler et al., 2002b; Kupr and Handschin, 2015; Lin et al., 2005; Lin et al., 2002a; Lin et al., 2003; Lin et al., 2002b; Lin et al., 2004a; Martinez-Redondo et al., 2015; Mootha et al., 2004; Pérez-Schindler, 2013; Puigserver and Spiegelman, 2003; Puigserver et al., 1998; Rowe et al., 2011; Schnyder et al., 2017b; Summermatter and Handschin, 2012; Zechner et al., 2010a). PGC-1α and PGC-1β regulate a large and complex transcriptional network by the interaction with numerous TFs (Baresic et al., 2014; Handschin and Spiegelman, 2006; Kupr and Handschin, 2015; Lin et al., 2005; Perez-Schindler et al., 2012; Salatino et al., 2016a). In this thesis, we investigated the molecular mechanism of SKM plasticity by multi-omics approaches such as transcriptomics and methylomics as well as ChIPseq in different PGC-1α and PGC-1β models *in vivo* and *in vitro* combined with two external stimuli, namely exercise and cold exposure.

The first manuscript discussed in this thesis is based on previous work performed by our group where the genome-wide transcriptional network and new binding partners of PGC-1α in SKM cells were elucidated (Baresic et al., 2014). Next to new binding partners as the activity protein 1 (AP-1), ERRα was found as strong partner of PGC-1α in the regulation of PGC-1α target genes (Baresic et al., 2014). The relationship between PGC-1α and ERRα in the control of nearly the whole mitochondrial and oxidative phosphorylation gene program was already shown earlier (Huss et al., 2002; Mootha et al., 2004; Schreiber et al., 2004). In addition, the interaction of PGC-1α and ERRα regulates angiogenesis in SMK by inducing VEGF (Arany et al., 2008). Hence, we were interested on the impact of ERRα on PGC-1α target genes and performed ChIPseq and gene expression analysis of ERRα in the context of PGC-1α overexpression in C2C12 myotubes. Surprisingly, we found that ERRα could be transcriptionally active and regulate PGC-1α target genes with and without coactivation by PGC-1α. This new observation might explain the fraction of indirectly regulated PGC-1α targets found in our previous study (Baresic et al., 2014). Even more, PGC-1α is able to

regulate ERRα gene expression and thus, indirectly regulate its target genes (Mootha et al., 2004). Furthermore, we discovered that ERRα might interact with the specificity protein 1 (SP1) to regulate PGC-1α target genes without coactivation by PGC-1α. Interestingly, the interaction of ERRα with SP1 was genomic context specific and favored high GC content genomic regions. Since GC level is often associated with DNA methylation (Moore et al., 2013; Schubeler, 2015; Stadler et al., 2011), we hypothesized that methylation might affect PGC-1α recruitment. However, previous studies in vascular smooth muscle cells observed binding of SP1 to the Mitofusin 2 promoter, which is a known PGC-1α target gene in SKM and hence, regulates its expression (Sorianello et al., 2012; Zorzano, 2009). Even more, it was reviewed that ERRα binds to the SP1 promoter and regulates its transcription in humans (Sumi and Ignarro, 2005). Further studies are needed to elucidate the exact role of ERRα interaction with or without PGC-1α as well as with other TFs, dependent on the ERRα response elements on the promoter site. It was already shown that changes in the ERRα binding site influence the conformation of ERRα and thus, the interaction with PGC-1α (Barry et al., 2006), which might as well be the case in our study. In addition, the motif similarity between the ERR family members could implicate that PGC-1α might coactivate as well ERRβ and ERRγ, as it was already shown that they are able to regulate PGC-1α target genes in hepatic and SKM cells (Cho et al., 2013; Zhang et al., 2006). Next to ERRα, other TFs might be induced by PGC-1α and regulate its target genes via interaction with other TFBPs, this would need further investigation. Interestingly, the role of PGC-1α is mostly discussed in its activator character, however, we observed that PGC-1α played a role in suppression as well (Baresic et al., 2014), which might reveal new aspects of the transcriptional control by PGC-1α and its partner usage. These findings show the complexity of the transcriptional network regulated by PGC-1α in SKM cells. The new aspect of genomic context leading to diverse coactivator - TF interaction brings new insights in the control of SKM plasticity by PGC-1α. Therefore, the interesting observation we made of diverse binding upon genomic GC content could indicate a new role of PGC-1α in DNA methylation regulation, which is associated with various GC and CpG content (Moore et al., 2013; Schubeler, 2015; Stadler et al., 2011). Regulation of DNA methylation by PGC-1α might serve as an additional layer of control for PGC-1α target genes and thus, allow to regulate the network influencing SKM plasticity and whole body homeostasis under external stimuli as e.g. exercise or disease conditions (Baar, 2010; Bajpeyi et al., 2017; Barres et al., 2009; Barres et al., 2012; Begue et al., 2017; Brunk et al., 1996; Carrió and Suelves, 2015; Howlett and McGee, 2016; Hupkes et al., 2011; Kanzleiter et al., 2015; Laker et al., 2014; Lochmann et al., 2015b; Murashov et al., 2016; Nitert et al., 2012; Voisin et al., 2015). Besides PGC-1α, the other PGC-1 family members as PGC-1β and PRC were not studied in detail yet. Therefore, genome-wide studies of these coactivators would further dissect the large and complex network regulated by the PGC-1 family of coactivators, not only in SKM cells. Finally, the whole project was performed in an *in vitro* model system,

which reflects the metabolic influences and pathways *in vivo* only to some extent. Therefore, the next step would be to dissect the transcriptional network of PGC-1α *in vivo* SKM, first under basal conditions and then with external stimuli as e.g. exercise or food and compare the findings to the *in vitro* approach.

As discussed above, not many studies were done about the role of PGC-1β (Arany et al., 2007; Brault et al., 2010; Gali Ramamoorthy et al., 2015; Lai et al., 2008; Lee et al., 2017; Lelliott et al., 2006; Lin et al., 2002a; Lin et al., 2003; Mortensen et al., 2007; Rowe et al., 2011; Shao et al., 2010; St-Pierre et al., 2003), especially on a genome-wide level to elucidate the transcriptional network as well as the binding partners of this coactivator in SKM. Therefore, the second manuscript aimed to reveal a global picture of the transcriptional network regulated by the coactivator PGC-1β in SKM cells, the TFBP interaction and compare it with the analysis performed for PGC-1α in muscle cells (Baresic et al., 2014; Salatino et al., 2016a). We combined genome-wide binding data from ChIPseq experiments with computational predictions of TFBSs and RNAseq gene expression profiles in response to PGC-1β overexpression in muscle cells. The transcriptional outline of PGC-1β resembled to a large extend the profile of PGC-1α in SKM cells with high involvement in mitochondrial biogenesis and energy homeostasis (Baresic et al., 2014; Handschin and Spiegelman, 2006; Lin et al., 2005; Puigserver and Spiegelman, 2003). In big contrast to the previously performed ChIPseq analysis of PGC-1α in muscle cells (Baresic et al., 2014; Salatino et al., 2016a), only mild recruitment of PGC-1β to the mouse genome could be found. These findings were inconsistent with the high level of differentially expressed genes measured in the RNAseq. Hence, this data indicated that most of the PGC-1β target genes were indirectly regulated. As our previous report for PGC-1α showed, there was control of PGC-1α target genes without direct coactivator - TF interaction (Salatino et al., 2016a). Some TFs, as e.g. ERRα, can interact with other TFs dependent on the genomic context and thus, regulate PGC-1α target genes (Salatino et al., 2016a). An explanation for the observed difference in the number of binding site detection between PGC-1α and PGC-1β ChIPseq as well as the discrepancies to the large number of regulated transcripts under PGC-1β overexpression might be the time point of the performed experiment. Hence, only a snapshot was taken from a large and complex network and thus by chance, a moment of low recruitment was harvested. Nevertheless, the large transcriptome detected by PGC-1β overexpression in myotubes indicated already an important role in metabolic balance, although our data directed towards that most of the genes were regulated indirectly by PGC-1β. However, we confirmed ERRα as the main interaction partner of PGC-1β, involved in the regulation of mitochondrial biogenesis and energy homeostasis, as it was already observed in other studies (Gali Ramamoorthy et al., 2015; Scarpulla, 2011; Shao et al., 2010) as well as for PGC-1α (Arany et al., 2008; Baresic et al., 2014; Huss et al., 2002; Mootha et al., 2004; Salatino et al., 2016a; Schreiber et al., 2004). In addition, we found

interactions with new binding partners as Ets-like and Hox-like TFs. Interestingly, literature already showed a role of Ets-like TFs in the NMJ formation (Hippenmeyer et al., 2007) and Hox-like TFs important for SKM differentiation and DNA methylation (Tsumagari et al., 2013a). However further evaluation has to be done to explain the biological output of this interactions, either by knockdown experiments of the TFs in the context of PGC-1β overexpression or by reporter assays. Even more, the detailed definition of the diverse function of PGC-1β compared to PGC-1α in muscle cells could not be fulfilled since the comparison of the two data sets was not possible as they were too different. Therefore, to clarify the transcriptional network overlap and diversity between PGC-1α and PGC-1β as well as to prove the interesting observation of indirect regulation by PGC-1β, a new experimental setup should be applied, where the ChIPseq and RNAseq of PGC-1β and PGC-1α overexpression in muscle cells will be performed together. This would allow a direct comparison between the two coactivators and would show if PGC-1β really controls only few genes directly. The repetition of the experiment would be of great importance to dissect in a clean and unbiased manner the very complex regulatory transcriptional network of PGC-1α and PGC-1β in SKM cells.

The third and fourth project were combined and resulted in two manuscripts, a main chapter 5.1 elucidating the role of acute and chronic exercise on the transcriptional and DNA methylation control in SKM as well as on muscle memory combined with PGC-1α involvement *in vivo* and *in vitro*. A supplemental chapter 5.2 analyzed the impact of PGC-1α and PGC-1β on the transcriptome and the methylome in an *in vitro* system. The aim of those projects was to dissect the mechanism how global as well as local DNA methylation is regulated in a specific tissue and whether external stimuli as exercise influence not only transcription but also DNA methylation and if these two events are coupled to each other (Barres et al., 2012; Lochmann et al., 2015a; Nitert et al., 2012). Even more, we aimed to understand the mechanism of SKM memory, an important feature in regard of therapeutic training after injury or disuse (Gundersen, 2016; Lindholm et al., 2016; Seaborne et al., 2018; Sharples et al., 2016). Finally, the role of PGC-1α was brought into the game as possible key mediator of DNA methylation combined with gene expressional adaptations upon exercise (Bajpeyi et al., 2017; Barres et al., 2009; Barres et al., 2012; Lochmann et al., 2015b). Our first study discussed in chapter 3 indicated that DNA methylation might affect PGC-1α recruitment (Salatino et al., 2016a), which is supported by other studies (Bajpeyi et al., 2017; Barres et al., 2009; Barres et al., 2012; Lochmann et al., 2015b). However, whether PGC-1α is able to manipulate methylation is not known yet.

We observed that acute exercise modified gene expression in a time course dependent manner and this was accompanied with DNA methylation changes. Even more, acute and chronic exercise led mostly to hypomethylation and gene activation, whereas hypermethylation tended to repress genes. The fact of

gene repression due to methylation by blocking the binding of TFs or changing the chromatin structure is known from literature, specifically in cancer cells (Jones and Takai, 2001; Robertson, 2005; Schubeler, 2015; Siegfried and Simon, 2010). Other studies analyzed the effect of exercise on DNA methylation and gene expression in SKM and observed mostly hypomethylation correlating with gene induction upon acute exercise (Barres et al., 2012; Lindholm et al., 2014). Nevertheless, there is still a debate whether acute exercise affects methylation and hence, gene expression and in which direction the methylation and transcript regulation goes (Kanzleiter et al., 2015; Lochmann et al., 2015b). We clearly identified that hypomethylation occurred more frequently compared to hypermethylation and this correlated nicely with gene activation in acute and chronic exercised mice. Even more, we could show that there was a strong time dependency of DNA methylation and transcriptional adaptation. Interestingly, the chicken or egg question arose, since it is not clear whether there is first DNA methylation and then gene expression adaptation or vice versa. We observed all possible combinations in our acute time course exercise data. Therefore, an acute exercise experiment where the system is not able to change its methylation status by blocking the DNMT and TETs would give the answer to this question. This huge combinatorial variety observed, opens new insides in the control of a large complex involved in SKM adaptations and plasticity. Interestingly, chronic training resulted in only mild transcriptional changes whereas the amount of DMRs was large. Since chronic exercise is a long-term adaptation, stable DNA methylation changes might occur leading to muscle memory and hence, reduced total transcriptional activity due to quicker response (Seaborne et al., 2018; Sharples et al., 2016). This fact was supported by the large overlap of chronic training induced DNA methylation with acute exercised transcriptional changes in our data set. Nevertheless, the exercise memory effect after chronic training has to be further characterized. Thus, we are currently performing a follow-up study with chronically exercised mice, which will be killed after a final acute exhausted test in a time course dependent manner of 0h, 4h, 6h, 8h, and 24h post exhaustion test. Transcriptome analysis of this data set will help to understand the potential memory effect in SKM after chronic training due to epigenetic markers on the DNA, allowing a much quicker adaptive response of the muscle. Furthermore, the exercise memory outcome could be tested by a chronic training paradigm followed by detraining and a possible faster retraining, as it was already performed for resistance exercise (Gundersen, 2016; Mutin-Carnino et al., 2014; Seaborne et al., 2018; Sharples et al., 2016). This knowledge may help to improve therapeutic trainings upon injury or disease (Alibegovic et al., 2010; Booth et al., 2012; Coffey and Hawley, 2007; Gabriel and Zierath, 2017; Jorge et al., 2011; Lindholm et al., 2016; Lindholm et al., 2014; Phillips and Mastaglia, 2000). In addition, the memory effect of parental training on the offspring in regard of methylome profile and performance would gain new insights in SKM memory and germline transmission. So far, only the effect of epigenetic changes and transfer to the next generation

in regard of obesity and T2D was studied (Carter et al., 2013; Laker et al., 2014; Murashov et al., 2016) but not during exercise. A parental transmission of “healthy epigenetic marks” to the offspring would allow a priming of the children either to have a heathier phenotype, be resistance to metabolic diseases or to be more sportive, which would open novel therapeutic strategies. Since PGC-1α and its target genes are induced by exercise and is hence, a main player in energy homeostasis and SKM plasticity by regulating a large transcriptional network, we elucidated the role of PGC-1α in acute exercise-induced transcriptional and methylation changes in wild type (WT) and skeletal muscle-specific PGC-1α knockout animals (MKO). PGC-1α was already shown to undergo methylation changes upon different stimuli as exercise leading to transcriptional adaptations (Barres et al., 2009; Barres et al., 2012; Lochmann et al., 2015b; Murashov et al., 2016). However, we showed the first time that PGC-1α plays a major role in the combined approach of DNA methylation and gene transcription not only during acute exercise but as well in sedentary conditions. MKO mice had reduced and distinct DMRs leading to changed and diminished transcription patterns following the acute exercise time course. Even more, the observed exercise pattern in WT animals of mostly hypomethylation was inversed in the knockout animals. Interestingly, both genotypes showed transcriptional regulation as most important function, although the genes used were distinct. The role of PGC-1α in the control of DNA methylation could even be strengthened by the large methylome and transcriptome in gain-of-function models of skeletal muscle-specific PGC-1α overexpressing mice and *in vitro* by PGC-1α overexpression in C2C12 myotubes. Both systems had an impact on transcription and on methylation, although the *in vitro* system exhibited only mild DNA methylation changes. It was shown that hypomethylation is essential to define muscle lineage and induce differentiation, hence, the methylation levels in differentiated myotubes are lower compared to myoblasts as mostly used for *in vitro* studies (Brunk et al., 1996; Carrió and Suelves, 2015; Hupkes et al., 2011; Lucarelli et al., 2001; Smith and Meissner, 2013). Finally, the role of PGC-1α in the control of DNMTs and TETs should be further elucidated under different conditions and in different genotypes. Combined approaches of exercise with knockout or overexpression of individual DNMTs and TETs in WT and MKO animals would show the regulatory dependency and power of PGC-1α on methylation and transcription. Furthermore, the importance of the DNMTs and TETs for the memory effect in muscle upon chronic training could be validated by chronic exercise in knockout models for DNMTs and TETs, followed by detraining and retraining. Combined approaches of methylomics and transcriptomics with morphological analysis would reveal more details. Taken together, our data provide inside into the close correlation of exercise, transcription and epigenetics. The importance of the exercise intervention, acute versus chronic, as well as the time dependency of DNA methylation and transcriptional output is an important feature, which has to be considered also in future studies. To understand the next layer of control by which PGC-1α is able to

regulate and fine-tune the complex transcriptional network in SKM, will help to adjust interventions and treatments used against metabolic disease or to support quality of life in myopathies and sarcopenia.

In the supplemental project, the transcriptional and the DNA methylation profile in C2C12 myotubes overexpressing PGC-1α and PGC-1β was elucidated. As already observed in the main chapter 5.1 and discussed above, PGC-1α regulates transcription and methylation in SKM *in vivo* and *in vitro*. We found that PGC-1β, as PGC-1α, was involved in the regulation of a large transcriptome and a smaller methylome in myotubes. Interestingly, both coactivators tended to more hypermethylation, which was opposite to the observations *in vivo*. Hence, the closed *in vitro* system might differentially regulate the metabolic pathways as the *in vivo* system, although several studies used both systems and revealed similar results (Brzeszczynska et al., 2018; Kurdiova et al., 2014; Lund et al., 2017; Salatino et al., 2016a). However, our observation might be explained by reduced methylation activity after development (Moore et al., 2013; Okano et al., 1999; Reik et al., 2001; Smith and Meissner, 2013), although this is in large contrast to the *in vivo* methylome measurements performed in the main chapter 5.1. Especially in the myogenic lineage, demethylation was shown to play a critical role to define muscle tissue and induce differentiation (Brunk et al., 1996; Hupkes et al., 2011; Lucarelli et al., 2001; Montesano et al., 2013; Tsumagari et al., 2013b). Nevertheless, a comparison of PGC-1α and PGC-1β regulated target genes and DMRs in differentiated myotubes would help to observe the overlapping as well as the distinct control and hence, support to define the role of each PGC-1 member in more detail. Furthermore, knockdown of one coactivator would indicate, whether there is a compensatory mechanism by the other family member in regard of DNA methylation and the corresponding gene regulation. Since the effect on methylation *in vitro* was not large, an *in vivo* approach with skeletal muscle-specific PGC-1β knockout and overexpressing animals combined with external stimuli as e.g. fasting, which was shown to be an important stimulus in regard of the control of PGC-1β target genes involved in muscle atrophy (Schnyder et al., 2018 (not published yet)), would further define the role of PGC-1β in the control of SKM metabolism. Finally, siRNA-based knockdown of different DNMTs and TETS revealed only very mild impact on PGC-1α and PGC-1β target genes. This might be due to compensatory functions, since the transcriptional network controlled by those coactivators is very large and is involved in essential metabolic signals, which has to be preserved (Arany et al., 2008; Cantó and Auwerx, 2009; Fernandez-Marcos and Auwerx, 2011; Handschin and Spiegelman, 2006, 2008; Kupr and Handschin, 2015; Lelliott et al., 2006; Lin et al., 2005; Puigserver et al., 1998; Rowe et al., 2011; Scarpulla, 2011). As already discussed above, an *in vivo* system with impaired DNMTs and TETs combined with PGC-1α/β under different conditions would give further ideas about the regulation of target genes. However, our data demonstrate a combined control of transcription and DNA methylation, which allows

a fine-tuned regulation of a large and complex transcriptional network in SKM cells by PGC-1α and PGC-1β.

The fifth project discussed in this thesis focused on the SKM contraction-induced transcriptional profile after different external stimuli as acute exercise and acute cold exposure combined with the PGC-1α dependency. Exercise is an widely accepted treatment to counteract metabolic diseases such as obesity or T2D and improve cardio vascular functions (Colberg et al., 2010a; Haskell et al., 2007) but also to increase quality of life in myopathies as well as in sarcopenia (Egan and Zierath, 2013; Gill et al., 2018; Law et al., 2016a; Phillips and Mastaglia, 2000). Many of the exercise-induced beneficial effects on whole body metabolism are mediated by SKM metabolic and molecular alterations (Egan and Zierath, 2013), which comprise adaptations in mitochondrial and metabolic function (Green et al., 1992; Spina et al., 1996), in the contractile apparatus (Adams et al., 1993; Widrick et al., 2002), in signaling cascades (Benziane et al., 2008) and in the transcriptional responses (Pilegaard et al., 2003). Several of these adaptations in SKM are discussed in context of exercise-induced muscle contraction, nevertheless, also cold-induced muscle shivering lead to numerous metabolic changes and adaptations. One of the most important mediators of the transcriptional adaptations to exercise and cold in SKM is PGC-1α (Catoire et al., 2012; Egan and Zierath, 2013; Lin et al., 2004a; Puigserver et al., 1998). However, the underlying mechanism of SKM contraction subsequent to exercise or cold is still largely unexplored and hence, it is not clear whether the same mechanisms and pathways are involved. We now defined for the first time the transcriptional profile of SKM during acute exercise in a time course dependent manner together with the acute cold transcriptional response. Furthermore, we observed a clear distinct transcriptional response to acute exercise and acute cold in SKM, showing that muscle contraction uses different molecular mechanisms dependent on the stimuli and biological output needed. Shivering, which is a repetitive contraction of muscle, is not sufficient to maintain body temperature over longer period of cold, thus non-shivering thermogenesis coming from BAT and from SKM has to be activated to generate sustained heat by uncoupling (Bal et al., 2012; Rowland et al., 2015). Nevertheless, the time-dependent switch from shivering to non-shivering thermogenesis in SKM is not defined yet. In addition to shivering, also exercise-induced muscle contraction was shown to generate heat (Henstridge et al., 2016; Kregel, 2002), specially maximal contraction as upon intense exercise or shivering bout was displayed to count up to 90% of oxygen consumption, hence massive heat production (Egan and Zierath, 2013; Rowland et al., 2015; Summermatter and Handschin, 2012; Zurlo et al., 1990). However, those mechanisms of heat production are very costly and limited by nutrition and are therefore, only acutely used (Egan et al., 2016; Egan and Zierath, 2013; Rowland et al., 2015). Anyway, the generated heat during cold is important as first line of

defense during acute cold to maintain body temperature (Rowland et al., 2015), contrarily, too much heat production during exercise is detrimental for the metabolism and reduces performance (Henstridge et al., 2016; Kregel, 2002; Noble and Shen, 2012). Hence, our data support those findings that different mechanism are controlled after exercise- or cold-induced muscle contraction. Even more, we observed PGC-1α as a major regulator of a proper and healthy response to acute cold- and acute exercise-induced stressors. In our cold experimental setup, we decided to use 6h cold exposure because PGC-1α gene expression peaked at this time point. From literature it is know that PGC-1α-Null mice are not able to survive longer than 6h during cold (Lin et al., 2004a). We observed no problems keeping body temperature in MKO animals due to induced uncoupling proteins in BAT and SKM to the same extend as in WT animals. However, in contrast to WT animals, the knockout mice had deficits on the transcriptional level, leading to transcriptional apoptotic responses. PGC-1α was already linked previously to apoptotic control and inflammatory processes, although not in association with cold (Adhihetty et al., 2009; Chen et al., 2011; Eisele et al., 2015; Handschin and Spiegelman, 2008). It seems that PGC-1α is important to cope with the switch from room temperature into cold in a healthy manner. Since we did not observe any body temperature related deficits in the MKO animals, further studies with chronic cold exposure or repetitive acute cold exposure would give more details about potential detrimental effects of the increased stress level and differentially regulated transcriptional profile in those mice compared to WT animals. The aim of this study was to elucidate the muscle contraction transcriptional profile following acute cold and acute exercise and elucidate the PGC-1α importance. Many studies already discussed the role of PGC-1α in SKM plasticity and energy homeostasis after exercise stimuli (Akimoto et al., 2008; Akimoto et al., 2005; Baar et al., 2002; Bajpeyi et al., 2017; Chinsomboon et al., 2009; Egan and Zierath, 2013; Gill et al., 2018; Handschin, 2016; Handschin et al., 2007a; Handschin and Spiegelman, 2008; Koves et al., 2005; Kupr et al., 2017; Miura et al., 2008; Miura et al., 2007; Pilegaard et al., 2003; Russell et al., 2005; Summermatter and Handschin, 2012; Tadaishi et al., 2011; Terada and Tabata, 2004; Ydfors et al., 2013a). However, a time course of acute exercise as well as the comparison of muscle contraction after external stimuli compared with the role of PGC-1α in this adaptation process was not investigated so far. We could confirm that MKO animals are not able to run as long as WT animals and that they have much higher lactate production following acute exercise (Handschin et al., 2007a; Summermatter et al., 2013). Importantly, we found massive transcriptional changes in both genotypes during all time points of the acute exercise time course, pointing the importance of time-dependent regulation, which should be considered for further studies instead of taking only a snapshot (Egan and Zierath, 2013; Gabriel and Zierath, 2017). The main response in WT animals upon acute exercise, regardless of any time point, was the cellular response to calcium as well as the response to stress including heat shock proteins (HSP). It is known that neuronal stimulation

increases cytoplasmic calcium levels and hence, activating different cascades such as Ca^{2+}/calmodulin-dependent protein kinases (Gehlert et al., 2015). In addition, cytosolic calcium concentrations can lead to hyperthermia, thus, a possible link of calcium concentration and HSP response might be considered since it has been shown that the heat shock TF (HSF) is able to regulate calcium (Mosser et al., 1990). Opposite, calcium was shown to induce some HSPs by inhibiting the Hsp90 in human keratinocytes (Chang et al., 2006; Wakita et al., 1994), which is missing in our MKO mice. Importantly, the core exercise response found in WT animals contained HSP, which were distinct from the response to stress in MKO animals containing different HSP. HSPs are chaperons that help to correctly fold newly synthesized proteins or to prevent protein aggregation and they have been shown to be upregulated upon an acute bout of exercise in different tissues, including SKM (Henstridge et al., 2016; Lancaster et al., 2004; Noble and Shen, 2012; Tsuzuki et al., 2017). Next to heat stress, they can be regulated also by other physiological stressors such as exercise, calcium, hypoxia, energy depletion or ischemia (Henstridge et al., 2016; Kregel, 2002). To elucidate whether the core exercise response of HSP induction found in our exercise model is only due to mechanical heat-stress or a mix of the mentioned stressors above is not clear yet and would need to be further analyzed. Due to our observation of induced calcium signaling in WT animals, the study of HSP regulation by increased cytosolic calcium level might be of interest in SKM and exercise physiology. Therefore, an exercise experiment such as treadmill running or swimming in a temperature-controlled room or pool should be performed to monitor and prevent overheating of SKM by mechanical contraction and hence, elucidate the role of the HSPs (Ishihara et al., 2009). Furthermore, it would be interesting to describe the role of SKM PGC-1α in this context, which is known to be regulated by calcium and has been shown to associate with HSF to induce the transcription of HSPs, which might explain the reduced and different response in the MKO animals (Handschin et al., 2003; Wu et al., 2002; Wu et al., 1999; Xu et al., 2016a). Recently, PGC-1α- and exercise-dependent myokines termed irisin, meteorin-like and β-aminoisobutyric acid have been identified to promote browning of white adipose tissue and thereby increasing energy expenditure (Bostrom et al., 2012; Rao et al., 2014; Roberts et al., 2014). It seems paradoxical that exercise triggers the release of myokines to induce thermogenesis and energy expenditure. The authors claim that this might be a possible evolutionary consequence of muscle shivering, however, direct correlations are missing yet. Therefore, these findings suggest that there might be overlap between SKM response to exercise and cold, although this is only a hypothesis so far. However, our combined analysis of acute cold and acute exercise revealed involvement of secreted peptides but none of the genes transcribing the three myokines mentioned above could be detected. Probably, plasma analysis would give more information than transcript levels. Interestingly, the combined analysis of acute exercise and acute cold response in SKM exposed the response to stress including HSPs as an exercise-

specific feature, which could not be found in the acute cold response. This might be due to different stress outputs needed during cold, as first line of defense, or exercise as already discussed before (Rowland et al., 2015). Contrary, a common attribute of general muscle contraction found in both stimuli was the term of transcription, which was depicted by a fraction of TFs. However, the TFs found were stimuli-specific and thus, mainly distinct from each other in acute exercise or acute cold. Nevertheless, the common "core SKM contractile response" in both conditions contained the TFs Nr4a1 (Nur77), Nr4a2 (Nurr1), and Nr4a3 (Nor1), which are known to play a role in SKM metabolism and have only been associated to exercise-induced muscle contraction but not to shivering thermogenesis yet (Chao et al., 2012; Kupr et al., 2017; Mahoney et al., 2005; Pearen et al., 2008; Tontonoz et al., 2015). This indicates that an important function upon acute muscle contraction is the maintenance of energy balance in the muscle and the whole body. Further evaluation of the nuclear receptor interaction during cold has to be considered. Mostly, the interaction of nuclear receptors with the coactivator PGC-1α has been studied so far. Thus, a combined new approach of PGC-1α with the Nr4a family of TFs would declare the interaction between those factors. ChIPseq would show whether there is direct interaction and if this interaction could be changed by different stimuli as exercise and cold. Even more, study of MKO mice would clarify the importance of PGC-1α in this context and whether there is compensation by other factors to still induce the Nr4a TFs. In addition, skeletal muscle-specific PGC-1α overexpressing mice could be used to elucidate if external stimuli and thus, PGC-1α induction is needed to activate this cascade or whether the high level of PGC-1α by overexpression is already enough to induce the same response as observed after exercise and cold. Taken together, our data demonstrate a distinct transcriptional response in SKM subsequent to acute exercise- or acute cold-induced contraction. Even more, we show the importance of PGC-1α in the normal and healthy response to acute muscle contraction as induced by cold or exercise. Hence, long-term exercise or cold exposure in WT and MKO mice combined with morphological and transcriptional analysis would reveal the detrimental effect of missing PGC-1α in SKM over a long period. Thus, a possible accumulation of stress factors, apoptotic markers and toxins might result in functional and morphological changes, which could be only discovered in aged and long-range treated animals. Since physical activity is already a well-established treatment against metabolic diseases, our results could help to improve and adapt treatments containing muscle contraction, such as exercise and cold, to improve further patients' quality of life.

The last and most pioneering chapter of this thesis, chapter 7, considered the generation of a multiplex epitope containing knock-in mouse at the Ppargc1a locus engineered by the CRISPR/Cas technology. We aimed to elucidate the promoter usage and the resulting isoforms of PGC-1α since the exact role of the proximal and distal PGC-1α promoters as well as the impact of the isoforms is not clear yet. PGC-1α can

be transcribed from two promoters, a proximal and a distal promoter, later one located 13.8 kilo base (kb) upstream (Martinez-Redondo et al., 2015; Miura et al., 2007; Ruas et al., 2012). Dependent on the promoter usage, different isoforms are generated, leading to diverse biological outputs. To date, it is not proven what isoform is generated by which promoter under changing conditions (Martinez-Redondo et al., 2016; Martinez-Redondo et al., 2015; Miura et al., 2007; Popov et al., 2015; Ruas et al., 2012; Ydfors et al., 2013b). However, recently PGC-1α4 was discovered to be transcribed from the distal promoter and contrarily to the so far described isoforms, involved in SKM hypertrophy (Ruas et al., 2012). By the CRSIPR/Cas technology, a non-tissue specific knock-in at the N-Terminus of Ppargc1a can be reached and thus, the promoter usage and the transcribed isoforms of PGC-1α can be studied in detail upon different stimuli and importantly and uniquely in different tissues. Nevertheless, several challenges had to be overcome in this project. First, the CRISPR/Cas genome editing technology to generate a knock-in model was mostly used in simpler organisms or when in mouse models then only for knockout. Only few studies reported successful knock-in approaches in the mouse genome yet (Singh et al., 2015; Wang et al., 2013; Yang et al., 2014). Secondly, the distance of the two PGC-1α promoters of 13.8kb did not allow to generate one knock-in construct, which could be inserted at once. Rather two independent constructs had to be designed for each promoter and each corresponding exon 1 individually, which had to be injected into pseudopregnant mice separately. Finally, the correct construct design and CRISPR/Cas system strategy to avoid off-targets, missing construct pieces, inactive gRNAs and the right conditions of all reagents and the template oligonucleotides to inject successfully into oocytes had to be tested and proved. Thus, the first goal was to generate at least one of the two new mouse lines, either with an epitope knock-in at the proximal promoter containing exon 1a or with the epitopes at the distal promoter containing exon 1b and exon 1c. For the first time, a mouse with a very complex multi-epitope construct at the proximal promoter of Ppargc1a could be generated, containing the construct in all cells of the body. Next, this mouse has to be mated with WT mice from the same genetic background to allow germline transmission. Once successful transmission could be achieved and the new mouse line increased in size, first validation experiments could be done. On one hand, it has to be proved that the mouse behaves still like a WT animal and that the expression of PGC-1α from the proximal promoter is still expressed like in WT mice and can react following external stimuli as e.g. exercise (Handschin and Spiegelman, 2006; Lin et al., 2002b; Pilegaard et al., 2003; Puigserver et al., 1998; Spiegelman and Heinrich, 2004). In addition, the second knock-in mouse line for the distal promoter should be generated individually, finally to have two stable knock-in lines. Thus, both lines can be used to already start experiments in regard of IP, ChIP and protein level characterization for each promoter individually. On the other hand, one of the stable mouse lines can be used to insert the second missing epitope tag construct for the other promoter by CRISPR/Cas

technology. The final goal of this project would be a mouse containing both epitope constructs for both promoters at once to have the full authority of promoter and isoform dissection of the PGC-1α protein. Taken together, the CRISPR/Cas technology is a new rising tool allowing innovative new genome editing approaches. Nevertheless, the theory and the practice do not always fit and thus, knowing all challenges we had to overcome at the beginning, we probably would have chosen the classical way of ES cells and homologous recombination, which would have been much faster in the end but would also involve limitations as tissue specificity. However, we managed half of the projects' aim with the generation of the first multiplex epitope knock-in mouse at the Ppargc1a proximal promoter, which is a great success for the whole PGC-1α community. Nevertheless, the main work with the characterization and experimental possibilities with this new mouse line as well as the generation of the second and finally the complete knock-in mouse, starts now.

9. Conclusion and Outlook

The PGC-1α and PGC-1β coactivators are involved in pleiotropic functions in SKM and whole body metabolism. The different projects discussed in this thesis illustrate the multiplicity of regulatory mechanisms in SKM plasticity and the impact of PGC-1α/β in those processes.

The first two projects revealed a genome-wide recruitment of PGC-1α and PGC-1β to the mouse genome in SKM cells. New TFBPs could be identified and novel regulations of PGC-1α target genes in new contexts were elucidated. Nevertheless, as already discussed in the section above, further studies need to be done in a combined PGC-1α/β ChIPseq approach in SKM cells to describe in detail the common and distinct features of those two coactivators. The projects three and four combined with project five revealed the first time a global overview of SKM controlled plasticity on transcriptional and methylation level *in vivo* and *in vitro* under diverse external stimuli as exercise and cold, associated with different PGC-1α and PGC-1β genotypes. Importantly, the transcriptional and methylation profiles following acute exercise, chronic exercise or cold-induced muscle shivering are distinct and PGC-1α dependent. The multi-omics approaches used revealed enormous new insides in the molecular mechanism of SKM plasticity and hence, opened new doors for novel studies. However, the combination of different projects, setups and analysis are important to dissect and understand the global molecular mechanism of SKM plasticity and the complex transcriptional network regulated by PGC-1α/β in this context. Finally, the last project focused on the generation of a unique multiplex epitope knock-in mouse at the Ppargc1a locus. This mouse, specially the complete knock-in mouse, will allow to dissect the molecular mechanism and control by PGC-1α under pleiotropic stimuli and in each cell of the body. A detailed dissection of promoter usage and isoform generation can be studied in detail. New TFBP can be identified by ChIPseq experiments for each generated isoform under different condition and various tissues. The new potential of this model is massive and will clearly have huge impact on the detailed global description of the PGC-1α coactivator.

Taken all together, we contributed many important new aspects to the current knowledge of the function and role of PGC-1α and PGC-1β coactivators in SKM metabolism. Nevertheless, numerous new questions arose and have to be further explored to fully understand the SKM plasticity and its impact on the whole body metabolism as well as the role of the PGC-1 coactivators. Still limited knowledge is around of PGC-1α protein, which now might be answered by the generated CRISPR mouse. Even less is known about PGC-1β and its transcriptional network in different physiological and pathophysiological conditions. Therefore, future studies have to focus more on the protein modification of PGC-1α and PGC-1β and their contribution to the body homeostasis. Since especially PGC-1α has been implicated to be a potential therapeutic target in metabolic disorders and other pathophysiological conditions, new findings will increase the knowledge and hence allow to develop new intervention strategies to specifically bring PGC-

1α and PGC-1β into the game in disease conditions to exert their beneficial effects on tissue- and whole body-specific metabolism.

References

Adams, G.R., Hather, B.M., Baldwin, K.M., and Dudley, G.A. (1993). Skeletal muscle myosin heavy chain composition and resistance training. Journal of applied physiology (Bethesda, Md. : 1985) *74*, 911-915.

Adcock, I.M., and Caramori, G. (2009). Chapter 31 - Transcription Factors A2 - Barnes, Peter J. In Asthma and COPD (Second Edition). J.M. Drazen, S.I. Rennard, and N.C. Thomson, eds. (Oxford: Academic Press), pp. 373-380.

Adhihetty, P.J., Uguccioni, G., Leick, L., Hidalgo, J., Pilegaard, H., and Hood, D.A. (2009). The role of PGC-1alpha on mitochondrial function and apoptotic susceptibility in muscle. American journal of physiology. Cell physiology *297*, C217-225.

Akalin, A., Kormaksson, M., Li, S., Garrett-Bakelman, F.E., Figueroa, M.E., Melnick, A., and Mason, C.E. (2012). methylKit: a comprehensive R package for the analysis of genome-wide DNA methylation profiles. Genome biology *13*, R87.

Akimoto, T., Li, P., and Yan, Z. (2008). Functional interaction of regulatory factors with the Pgc-1alpha promoter in response to exercise by in vivo imaging. American journal of physiology. Cell physiology *295*, C288-292.

Akimoto, T., Pohnert, S.C., Li, P., Zhang, M., Gumbs, C., Rosenberg, P.B., Williams, R.S., and Yan, Z. (2005). Exercise stimulates Pgc-1alpha transcription in skeletal muscle through activation of the p38 MAPK pathway. The Journal of biological chemistry *280*, 19587-19593.

Alibegovic, A.C., Sonne, M.P., Hojbjerre, L., Bork-Jensen, J., Jacobsen, S., Nilsson, E., Faerch, K., Hiscock, N., Mortensen, B., Friedrichsen, M., et al. (2010). Insulin resistance induced by physical inactivity is associated with multiple transcriptional changes in skeletal muscle in young men. Am J Physiol Endocrinol Metab *299*, E752-763.

Anderson, R.M., Barger, J.L., Edwards, M.G., Braun, K.H., O'Connor, C.E., Prolla, T.A., and Weindruch, R. (2008). Dynamic regulation of PGC-1alpha localization and turnover implicates mitochondrial adaptation in calorie restriction and the stress response. Aging cell *7*, 101-111.

Andersson, U., and Scarpulla, R.C. (2001). Pgc-1-related coactivator, a novel, serum-inducible coactivator of nuclear respiratory factor 1-dependent transcription in mammalian cells. Molecular and cellular biology *21*, 3738-3749.

Arany, Z. (2008). PGC-1 coactivators and skeletal muscle adaptations in health and disease. Current opinion in genetics & development *18*, 426-434.

Arany, Z., Foo, S.Y., Ma, Y., Ruas, J.L., Bommi-Reddy, A., Girnun, G., Cooper, M., Laznik, D., Chinsomboon, J., Rangwala, S.M., et al. (2008). HIF-independent regulation of VEGF and angiogenesis by the transcriptional coactivator PGC-1alpha. Nature *451*, 1008-1012.

Arany, Z., He, H., Lin, J., Hoyer, K., Handschin, C., Toka, O., Ahmad, F., Matsui, T., Chin, S., Wu, P.H., et al. (2005). Transcriptional coactivator PGC-1 alpha controls the energy state and contractile function of cardiac muscle. Cell metabolism *1*, 259-271.

Arany, Z., Lebrasseur, N., Morris, C., Smith, E., Yang, W., Ma, Y., Chin, S., and Spiegelman, B.M. (2007). The transcriptional coactivator PGC-1beta drives the formation of oxidative type IIX fibers in skeletal muscle. Cell metabolism *5*, 35-46.

Assenov, Y., Muller, F., Lutsik, P., Walter, J., Lengauer, T., and Bock, C. (2014). Comprehensive analysis of DNA methylation data with RnBeads. Nature methods *11*, 1138-1140.

Baar, K. (2010). Epigenetic control of skeletal muscle fibre type. Acta physiologica (Oxford, England) *199*, 477-487.

Baar, K., Wende, A.R., Jones, T.E., Marison, M., Nolte, L.A., Chen, M., Kelly, D.P., and Holloszy, J.O. (2002). Adaptations of skeletal muscle to exercise: rapid increase in the transcriptional coactivator PGC-1. FASEB journal : official publication of the Federation of American Societies for Experimental Biology *16*, 1879-1886.

Bajpeyi, S., Covington, J.D., Taylor, E.M., Stewart, L.K., Galgani, J.E., and Henagan, T.M. (2017). Skeletal Muscle PGC1α −1 Nucleosome Position and −260 nt DNA Methylation Determine Exercise Response and Prevent Ectopic Lipid Accumulation in Men. Endocrinology *158*, 2190-2199.

Bal, N.C., Maurya, S.K., Sopariwala, D.H., Sahoo, S.K., Gupta, S.C., Shaikh, S.A., Pant, M., Rowland, L.A., Bombardier, E., Goonasekera, S.A., et al. (2012). Sarcolipin is a newly identified regulator of muscle-based thermogenesis in mammals. Nature medicine *18*, 1575-1579.

Balwierz, P.J., Pachkov, M., Arnold, P., Gruber, A.J., Zavolan, M., and van Nimwegen, E. (2014). ISMARA: automated modeling of genomic signals as a democracy of regulatory motifs. Genome research *24*, 869-884.

Baresic, M., Salatino, S., Kupr, B., van Nimwegen, E., and Handschin, C. (2014). Transcriptional network analysis in muscle reveals AP-1 as a partner of PGC-1alpha in the regulation of the hypoxic gene program. Molecular and cellular biology *34*, 2996-3012.

Barnes, W.M. (1994). PCR amplification of up to 35-kb DNA with high fidelity and high yield from lambda bacteriophage templates. Proceedings of the National Academy of Sciences *91*, 2216-2220.

Barres, R., Osler, M.E., Yan, J., Rune, A., Fritz, T., Caidahl, K., Krook, A., and Zierath, J.R. (2009). Non-CpG methylation of the PGC-1alpha promoter through DNMT3B controls mitochondrial density. Cell metabolism *10*, 189-198.

Barres, R., Yan, J., Egan, B., Treebak, J.T., Rasmussen, M., Fritz, T., Caidahl, K., Krook, A., O'Gorman, D.J., and Zierath, J.R. (2012). Acute exercise remodels promoter methylation in human skeletal muscle. Cell metabolism *15*, 405-411.

Barry, J.B., Laganiere, J., and Giguere, V. (2006). A single nucleotide in an estrogen-related receptor alpha site can dictate mode of binding and peroxisome proliferator-activated receptor gamma coactivator 1alpha activation of target promoters. Molecular endocrinology *20*, 302-310.

Begue, G., Raue, U., Jemiolo, B., and Trappe, S. (2017). DNA methylation assessment from human slow- and fast-twitch skeletal muscle fibers. Journal of applied physiology (Bethesda, Md. : 1985) *122*, 952-967.

Benziane, B., Burton, T.J., Scanlan, B., Galuska, D., Canny, B.J., Chibalin, A.V., Zierath, J.R., and Stepto, N.K. (2008). Divergent cell signaling after short-term intensified endurance training in human skeletal muscle. Am J Physiol Endocrinol Metab *295*, E1427-1438.

Berger, S., Omidi, S., Pachkov, M., Arnold, P., Kelley, N., Salatino, S., and van Nimwegen, E. (2016). Crunch: Completely Automated Analysis of ChIP-seq Data. In bioRvix.

Blattler, A., and Farnham, P.J. (2013). Cross-talk between site-specific transcription factors and DNA methylation states. The Journal of biological chemistry *288*, 34287-34294.

Blattler, S.M., Verdeguer, F., Liesa, M., Cunningham, J.T., Vogel, R.O., Chim, H., Liu, H., Romanino, K., Shirihai, O.S., Vazquez, F., et al. (2012). Defective mitochondrial morphology and bioenergetic function in mice lacking the transcription factor Yin Yang 1 in skeletal muscle. Molecular and cellular biology *32*, 3333-3346.

Bodine, S.C., Latres, E., Baumhueter, S., Lai, V.K., Nunez, L., Clarke, B.A., Poueymirou, W.T., Panaro, F.J., Na, E., Dharmarajan, K., et al. (2001). Identification of ubiquitin ligases required for skeletal muscle atrophy. Science *294*, 1704-1708.

Booth, F.W., Roberts, C.K., and Laye, M.J. (2012). Lack of exercise is a major cause of chronic diseases. Comprehensive Physiology *2*, 1143-1211.

Bostrom, P., Wu, J., Jedrychowski, M.P., Korde, A., Ye, L., Lo, J.C., Rasbach, K.A., Bostrom, E.A., Choi, J.H., Long, J.Z., et al. (2012). A PGC1-alpha-dependent myokine that drives brown-fat-like development of white fat and thermogenesis. Nature *481*, 463-468.

Brault, J.J., Jespersen, J.G., and Goldberg, A.L. (2010). Peroxisome proliferator-activated receptor gamma coactivator 1alpha or 1beta overexpression inhibits muscle protein degradation, induction of ubiquitin ligases, and disuse atrophy. The Journal of biological chemistry *285*, 19460-19471.

Brunk, B.P., Goldhamer, D.J., and Emerson, C.P., Jr. (1996). Regulated demethylation of the myoD distal enhancer during skeletal myogenesis. Developmental biology *177*, 490-503.

Bruusgaard, J.C., Johansen, I.B., Egner, I.M., Rana, Z.A., and Gundersen, K. (2010). Myonuclei acquired by overload exercise precede hypertrophy and are not lost on detraining. Proceedings of the National Academy of Sciences of the United States of America *107*, 15111-15116.

Brzeszczynska, J., Meyer, A., McGregor, R., Schilb, A., Degen, S., Tadini, V., Johns, N., Langen, R., Schols, A., Glass, D.J., et al. (2018). Alterations in the in vitro and in vivo regulation of muscle regeneration in healthy ageing and the influence of sarcopenia. Journal of cachexia, sarcopenia and muscle *9*, 93-105.

Canto, C., and Auwerx, J. (2009). PGC-1alpha, SIRT1 and AMPK, an energy sensing network that controls energy expenditure. Current opinion in lipidology *20*, 98-105.

Cantó, C., and Auwerx, J. (2009). PGC-1alpha, SIRT1 and AMPK, an energy sensing network that controls energy expenditure. Current opinion in lipidology *20*, 98-105.

Canto, C., Gerhart-Hines, Z., Feige, J.N., Lagouge, M., Noriega, L., Milne, J.C., Elliott, P.J., Puigserver, P., and Auwerx, J. (2009). AMPK regulates energy expenditure by modulating NAD+ metabolism and SIRT1 activity. Nature *458*, 1056-1060.

Canto, C., Jiang, L.Q., Deshmukh, A.S., Mataki, C., Coste, A., Lagouge, M., Zierath, J.R., and Auwerx, J. (2010). Interdependence of AMPK and SIRT1 for metabolic adaptation to fasting and exercise in skeletal muscle. Cell metabolism *11*, 213-219.

Carmona-Saez, P., Chagoyen, M., Tirado, F., Carazo, J.M., and Pascual-Montano, A. (2007). GENECODIS: a web-based tool for finding significant concurrent annotations in gene lists. Genome biology *8*, R3.

Carrio, E., and Suelves, M. (2015). DNA methylation dynamics in muscle development and disease. Frontiers in aging neuroscience *7*, 19.

Carrió, E., and Suelves, M. (2015). DNA methylation dynamics in muscle development and disease. Frontiers in aging neuroscience *7*, 19.

Carter, L.G., Qi, N.R., De Cabo, R., and Pearson, K.J. (2013). Maternal exercise improves insulin sensitivity in mature rat offspring. Medicine and science in sports and exercise *45*, 832-840.

Catoire, M., Mensink, M., Boekschoten, M.V., Hangelbroek, R., Muller, M., Schrauwen, P., and Kersten, S. (2012). Pronounced effects of acute endurance exercise on gene expression in resting and exercising human skeletal muscle. PLoS One *7*, e51066.

Cedar, H., and Bergman, Y. (2009). Linking DNA methylation and histone modification: patterns and paradigms. Nature Reviews Genetics *10*, 295.

Chang, Y.S., Lee, L.C., Sun, F.C., Chao, C.C., Fu, H.W., and Lai, Y.K. (2006). Involvement of calcium in the differential induction of heat shock protein 70 by heat shock protein 90 inhibitors, geldanamycin and radicicol, in human non-small cell lung cancer H460 cells. Journal of cellular biochemistry *97*, 156-165.

Chao, L.C., Wroblewski, K., Ilkayeva, O.R., Stevens, R.D., Bain, J., Meyer, G.A., Schenk, S., Martinez, L., Vergnes, L., Narkar, V.A., et al. (2012). Skeletal muscle Nur77 expression enhances oxidative metabolism and substrate utilization. Journal of lipid research *53*, 2610-2619.

Chappuis, S., Ripperger, J.A., Schnell, A., Rando, G., Jud, C., Wahli, W., and Albrecht, U. (2013). Role of the circadian clock gene Per2 in adaptation to cold temperature. Molecular Metabolism *2*, 184-193.

Chen, S.-D., Yang, D.-I., Lin, T.-K., Shaw, F.-Z., Liou, C.-W., and Chuang, Y.-C. (2011). Roles of Oxidative Stress, Apoptosis, PGC-1α and Mitochondrial Biogenesis in Cerebral Ischemia. International Journal of Molecular Sciences *12*, 7199-7215.

Chinsomboon, J., Ruas, J., Gupta, R.K., Thom, R., Shoag, J., Rowe, G.C., Sawada, N., Raghuram, S., and Arany, Z. (2009). The transcriptional coactivator PGC-1α mediates exercise-induced angiogenesis in skeletal muscle. Proceedings of the National Academy of Sciences of the United States of America *106*, 21401-21406.

Cho, Y., Hazen, B.C., Russell, A.P., and Kralli, A. (2013). Peroxisome proliferator-activated receptor gamma coactivator 1 (PGC-1)- and estrogen-related receptor (ERR)-induced regulator in muscle 1 (Perm1) is a tissue-specific regulator of oxidative capacity in skeletal muscle cells. The Journal of biological chemistry *288*, 25207-25218.

Coffey, V.G., and Hawley, J.A. (2007). The molecular bases of training adaptation. Sports medicine *37*, 737-763.

Colberg, S.R., Sigal, R.J., Fernhall, B., Regensteiner, J.G., Blissmer, B.J., Rubin, R.R., Chasan-Taber, L., Albright, A.L., Braun, B., American College of Sports, M., et al. (2010a). Exercise and type 2 diabetes: the American College of Sports Medicine and the American Diabetes Association: joint position statement. Diabetes Care *33*, e147-167.

Colberg, S.R., Sigal, R.J., Fernhall, B., Regensteiner, J.G., Blissmer, B.J., Rubin, R.R., Chasan-Taber, L., Albright, A.L., Braun, B., American College of Sports, M., et al. (2010b). Exercise and type 2 diabetes: the American College of Sports Medicine and the American Diabetes Association: joint position statement executive summary. Diabetes care *33*, 2692-2696.

Cong, L., Ran, F.A., Cox, D., Lin, S.L., Barretto, R., Habib, N., Hsu, P.D., Wu, X.B., Jiang, W.Y., Marraffini, L.A., et al. (2013). Multiplex Genome Engineering Using CRISPR/Cas Systems. Science *339*, 819-823.

Crick, F.H. (1966). Codon--anticodon pairing: the wobble hypothesis. Journal of molecular biology *19*, 548-555.

Cunningham, J.T., Rodgers, J.T., Arlow, D.H., Vazquez, F., Mootha, V.K., and Puigserver, P. (2007). mTOR controls mitochondrial oxidative function through a YY1-PGC-1alpha transcriptional complex. Nature *450*, 736-740.

Dahl, C., Gronbaek, K., and Guldberg, P. (2011). Advances in DNA methylation: 5-hydroxymethylcytosine revisited. Clinica chimica acta; international journal of clinical chemistry *412*, 831-836.

Deaton, A.M., and Bird, A. (2011). CpG islands and the regulation of transcription. Genes & development *25*, 1010-1022.

Deng, C., Wang, P., Zhang, X., and Wang, Y. (2015). Short-term, daily exposure to cold temperature may be an efficient way to prevent muscle atrophy and bone loss in a microgravity environment. Life sciences in space research *5*, 1-5.

Doudna, J.A., and Charpentier, E. (2014). The new frontier of genome engineering with CRISPR-Cas9. Science *346*.

Egan, B., Hawley, J.A., and Zierath, J.R. (2016). SnapShot: Exercise Metabolism. Cell metabolism *24*, 342-342 e341.

Egan, B., and Zierath, J.R. (2013). Exercise metabolism and the molecular regulation of skeletal muscle adaptation. Cell metabolism *17*, 162-184.

Eisele, P.S., Furrer, R., Beer, M., and Handschin, C. (2015). The PGC-1 coactivators promote an anti-inflammatory environment in skeletal muscle in vivo. Biochemical and biophysical research communications *464*, 692-697.

Fan, M., Rhee, J., St-Pierre, J., Handschin, C., Puigserver, P., Lin, J., Jaeger, S., Erdjument-Bromage, H., Tempst, P., and Spiegelman, B.M. (2004). Suppression of mitochondrial respiration through recruitment of p160 myb binding protein to PGC-1alpha: modulation by p38 MAPK. Genes & development *18*, 278-289.

Feng, J., Chang, H., Li, E., and Fan, G. (2005). Dynamic expression of de novo DNA methyltransferases Dnmt3a and Dnmt3b in the central nervous system. Journal of neuroscience research *79*, 734-746.

Fernandez-Marcos, P.J., and Auwerx, J. (2011). Regulation of PGC-1alpha, a nodal regulator of mitochondrial biogenesis. The American journal of clinical nutrition *93*, 884S-890.

Gabriel, B.M., and Zierath, J.R. (2017). The Limits of Exercise Physiology: From Performance to Health. Cell metabolism *25*, 1000-1011.

Gali Ramamoorthy, T., Laverny, G., Schlagowski, A.I., Zoll, J., Messaddeq, N., Bornert, J.M., Panza, S., Ferry, A., Geny, B., and Metzger, D. (2015). The transcriptional coregulator PGC-1beta controls mitochondrial function and anti-oxidant defence in skeletal muscles. Nature communications *6*, 10210.

Gasiunas, G., Barrangou, R., Horvath, P., and Siksnys, V. (2012). Cas9–crRNA ribonucleoprotein complex mediates specific DNA cleavage for adaptive immunity in bacteria. Proceedings of the National Academy of Sciences *109*, E2579-E2586.

Gehlert, S., Bloch, W., and Suhr, F. (2015). Ca2+-dependent regulations and signaling in skeletal muscle: from electro-mechanical coupling to adaptation. Int J Mol Sci *16*, 1066-1095.

Gerhart-Hines, Z., Feng, D., Emmett, M.J., Everett, L.J., Loro, E., Briggs, E.R., Bugge, A., Hou, C., Ferrara, C., Seale, P., et al. (2013). The nuclear receptor Rev-erbalpha controls circadian thermogenic plasticity. Nature *503*, 410-413.

Gibson, D.G., Smith, H.O., Hutchison, C.A., 3rd, Venter, J.C., and Merryman, C. (2010). Chemical synthesis of the mouse mitochondrial genome. Nature methods *7*, 901-903.

Gibson, D.G., Young, L., Chuang, R.Y., Venter, J.C., Hutchison, C.A., 3rd, and Smith, H.O. (2009). Enzymatic assembly of DNA molecules up to several hundred kilobases. Nature methods *6*, 343-345.

Gill, J.F., Santos, G., Schnyder, S., and Handschin, C. (2018). PGC-1alpha affects aging-related changes in muscle and motor function by modulating specific exercise-mediated changes in old mice. Aging cell *17*.

Glass, C.K., and Rosenfeld, M.G. (2000). The coregulator exchange in transcriptional functions of nuclear receptors. Genes & development *14*, 121-141.

Glass, D., and Roubenoff, R. (2010). Recent advances in the biology and therapy of muscle wasting. Annals of the New York Academy of Sciences *1211*, 25-36.

Green, H.J., Helyar, R., Ball-Burnett, M., Kowalchuk, N., Symon, S., and Farrance, B. (1992). Metabolic adaptations to training precede changes in muscle mitochondrial capacity. Journal of applied physiology (Bethesda, Md. : 1985) *72*, 484-491.

Gundersen, K. (2011). Excitation-transcription coupling in skeletal muscle: the molecular pathways of exercise. Biological reviews of the Cambridge Philosophical Society *86*, 564-600.

Gundersen, K. (2016). Muscle memory and a new cellular model for muscle atrophy and hypertrophy. The Journal of experimental biology *219*, 235-242.

Hamrick, M.W., McNeil, P.L., and Patterson, S.L. (2010). Role of muscle-derived growth factors in bone formation. Journal of musculoskeletal & neuronal interactions *10*, 64-70.

Handschin, C. (2010). Regulation of skeletal muscle cell plasticity by the peroxisome proliferator-activated receptor gamma coactivator 1alpha. Journal of receptor and signal transduction research *30*, 376-384.

Handschin, C. (2016). Caloric restriction and exercise "mimetics'': Ready for prime time? Pharmacological research *103*, 158-166.

Handschin, C., Chin, S., Li, P., Liu, F., Maratos-Flier, E., Lebrasseur, N.K., Yan, Z., and Spiegelman, B.M. (2007a). Skeletal muscle fiber-type switching, exercise intolerance, and myopathy in PGC-1alpha muscle-specific knock-out animals. The Journal of biological chemistry *282*, 30014-30021.

Handschin, C., Kobayashi, Y.M., Chin, S., Seale, P., Campbell, K.P., and Spiegelman, B.M. (2007b). PGC-1alpha regulates the neuromuscular junction program and ameliorates Duchenne muscular dystrophy. Genes & development *21*, 770-783.

Handschin, C., Lin, J., Rhee, J., Peyer, A.K., Chin, S., Wu, P.H., Meyer, U.A., and Spiegelman, B.M. (2005). Nutritional regulation of hepatic heme biosynthesis and porphyria through PGC-1alpha. Cell *122*, 505-515.

Handschin, C., Rhee, J., Lin, J., Tarr, P.T., and Spiegelman, B.M. (2003). An autoregulatory loop controls peroxisome proliferator-activated receptor gamma coactivator 1alpha expression in muscle. Proceedings of the National Academy of Sciences of the United States of America *100*, 7111-7116.

Handschin, C., and Spiegelman, B.M. (2006). Peroxisome proliferator-activated receptor gamma coactivator 1 coactivators, energy homeostasis, and metabolism. Endocrine reviews *27*, 728-735.

Handschin, C., and Spiegelman, B.M. (2008). The role of exercise and PGC1alpha in inflammation and chronic disease. Nature *454*, 463-469.

Haskell, W.L., Lee, I.M., Pate, R.R., Powell, K.E., Blair, S.N., Franklin, B.A., Macera, C.A., Heath, G.W., Thompson, P.D., Bauman, A., et al. (2007). Physical activity and public health: updated recommendation for adults from the American College of Sports Medicine and the American Heart Association. Circulation *116*, 1081-1093.

Haueter, S., Kawasumi, M., Asner, I., Brykczynska, U., Cinelli, P., Moisyadi, S., Burki, K., Peters, A.H., and Pelczar, P. (2010). Genetic vasectomy-overexpression of Prm1-EGFP fusion protein in elongating spermatids causes dominant male sterility in mice. Genesis (New York, N.Y. : 2000) *48*, 151-160.

Heberle, H., Meirelles, G.V., da Silva, F.R., Telles, G.P., and Minghim, R. (2015). InteractiVenn: a web-based tool for the analysis of sets through Venn diagrams. BMC bioinformatics *16*, 169.

Heim-Kupr, B., Nordström, K., Schnyder, S., Furrer, R., Steurer, S., Walter, J., and Handschin, C. (2018 (not published yet)). Acute and chronic exercise regulate skeletal muscle DNA methylation and transcription in a time and PGC-1α dependent manner. not published yet.

Henagan, T.M., Stewart, L.K., Forney, L.A., Sparks, L.M., Johannsen, N., and Church, T.S. (2014). PGC1α −1 Nucleosome Position and Splice Variant Expression and Cardiovascular Disease Risk in Overweight and Obese Individuals. PPAR Research *2014*, 895734.

Henstridge, D.C., Febbraio, M.A., and Hargreaves, M. (2016). Heat shock proteins and exercise adaptations. Our knowledge thus far and the road still ahead. Journal of applied physiology (Bethesda, Md. : 1985) *120*, 683-691.

Herman, J.G., and Baylin, S.B. (2003). Gene silencing in cancer in association with promoter hypermethylation. The New England journal of medicine *349*, 2042-2054.

Hermanson, O., Glass, C.K., and Rosenfeld, M.G. (2002). Nuclear receptor coregulators: multiple modes of modification. Trends in endocrinology and metabolism: TEM *13*, 55-60.

Hille, F., Richter, H., Wong, S.P., Bratovic, M., Ressel, S., and Charpentier, E. (2018). The Biology of CRISPR-Cas: Backward and Forward. Cell *172*, 1239-1259.

Hiller, K., Grote, A., Scheer, M., Munch, R., and Jahn, D. (2004). PrediSi: prediction of signal peptides and their cleavage positions. Nucleic acids research *32*, W375-379.

Himeda, C.L., Ranish, J.A., and Hauschka, S.D. (2008). Quantitative proteomic identification of MAZ as a transcriptional regulator of muscle-specific genes in skeletal and cardiac myocytes. Molecular and cellular biology *28*, 6521-6535.

Hippenmeyer, S., Huber, R.M., Ladle, D.R., Murphy, K., and Arber, S. (2007). ETS transcription factor Erm controls subsynaptic gene expression in skeletal muscles. Neuron *55*, 726-740.

Hoier, B., Nordsborg, N., Andersen, S., Jensen, L., Nybo, L., Bangsbo, J., and Hellsten, Y. (2012). Pro- and anti-angiogenic factors in human skeletal muscle in response to acute exercise and training. The Journal of physiology *590*, 595-606.

Holliday, R., and Pugh, J.E. (1975). DNA modification mechanisms and gene activity during development. Science *187*, 226-232.

Horvath, P., and Barrangou, R. (2010). CRISPR/Cas, the Immune System of Bacteria and Archaea. Science *327*, 167-170.

Hovestadt, V., Jones, D.T., Picelli, S., Wang, W., Kool, M., Northcott, P.A., Sultan, M., Stachurski, K., Ryzhova, M., Warnatz, H.J., et al. (2014). Decoding the regulatory landscape of medulloblastoma using DNA methylation sequencing. Nature *510*, 537-541.

Howlett, K.F., and McGee, S.L. (2016). Epigenetic regulation of skeletal muscle metabolism. Clinical science (London, England : 1979) *130*, 1051-1063.

Hupkes, M., Jonsson, M.K., Scheenen, W.J., van Rotterdam, W., Sotoca, A.M., van Someren, E.P., van der Heyden, M.A., van Veen, T.A., van Ravestein-van Os, R.I., Bauerschmidt, S., et al. (2011). Epigenetics: DNA demethylation promotes skeletal myotube maturation. FASEB journal : official publication of the Federation of American Societies for Experimental Biology *25*, 3861-3872.

Huss, J.M., Kopp, R.P., and Kelly, D.P. (2002). Peroxisome proliferator-activated receptor coactivator-1alpha (PGC-1alpha) coactivates the cardiac-enriched nuclear receptors estrogen-related receptor-alpha and -gamma. Identification of novel leucine-rich interaction motif within PGC-1alpha. The Journal of biological chemistry *277*, 40265-40274.

Huss, J.M., Torra, I.P., Staels, B., Giguere, V., and Kelly, D.P. (2004). Estrogen-related receptor alpha directs peroxisome proliferator-activated receptor alpha signaling in the transcriptional control of energy metabolism in cardiac and skeletal muscle. Molecular and cellular biology *24*, 9079-9091.

Iepsen, U.W., Jorgensen, K.J., Ringbaek, T., Hansen, H., Skrubbeltrang, C., and Lange, P. (2015). A combination of resistance and endurance training increases leg muscle strength in COPD: An evidence-based recommendation based on systematic review with meta-analyses. Chronic respiratory disease *12*, 132-145.

Ishihara, K., Yamada, A., Mita, Y., Goto, A., Ishimi, T., Mabuchi, H., Inoue, K., Fushiki, T., and Yasumoto, K. (2009). Improved swimming pool achieves higher reproducibility and sensitivity to effect of food components as ergogenic AIDS. Journal of nutritional science and vitaminology *55*, 301-308.

Ito, S., D'Alessio, A.C., Taranova, O.V., Hong, K., Sowers, L.C., and Zhang, Y. (2010). Role of Tet proteins in 5mC to 5hmC conversion, ES-cell self-renewal and inner cell mass specification. Nature *466*, 1129-1133.

Iyer, L.M., Zhang, D., and Aravind, L. (2016). Adenine methylation in eukaryotes: Apprehending the complex evolutionary history and functional potential of an epigenetic modification. BioEssays : news and reviews in molecular, cellular and developmental biology *38*, 27-40.

Jager, S., Handschin, C., St-Pierre, J., and Spiegelman, B.M. (2007). AMP-activated protein kinase (AMPK) action in skeletal muscle via direct phosphorylation of PGC-1alpha. Proceedings of the National Academy of Sciences of the United States of America *104*, 12017-12022.

Jin, B., Li, Y., and Robertson, K.D. (2011). DNA methylation: superior or subordinate in the epigenetic hierarchy? Genes & cancer *2*, 607-617.

Jinek, M., Chylinski, K., Fonfara, I., Hauer, M., Doudna, J.A., and Charpentier, E. (2012). A Programmable Dual-RNA–Guided DNA Endonuclease in Adaptive Bacterial Immunity. Science *337*, 816-821.

Jones, P.A., and Takai, D. (2001). The role of DNA methylation in mammalian epigenetics. Science *293*, 1068-1070.

Jorge, M.L., de Oliveira, V.N., Resende, N.M., Paraiso, L.F., Calixto, A., Diniz, A.L., Resende, E.S., Ropelle, E.R., Carvalheira, J.B., Espindola, F.S., et al. (2011). The effects of aerobic, resistance, and combined exercise on metabolic control, inflammatory markers, adipocytokines, and muscle insulin signaling in patients with type 2 diabetes mellitus. Metabolism: clinical and experimental *60*, 1244-1252.

Kang, S., Bajnok, L., Longo, K.A., Petersen, R.K., Hansen, J.B., Kristiansen, K., and MacDougald, O.A. (2005). Effects of Wnt signaling on brown adipocyte differentiation and metabolism mediated by PGC-1alpha. Molecular and cellular biology *25*, 1272-1282.

Kanzleiter, T., Jahnert, M., Schulze, G., Selbig, J., Hallahan, N., Schwenk, R.W., and Schurmann, A. (2015). Exercise training alters DNA methylation patterns in genes related to muscle growth and differentiation in mice. Am J Physiol Endocrinol Metab *308*, E912-920.

Knutti, D., Kaul, A., and Kralli, A. (2000). A Tissue-Specific Coactivator of Steroid Receptors, Identified in a Functional Genetic Screen. Molecular and cellular biology *20*, 2411-2422.

Knutti, D., and Kralli, A. (2001). PGC-1, a versatile coactivator. Trends in endocrinology and metabolism: TEM *12*, 360-365.

Koves, T.R., Li, P., An, J., Akimoto, T., Slentz, D., Ilkayeva, O., Dohm, G.L., Yan, Z., Newgard, C.B., and Muoio, D.M. (2005). Peroxisome proliferator-activated receptor-gamma co-activator 1alpha-mediated metabolic

remodeling of skeletal myocytes mimics exercise training and reverses lipid-induced mitochondrial inefficiency. The Journal of biological chemistry *280*, 33588-33598.

Kregel, K.C. (2002). Heat shock proteins: modifying factors in physiological stress responses and acquired thermotolerance. Journal of applied physiology (Bethesda, Md. : 1985) *92*, 2177-2186.

Kressler, D., Schreiber, S.N., Knutti, D., and Kralli, A. (2002a). The PGC-1-related protein PERC is a selective coactivator of estrogen receptor alpha. The Journal of biological chemistry *277*, 13918-13925.

Kressler, D., Schreiber, S.N., Knutti, D., and Kralli, A. (2002b). The PGC-1-related Protein PERC Is a Selective Coactivator of Estrogen Receptor α. Journal of Biological Chemistry *277*, 13918-13925.

Kupr, B., and Handschin, C. (2015). Complex Coordination of Cell Plasticity by a PGC-1alpha-controlled Transcriptional Network in Skeletal Muscle. Frontiers in physiology *6*, 325.

Kupr, B., Schnyder, S., and Handschin, C. (2017). Role of Nuclear Receptors in Exercise-Induced Muscle Adaptations. Cold Spring Harbor perspectives in medicine *7*.

Kurdiova, T., Balaz, M., Vician, M., Maderova, D., Vlcek, M., Valkovic, L., Srbecky, M., Imrich, R., Kyselovicova, O., Belan, V., et al. (2014). Effects of obesity, diabetes and exercise on Fndc5 gene expression and irisin release in human skeletal muscle and adipose tissue: in vivo and in vitro studies. The Journal of physiology *592*, 1091-1107.

Lai, L., Leone, T.C., Zechner, C., Schaeffer, P.J., Kelly, S.M., Flanagan, D.P., Medeiros, D.M., Kovacs, A., and Kelly, D.P. (2008). Transcriptional coactivators PGC-1alpha and PGC-lbeta control overlapping programs required for perinatal maturation of the heart. Genes & development *22*, 1948-1961.

Laker, R.C., Lillard, T.S., Okutsu, M., Zhang, M., Hoehn, K.L., Connelly, J.J., and Yan, Z. (2014). Exercise prevents maternal high-fat diet-induced hypermethylation of the Pgc-1alpha gene and age-dependent metabolic dysfunction in the offspring. Diabetes *63*, 1605-1611.

Lancaster, G.I., Møller, K., Nielsen, B., Secher, N.H., Febbraio, M.A., and Nybo, L. (2004). Exercise induces the release of heat shock protein 72 from the human brain in vivo. Cell Stress & Chaperones *9*, 276-280.

Langemeijer, S.M., Aslanyan, M.G., and Jansen, J.H. (2009). TET proteins in malignant hematopoiesis. Cell cycle *8*, 4044-4048.

Law, T.D., Clark, L.A., and Clark, B.C. (2016a). Resistance Exercise to Prevent and Manage Sarcopenia and Dynapenia. Annual review of gerontology & geriatrics *36*, 205-228.

Law, T.D., Clark, L.A., and Clark, B.C. (2016b). Resistance Exercise to Prevent and Manage Sarcopenia and Dynapenia. Annu Rev Gerontol Geriatr *36*, 205-228.

Lee, P., Brychta, R.J., Linderman, J., Smith, S., Chen, K.Y., and Celi, F.S. (2013). Mild Cold Exposure Modulates Fibroblast Growth Factor 21 (FGF21) Diurnal Rhythm in Humans: Relationship between FGF21

Levels, Lipolysis, and Cold-Induced Thermogenesis. The Journal of Clinical Endocrinology & Metabolism *98*, E98-E102.

Lee, S., Leone, T.C., Rogosa, L., Rumsey, J., Ayala, J., Coen, P.M., Fitts, R.H., Vega, R.B., and Kelly, D.P. (2017). Skeletal muscle PGC-1beta signaling is sufficient to drive an endurance exercise phenotype and to counteract components of detraining in mice. Am J Physiol Endocrinol Metab *312*, E394-e406.

Lelliott, C.J., Medina-Gomez, G., Petrovic, N., Kis, A., Feldmann, H.M., Bjursell, M., Parker, N., Curtis, K., Campbell, M., Hu, P., et al. (2006). Ablation of PGC-1beta results in defective mitochondrial activity, thermogenesis, hepatic function, and cardiac performance. PLoS biology *4*, e369.

Leone, T.C., Lehman, J.J., Finck, B.N., Schaeffer, P.J., Wende, A.R., Boudina, S., Courtois, M., Wozniak, D.F., Sambandam, N., Bernal-Mizrachi, C., et al. (2005). PGC-1alpha deficiency causes multi-system energy metabolic derangements: muscle dysfunction, abnormal weight control and hepatic steatosis. PLoS biology *3*, e101.

Lerin, C., Rodgers, J.T., Kalume, D.E., Kim, S.-h., Pandey, A., and Puigserver, P. (2006). GCN5 acetyltransferase complex controls glucose metabolism through transcriptional repression of PGC-1α. Cell metabolism *3*, 429-438.

Li, E., Beard, C., Forster, A.C., Bestor, T.H., and Jaenisch, R. (1993). DNA methylation, genomic imprinting, and mammalian development. Cold Spring Harbor symposia on quantitative biology *58*, 297-305.

Li, E., Bestor, T.H., and Jaenisch, R. (1992). Targeted mutation of the DNA methyltransferase gene results in embryonic lethality. Cell *69*, 915-926.

Li, H., and Durbin, R. (2009). Fast and accurate short read alignment with Burrows-Wheeler transform. Bioinformatics (Oxford, England) *25*, 1754-1760.

Li, S., Liu, C., Li, N., Hao, T., Han, T., Hill, D.E., Vidal, M., and Lin, J.D. (2008). Genome-wide Coactivation Analysis of PGC-1α Identifies BAF60a as a Regulator of Hepatic Lipid Metabolism. Cell metabolism *8*, 105-117.

Liang, H., and Ward, W.F. (2006). PGC-1alpha: a key regulator of energy metabolism. Advances in physiology education *30*, 145-151.

Lin, J., Handschin, C., and Spiegelman, B.M. (2005). Metabolic control through the PGC-1 family of transcription coactivators. Cell metabolism *1*, 361-370.

Lin, J., Puigserver, P., Donovan, J., Tarr, P., and Spiegelman, B.M. (2002a). Peroxisome proliferator-activated receptor gamma coactivator 1beta (PGC-1beta), a novel PGC-1-related transcription coactivator associated with host cell factor. The Journal of biological chemistry *277*, 1645-1648.

Lin, J., Tarr, P.T., Yang, R., Rhee, J., Puigserver, P., Newgard, C.B., and Spiegelman, B.M. (2003). PGC-1beta in the regulation of hepatic glucose and energy metabolism. The Journal of biological chemistry *278*, 30843-30848.

Lin, J., Wu, H., Tarr, P.T., Zhang, C.Y., Wu, Z., Boss, O., Michael, L.F., Puigserver, P., Isotani, E., Olson, E.N., et al. (2002b). Transcriptional co-activator PGC-1 alpha drives the formation of slow-twitch muscle fibres. Nature *418*, 797-801.

Lin, J., Wu, P.-H., Tarr, P.T., Lindenberg, K.S., St-Pierre, J., Zhang, C.-y., Mootha, V.K., Jäger, S., Vianna, C.R., Reznick, R.M., et al. (2004a). Defects in Adaptive Energy Metabolism with CNS-Linked Hyperactivity in PGC-1α Null Mice. Cell *119*, 121-135.

Lin, J., Wu, P.H., Tarr, P.T., Lindenberg, K.S., St-Pierre, J., Zhang, C.Y., Mootha, V.K., Jager, S., Vianna, C.R., Reznick, R.M., et al. (2004b). Defects in adaptive energy metabolism with CNS-linked hyperactivity in PGC-1alpha null mice. Cell *119*, 121-135.

Lin, M.T., and Beal, M.F. (2006). Mitochondrial dysfunction and oxidative stress in neurodegenerative diseases. Nature *443*, 787-795.

Lindholm, M.E., Giacomello, S., Werne Solnestam, B., Fischer, H., Huss, M., Kjellqvist, S., and Sundberg, C.J. (2016). The Impact of Endurance Training on Human Skeletal Muscle Memory, Global Isoform Expression and Novel Transcripts. PLoS genetics *12*, e1006294.

Lindholm, M.E., Marabita, F., Gomez-Cabrero, D., Rundqvist, H., Ekstrom, T.J., Tegner, J., and Sundberg, C.J. (2014). An integrative analysis reveals coordinated reprogramming of the epigenome and the transcriptome in human skeletal muscle after training. Epigenetics *9*, 1557-1569.

Liu, C., and Lin, J.D. (2011). PGC-1 coactivators in the control of energy metabolism. Acta biochimica et biophysica Sinica *43*, 248-257.

Liu, Y., Siegmund, K.D., Laird, P.W., and Berman, B.P. (2012). Bis-SNP: combined DNA methylation and SNP calling for Bisulfite-seq data. Genome biology *13*, R61.

Lochmann, T.L., Thomas, R.R., Bennett, J.P., Jr., and Taylor, S.M. (2015a). Epigenetic Modifications of the PGC-1alpha Promoter during Exercise Induced Expression in Mice. PLoS One *10*, e0129647.

Lochmann, T.L., Thomas, R.R., Bennett, J.P., and Taylor, S.M. (2015b). Epigenetic Modifications of the PGC-1α Promoter during Exercise Induced Expression in Mice. PLoS ONE *10*, e0129647.

Lonard, D.M., and O'Malley, B.W. (2007). Nuclear Receptor Coregulators: Judges, Juries, and Executioners of Cellular Regulation. Molecular cell *27*, 691-700.

Lucarelli, M., Fuso, A., Strom, R., and Scarpa, S. (2001). The dynamics of myogenin site-specific demethylation is strongly correlated with its expression and with muscle differentiation. The Journal of biological chemistry *276*, 7500-7506.

Lund, J., Rustan, A.C., Lovsletten, N.G., Mudry, J.M., Langleite, T.M., Feng, Y.Z., Stensrud, C., Brubak, M.G., Drevon, C.A., Birkeland, K.I., et al. (2017). Exercise in vivo marks human myotubes in vitro: Training-induced increase in lipid metabolism. PLoS One *12*, e0175441.

Luo, G.Z., Blanco, M.A., Greer, E.L., He, C., and Shi, Y. (2015). DNA N(6)-methyladenine: a new epigenetic mark in eukaryotes? Nature reviews. Molecular cell biology *16*, 705-710.

Lustig, Y., Ruas, J.L., Estall, J.L., Lo, J.C., Devarakonda, S., Laznik, D., Choi, J.H., Ono, H., Olsen, J.V., and Spiegelman, B.M. (2011). Separation of the gluconeogenic and mitochondrial functions of PGC-1{alpha} through S6 kinase. Genes & development *25*, 1232-1244.

Lyko, F., Ramsahoye, B.H., and Jaenisch, R. (2000). DNA methylation in Drosophila melanogaster. Nature *408*, 538-540.

Mahoney, D.J., Parise, G., Melov, S., Safdar, A., and Tarnopolsky, M.A. (2005). Analysis of global mRNA expression in human skeletal muscle during recovery from endurance exercise. FASEB journal : official publication of the Federation of American Societies for Experimental Biology *19*, 1498-1500.

Martin, M. (2011). Cutadapt removes adapter sequences from high-throughput sequencing reads. EMBnet.journal *17*.

Martinez-Redondo, V., Jannig, P.R., Correia, J.C., Ferreira, D.M., Cervenka, I., Lindvall, J.M., Sinha, I., Izadi, M., Pettersson-Klein, A.T., Agudelo, L.Z., et al. (2016). Peroxisome Proliferator-activated Receptor gamma Coactivator-1 alpha Isoforms Selectively Regulate Multiple Splicing Events on Target Genes. The Journal of biological chemistry *291*, 15169-15184.

Martinez-Redondo, V., Pettersson, A.T., and Ruas, J.L. (2015). The hitchhiker's guide to PGC-1alpha isoform structure and biological functions. Diabetologia *58*, 1969-1977.

Maston, G.A., Evans, S.K., and Green, M.R. (2006). Transcriptional regulatory elements in the human genome. Annual review of genomics and human genetics *7*, 29-59.

McGee, S.L., and Walder, K.R. (2017). Exercise and the Skeletal Muscle Epigenome. Cold Spring Harbor perspectives in medicine *7*.

Meissner, A., Gnirke, A., Bell, G.W., Ramsahoye, B., Lander, E.S., and Jaenisch, R. (2005). Reduced representation bisulfite sequencing for comparative high-resolution DNA methylation analysis. Nucleic acids research *33*, 5868-5877.

Metsalu, T., and Vilo, J. (2015). ClustVis: a web tool for visualizing clustering of multivariate data using Principal Component Analysis and heatmap. Nucleic acids research *43*, W566-570.

Miura, S., Kai, Y., Kamei, Y., and Ezaki, O. (2008). Isoform-specific increases in murine skeletal muscle peroxisome proliferator-activated receptor-gamma coactivator-1alpha (PGC-1alpha) mRNA in response to beta2-adrenergic receptor activation and exercise. Endocrinology *149*, 4527-4533.

Miura, S., Kawanaka, K., Kai, Y., Tamura, M., Goto, M., Shiuchi, T., Minokoshi, Y., and Ezaki, O. (2007). An increase in murine skeletal muscle peroxisome proliferator-activated receptor-gamma coactivator-1alpha (PGC-1alpha) mRNA in response to exercise is mediated by beta-adrenergic receptor activation. Endocrinology *148*, 3441-3448.

Monsalve, M., Wu, Z., Adelmant, G., Puigserver, P., Fan, M., and Spiegelman, B.M. (2000). Direct coupling of transcription and mRNA processing through the thermogenic coactivator PGC-1. Molecular cell *6*, 307-316.

Montesano, A., Luzi, L., Senesi, P., and Terruzzi, I. (2013). Modulation of cell cycle progression by 5-azacytidine is associated with early myogenesis induction in murine myoblasts. International journal of biological sciences *9*, 391-402.

Moore, L.D., Le, T., and Fan, G. (2013). DNA methylation and its basic function. Neuropsychopharmacology : official publication of the American College of Neuropsychopharmacology *38*, 23-38.

Mootha, V.K., Handschin, C., Arlow, D., Xie, X., St Pierre, J., Sihag, S., Yang, W., Altshuler, D., Puigserver, P., Patterson, N., et al. (2004). Erralpha and Gabpa/b specify PGC-1alpha-dependent oxidative phosphorylation gene expression that is altered in diabetic muscle. Proceedings of the National Academy of Sciences of the United States of America *101*, 6570-6575.

Mortensen, O.H., Plomgaard, P., Fischer, C.P., Hansen, A.K., Pilegaard, H., and Pedersen, B.K. (2007). PGC-1beta is downregulated by training in human skeletal muscle: no effect of training twice every second day vs. once daily on expression of the PGC-1 family. Journal of applied physiology (Bethesda, Md. : 1985) *103*, 1536-1542.

Mosser, D.D., Kotzbauer, P.T., Sarge, K.D., and Morimoto, R.I. (1990). In vitro activation of heat shock transcription factor DNA-binding by calcium and biochemical conditions that affect protein conformation. Proceedings of the National Academy of Sciences of the United States of America *87*, 3748-3752.

Munzel, M., Lischke, U., Stathis, D., Pfaffeneder, T., Gnerlich, F.A., Deiml, C.A., Koch, S.C., Karaghiosoff, K., and Carell, T. (2011). Improved synthesis and mutagenicity of oligonucleotides containing 5-hydroxymethylcytosine, 5-formylcytosine and 5-carboxylcytosine. Chemistry *17*, 13782-13788.

Murashov, A.K., Pak, E.S., Koury, M., Ajmera, A., Jeyakumar, M., Parker, M., Williams, O., Ding, J., Walters, D., and Neufer, P.D. (2016). Paternal long-term exercise programs offspring for low energy expenditure and increased risk for obesity in mice. FASEB journal : official publication of the Federation of American Societies for Experimental Biology *30*, 775-784.

Mutin-Carnino, M., Carnino, A., Roffino, S., and Chopard, A. (2014). Effect of muscle unloading, reloading and exercise on inflammation during a head-down bed rest. International journal of sports medicine *35*, 28-34.

Nitert, M.D., Dayeh, T., Volkov, P., Elgzyri, T., Hall, E., Nilsson, E., Yang, B.T., Lang, S., Parikh, H., Wessman, Y., et al. (2012). Impact of an exercise intervention on DNA methylation in skeletal muscle from first-degree relatives of patients with type 2 diabetes. Diabetes *61*, 3322-3332.

Noble, E.G., and Shen, G.X. (2012). Impact of Exercise and Metabolic Disorders on Heat Shock Proteins and Vascular Inflammation. Autoimmune Diseases *2012*, 836519.

Nogales-Cadenas, R., Carmona-Saez, P., Vazquez, M., Vicente, C., Yang, X., Tirado, F., Carazo, J.M., and Pascual-Montano, A. (2009). GeneCodis: interpreting gene lists through enrichment analysis and integration of diverse biological information. Nucleic acids research *37*, W317-322.

Ntanasis-Stathopoulos, J., Tzanninis, J.G., Philippou, A., and Koutsilieris, M. (2013). Epigenetic regulation on gene expression induced by physical exercise. Journal of musculoskeletal & neuronal interactions *13*, 133-146.

Okano, M., Bell, D.W., Haber, D.A., and Li, E. (1999). DNA methyltransferases Dnmt3a and Dnmt3b are essential for de novo methylation and mammalian development. Cell *99*, 247-257.

Oliveira, R.L., Ueno, M., de Souza, C.T., Pereira-da-Silva, M., Gasparetti, A.L., Bezzera, R.M., Alberici, L.C., Vercesi, A.E., Saad, M.J., and Velloso, L.A. (2004). Cold-induced PGC-1alpha expression modulates muscle glucose uptake through an insulin receptor/Akt-independent, AMPK-dependent pathway. American journal of physiology. Endocrinology and metabolism *287*, E686-695.

Olson, B.L., Hock, M.B., Ekholm-Reed, S., Wohlschlegel, J.A., Dev, K.K., Kralli, A., and Reed, S.I. (2008). SCFCdc4 acts antagonistically to the PGC-1alpha transcriptional coactivator by targeting it for ubiquitin-mediated proteolysis. Genes & development *22*, 252-264.

Olson, E.N., and Williams, R.S. (2000). Calcineurin signaling and muscle remodeling. Cell *101*, 689-692.

Pearen, M.A., Myers, S.A., Raichur, S., Ryall, J.G., Lynch, G.S., and Muscat, G.E.O. (2008). The Orphan Nuclear Receptor, NOR-1, a Target of β-Adrenergic Signaling, Regulates Gene Expression that Controls Oxidative Metabolism in Skeletal Muscle. Endocrinology *149*, 2853-2865.

Perez-Schindler, J., Summermatter, S., Salatino, S., Zorzato, F., Beer, M., Balwierz, P.J., van Nimwegen, E., Feige, J.N., Auwerx, J., and Handschin, C. (2012). The corepressor NCoR1 antagonizes PGC-1alpha and estrogen-related receptor alpha in the regulation of skeletal muscle function and oxidative metabolism. Molecular and cellular biology *32*, 4913-4924.

Pérez-Schindler, J.a.C.H. (2013). New insights in the regulation of skeletal muscle PGC-1α by exercise and metabolic diseases. Drug Discovery Today: Disease Models 10(2): e79-e85.

Perry, C.G., Lally, J., Holloway, G.P., Heigenhauser, G.J., Bonen, A., and Spriet, L.L. (2010). Repeated transient mRNA bursts precede increases in transcriptional and mitochondrial proteins during training in human skeletal muscle. The Journal of physiology *588*, 4795-4810.

Phillips, B.A., and Mastaglia, F.L. (2000). Exercise therapy in patients with myopathy. Current opinion in neurology *13*, 547-552.

Philp, A., Belew, M.Y., Evans, A., Pham, D., Sivia, I., Chen, A., Schenk, S., and Baar, K. (2011). The PGC-1alpha-related coactivator promotes mitochondrial and myogenic adaptations in C2C12 myotubes. American journal of physiology. Regulatory, integrative and comparative physiology *301*, R864-872.

Pilegaard, H., Saltin, B., and Neufer, P.D. (2003). Exercise induces transient transcriptional activation of the PGC-1alpha gene in human skeletal muscle. The Journal of physiology *546*, 851-858.

Popov, D.V., Lysenko, E.A., Kuzmin, I.V., Vinogradova, V., and Grigoriev, A.I. (2015). Regulation of PGC-1α Isoform Expression in Skeletal Muscles. Acta Naturae *7*, 48-59.

Puigserver, P., Adelmant, G., Wu, Z., Fan, M., Xu, J., O'Malley, B., and Spiegelman, B.M. (1999). Activation of PPARγ Coactivator-1 Through Transcription Factor Docking. Science *286*, 1368-1371.

Puigserver, P., Rhee, J., Lin, J., Wu, Z., Yoon, J.C., Zhang, C.Y., Krauss, S., Mootha, V.K., Lowell, B.B., and Spiegelman, B.M. (2001). Cytokine stimulation of energy expenditure through p38 MAP kinase activation of PPARgamma coactivator-1. Molecular cell *8*, 971-982.

Puigserver, P., and Spiegelman, B.M. (2003). Peroxisome proliferator-activated receptor-gamma coactivator 1 alpha (PGC-1 alpha): transcriptional coactivator and metabolic regulator. Endocrine reviews *24*, 78-90.

Puigserver, P., Wu, Z., Park, C.W., Graves, R., Wright, M., and Spiegelman, B.M. (1998). A cold-inducible coactivator of nuclear receptors linked to adaptive thermogenesis. Cell *92*, 829-839.

Rao, R.R., Long, J.Z., White, J.P., Svensson, K.J., Lou, J., Lokurkar, I., Jedrychowski, M.P., Ruas, J.L., Wrann, C.D., Lo, J.C., et al. (2014). Meteorin-like is a hormone that regulates immune-adipose interactions to increase beige fat thermogenesis. Cell *157*, 1279-1291.

Reik, W., Dean, W., and Walter, J. (2001). Epigenetic reprogramming in mammalian development. Science *293*, 1089-1093.

Riggs, A.D. (1975). X inactivation, differentiation, and DNA methylation. Cytogenetics and cell genetics *14*, 9-25.

Roberts, L.D., Bostrom, P., O'Sullivan, J.F., Schinzel, R.T., Lewis, G.D., Dejam, A., Lee, Y.K., Palma, M.J., Calhoun, S., Georgiadi, A., et al. (2014). beta-Aminoisobutyric acid induces browning of white fat and hepatic beta-oxidation and is inversely correlated with cardiometabolic risk factors. Cell metabolism *19*, 96-108.

Robertson, K.D. (2005). DNA methylation and human disease. Nature reviews. Genetics *6*, 597-610.

Robinson, M.M., Dasari, S., Konopka, A.R., Johnson, M.L., Manjunatha, S., Esponda, R.R., Carter, R.E., Lanza, I.R., and Nair, K.S. (2017). Enhanced Protein Translation Underlies Improved Metabolic and Physical Adaptations to Different Exercise Training Modes in Young and Old Humans. Cell metabolism *25*, 581-592.

Rowe, G.C., Jang, C., Patten, I.S., and Arany, Z. (2011). PGC-1beta regulates angiogenesis in skeletal muscle. Am J Physiol Endocrinol Metab *301*, E155-163.

Rowe, G.C., Patten, I.S., Zsengeller, Z.K., El-Khoury, R., Okutsu, M., Bampoh, S., Koulisis, N., Farrell, C., Hirshman, M.F., Yan, Z., et al. (2013). Disconnecting mitochondrial content from respiratory chain capacity in PGC-1-deficient skeletal muscle. Cell reports *3*, 1449-1456.

Rowland, L.A., Bal, N.C., and Periasamy, M. (2015). The role of skeletal-muscle-based thermogenic mechanisms in vertebrate endothermy. Biological reviews of the Cambridge Philosophical Society *90*, 1279-1297.

Ruas, J.L., White, J.P., Rao, R.R., Kleiner, S., Brannan, K.T., Harrison, B.C., Greene, N.P., Wu, J., Estall, J.L., Irving, B.A., et al. (2012). A PGC-1alpha isoform induced by resistance training regulates skeletal muscle hypertrophy. Cell *151*, 1319-1331.

Russell, A.P., Hesselink, M.K., Lo, S.K., and Schrauwen, P. (2005). Regulation of metabolic transcriptional co-activators and transcription factors with acute exercise. FASEB journal : official publication of the Federation of American Societies for Experimental Biology *19*, 986-988.

Rytinki, M.M., and Palvimo, J.J. (2009). SUMOylation attenuates the function of PGC-1alpha. The Journal of biological chemistry *284*, 26184-26193.

Salatino, S., Kupr, B., Baresic, M., van Nimwegen, E., and Handschin, C. (2016a). The Genomic Context and Corecruitment of SP1 Affect ERRalpha Coactivation by PGC-1alpha in Muscle Cells. Molecular endocrinology *30*, 809-825.

Salatino, S., Kupr, B., Baresic, M., van Nimwegen, E., and Handschin, C. (2016b). The Genomic Context and Corecruitment of SP1 Affect ERRα Coactivation by PGC-1α in Muscle Cells. Molecular Endocrinology *30*, 809-825.

Sandri, M., Lin, J., Handschin, C., Yang, W., Arany, Z.P., Lecker, S.H., Goldberg, A.L., and Spiegelman, B.M. (2006). PGC-1alpha protects skeletal muscle from atrophy by suppressing FoxO3 action and atrophy-specific gene transcription. Proceedings of the National Academy of Sciences of the United States of America *103*, 16260-16265.

Sandri, M., Sandri, C., Gilbert, A., Skurk, C., Calabria, E., Picard, A., Walsh, K., Schiaffino, S., Lecker, S.H., and Goldberg, A.L. (2004). Foxo transcription factors induce the atrophy-related ubiquitin ligase atrogin-1 and cause skeletal muscle atrophy. Cell *117*, 399-412.

Sapru, M.K. (2001). Neuregulin-1 regulates expression of the Ets-2 transcription factor. Life sciences *69*, 2663-2674.

Scarpulla, R.C. (2008). Transcriptional Paradigms in Mammalian Mitochondrial Biogenesis and Function. Physiological reviews *88*, 611-638.

Scarpulla, R.C. (2011). Metabolic control of mitochondrial biogenesis through the PGC-1 family regulatory network. Biochimica et biophysica acta *1813*, 1269-1278.

Scarpulla, R.C., Vega, R.B., and Kelly, D.P. (2012). Transcriptional integration of mitochondrial biogenesis. Trends in endocrinology and metabolism: TEM *23*, 459-466.

Schiaffino, S., and Reggiani, C. (2011). Fiber types in mammalian skeletal muscles. Physiological reviews *91*, 1447-1531.

Schnyder, S., and Handschin, C. (2015). Skeletal muscle as an endocrine organ: PGC-1alpha, myokines and exercise. Bone *80*, 115-125.

Schnyder, S., Heim-Kupr, B., Beer, M., Mittal, N., Ehrenfeuchter, N., and Handschin, C. (2018 (not published yet)). PGC-1β is involved in the response to fasting-induced skeletal muscle atrophy by inhibiting Nfatc1 activity. not published yet.

Schnyder, S., Kupr, B., and Handschin, C. (2017a). Coregulator-mediated control of skeletal muscle plasticity - A mini-review. Biochimie *136*, 49-54.

Schnyder, S., Svensson, K., Cardel, B., and Handschin, C. (2017b). Muscle PGC-1α is required for long term systemic and local adaptations to a ketogenic diet in mice. American journal of physiology. Endocrinology and metabolism *312*, E437-E446.

Schreiber, S.N., Emter, R., Hock, M.B., Knutti, D., Cardenas, J., Podvinec, M., Oakeley, E.J., and Kralli, A. (2004). The estrogen-related receptor alpha (ERRalpha) functions in PPARgamma coactivator 1alpha (PGC-1alpha)-induced mitochondrial biogenesis. Proceedings of the National Academy of Sciences of the United States of America *101*, 6472-6477.

Schubeler, D. (2015). Function and information content of DNA methylation. Nature *517*, 321-326.

Seaborne, R.A., Strauss, J., Cocks, M., Shepherd, S., O'Brien, T.D., van Someren, K.A., Bell, P.G., Murgatroyd, C., Morton, J.P., Stewart, C.E., et al. (2018). Human Skeletal Muscle Possesses an Epigenetic Memory of Hypertrophy. Scientific reports *8*, 1898.

Shao, D., Liu, Y., Liu, X., Zhu, L., Cui, Y., Cui, A., Qiao, A., Kong, X., Liu, Y., Chen, Q., et al. (2010). PGC-1 beta-regulated mitochondrial biogenesis and function in myotubes is mediated by NRF-1 and ERR alpha. Mitochondrion *10*, 516-527.

Sharples, A.P., Stewart, C.E., and Seaborne, R.A. (2016). Does skeletal muscle have an 'epi'-memory? The role of epigenetics in nutritional programming, metabolic disease, aging and exercise. Aging cell *15*, 603-616.

Siegfried, Z., and Simon, I. (2010). DNA methylation and gene expression. Wiley interdisciplinary reviews. Systems biology and medicine *2*, 362-371.

Singh, P., Schimenti, J.C., and Bolcun-Filas, E. (2015). A Mouse Geneticist's Practical Guide to CRISPR Applications. Genetics *199*, 1-U402.

Skrypnik, D., Bogdanski, P., Madry, E., Karolkiewicz, J., Ratajczak, M., Krysciak, J., Pupek-Musialik, D., and Walkowiak, J. (2015). Effects of Endurance and Endurance Strength Training on Body Composition and Physical Capacity in Women with Abdominal Obesity. Obesity facts *8*, 175-187.

Smigielski, E.M., Sirotkin, K., Ward, M., and Sherry, S.T. (2000). dbSNP: a database of single nucleotide polymorphisms. Nucleic acids research *28*, 352-355.

Smith, Z.D., and Meissner, A. (2013). DNA methylation: roles in mammalian development. Nature reviews. Genetics *14*, 204-220.

Song, F., Smith, J.F., Kimura, M.T., Morrow, A.D., Matsuyama, T., Nagase, H., and Held, W.A. (2005). Association of tissue-specific differentially methylated regions (TDMs) with differential gene expression. Proceedings of the National Academy of Sciences of the United States of America *102*, 3336-3341.

Sonoda, J., Mehl, I.R., Chong, L.-W., Nofsinger, R.R., and Evans, R.M. (2007). PGC-1β controls mitochondrial metabolism to modulate circadian activity, adaptive thermogenesis, and hepatic steatosis. Proceedings of the National Academy of Sciences of the United States of America *104*, 5223-5228.

Sorianello, E., Soriano, F.X., Fernandez-Pascual, S., Sancho, A., Naon, D., Vila-Caballer, M., Gonzalez-Navarro, H., Portugal, J., Andres, V., Palacin, M., et al. (2012). The promoter activity of human Mfn2 depends on Sp1 in vascular smooth muscle cells. Cardiovascular research *94*, 38-47.

Spiegelman, B.M., and Heinrich, R. (2004). Biological control through regulated transcriptional coactivators. Cell *119*, 157-167.

Spina, R.J., Chi, M.M., Hopkins, M.G., Nemeth, P.M., Lowry, O.H., and Holloszy, J.O. (1996). Mitochondrial enzymes increase in muscle in response to 7-10 days of cycle exercise. Journal of applied physiology (Bethesda, Md. : 1985) *80*, 2250-2254.

St-Pierre, J., Lin, J., Krauss, S., Tarr, P.T., Yang, R., Newgard, C.B., and Spiegelman, B.M. (2003). Bioenergetic analysis of peroxisome proliferator-activated receptor gamma coactivators 1alpha and 1beta (PGC-1alpha and PGC-1beta) in muscle cells. The Journal of biological chemistry *278*, 26597-26603.

Stadler, M.B., Murr, R., Burger, L., Ivanek, R., Lienert, F., Scholer, A., van Nimwegen, E., Wirbelauer, C., Oakeley, E.J., Gaidatzis, D., et al. (2011). DNA-binding factors shape the mouse methylome at distal regulatory regions. Nature *480*, 490-495.

Stepto, N.K., Coffey, V.G., Carey, A.L., Ponnampalam, A.P., Canny, B.J., Powell, D., and Hawley, J.A. (2009). Global gene expression in skeletal muscle from well-trained strength and endurance athletes. Medicine and science in sports and exercise *41*, 546-565.

Sternberg, S.H., and Doudna, J.A. (2015). Expanding the Biologist's Toolkit with CRISPR-Cas9. Molecular cell *58*, 568-574.

Su, T., Liu, F., Gu, P., Jin, H., Chang, Y., Wang, Q., Liang, Q., and Qi, Q. (2016). A CRISPR-Cas9 Assisted Non-Homologous End-Joining Strategy for One-step Engineering of Bacterial Genome. Scientific reports *6*, 37895.

Suetta, C., Frandsen, U., Jensen, L., Jensen, M.M., Jespersen, J.G., Hvid, L.G., Bayer, M., Petersson, S.J., Schroder, H.D., Andersen, J.L., et al. (2012). Aging affects the transcriptional regulation of human skeletal muscle disuse atrophy. PLoS One *7*, e51238.

Sumi, D., and Ignarro, L.J. (2005). Sp1 transcription factor expression is regulated by estrogen-related receptor alpha1. Biochem Biophys Res Commun *328*, 165-172.

Summermatter, S., Baum, O., Santos, G., Hoppeler, H., and Handschin, C. (2010). Peroxisome proliferator-activated receptor {gamma} coactivator 1{alpha} (PGC-1{alpha}) promotes skeletal muscle lipid refueling in vivo by activating de novo lipogenesis and the pentose phosphate pathway. The Journal of biological chemistry *285*, 32793-32800.

Summermatter, S., and Handschin, C. (2012). PGC-1alpha and exercise in the control of body weight. International journal of obesity *36*, 1428-1435.

Summermatter, S., Santos, G., Perez-Schindler, J., and Handschin, C. (2013). Skeletal muscle PGC-1alpha controls whole-body lactate homeostasis through estrogen-related receptor alpha-dependent activation of LDH B and repression of LDH A. Proceedings of the National Academy of Sciences of the United States of America *110*, 8738-8743.

Svingen, T., and Tonissen, K.F. (2006). Hox transcription factors and their elusive mammalian gene targets. Heredity *97*, 88-96.

Taaffe, D.R., Henwood, T.R., Nalls, M.A., Walker, D.G., Lang, T.F., and Harris, T.B. (2009). Alterations in muscle attenuation following detraining and retraining in resistance-trained older adults. Gerontology *55*, 217-223.

Tabas-Madrid, D., Nogales-Cadenas, R., and Pascual-Montano, A. (2012). GeneCodis3: a non-redundant and modular enrichment analysis tool for functional genomics. Nucleic acids research *40*, W478-483.

Tadaishi, M., Miura, S., Kai, Y., Kano, Y., Oishi, Y., and Ezaki, O. (2011). Skeletal Muscle-Specific Expression of PGC-1α-b, an Exercise-Responsive Isoform, Increases Exercise Capacity and Peak Oxygen Uptake. PLoS ONE *6*, e28290.

Tahiliani, M., Koh, K.P., Shen, Y., Pastor, W.A., Bandukwala, H., Brudno, Y., Agarwal, S., Iyer, L.M., Liu, D.R., Aravind, L., et al. (2009). Conversion of 5-methylcytosine to 5-hydroxymethylcytosine in mammalian DNA by MLL partner TET1. Science *324*, 930-935.

Taylor, S.M., and Jones, P.A. (1979). Multiple new phenotypes induced in 10T1/2 and 3T3 cells treated with 5-azacytidine. Cell *17*, 771-779.

Terada, S., and Tabata, I. (2004). Effects of acute bouts of running and swimming exercise on PGC-1alpha protein expression in rat epitrochlearis and soleus muscle. Am J Physiol Endocrinol Metab *286*, E208-216.

Teyssier, C., Ma, H., Emter, R., Kralli, A., and Stallcup, M.R. (2005). Activation of Nuclear Receptor Coactivator PGC-1α by Arginine Methylation. Genes & development *19*, 1466-1473.

Tiraby, C., Hazen, B.C., Gantner, M.L., and Kralli, A. (2011). Estrogen-related receptor gamma promotes mesenchymal-to-epithelial transition and suppresses breast tumor growth. Cancer research *71*, 2518-2528.

Tontonoz, P., Cortez-Toledo, O., Wroblewski, K., Hong, C., Lim, L., Carranza, R., Conneely, O., Metzger, D., and Chao, L.C. (2015). The orphan nuclear receptor Nur77 is a determinant of myofiber size and muscle mass in mice. *35*, 1125-1138.

Tsumagari, K., Baribault, C., Terragni, J., Chandra, S., Renshaw, C., Sun, Z., Song, L., Crawford, G.E., Pradhan, S., Lacey, M., et al. (2013a). DNA methylation and differentiation: HOX genes in muscle cells. Epigenetics & chromatin *6*, 25.

Tsumagari, K., Baribault, C., Terragni, J., Varley, K.E., Gertz, J., Pradhan, S., Badoo, M., Crain, C.M., Song, L., Crawford, G.E., et al. (2013b). Early de novo DNA methylation and prolonged demethylation in the muscle lineage. Epigenetics *8*, 317-332.

Tsuzuki, T., Kobayashi, H., Yoshihara, T., Kakigi, R., Ichinoseki-Sekine, N., and Naito, H. (2017). Attenuation of exercise-induced heat shock protein 72 expression blunts improvements in whole-body insulin resistance in rats with type 2 diabetes. Cell Stress Chaperones *22*, 263-269.

Vercauteren, K., Gleyzer, N., and Scarpulla, R.C. (2009). Short hairpin RNA-mediated silencing of PRC (PGC-1-related coactivator) results in a severe respiratory chain deficiency associated with the proliferation of aberrant mitochondria. The Journal of biological chemistry *284*, 2307-2319.

Vercauteren, K., Pasko, R.A., Gleyzer, N., Marino, V.M., and Scarpulla, R.C. (2006). PGC-1-related coactivator: immediate early expression and characterization of a CREB/NRF-1 binding domain associated with cytochrome c promoter occupancy and respiratory growth. Molecular and cellular biology *26*, 7409-7419.

Voisin, S., Eynon, N., Yan, X., and Bishop, D.J. (2015). Exercise training and DNA methylation in humans. Acta physiologica (Oxford, England) *213*, 39-59.

Wakita, H., Tokura, Y., Furukawa, F., and Takigawa, M. (1994). High calcium induces heat shock proteins 72 and 60 in cultured human keratinocytes: comparative study with heat shock and sunlamp light irradiation. Journal of dermatological science *8*, 136-144.

Wallberg, A.E., Yamamura, S., Malik, S., Spiegelman, B.M., and Roeder, R.G. (2003a). Coordination of p300-mediated chromatin remodeling and TRAP/mediator function through coactivator PGC-1alpha. Molecular cell *12*, 1137-1149.

Wallberg, A.E., Yamamura, S., Malik, S., Spiegelman, B.M., and Roeder, R.G. (2003b). Coordination of p300-Mediated Chromatin Remodeling and TRAP/Mediator Function through Coactivator PGC-1α. Molecular cell *12*, 1137-1149.

Wang, H.Y., Yang, H., Shivalila, C.S., Dawlaty, M.M., Cheng, A.W., Zhang, F., and Jaenisch, R. (2013). One-Step Generation of Mice Carrying Mutations in Multiple Genes by CRISPR/Cas-Mediated Genome Engineering. Cell *153*, 910-918.

Widrick, J.J., Stelzer, J.E., Shoepe, T.C., and Garner, D.P. (2002). Functional properties of human muscle fibers after short-term resistance exercise training. American journal of physiology. Regulatory, integrative and comparative physiology *283*, R408-416.

Wiedenheft, B., Sternberg, S.H., and Doudna, J.A. (2012). RNA-guided genetic silencing systems in bacteria and archaea. Nature *482*, 331-338.

Wu, H., Kanatous, S.B., Thurmond, F.A., Gallardo, T., Isotani, E., Bassel-Duby, R., and Williams, R.S. (2002). Regulation of mitochondrial biogenesis in skeletal muscle by CaMK. Science *296*, 349-352.

Wu, Z., Puigserver, P., Andersson, U., Zhang, C., Adelmant, G., Mootha, V., Troy, A., Cinti, S., Lowell, B., Scarpulla, R.C., et al. (1999). Mechanisms controlling mitochondrial biogenesis and respiration through the thermogenic coactivator PGC-1. Cell *98*, 115-124.

Xu, L., Ma, X., Bagattin, A., and Mueller, E. (2016a). The transcriptional coactivator PGC1alpha protects against hyperthermic stress via cooperation with the heat shock factor HSF1. Cell Death Dis *7*, e2102.

Xu, W., Wang, F., Yu, Z., and Xin, F. (2016b). Epigenetics and Cellular Metabolism. Genetics & Epigenetics *8*, 43-51.

Yang, H., Wang, H.Y., and Jaenisch, R. (2014). Generating genetically modified mice using CRISPR/Cas-mediated genome engineering. Nat Protoc *9*, 1956-1968.

Yang, H., Wang, H.Y., Shivalila, C.S., Cheng, A.W., Shi, L.Y., and Jaenisch, R. (2013). One-Step Generation of Mice Carrying Reporter and Conditional Alleles by CRISPR/Cas-Mediated Genome Engineering. Cell *154*, 1370-1379.

Yang, Y., Creer, A., Jemiolo, B., and Trappe, S. (2005). Time course of myogenic and metabolic gene expression in response to acute exercise in human skeletal muscle. Journal of applied physiology *98*, 1745-1752.

Ydfors, M., Fischer, H., Mascher, H., Blomstrand, E., Norrbom, J., and Gustafsson, T. (2013a). The truncated splice variants, NT-PGC-1alpha and PGC-1alpha4, increase with both endurance and resistance exercise in human skeletal muscle. Physiological reports *1*, e00140.

Ydfors, M., Fischer, H., Mascher, H., Blomstrand, E., Norrbom, J., and Gustafsson, T. (2013b). The truncated splice variants, NT-PGC-1α and PGC-1α4, increase with both endurance and resistance exercise in human skeletal muscle. Physiological reports *1*, e00140.

Yong, W.S., Hsu, F.M., and Chen, P.Y. (2016). Profiling genome-wide DNA methylation. Epigenetics & chromatin *9*, 26.

Yoon, J.C., Puigserver, P., Chen, G., Donovan, J., Wu, Z., Rhee, J., Adelmant, G., Stafford, J., Kahn, C.R., Granner, D.K., et al. (2001). Control of hepatic gluconeogenesis through the transcriptional coactivator PGC-1. Nature *413*, 131-138.

Zechner, C., Lai, L., Fong, J.L., Geng, T., Yan, Z., Rumsey, J.W., Collia, D., Chen, Z., Wozniak, D.F., Leone, T.C., et al. (2010a). Total Skeletal Muscle PGC-1 Deficiency Uncouples Mitochondrial Derangements from Fiber Type Determination and Insulin Sensitivity. Cell metabolism *12*, 633-642.

Zechner, C., Lai, L., Zechner, J.F., Geng, T., Yan, Z., Rumsey, J.W., Collia, D., Chen, Z., Wozniak, D.F., Leone, T.C., et al. (2010b). Total skeletal muscle PGC-1 deficiency uncouples mitochondrial derangements from fiber type determination and insulin sensitivity. Cell metabolism *12*, 633-642.

Zhang, H.M., Chen, H., Liu, W., Liu, H., Gong, J., Wang, H., and Guo, A.Y. (2012). AnimalTFDB: a comprehensive animal transcription factor database. Nucleic acids research *40*, D144-149.

Zhang, H.M., Liu, T., Liu, C.J., Song, S., Zhang, X., Liu, W., Jia, H., Xue, Y., and Guo, A.Y. (2015). AnimalTFDB 2.0: a resource for expression, prediction and functional study of animal transcription factors. Nucleic acids research *43*, D76-81.

Zhang, Y., Huypens, P., Adamson, A.W., Chang, J.S., Henagan, T.M., Boudreau, A., Lenard, N.R., Burk, D., Klein, J., Perwitz, N., et al. (2009). Alternative mRNA splicing produces a novel biologically active short isoform of PGC-1alpha. The Journal of biological chemistry *284*, 32813-32826.

Zhang, Y., Ma, K., Sadana, P., Chowdhury, F., Gaillard, S., Wang, F., McDonnell, D.P., Unterman, T.G., Elam, M.B., and Park, E.A. (2006). Estrogen-related receptors stimulate pyruvate dehydrogenase kinase isoform 4 gene expression. The Journal of biological chemistry *281*, 39897-39906.

Zorzano, A. (2009). Regulation of mitofusin-2 expression in skeletal muscle. Applied physiology, nutrition, and metabolism = Physiologie appliquee, nutrition et metabolisme *34*, 433-439.

Zurlo, F., Larson, K., Bogardus, C., and Ravussin, E. (1990). Skeletal muscle metabolism is a major determinant of resting energy expenditure. The Journal of clinical investigation *86*, 1423-1427.

Appendices

Appendix 1: Transcriptional Network Analysis in Muscle Reveals AP-1 as a Partner of PGC-1α in the Regulation of the Hypoxic Gene Program

MCB
Journals.ASM.org

Transcriptional Network Analysis in Muscle Reveals AP-1 as a Partner of PGC-1α in the Regulation of the Hypoxic Gene Program

Mario Baresic,[a] Silvia Salatino,[a,b,c] Barbara Kupr,[a] Erik van Nimwegen,[b,c] Christoph Handschin[a]

Focal Area Growth and Development[a] and Focal Area Computational and Systems Biology,[b] Biozentrum, University of Basel, Basel, Switzerland; Swiss Institute of Bioinformatics, Basel, Switzerland[c]

Skeletal muscle tissue shows an extraordinary cellular plasticity, but the underlying molecular mechanisms are still poorly understood. Here, we use a combination of experimental and computational approaches to unravel the complex transcriptional network of muscle cell plasticity centered on the peroxisome proliferator-activated receptor γ coactivator 1α (PGC-1α), a regulatory nexus in endurance training adaptation. By integrating data on genome-wide binding of PGC-1α and gene expression upon PGC-1α overexpression with comprehensive computational prediction of transcription factor binding sites (TFBSs), we uncover a hitherto-underestimated number of transcription factor partners involved in mediating PGC-1α action. In particular, principal component analysis of TFBSs at PGC-1α binding regions predicts that, besides the well-known role of the estrogen-related receptor α (ERRα), the activator protein 1 complex (AP-1) plays a major role in regulating the PGC-1α-controlled gene program of the hypoxia response. Our findings thus reveal the complex transcriptional network of muscle cell plasticity controlled by PGC-1α.

A sedentary lifestyle can lead to an imbalance between energy intake and expenditure and favors the development of a number of chronic diseases like obesity and type 2 diabetes. Regular exercise, on the other hand, is an effective way to reduce the risk for these lifestyle-related pathologies (1). The health benefits of exercise are at least in part induced by changes in skeletal muscle tissue. Muscle cells exhibit a high plasticity and thus a remarkably complex adaptation to increased contractile activity. For example, endurance training induces mitochondrial biogenesis, increases capillary density, and improves insulin sensitivity (1, 2). To achieve such a complex plastic response, a number of different signaling pathways are activated in an exercising muscle, for example, p38 mitogen-activated protein kinase (MAPK)-mediated protein phosphorylation events, increased intracellular calcium levels, or the activation of the metabolic sensors AMP-dependent protein kinase (AMPK) and sirtuin-1 (SIRT1) (3). While the temporal coordination of the numerous inputs is not clear, all of the major signaling pathways converge on the peroxisome proliferator-activated receptor (PPAR) γ coactivator 1α (PGC-1α) to either induce *Ppargc1a* gene expression, promote posttranslational modifications of the PGC-1α protein, or do both (4, 5). Upon activation, PGC-1α mediates the muscular adaptations to endurance exercise by coactivating various transcription factors (TFs) involved in the regulation of diverse biological programs such as mitochondrial biogenesis, angiogenesis, reactive oxygen species (ROS) detoxification, or glucose uptake (3). Accordingly, transgenic (TG) expression of PGC-1α in mouse skeletal muscle at physiological levels not only induces mitochondrial biogenesis but also drives a fiber-type conversion toward a more oxidative, slow-twitch phenotype (6), while muscle-specific *Ppargc1a*-knockout animals exhibit several symptoms of pathological inactivity (7, 8).

Coregulators are part of multicomponent regulatory protein complexes that are well suited to translate external stimuli into changes in promoter and enhancer activities by combining various enzymatic activities to modulate histones and chromatin structure and recruit other TFs (9). Thus, dynamic assembly of distinct coregulator complexes enables the integration of many different signaling pathways, leading to a coordinated and specific regulation of entire biological programs by multiple TFs (10, 11). For example, PGC-1α not only recruits histone acetylases (12), the TRAP/DRIP/Mediator (13), and the SWI/SNF protein complexes (14) but also binds to and coactivates a myriad of different transcription factors, even though a systematic inventory of TF binding partners has not been compiled yet (15). Thus, the specific control exerted by the PGC-1α-dependent transcriptional network might provide an explanation for the dynamic and coordinated muscle adaptation to exercise. Since PGC-1α in skeletal muscle not only confers a trained phenotype but also ameliorates several different muscle diseases (16), the unraveling of the PGC-1α-controlled transcriptional network in skeletal muscle would be of great interest to identify putative therapeutic targets within this pathway.

Therefore, we aimed at obtaining a global picture of the coregulatory activity of PGC-1α in skeletal muscle cells. More precisely, by combining data on the genome-wide binding locations of PGC-1α and the gene expression profiles in response to PGC-1α overexpression with comprehensive computational prediction of transcription factor binding site (TFBS) occurrence, we sought to unveil the biological processes that are regulated by PGC-1α, to identify the transcription factors that partner with

Received 26 December 2013 Returned for modification 26 January 2014
Accepted 3 June 2014
Published ahead of print 9 June 2014
Address correspondence to Erik van Nimwegen, erik.vannimwegen@unibas.ch, or Christoph Handschin, christoph.handschin@unibas.ch.
M.B. and S.S. contributed equally to this article.
Supplemental material for this article may be found at http://dx.doi.org/10.1128/MCB.01710-13.

doi:10.1128/MCB.01710-13

PGC-1α, and to determine the mechanistic details of PGC-1α-regulated transcription. We not only mapped the locations on the DNA where PGC-1α was bound but also delineated the target genes whose expression is either directly or indirectly affected by PGC-1α and identified novel putative transcription factor partners that mediated PGC-1α's action. In particular, our results strongly suggest that the activator protein 1 (AP-1) complex is a major regulatory partner of PGC-1α, with AP-1 and PGC-1α together regulating the hypoxic response gene program in muscle cells *in vitro* and *in vivo*.

MATERIALS AND METHODS

Cell culture and small interfering RNA (siRNA) transfection. C2C12 cells were grown in Dulbecco's modified Eagle's medium (DMEM) supplemented with 10% fetal bovine serum (FBS), 100 units/ml penicillin, and 100 μg/ml streptomycin. To obtain myotubes, the C2C12 myoblasts were allowed to reach 90% confluence and the medium was changed to DMEM supplemented with 2% horse serum (differentiation medium) for 72 h.

The siRNAs for the knockdown of NFE2L2, FOS, JUN, ATF3, NFYC, ZFP143, GTF2I, the nontargeting siRNA pool, and the DharmaFECT1 transfection reagent were purchased from Dharmacon (Fisher Scientific), and the siRNA transfection was performed according to the Thermo Scientific DharmaFECT transfection reagent siRNA transfection protocol. Briefly, after 3 days of differentiation, the respective siRNAs (50 nM final concentration) were added to the medium. Twenty-four hours after siRNA transfection, the cells were infected with adenovirus (AV) expressing either PGC-1α (AV-PGC-1α) or the green fluorescent protein (AV-GFP). Then, 48 h after adenoviral infection, the cells were harvested.

Differentiated C2C12 cells were infected with AV expressing short hairpin RNA (shRNA) for estrogen-related receptor α (AV-shERRα) (kindly provided by Anastasia Kralli, Scripps Research Institute, La Jolla, CA) to knock down and inactivate ERRα or shGFP as a control. The infected cells were kept in culture for 4 days. Afterwards, cells were infected with the AV-Flag-PGC-1α or AV-GFP and kept in culture for two additional days. As a supplement to the previously infected AV shERRα cells, 2 μM ERRα inverse agonist XCT-790 was added. To the remaining cells, 0.02% dimethyl sulfoxide (DMSO) as a vehicle was added to the differentiated medium. All the experiments have been performed in biological triplicates. For RNA isolation, TRIzol was used according to the TRIzol reagent RNA isolation protocol (Invitrogen). Three conditions were used for further analysis: AV-shGFP plus AV-GFP plus vehicle, AV-shGFP plus AV-Flag-PGC-1α plus vehicle, and AV-shERRα plus AV-Flag-PGC-1α plus 2 μM XCT-790.

ChIP and ChIP sequencing (ChIP-Seq). Chromatin immunoprecipitation (ChIP) was performed according to the Agilent Mammalian ChIP-on-chip protocol, version 10.0. For each immunoprecipitation, approximately 1×10^8 C2C12 cells were differentiated into myotubes and infected with AV-Flag-PGC-1α. For cross-linking protein complexes to DNA-binding elements, the cells were incubated in a 1% formaldehyde solution for 10 min, followed by the addition of glycine to a final concentration of 125 mM to quench the effect of the formaldehyde. The cells were rinsed in 1× phosphate-buffered saline (PBS), harvested in ice-cold 1× PBS using a silicone scraper, and pelleted by centrifugation. The pelleted cells were either used immediately or flash frozen and stored for later. The cells were then lysed at 4°C using two lysis buffers containing 0.5% NP-40–0.25% Triton X-100 and 0.1% sodium deoxycholate–0.5% *N*-lauroylsarcosine, respectively. The chromatin was then sheared by sonication to obtain DNA fragments of about 100 to 600 bp in length. Fifty microliters of the sonicated lysate was saved as input DNA. The immunoprecipitation was performed overnight at 4°C using magnetic beads (protein G Dynabeads; Invitrogen), which were previously coated with monoclonal antibodies like the monoclonal anti-Flag M2 antibody (Sigma) for the ChIP of PGC-1α or with the monoclonal anti-c-Fos (9F6) rabbit antibody (catalog no. 2250; Cell Signaling) for the ChIP of FOS. The beads carrying the precipitate were washed five times for the c-Fos antibody and six times for the Flag antibody with radioimmunoprecipitation assay (RIPA) buffer and once with Tris-EDTA (TE) that contained 50 mM NaCl to eliminate unspecific binding of DNA to the beads. For elution, the beads were resuspended in elution buffer containing 1% SDS, placed in a 65°C water bath for 15 min, and vortexed every 2 min. To reverse the cross-links, the samples were incubated at 65°C overnight. The following day, the RNA and the cellular proteins were digested using RNase A and proteinase K. The DNA was precipitated, and the success of the chromatin immunoprecipitation was validated by semiquantitative real-time PCR. The ChIP experiments were performed in triplicates. The ChIP of PGC-1α was further used for sequencing. The ChIP-Seq experiment on overexpressed PGC-1α in C2C12 cells was performed in biological duplicates. At the joint Quantitative Genomics core facility of the University of Basel and the Department of Biosystems Science and Engineering (D-BSSE) of the ETH Zurich in Basel, Switzerland, DNA libraries were prepared using the standard Illumina ChIP-Seq protocol, as described by the manufacturer, and the immunoprecipitated samples were sequenced on the Genome Analyzer II. In order to keep only high-quality data, the sequenced reads were filtered based on the quality score of each read and its alignments. Reads were retained when the Phred score was ≥20, the read length was ≥25 bp, and the number of wrongly called nucleotides (Ns) was ≤2. Those reads that passed the filter (6,711,717 for the first immunoprecipitated sample [IP], 36,580,431 for the second IP, 17,899,074 for the first whole-cell extract [WCE], and 35,525,221 for the second WCE) were aligned with the mouse genome (UCSC mm9 assembly), using Bowtie version 0.12.7 (17) with parameters –best –strata -a –m 100. The number of aligned reads equaled 5,699,648 for the first IP sample, 16,053,370 for the first WCE, 21,448,059 for the second IP, and 32,244,584 for the second WCE.

Identification of bound regions. To identify regions that were significantly enriched in the ChIP, we passed a 200-bp-long sliding window along the genome, sliding by 25 bp between consecutive windows, and estimated the fraction of all ChIP reads (f_{IP}) that fall within the window, as well as the fraction f_{WCE} of reads from the whole-cell extract that fall in the same window (which we estimate from a 2,000-bp-long window centered on the same genomic location). A Z score quantifying the enrichment in the ChIP of each window was computed as

$$Z = \frac{f_{IP} - f_{WCE}}{\sqrt{\sigma^2_{IP} + \sigma^2_{WCE}}}$$

where σ^2_{IP} and σ^2_{WCE} are the variances of the IP and WCE read frequencies, respectively, which are given by

$$\sigma^2_{IP} = \frac{f_{IP} \times (1 - f_{IP})}{N_{IP}} \text{ and } \sigma^2_{WCE} = \frac{f_{WCE} \times (1 - f_{WCE})}{N_{WCE}}$$

respectively.

The enrichments were reproducible across biological replicates. Using only the first sequencing data set, we called peaks at a Z cutoff of 4.5; we then compared these with the Z scores from the corresponding regions of the second data set, and the Pearson correlation coefficient was found to be 0.778. Similarly, we called peaks at a Z cutoff of 4.5 using only the second sequencing data set; when we compared these peaks with the Z scores of the corresponding regions from the first data set, the Pearson correlation coefficient was found to be 0.782.

To obtain a final set of binding peaks, we combined the reads from the two biological replicates, computing the Z score of each window as

$$Z = \frac{f_{IP_1} + f_{IP_2} - f_{WCE_1} - f_{WCE_2}}{\sqrt{\sigma^2_{IP_1} + \sigma^2_{IP_2} + \sigma^2_{WCE_1} + \sigma^2_{WCE_2}}}$$

We conservatively considered all windows with a Z score larger than 4.5 to be significantly enriched (false discovery rate [FDR], 0.6%). The final binding peaks were obtained by merging consecutive windows that all passed the cutoff and by considering the "peak" to correspond to the top-scoring window, i.e., corresponding to the summit of the ChIP-Seq signal. To determine the PGC-1α distribution genome-wide, peaks were

annotated according to their closest *Mus musculus* RefSeq transcripts. We defined peaks as "intronic" (peak center lying inside an intron), "exonic" (peak center lying inside an exon), "upstream of TSS" (peak center lying between kb −10 and 0 relative to the closest transcription start site [TSS]), "downstream of TES" (peak center lying between kb 0 and +10 relative to the closest transcription end site [TES]), or "intergenic" (peak center located farther than 10 kb from the nearest transcript). Moreover, we computed the ratio between observed and expected peak location distributions, obtained by generating 100 peak sets composed of 7,512 random peaks each.

Motif finding and TFBS overrepresentation. The binding peak regions were aligned with orthologous regions from 6 other mammalian species—human (hg18), rhesus macaque (rheMac2), dog (canFam2), horse (equCab1), cow (bosTau3), and opossum (monDom4)—using T-Coffee (18). A collection of 190 mammalian regulatory motifs (position weight matrices [WMs]) representing the binding specificities of approximate 350 mouse TFs (in many cases, sequence specificities of multiple closely related TFs were represented with the same WM) were downloaded from the SwissRegulon website (19). TFBSs for all known motifs were predicted using the MotEvo algorithm (20) on the alignments of all 7,512 peak sequences. Only binding sites with a posterior probability of ≥0.1 were considered for the further steps of the analysis. In order to create a background set of regions to assess the overrepresentation of binding sites within our regions, we created randomized alignments by shuffling the multiple alignment columns, maintaining both the gap patterns and the conservation patterns of the original alignments. TFBSs were predicted on the shuffled alignments using the same MotEvo settings as those for the original peak alignments. Overrepresentation of motifs in the PGC-1α binding peaks was calculated by comparing total predicted TFBS occurrence within binding peaks with the predicted TFBS occurrence in the shuffled alignments. We evaluated the enrichment of TFBSs for each motif x by collecting the sum n_x of the posterior probabilities of its predicted sites in the peak alignments as well as the corresponding sum n'_x in the shuffled alignments and computed a Z score:

$$Z = \frac{f_x - f'_x}{\sqrt{\frac{f_x \times (1 - f_x)}{L_x} + \frac{f'_x \times (1 - f'_x)}{L'_x}}}$$

where L_x and L'_x are the total lengths of the original and shuffled alignments, respectively, while f_x and f'_x are given by the equations $n_x \times l_x = f_x \times L_x$ and $n'_x \times l_x = f'_x \times L'_x$, with l_x being the length of motif x.

PCA of TFBS occurrence in binding peaks. The input matrix N for the principal component analysis (PCA) contained the total number of predicted binding sites N_{pm} in each of the 7,512 binding peaks p (rows) for each of the 190 mammalian regulatory motifs m (columns). After mean centering the columns of this matrix, $\tilde{N}_{pm} = N_{pm} - \langle N_m \rangle$, i.e., subtracting the average site count for each motif, singular value decomposition (SVD) was used to factorize this matrix: $\tilde{N} = U \cdot S \cdot V^T$, where U is a $P \times M$ matrix whose columns are the left singular vectors of $\tilde{N}$; S is an $M \times M$ diagonal matrix containing the singular values, and V^T (the transpose of V) is an $M \times M$ matrix whose rows are the right singular vectors, with P the number of peaks and M the number of motifs. The SVD was performed using the "svd" package of the "R" programming language.

Gene expression arrays. Whole-gene expression after 48 h of transfection with adenovirus was measured in C2C12 cells with Affymetrix GeneChip Mouse Gene 1.0 ST microarrays at the Life Science Training core facility of the University of Basel. Raw probe intensities were corrected for background and unspecific binding using the Bioconductor package "affy" (21). Subsequently, probes were classified as expressed or nonexpressed by using the "Mclust" R package (22), and after removal of nonexpressed probes, the intensity values were quantile normalized across all samples. Using mapping of the probes to the UCSC collection of mouse mRNAs, probes were then associated with a comprehensive collection of mouse promoters available from the SwissRegulon database (19). The $\log_2$ expression level of a given promoter was calculated as the weighted average of the expression levels of all probes associated with it. $\log_2$ expression levels were then compared between overexpressed PGC-1α and the control GFP sample; for each promoter, the change in expression level across the two conditions was measured by $\log_2$ fold change ($\log_2$FC), computed as the difference between the mean of the $\log_2$ values in PGC-1α and the mean of the $\log_2$ values in GFP. The significance of the expression change was assessed by a Z score, which was computed as

$$Z = \frac{\bar{E}_{PGC1\alpha} - \bar{E}_{GFP}}{\sqrt{\frac{\sigma^2_{PGC1\alpha}}{n} + \frac{\sigma^2_{GFP}}{n}}}$$

where $n = 3$ is the number of replicate samples, $\bar{E}_{PGC1\alpha}$ is the mean $\log_2$ expression across the PGC-1α samples, $\bar{E}_{GFP}$ is the mean $\log_2$ expression across the GFP samples, and $\sigma^2_{PGC1\alpha}$ and σ^2_{GFP} are the variances of $\log_2$ expression levels across the replicates for the PGC-1α and control samples, respectively. Promoters were considered significantly upregulated when $\log_2$FC was ≥1 and Z was ≥3 and significantly downregulated when $\log_2$FC was ≤−1 and Z was ≤−3.

Peaks were assigned to promoters by proximity. To assign each peak to a promoter, we calculated the distance from the center of the peak to the center of neighboring promoters; whenever the peak was closer than 10 kb from at least one promoter, it was assigned to the nearest promoter and, thus, to its associated gene.

GO enrichment analysis. Gene identifiers (IDs) were extracted from differentially regulated promoters and divided into four groups: upregulated promoters with an assigned binding peak, upregulated promoters without an assigned binding peak, downregulated promoters with an assigned peak, and downregulated promoters without an assigned peak. These four gene sets were used as input for the functional analysis tool FatiGO (23) to identify significantly overrepresented gene ontology (GO) categories compared to all *Mus musculus* genes. Only GO terms having an FDR-adjusted P value of ≤0.05 were considered significant.

Motif activity at direct and indirect targets of PGC-1α. To integrate the information from the PGC-1α binding peaks, we extended motif activity response analysis (MARA) (24) to model the direct and indirect regulatory effects of PGC-1α. Given the input expression data and the computationally predicted binding sites, MARA infers, for each of 190 regulatory motifs m, the activity A_{ms} of the motif in each sample s when the motif occurs outside a region of PGC-1α and the activities A^*_{ms} of the motifs when they occur within a PGC-1α binding peak. That is, changes in the motif activities A_{ms} upon overexpression of PGC-1α indicate indirect regulatory effects of PGC-1α on each motif m, whereas changes in the motif activities A^*_{ms} reflect direct regulatory effects of PGC-1α as mediated by each motif m. For each promoter p that was not associated with any PGC-1α binding peak (which we designate indirect targets), we modeled its log-expression in sample s, e_{ps}, in terms of the predicted number of TFBSs N_{pm} that occur in the proximal promoter region (running from −500 to +500 relative to the TSS) for each regulatory motif m. That is, MARA assumes the linear model

$$e_{ps} = c_p + \tilde{c}_s + \sum_m N_{pm} A_{ms}$$

where c_p is the basal expression of promoter p, $\tilde{c}_s$ is a sample-dependent normalization constant, and A_{ms} is the regulatory activity of motif m in sample s, which is inferred by the model. Formally, A_{ms} quantifies the amount by which the expression of promoter p in sample s would be reduced if a binding site for motif m were to be deleted from the promoter.

For each "direct target" promoter p that has an associated PGC-1α binding peak, which we defined as promoters with a peak within 1 kb or with a peak within 100 kb that was highly conserved according to the PhastCons score of the region (25), we model its expression in terms of the predicted TFBSs in the binding peak, i.e.,

$$e_{ps} = c_p + \tilde{c}_s + \sum_m N^*_{pm} A^*_{ms}$$

where N^*_{pm} is the number of predicted TFBSs for motif m in the peak

associated with promoter p and A^*_{ms} is the motif activity of regulator m in sample s when this motif occurs in the context of PGC-1α binding. That is, the inferred motif activities A_{ms} quantify the activities of regulatory motifs when they occur independently of PGC-1α binding, and the motif activities A^*_{ms} quantify the activities of motifs when they occur in a PGC-1α binding peak, i.e., the latter activities reflect direct effects of a PGC-1α while the former activities reflect indirect effects.

MARA predicts activities for 190 different mammalian regulatory motifs, associated with roughly 350 mouse TFs. Besides motif activities, MARA also calculates error bars δ_{ms} for each motif m in each sample s. Using these, MARA calculates, for each motif m, an overall significance measure for the variation in motif activities across the samples analogous to a Z statistic:

$$z_m = \sqrt{\frac{1}{S}\sum_{s=1}^{S}\left(\frac{A_{ms}}{\delta_{ms}}\right)^2}$$

For each motif, we calculate both a Z score z_m associated with its indirect activity changes and a Z score z^*_m associated with its direct activity changes. MARA also ranks the confidence on predicted target promoters of each motif by a Bayesian procedure that quantifies the contribution of that factor to explaining the promoter's expression variation by a chi-square value (for details, see reference 24). The parameters used for motif stratification were (i) the Z score z^*_m for direct activity changes; (ii) the Z score z_m for indirect motif activity changes; (iii) the Z score $\bar{z}^*_m$ for direct motif activity changes, computed by averaging the sample replicates; and (iv) the Z score $\bar{z}_m$ for indirect motif activity changes, computed by averaging the sample replicates. The latter two measures were used to show which in direction the motif activity changes when overexpressing PGC-1α with respect to the control condition. All motifs m for which either the direct or indirect motif activities were changing significantly ($z \geq 2$) were subsequently selected.

***De novo* motif finding.** PhyloGibbs (26) was used to identify *de novo* motifs across the 200 top enriched PGC-1α peaks. The parameters used were -D 1 -z 1 -y 200 -m 10, corresponding to searching on multiple alignments for a single motif of length 10 with a total of 200 sites. The resulting motif was scanned for similarity to the other known motifs from our data set using STAMP (27), with the following settings: Pearson correlation coefficient for column comparison metric, Smith-Waterman for the alignment method, and penalty of 0.5 and 0.25 for gap opening and gap extension, respectively.

Real-time PCR and target gene validation. Putative target genes of distinct transcription factor–PGC-1α combinations were chosen according to three criteria: first, positive transcriptional regulation by PGC-1α by more than 2-fold; second, presence of a PGC-1α binding peak within a 10-kb distance from the TSS; and third, prediction of targeting by MARA with a positive chi-square score. The sequences of the primers used in real-time PCR experiments are depicted in Table S1 in the supplemental material. Relative mRNA was quantified by quantitative PCR (qPCR) on a StepOnePlus system (Applied Biosystems) using Power SYBR green PCR master mix (Applied Biosystems).

The values are presented as the mean ± standard error of the mean (SEM). Student's t test was performed, and a P value of <0.05 was considered significant (*, $P < 0.05$; **, $P < 0.01$; ***, $P < 0.001$).

Animals. Mice were housed in a conventional facility with a 12-h night/12-h day cycle with free access to chow diet pellet and water. For the experiments, 22- to 23-week-old skeletal muscle-specific HSA-PGC-1α knockout (MKO) male mice and 8-week-old PGC-1α muscle-specific transgenic (TG) male mice were used as previously described (6–8). All experiments were performed according to the criteria outlined for the care and use of laboratory animals and with approval of the veterinary office of the Basel canton and the Swiss authorities.

Treadmill running. Treadmill running was performed with the TG mice on the Columbus Instruments motorized treadmill with an electric shock grid. The mice were acclimatized to the treadmill and then allowed to run till exhaustion. The running protocol is as follows: 10 m/min for 5 min with an increase of 2 m/min every 5 min until 26 m/min and an inclination of 5 degrees. The speed of 26 m/min was kept until exhaustion of the mice (7, 28, 29). Mice were killed and tissues were collected 3 h after exercise.

RNA isolation of muscle tissue. Gastrocnemius and quadriceps were used to isolate RNA by TRIzol according to the TRIzol reagent RNA isolation protocol (Invitrogen).

Microarray data accession number. The Gene Expression Omnibus (GEO) accession number for the ChIP-Seq and gene expression array data reported in this paper is GSE51191.

RESULTS

Broad recruitment of PGC-1α to the mouse genome. PGC-1α-dependent gene transcription has been studied in many different experimental contexts. In isolation, gene expression arrays, however, are unable to distinguish direct from indirect targets or to reveal the genomic sites where PGC-1α is recruited to enhancer and promoter elements, i.e., by coactivating TFs that directly bind to the DNA. Thus, we first performed chromatin immunoprecipitation followed by deep sequencing (ChIP-Seq) of PGC-1α in differentiated C2C12 mouse myotubes to identify the locations where PGC-1α is bound to the genome. To identify genomic regions that are significantly enriched in the ChIP, we slid a 200-bp window across the genome comparing the local ChIP read density with the read density from a background whole-cell extract sample. We selected all regions with a Z-statistic larger than 4.5 as significantly enriched (FDR, 0.6%) (see Fig. S1A in the supplemental material). Using this stringent cutoff, we identified 7,512 binding regions for PGC-1α via interaction with a TF genome-wide, which include binding regions in the promoters of known PGC-1α target genes (Fig. 1A), such as medium-chain-specific acyl coenzyme A (acyl-CoA) dehydrogenase (*Acadm*) and cytochrome *c* (*Cycs*) (30, 31). The enrichment of immunoprecipitated DNA fragments from the ChIP-Seq was validated for these and other PGC-1α target genes by semiquantitative real-time PCR (Fig. 1B). In absolute terms, the distribution of the ChIP-Seq peaks revealed that PGC-1α is mostly recruited at distal sites from the assigned targets and, to a lesser extent, to proximal regions of the gene or within an intronic sequence (Fig. 1C). However, compared to randomly selected DNA regions of equal size and number, PGC-1α binding peaks occur twice as often within 10 kb upstream of the transcription start site (TSS).

In parallel to the ChIP-Seq experiment, we furthermore analyzed gene expression patterns in differentiated muscle cells both under control conditions and under PGC-1α overexpression. Using a reference set of mouse promoters (19) and associating microarray probes with promoters by mapping to known transcripts, we found 1,566 promoters (corresponding to 984 genes) to be significantly upregulated ($\log_2$ fold change, ≥ 1; Z score, ≥ 3) and 1,165 promoters (corresponding to 727 genes) to be significantly downregulated ($\log_2$ fold change, ≤ -1; Z score, ≤ -3). Thus, similarly to previous reports, PGC-1α induced and repressed the transcription of almost the same number of genes, respectively, indicating that the physiological function of PGC-1α includes both the activation and the inhibition of substantial numbers of genes.

To combine the DNA-binding results from the ChIP-Seq with the data of the gene expression arrays, we then assigned ChIP-Seq peaks to the closest promoter (and the associated gene) within a maximum distance of 10 kb. In this way, about 30% of all peaks (2,295 of 7,512) could be associated with a target promoter. In-

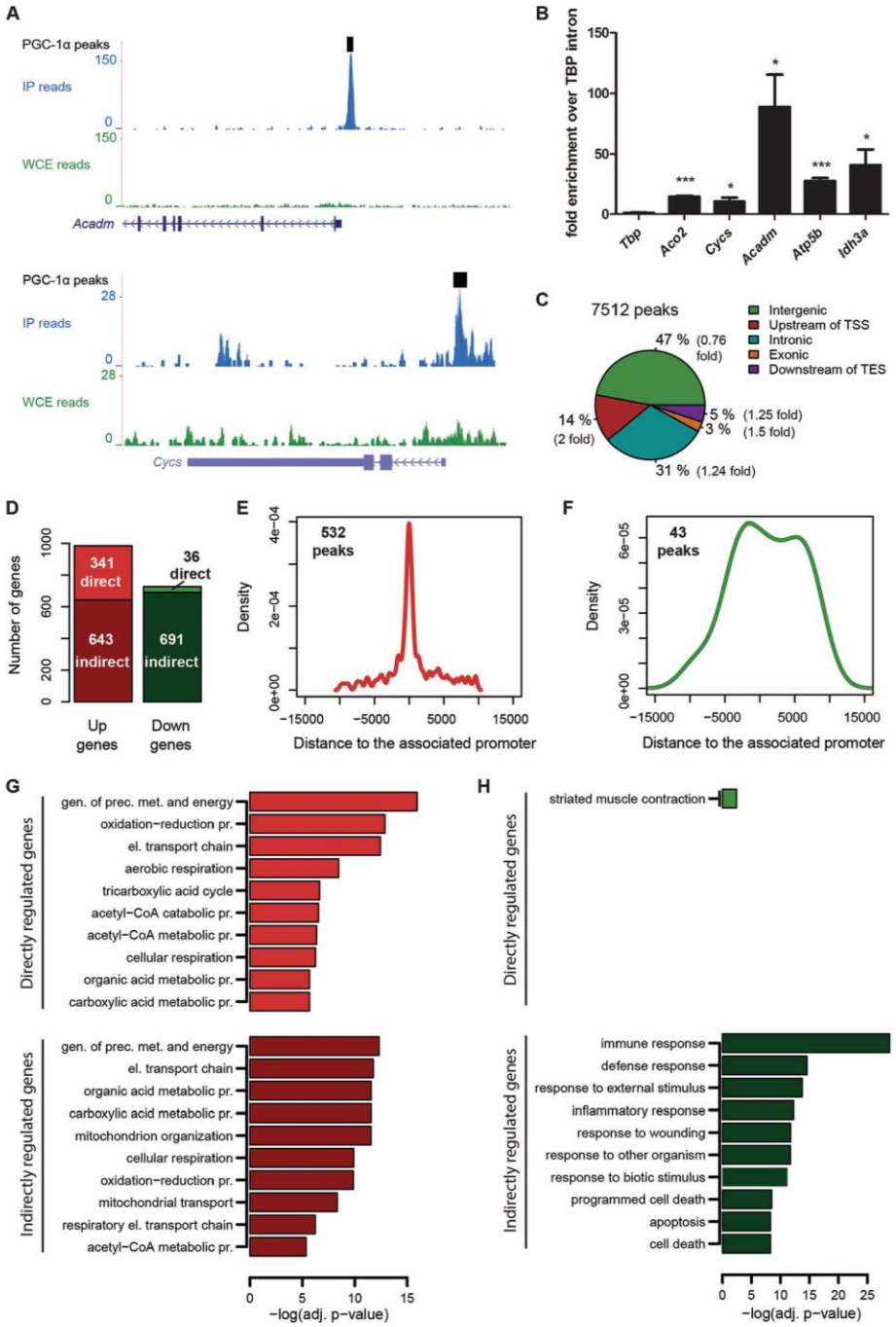

FIG 1 Genome-wide DNA recruitment of PGC-1α in mouse muscle cells. (A) PGC-1α ChIP-Seq binding peaks (read densities) around the TSSs of the genes *Acadm* and *Cycs* obtained from the UCSC Genome Browser. (B) Real-time PCR validation of the ChIP enrichment measured at the promoter of a set of PGC-1α target genes. Bars represent fold enrichment over that of the *Tbp* intron; error bars represent SEMs. *, $P < 0.05$; **, $P < 0.01$; ***, $P < 0.001$. (C) Mapping

versely, for about 35% of all significantly upregulated genes (341 of 984), a PGC-1α binding peak is found within 10 kb of the promoter. Since some of the upregulated promoters may be regulated by more distal peaks, this is only a lower bound on the fraction of genes that are directly regulated. In stark contrast, only about 5% of all repressed genes harbor one or more PGC-1α DNA recruitment peaks in their vicinity (36 of 727), compared with 95% indirectly downregulated PGC-1α target genes (691 genes) (Fig. 1D). Moreover, the distribution of the distances between PGC-1α peaks and their associated promoters revealed a tight cluster of 532 peaks close to promoter regions for upregulated, direct PGC-1α target genes (Fig. 1E), whereas the distribution of the 43 peaks associated with downregulated genes was much wider, raising the possibility that the association of peaks with transcriptionally repressed genes was spurious (Fig. 1F). In summary, the strong enrichment of binding peaks near upregulated genes and the almost complete absence of binding peaks near downregulated genes suggest that direct regulation of transcription by PGC-1α is almost exclusively activating. We note that there is a large fraction of binding peaks (75%) that are associated with target genes that do not significantly alter their expression. These peaks may have been wrongly assigned, their functionality may be dependent on additional factors not active in these cells, or they may simply be spurious binding events that are not functional.

We next used this stratification of peaks and genes to study whether direct (i.e., with an associated binding peak) and indirect PGC-1α target genes exert different biological functions and identified gene ontology (GO) terms that were overrepresented in any of the four categories. First, we observed that the most significantly enriched functional categories for directly and indirectly upregulated genes were those related to mitochondria, oxidative phosphorylation, and energy production (Fig. 1G; see also Fig. S1B in the supplemental material). In contrast, GO analysis of indirectly downregulated PGC-1α target genes revealed a high prevalence of terms related to inflammation and immune response (Fig. 1H; see also Fig. S1C). Assuming that the assignment of peaks to repressed genes is not spurious, the few directly repressed PGC-1α targets exhibit an enrichment in functions related to muscle contraction, in particular for genes that are linked to contractile and metabolic properties of glycolytic, fast-twitch muscle fibers (Fig. 1H; see also Fig. S1D), as would be expected from the observed shift from glycolytic to oxidative fibers mediated by PGC-1α in muscle (6).

Modeling the direct and indirect gene regulatory effects of PGC-1α. As a next step, we rigorously modeled the effects of PGC-1α on its target genes in terms of the occurrence of TFBSs for a large collection of mammalian regulatory motifs. We previously introduced a general framework, called motif activity response analysis (MARA) (24), for modeling the gene expression profiles as a linear function of the TFBSs occurring in the promoters and unknown regulatory "activities" of each of the regulators. As detailed in Materials and Methods, we here extended MARA to incorporate information from the PGC-1α ChIP-Seq data, with the aim of identifying which other TFs are involved in mediating both the direct and indirect regulatory effects of PGC-1α. Specifically, for all "direct target" promoters that were associated with a PGC-1α binding peak, we modeled the expression of the promoter in terms of the predicted TFBSs in the neighborhood of the binding peak, while for "indirect target" promoters, we modeled the promoter's expression in terms of the predicted TFBSs in the proximal promoter region, according to the conventional MARA approach (Fig. 2A and B).

First, further supporting our analysis above, direct target promoters were almost exclusively upregulated and only in a few exceptional cases reached statistical significance for PGC-1α-repressed transcripts (Fig. 2C). Among the direct motif activities, the ESRRA position weight matrix was the top-ranking motif with a Z score of 6.04 (see Fig. S2 in the supplemental material). The corresponding TF estrogen-related receptor α (ERRα), an orphan nuclear receptor, has been extensively studied as a central binding partner for PGC-1α in the regulation of mitochondrial gene expression (30–32). To stratify the different motifs according to their predicted functions, we then divided all motifs into groups according to the behavior of both their direct and indirect activity changes. Strikingly, all motifs exhibited one of only four different motif activity patterns. First, 6 TFs (see Fig. S2) were predicted to positively regulate PGC-1α target genes only in the presence of PGC-1α (Fig. 2D). Second, we found 6 motifs (see Fig. S2) with significantly upregulated direct and indirect motif activities upon PGC-1α overexpression (Fig. 2E). To our surprise, ERRα was predicted to regulate PGC-1α target genes in this manner, even though in previous reports gene regulation by ERRα in the context of activated PGC-1α was suggested to be dependent on PGC-1α coactivation (30–32). Third, we found 13 motifs (see Fig. S2) that were predicted to regulate PGC-1α target genes but, however, only in the absence of PGC-1α (Fig. 2F). Fourth, there was a group of 28 motifs (see Fig. S2) that showed a significant decrease of indirect motif activity upon PGC-1α overexpression, but no significant change of their direct motif activity, including NF-κB (Fig. 2G), a central regulator of inflammation which is indirectly repressed by PGC-1α (33). Intriguingly, however, no motif was found that showed significant direct repression of target genes, reinforcing the hypothesis that PGC-1α-dependent gene repression is an indirect event.

Nuclear receptors and activator protein-1-like leucine zipper proteins are the main functional partners of PGC-1α in muscle cells. As a next step, we analyzed the occurrence of TF DNA-binding motifs in the PGC-1α peaks identified by ChIP-Seq. We first performed *de novo* motif prediction on the top 200 peaks, using PhyloGibbs (26). As shown in Fig. 3A, the motif that PhyloGibbs identified matches significantly (E value = 7.7834e−10, as calculated by STAMP [27]) the canonical ESRRA motif. In addition to the *de novo* prediction, we also used the same collection

ChIP-Seq PGC-1α peaks across the genome. Transcription start site (TSS) and transcription end site (TES) are relative to mm9 RefSeq transcripts. "Intergenic," ≥10 kb from the nearest transcript; "Upstream of TSS," kb −10 to 0 relative to the TSS; "Downstream of TES," kb 0 to +10 relative to the TES. Numbers in parentheses indicate, for each category, the ratio between the percentage of PGC-1α peaks and the percentage of the same number of randomly distributed peaks. (D) Histogram illustrating the number of direct and indirect genes either up- or downregulated by overexpression of PGC-1α in muscle cells. Direct genes are those associated with promoters found within ±10 kb relative to the nearest peak. (E) Distribution of the distances of 532 peaks from their associated upregulated gene promoters. (F) Distribution of the distances of 43 peaks from their associated downregulated gene promoters. (G and H) Subset of the top significantly enriched GO Biological Process terms identified for directly and indirectly upregulated (G) and downregulated (H) PGC-1α target genes.

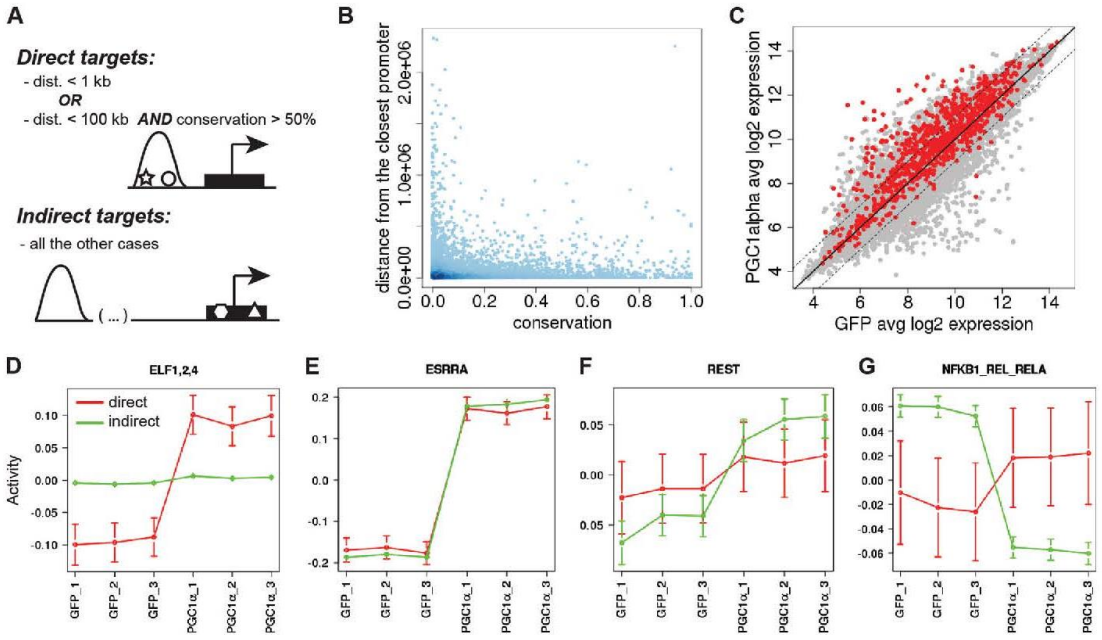

FIG 2 Four distinct mechanistic modes of action for gene expression regulated by PGC-1α and TF partners. (A) Classification of direct and indirect target genes in MARA (see Materials and Methods). (B) Distribution of peak distance from the closest promoter and PhastCons conservation score of the peak. (C) Distribution of $\log_2$ expression values for all mouse promoters. Expression values were averaged across the 3 GFP and the 3 PGC-1α samples. Direct targets are depicted in red; indirect targets are depicted in gray. (D to G) Activity plot of the motifs ELF1,2,4 (D), ESRRA (E), REST (F), and NFKB1_REL_RELA (G) as predicted by MARA (motif activity response analysis). Red, direct targets; green, indirect targets.

of 190 mammalian regulatory motifs used by MARA (19) to check which known TF DNA-binding motifs were significantly overrepresented in the PGC-1α peaks relative to a set of background regions. Many of the most significantly enriched motifs represent variations of nuclear receptor binding sequences that are based on the "AG$^{T}/_{G}$TCA" core hexamer and occur either alone or in direct, inverted, or everted repeats with variable spacing (Fig. 3B). Of these, the most significantly enriched motif was ESRRA, which is present in ~20% of all peaks. Moreover, among all genes with at least one associated binding peak within 10 kb, ~28% are associated with a peak containing a predicted ERRα site. Interestingly, besides the nuclear receptor motifs, we also found the DNA-binding element of the insulator protein CCCTC-binding factor (CTCF), and a set of highly similar DNA elements sharing the FOS-JUN-like recognition sequence "TGA(G/C)TCA" was bound by the TFs BACH2, FOS, FOSB, FOSL1, JUN, JUNB, JUND, FOSL2, NFE2, and NFE2L2 among the top 15 motifs enriched in PGC-1α peaks (Fig. 3B).

The identity of the exact nuclear receptor binding partner that is bound at each peak is difficult to deduce from DNA-binding motifs, since considerable promiscuity exists between receptors and DNA-binding elements in different configurations of hexameric repeats (34). Moreover, non-nuclear receptor-like TFs are less well studied in the context of PGC-1α-controlled gene expression. Thus, to identify which regulatory motifs are most overrepresented among peaks that do not contain nuclear receptor-like sites, we first manually grouped all of the motifs with a sequence logo very similar to that of ESRRA. Next, we discarded all peaks that had one or more predicted TFBSs for any of the motifs in this set. With the remaining 3,856 DNA sequences (51.33% of the peaks), we then again assessed the overrepresentation of each of the 190 mammalian regulatory motifs. In this analysis, "TGA(G/C)TCA" recognition elements, hence, FOS-JUN-like motifs, were the most significantly enriched among these peaks (Fig. 3C). This result suggests that PGC-1α peaks naturally fall into two classes: those containing ESRRA-like sites and those containing sites for FOS-JUN-like motifs.

We then constructed a matrix N, whose elements N_{pm} contain the number of predicted TFBSs for each motif m in each peak region p. We then performed principal component analysis (PCA) on this site-count matrix to identify linear combinations of regulatory motifs that explain most of the variation in site-counts across the PGC-1α peaks. The first two components (out of 190 in total) clearly proved to be the most relevant ones, accounting for 10% and 9.6% of the total variation in our data set, respectively (Fig. 3D). Figure 3E shows the projection of all motifs on these first two principal components, with the names of the motifs with the largest projections indicated in the figure. Whereas most motifs have projections close to zero along the first component, there is one group of motifs with strong negative projections (ESRRA, NR1H4, NR5A1,2, and NR6A1) and one group of motifs with strong positive projections [BACH2, FOS_FOS(B,L1)_JUN(B,D), FOSL2, NFE2, NFE2L1, and NFE2L2]. These two sets of sites correspond precisely to the two classes of motifs identified above,

A

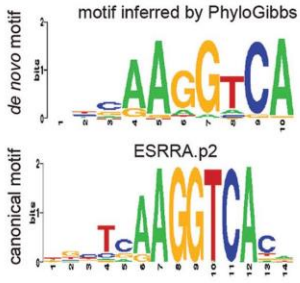

B

Motif name	Z score	TFBSs count	Peaks percentage	Genes in the associated peaks
ESRRA	96.95	1709	19.76%	461 (28.47%)
BACH2	81.74	1300	16.01%	286 (17.67%)
NR5A1,2	80.48	2007	22.58%	522 (32.24%)
NR6A1	72.63	767	8.24%	200 (12.35%)
FOS_FOS{B,L1}_JUN{B,D}	69.89	2030	19.18%	341 (21.06%)
FOSL2	68.06	1360	16.05%	308 (19.02%)
NFE2	62.78	1006	12.15%	229 (14.14%)
NFE2L2	56.66	697	8.53%	174 (10.75%)
HNF4A_NR2F1,2	47.20	766	9.15%	209 (12.91%)
CTCF	47.10	188	2.46%	73 (4.51%)
PPARG	40.61	389	4.30%	101 (6.24%)
REST	40.00	98	0.71%	15 (0.93%)
NR1H4	38.91	586	7.08%	156 (9.64%)
RXRA_VDR{dimer}	35.02	364	4.26%	100 (6.18%)
RREB1	34.23	180	1.78%	42 (2.59%)

C

Motif name	Z score	TFBSs count	Peaks percentage
BACH2	59.05	712	16.96%
FOS_FOS{B,L1}_JUN{B,D}	51.92	1125	20.18%
FOSL2	49.84	724	16.55%
NFE2	46.72	548	12.76%
NFE2L2	39.79	372	8.84%
REST	35.42	71	0.93%
CTCF	33.65	97	2.46%
CDX1,2,4	27.37	218	4.59%
MZF1	23.94	228	4.95%
RREB1	22.80	108	2.02%
SPI1	21.90	218	5.50%
BPTF	21.88	278	4.80%
GTF2I	21.17	228	4.95%
PATZ1	20.97	162	3.92%
FOX{I1,J2}	20.47	211	4.33%

D

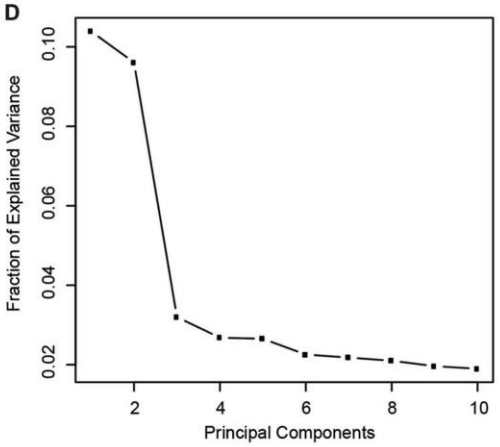

E

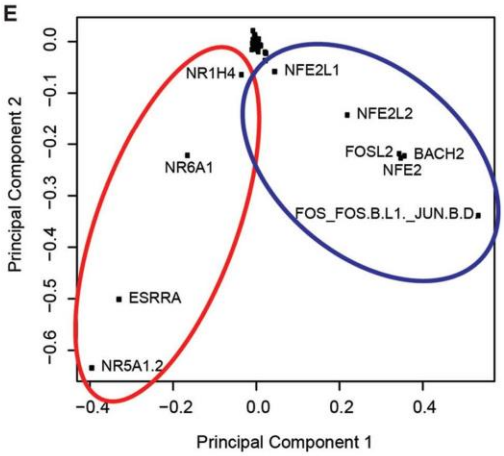

F

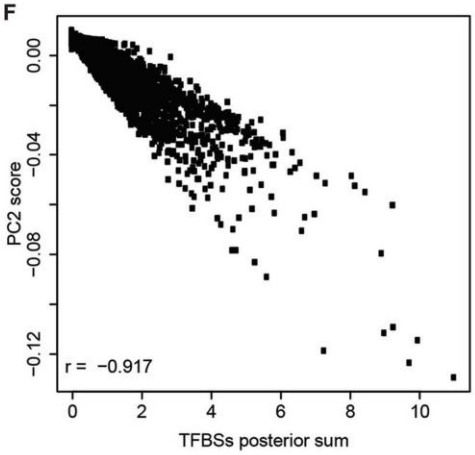

FIG 3 PCA reveals FOS-JUN-like leucine zippers as a new class of putative functional PGC-1α partners. (A) Sequence logo of the top position weight matrix discovered *de novo* by PhyloGibbs in the top 200 scoring peaks and of the corresponding canonical motif of ERRα as predicted by STAMP. (B) Top-scoring results of motif search performed on all 7,512 PGC-1α peaks with MotEvo. Motifs depicted in red and blue correspond to the clusters identified by PCA in panel D. (C) Top-scoring results of motif search performed on the 3,656 "non-ESRRA-like" peaks with MotEvo. (D) Fraction of explained variance of the top 10 PCA components. (E) PCA of the 7,512 PGC-1α peaks. Eigenmotif scores across principal component 1 (PC1) and principal component 2 (PC2) are shown. Red and blue ellipses highlight motif clusters, as identified by PC1, of nuclear hormone receptor-like zinc finger and FOS-JUN-like leucine zipper proteins, respectively. (F) Correlation between principal component 2 scores and binding site posterior sum for each peak relative to the top 10 PCA motifs. "r" refers to the Pearson correlation coefficient.

TABLE 1 Global summary of all analyses performed on PGC-1α peaks[f]

Motif name	PCA[a]	Overrepresentation in[b]: All PGC-1α peaks	Overrepresentation in[b]: "Non ESRRA-like" peaks	MARA activity Z score[c]: Direct	MARA activity Z score[c]: Indirect	Log_2 FC in expression array[d]	Absolute expression in PGC-1α sample[e]	Final ranking
ESRRA	Yes	1	182	6.04 (14.78)	15.49 (37.94)	2.31	1,829.45	6
FOS_FOS(B,L1)_JUN(B,D)	**Yes**	**5**	**2**	0.88 (2.14)	1.81 (−4.34)	**1.78**	**1,508.85**	**5**
ZNF143		**27**	**28**	**2.48 (6.05)**	**4.65 (9.68)**	0.38	**384.36**	**5**
BPTF		21	12	1.38 (3.37)	2.56 (−6.25)	−0.56	333.34	4
ESR1		17	50	2.33 (5.69)	4.53 (11.04)	−0.47	232.42	4
FOSL2	Yes	6	3	0.88 (2.14)	1.51 (3.65)	−0.98	717.09	4
GTF2I		34	**13**	**2.09 (5.10)**	**2.38 (−5.80)**	−0.55	**1,207.81**	**4**
NFE2L2	**Yes**	**8**	**5**	0.57 (1.38)	1.01 (−2.37)	−0.38	**3,673.63**	**4**
NFY(A,B,C)		96	116	**2.37 (5.80)**	**3.56 (7.62)**	**1.07**	**2,409.48**	**4**
NR5A1,2	Yes	3	188	3.53 (8.66)	7.73 (17.00)	−0.08	80.97	4
REST		12	6	0.48 (1.15)	2.41 (5.70)	−0.89	328.04	4
RREB1		15	10	1.56 (3.82)	2.39 (−5.42)	0.05	678.44	4
SP1		24	22	3.99 (9.76)	0.61 (0.33)	−0.32	751.98	4
STAT2,4,6		29	23	0.35 (0.52)	4.81 (−9.67)	−2.72	380.12	4
TLX1.3_NFIC (dimer)		19	17	0.84 (−2.05)	4.91 (−11.97)	−0.34	2,339.33	4

[a] Requirement for PCA: being among the top 10 motifs contributing most to PC1 and PC2.
[b] Requirement for motif overrepresentation: being among the top 30 significant motifs; ranking position shown.
[c] Requirement for MARA: having a Z score of ≥2.0. Numbers in parentheses show the difference between the PGC-1α state and the GFP state, representing the direction in which the motif activity changes following PGC-1α overexpression.
[d] Requirement for the expression array (i): having a log_2 fold change value of ≥1.0 (corresponding to 2-fold upregulation).
[e] Requirement for the expression array (ii): having an absolute expression in the PGC-1α sample of ≥100.
[f] The final score is the count of all analyses where a certain motif passed the defined cutoffs. The motifs chosen for validation and their corresponding values which satisfied the cutoffs are shown in bold.

confirming that the most significant variation in TFBSs across PGC-1α peaks is caused by the occurrence of either ESRRA-like motifs or FOS-JUN-like motifs. Most interestingly, these two clusters of motifs reflect structurally distinct classes of TFs; the negatively scoring eigenmotifs are characterized by binding of nuclear receptor-type zinc finger domains, while the eigenmotifs with a positive score correspond to activator protein 1 (AP-1)-like leucine zipper domains.

The second principal component corresponds to the strength of the binding signal for these 10 motifs, as confirmed by the robust negative correlation ($r = -0.92$) between the TFBS posterior sum per peak and the peak's projection along the second principal component (Fig. 3F).

Validation of top-scoring motifs reveals novel functional partners of PGC-1α. Our analysis identified a number of so-far-uncharacterized TFs as potentially functional partners for PGC-1α-controlled gene expression in skeletal muscle cells. In order to experimentally validate some of these candidates, we sorted all TFs by a number of criteria, including TFBS overrepresentation in binding peaks, MARA activity upon PGC-1α overexpression, and the expression pattern of the TFs themselves. Table 1 shows the top 15 ranked TFs according to this selection. As expected, the well-known PGC-1α partner ERRα was identified as the most important factor. For our validation experiments, we chose the next two motifs [FOS_FOS(B,L1)_JUN(B,D) and ZNF143, which is also known as ZFP143] as well as three motifs from further down the list of the top 15 motifs (GTF2I, NFE2L2, and NFYC).

FOS, the most upregulated TF (log_2 fold change = 1.78) among the TFs associated with the motif FOS_FOS(B,L1)_JUN(B,D), is a basic leucine zipper transcription factor known to heterodimerize with other leucine zipper proteins in order to form the AP-1 complex (35). The AP-1 complex furthermore contains JUN as well as ATF proteins. Thus, to dissect the function of the AP-1 protein complex, we also included JUN and ATF3, the most highly expressed isoforms of their respective protein families in muscle cells.

For each of these 7 TFs (ATF3, FOS, GTF2I, JUN, NFE2L2, NFYC, and ZFP143), we selected a dozen target genes based on the chi-square score of the MARA prediction, the presence of a PGC-1α binding peak with at least one predicted binding site for the factor of interest, and the presence of at least a 2-fold induction upon overexpression of PGC-1α. As summarized in Fig. 4 and Fig. S3 in the supplemental material, siRNA-based knockdown of all TFs resulted in a robust reduction of the target mRNAs from −40% to −75%. With the exception of NFYC and JUN, we found that the large majority of predicted target genes were downregulated upon knockdown of the factor, confirming our predictions (Fig. 4). The most consistent effects were observed for FOS and ZFP143 (all targets downregulated), followed by GTF2I (11 out of 12 downregulated) and NFE2L2 and ATF3 (10 out of 12 downregulated). Interestingly, distinct target genes of the AP-1 complex showed differential responsiveness to knockdown of the three AP-1 complex components FOS, JUN, and ATF3 (Fig. 4B, C, and D). Similarly, PGC-1α-mediated induction of a majority of the predicted target genes for NFE2L2 (Fig. 4E), ZFP143 (Fig. 4F), and GTF2I (Fig. 4G) was reduced upon knockdown of the respective TF compared to the expression in cells with overexpressed PGC-1α and a scrambled siRNA control. Surprisingly, only 1 of the 11 predicted target genes for NFYC that have been chosen for validation was significantly repressed by siRNA-induced reduction of this TF (Fig. 4H), suggesting that other TFs may be involved in mediating the regulatory effects of the NFYC regulatory motif.

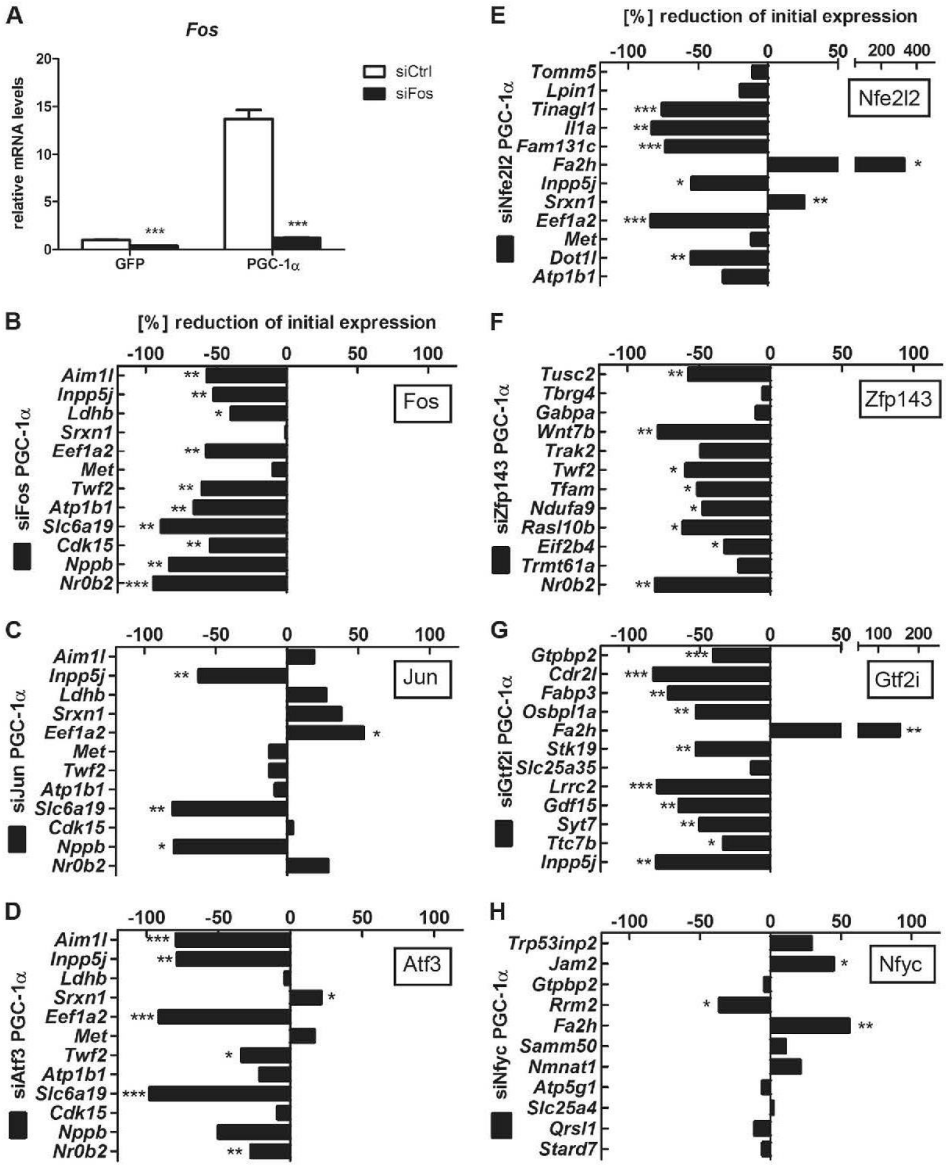

FIG 4 Validation of TFs associated with top-scoring motifs reveals novel functional PGC-1α partners. (A) siRNA-mediated knockdown efficiency for FOS. Bars represent fold induction over GFP/siCtrl value; error bars represent SEMs. *, $P < 0.05$; **, $P < 0.01$; ***, $P < 0.001$. See also Fig. S3 in the supplemental material. (B to H) Quantitative real-time PCR analysis of PGC-1α target genes whose associated peak contains at least one binding site for the motif FOS_FOS(B,L1)_JUN(B,D) (B to D), NFE2L2 (E), ZNF143, also known as ZFP143 (F), GTF2I (G), or NFY(A,B,C) (H). Bars represent % change compared to PGC-1α/siCtrl values. Error bars represent SEMs. *, $P < 0.05$; **, $P < 0.01$; ***, $P < 0.001$.

Functional interaction between PGC-1α and different compositions of the AP-1 protein complex. Our targeted validation strategy revealed that PGC-1α target genes predicted to be regulated by the FOS-JUN-like motif react in distinct manners to siRNA-mediated knockdown of individual components of the AP-1 transcription factor protein complex. For example, some genes reacted only to reduction of FOS (Fig. 5A), while others were responsive to the knockdown of two (Fig. 5B) or even all

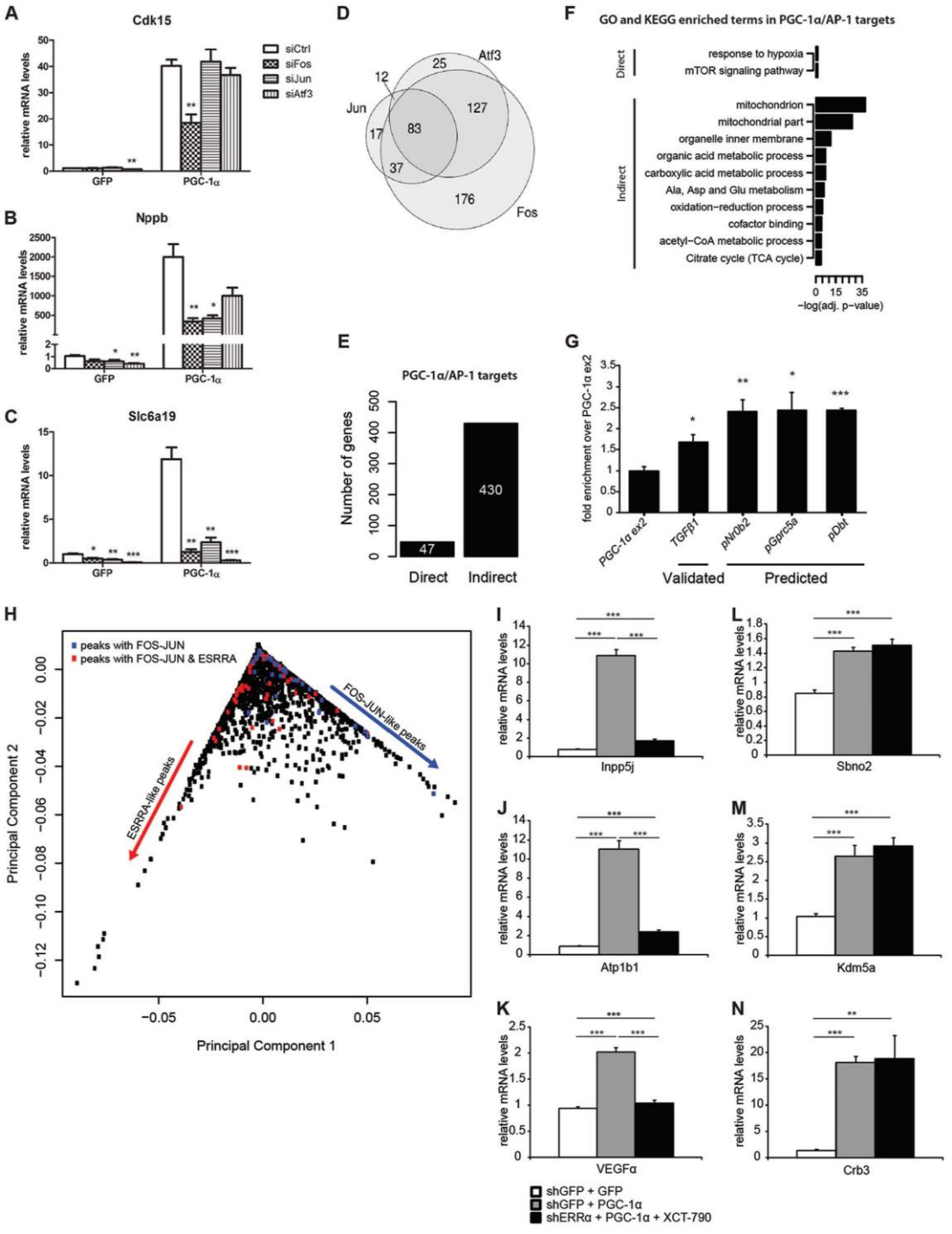
A
Cdk15
relative mRNA levels
siCtrl
siFos
siJun
siAtf3
GFP
PGC-1α
B
Nppb
C
Slc6a19
D
Atf3
Jun
Fos
25
12
127
17
83
37
176
E
PGC-1α/AP-1 targets
Number of genes
47
430
Direct
Indirect
F
GO and KEGG enriched terms in PGC-1α/AP-1 targets
Direct
response to hypoxia
mTOR signaling pathway
Indirect
mitochondrion
mitochondrial part
organelle inner membrane
organic acid metabolic process
carboxylic acid metabolic process
Ala, Asp and Glu metabolism
oxidation−reduction process
cofactor binding
acetyl−CoA metabolic process
Citrate cycle (TCA cycle)
−log(adj. p−value)
G
fold enrichment over PGC-1α ex2
PGC-1α ex2
TGFβ1
pNr0b2
pGprc5a
pDbt
Validated
Predicted
H
peaks with FOS-JUN
peaks with FOS-JUN & ESRRA
ESRRA-like peaks
FOS-JUN-like peaks
Principal Component 2
Principal Component 1
I
Inpp5j
L
Sbno2
J
Atp1b1
M
Kdm5a
K
VEGFα
N
Crb3
shGFP + GFP
shGFP + PGC-1α
shERRα + PGC-1α + XCT-790

three (Fig. 5C) AP-1 protein partners that we have tested using the siRNA-based approach. To further dissect the responsiveness of PGC-1α target genes to different AP-1 protein complexes, we performed global gene expression arrays upon knockdown of each of the three TF components of the AP-1 complex. Figure 5D depicts the number of genes that were induced by PGC-1α and that were, at the same time, downregulated by the siRNA knockdown of any of the three AP-1 complex members. Among a total of 477 genes, 89% responded to FOS knockdown, 52% to ATF3 knockdown, and 31% to JUN knockdown. Moreover, while 37% of all targets responded exclusively to FOS, the fraction of targets responding exclusively to either JUN or ATF3 was at most 5%. This analysis shows that, whereas different target genes respond differently to the knockdown of distinct AP-1 components, FOS is the dominant factor in determining AP-1 function under these conditions.

As shown in Fig. 3B, 341 genes were associated with a PGC-1α binding peak containing a predicted site for the FOS-JUN-like motif bound by the AP-1 complex. Of these genes, the expression of 55 was significantly induced by PGC-1α overexpression in muscle cells. In our siRNA-based validation experiment, we found that 47 out of these 55 PGC-1α-induced/AP-1 predicted targets were significantly downregulated by knockdown of the AP-1 complex components, and we called these genes "direct PGC-1α/AP-1 targets." The remaining 430 genes out of 477 (Fig. 5D) were defined accordingly as "indirect PGC-1α/AP-1 targets" that lack a PGC-1α peak containing a FOS-JUN-like motif but still are regulated by PGC-1α and the AP-1 protein components (Fig. 5E). To reveal whether these gene categories exert distinct functions, GO and KEGG enrichment analyses were performed. Surprisingly, the 47 direct PGC-1α/AP-1 target genes showed a distinct and significant overrepresentation of the terms "response to hypoxia" (GO ID, 0001666; adjusted *P* value, 0.0247542) and "mTOR signaling pathway" (KEGG ID, mmu04150; adjusted *P* value, 0.030674) that were absent in the GO analysis of the remaining PGC-1α/AP-1 targets (Fig. 5F). Recruitment of FOS to the same regulatory regions as PGC-1α in the direct AP-1/PGC-1α target genes was subsequently validated by ChIP (Fig. 5G). These results suggest that AP-1, when interacting with PGC-1α, drives a synergic effect of response to hypoxia; on the other hand, when AP-1 and PGC-1α act separately and, furthermore, through downstream intermediate TFs, they regulate the expression of genes involved in mitochondrial organization and energy metabolism.

Intriguingly, several of the predicted AP-1/PGC-1α target genes are also under the control of PGC-1α working with other transcription factors. For example, the vascular endothelial growth factor (VEGF) or, based on the gene expression arrays, 8 OXPHOS genes seem likewise to be under the control of AP-1 as well as ERRα in the context of elevated PGC-1α in skeletal muscle (31, 36). We therefore assessed the predicted and experimental overlap of these two transcription factors in the regulation of AP-1/PGC-1α target genes. Interestingly, when the PCA of the PGC-1α peaks was stratified in terms of eigenpeaks, we observed two distinct groups of peaks associated with AP-1/PGC-1α target genes (Fig. 5H). First, some of these genes exclusively harbored peaks with FOS-JUN-like TFBSs, whereas the second group exhibited either peaks with both FOS-JUN- and ESRRA-like TFBSs or a combination of distinct peaks with either of these sites within 10 kb from their promoters (Fig. 5H). Next, we validated this prediction by investigating the change in expression of different AP-1/PGC-1α target genes in the context of reduced ERRα expression and function, elicited by a combination of shRNA-mediated knockdown and pharmacological treatment of muscle cells with the ERRα inverse agonist XCT-790 (31). In line with the PCA, two distinct groups of ERRα inhibition-sensitive (Fig. 5I to K) and -insensitive (Fig. 5L to N) AP-1/PGC-1α target genes were found.

Finally, since all of the experiments were performed in differentiated myotubes in culture, we assessed whether similar gene expression changes of the direct AP-1/PGC-1α targets involved in hypoxic gene regulation are also observed in skeletal muscle tissue of different gain-of-function (6) and loss-of-function (7, 8) mouse models *in vivo*. In skeletal muscle-specific PGC-1α knockout mice, the expression of several of these genes was reduced significantly (Fig. 6A to F). Surprisingly, however, some of the predicted transcripts were not altered in this loss-of-function model for PGC-1α, for example, Nr0b2 (Fig. 6E). To further clarify the role of PGC-1α in the regulation of these genes, relative transcript levels were next assessed in muscle-specific transgenic mice for PGC-1α (Fig. 6G to L). In most cases, the genes with a reduction in their transcription in the PGC-1α muscle-specific knockout animals were inversely elevated in the PGC-1α muscle-specific transgenic mice. Moreover, some of these genes were likewise induced by exercise (Fig. 6G to L), and at least in some cases, for example, Twf2 and Nr0b2 (Fig. 6J and K), PGC-1α overexpression and physical activity synergistically boosted gene expression; for Nr0b2, this occurred even in the absence of any effect of the muscle-specific PGC-1α transgene *per se* (Fig. 6K).

FIG 5 PGC-1α controls the hypoxia gene program via a functional interaction with different configurations of the AP-1 protein complex. (A to C) Quantitative real-time PCR analysis of *Cdk15* (A), *Nppb* (B), and *Slc6a19* (C) mRNA levels in response to PGC-1α overexpression and either siFos, siJun, or siAtf3 knockdown. Data are normalized to mRNA levels in GFP adenovirus-infected cells. Error bars represent ±SEMs. *, $P < 0.05$; **, $P < 0.01$; ***, $P < 0.001$. (D) Venn diagram illustrating the overlap in number of genes upregulated by PGC-1α and downregulated by either FOS, JUN, or ATF3 knockdown. (E) Histogram illustrating the number of direct and indirect PGC-1α/AP-1 target genes. (F) Subset of the top significantly enriched Gene Ontology and KEGG terms identified for the two gene groups illustrated in panel E. TCA, tricarboxylic acid. (G) Quantitative real-time PCR validation of the ChIP enrichment of c-Fos measured at the gene *TGFβ1* (validated) and at the promoters of *Nr0b2*, *Gprc5a*, and *Dbt* (predicted) target genes. Bars represent fold enrichment over PGC-1α exon 2 set as 1. Error bars represent SEMs. *, $P < 0.05$; **, $P < 0.01$; ***, $P < 0.001$. (H) PCA of the 7,512 PGC-1α peaks. Eigenpeak scores across principal component 1 and principal component 2 are shown. Colored dots correspond to peaks associated to the 47 direct PGC-1α/AP-1 targets. Blue dots refer to genes associated with peaks containing only FOS-JUN TFBSs, while red dots refer to genes associated with peaks with FOS-JUN and ESRRA TFBSs, located either in the same peak or in distinct PGC-1α peaks. (I to K) Quantitative real-time PCR analysis of PGC-1α/AP-1 targets whose associated peaks contain an ESRRA binding site. The bars represent relative mRNA levels compared to AV-shGFP plus AV-GFP plus vehicle, which is set as 1. The error bars represent SEMs. *, $P < 0.05$; **, $P < 0.01$; ***, $P < 0.001$. (L to N) Quantitative real-time PCR analysis of PGC-1α/AP-1 targets whose associated peaks (if any) do not contain an ESRRA binding site. The bars represent relative mRNA levels compared to AV-shGFP plus AV-GFP plus vehicle, which is set as 1. The error bars represent SEMs. *, $P < 0.05$; **, $P < 0.01$; ***, $P < 0.001$.

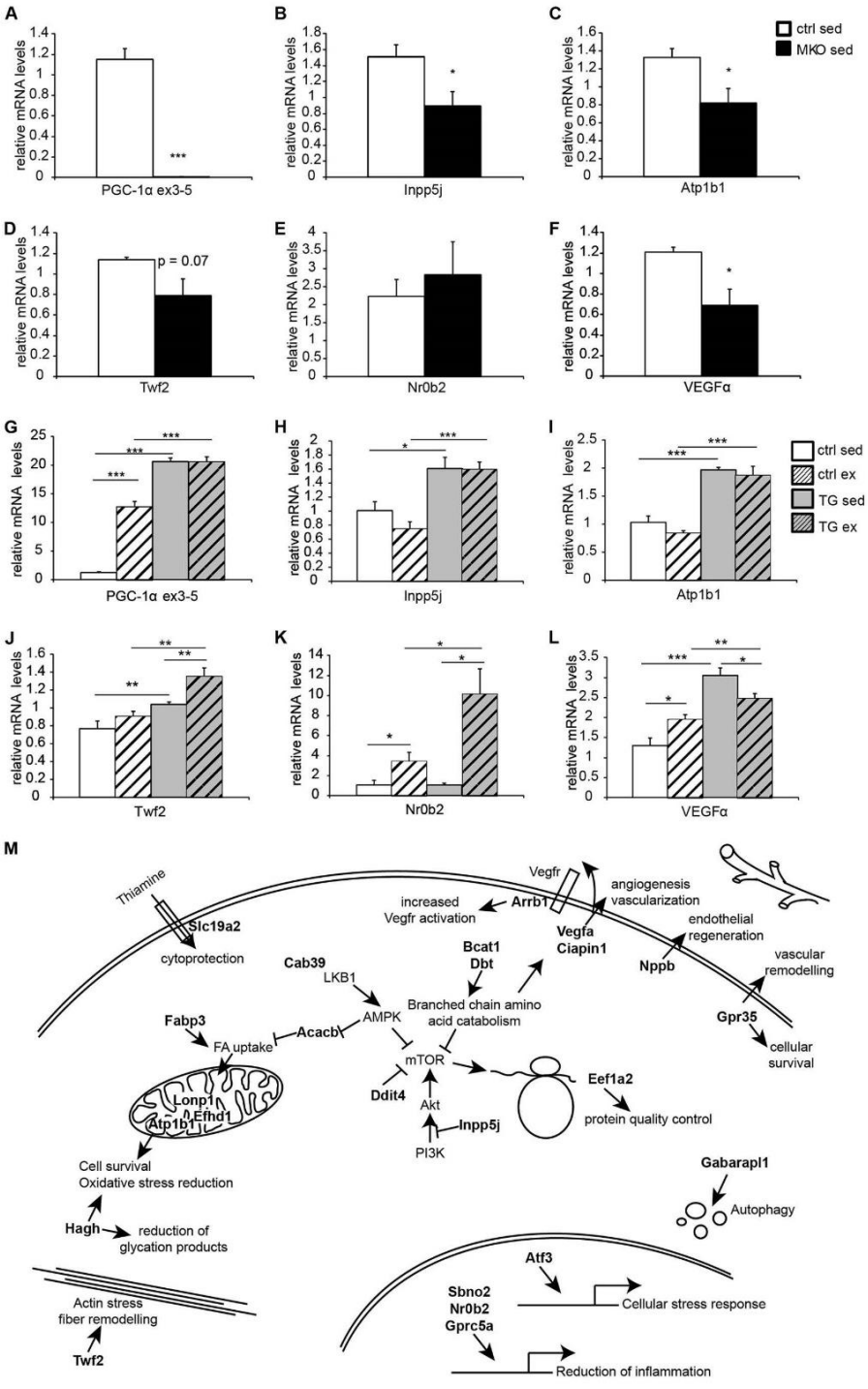
A
B
C
D
E
F
G
H
I
J
K
L
M
relative mRNA levels
PGC-1α ex3-5
Inpp5j
Atp1b1
Twf2
Nr0b2
VEGFα
ctrl sed
MKO sed
ctrl ex
TG sed
TG ex
p = 0.07
Thiamine
Slc19a2
cytoprotection
Vegfr
angiogenesis
vascularization
increased
Vegfr activation
Arrb1
Vegfa
Ciapin1
endothelial
regeneration
Nppb
vascular
remodelling
Cab39
LKB1
Bcat1
Dbt
Branched chain amino
acid catabolism
AMPK
Acacb
Fabp3
FA uptake
mTOR
Gpr35
cellular
survival
Ddit4
Akt
Eef1a2
protein quality control
Lonp1
Efhd1
Atp1b1
Inpp5j
PI3K
Cell survival
Oxidative stress reduction
Hagh
reduction of
glycation products
Gabarapl1
Autophagy
Atf3
Sbno2
Nr0b2
Gprc5a
Cellular stress response
Reduction of inflammation
Actin stress
fiber remodelling
Twf2

DISCUSSION

Exercise-induced skeletal muscle cell plasticity is a highly complex biological program that involves the remodeling of a number of fundamental cellular properties. Since PGC-1α function has been strongly linked to the induction of an endurance-trained muscle phenotype, we here dissected the PGC-1α-controlled transcriptional network in muscle cells. First, our results reveal a broad recruitment of PGC-1α to many different sites in the mouse genome (7,512 peaks), the majority of which were either not located within 10 kb from a promoter or close to a gene that was not regulated by PGC-1α overexpression at the time of harvest of the cells, as has analogously been observed in many other ChIP-Seq experiments (for example, see reference 37). Apart from the fact that PGC-1α could mediate long-range enhancer effects that were excluded in our peak-gene assignment, it is conceivable that PGC-1α recruitment is transcriptionally silent in some binding peaks because it requires the recruitment of additional cofactors for activation, which are not present under the conditions or in the cell type in which our experiments were performed. In addition, it is possible that a large fraction of PGC-1α binding peaks are "neutral" in the sense of not having any direct role in regulating gene expression.

Second, while an almost equally strong effect of PGC-1α on gene induction and repression has been reported (31), our analysis now indicates that direct PGC-1α-mediated gene expression is restricted almost exclusively to positively regulated PGC-1α target genes, whereas the vast majority of gene repression is indirect, i.e., not associated with PGC-1α recruitment within a 10-kb distance to the genes' promoters. Thus, the fact that almost 95% of all repressed genes were not linked to PGC-1α recruitment strongly implies that this coregulator primarily acts as a coactivator, and not as a corepressor, as suggested by the data of some studies (38–40). Importantly, indirect repression of PGC-1α target genes was also supported by the MARA prediction. The strong indirect inhibition of genes, many of which are involved in inflammatory processes, is predicted by MARA to be mediated by TFs such as NF-κB and interferon regulatory factor (IRF). Such an indirect inhibition of NF-κB and proinflammatory genes by PGC-1α in muscle cells has been reported previously (33).

One of the main functions of PGC-1α in all cells and organs is to boost mitochondrial gene transcription and oxidative metabolism. Accordingly, we observed that Gene Ontology terms related to these pathways were highly enriched when analyzing positively regulated PGC-1α target genes in muscle cells. Based on previous studies, the regulation of this core function could have been assigned to the direct interaction of PGC-1α and ERRα binding to regulatory elements of these genes (31, 32). Surprisingly, our data indicate that many of the genes that are involved in oxidative metabolic pathways are indirectly controlled by PGC-1α and, hence, do not require PGC-1α recruitment to enhancer and promoter elements. Likewise unexpectedly, the MARA implies ERRα action on direct and indirect PGC-1α-induced target genes, i.e., in the presence or absence of PGC-1α coactivation. Thus, while these observations might obviously reflect a temporally distinct control of different PGC-1α target genes that is not represented in our simultaneous analysis of DNA binding and gene expression at one time point, it is conceivable that PGC-1α acts primarily as an upstream regulator of other factors that are subsequently controlling more downstream PGC-1α target genes without direct involvement of PGC-1α itself.

In skeletal muscle, PGC-1α has been reported to interact with ERRs, peroxisome proliferator-activated receptors (PPARs), and other nuclear receptors, as well as myocyte enhancer and nuclear respiratory factors, to mediate transcriptional regulation (3). Accordingly, ERRα and other nuclear receptor binding motifs were among the most highly significant binding elements in our present report. Importantly, however, we also predict a number of so-far unknown TFs to functionally interact with PGC-1α and thereby contribute to PGC-1α-controlled gene expression in skeletal muscle. Since a complete functional validation of all new putative TF partners is beyond the scope of this paper, we combined the high-throughput results with several computational analyses (Table 1) to select and test some of the potentially most important factors together with predicted target genes. Notably, in siRNA-based knockdown experiments, we could show that depletion of FOS and its putative AP-1 multimerization partners JUN and ATF3 as well as NFE2L2, ZFP143, and GTF2I in muscle cells reduced the ability of PGC-1α to positively regulate target genes. Second, we could provide evidence of a corecruitment of FOS and PGC-1α to the same regulatory sites in the vicinity of AP-1/PGC-1α target genes, confirming a functional interaction between these TFs and PGC-1α. Thus, our results indicate that the coactivation repertoire of PGC-1α in muscle exceeds the prediction of previous studies by far. For example, even in our list of the top 15 motifs, several predicted TFs have not yet been investigated in the context of PGC-1α-controlled gene expression, including BPTF, FOSL2, REST, or RREB1. Future studies will aim at a more detailed dissection of the global functional consequences of PGC-1α coactivation of these TFs in muscle cells.

Curiously, almost all of our analyses, and in particular the principal component analysis, highlighted the relevance of FOS-JUN-like motifs. In fact, the largest amount of variation in TFBS occurrence within PGC-1α binding peaks results from either ESRRA-like or FOS-JUN-like motifs. The FOS-JUN-like motif, in particular, embodies the main binding elements of the AP-1 complex, which consist of different configurations of FOS, JUN, ATF, and MAF proteins (35, 41). Our data comparing gene expression in cells with reduced FOS, JUN, and ATF3 levels indicate that PGC-1α functionally interacts with the AP-1 complex in different configurations in the regulation of specific genes. The differential requirement observed for distinct AP-1 components might provide an additional layer of control for specific PGC-1α target gene regulation.

AP-1 function itself is regulated by a variety of stimuli, includ-

FIG 6 PGC-1α controls the hypoxic gene program in muscle *in vivo*. (A to F) Quantitative real-time PCR analysis of hypoxic genes in sedentary control (ctrl) and muscle-specific knockout (MKO) mice. The control group is set as 1. Error bars represent SEMs. *, $P < 0.05$; **, $P < 0.01$; ***, $P < 0.001$. (G to L) Quantitative real-time PCR analysis of hypoxic genes in treadmill-running mice. Control (ctrl) and muscle-specific transgenic (TG) mice were used under sedentary and exercise conditions. The control group under sedentary conditions is set as 1. Error bars represent SEMs. *, $P < 0.05$; **, $P < 0.01$; ***, $P < 0.001$. (M) Schematic representation depicting the downstream effects of the functional interaction between PGC-1α and the AP-1 complex in the context of the hypoxia gene program. Direct targets of PGC-1α and AP-1 are indicated in bold.

ing cytokines, growth factors, and stress, and subsequently controls a number of cellular processes, including apoptosis, cell proliferation and differentiation, stress response, and hypoxia (41, 42). Mechanistically, we classified PGC-1α-induced/AP-1-knockdown targets in either direct or indirect genes. Most interestingly, functional analysis of these two groups of genes revealed that when AP-1 and PGC-1α act disjointedly, they are involved in the regulation of mitochondrial and other metabolic genes, while when coactivated by PGC-1α, AP-1 distinctly alters the expression of genes that are enriched in the ontology terms "response to hypoxia" and "mTOR signaling" (Fig. 5F). Intriguingly, a closer analysis of all 47 direct AP-1/PGC-1α target genes revealed 24 genes that are induced by hypoxia, are effectors of hypoxia, or attenuate the detrimental consequences of hypoxia (Fig. 6M). For example, several inhibitors of the mTOR signaling pathways are included in this group of genes, and hypoxia has been described as a suppressor of mTORC1 activity (43). Another group of genes contributes to the reduction of cellular stress, detrimental metabolites, and reactive oxygen species and an increase in cellular survival to reduce potential harmful consequences of prolonged hypoxia (44). Furthermore, several genes promote endothelial regeneration, vascular remodeling, and vascularization (45). In this context, PGC-1α has previously been shown to promote VEGF-induced angiogenesis in skeletal muscle in a hypoxia-inducible factor 1α (HIF-1α)-independent, ERRα-dependent manner (36). Similarly, PGC-1α regulates the hypoxic response of brown fat (46) and neuronal and endothelial cells (47), even though the mechanisms of cellular protection exerted by PGC-1α in these experimental contexts have not been elucidated. Our findings now indicate that, to ensure adequate oxygen and nutrient supplies for oxidative metabolism in skeletal muscle cells, PGC-1α might coordinate metabolic needs through ERRα-induced *Vegf* expression with a broad, stress-induced AP-1-dependent hypoxia program. Such a functional convergence was found for a subset of the direct AP-1/PGC-1α target genes that likewise seem to be under the control of ERRα together with PGC-1α (Fig. 5H and I to K). Inversely, for the complementary subset of these genes, the functional interaction between AP-1 and PGC-1α seems distinct from the ERRα-dependent PGC-1α target gene regulation. Finally, *in vivo* evidence supports our muscle cell culture-based prediction, considering that many of the AP-1/PGC-1α hypoxia-related target genes exhibit reduced and elevated transcript levels in PGC-1α muscle-specific knockout and transgenic animals, respectively. As previously demonstrated for VEGF and skeletal muscle vascularization (36), many aspects of the phenotypic consequences of exercise-induced muscle hypoxia occur in the muscle-specific transgenic mice even in the absence of physical activity. In an extension of these studies, we now, however, found additional genes involved in this process that show an additional, or in the case of Nr0b2, even an exclusive synergistic activation by exercise in the PGC-1α transgenic animals. Thus, combined with previous descriptions of muscle plasticity in these mice postexercise in regard to insulin sensitivity (29), our present findings reiterate the importance of bona fide exercise even in a genetic model for endurance training such as the PGC-1α muscle-specific transgenic animals.

In summary, our data provide a first insight into the transcriptional network controlled by PGC-1α in muscle cells. While one other study of global DNA recruitment of PGC-1α has been performed in the human hepatoma cell line HepG2 (48), our results highlight the importance of combining ChIP-Seq experiments and transcriptional data together with a comprehensive computational modeling approach and experimental validation of predicted key regulators, in order to be able to discover mechanistic as well as functional outcomes of such a network. Combined with the knowledge of transcriptional regulation, posttranslational modifications, alternative splicing, and recruitment of different chromatin remodeling protein complexes, a scenario can thus be conceived in which PGC-1α is able to control and integrate different signaling pathways using a multitude of different transcription factor binding partners (10, 11). A better understanding of such regulatory networks will eventually allow the targeting of whole biological programs or specific submodules in pathological states of dysregulation.

ACKNOWLEDGMENTS

We thank Anastasia Kralli, Svenia Schnyder, Gesa Santos, Kristoffer Svensson, and Markus Beer for reagents, help, and input in the preparation of the manuscript. We are grateful to the [BC]2 Basel Computational Biology Center for providing computational resources.

This project was funded by ERC Consolidator grant 616830-MUSCLE_NET to C.H., the Swiss National Science Foundation (31003A_135397 to E.V.N. and 310030_132900 to C.H.), SystemsX.ch (CellPlasticity, StoNets, and BrainstemX research projects to E.V.N.), the Swiss Society for Research on Muscle Diseases (SSEM), the Neuromuscular Research Association Basel (NeRAB), the Gebert-Rüf Foundation "Rare Diseases" Program, the University of Basel, and the Biozentrum. S.S. was supported by an IPhD fellowship of the SystemsX.ch Swiss Initiative in Systems Biology.

We have no conflict of interest in regard to this paper.

REFERENCES

1. Handschin C, Spiegelman BM. 2008. The role of exercise and PGC1alpha in inflammation and chronic disease. Nature 454:463–469. http://dx.doi.org/10.1038/nature07206.
2. Pedersen BK, Febbraio MA. 2012. Muscles, exercise and obesity: skeletal muscle as a secretory organ. Nat. Rev. Endocrinol. 8:457–465. http://dx.doi.org/10.1038/nrendo.2012.49.
3. Handschin C. 2010. Regulation of skeletal muscle cell plasticity by the peroxisome proliferator-activated receptor gamma coactivator 1alpha. J. Recept. Signal Transduct. Res. 30:376–384. http://dx.doi.org/10.3109/10799891003641074.
4. Handschin C, Spiegelman BM. 2006. Peroxisome proliferator-activated receptor gamma coactivator 1 coactivators, energy homeostasis, and metabolism. Endocr. Rev. 27:728–735. http://dx.doi.org/10.1210/er.2006-0037.
5. Finck BN, Kelly DP. 2006. PGC-1 coactivators: inducible regulators of energy metabolism in health and disease. J. Clin. Invest. 116:615–622. http://dx.doi.org/10.1172/JCI27794.
6. Lin J, Wu H, Tarr PT, Zhang CY, Wu Z, Boss O, Michael LF, Puigserver P, Isotani E, Olson EN, Lowell BB, Bassel-Duby R, Spiegelman BM. 2002. Transcriptional co-activator PGC-1 alpha drives the formation of slow-twitch muscle fibres. Nature 418:797–801. http://dx.doi.org/10.1038/nature00904.
7. Handschin C, Chin S, Li P, Liu F, Maratos-Flier E, Lebrasseur NK, Yan Z, Spiegelman BM. 2007. Skeletal muscle fiber-type switching, exercise intolerance, and myopathy in PGC-1alpha muscle-specific knock-out animals. J. Biol. Chem. 282:30014–30021. http://dx.doi.org/10.1074/jbc.M704817200.
8. Handschin C, Choi CS, Chin S, Kim S, Kawamori D, Kurpad AJ, Neubauer N, Hu J, Mootha VK, Kim YB, Kulkarni RN, Shulman GI, Spiegelman BM. 2007. Abnormal glucose homeostasis in skeletal muscle-specific PGC-1alpha knockout mice reveals skeletal muscle-pancreatic beta cell crosstalk. J. Clin. Invest. 117:3463–3474. http://dx.doi.org/10.1172/JCI31785.
9. Lonard DM, O'Malley BW. 2006. The expanding cosmos of nuclear receptor coactivators. Cell 125:411–414. http://dx.doi.org/10.1016/j.cell.2006.04.021.

10. Lonard DM, O'Malley BW. 2007. Nuclear receptor coregulators: judges, juries, and executioners of cellular regulation. Mol. Cell 27:691–700. http://dx.doi.org/10.1016/j.molcel.2007.08.012.
11. Spiegelman BM, Heinrich R. 2004. Biological control through regulated transcriptional coactivators. Cell 119:157–167. http://dx.doi.org/10.1016/j.cell.2004.09.037.
12. Puigserver P, Adelmant G, Wu Z, Fan M, Xu J, O'Malley B, Spiegelman BM. 1999. Activation of PPARgamma coactivator-1 through transcription factor docking. Science 286:1368–1371. http://dx.doi.org/10.1126/science.286.5443.1368.
13. Wallberg AE, Yamamura S, Malik S, Spiegelman BM, Roeder RG. 2003. Coordination of p300-mediated chromatin remodeling and TRAP/mediator function through coactivator PGC-1alpha. Mol. Cell 12:1137–1149. http://dx.doi.org/10.1016/S1097-2765(03)00391-5.
14. Li S, Liu C, Li N, Hao T, Han T, Hill DE, Vidal M, Lin JD. 2008. Genome-wide coactivation analysis of PGC-1alpha identifies BAF60a as a regulator of hepatic lipid metabolism. Cell Metab. 8:105–117. http://dx.doi.org/10.1016/j.cmet.2008.06.013.
15. Lin J, Handschin C, Spiegelman BM. 2005. Metabolic control through the PGC-1 family of transcription coactivators. Cell Metab. 1:361–370. http://dx.doi.org/10.1016/j.cmet.2005.05.004.
16. Handschin C. 2009. The biology of PGC-1alpha and its therapeutic potential. Trends Pharmacol. Sci. 30:322–329. http://dx.doi.org/10.1016/j.tips.2009.03.006.
17. Langmead B, Trapnell C, Pop M, Salzberg SL. 2009. Ultrafast and memory-efficient alignment of short DNA sequences to the human genome. Genome Biol. 10:R25. http://dx.doi.org/10.1186/gb-2009-10-3-r25.
18. Notredame C, Higgins DG, Heringa J. 2000. T-Coffee: a novel method for fast and accurate multiple sequence alignment. J. Mol. Biol. 302:205–217. http://dx.doi.org/10.1006/jmbi.2000.4042.
19. Perez-Schindler J, Summermatter S, Santos G, Zorzato F, Handschin C. 2013. The transcriptional coactivator PGC-1alpha is dispensable for chronic overload-induced skeletal muscle hypertrophy and metabolic remodeling. Proc. Natl. Acad. Sci. U. S. A. 110:20314–20319. http://dx.doi.org/10.1073/pnas.1312039110.
20. Arnold P, Erb I, Pachkov M, Molina N, van Nimwegen E. 2012. MotEvo: integrated Bayesian probabilistic methods for inferring regulatory sites and motifs on multiple alignments of DNA sequences. Bioinformatics 28:487–494. http://dx.doi.org/10.1093/bioinformatics/btr695.
21. Gentleman RC, Carey VJ, Bates DM, Bolstad B, Dettling M, Dudoit S, Ellis B, Gautier L, Ge Y, Gentry J, Hornik K, Hothorn T, Huber W, Iacus S, Irizarry R, Leisch F, Li C, Maechler M, Rossini AJ, Sawitzki G, Smith C, Smyth G, Tierney L, Yang JY, Zhang J. 2004. Bioconductor: open software development for computational biology and bioinformatics. Genome Biol. 5:R80. http://dx.doi.org/10.1186/gb-2004-5-10-r80.
22. R Development Core Team. 2012. R: a language and environment for statistical computing. R Foundation for Statistical Computing, Vienna, Austria.
23. Al-Shahrour F, Diaz-Uriarte R, Dopazo J. 2004. FatiGO: a web tool for finding significant associations of Gene Ontology terms with groups of genes. Bioinformatics 20:578–580. http://dx.doi.org/10.1093/bioinformatics/btg455.
24. Suzuki H, Forrest AR, van Nimwegen E, Daub CO, Balwierz PJ, Irvine KM, Lassmann T, Ravasi T, Hasegawa Y, de Hoon MJ, Katayama S, Schroder K, Carninci P, Tomaru Y, Kanamori-Katayama M, Kubosaki A, Akalin A, Ando Y, Arner E, Asada M, Asahara H, Bailey T, Bajic VB, Bauer D, Beckhouse AG, Bertin N, Bjorkegren J, Brombacher F, Bulger E, Chalk AM, Chiba J, Cloonan N, Dawe A, Dostie J, Engstrom PG, Essack M, Faulkner GJ, Fink JL, Fredman D, Fujimori K, Furuno M, Gojobori T, Gough J, Grimmond SM, Gustafsson M, Hashimoto M, Hashimoto T, Hatakeyama M, Heinzel S, Hide W, Hofmann O, Hornquist M, Huminiecki L, et al. 2009. The transcriptional network that controls growth arrest and differentiation in a human myeloid leukemia cell line. Nat. Genet. 41:553–562. http://dx.doi.org/10.1038/ng.375.
25. Siepel A, Bejerano G, Pedersen JS, Hinrichs AS, Hou M, Rosenbloom K, Clawson H, Spieth J, Hillier LW, Richards S, Weinstock GM, Wilson RK, Gibbs RA, Kent WJ, Miller W, Haussler D. 2005. Evolutionarily conserved elements in vertebrate, insect, worm, and yeast genomes. Genome Res. 15:1034–1050. http://dx.doi.org/10.1101/gr.3715005.
26. Siddharthan R, Siggia ED, van Nimwegen E. 2005. PhyloGibbs: a Gibbs sampling motif finder that incorporates phylogeny. PLoS Comput. Biol. 1:e67. http://dx.doi.org/10.1371/journal.pcbi.0010067.
27. Mahony S, Benos PV. 2007. STAMP: a web tool for exploring DNA-binding motif similarities. Nucleic Acids Res. 35:W253–W258. http://dx.doi.org/10.1093/nar/gkm272.
28. Summermatter S, Santos G, Perez-Schindler J, Handschin C. 2013. Skeletal muscle PGC-1alpha controls whole-body lactate homeostasis through estrogen-related receptor alpha-dependent activation of LDH B and repression of LDH A. Proc. Natl. Acad. Sci. U. S. A. 110:8738–8743. http://dx.doi.org/10.1073/pnas.1212976110.
29. Summermatter S, Shui G, Maag D, Santos G, Wenk MR, Handschin C. 2013. PGC-1alpha improves glucose homeostasis in skeletal muscle in an activity-dependent manner. Diabetes 62:85–95. http://dx.doi.org/10.2337/db12-0291.
30. Huss JM, Torra IP, Staels B, Giguere V, Kelly DP. 2004. Estrogen-related receptor alpha directs peroxisome proliferator-activated receptor alpha signaling in the transcriptional control of energy metabolism in cardiac and skeletal muscle. Mol. Cell. Biol. 24:9079–9091. http://dx.doi.org/10.1128/MCB.24.20.9079-9091.2004.
31. Mootha VK, Handschin C, Arlow D, Xie X, St. Pierre J, Sihag S, Yang W, Altshuler D, Puigserver P, Patterson N, Willy PJ, Schulman IG, Heyman RA, Lander ES, Spiegelman BM. 2004. Erralpha and Gabpa/b specify PGC-1alpha-dependent oxidative phosphorylation gene expression that is altered in diabetic muscle. Proc. Natl. Acad. Sci. U. S. A. 101:6570–6575. http://dx.doi.org/10.1073/pnas.0401401101.
32. Schreiber SN, Emter R, Hock MB, Knutti D, Cardenas J, Podvinec M, Oakeley EJ, Kralli A. 2004. The estrogen-related receptor alpha (ERRalpha) functions in PPARgamma coactivator 1alpha (PGC-1alpha)-induced mitochondrial biogenesis. Proc. Natl. Acad. Sci. U. S. A. 101:6472–6477. http://dx.doi.org/10.1073/pnas.0308686101.
33. Eisele PS, Salatino S, Sobek J, Hottiger MO, Handschin C. 2013. The peroxisome proliferator-activated receptor gamma coactivator 1alpha/beta (PGC-1) coactivators repress the transcriptional activity of NF-kappaB in skeletal muscle cells. J. Biol. Chem. 288:2246–2260. http://dx.doi.org/10.1074/jbc.M112.375253.
34. Mangelsdorf DJ, Evans RM. 1995. The RXR heterodimers and orphan receptors. Cell 83:841–850. http://dx.doi.org/10.1016/0092-8674(95)90200-7.
35. Hai T, Curran T. 1991. Cross-family dimerization of transcription factors Fos/Jun and ATF/CREB alters DNA binding specificity. Proc. Natl. Acad. Sci. U. S. A. 88:3720–3724. http://dx.doi.org/10.1073/pnas.88.9.3720.
36. Arany Z, Foo SY, Ma Y, Ruas JL, Bommi-Reddy A, Girnun G, Cooper M, Laznik D, Chinsomboon J, Rangwala SM, Baek KH, Rosenzweig A, Spiegelman BM. 2008. HIF-independent regulation of VEGF and angiogenesis by the transcriptional coactivator PGC-1alpha. Nature 451:1008–1012. http://dx.doi.org/10.1038/nature06613.
37. Ma Z, Swigut T, Valouev A, Rada-Iglesias A, Wysocka J. 2011. Sequence-specific regulator Prdm14 safeguards mouse ESCs from entering extraembryonic endoderm fates. Nat. Struct. Mol. Biol. 18:120–127. http://dx.doi.org/10.1038/nsmb.2000.
38. Qian J, Chen S, Huang Y, Shi X, Liu C. 2013. PGC-1alpha regulates hepatic hepcidin expression and iron homeostasis in response to inflammation. Mol. Endocrinol. 27:683–692. http://dx.doi.org/10.1210/me.2012-1345.
39. Jang WG, Kim EJ, Park KG, Park YB, Choi HS, Kim HJ, Kim YD, Kim KS, Lee KU, Lee IK. 2007. Glucocorticoid receptor mediated repression of human insulin gene expression is regulated by PGC-1alpha. Biochem. Biophys. Res. Commun. 352:716–721. http://dx.doi.org/10.1016/j.bbrc.2006.11.074.
40. Sandri M, Lin J, Handschin C, Yang W, Arany ZP, Lecker SH, Goldberg AL, Spiegelman BM. 2006. PGC-1alpha protects skeletal muscle from atrophy by suppressing FoxO3 action and atrophy-specific gene transcription. Proc. Natl. Acad. Sci. U. S. A. 103:16260–16265. http://dx.doi.org/10.1073/pnas.0607795103.
41. Shaulian E, Karin M. 2002. AP-1 as a regulator of cell life and death. Nat. Cell Biol. 4:E131–E136. http://dx.doi.org/10.1038/ncb0502-e131.
42. Curran T, Franza BR, Jr. 1988. Fos and Jun: the AP-1 connection. Cell 55:395–397. http://dx.doi.org/10.1016/0092-8674(88)90024-4.
43. Cam H, Easton JB, High A, Houghton PJ. 2010. mTORC1 signaling under hypoxic conditions is controlled by ATM-dependent phosphorylation of HIF-1alpha. Mol. Cell 40:509–520. http://dx.doi.org/10.1016/j.molcel.2010.10.030.
44. Majmundar AJ, Wong WJ, Simon MC. 2010. Hypoxia-inducible factors and the response to hypoxic stress. Mol. Cell 40:294–309. http://dx.doi.org/10.1016/j.molcel.2010.09.022.
45. Wagner PD. 2001. Skeletal muscle angiogenesis. A possible role for hyp-

oxia. Adv. Exp. Med. Biol. 502:21–38. http://dx.doi.org/10.1007/978-1-4757-3401-0_4.
46. Pino E, Wang H, McDonald ME, Qiang L, Farmer SR. 2012. Roles for peroxisome proliferator-activated receptor gamma (PPARgamma) and PPARgamma coactivators 1alpha and 1beta in regulating response of white and brown adipocytes to hypoxia. J. Biol. Chem. 287:18351–18358. http://dx.doi.org/10.1074/jbc.M112.350918.
47. Zhao J, Li L, Pei Z, Li C, Wei H, Zhang B, Peng Y, Wang Y, Tao Y, Huang R. 2012. Peroxisome proliferator activated receptor (PPAR)-gamma co-activator 1-alpha and hypoxia induced factor-1alpha mediate neuro- and vascular protection by hypoxic preconditioning in vitro. Brain Res. 1447:1–8. http://dx.doi.org/10.1016/j.brainres.2012.01.059.
48. Charos AE, Reed BD, Raha D, Szekely AM, Weissman SM, Snyder M. 2012. A highly integrated and complex PPARGC1A transcription factor binding network in HepG2 cells. Genome Res. 22:1668–1679. http://dx.doi.org/10.1101/gr.127761.111.

SUPPLEMENTAL FIGURES AND TABLES

Fig.S1

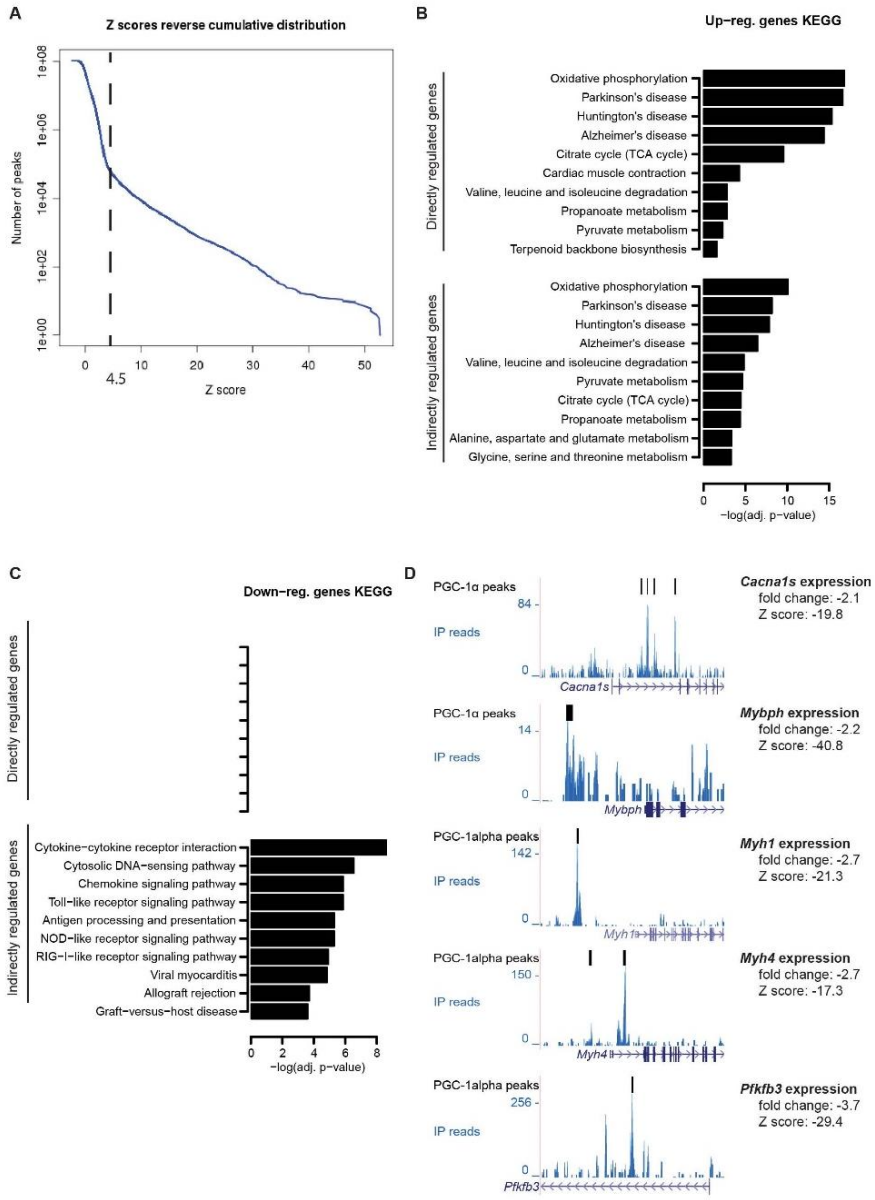

Suppl. Fig. S1. Peak Z score distribution and KEGG functional analysis. Related to Figure 1.

(A) Distribution of the Z scores for all sliding windows considered by the peak-finding algorithm along the mouse genome. The chosen cutoff for peak calling is depicted by the dotted line.

(B) Subset of the top significantly enriched KEGG terms identified for direct and indirect up-regulated PGC-1α target genes.

(C) Subset of the top significantly enriched KEGG terms identified for direct and indirect down-regulated PGC-1α target genes.

(D) ChIP-Seq signal around the promoter region of the five directly down-regulated genes (*Cacna1s*, *Mybph*, *Myh1*, *Myh4*, *Pfkfb3*) involved in regulating the contractile properties of fast-twitch muscle fibers.

Fig.S2

A

Motif name	Z direct	Z indirect	Z avg. direct	Z avg. indirect	Directly activated	Indirectly activated	Directly repressed	Indirectly repressed
Group 1: motifs only directly activated by PGC-1alpha								
SP1.p2	3.99	0.61	9.76	0.33	1	0	0	0
ELF1,2,4.p2	3.11	1.32	7.59	3.13	1	0	0	0
PAX4.p2	2.50	1.53	6.11	-3.68	1	0	0	0
LMO2.p2	2.36	1.65	5.78	3.98	1	0	0	0
HNF4A_NR2F1,2.p2	2.26	1.54	5.52	3.64	1	0	0	0
GTF2I.p2	2.09	2.38	5.10	-5.80	1	0	0	1
Group 2: motifs directly and indirectly activated by PGC-1alpha								
ESRRA.p2	6.04	15.49	14.78	37.94	1	1	0	0
NR5A1,2.p2	3.53	7.73	8.66	17.00	1	1	0	0
ZNF143.p2	2.48	4.65	6.05	9.68	1	1	0	0
NFY{A,B,C}.p2	2.37	3.56	5.80	7.62	1	1	0	0
ESR1.p2	2.33	4.53	5.69	11.04	1	1	0	0
RXR{A,B,G}.p2	2.29	4.30	5.59	10.50	1	1	0	0
Group 3: motifs only indirectly activated by PGC-1alpha								
NRF1.p2	1.60	4.61	3.91	6.21	0	1	0	0
YY1.p2	0.88	2.97	2.09	5.77	0	1	0	0
EHF.p2	0.73	2.77	1.77	6.35	0	1	0	0
RXRA_VDR{dimer}.p2	0.71	2.54	1.71	6.20	0	1	0	0
HES1.p2	0.34	2.52	0.84	6.10	0	1	0	0
FOXO1,3,4.p2	0.46	2.51	1.13	6.12	0	1	0	0
ELK1,4_GABP{A,B1}.p3	1.18	2.46	2.89	5.95	0	1	0	0
NKX3-1.p2	0.60	2.43	1.48	5.93	0	1	0	0
REST.p3	0.48	2.41	1.15	5.70	0	1	0	0
NFE2L1.p2	1.79	2.32	4.36	5.23	0	1	0	0
POU5F1_SOX2{dimer}.p2	0.24	2.32	0.57	5.65	0	1	0	0
AIRE.p2	0.38	2.24	-0.91	5.40	0	1	0	0
RXRG_dimer.p3	1.67	2.01	4.09	4.89	0	1	0	0
Group 4: motifs only indirectly repressed by PGC-1alpha								
IRF1,2,7.p3	1.77	24.23	4.34	-14.48	0	0	0	1
NFKB1_REL_RELA.p2	0.50	6.54	1.19	-16.01	0	0	0	1
TLX1..3_NFIC{dimer}.p2	0.84	4.91	-2.05	-11.97	0	0	0	1
STAT2,4,6.p2	0.35	4.81	0.52	-9.67	0	0	0	1
DMAP1_NCOR{1,2}_SMARC.p	0.25	4.22	-0.60	-8.73	0	0	0	1
RUNX1..3.p2	0.09	3.94	0.11	-9.61	0	0	0	1
NFATC1..3.p2	0.16	3.46	-0.24	-8.42	0	0	0	1
GATA1..3.p2	1.21	3.39	-2.92	-8.04	0	0	0	1
TBP.p2	1.11	3.20	2.71	-4.04	0	0	0	1
ZIC1..3.p2	0.20	2.99	-0.46	-7.24	0	0	0	1
ATF6.p2	0.24	2.97	-0.51	-7.25	0	0	0	1
TLX2.p2	0.57	2.86	1.37	-6.76	0	0	0	1
TFAP2B.p2	1.75	2.72	4.26	-6.61	0	0	0	1
SPI1.p2	1.69	2.70	4.14	-6.19	0	0	0	1
MEF2{A,B,C,D}.p2	0.97	2.67	2.35	-6.51	0	0	0	1
TFCP2.p2	1.07	2.62	2.57	-5.80	0	0	0	1
BPTF.p2	1.38	2.56	3.37	-6.25	0	0	0	1
LEF1_TCF7_TCF7L1,2.p2	0.17	2.55	0.37	-6.11	0	0	0	1
STAT1,3.p3	0.74	2.53	1.79	-6.17	0	0	0	1
RREB1.p2	1.56	2.39	3.82	-5.42	0	0	0	1
GTF2I.p2	2.09	2.38	5.10	-5.80	1	0	0	1
MYFfamily.p2	0.36	2.38	0.79	-5.12	0	0	0	1
ZNF384.p2	0.64	2.34	-1.55	-5.27	0	0	0	1
TGIF1.p2	0.57	2.34	1.34	-5.68	0	0	0	1
TEAD1.p2	0.99	2.23	-2.43	-5.43	0	0	0	1
SOX{8,9,10}.p2	0.16	2.17	0.30	-5.28	0	0	0	1
CEBPA,B_DDIT3.p2	1.03	2.13	2.51	-5.20	0	0	0	1
MYOD1.p2	1.49	2.05	3.65	-4.99	0	0	0	1

Suppl. Fig. S2. Motif activities clustered by Z score in direct/indirect activation/repression. Related to Figure 2.

(A) Motifs showing different types of regulation (1=yes, 0=not).

Fig.S3

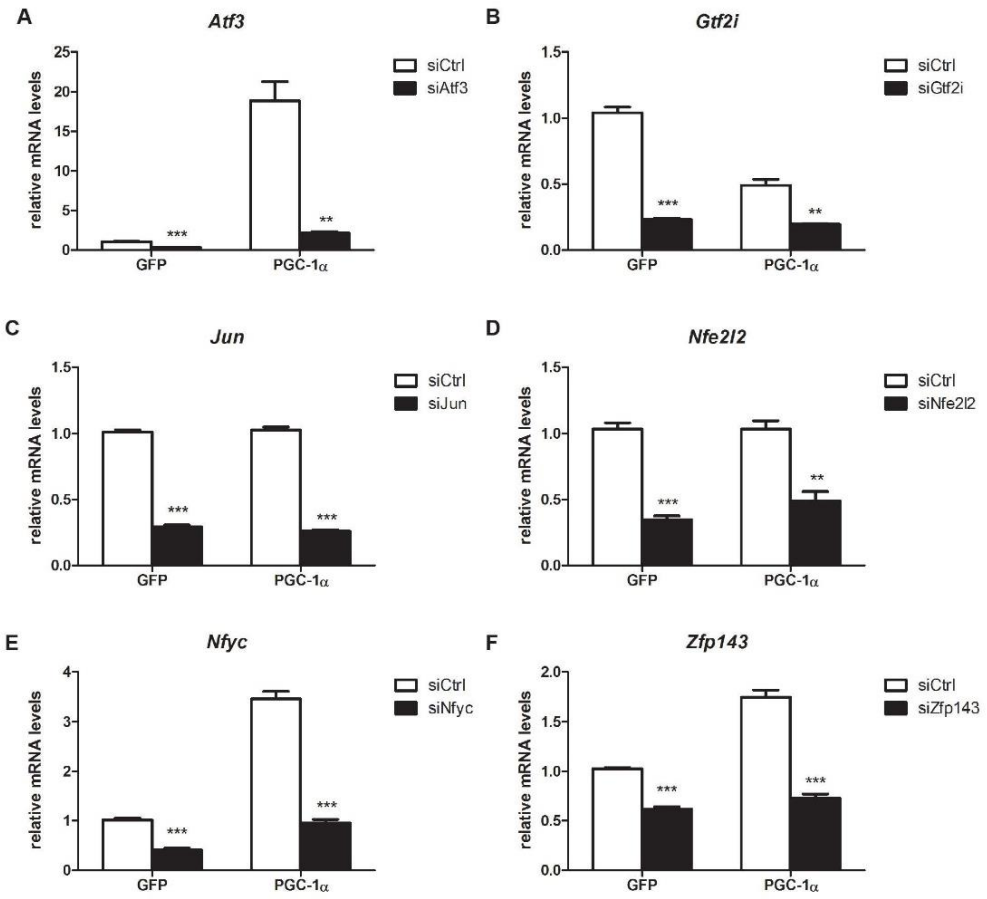

Suppl. Fig. S3. siRNA knockdown efficiency for the putative PGC-1α partner TFs. Related to Figure 4

(A-F) siRNA knockdown efficiency for ATF3 (A), GTF2I (B), JUN (C), NFE2L2 (D), NFYC (E) and ZFP143 (F) knockdown. Bars represent fold change over GFP/siCtrl levels. Error bars represent SEM. *p < 0.05; **p < 0.01; ***p < 0.001.

Suppl. Table 1. Real-time primer sequences. Semiquantitative real-time PCR primers used for validation experiments.

Real-time PCR primers used for testing the efficiency of the ChIP		
Gene promoter or intron	Forward primer	Reverse primer
Tbp intron	TGTGAGCTCCTTGGCTTTTT	ATAGTTGCCCAGCAATCAGG
promoter of *Aco2*	CACCGATAGTTGCTTTCCAGATAC	AACCATCTGACAGGCATAGTCAAT
promoter of *Cycs*	AAGGGCGCCCTCTGGGCACATC	ATCCCCGTCGCGCGCTCACCG
promoter of *Acadm*	CCTTGCCCGAGCCTAAAC	GTCTGGCTGCGCCCTCT
promoter of *Atp5b*	CTGGAAACTTCCACCCTCACTA	GAGAGGTTTTTGGCGGAACTA
promoter of *Idh3a*	GGACGGCGTCAAGGTCAAG	GCCTAGGTGGCCTGTCTGTG
PGC-1α exon 2	TGAGGACCAGCCTCTTTGCCC A	CGCTACACCACTTCAATCCACCC

Gene or gene promoter	Forward + reverse primer		FOS binding site	Peak position
TGF61[*1]	F:	TTTGAGACTTTTCCGCTGCT	chr7:26472349-26472356	(see reference 1)
	R:	GGTCCTGCCTCCTTGCGA		
Nr0b2 promoter	F:	GGTACAGCCTGGGTTAATGAC	chr4:133109008-133109015	chr4:133108962-133109162
	R:	ACTGCCTGGATGCCCTTTAT		
Gprc5a promoter	F:	TGATGTCATGAGCCTCACCC	chr6:135011471-135011478	chr6: 135011398-135011598
	R:	TAGCTGTCATTGAGGGCACT		
Dbt promoter	F:	AAGGGGCAAAGCAATTCAGG	chr3: 116215241-116215248 chr3: 116215242-116215249	chr3: 116215152-116215352 chr3: 116215152-116215352
	R:	CTTAGAAAATGTGGTCAGATGCA		

Real-time PCR primers used for testing the knockdown efficiency by siRNAs		
Gene	Forward primer	Reverse primer
Rn18s	AGTCCCTGCCCTTTGTACACA	CGATCCGAGGGCCTCACTA
Fos	TACTACCATTCCCCAGCCGA	GCTGTCACCGTGGGGATAAA
Jun	TGGGCACATCACCACTACAC	TCTGGCTATGCAGTTCAGCC
Atf3	TCTGCGCTGGAGTCAGTTAC	CCGCCTCCTTTTCCTCTCAT
Gtf2i	TTCGAAGGCTTTGCAAGGAAG	TTCGGGGTCCTCACTGGTTT
Nfe2l2	AGTGGATCCGCCAGCTACTC	ATGGGAATGTCTCTGCCAAA
Nfyc	CCACCAGTTCTACGACCACC	GGCCTGTACAATCTGCACCT
Zfp143	GTGGTCGGTCCTTTACCACA	AAATGCCCTCCCACATCCAG

Real-time primers used for target gene validation		
Gene	Forward primer	Reverse primer
Aim1l	CCTGTTGCGTCCATAAGGGT	GCTCTGAGTTCCACATCCCC
Atp1b1	GCTACGAGGCCTACGTGCTA	TGCCACAGTCCTCGAAAATC
Atp5g1	CAGAGGCCCCATCTAAGCAG	TGTCCCGGGAAATGACACTG
Cdk15	ATGCAGTTGCTACCACCGTT	CCGTGGAACTGGATGCTTCT
Cdr2l	GGAACAGGAAAACGAACGGC	ACCACCGTGTACTCACGTTC
Crb3	CCGGACCCTTTCACAAATAGC	CTCTGTCTGCCGCTTTTCC

Dot1l	TGACCTCAGATGAGGAGCCA	TGTCTTCGGGGGAGATTTGC
Eef1a2	CAAGATGGACTCCACGGAAC	CTGGGTTGTAGCCGATCTTC
Eif2b4	ACGGCAAGACCCAATCAGAG	AAGTTCTGCCTTACTCCGGC
Fa2h	GTGGACTGGCAGAAACCTCT	TCTGAGTGGAAGAGGCGAAT
Fabp3	CATGTGCAGAAGTGGAACGG	CTCACCACACTGCCATGAGT
Fam131c	CTGGCTACGTCATCCCTTGT	TCCAGCCTTTCCACTCGAT
Gabpa	GTCGAGGTGGTCATCGATCC	GTAATGTGCTTGGTGCCGTC
Gdf15	CACGCATGCGCAGATCAAAG	TGTGCATAAGAACCACCGGG
Gtpbp2	TGGAAACCTCAAAGCTCGGG	GTACGGAGGGTTGTTGGCTT
Il1a	TGCAAGCTATGGCTCACTTC	GATACTGTCACCCGGCTCTC
Inpp5j	ACAAGGGCGGAGTAAGTGTG	TGAAAGTTATCCTTGCGCTGT
Jam2	GTATTACTGCGAAGCCCGGA	CAACCGTTGCTATGATGCCG
Kdm5a	GTCTTCCGTGTGTCATCAGC	TTAGTCGGGGCAATTCAGGT
Ldhb	GACTCCGAAAATTGTGGCCG	TTCTCTGCACCAGGTTGAGC
Lpin1	CGGCCCTCAACACCAAAAAG	AATTCACCCCACAGCCAGAG
Lrrc2	GTGGAAGGAGCTGCCTGATT	AACAGCTCGATGTACGTGGG
Met	GCTGAGAAACTCTTCCGGCT	AGCCGGCCCATGAATAAGTC
Ndufa9	TTCTGTGGCTCATCCCATCG	TGTAGCCCCAAACACAGTGG
Nmnat1	GGTCGGTGATGCGTACAAGA	CCACGTATCCACTTCCACCC
Nppb	GGCCTCACAAAAGAACACCC	TGCCCAAAGCAGCTTGAGAT
Nr0b2	CCTCTTCAACCCAGATGTGC	GGGCTCCAAGACTTCACACA
Osbpl1a	TCCCCCAATCAGTGCATTCC	GCTTCTACACTCTTGCCCCA
Qrsl1	GTTGGATCAGGGTGCCCTAC	GGGGTTTCTAACTGGCCCAA
Rasl10b	AGACCTGGAAGTGCGGCTAC	GGCAGCGTGCACGTGTTT
Rrm2	TTGCAGCGAGTGATGGCATA	CCATGGCAATTTGGAAGCCA
Samm50	TTTTGATGGACTTGGGCGGA	TGAGATCGCCGCATTACCTC
Sbno2	AGACATCCCAGACACACCTG	TGAGAAGTGGAGTGCTGGAG
Slc25a4	GGTACTTCCCCACTCAAGCC	AGCAAAGTAGCGCCAGAACT
Slc25a35	TAGTCGTGGCAATGACACCC	TCCAAGATCCCCCGGTACAT
Slc6a19	TCCACTCAACCAGAACCAGAC	TGAGTCACTGATGGAAGTGGAG
Srxn1	CCAGGGTGGCGACTACTACT	AGGTCTGAAAGGGTGGACCTC
Stard7	CTCTACGGCCGCCTGTATTC	CGCCATCAAAACAGAGGCAT
Stk19	GTCCTCACTGTCCGAGATGC	CACCATGCTCAGTACAGCCT
Syt7	ACTGGGCAAACGCTACAAGA	TGCAGGCAACTTGATGGCTT
Tbrg4	AACGACAGCCGTACATTGGT	AGCTCCAGGCACTTGTCTTC
Tfam	GAGCGTGCTAAAAGCACTGG	GCTACCCATGCTGGAAAAACA
Tinagl1	TTCTTGTACCAGCGTGGCAT	CCCCACCCAGTGATCTTGAC
Tomm5	CGGAGGAGATGAAGCGGAAG	TATGGAGTGACTCGCAGCAG
Trak2	GCTGAAGAGACGTTCCGCTA	ATCTCGATCCCTCTCTGCCA
Trmt61a	GCTCCTTCTCTCCGTGCATT	TGCGCACATTGTAGACCTGT
Trp53inp2	TACCCCTCCCGCCTGTTTTA	CTGCCGGTGACATAAACGGA
Ttc7b	TGCTCCCCACGATCAAGAAC	ATCTCCCGACTCCTCTCGTC
Tusc2	GCAGTGCCTCCCTTCGTATT	CTGCCCATTCTTGGTGACGA
Twf2	TGCTACCTCCTCTTCCGACT	ATAGCATCTTCAGCCGCACC
VEGFα	CACGACAGAAGGAGAGCAGA	GGGCTTCATCGTTACAGCAG
Wnt7b	TTTCTCTGCTTTGGCGTCCT	GGCCAGGAATCTTGTTGCAG

SUPPLEMENTAL REFERENCES

[1] Liu, G., Ding, W., Liu, X., and Mulder, K.M. (2006). c-Fos is required for TGFbeta1 production and the associated paracrine migratory effects of human colon carcinoma cells. Mol Carcinog *45*, 582-593

Appendix 2: Role of Nuclear Receptors in Exercise-Induced Muscle Adaptations

Role of Nuclear Receptors in Exercise-Induced Muscle Adaptations

Barbara Kupr, Svenia Schnyder, and Christoph Handschin

Biozentrum, University of Basel, Basel 4056, Switzerland

Correspondence: christoph.handschin@unibas.ch

Cold Spring Harbor Perspectives in Medicine
www.perspectivesinmedicine.org

Skeletal muscle is not only one of the largest, but also one of the most dynamic organs. For example, plasticity elicited by endurance or resistance exercise entails complex transcriptional programs that are still poorly understood. Various signaling pathways are engaged in the contracting muscle fiber and collectively culminate in the modulation of the activity of numerous transcription factors (TFs) and coregulators. Because exercise confers many benefits for the prevention and treatment of a wide variety of pathologies, pharmacological activation of signaling pathways and TFs is an attractive avenue to elicit therapeutic effects. Members of the nuclear receptor (NR) superfamily are of particular interest owing to the presence of well-defined DNA- and ligand-binding domains. In this review, we summarize the current understanding of the involvement of NRs in muscle biology and exercise adaptation.

Skeletal muscle is the largest organ in our body, accounts for ~40% of body mass, contains ~50%–75% of all body proteins, and takes up ~85% of glucose on insulin stimulation (Frontera and Ochala 2015). Moreover, even though skeletal muscle only contributes ~30% to energy expenditure at rest, 90% of the 20-fold peak increase in energy expenditure during physical activity can be attributed to muscle. Accordingly, skeletal muscle is one of the main sites of metabolism of glucose, fatty acids, ketone bodies, and lactate. The energy generated in this process is used for contraction and hence the generation of force, including that which is required to maintain posture and breathing. In addition, skeletal muscle function is instrumental to maintain body temperature, and is one of the main storage sites for glucose (in the form of glycogen), lipids (as neutral triglyceride lipid droplets), and amino acids. With the detection of myokines, muscle has also been defined as endocrine organ exerting auto-, para-, and endocrine effects (Schnyder and Handschin 2015). Finally, skeletal muscle can contribute to the detoxification of predominantly endogenous metabolites, such as L-kynurenine or excessive ketone bodies (Svensson et al. 2016).

To be able to cope with these diverse functions, skeletal muscle is one of the most dynamic tissues. On different stimuli, massive adaptations are initiated and, if the respective stimuli persist, maintained chronically. Most strikingly, biochemical, metabolic, and contractile properties are modulated by physical activity. Many different signaling pathways are activated during and after exercise bouts and collectively result in the regulation of a complex transcriptional program (Egan and Zierath 2013; Kupr and Hand-

Editors: Juleen R. Zierath, Michael J. Joyner, and John A. Hawley
Additional Perspectives on The Biology of Exercise available at www.perspectivesinmedicine.org

 doi: 10.1101/cshperspect.a029835
Cite this article as *Cold Spring Harb Perspect Med* 2017;7:a029835

schin 2015; Hoppeler 2016) that varies between endurance and resistance exercise resulting in distinct and specific outcomes (Hawley et al. 2014; Camera et al. 2016; Qaisar et al. 2016). Importantly, these two types of exercise not only improve muscle endurance and strength, respectively, but also confer beneficial effects for the prevention and treatment of many different pathologies (Handschin and Spiegelman 2008; Booth et al. 2012; Pedersen and Saltin 2015).

Even though the epidemiological association of a sedentary lifestyle with the increased risk for many chronic diseases is clear, and inversely, the benefits of exercise have been shown (Pedersen and Saltin 2015), the incidence of most of these pathologies is on the rise worldwide. Exercise interventions often fail because of lack of adherence and compliance. Moreover, subgroups of patients exist with exercise intolerance, defined either as the inability to train or as a detrimental outcome of physical activity. It is therefore intriguing to speculate that a better knowledge of the complex molecular mechanisms that underlie exercise adaptations in skeletal muscle could be leveraged to design so-called "exercise mimetics," pharmacological interventions that elicit exercise-like effects (Handschin 2016). Of the transcription factors (TFs) that have been described in skeletal muscle plasticity, those belonging to the superfamily of nuclear receptors (NRs) are of particular interest in this regard. NRs are the largest family of TFs in metazoans (Escriva et al. 2004; Bookout et al. 2006). With few exceptions, all of the NRs are characterized by a highly conserved domain structure (Fig. 1A) (Germain et al. 2006). An amino-terminal A/B domain, often with an intrinsic transcriptional activation function (AF-1), is followed by a DNA-binding domain C that entails a zinc finger–based DNA-binding domain. A hinge region D then links to the ligand-binding and dimerization domain E/F, of which helix 12 includes the activation function 2 (AF-2). The NR superfamily includes the classic steroid hormone receptors, "orphan" receptors with no known endogenous ligand, and "adopted" NRs for which endogenous ligands have been identified. All of the NRs with functional DNA-binding domains are recruited to either individual or direct, inverted or everted repeats of canonical nucleotide hexamer half-sites with variable spacing (Fig. 1B). Although most of the steroid hormone receptors bind as homodimers, other NRs can also be recruited to target sites as monomers or as heterodimers with the common binding partners retinoid X receptors α, β, or γ (RXRα/β/γ, official no-

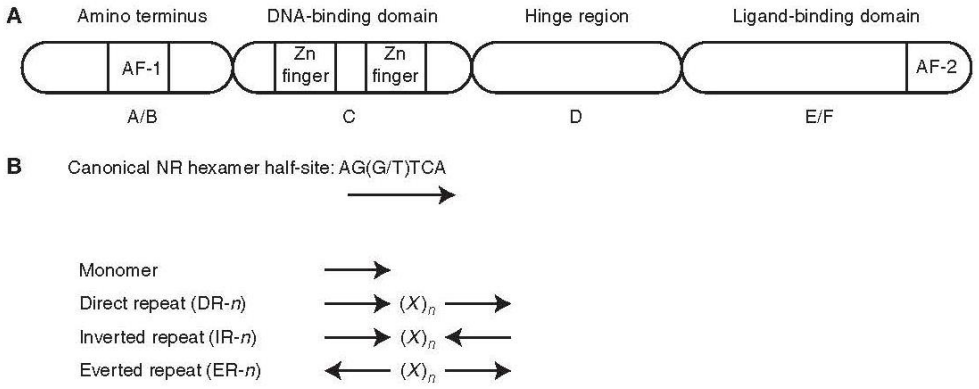

Figure 1. Structure and DNA-binding sites of nuclear receptors (NRs). (*A*) Schematic representation of the different NR domains. (*B*) Arrangements of DNA-binding sites of NRs. $(X)_n$ indicates a spacer of *n* arbitrary nucleotides *X* between the hexamer half-sites. The repeats are accordingly designated as DR-*n*, IR-*n*, or ER-*n*, for example, DR-1 for a direct repeat with a spacer of one nucleotide.

Cold Spring Harbor Perspectives in Medicine
www.perspectivesinmedicine.org

menclature NR2B1/2/3) (see Auwerx et al. 1999). Type I NRs reside in the cytoplasm and translocate into the nucleus on ligand binding and activation. Type II NRs are found in the nucleus, heterodimerize with RXRs, often sit on response elements and then exchange corepressors for coactivators when activated by ligands. Similarly, the type III and type IV NRs are retained in the nucleus and bind to DNA-response elements as homodimers to hexamer repeats (type III) or as monomers or dimers, but only to a single hexamer half site (type IV). NR ligands include hormones, lipids, steroids, retinoids, xenobiotics, and synthetic compounds. Accordingly, many NRs sense the energy or the dietary status of a cell and regulate metabolism and energy expenditure (Pardee et al. 2011). Not surprisingly, various NRs have thus also been implicated in the regulation of myogenesis, skeletal muscle function, and plasticity. In this review, these NRs and important cofactors are highlighted and their role in exercise-induced muscle adaptations as well as their potential as drug targets is discussed.

THE NR SUPERFAMILY AND ITS ROLE IN EXERCISE-INDUCED SKELETAL MUSCLE ADAPTATION

A surprisingly high proportion of NRs in mice, 35 out of 49, shows detectable gene expression in skeletal muscle (Table 1) (Bookout et al. 2006). However, a potential role in skeletal muscle function and exercise adaptation has been studied for only a subset of those (Fig. 2). Current knowledge and recent updates about these NRs are summarized in the following paragraphs and in Table 2. (Further information and primary literature can be found in additional excellent review articles on this topic, for example, Smith and Muscat 2005; Fan et al. 2011, 2013; Fan and Evans 2015; Mizunoya 2015.)

Subfamily 1, Group A: Thyroid Hormone Receptors—Type II

Hypo- and hyperthyroidism have profound effects on whole body metabolism. The effect of thyroid hormone is mediated by two thyroid hormone receptors (TRs), TRα (NR1A1) and TRβ (NR1A2). In skeletal muscle, hypothyroidism promotes a shift toward slow, oxidative, while injection of thyroid hormone to fast, glycolytic muscle fibers, respectively (Smith and Muscat 2005; Mizunoya 2015). In loss-of-function studies, knockout of TRα, but not of TRβ, was likewise associated with an increase in oxidative muscle fibers (Yu et al. 2000). Interestingly, however, concomitant ablation of both TRs exacerbated the switch from type II to type I fibers, indicating that TRβ might boost the action of TRα in skeletal muscle. TRα is furthermore induced by contraction in skeletal muscle leading to a modulation of carbohydrate and lipid metabolism (Lima et al. 2009). At least some of the effects of low levels of thyroid hormone on tricarboxylic acid (TCA) cycle activity and mitochondrial oxidative phosphorylation (OXPHOS) in skeletal muscle could be meditated by activation of the peroxisome proliferator-activated receptor γ coactivator-1α (PGC-1α) (Irrcher et al. 2003), a master regulator of mitochondrial function and oxidative metabolism, potentially in a fiber type–specific manner (Bahi et al. 2005).

Subfamily 1, Group C: Peroxisome Proliferator-Activated Receptors—Type II

In mammals, three peroxisome proliferator-activated receptors (PPARs) PPARα (NR1C1), PPARβ/δ (NR1C2), and PPARγ (NR1C3) have been identified, all of which are expressed in skeletal muscle and have been implicated in regulating lipid metabolism. The PPARs heterodimerize with RXRs and bind to PPAR-response elements consisting of a core of a direct repeat of two hexamer half sites with a spacing of 1 nucleotide (DR-1) in promoter and enhancer regions of their target genes.

PPARα, activated by free fatty acids and fibrate drugs, strongly controls fatty acid oxidation, TCA cycle activity, and mitochondrial OXPHOS. Interestingly, however, muscle lipid metabolism is only slightly altered in PPARα knockout animals, implying a functional compensation by PPARβ/δ, which shares many common target genes with PPARα (Muoio

Cold Spring Harbor Perspectives in Medicine
www.perspectivesinmedicine.org

Table 1. Human and mouse nuclear receptors

NR subfamily and group	NR nomenclature	Trivial name	Muscle expression (*Mus musculus*)[a]
1A	NR1A1	TRα	H
	NR1A2	TRβ	L
1B	NR1B1	RARα	H
	NR1B2	RARβ	I
	NR1B3	RARγ	I
1C	NR1C1	PPARα	I
	NR1C2	PPARβ/δ	I
	NR1C3	PPARγ	I
1D	NR1D1	REVERBα	H
	NR1D2	REVERBβ	I
1F	NR1F1	RORα	H
	NR1F2	RORβ	L
	NR1F3	RORγ	H
1H	NR1H2	LXRβ	I
	NR1H3	LXRα	H
	NR1H4	FXRα	nd
	NR1H5[b]	FXRβ[b]	nd
1I	NR1I1	VDR	L
	NR1I2	PXR	nd
	NR1I3	CAR	nd
2A	NR2A1	HNF4α	nd
	NR2A2	HNF4γ	nd
2B	NR2B1	RXRα	H
	NR2B2	RXRβ	H
	NR2B3	RXRγ	H
2C	NR2C1	TR2	L
	NR2C2	TR4	I
2E	NR2E1	TLX	nd
	NR2E3	PNR	nd
2F	NR2F1	COUP-TFI	L
	NR2F2	COUP-TFII	I
	NR2F6	EAR2	I[c]
3A	NR3A1	ERα	I
	NR3A2	ERβ	nd
3B	NR3B1	ERRα	H
	NR3B2	ERRβ	I
	NR3B3	ERRγ	I
3C	NR3C1	GR	H
	NR3C2	MR	I
	NR3C3	PR	nd
	NR3C4	AR	H
4A	NR4A1	NUR77	H
	NR4A2	NURR1	I
	NR4A3	NOR1	H
5A	NR5A1	SF1	nd
	NR5A2	LRH1	nd
6A	NR6A1	GCNF1	L
0B	NR0B1	DAX1	nd
	NR0B2	SHP	nd

NRs highlighted by gray shading are discussed in this review.

H, High expression; I, intermediate expression; L, low expression; nd, not detected.

[a]NR gene expression in mouse muscle according to Bookout et al. (2006).

[b]FXRβ is a pseudogene in the human genome.

[c]The expression of NR2F6/Ear2 was not reported in to Bookout et al. (2006) and muscle expression confirmed using BioGPS and GeneCards.

Cold Spring Harbor Perspectives in Medicine
www.perspectivesinmedicine.org

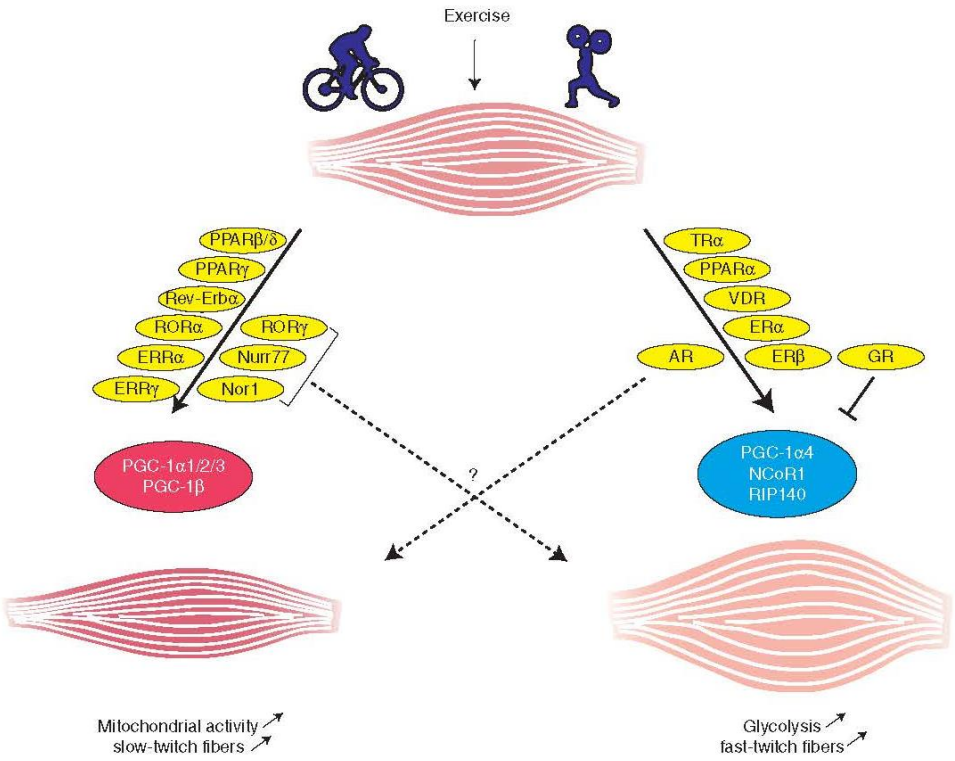

Figure 2. Regulation of endurance and resistance exercise adaptations in skeletal muscle by nuclear receptors (NRs) and coregulators. For some NRs, including RORγ, Nur77, Nor1, or AR, a role in both the promotion of an oxidative and a glycolytic muscle phenotype has been proposed in different experimental models.

et al. 2002). Accordingly, muscle-specific overexpression of either of these PPARs results in elevated oxidative metabolism of fatty acids (Luquet et al. 2003; Finck et al. 2005). However, unexpectedly and diametrically opposite to PPARβ/δ, muscle-specific PPARα transgenic mice are susceptible to the development of insulin resistance, have a reduced endurance capacity, and depict an oxidative to glycolytic fiber type switch (Gan et al. 2013). Inversely, more oxidative fibers are detected in muscle-specific PPARα knockout animals (Gan et al. 2013). This negative cross talk between PPARα and PPARβ/δ is mediated by the miRNAs miR-208b and miR-499, which boost oxidative and repress glycolytic fiber determination (Gan et al. 2013).

The transcription of PPARβ/δ is induced by acute and chronic endurance exercise and subsequently promotes a glycolytic to oxidative fiber-type switch linked to higher OXPHOS activity, reduced fat mass, and improved glucose tolerance (Fan and Evans 2015). Muscle-specific overexpression of PPARβ/δ (Gan et al. 2011) or of PPARβ/δ fused to the strong VP16 transcriptional activation domain (Wang et al. 2004) accordingly enhances endurance exercise performance. Similarly, administration of the synthetic PPARβ/δ ligand GW501516 improves oxidative metabolism and enhances the effect of endurance exercise training (Narkar et al. 2008). In contrast, skeletal muscle–specific ablation of the PPARβ/δ gene results in a shift toward glycolytic fibers, reduced fatty acid catabolism and OXPHOS activity, decreased exercise performance, as well as exacerbated insulin resistance, glucose intolerance,

Table 2. Muscle phenotype of gain- and loss-of-function models for selected NRs

NR nomenclature	Trivial name	Loss-of-function model	Muscle phenotype	Gain-of-function model	Muscle phenotype	Ligands (examples)
NR1A1	TRα	KO	Oxidative fibers	Pharm	Mitochondrial biogenesis	Thyroid hormone
NR1C1	PPARα	mKO	Oxidative fibers	mTG	Glycolytic fibers, reduced endurance	Fibrate drugs, fatty acids
NR1C2	PPARβ/δ	mKO	Glycolytic fibers	mTG	Oxidative fibers, improved endurance	GW501516, fatty acids
NR1C3	PPARγ	mKO	Glucose intolerance and insulin resistance	mTG	Oxidative fibers	Thiazolidinediones, fatty acids
NR1D1	REVERBα	mKO	Reduced endurance exercise performance	mTG	Oxidative fibers, improved endurance	SR9009
NR1F1	RORα	KO	Atrophy	mTG	Oxidative fibers, lipid metabolism	
NR1F3	RORγ	KO	Atrophy	mTG	Lipid and carbohydrate metabolism	
NR1H2	LXRβ	KO	Impaired glycogen buildup and lipogenesis			T0901317, oxysterols
NR1H3	LXRα	KO	Impaired glycogen buildup and lipogenesis			T0901317, oxysterols
NR1I1	VDR	KO	Atrophy, NMJ disruption			Vitamin D_3
NR2B3	RXRγ	KO	Lipolysis			9-*cis* retinoic acid
NR3A1	ERα	mKO	Muscle weakness	Pharm	Hypertrophy	Estradiol
NR3B1	ERRα	mKO	Glycolytic, reduced endurance exercise tolerance and regeneration			
NR3B3	ERRγ	mKO	Reduced endurance exercise capacity	mTG	Oxidative fibers, improved endurance	GSK4716
NR3C1	GR	mKO	Regulation of protein metabolism and prevention of atrophy	Pharm	Atrophy	Glucocorticoids
NR3C4	AR	mKO	Shift from slow to fast fibers	Pharm	Hypertrophy	Testosterone
NR4A1	NUR77	mKO	Atrophy	mTG	Hypertrophy, glucose utilization vs. oxidative metabolism[a]	
NR4A2	NURR1			mTG	Oxidative phenotype versus glycolytic fibers, high endurance, hypertrophy[a]	
NR4A3	NOR1			mTG	Oxidative phenotype versus glycolytic fibers, high endurance, hypertrophy[a]	

KO, Global knockout; mKO, muscle-specific knockout; mTG, muscle-specific transgenic; Pharm, pharmacological modulation.
[a]Conflicting data from different studies.

and obesity when fed a high-fat diet (Schuler et al. 2006). Interestingly, PPARβ/δ controls the expression of PGC-1α and thereby enhances its own activity by boosting transcriptional coactivation (Schuler et al. 2006). Thus, as a downstream effector from PPARβ/δ, PGC-1α exerts potent effects on endurance exercise adaptations even in the absence of PPARβ/δ in skeletal muscle (Pérez-Schindler et al. 2014).

Of the three PPARs, PPARγ depicts the lowest expression in skeletal muscle. Nevertheless, a role in the control of muscle metabolism was implied by observations in muscle-specific PPARγ knockout mice that develop adiposity and at least a mild insulin resistance under high-fat diet (Hevener et al. 2003; Norris et al. 2003). Animals with a muscle-specific transgenic overexpression of a modified PPARγ (harboring a mutation in the inhibitory phosphorylation site Ser86 and a carboxy-terminal fusion to the CR1 region of the adenovirus E1a gene that strongly promotes transcriptional activity) are protected against diet-induced insulin resistance and glucose intolerance, secrete elevated levels of adiponectin from muscle, and show a switch toward more oxidative fibers, similar to PPARβ/δ (Amin et al. 2010).

Subfamily 1, Group D: Rev-Erb—Type IV

Rev-Erbα (NR1D1) and Rev-Erbβ (NR1D2) are NRs with a dual role regulating the circadian clock and cellular metabolism (Cho et al. 2012). On binding of heme, the endogenous ligand of these NRs (Yin et al. 2007), the Rev-Erbs recruit corepressors such as the NR corepressor 1 (NCoR1) or the histone deacetylase 3 (HDAC3) and thus transcriptionally repress target genes. Gain- and loss-of-function studies of muscle Rev-Erbα revealed a prominent involvement in the regulation of mitochondrial biogenesis, mitophagy, promotion of a slow fiber type, and, ultimately, higher endurance capacity (Woldt et al. 2013). Mechanistically, muscle-specific ablation of the Rev-Erbα gene was associated with reduced activity of the AMP-dependent protein kinase (AMPK)–sirtuin 1 (SIRT1)–PGC-1α signaling axis (Woldt et al. 2013). Accordingly, mice treated with the Rev-Erbα agonist SR9009 show increased activation of these factors (Woldt et al. 2013). A contribution of Rev-Erbβ to the control of lipid uptake has been postulated (Ramakrishnan et al. 2005). However, in contrast to the well-established role of Rev-Erbα in the control of oxidative muscle function, the function of Rev-Erbβ in skeletal muscle remains poorly understood.

Subfamily 1, Group F: Retinoid-Related Orphan Receptors—Type IV

The transcriptional activity of the retinoid-related orphan receptors (RORs) is negatively affected by the Rev-Erb receptors, at least in the control of the circadian clock. However, with regard to skeletal muscle function, RORα (NR1F1) elicits changes that are in part similar to those described for Rev-Erbα, in particular in the regulation of lipid metabolism (Fitzsimmons et al. 2012). In addition, RORα also affects muscle lipogenesis, cholesterol efflux, insulin sensitivity, and glucose uptake. Mechanistically, these observations have been linked to a modulation of protein kinase B (PKB/Akt) and AMPK signaling coupled to a change in PGC-1α gene expression (Fitzsimmons et al. 2012). RORγ (NR1F3) is also highly expressed in skeletal muscle, but the function is less clear. Overexpression studies in muscle have linked RORγ to the regulation of genes involved in lipid and carbohydrate metabolism, and possibly muscle mass through the induction of the myostatin gene (Raichur et al. 2010). However, the physiological relevance of these observations is unknown. Moreover, because RORγ induces RORα and Rev-Erbα, it is not clear whether these effects are direct or indirect (Raichur et al. 2010).

Subfamily 1, Group H: Liver X Receptor—Type II

Liver X receptors (LXR) LXRα (NR1H3) and LXRβ (NR1H2) have potent effects on cholesterol efflux in various tissues and cell types. Both receptors have been linked to anabolic pathways in skeletal muscle, including glycogen buildup and lipogenesis (Archer et al. 2014). Long-term treatment of mice with the synthetic

Cold Spring Harbor Perspectives in Medicine
www.perspectivesinmedicine.org

LXR agonist T0901317 elevated lipogenesis and reverse cholesterol transport in wild-type and in LXRα, but to a lesser extent in LXRβ knockout animals, indicating that LXRβ might constitute the more relevant LXR variant in skeletal muscle (Hessvik et al. 2010). The anabolic function of the LXRs indicate that these receptors are involved in regeneration processes between exercise bouts to replenish intramuscular glycogen and lipid stores, for example, when coactivated by PGC-1α (Summermatter et al. 2010).

Subfamily 1, Group I: Vitamin D Receptor—Type II

The vitamin D receptor (VDR, NR1I1) is involved in regulating mineral metabolism. In humans, polymorphisms of the VDR gene are associated with aberrations in muscle strength (Pojednic and Ceglia 2014). In mice, VDR gene ablation results in muscle fiber atrophy, motor deficits, decreased locomotive activity after exercise and reduced neuromuscular maintenance (Girgis et al. 2014; Sakai et al. 2015). Endogenous VDR gene expression is induced after resistance training in rats (Makanae et al. 2015). Combined with studies using vitamin D administration in human patients, a positive role of the VDR in the control of muscle mass, fiber hypertrophy, and anabolic capacity can be predicted (Pojednic and Ceglia 2014).

Subfamily 2, Group B: Retinoid X Receptors—Type III

In addition to their ability to homodimerize, the retinoid X receptor (RXR) family members RXRα (NR2B1), RXRβ (NR2B2), and RXRγ (NR2B3) are obligate heterodimerization partners for a number of NRs and thus play a unique role in modulating and integrating the function of these different receptors (Perez et al. 2012; Evans and Mangelsdorf 2014). Although RXRβ is ubiquitously expressed, RXRα and RXRγ levels are enriched in some tissues, including skeletal muscle. Global RXRγ knockout animals have a leaner phenotype after a high-fat diet feeding, which is most likely attributed to an up-regulation of lipoprotein lipase in skeletal muscle (Haugen et al. 2004). However, little is known about the specific functions of all three RXRs in skeletal muscle. Intriguingly, NR/RXR heterodimers are classified as "permissive" and "nonpermissive." Permissive RXR heterodimers include the interactions with PPARs or LXRs and thus are activated by either RXR or PPAR/LXR ligands. In contrast, TR and VDR interact with RXR in a nonpermissive manner and therefore are not activated by 9-*cis* retinoic acid or other RXR ligands (Perez et al. 2012). Activation of RXRs in skeletal muscle would thus be expected to be linked to increased action of permissive but not of nonpermissive NR heterodimerization partners.

Subfamily 3, Groups A and C: Estrogen Receptor, Androgen Receptor, Glucocorticoid Receptor—Type I

Estrogens have primarily been linked to reduced inflammation and enhanced regeneration of skeletal muscle in ovariectomized rodents or postmenopausal women (Lowe et al. 2010; Diel 2014). In addition, it is now clear that estrogens also improve muscle mass and strength even though it is disputed whether increased quantity or quality of muscle is the driver of these changes. Both estrogen receptors (ERs) ERα (NR3A1) and ERβ (NR3A2) are expressed in skeletal muscle, are induced by exercise (Wiik et al. 2005) and thought to contribute to the effects of estrogen in this tissue. Intriguingly, at least some of the effects of estrogen, for example, activation of AMPK, might be mediated by nongenomic signaling pathways and thereby reinforce the receptor-dependent adaptations (Oosthuyse and Bosch 2012).

Male sex hormones elicit potent anabolic effects on skeletal muscle tissue, but also enhance muscle regeneration (O'Connell and Wu 2014). Most of these effects are mediated by activation of the androgen receptor (AR) NR3C4, in particular, the strong boost in muscle protein synthesis. Accordingly, muscle hypertrophy elicited by resistance training is attenuated by AR blockage (Inoue et al. 1994). Regulation of AR levels after resistance exercise seems to depend on a complex control of contractile and

Cold Spring Harbor Perspectives in Medicine
www.perspectivesinmedicine.org

nutritional cues, and can vary between different fiber types (Gonzalez et al. 2016). Similarly, the contradicting results of physiological testosterone fluctuations and muscle hypertrophy in different human studies imply a more complex interaction between androgens, growth hormone, and insulin-like growth factor 1 (IGF1) in this context (Gonzalez et al. 2016). However, the anabolic effect of superphysiological concentrations of testosterone consistently includes an improvement of muscle mass caused by hypertrophy of type I and type II fibers as well as muscle strength and power, whereas fatigability and muscle quality, defined as ratio between muscle strength to size, are less affected in humans (O'Connell and Wu 2014). The central role for the AR to regulate muscle development, mass, strength, and fatigue resistance was confirmed by experiments in male AR knockout mice (MacLean et al. 2008). Somewhat contradictory, a different AR knockout mouse model depicted a shift from oxidative toward glycolytic muscle fibers, thereby also linking the AR to the maintenance of slow-twitch oxidative fibers (Altuwaijri et al. 2004).

In contrast to the positive effects of ERs and the AR on muscle mass and function, the glucocorticoid receptor (GR), NR3C1, has been associated with atrophy of primarily type II muscle fibers (Kuo et al. 2013; Schakman et al. 2013). Cortisol, the ligand of the GR, is a stress hormone released during exercise, starvation, or sepsis that contributes to the metabolic remodeling in various tissues (Kraemer and Ratamess 2005). In skeletal muscle, one effect of cortisol is the stimulation of protein breakdown and the inhibition of protein synthesis (Schakman et al. 2013). Although short-term elevation of cortisol is a normal response to acute exercise bouts, chronic elevation can be an indicator of overtraining or training-induced stress. The ratio between testosterone and cortisol has been proposed to correlate with the anabolic and catabolic state of skeletal muscle, respectively, even though this interpretation is debated (Kraemer and Ratamess 2005). The GR is up-regulated by physical activity, most notably by eccentric resistance exercise bouts, but this induction is attenuated by chronic training, as is the increase in circulating cortisol. In line, a reduction in muscle mass is a common side effect in patients treated with corticosteroids. However, paradoxically, Duchenne muscular dystrophy patients profit from administration of glucocorticoids. Even though the mechanisms behind this therapeutic effect is unclear, anti-inflammatory properties, up-regulation of utrophin, normalization of intramyocellular calcium homeostasis, and stabilization of the muscle fiber membrane have been proposed to contribute to the positive outcome of glucocorticoid treatment in Duchenne patients (Matthews et al. 2016).

Subfamily 3, Group B: Estrogen-Related Receptors—Type IV

Estrogen-related receptors (ERRs) ERRα (NR3B1), ERRβ (NR3B2), and ERRγ (NR3B3) are all substantially expressed in tissues with a high energetic demand, for example, skeletal muscle (Fan and Evans 2015). Muscle-specific ERRα knockout animals show an impaired muscle regeneration capacity, compromised antioxidant response, reduced oxidative capacity, and angiogenesis (LaBarge et al. 2014). Moreover, these mice have a blunted response to high-fat diet and exercise, including impaired exercise tolerance, and muscle fitness (LaBarge et al. 2014; Perry et al. 2014; Huss et al. 2015). ERRα gene expression is induced by physical activity in animals and humans, and this receptor then coordinates the expression of genes involved in lipid uptake, metabolism, and mitochondrial OXPHOS (Huss et al. 2015). Even though cholesterol has been recently postulated as endogenous ERRα ligand (Wei et al. 2016), the transcriptional activity of all three ERRs is thought to be mainly driven by coregulator binding. In the case of ERRα, the coactivator PGC-1α seems of particular relevance for the regulation of target genes in skeletal muscle (Mootha et al. 2004). In fact, the genomic context of regulatory elements in target gene enhancers and promoters might dynamically determine the interaction and activity of these two proteins (Salatino et al. 2016).

ERRα and ERRγ have a considerable overlap in binding sites and accordingly regulate similar metabolic genes (Fan and Evans 2015).

Nevertheless, differences in the regulation of the TCA cycle and the inability of ERRα to compensate for the loss of ERRγ in null mice highlight the specific roles for these two receptors (Eichner and Giguere 2011). Like ERRα, ERRγ is induced by exercise. Skeletal muscle-specific overexpression of ERRγ alone or when fused to VP16 leads to a switch to oxidative fiber types and induces mitochondrial biogenesis and angiogenesis, collectively resulting in an improved endurance capacity (Rangwala et al. 2010; Narkar et al. 2011). Many of these effects can also be elicited by treatment with the ERRγ-specific synthetic activator GSK4716 (Rangwala et al. 2010). Inversely, a reduced exercise capacity was observed in ERRγ muscle-specific knockouts (Gan et al. 2013).

ERRβ is the least characterized receptor of this group and, despite high expression in skeletal muscle, regulation and function are largely unexplored. A partial redundancy between ERRβ and ERRγ with regard to the maintenance of type I fibers in mixed muscle beds has been proposed (Gan et al. 2013), but mechanistic aspects and a comprehensive analysis remain elusive.

Subfamily 4, Group A: Neuron-Derived Clone 77/Nerve Growth Factor IB, Neuron-Derived Orphan Receptor 1—Type IV

All three mammalian members of this group of NRs, neuron-derived Clone 77/nerve growth factor IB (Nur77) NR4A1, NR related 1 protein (Nurr1) NR4A2, and neuron-derived orphan receptor 1 (Nor1) NR4A3 are induced by a single bout of exhaustive endurance exercise in human skeletal muscle (Mahoney et al. 2005); however, little is known about the role of Nurr1 in this tissue. Nur77 is predominantly expressed in glycolytic muscle fibers and was first postulated to be involved in the control of glucose metabolism (Chao et al. 2007). Later findings surprisingly implied an involvement of Nur77 in the regulation of oxidative metabolism and, accordingly, muscle-specific overexpression of Nur77 results in an increase in the proportion of oxidative muscle fibers, and mitochondrial DNA content with a concomitant shift from glucose utilization to fatty acid oxidation and improved fatigue resistance (Chao et al. 2012). Recently, however, Nur77 activity was associated with muscle growth, most likely controlled by activation of the IGF1-Akt-mammalian target of rapamycin (mTOR) signaling axis leading to the up-regulation of a hypertrophic gene program and an attenuation of the expression of the proatrophic myostatin as well as the E3 ubiquitin ligases MAFbx and MuRF1 (Tontonoz et al. 2015). However, while skeletal muscle–specific Nur77 mice do not depict increased muscle mass despite fiber hypertrophy, animals with a specific gene ablation of Nur77 in skeletal muscle show reduced myofiber size and muscle mass (Tontonoz et al. 2015).

Like Nur77, Nor1 is also induced by acute exercise and β2-adrenergic signaling however, both in glycolytic and oxidative muscle fibers (Fan et al. 2013). Skeletal muscle-specific overexpression of Nor1 in mice results in an oxidative, high-endurance phenotype with increased mitochondrial number and DNA, elevated myoglobin, enhanced ATP production, and PGC-1α gene expression (Pearen et al. 2013). Intriguingly, a shift from type I and IIb toward type IIa and IIx muscle fibers is observed in these animals (Mizunoya 2015). These fatigue-resistant Nor1 transgenic animals also show improved autophagy after endurance exercise, leading to better clearing of debris in the tissue (Goode et al. 2016). Unexpectedly, Nor1 overexpression was recently also linked to muscle hypertrophy and increased vascularization in skeletal muscle via activation of the mTOR signaling pathway (Goode et al. 2016).

NR COREGULATORS

The transcriptional activity of NRs is affected by recruitment of coactivator and corepressor proteins, which can occur in a ligand-dependent and ligand-independent manner. In skeletal muscle, several coregulators have been identified that modulate metabolic and contractile properties at least in part by binding to the NRs described in this review. Most prominently, muscle-specific overexpression of PGC-1α and the related PGC-1β are sufficient to promote a

Cold Spring Harbor Perspectives in Medicine
www.perspectivesinmedicine.org

fiber-type switch toward type I/IIa and IIx, respectively, even though it is not clear whether the latter occurs under physiological conditions (Eisele and Handschin 2014). Of these two coactivators, only PGC-1α levels and activity are clearly associated with physical activity (Lin et al. 2002; Kupr and Handschin 2015), and gain- and loss-of-function in skeletal muscle result in improved and impaired endurance capacity, respectively (Lin et al. 2002; Handschin et al. 2007). Recently, the PGC-1α4 isoform was identified to promote a hypertrophic response in skeletal muscle (Ruas et al. 2012) in contrast to the PGC-1α1, -1α2, and -1α3 isoforms that have been linked to an endurance program (Martinez-Redondo et al. 2015). The expression of the corepressor NCoR1 is higher in inactive skeletal muscle, and NCoR1 competes with PGC-1α for binding to ERRα (Pérez-Schindler et al. 2012). Accordingly, muscle-specific NCoR1 knockout mice recapitulate many of the metabolic adaptations that are also observed in PGC-1α transgenic animals (Pérez-Schindler et al. 2012). Similarly, overexpression and knockout of the corepressor receptor-interacting protein 140 (RIP140) results in decreased and elevated numbers of oxidative muscle fibers, respectively (Seth et al. 2007). This complex still poorly understood regulatory network of coactivator and corepressor proteins is thus intricately linked to NR action in skeletal muscle plasticity (Schnyder et al. 2016).

EXERCISE MIMETICS

Several pharmacological agents have already been proposed to act as "exercise mimetics," including three that activate NRs: SR9009 (Rev-Erbα), GSK4716 (ERRγ), and GW501516 (PPARβ/δ) (Handschin 2016). With well-defined and conserved ligand-binding domains, it is conceivable that other NRs could also be targeted to take advantage of their function in skeletal muscle. Importantly, however, for none of the currently proposed "exercise mimetics," have efficacy and safety been tested in humans to date. The alarming use of some of these compounds as performance-enhancing drugs in athletes with a subsequent ban by the World Anti-Doping Agency underlines the need for a better understanding of the mechanisms, side effects, toxicity, and dosage (Wall et al. 2016). The summary of NRs and coregulators in this review should further illustrate the regulatory complexity of skeletal muscle plasticity, which is vastly expanded by non-NR TFs and signaling pathways (Hoppeler 2016). Despite the results in animal models with a higher endurance capacity, the expected effects of pharmacological modulation of one NR in skeletal muscle are difficult to reconcile with the myriad of muscular and nonmuscular adaptations elicited by bona fide physical activity (Booth and Laye 2009).

OPEN QUESTIONS

Of the 35 NRs expressed in mouse skeletal muscle, we have discussed here 26 with a potential role in exercise adaptation and skeletal muscle plasticity. A majority of these promote an oxidative, high-endurance phenotype (Fig. 2). The signaling networks and transcriptional hierarchies between these receptors are, however, not clear. Moreover, it is unknown whether the high number of NRs with seemingly overlapping function is a sign of transcriptional redundancy or represents specific regulation of highly specialized adaptations. An oxidative phenotype can, for example, be achieved by a down-regulation of type I and IIb fibers in the case of Nor1 or by the more classic shift from type IIb and IIx toward IIa and I as seen in overexpression studies with PPARβ/δ or ERRγ. Furthermore, the alternating classification of Nur77 and Nor1 as pro-oxidative and proglycolytic NRs highlight a potential discrepancy between the results obtained in different experimental contexts, for example, cultured muscle cells compared with the constitutive transgenic elevation in skeletal muscle in vivo. These somewhat contradictory results with regard to the effects on glucose and lipid oxidation as well as glycolytic and oxidative fiber promotion, respectively, will therefore have to be clarified in future studies. Furthermore, whether the effects of Nur77 and Nor1 on muscle mass are primarily mediated by altered myogenesis or represent a bona fide modulation of atrophy and hypertrophy in regeneration and exercise in

Cold Spring Harbor Perspectives in Medicine
www.perspectivesinmedicine.org

adult muscle remains to be shown. Similarly, the extensive study of anabolic steroids emerged with a consensus of increased muscle hypertrophy in humans. Nevertheless, results obtained in some but not all AR knockout mouse models imply a role for the AR in promoting an oxidative, high-endurance phenotype. Similarly, the effect of genetic ablation of the TRs on fiber-type distribution might appear contradictory vis-à-vis the mitochondrial boost elicited by short-term treatment with thyroid hormone. These and other examples show that the choice of model and the way of treatment might significantly alter the outcome. Therefore, caution should be used for the extrapolation of results from cell culture, nonconditional knockouts, and transgenic animals to the physiological role of NRs in skeletal muscle in humans.

CONCLUDING REMARKS

Endurance and resistance exercise confer many beneficial health effects, which substantially lower the risk for many chronic diseases and are a therapeutic pillar for a number of different pathologies. Even though the molecular mechanisms of muscle plasticity are still poorly understood, NRs are attractive drug targets to take advantage of some of the therapeutic effects of exercise. The ever-increasing prevalence of chronic diseases, age-related afflictions and pathologies associated with exercise intolerance indicate that even partial "exercise mimetics" might confer a significant relief for patients and overburdened health care systems. However, at the moment, it is not clear whether such drugs exist and, if so, whether they can be effectively and safely used in patients. Therefore, physical activity and diet should stay at the forefront of disease prevention and treatment wherever possible (Booth et al. 2012; Pedersen and Saltin 2015) until better pharmacological interventions targeted at improving muscle function are available.

ACKNOWLEDGMENTS

We apologize for omission of a copious amount of primary literature because of space limitations. We thank Regula Furrer for critical comments on our manuscript. Work in our group is supported by the Swiss National Science Foundation, the European Research Council (ERC) Consolidator Grant 616830-MUSCLE_NET, Swiss Cancer Research Grant KFS-3733-08-2015, the Swiss Society for Research on Muscle Diseases (SSEM), SystemsX.ch, the Novartis Stiftung für Medizinisch-Biologische Forschung and the University of Basel. B.K. is the recipient of a Fellowship for Excellence of the International PhD Program of the Biozentrum, University of Basel.

The authors declare no conflict of interest.

REFERENCES

Altuwaijri S, Lee DK, Chuang KH, Ting HJ, Yang Z, Xu Q, Tsai MY, Yeh S, Hanchett LA, Chang HC, et al. 2004. Androgen receptor regulates expression of skeletal muscle-specific proteins and muscle cell types. *Endocrine* **25**: 27–32.

Amin RH, Mathews ST, Camp HS, Ding L, Leff T. 2010. Selective activation of PPARγ in skeletal muscle induces endogenous production of adiponectin and protects mice from diet-induced insulin resistance. *Am J Physiol Endorinol Metab* **298**: E28–E37.

Archer A, Laurencikiene J, Ahmed O, Steffensen KR, Parini P, Gustafsson JA, Korach-Andre M. 2014. Skeletal muscle as a target of LXR agonist after long-term treatment: Focus on lipid homeostasis. *Am J Physiol Endocrinol Metab* **306**: E494–E502.

Auwerx J, Baulieu E, Beato M, Becker-Andre M, Burbach PH, Camerino G, Chambon P, Cooney A, Dejean A, Dreyer C, et al. 1999. A unified nomenclature system for the nuclear receptor superfamily. *Cell* **97**: 161–163.

Bahi L, Garnier A, Fortin D, Serrurier B, Veksler V, Bigard AX, Ventura-Clapier R. 2005. Differential effects of thyroid hormones on energy metabolism of rat slow- and fast-twitch muscles. *J Cell Physiol* **203**: 589–598.

Bookout AL, Jeong Y, Downes M, Yu RT, Evans RM, Mangelsdorf DJ. 2006. Anatomical profiling of nuclear receptor expression reveals a hierarchical transcriptional network. *Cell* **126**: 789–799.

Booth FW, Laye MJ. 2009. Lack of adequate appreciation of physical exercise's complexities can pre-empt appropriate design and interpretation in scientific discovery. *J Physiol* **587**: 5527–5539.

Booth FW, Roberts CK, Laye MJ. 2012. Lack of exercise is a major cause of chronic diseases. *Compr Physiol* **2**: 1143–1211.

Camera DM, Smiles WJ, Hawley JA. 2016. Exercise-induced skeletal muscle signaling pathways and human athletic performance. *Free Radic Biol Med* **98**: 131–143.

Chao LC, Zhang Z, Pei L, Saito T, Tontonoz P, Pilch PF. 2007. Nur77 coordinately regulates expression of genes linked

to glucose metabolism in skeletal muscle. *Mol Endocrinol* **21**: 2152–2163.

Chao LC, Wroblewski K, Ilkayeva OR, Stevens RD, Bain J, Meyer GA, Schenk S, Martinez L, Vergnes L, Narkar VA, et al. 2012. Skeletal muscle Nur77 expression enhances oxidative metabolism and substrate utilization. *J Lipid Res* **53**: 2610–2619.

Cho H, Zhao X, Hatori M, Yu RT, Barish GD, Lam MT, Chong LW, DiTacchio L, Atkins AR, Glass CK, et al. 2012. Regulation of circadian behaviour and metabolism by REV-ERB-α and REV-ERB-β. *Nature* **485**: 123–127.

Diel P. 2014. The role of the estrogen receptor in skeletal muscle mass homeostasis and regeneration. *Acta Physiol (Oxf)* **212**: 14–16.

Egan B, Zierath JR. 2013. Exercise metabolism and the molecular regulation of skeletal muscle adaptation. *Cell Metab* **17**: 162–184.

Eichner LJ, Giguere V. 2011. Estrogen related receptors (ERRs): A new dawn in transcriptional control of mitochondrial gene networks. *Mitochondrion* **11**: 544–552.

Eisele PS, Handschin C. 2014. Functional crosstalk of PGC-1 coactivators and inflammation in skeletal muscle pathophysiology. *Semin Immunopathol* **36**: 27–53.

Escriva H, Bertrand S, Laudet V. 2004. The evolution of the nuclear receptor superfamily. *Essays Biochem* **40**: 11–26.

Evans RM, Mangelsdorf DJ. 2014. Nuclear receptors, RXR, and the big bang. *Cell* **157**: 255–266.

Fan W, Evans R. 2015. PPARs and ERRs: Molecular mediators of mitochondrial metabolism. *Curr Opin Cell Biol* **33**: 49–54.

Fan W, Downes M, Atkins A, Yu R, Evans RM. 2011. Nuclear receptors and AMPK: Resetting metabolism. *Cold Spring Harb Symp Quant Biol* **76**: 17–22.

Fan W, Atkins AR, Yu RT, Downes M, Evans RM. 2013. Road to exercise mimetics: Targeting nuclear receptors in skeletal muscle. *J Mol Endocrinol* **51**: T87–T100.

Finck BN, Bernal-Mizrachi C, Han DH, Coleman T, Sambandam N, LaRiviere LL, Holloszy JO, Semenkovich CF, Kelly DP. 2005. A potential link between muscle peroxisome proliferator-activated receptor-α signaling and obesity-related diabetes. *Cell Metab* **1**: 133–144.

Fitzsimmons RL, Lau P, Muscat GE. 2012. Retinoid-related orphan receptor α and the regulation of lipid homeostasis. *J Steroid Biochem Mol Biol* **130**: 159–168.

Frontera WR, Ochala J. 2015. Skeletal muscle: A brief review of structure and function. *Calcif Tissue Int* **96**: 183–195.

Gan Z, Burkart-Hartman EM, Han DH, Finck B, Leone TC, Smith EY, Ayala JE, Holloszy J, Kelly DP. 2011. The nuclear receptor PPARβ/δ programs muscle glucose metabolism in cooperation with AMPK and MEF2. *Genes Dev* **25**: 2619–2630.

Gan Z, Rumsey J, Hazen BC, Lai L, Leone TC, Vega RB, Xie H, Conley KE, Auwerx J, Smith SR, et al. 2013. Nuclear receptor/microRNA circuitry links muscle fiber type to energy metabolism. *J Clin Invest* **123**: 2564–2575.

Germain P, Staels B, Dacquet C, Spedding M, Laudet V. 2006. Overview of nomenclature of nuclear receptors. *Pharmacol Rev* **58**: 685–704.

Girgis CM, Mokbel N, Cha KM, Houweling PJ, Abboud M, Fraser DR, Mason RS, Clifton-Bligh RJ, Gunton JE. 2014. The vitamin D receptor (VDR) is expressed in skeletal muscle of male mice and modulates 25-hydroxyvitamin D (25OHD) uptake in myofibers. *Endocrinology* **155**: 3227–3237.

Gonzalez AM, Hoffman JR, Stout JR, Fukuda DH, Willoughby DS. 2016. Intramuscular anabolic signaling and endocrine response following resistance exercise: Implications for muscle hypertrophy. *Sports Med* **46**: 671–685.

Goode JM, Pearen MA, Tuong ZK, Wang SC, Oh TG, Shao EX, Muscat GE. 2016. The nuclear receptor, Nor-1, induces the physiological responses associated with exercise. *Mol Endocrinol* **30**: 660–676.

Handschin C. 2016. Caloric restriction and exercise "mimetics": Ready for prime time? *Pharmacol Res* **103**: 158–166.

Handschin C, Spiegelman BM. 2008. The role of exercise and PGC1α in inflammation and chronic disease. *Nature* **454**: 463–469.

Handschin C, Chin S, Li P, Liu F, Maratos-Flier E, Lebrasseur NK, Yan Z, Spiegelman BM. 2007. Skeletal muscle fiber-type switching, exercise intolerance, and myopathy in PGC-1α muscle-specific knock-out animals. *J Biol Chem* **282**: 30014–30021.

Haugen BR, Jensen DR, Sharma V, Pulawa LK, Hays WR, Krezel W, Chambon P, Eckel RH. 2004. Retinoid X receptor γ-deficient mice have increased skeletal muscle lipoprotein lipase activity and less weight gain when fed a high-fat diet. *Endocrinology* **145**: 3679–3685.

Hawley JA, Hargreaves M, Joyner MJ, Zierath JR. 2014. Integrative biology of exercise. *Cell* **159**: 738–749.

Hessvik NP, Boekschoten MV, Baltzersen MA, Kersten S, Xu X, Andersen H, Rustan AC, Thoresen GH. 2010. LXRβ is the dominant LXR subtype in skeletal muscle regulating lipogenesis and cholesterol efflux. *Am J Physiol Endocrinol Metab* **298**: E602–E613.

Hevener AL, He WM, Barak Y, Le J, Bandyopadhyay G, Olson P, Wilkes J, Evans RM, Olefsky J. 2003. Muscle-specific *Pparg* deletion causes insulin resistance. *Nat Med* **9**: 1491–1497.

Hoppeler H. 2016. Molecular networks in skeletal muscle plasticity. *J Exp Biol* **219**: 205–213.

Huss JM, Garbacz WG, Xie W. 2015. Constitutive activities of estrogen-related receptors: Transcriptional regulation of metabolism by the ERR pathways in health and disease. *Biochim Biophys Acta* **1852**: 1912–1927.

Inoue K, Yamasaki S, Fushiki T, Okada Y, Sugimoto E. 1994. Androgen receptor antagonist suppresses exercise-induced hypertrophy of skeletal muscle. *Eur J Appl Physiol Occup Physiol* **69**: 88–91.

Irrcher I, Adhihetty PJ, Sheehan T, Joseph AM, Hood DA. 2003. PPARγ coactivator-1α expression during thyroid hormone- and contractile activity-induced mitochondrial adaptations. *Am J Physiol Cell Physiol* **284**: C1669–C1677.

Kraemer WJ, Ratamess NA. 2005. Hormonal responses and adaptations to resistance exercise and training. *Sports Med* **35**: 339–361.

Kuo T, Harris CA, Wang JC. 2013. Metabolic functions of glucocorticoid receptor in skeletal muscle. *Mol Cell Endocrinol* **380**: 79–88.

Kupr B, Handschin C. 2015. Complex coordination of cell plasticity by a PGC-1α-controlled transcriptional network in skeletal muscle. *Front Physiol* **6**: 325.

LaBarge S, McDonald M, Smith-Powell L, Auwerx J, Huss JM. 2014. Estrogen-related receptor-α (ERRα) deficiency in skeletal muscle impairs regeneration in response to injury. *FASEB J* **28**: 1082–1097.

Lima GA, Anhe GF, Giannocco G, Nunes MT, Correa-Giannella ML, Machado UF. 2009. Contractile activity per se induces transcriptional activation of SLC2A4 gene in soleus muscle: Involvement of MEF2D, HIF-1a, and TRα transcriptional factors. *Am J Physiol Endocrinol Metab* **296**: E132–E138.

Lin J, Wu H, Tarr PT, Zhang CY, Wu Z, Boss O, Michael LF, Puigserver P, Isotani E, Olson EN, et al. 2002. Transcriptional co-activator PGC-1α drives the formation of slow-twitch muscle fibres. *Nature* **418**: 797–801.

Lowe DA, Baltgalvis KA, Greising SM. 2010. Mechanisms behind estrogen's beneficial effect on muscle strength in females. *Exerc Sport Sci Rev* **38**: 61–67.

Luquet S, Lopez-Soriano J, Holst D, Fredenrich A, Melki J, Rassoulzadegan M, Grimaldi PA. 2003. Peroxisome proliferator-activated receptor δ controls muscle development and oxidative capability. *FASEB J* **17**: 2299–2301.

MacLean HE, Chiu WS, Notini AJ, Axell AM, Davey RA, McManus JF, Ma C, Plant DR, Lynch GS, Zajac JD. 2008. Impaired skeletal muscle development and function in male, but not female, genomic androgen receptor knockout mice. *FASEB J* **22**: 2676–2689.

Mahoney DJ, Parise G, Melov S, Safdar A, Tarnopolsky MA. 2005. Analysis of global mRNA expression in human skeletal muscle during recovery from endurance exercise. *FASEB J* **19**: 1498–1500.

Makanae Y, Ogasawara R, Sato K, Takamura Y, Matsutani K, Kido K, Shiozawa N, Nakazato K, Fujita S. 2015. Acute bout of resistance exercise increases vitamin D receptor protein expression in rat skeletal muscle. *Exp Physiol* **100**: 1168–1176.

Martinez-Redondo V, Pettersson AT, Ruas JL. 2015. The hitchhiker's guide to PGC-1α isoform structure and biological functions. *Diabetologia* **58**: 1969–1977.

Matthews E, Brassington R, Kuntzer T, Jichi F, Manzur AY. 2016. Corticosteroids for the treatment of Duchenne muscular dystrophy. *Cochrane Database Syst Rev* **5**: CD003725.

Mizunoya W. 2015. Nuclear receptors and skeletal muscle fiber type. *J Phys Fitness Sports Med* **4**: 259–270.

Mootha VK, Handschin C, Arlow D, Xie X, St Pierre J, Sihag S, Yang W, Altshuler D, Puigserver P, Patterson N, et al. 2004. Errα and Gabpa/b specify PGC-1α-dependent oxidative phosphorylation gene expression that is altered in diabetic muscle. *Proc Natl Acad Sci* **101**: 6570–6575.

Muoio DM, MacLean PS, Lang DB, Li S, Houmard JA, Way JM, Winegar DA, Corton JC, Dohm GL, Kraus WE. 2002. Fatty acid homeostasis and induction of lipid regulatory genes in skeletal muscles of peroxisome proliferator-activated receptor (PPAR) α knock-out mice. Evidence for compensatory regulation by PPARδ. *J Biol Chem* **277**: 26089–26097.

Narkar VA, Downes M, Yu RT, Embler E, Wang YX, Banayo E, Mihaylova MM, Nelson MC, Zou Y, Juguilon H, et al. 2008. AMPK and PPARδ agonists are exercise mimetics. *Cell* **134**: 405–415.

Narkar VA, Fan W, Downes M, Yu RT, Jonker JW, Alaynick WA, Banayo E, Karunasiri MS, Lorca S, Evans RM. 2011. Exercise and PGC-1α-independent synchronization of type I muscle metabolism and vasculature by ERRγ. *Cell Metab* **13**: 283–293.

Norris AW, Chen L, Fisher SJ, Szanto I, Ristow M, Jozsi AC, Hirshman MF, Rosen ED, Goodyear LJ, Gonzalez FJ, et al. 2003. Muscle-specific PPARγ-deficient mice develop increased adiposity and insulin resistance but respond to thiazolidinediones. *J Clin Invest* **112**: 608–618.

O'Connell MD, Wu FC. 2014. Androgen effects on skeletal muscle: Implications for the development and management of frailty. *Asian J Androl* **16**: 203–212.

Oosthuyse T, Bosch AN. 2012. Oestrogen's regulation of fat metabolism during exercise and gender specific effects. *Curr Opin Pharmacol* **12**: 363–371.

Pardee K, Necakov AS, Krause H. 2011. Nuclear receptors: Small molecule sensors that coordinate growth, metabolism and reproduction. *Subcell Biochem* **52**: 123–153.

Pearen MA, Goode JM, Fitzsimmons RL, Eriksson NA, Thomas GP, Cowin GJ, Wang SC, Tuong ZK, Muscat GE. 2013. Transgenic muscle-specific Nor-1 expression regulates multiple pathways that effect adiposity, metabolism, and endurance. *Mol Endocrinol* **27**: 1897–1917.

Pedersen BK, Saltin B. 2015. Exercise as medicine—Evidence for prescribing exercise as therapy in 26 different chronic diseases. *Scand J Med Sci Sports* **25**: 1–72.

Perez E, Bourguet W, Gronemeyer H, de Lera AR. 2012. Modulation of RXR function through ligand design. *Biochim Biophys Acta* **1821**: 57–69.

Pérez-Schindler J, Summermatter S, Salatino S, Zorzato F, Beer M, Balwierz PJ, van Nimwegen E, Feige JN, Auwerx J, Handschin C. 2012. The corepressor NCoR1 antagonizes PGC-1α and estrogen-related receptor α in the regulation of skeletal muscle function and oxidative metabolism. *Mol Cell Biol* **32**: 4913–4924.

Pérez-Schindler J, Svensson K, Vargas-Fernandez E, Santos G, Wahli W, Handschin C. 2014. The coactivator PGC-1α regulates skeletal muscle oxidative metabolism independently of the nuclear receptor PPARβ/δ in sedentary mice fed a regular chow diet. *Diabetologia* **57**: 2405–2412.

Perry MC, Dufour CR, Tam IS, B'chir W, Giguere V. 2014. Estrogen-related receptor-α coordinates transcriptional programs essential for exercise tolerance and muscle fitness. *Mol Endocrinol* **28**: 2060–2071.

Pojednic RM, Ceglia L. 2014. The emerging biomolecular role of vitamin D in skeletal muscle. *Exerc Sport Sci Rev* **42**: 76–81.

Qaisar R, Bhaskaran S, Van Remmen H. 2016. Muscle fiber type diversification during exercise and regeneration. *Free Radic Biol Med* **98**: 56–67.

Raichur S, Fitzsimmons RL, Myers SA, Pearen MA, Lau P, Eriksson N, Wang SM, Muscat GE. 2010. Identification and validation of the pathways and functions regulated by the orphan nuclear receptor, ROR α1, in skeletal muscle. *Nucleic Acids Res* **38**: 4296–4312.

Ramakrishnan SN, Lau P, Burke LJ, Muscat GE. 2005. Rev-erbβ regulates the expression of genes involved in lipid

absorption in skeletal muscle cells: Evidence for crosstalk between orphan nuclear receptors and myokines. *J Biol Chem* **280**: 8651–8659.

Rangwala SM, Wang X, Calvo JA, Lindsley L, Zhang Y, Deyneko G, Beaulieu V, Gao J, Turner G, Markovits J. 2010. Estrogen-related receptor γ is a key regulator of muscle mitochondrial activity and oxidative capacity. *J Biol Chem* **285**: 22619–22629.

Ruas JL, White JP, Rao RR, Kleiner S, Brannan KT, Harrison BC, Greene NP, Wu J, Estall JL, Irving BA, et al. 2012. A PGC-1α isoform induced by resistance training regulates skeletal muscle hypertrophy. *Cell* **151**: 1319–1331.

Sakai S, Suzuki M, Tashiro Y, Tanaka K, Takeda S, Aizawa K, Hirata M, Yogo K, Endo K. 2015. Vitamin D receptor signaling enhances locomotive ability in mice. *J Bone Miner Res* **30**: 128–136.

Salatino S, Kupr B, Baresic M, van Nimwegen E, Handschin C. 2016. The genomic context and corecruitment of SP1 affect ERRα coactivation by PGC-1α in muscle cells. *Mol Endocrinol* **30**: 809–825.

Schakman O, Kalista S, Barbe C, Loumaye A, Thissen JP. 2013. Glucocorticoid-induced skeletal muscle atrophy. *Int J Biochem Cell Biol* **45**: 2163–2172.

Schnyder S, Handschin C. 2015. Skeletal muscle as an endocrine organ: PGC-1α, myokines and exercise. *Bone* **80**: 115–125.

Schnyder S, Kupr B, Handschin C. 2016. Coregulator-mediated control of skeletal muscle plasticity—A mini-review. *Biochimie* doi: 10.1016/j.biochi.2016.12.011.

Schuler M, Ali F, Chambon C, Duteil D, Bornert JM, Tardivel A, Desvergne B, Wahli W, Chambon P, Metzger D. 2006. PGC1α expression is controlled in skeletal muscles by PPARβ, whose ablation results in fiber-type switching, obesity, and type 2 diabetes. *Cell Metab* **4**: 407–414.

Seth A, Steel JH, Nichol D, Pocock V, Kumaran MK, Fritah A, Mobberley M, Ryder TA, Rowlerson A, Scott J, et al. 2007. The transcriptional corepressor RIP140 regulates oxidative metabolism in skeletal muscle. *Cell Metab* **6**: 236–245.

Smith AG, Muscat GE. 2005. Skeletal muscle and nuclear hormone receptors: Implications for cardiovascular and metabolic disease. *Int J Biochem Cell Biol* **37**: 2047–2063.

Summermatter S, Baum O, Santos G, Hoppeler H, Handschin C. 2010. Peroxisome proliferator-activated receptor γ coactivator 1α (PGC-1α) promotes skeletal muscle lipid refueling in vivo by activating de novo lipogenesis and the pentose phosphate pathway. *J Biol Chem* **285**: 32793–32800.

Svensson K, Albert V, Cardel B, Salatino S, Handschin C. 2016. Skeletal muscle PGC-1α modulates systemic ketone body homeostasis and ameliorates diabetic hyperketonemia in mice. *FASEB J* **30**: 1976–1986.

Tontonoz P, Cortez-Toledo O, Wroblewski K, Hong C, Lim L, Carranza R, Conneely O, Metzger D, Chao LC. 2015. The orphan nuclear receptor Nur77 is a determinant of myofiber size and muscle mass in mice. *Mol Cell Biol* **35**: 1125–1138.

Wall CE, Yu RT, Atkins AR, Downes M, Evans RM. 2016. Nuclear receptors and AMPK: Can exercise mimetics cure diabetes? *J Mol Endocrinol* **57**: R49–R58.

Wang YX, Zhang CL, Yu RT, Cho HK, Nelson MC, Bayuga-Ocampo CR, Ham J, Kang H, Evans RM. 2004. Regulation of muscle fiber type and running endurance by PPARδ. *PLoS Biol* **2**: e294.

Wei W, Schwaid AG, Wang X, Wang X, Chen S, Chu Q, Saghatelian A, Wan Y. 2016. Ligand activation of ERRα by cholesterol mediates statin and bisphosphonate effects. *Cell Metab* **23**: 479–491.

Wiik A, Gustafsson T, Esbjornsson M, Johansson O, Ekman M, Sundberg CJ, Jansson E. 2005. Expression of oestrogen receptor α and β is higher in skeletal muscle of highly endurance-trained than of moderately active men. *Acta Physiol Scand* **184**: 105–112.

Woldt E, Sebti Y, Solt LA, Duhem C, Lancel S, Eeckhoute J, Hesselink MK, Paquet C, Delhaye S, Shin Y, et al. 2013. Rev-erb-α modulates skeletal muscle oxidative capacity by regulating mitochondrial biogenesis and autophagy. *Nat Med* **19**: 1039–1046.

Yin L, Wu N, Curtin JC, Qatanani M, Szwergold NR, Reid RA, Waitt GM, Parks DJ, Pearce KH, Wisely GB, et al. 2007. Rev-erbα, a heme sensor that coordinates metabolic and circadian pathways. *Science* **318**: 1786–1789.

Yu F, Gothe S, Wikstrom L, Forrest D, Vennstrom B, Larsson L. 2000. Effects of thyroid hormone receptor gene disruption on myosin isoform expression in mouse skeletal muscles. *Am J Physiol Regul Integr Comp Physiol* **278**: R1545–R1554.

Cold Spring Harbor Perspectives in Medicine
www.perspectivesinmedicine.org

Appendix 3: Complex Coordination of Cell Plasticity by PGC-1α-controlled Transcriptional Network in skeletal Muscle

frontiers in Physiology

MINI REVIEW
published: 09 November 2015
doi: 10.3389/fphys.2015.00325

Complex Coordination of Cell Plasticity by a PGC-1α-controlled Transcriptional Network in Skeletal Muscle

Barbara Kupr and Christoph Handschin **

Biozentrum, University of Basel, Basel, Switzerland

Skeletal muscle cells exhibit an enormous plastic capacity in order to adapt to external stimuli. Even though our overall understanding of the molecular mechanisms that underlie phenotypic changes in skeletal muscle cells remains poor, several factors involved in the regulation and coordination of relevant transcriptional programs have been identified in recent years. For example, the peroxisome proliferator-activated receptor γ coactivator-1α (PGC-1α) is a central regulatory nexus in the adaptation of muscle to endurance training. Intriguingly, PGC-1α integrates numerous signaling pathways and translates their activity into various transcriptional programs. This selectivity is in part controlled by differential expression of PGC-1α variants and post-translational modifications of the PGC-1α protein. PGC-1α-controlled activation of transcriptional networks subsequently enables a spatio-temporal specification and hence allows a complex coordination of changes in metabolic and contractile properties, protein synthesis and degradation rates and other features of trained muscle. In this review, we discuss recent advances in our understanding of PGC-1α-regulated skeletal muscle cell plasticity in health and disease.

Keywords: skeletal muscle, transcriptional regulation, PGC-1α, exercise, metabolism, co-regulator

OPEN ACCESS

Edited by:
Russell T. Hepple, McGill University, Canada

Reviewed by:
Espen Spangenburg, East Carolina University, USA
Aaron Paul Russell, Aaron Russell, Australia

***Correspondence:**
Christoph Handschin
christoph.handschin@unibas.ch

Specialty section:
This article was submitted to Striated Muscle Physiology, a section of the journal Frontiers in Physiology

Received: *31 August 2015*
Accepted: *27 October 2015*
Published: *09 November 2015*

Citation:
Kupr B and Handschin C (2015) Complex Coordination of Cell Plasticity by a PGC-1α-controlled Transcriptional Network in Skeletal Muscle. Front. Physiol. 6:325. doi: 10.3389/fphys.2015.00325

INTRODUCTION

Cell plasticity is often controlled by complex transcriptional networks. While traditionally, much of the research on such networks was focused on transcription factors, the important role of co-regulators has been increasingly appreciated in recent years (Dasgupta et al., 2014; Mouchiroud et al., 2014). Co-regulator proteins have no intrinsic DNA-binding domain and thus rely on transcription factors to be recruited to regulatory elements. The ability of co-regulators to bind to various partners enables the regulation of broad, complex transcriptional programs. The peroxisome proliferator-activated receptor γ (PPARγ) coactivator-1α (PGC-1α) is a prototypical member of this class of proteins. Initially discovered in a screen comparing white and brown adipose tissue, expression of PGC-1α has subsequently been documented in all tissues with a high energetic demand, including brain, kidney, skeletal, and cardiac muscle, liver, pancreas, or the retina (Martínez-Redondo et al., 2015). The core function of PGC-1α centers on the induction of mitochondrial biogenesis and oxidative metabolism. PGC-1α likewise controls highly tissue-specific programs, such as hepatic gluconeogenesis or mitochondrial uncoupling in brown adipose tissue. Since the phenotype of global PGC-1α transgenic and

knockout mice is complex (Lin et al., 2004; Liang et al., 2009), many insights into organ-specific function and regulation of PGC-1α, including those discussed in this review unless otherwise stated, have mostly been obtained from murine tissue-specific gain- and loss-of-function models (Handschin et al., 2005). In skeletal muscle, specific overexpression of PGC-1α at physiological levels is sufficient to induce an endurance-trained phenotype (Lin et al., 2002) while super-physiological overexpression promotes fiber damage and impaired muscle function (Lin et al., 2002; Miura et al., 2006). Inversely, ablation of PGC-1α gene expression in this tissue promotes several typical signs of pathological inactivity, including a local and systemic chronic inflammation (Handschin et al., 2007a,b). A reduction in PGC-1α gene expression in human skeletal muscle has been associated with insulin resistance and type 2 diabetes, at least in some patient cohorts (Patti et al., 2003). Of note, mice with a heterozygous deletion of PGC-1α in skeletal muscle also exhibit a dysregulation of glucose homeostasis (Handschin et al., 2007b).

PGC-1α integrates the activity of the major signaling pathways that are important in a contracting muscle fiber and accordingly, PGC-1α transcript and protein levels are elevated after a training bout (Pérez-Schindler and Handschin, 2013). As consequence, PGC-1α then controls the biological program encompassing all plastic changes of the muscle cell to endurance exercise. For example, mice with elevated muscle PGC-1α levels exhibit a higher number of mitochondria, a switch toward oxidative, slow-twitch muscle fiber types, altered substrate synthesis and metabolism, and a reduction in muscle protein breakdown (Handschin, 2010). Importantly, the effects of PGC-1α extend beyond muscle cells: elevation of PGC-1α in muscle leads to higher tissue vascularization (Arany et al., 2008) and a remodeling of the post- and presynaptic side of the neuromuscular junction (Handschin et al., 2007c; Arnold et al., 2014). Furthermore, PGC-1α-regulated endocrine mediators, members of the so-called myokine protein family, promote beige fat cell differentiation and activation in white adipose tissue or neurogenesis in the hippocampus and thereby dramatically extend the reach of muscle PGC-1α (Schnyder and Handschin, 2015). Surprisingly, while overexpression of PGC-1α is sufficient to induce an endurance-trained muscle phenotype, several aspects of training adaptation seem to be retained even in mice with a global or muscle-specific knockout of this coactivator, respectively (Leick et al., 2008; Rowe et al., 2012). Discrepancies in such studies however indicate that the specific animal model, training type, timing, intensity, and other aspects of the exercise protocol are important for the assessment of the requirement of PGC-1α in exercise adaptation (Geng et al., 2010). Furthermore, these studies imply a redundant regulation of these evolutionarily extremely important plastic changes in skeletal muscle in which PGC-1α can be partially replaced by other, so far unknown regulators. Thus, in a physiological setting, PGC-1α controls a highly complex transcriptional network that requires spatial and temporal specification, coordination of anabolic and catabolic pathways as well as precise activation and termination. In this mini review, we highlight some of the recent mechanistic findings that contribute to the ability of PGC-1α to regulate transcription in such a broad and precise manner.

INTEGRATION OF CONTRACTION-INDUCED SIGNALING PATHWAYS BY PGC-1α IN SKELETAL MUSCLE

Muscle fiber contraction is linked to activation by the motor neuron, mechanical stress, relative tissue physoxia, an altered neuroendocrine milieu, changes in metabolic demand and other stimuli that engage various signaling pathways. All of these signals converge on PGC-1α and promote a transcriptional induction of the gene or induce posttranslational modifications (PTM) of the protein (**Figure 1A**), including PGC-1α protein phosphorylation by various kinases on different phosphorylation sites, acetylation, methylation, sumoylation, ubiquitination, and acetylglucosamination (**Figure 1B**; Fernandez-Marcos and Auwerx, 2011). The effects of most of these modifications on PGC-1α function are still poorly understood. Some of the PTMs can alter the stability of the PGC-1α protein or modulate the interaction with transcription factors or other co-regulators. For example, phosphorylation by the p38 mitogen-activated protein kinase (p38 MAPK) results in a prolongation of the normally very short half-life of the PGC-1α protein of ~2.5 h (Puigserver et al., 2001), at least in part by preventing ubiquitination of PGC-1α and therefore stabilizing the protein (Olson et al., 2008). The AMP-dependent protein kinase (AMPK) likewise phosphorylates the PGC-1α protein in addition to its positive effect on PGC-1α gene transcription and predominantly triggers catabolic pathways to rectify a relative energy deficit, e.g., in exercise (Jager et al., 2007). Such a temporal specification is extremely important to avoid futile cycles of PGC-1α-controlled anabolic and catabolic pathways, e.g., fatty acid β-oxidation and *de novo* lipogenesis (Summermatter et al., 2010). Moreover, PTMs could also determine spatial differentiation of PGC-1α function. For example, the interaction between PGC-1α and the GA-binding protein (GABP, also called nuclear respiratory factor 2 or NRF2) not only requires the presence of host cell factor (HCF) as an additional adaptor protein, but also specific phosphorylation events both on PGC-1α as well as the GABPB1 subunit of the GABP complex (Handschin et al., 2007c). These PTMs can be triggered by motor neuron-evoked neuregulin stimulation of the muscle fiber and thereby control a specific transcriptional activation of post-synaptic neuromuscular junction genes by PGC-1α and GABP exclusively in sub-synaptic nuclei (Handschin et al., 2007c). Thus, in addition to the modulation of protein stability, PTMs might alter the activity and stability of PGC-1α as well as the ability to interact with transcription factors and thereby regulate specific transcriptional programs (Handschin and Spiegelman, 2006). For most modifications of the PGC-1α protein, a "PTM code" (Lonard and O'malley, 2007) that determines transcription factor interaction specificity has not been elucidated. A prototypical example for a PGC-1α PTM code however is provided by the S6 kinase (S6K)-mediated phosphorylation that selectively

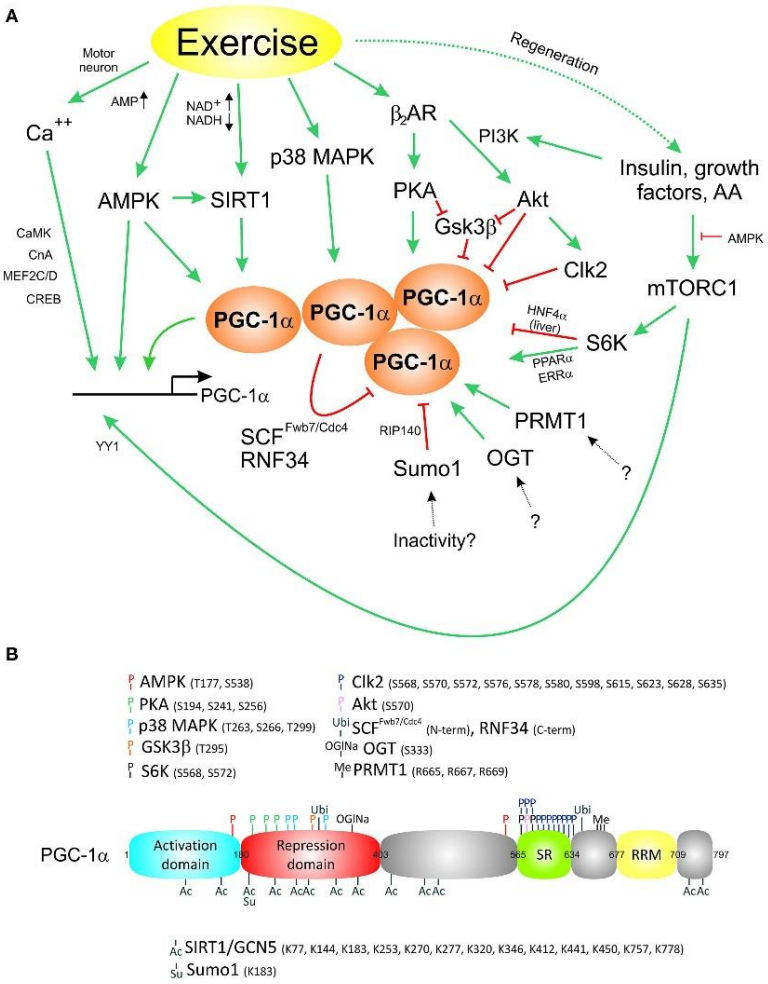

FIGURE 1 | Complex activation of the transcriptional co-activator PGC-1α by different signaling pathways. (A) Exercise triggers a complex transcriptional activation as well as various posttranslational modifications to control PGC-1α levels and activity. **(B)**, Posttranslational modifications of the PGC-1α protein. AA, amino acids; Ac, acetylation; Akt, protein kinase B; AMPK, AMP-activated protein kinase; β2AR, β2 adrenergic receptor; CaMK, Ca^{2+}/calmodulin-dependent protein kinase; CnA, calcineurin A; Clk2, Cdc2-like kinase 2; CREB, cAMP response element binding protein; ERRα, estrogen-related receptor α; Gsk3β, glycogen synthase kinase 3 beta; HNF4 α, hepatic nuclear factor 4 α; MEF2C/2D, myocyte enhancer factors 2C/D; Me, methylation; mTORC1, mammalian target of rapamycin complex 1; OGlNa, O-linked β-N-acetylglucosamination; OGT, O-linked β-N-acetylglucosamine transferase; p38 MAPK, p38 mitogen-activated protein kinase; PI3K, phosphoinositide 3 kinase; PKA, protein kinase A; P, phosphorylation; PPARα, peroxisome proliferator-activated receptor α; PRMT1, protein arginine methyltransferase 1; RIP140, receptor interacting protein 140; RNF34, ring finger protein 34; S6K, S6-kinase; $SCF^{Fwb7/Cdc4}$, SCF ubiquitin ligase complex subunit Fwb7/Cdc4; SIRT1, sirtuin-1; Su, sumoylation; Sumo1, small ubiquitin related modifier 1; Ubi, ubiquitination; YY1, yin yang 1.

retains the ability of PGC-1α to boost fatty acid oxidation and mitochondrial function while attenuating its effect on gluconeogenesis in the liver (Lustig et al., 2011). Mechanistically, these PTMs reduce the interaction between PGC-1α and the hepatic nuclear factor 4 α (HNF4α), but not co-activation of the estrogen-related receptor α (ERRα) or PPARα. In addition to binding to transcription factors, PTMs of the PGC-1α protein can also affect the interaction with other co-regulators. For example, the co-repressors p160 myb binding protein (p160MBP) and receptor interacting protein 140 (RIP140) are recruited to PGC-1α in a PTM-dependent manner: p160MBP inhibits the ability of PGC-1α to regulate mitochondrial gene expression in the absence of p38 MAPK-mediated phosphorylation (Fan et al., 2004) while RIP140 associates with and represses sumoylated

PGC-1α (Rytinki and Palvimo, 2009). Other co-repressors reduce PGC-1α activity by competing for binding to transcription factors, for example modulation of ERRα co-activation by the nuclear receptor co-repressor 1 (NCoR1; Pérez-Schindler et al., 2012) or of the glucocorticoid receptor by the small heterodimer partner (SHP; Borgius et al., 2002). PTM-dependent binding events are also observed for co-activators as exemplified by the interaction of PGC-1α with the Mediator 1 (MED1) subunit of the TRAP/DRIP/mediator complex that is disrupted after phosphorylation of PGC-1α by the Cdc2-like kinase 2 (Clk2; Tabata et al., 2014). Ubiquitination and subsequent proteasomal degradation of the PGC-1α protein form a negative feedback loop to ensure timely termination of the PGC-1α response (Sano et al., 2007). This process might be triggered by PGC-1α protein self-aggregation upon reaching a critical threshold (Sano et al., 2007). Thus, PGC-1α serves as recipient of a multitude of PTMs, thereby integrates the activity of the respective signaling pathways and subsequently triggers a transcriptional response that is adapted to the specific cellular context.

REGULATORY AND FUNCTIONAL DIVERSITY BASED ON THE PGC-1α GENE STRUCTURE AND TRANSCRIPT VARIANTS

PGC-1α gene expression is rapidly and robustly increased in response to external stimuli that increase the energy demand such as cold in brown fat, fasting in the liver, or contraction in skeletal muscle (Lin et al., 2005). The cAMP response element binding protein (CREB) and the activating transcription factor-2 (ATF-2), both of which bind to cAMP response elements (CRE), are common regulators of PGC-1α transcription in most tissues. In addition, tissue-specific transcription factors provide an additional layer of control, e.g., myocyte enhancer factors 2C/D (MEF2C and -2D) in muscle cells (Pérez-Schindler and Handschin, 2013). A positive autoregulatory loop of MEF2C/D co-activation by PGC-1α on its own promoter furthermore contributes to adequate and controlled induction of PGC-1α transcription in this tissue (Handschin et al., 2003). Intriguingly, this theme of using cross- and autoregulatory loops, thus forming biological switches, is also observed in early downstream target gene regulation, for example in the induction of ERRα and GABPA by PGC-1α (Mootha et al., 2004).

PGC-1α transcription can be initiated from three start sites on two alternative promoters. Moreover, alternative RNA processing further increases the number of PGC-1α transcripts and, as a consequence, protein variants (Martínez-Redondo et al., 2015). Even though the regulatory elements of the two promoters have not yet been studied in detail, the proximal promoter seems to provide a more robust basal expression while the distal promoter that is approximately 13 kb upstream exhibits a higher dynamic range in gene expression, at least in skeletal muscle (Martínez-Redondo et al., 2015). It is still unclear whether alternative promoter usage is closely linked to the transcription of PGC-1α isoforms. Moreover, the functional consequence of the selective expression of most PGC-1α transcript variants is unknown. Surprisingly however, the PGC-1α4 variant seems to regulate a highly distinct transcriptional program with very little overlap compared to that of the other variants (Ruas et al., 2012). PGC-1α4 contributes to skeletal muscle adaptation to resistance training and the ensuing fiber hypertrophy (Ruas et al., 2012), at least in certain contexts (Pérez-Schindler et al., 2013), diametrically opposite to the endurance exercise-like phenotype triggered by the other PGC-1α isoforms. In humans however, some studies questioned an exclusive correlation between PGC-1α4 expression and resistance training (Lundberg et al., 2014) warranting further studies. In any case however, the gene structure and transcript processing of PGC-1α thus provide an additional layer of regulatory and functional specification (Handschin and Spiegelman, 2006).

PGC-1α-CONTROLLED TRANSCRIPTIONAL NETWORK REGULATION ALLOWS CONTEXT-DEPENDENT CONTROL AND SPECIFICATION

Originally, PGC-1α has been discovered as a coactivator of PPARγ and was hence named accordingly (Puigserver et al., 1998). It however became clear that PGC-1α not only interacts with this, but also a number of other nuclear receptors and non-nuclear receptor transcription factors. Intriguingly, these interactions are mediated by different structural domains within the PGC-1α protein, with a more N-terminal preference for nuclear receptor co-activation while others, for example MEF2 or forkhead box protein 1 (Foxo1) bind PGC-1α closer to the C-terminus (Lin et al., 2005). Therefore, the functional specificity of PGC-1α isoforms that lack certain domains of the full-length protein could stem from the specific ablation and enhancement of binding to transcription factor partners (Handschin and Spiegelman, 2006; Martínez-Redondo et al., 2015). Despite the identification of various interaction partners, PGC-1α seems to have a special relationship with ERRα, at least in the regulation of mitochondrial genes (Mootha et al., 2004). ERRα is an orphan nuclear receptor that is mainly activated by co-activator binding in a ligand-independent manner (Kallen et al., 2004). Moreover, PGC-1α rapidly induces the transcription of ERRα as an early response target gene (Mootha et al., 2004). It thus is not surprising that pharmacological inhibition of the interaction between PGC-1α and ERRα or knockdown of ERRα has a potent effect on many PGC-1α target genes in muscle cells (Mootha et al., 2004; Schreiber et al., 2004). A global analysis of PGC-1α recruitment to regulatory elements in the mouse genome combined with an expression analysis however revealed a so-far largely underestimated number of putative transcription factor partners beyond ERRα to be involved in PGC-1α-mediated target gene regulation in muscle cells (Baresic et al., 2014). Furthermore, transcription factor motif activity response analysis not only predicts ERRα to be involved in the regulation of primary, but also secondary PGC-1α target genes, thus both in the co-activated state but also working without PGC-1α in this context. These data indicate a much higher complexity of transcription factor engagement by PGC-1α than previously

suggested. Second, the combination of PGC-1α ChIPseq and gene expression data revealed that of the high number of PGC-1α repressed genes, only a small minority, ~5%, have a PGC-1α DNA recruitment peak within a distance of ±10 kb of their promoter. Accordingly, the findings imply that the effect of PGC-1α on gene repression is predominantly indirect and that PGC-1α lacks an intrinsic inhibitory function (Baresic et al., 2014). While a systematic analysis of gene repression by PGC-1α remains to be done, PGC-1α-dependent reduction of the activating phosphorylation of the p65 subunit of the nuclear factor κB (NF-κB; Eisele et al., 2013) could account for at least some of the indirect inhibitory effect of PGC-1α on pro-inflammatory muscle gene expression (Eisele and Handschin, 2014). Third, this systematic study revealed novel insights into the mechanisms that ensure functional redundancy and complementation of PGC-1α-mediated transcriptional control. Principal component analysis of the transcription factor binding motifs within the regions of PGC-1α DNA recruitment implied an important role for the activator protein-1 (AP-1) transcription factor complex in PGC-1α-controlled gene expression (Baresic et al., 2014). AP-1 is a well-studied stress response gene in various cellular contexts, but has so far never been associated with PGC-1α function in muscle. Interestingly, the group of direct targets for AP-1 and PGC-1α was significantly enriched in genes associated with the cellular response to hypoxia, including several regulators of vascularization. This regulation complements the previously discovered control of the expression of the vascular endothelial growth factor (VEGF) by PGC-1α and ERRα (Arany et al., 2008). These findings imply that this seemingly redundant usage of different transcription factors to regulate the same biological program ensures adequate regulation of this critical process. Alternatively, the ability of PGC-1α to enhance the transcriptional activity of different partners might also indicate that PGC-1α is able to regulate the respective target genes in different cellular contexts, e.g., by binding to ERRα in a metabolically stressed muscle cell and acting together with AP-1 upon reduced physoxic conditions (**Figure 2**). Exercise triggers a hypoxic response including an activation of the hypoxia-inducible factor-1 (HIF-1) in muscle cells by a lowering of the relative tissue oxygen availability due to a dysbalance between oxygen consumption and supply, exacerbated by contraction-mediated constriction of blood vessels (Lindholm and Rundqvist, 2015). Together, the current data highlight the vast complexity of diverse mechanisms by which PGC-1α exerts a pleiotropic response in muscle cells.

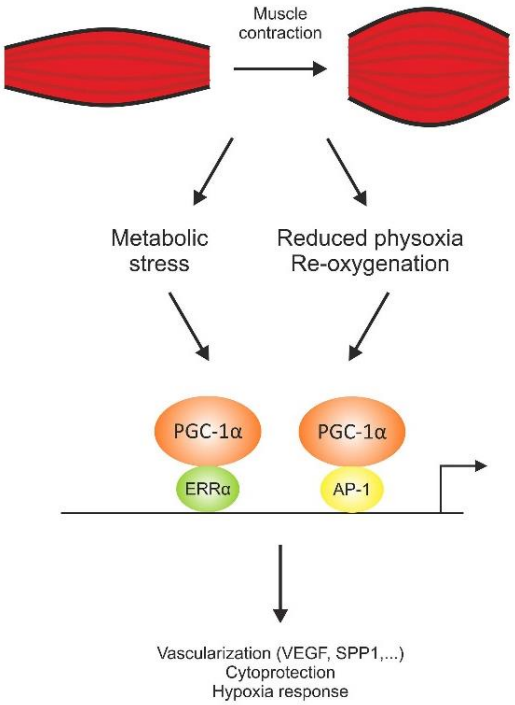

FIGURE 2 | PGC-1α engages different transcription factors to robustly regulate biological programs. Co-activation of the estrogen-related receptor α (ERRα) and the activator protein-1 transcription factor complex (AP-1) allow a differential regulation of the gene program for vascularization, cytoprotection, and hypoxia response triggered by different stimuli, e.g., a change in the metabolic demand and the ensuing angiogenesis to improve substrate availability or neovascularization as a response to a contraction-mediated reduction in tissue physoxia and an ensuing re-oxygenation for adequate oxygen supply. SPP1, secreted phosphoprotein 1; VEGF, vascular endothelial growth factor.

CONCLUSIONS AND OUTLOOK

In essence, PGC-1α is a protein docking platform that on one side is recruited to transcription factors bound to their target gene promoters and enhancers, and on the other side interacts with components of the histone acetyltransferase (Puigserver et al., 1999), TRAP/DRIP/mediator (Wallberg et al., 2003), and SWI/SNF (Li et al., 2008) co-regulator protein complexes. Thereby, PGC-1α greatly boosts transcription even though PGC-1α lacks any discernable intrinsic enzymatic activity. Despite this ostensible simplicity in function, PGC-1α can control highly complex transcriptional programs in various tissues with a significant impact on organ plasticity. The ability of PGC-1α to integrate different signaling pathways through a multitude of PTMs, selective activation of alternative promoters and expression of transcript variants could provide a mechanistic explanation for the key regulatory function of PGC-1α in the regulation of tissue phenotypes. However, more studies will be required to obtain a better understanding and overview on the different aspects of the regulation of a co-activator-controlled transcriptional network, which not only is of high interest to understand the basic biology, but could also have a significant clinical impact. In a physiological and pathophysiological context, elevation of PGC-1α in muscle promotes a high endurance phenotype and ameliorates various muscle diseases with different etiologies, including Duchenne muscular dystrophy (Handschin et al., 2007c), denervation-induced fiber atrophy (Sandri et al., 2006), or sarcopenia (Wenz et al., 2014), respectively. To date, it is not clear which functions

of muscle PGC-1α are responsible for such a broad therapeutic effect (Handschin, 2009). Similarly, pharmacological agents that robustly, specifically and safely elevate PGC-1α in skeletal muscle in the desired therapeutic window remain elusive (Svensson and Handschin, 2014). Finally, based on studies with muscle-specific PGC-1α transgenic animals that have an accelerated development of insulin resistance on a high fat diet (Choi et al., 2008), which can only be rectified by *bona fide* physical activity (Summermatter et al., 2013), the application of so-called "exercise mimetics," compounds that elicit exercise-like effects in muscle and other tissues, might be problematic. Therefore, to design partial exercise mimetics or new compounds that specifically activate certain functions of PGC-1α, better knowledge about upstream regulators and downstream effects on the transcriptional network are needed. In particular, even though a strong correlation between muscle PGC-1α expression, exercise, and diseases states has been repeatedly documented in humans (e.g., see Silvennoinen et al., 2015), information about the regulation and function of human muscle PGC-1α so far remains largely descriptive. Until further insights are obtained, physical activity thus remains a cheap and effective way for the prevention and treatment of many chronic diseases (Handschin and Spiegelman, 2008), at least in exercise-tolerant patients.

ACKNOWLEDGMENTS

We thank Svenia Schnyder for critical comments on the manuscript. Work in our lab is supported by the ERC Consolidator grant 616830-MUSCLE_NET, the Swiss National Science Foundation, SystemsX.ch, the Swiss Society for Research on Muscle Diseases (SSEM), the "Novartis Stiftung für medizinisch-biologische Forschung," the University of Basel and the Biozentrum. BK is supported by the Biozentrum Basel International PhD Program "Fellowships for Excellence."

REFERENCES

Arany, Z., Foo, S. Y., Ma, Y. H., Ruas, J. L., Bommi-Reddy, A., Girnun, G., et al. (2008). HIF-independent regulation of VEGF and angiogenesis by the transcriptional coactivator PGC-1 alpha. *Nature* 451, 1008–1012. doi: 10.1038/nature06613

Arnold, A. S., Gill, J., Christe, M., Ruiz, R., McGuirk, S., St-Pierre, J., et al. (2014). Morphological and functional remodelling of the neuromuscular junction by skeletal muscle PGC-1alpha. *Nat. Commun.* 5, 3569. doi: 10.1038/ncomms4569

Baresic, M., Salatino, S., Kupr, B., van Nimwegen, E., and Handschin, C. (2014). Transcriptional network analysis in muscle reveals ap-1 as a partner of PGC-1 alpha in the regulation of the hypoxic gene program. *Mol. Cell. Biol.* 34, 2996–3012. doi: 10.1128/MCB.01710-13

Borgius, L. J., Steffensen, K. R., Gustafsson, J. A., and Treuter, E. (2002). Glucocorticoid signaling is perturbed by the atypical orphan receptor and corepressor SHP. *J. Biol. Chem.* 277, 49761–49766. doi: 10.1074/jbc.M205641200

Choi, C. S., Befroy, D. E., Codella, R., Kim, S., Reznick, R. M., Hwang, Y. J., et al. (2008). Paradoxical effects of increased expression of PGC-1alpha on muscle mitochondrial function and insulin-stimulated muscle glucose metabolism. *Proc. Natl. Acad. Sci. U.S.A.* 105, 19926–19931. doi: 10.1073/pnas.0810339105

Dasgupta, S., Lonard, D. M., and O'Malley, B. W. (2014). Nuclear receptor coactivators: master regulators of human health and disease. *Annu. Rev. Med.* 65, 279–292. doi: 10.1146/annurev-med-051812-145316

Eisele, P. S., and Handschin, C. (2014). Functional crosstalk of PGC-1 coactivators and inflammation in skeletal muscle pathophysiology. *Semin. Immunopathol.* 36, 27–53. doi: 10.1007/s00281-013-0406-4

Eisele, P. S., Salatino, S., Sobek, J., Hottiger, M. O., and Handschin, C. (2013). The peroxisome proliferator-activated receptor gamma coactivator 1alpha/beta (PGC-1) coactivators repress the transcriptional activity of NF-kappaB in skeletal muscle cells. *J. Biol. Chem.* 288, 2246–2260. doi: 10.1074/jbc.M112.375253

Fan, M., Rhee, J., St-Pierre, J., Handschin, C., Puigserver, P., Lin, J., et al. (2004). Suppression of mitochondrial respiration through recruitment of p160 myb binding protein to PGC-1alpha: modulation by p38 MAPK. *Genes Dev.* 18, 278–289. doi: 10.1101/gad.1152204

Fernandez-Marcos, P. J., and Auwerx, J. (2011). Regulation of PGC-1alpha, a nodal regulator of mitochondrial biogenesis. *Am. J. Clin. Nutr.* 93, 884S-890S. doi: 10.3945/ajcn.110.001917

Geng, T., Li, P., Okutsu, M., Yin, X., Kwek, J., Zhang, M., et al. (2010). PGC-1alpha plays a functional role in exercise-induced mitochondrial biogenesis and angiogenesis but not fiber-type transformation in mouse skeletal muscle. *Am. J. Physiol. Cell Physiol.* 298, C572–C579. doi: 10.1152/ajpcell.00481.2009

Handschin, C. (2009). The biology of PGC-1alpha and its therapeutic potential. *Trends Pharmacol. Sci.* 30, 322–329. doi: 10.1016/j.tips.2009.03.006

Handschin, C. (2010). Regulation of skeletal muscle cell plasticity by the peroxisome proliferator-activated receptor gamma coactivator 1alpha. *J. Recept. Signal Transduct. Res.* 30, 376–384. doi: 10.3109/10799891003641074

Handschin, C., Chin, S., Li, P., Liu, F., Maratos-Flier, E., Lebrasseur, N. K., et al. (2007a). Skeletal muscle fiber-type switching, exercise intolerance, and myopathy in PGC-1 alpha muscle-specific knock-out animals. *J. Biol. Chem.* 282, 30014–30021. doi: 10.1074/jbc.M704817200

Handschin, C., Choi, C. S., Chin, S., Kim, S., Kawamori, D., Kurpad, A. J., et al. (2007b). Abnormal glucose homeostasis in skeletal muscle-specific PGC-1 alpha knockout mice reveals skeletal muscle-pancreatic beta cell crosstalk. *J. Clin. Invest.* 117, 3463–3474. doi: 10.1172/JCI31785

Handschin, C., Kobayashi, Y. M., Chin, S., Seale, P., Campbell, K. P., and Spiegelman, B. M. (2007c). PGC-1 alpha regulates the neuromuscular junction program and ameliorates Duchenne muscular dystrophy. *Genes Dev.* 21, 770–783. doi: 10.1101/gad.1525107

Handschin, C., Lin, J., Rhee, J., Peyer, A. K., Chin, S., Wu, P. H., et al. (2005). Nutritional regulation of hepatic heme biosynthesis and porphyria through PGC-1alpha. *Cell* 122, 505–515. doi: 10.1016/j.cell.2005.06.040

Handschin, C., Rhee, J., Lin, J., Tarr, P. T., and Spiegelman, B. M. (2003). An autoregulatory loop controls peroxisome proliferator-activated receptor gamma coactivator 1alpha expression in muscle. *Proc. Natl. Acad. Sci. U.S.A.* 100, 7111–7116. doi: 10.1073/pnas.1232352100

Handschin, C., and Spiegelman, B. M. (2006). Peroxisome proliferator-activated receptor gamma coactivator 1 coactivators, energy homeostasis, and metabolism. *Endocr. Rev.* 27, 728–735. doi: 10.1210/er.2006-0037

Handschin, C., and Spiegelman, B. M. (2008). The role of exercise and PGC1 alpha in inflammation and chronic disease. *Nature* 454, 463–469. doi: 10.1038/nature07206

Jager, S., Handschin, C., Pierre, J., and Spiegelman, B. M. (2007). AMP-activated protein kinase (AMPK) action in skeletal muscle via direct phosphorylation of PGC-1 alpha. *Proc. Natl. Acad. Sci. U.S.A.* 104, 12017–12022. doi: 10.1073/pnas.0705070104

Kallen, J., Schlaeppi, J. M., Bitsch, F., Filipuzzi, I., Schilb, A., Riou, V., et al. (2004). Evidence for ligand-independent transcriptional activation of the human estrogen-related receptor alpha (ERRalpha): crystal structure of ERRalpha ligand binding domain in complex with peroxisome proliferator-activated receptor coactivator-1alpha. *J. Biol. Chem.* 279, 49330–49337. doi: 10.1074/jbc.M407999200

Leick, L., Wojtaszewski, J. F., Johansen, S. T., Kiilerich, K., Comes, G., Hellsten, Y., et al. (2008). PGC-1alpha is not mandatory for exercise- and training-induced adaptive gene responses in mouse skeletal muscle. *Am. J. Physiol. Endocrinol. Metab.* 294, E463–E474. doi: 10.1152/ajpendo.00666.2007

Li, S., Liu, C., Li, N., Hao, T., Han, T., Hill, D. E., et al. (2008). Genome-wide coactivation analysis of PGC-1alpha identifies BAF60a as a regulator of hepatic lipid metabolism. *Cell Metab.* 8, 105–117. doi: 10.1016/j.cmet.2008.06.013

Liang, H., Balas, B., Tantiwong, P., Dube, J., Goodpaster, B. H., O'Doherty, R. M., et al. (2009). Whole body overexpression of PGC-1alpha has opposite effects on hepatic and muscle insulin sensitivity. *Am. J. Physiol. Endocrinol. Metab.* 296, E945–E954. doi: 10.1152/ajpendo.90292.2008

Lin, J., Handschin, C., and Spiegelman, B. M. (2005). Metabolic control through the PGC-1 family of transcription coactivators. *Cell Metab.* 1, 361–370. doi: 10.1016/j.cmet.2005.05.004

Lin, J., Wu, H., Tarr, P. T., Zhang, C. Y., Wu, Z., Boss, O., et al. (2002). Transcriptional co-activator PGC-1 alpha drives the formation of slow-twitch muscle fibres. *Nature* 418, 797–801. doi: 10.1038/nature00904

Lin, J., Wu, P. H., Tarr, P. T., Lindenberg, K. S., St-Pierre, J., Zhang, C. Y., et al. (2004). Defects in adaptive energy metabolism with CNS-linked hyperactivity in PGC-1alpha null mice. *Cell* 119, 121–135. doi: 10.1016/j.cell.2004.09.013

Lindholm, M. E., and Rundqvist, H. (2015). Skeletal muscle HIF-1 and exercise. *Exp. Physiol.* doi: 10.1113/EP085318. [Epub ahead of print].

Lonard, D. M., and O'malley, B. W. (2007). Nuclear receptor coregulators: judges, juries, and executioners of cellular regulation. *Mol. Cell* 27, 691–700. doi: 10.1016/j.molcel.2007.08.012

Lundberg, T. R., Fernandez-Gonzalo, R., Norrbom, J., Fischer, H., Tesch, P. A., and Gustafsson, T. (2014). Truncated splice variant PGC-1alpha4 is not associated with exercise-induced human muscle hypertrophy. *Acta Physiol.* 212, 142–151. doi: 10.1111/apha.12310

Lustig, Y., Ruas, J. L., Estall, J. L., Lo, J. C., Devarakonda, S., Laznik, D., et al. (2011). Separation of the gluconeogenic and mitochondrial functions of PGC-1 alpha through S6 kinase. *Genes Dev.* 25, 1232–1244. doi: 10.1101/gad.2054711

Martínez-Redondo, V., Pettersson, A. T., and Ruas, J. L. (2015). The hitchhiker's guide to PGC-1alpha isoform structure and biological functions. *Diabetologia* 58, 1969–1977. doi: 10.1007/s00125-015-3671-z

Miura, S., Tomitsuka, E., Kamei, Y., Yamazaki, T., Kai, Y., Tamura, M., et al. (2006). Overexpression of peroxisome proliferator-activated receptor gamma co-activator-1alpha leads to muscle atrophy with depletion of ATP. *Am. J. Pathol.* 169, 1129–1139. doi: 10.2353/ajpath.2006.060034

Mootha, V. K., Handschin, C., Arlow, D., Xie, X., St Pierre, J., Sihag, S., et al. (2004). Erralpha and Gabpa/b specify PGC-1alpha-dependent oxidative phosphorylation gene expression that is altered in diabetic muscle. *Proc. Natl. Acad. Sci. U.S.A.* 101, 6570–6575. doi: 10.1073/pnas.0401401101

Mouchiroud, L., Eichner, L. J., Shaw, R. J., and Auwerx, J. (2014). Transcriptional coregulators: fine-tuning metabolism. *Cell Metab.* 20, 26–40. doi: 10.1016/j.cmet.2014.03.027

Olson, B. L., Hock, M. B., Ekholm-Reed, S., Wohlschlegel, J. A., Dev, K. K., Kralli, A., et al. (2008). SCFCdc4 acts antagonistically to the PGC-1alpha transcriptional coactivator by targeting it for ubiquitin-mediated proteolysis. *Genes Dev.* 22, 252–264. doi: 10.1101/gad.1624208

Patti, M. E., Butte, A. J., Crunkhorn, S., Cusi, K., Berria, R., Kashyap, S., et al. (2003). Coordinated reduction of genes of oxidative metabolism in humans with insulin resistance and diabetes: potential role of PGC1 and NRF1. *Proc. Natl. Acad. Sci. U.S.A.* 100, 8466–8471. doi: 10.1073/pnas.1032913100

Pérez-Schindler, J., and Handschin, C. (2013). New insights in the regulation of skeletal muscle PGC-1α by exercise and metabolic diseases. *Drug Discov. Today Dis. Models* 10, e79–e85. doi: 10.1016/j.ddmod.2012.12.002

Pérez-Schindler, J., Summermatter, S., Salatino, S., Zorzato, F., Beer, M., Balwierz, P. J., et al. (2012). The corepressor NCoR1 antagonizes PGC-1alpha and estrogen-related receptor alpha in the regulation of skeletal muscle function and oxidative metabolism. *Mol. Cell. Biol.* 32, 4913–4924. doi: 10.1128/MCB.00877-12

Pérez-Schindler, J., Summermatter, S., Santos, G., Zorzato, F., and Handschin, C. (2013). The transcriptional coactivator PGC-1 alpha is dispensable for chronic overload-induced skeletal muscle hypertrophy and metabolic remodeling. *Proc. Natl. Acad. Sci. U.S.A.* 110, 20314–20319. doi: 10.1073/pnas.1312039110

Puigserver, P., Adelmant, C., Wu, Z. D., Fan, M., Xu, J. M., O'malley, B., et al. (1999). Activation of PPAR gamma coactivator-1 through transcription factor docking. *Science* 286, 1368–1371. doi: 10.1126/science.286.5443.1368

Puigserver, P., Rhee, J., Lin, J. D., Wu, Z. D., Yoon, J. C., Zhang, C. Y., et al. (2001). Cytokine stimulation of energy expenditure through p38 MAP kinase activation of PPAR gamma coactivator-1. *Mol. Cell* 8, 971–982. doi: 10.1016/S1097-2765(01)00390-2

Puigserver, P., Wu, Z., Park, C. W., Graves, R., Wright, M., and Spiegelman, B. M. (1998). A cold-inducible coactivator of nuclear receptors linked to adaptive thermogenesis. *Cell* 92, 829–839.

Rowe, G. C., El-Khoury, R., Patten, I. S., Rustin, P., and Arany, Z. (2012). PGC-1alpha is dispensable for exercise-induced mitochondrial biogenesis in skeletal muscle. *PLoS ONE* 7:e41817. doi: 10.1371/journal.pone.0041817

Ruas, J. L., White, J. P., Rao, R. R., Kleiner, S., Brannan, K. T., Harrison, B. C., et al. (2012). A PGC-1 alpha isoform induced by resistance training regulates skeletal muscle hypertrophy. *Cell* 151, 1319–1331. doi: 10.1016/j.cell.2012.10.050

Rytinki, M. M., and Palvimo, J. J. (2009). SUMOylation attenuates the function of PGC-1alpha. *J. Biol. Chem.* 284, 26184–26193. doi: 10.1074/jbc.M109.038943

Sandri, M., Lin, J. D., Handschin, C., Yang, W. L., Arany, Z. P., Lecker, S. H., et al. (2006). PGC-1 alpha a protects skeletal muscle from atrophy by suppressing Fox03 action and atrophy-specific gene transcription. *Proc. Natl. Acad. Sci. U.S.A.* 103, 16260–16265. doi: 10.1073/pnas.0607795103

Sano, M., Tokudome, S., Shimizu, N., Yoshikawa, N., Ogawa, C., Shirakawa, K., et al. (2007). Intramolecular control of protein stability, subnuclear compartmentalization, and coactivator function of peroxisome proliferator-activated receptor gamma coactivator 1alpha. *J. Biol. Chem.* 282, 25970–25980. doi: 10.1074/jbc.M703634200

Schnyder, S., and Handschin, C. (2015). Skeletal muscle as an endocrine organ: PGC-1α, myokines and exercise. *Bone* 80, 115–125. doi: 10.1016/j.bone.2015.02.008

Schreiber, S. N., Emter, R., Hock, M. B., Knutti, D., Cardenas, J., Podvinec, M., et al. (2004). The estrogen-related receptor alpha (ERRalpha) functions in PPARgamma coactivator 1alpha (PGC-1alpha)-induced mitochondrial biogenesis. *Proc. Natl. Acad. Sci. U.S.A.* 101, 6472–6477. doi: 10.1073/pnas.0308686101

Silvennoinen, M., Ahtiainen, J. P., Hulmi, J. J., Pekkala, S., Taipale, R. S., Nindl, B. C., et al. (2015). PGC-1 isoforms and their target genes are expressed differently in human skeletal muscle following resistance and endurance exercise. *Physiol. Rep.* 3:e12563. doi: 10.14814/phy2.12563

Summermatter, S., Baum, O., Santos, G., Hoppeler, H., and Handschin, C. (2010). Peroxisome proliferator-activated receptor gamma coactivator 1 alpha (PGC-1 alpha) promotes skeletal muscle lipid refueling *in vivo* by activating de novo lipogenesis and the pentose phosphate pathway. *J. Biol. Chem.* 285, 32793–32800. doi: 10.1074/jbc.M110.145995

Summermatter, S., Shui, G. H., Maag, D., Santos, G., Wenk, M. R., and Handschin, C. (2013). PGC-1 alpha improves glucose homeostasis in skeletal muscle in an activity-dependent manner. *Diabetes* 62, 85–95. doi: 10.2337/db12-0291

Svensson, K., and Handschin, C. (2014). Modulation of PGC-1alpha activity as a treatment for metabolic and muscle-related diseases. *Drug Discov. Today* 19, 1024–1029. doi: 10.1016/j.drudis.2014.02.013

Tabata, M., Rodgers, J. T., Hall, J. A., Lee, Y., Jedrychowski, M. P., Gygi, S. P., et al. (2014). Cdc2-like kinase 2 suppresses hepatic fatty acid oxidation and ketogenesis through disruption of the PGC-1alpha and MED1 complex. *Diabetes* 63, 1519–1532. doi: 10.2337/db13-1304

Wallberg, A. E., Yamamura, S., Malik, S., Spiegelman, B. M., and Roeder, R. G. (2003). Coordination of p300-mediated chromatin remodeling and TRAP/mediator function through coactivator PGC-1alpha. *Mol. Cell* 12, 1137–1149. doi: 10.1016/S1097-2765(03)00391-5

Wenz, T., Rossi, S. G., Rotundo, R. L., Spiegelman, B. M., and Moraes, C. T. (2014). Increased muscle PGC-1 alpha expression protects from sarcopenia and metabolic disease during aging (vol 106, pg 20405, 2009). *Proc. Natl. Acad. Sci. U.S.A.* 111, 15851–15851. doi: 10.1073/pnas.1419095111

Conflict of Interest Statement: The authors declare that the research was conducted in the absence of any commercial or financial relationships that could be construed as a potential conflict of interest.

Acknowledgments

First, I would like to thank Prof. Dr. Christoph Handschin, my supervisor, for giving me the opportunity to complete my PhD in his lab. I am very thankful for his support and that he allowed me to work independently and bring in my own ideas. Whenever I needed to discuss results, develop new hypotheses or to get advices, his door was always open.

Furthermore, I am grateful to my thesis committee members Prof. Dr. Markus Rüegg, who supported me already during my Master thesis and now during the course of my PhD, and Prof. Dr. Martin Spiess.

A big thank to all current and former Handschin lab members as well as the Rüegg lab members, which created a great working atmosphere and shared their knowledge about various experiments and techniques with me.

I would also like to thank the collaborators Dr. Pawel Pelczar, who helped me to generate the multiplex epitope tag Ppargc1a knock-in mouse and Dr. Karl Nordström, who analyzed the RRBS data.

A very special thank goes to Svenia Schnyder, Bettina Karrer, Regula Furrer and Jny Wittker for their great support and an awesome time in- and outside the lab.

Last but not least, the biggest thank goes to my family and specially to my husband Philippe Heim, who, went through and survived all the ups and downs I faced during my PhD. They always encouraged and supported me with great patience and enthusiasm.

Curriculum Vitae

PERSONAL INFORMATION

Barbara Heim-Kupr
MSc in Molecular Biology

Schlettstadterstrasse 35
CH-4055 Basel
E-Mail: barbara.heim17@gmail.com
Phone: +41 79 257 22 32

Date of birth: 29th July 1988
Nationality: Swiss

PRACTICAL EXPERIENCE

09/2013 – expected 06/2018	**PhD in Biochemistry, Biozentrum, University of Basel** Scientific research, project management and organization in the field of biochemistry and molecular biology, laboratory work - High Throughput processing and sequencing: RNAseq, ChIPseq, Reduced Representation Bisulfite Sequencing (RRBS) - Arrangement of collaborations for Big Data analysis - Big Data processing and management by CLC, RStudio, ISMARA, Crunch - *In vivo*: LTK1 Certificate, mouse work, biochemical analysis - *In vitro*: cell culture, adenoviral transduction, siRNA, Seahorse assay, diverse biochemical applications
03/2013 – 06/2013	**Scientific Associate, Biozentrum, University of Basel** Laboratory work in the scientific field of biochemistry and molecular biology
09/2011 – 03/2013	**Master of Science in Molecular Biology, Biozentrum, University of Basel** Scientific research in the field of biochemical pathways and molecular biology

WORK EXPERIENCE

09/2013 – expected 06/2018 of	PhD in Biochemistry, Prof. Christoph Handschin, Biozentrum, University Basel
03/2013 – 06/2013	Scientific Associate, Prof. Markus A. Rüegg, Biozentrum, University of Basel
Since 2003	Captain of the 1st League Team Ladies, Tennis Club Old Boys Basel
01/2011 – 09/2013	Hostess Messe CH, Basel
09/2009 – 10/2010	Agency Assistant, Swisscanto Vorsorge, Basel

EDUCATION

09/2013 – expected 06/2018	PhD in Biochemistry, Biozentrum, University of Basel
09/2011 – 03/2013	Master of Science in Molecular Biology, University of Basel Title: "The Skeletal Muscle-Specific Inactivation of mTORC1 Affects Whole Body Metabolism"
08/2008 – 08/2011	Bachelor of Science in Molecular Biology, University of Basel
07/2004 – 12/2007	Matura, Biology and Chemistry, Gymnasium Oberwil BL

HONORS AND CERTIFICATES

2018	**Project Management Certificate**, SPOL AG, Schweiz
2017	Presentation at the **Diabetes Keystone Symposia**, Colorado, USA
2014	Presentation at the **TriRhena Metabolism Club Meeting**, Strasbourg, France
2013	Selected for the **Fellowship for Excellence International PhD Program**, Biozentrum, University of Basel

LANGUAGE SKILLS

German	Native
English	Fluent (spoken and written)
French	Intermediate (spoken and written)
Czech	Fluent (spoken)

PERSONAL INTERESSTS

Competitive Tennis and Squash single and team, skiing, hiking

REFERENCE

Prof. Dr. Christoph Handschin, University of Basel, christoph.handschin@unibas.ch

PUBLICATIONS

B. Kupr, S. Schnyder and C. Handschin (2017). "Role of Nuclear Receptors in Exercise-Induced Muscle Adaptations", Cold Spring Harbor Perspectives in Medicine, The Biology of Exercise

S. Schnyder, **B. Kupr**, C. Handschin (2017). "Coregulator-mediated control of skeletal muscle plasticity - A mini-review", Biochimie

S. Salatino and **B. Kupr**, M. Baresic, E. van Nimwegen, C. Handschin (2016). "The genomic context and co-recruitment of SP1 affect ERRα co-activation by PGC-1α in muscle cells", Molecular Endocrinology

M. Guridi M, **B. Kupr**, K. Romanino, S. Lin, D. Falcetta, L. Tintignac, M. A. Rüegg (2016). "Alterations to mTORC1 signaling in the skeletal muscle differentially affect whole-body metabolism", Skeletal muscle

M. Guridi, L. Tintignac, S. Lin, **B. Kupr**, P. Castets, M. A. Rüegg (2015). "Activation of mTORC1 in skeletal muscle regulates whole-body metabolism through FGF21", Science signaling

B. Kupr and C. Handschin (2015). "Complex Coordination of Cell Plasticity by a PGC-1alpha-controlled Transcriptional Network in Skeletal Muscle", Frontiers in physiology

M. Baresic and S. Salatino, **B. Kupr**, E. van Nimwegen, C. Handschin (2014). "Transcriptional network analysis in muscle reveals AP-1 as a partner of PGC-1α in the regulation of the hypoxic gene program", Molecular and Cellular Biology